ROOF FRAMING DESIGN GUIDE for Metal Building Systems

2nd Edition

MBMA
METAL BUILDING MANUFACTURERS ASSOCIATION®
Research | Leadership | Education

DISCLAIMER

This design guide has been developed under the direction of the American Iron and Steel Institute (AISI) Education Committee and the Metal Building Manufacturers Association (MBMA). The AISI Education Committee and MBMA wish to acknowledge and express gratitude to Dr. Michael Seek, P.E., Old Dominion University for developing this design guide. This guide is an update of the 2009 edition of the Design Guide for Cold-Formed Steel Purlin Roof Framing Systems, AISI D111, authored by Dr. Thomas Murray, P.E., Emeritus Professor, Virginia Tech, Mr. Jeff Sears, S.E., Kirkpatrick Forest Curtis, and Dr. Michael Seek.

With anticipated improvements in understanding of the behavior of cold-formed steel and the continuing development of new technology, this material might become dated. It is possible that MBMA will attempt to produce updates of this guide, but it is not guaranteed.

The information contained in this document is believed to be accurate; however, it is being provided for informational purposes only and is intended for use only as a guide. Publication of this document by MBMA should not be construed as MBMA engaging in or rendering engineering, legal, or other professional services. Use of the information contained in this document should not be considered a substitute for the advice of a registered professional engineer, attorney, or other professional. If such advice is required, seek the services of a registered professional engineer, licensed attorney, or other professional.

1st Printing – June 2024

Published by Metal Building Manufacturers Association

PREFACE

This document provides engineers with practical guidance on the design of cold-formed steel purlin roof framing systems. Substantive changes and updates were made from the 2009 edition of the Design Guide for Cold-Formed Steel Purlin Roof Framing Systems, AISI D111.

The material presented in this publication has been prepared as general information for the reader. While the material is believed to be technically correct and in accordance with recognized good practice at the time of publication, it should not be used without first securing competent advice with respect to its suitability for any given application. Neither the Metal Building Manufacturers Association (MBMA) and its members nor Old Dominion University and its faculty warrant or assume liability for the suitability of the material for any general or particular use.

Funding for the update of this guide was provided to Dr. Seek at Old Dominion University by the MBMA. Members of the AISI Committee on Specifications for the Design of Cold-Formed Steel Structural Members and MBMA provided valuable comments that greatly improved the guide. In particular, the members of the MBMA Steering Group members that performed an extensive review are Dennis Watson, Alliance Steel, Inc, Jeff Sears, Kirkpatrick Forest Curtis, Jim Fisher Computerized Structural Design, Joe Nunnery, Mark Detwiler, Cornerstone Building Brands, Rae Limerick, Nucor Building Systems, Roger LaBoube, Missouri University of Science & Technology, Thomas Murray, Virginia Tech, Al Harrold and Don Tobler.

TABLE OF CONTENTS

ROOF FRAMING DESIGN GUIDE FOR METAL BUILDING SYSTEMS

CHAPTER 1 INTRODUCTION

A typical cold-formed steel purlin roof framing system consists of four primary components: roof panels, purlins, purlin braces, and system anchorage. These components interact to create a structural system: the roof panels support both gravity and wind uplift loading while providing lateral support to the purlins. In turn, the purlins support the roof panels and provide lateral and, together with flange braces, flexural-torsional support to the supporting building frame members. The system anchorage restrains displacements of the purlin in the plane of the roof with the resulting forces resisted by anchorage devices (anti-roll clips) at the building frames or by restraint braces within the purlin spans. Optional in-plane or torsional braces provide lateral support to purlins at discrete locations. Figure 1-1 shows cold-formed steel roof framing for a typical metal building.

While the roof panels create a diaphragm that stabilizes the purlins, this diaphragm is not relied upon for overall building stability. Bracing in the plane of the roof is used to create a horizontal lateral force resisting system to transfer wind and seismic loads. Some purlins, referred to as strut purlins, are incorporated into this in-plane bracing to transfer axial forces from the building end walls to the longitudinal bracing system. Note that this in-plane bracing is not shown in Figure 1-1.

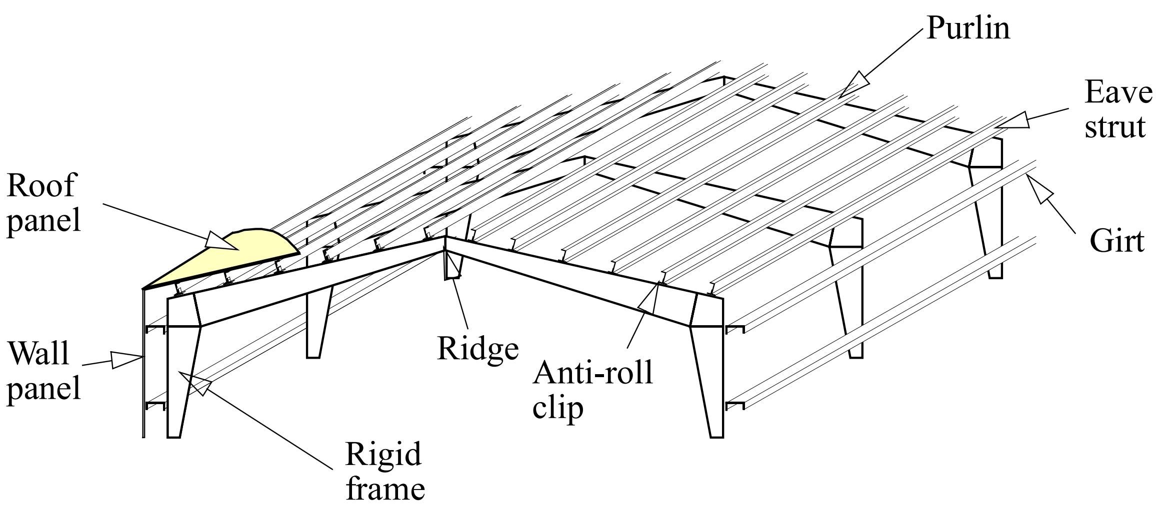

Figure 1-1 Typical Metal Building Framing

1.1 Roof Panels

Steel roof panels serve as an environmental barrier as well as provide lateral and rotational restraint to the supporting purlins. Roof panels are one of two basic types: through-fastened (sometimes referred to as screw-fastened) and standing seam. Through-fastened panels are attached directly to the supporting purlins using self-drilling screws as shown in Figure 1.1-1(a). For standing seam systems, the panel is connected to the purlins by specially designed clips with a tab that is embedded into the panel seam during field assembly as shown in Figure 1.1-1(b). The clips are attached to the purlin flange using self-drilling screws. With the clip concealed within the seam, standing seam panels provide a water-tight membrane where the only penetrations in the panels are at the building eave or ridge and at panel end laps.

Standing seam panel profiles are commonly referred to as pan-type as shown in Figure 1.1-2(a), or rib-type as shown in Figure 1.1-2(b). There are two basic clip types: fixed, Figure 1.1-3(a) and sliding or two-piece clip, Figure 1.1-3(b). For a system constructed with fixed clips, thermal movement is accommodated through slippage between the roof panel and the fixed clip or by bending of the fixed clip. The sliding clips on the other hand are designed for movement between the components of the clip itself. The trade-off with the standing seam system's ability to accommodate thermal movement is that the purlin lateral support provided by the system is compromised. This purlin lateral support is highly dependent on the panel profile and clip details. The requirements of the panels to provide diaphragm strength and stiffness are discussed in Chapter 4.

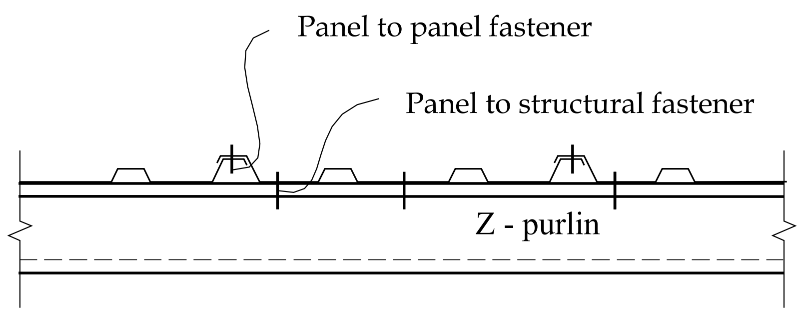

(a) Through-Fastened Panel

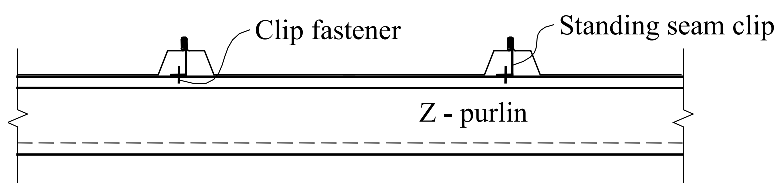

(b) Standing Seam Panel

Figure 1.1-1 Roof Panel Profiles

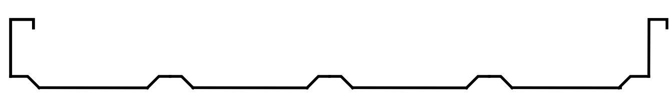

(a) Pan-Type Panel Profile

(b) Rib-Type Panel Profile

Figure 1.1-2 Panel Profiles

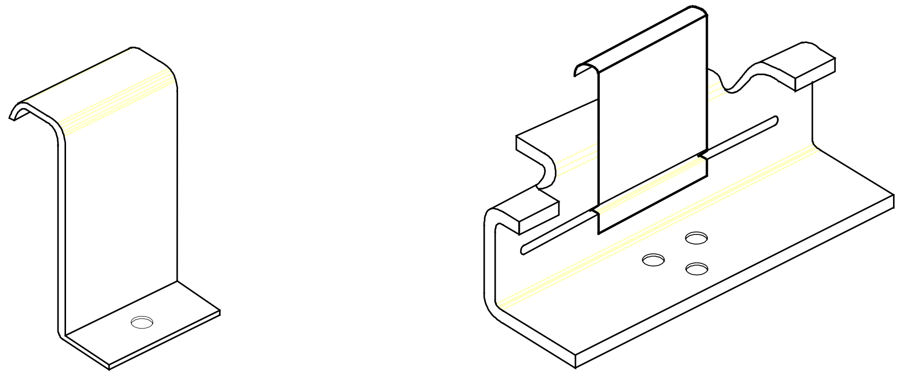

(a) Fixed Clip **(b) Sliding or Two-Piece Clip**

Figure 1.1-3 Types of Standing Seam Clips

Insulation of the building envelope at the roof is accomplished in several ways. Batts of insulation may be installed between the purlin and the panels as shown in Figure 1.1-4(a). For standing seam systems, the insulation is compressed under the purlin clips. As insulation thickness requirements increase, blocks of rigid insulation may be placed between the purlin and the panels. Insulated sandwich panels that have a layer of rigid insulation sandwiched between two cold-formed steel membranes may also be used. These sandwich panels may be either a through-fastened system with self-drilling fasteners through the entire panel assembly or a standing seam system with concealed clips and fasteners as shown in Figure 1.1-4(b). A combined system as shown in Figure 1.1-4(c) has through-fastened panels attached directly to the purlins, layers of batt or rigid insulation, and standing seam panels on the exterior. The insulation method and the amount of insulation will impact the ability of the panels to brace the purlin.

1.2 Purlins

Cold-formed steel roof framing systems are commonly constructed using cold-formed steel C- or Z-sections, referred to as purlins. Although purlins are the primary load carrying components of the roof system, they are commonly called secondary members with respect to the entire building system. Generally, purlins are lapped as shown in Figure 1.2-1 to provide continuity and therefore greater efficiency. Z-section purlins are essentially point-symmetric; however, some manufacturers produce Z-sections with slightly unequal width flanges to facilitate nesting in the lapped region. These unequal flange purlins are still considered as point symmetric. The lap connection is usually made with at least two structural bolts through the webs of the lapped purlins near each end of the lap as shown in Figure 1.2-1. In addition, the purlins are connected to the supporting rafter by either flange bolts or connected as shown in Figure 1.2-2. Cold-formed steel purlins are most efficient for spans less than 40 feet. For longer spans, steel joists are more economical.

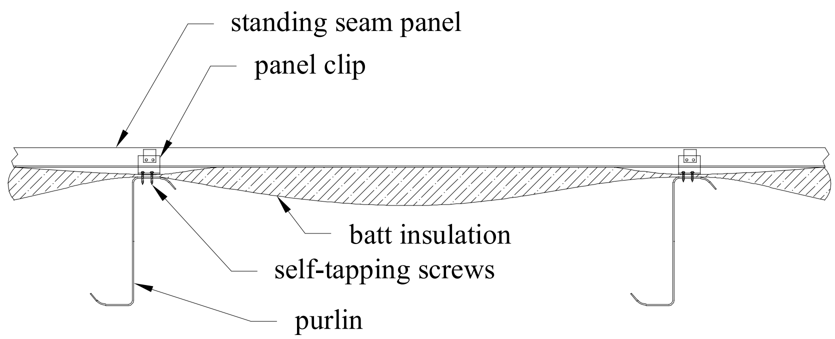

(a) Insulation Batts

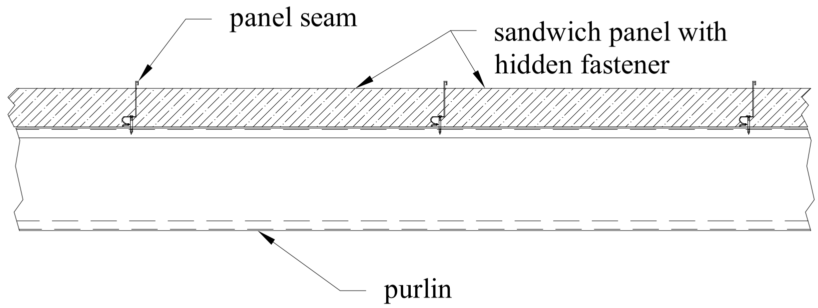

(b) Sandwich Panel

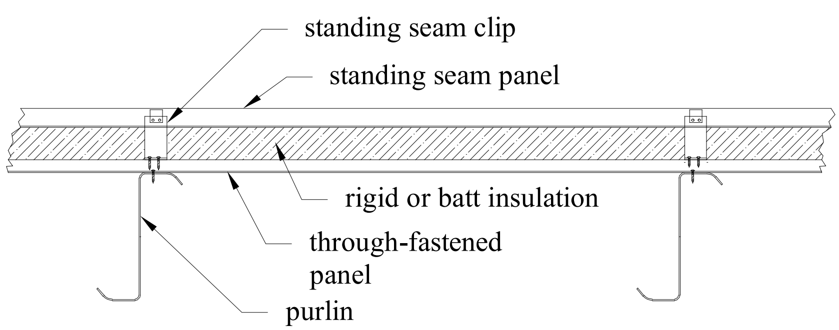

(c) Multi-Panel Layered System

Figure 1.1-4 Insulation Strategies

1.3 Purlin Bracing

Purlin braces are elements within a roof system that provide lateral and/or torsion restraint to the purlin. The braces may be continuous or discrete.

Continuous bracing is provided by the panels attached to the exterior flange of the purlin. The effective lateral support provided by the panel and the system anchorage is a function of the loading direction (gravity or uplift), purlin attachment details (flange or web bolted) and the system details (panel type, clip type, insulation level).

Generally, through-fastened panels are assumed to provide full lateral and torsional restraint for gravity loading in the positive moment region (the portion of the span where the panel is attached to the purlin compression flange). Design assumptions for the negative moment region (the portion of the span where the panel is attached to the purlin tension flange) vary from unrestrained to fully restrained. A common assumption is that the purlin is unbraced between the end of the lap and the adjacent inflection point, but this assumption may be unduly conservative as is discussed in Chapter 3.

For uplift loading, through-fastened panels provide partial lateral torsional restraint. Attempts have been made to develop test methods to determine the torsional restraint provided by specific panel profile/screw combinations. However, the variability of the methods and their complexity necessitated something simpler for routine use. Consequently, the empirical R-factor method was developed for determining the flexural strength of through-fastened roof purlins under uplift loading. The design methods for purlins with through-fastened panels are discussed further in Section 2.2.

The lateral and torsional restraint provided by standing seam roof systems varies considerably depending on the panel profile and the clip details. Consequently, a generic solution is not possible and AISI S908, *Test Standard for Determining the Flexural Strength Reduction Factor of Purlins Supporting a Standing Seam Roof System* (AISI, 2017d), also known as the Base Test Method was therefore developed. Purlin design by the base test method is discussed in Section 2.3.2.

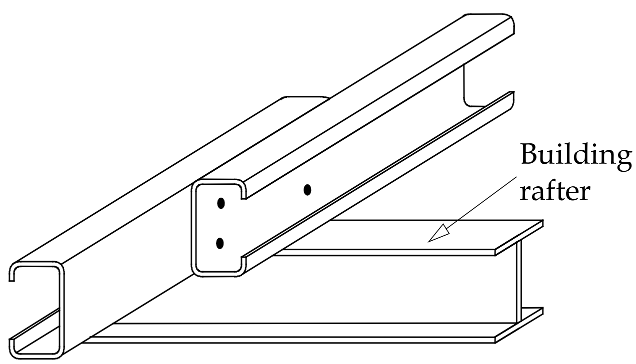

(a) Lapped C-Purlins

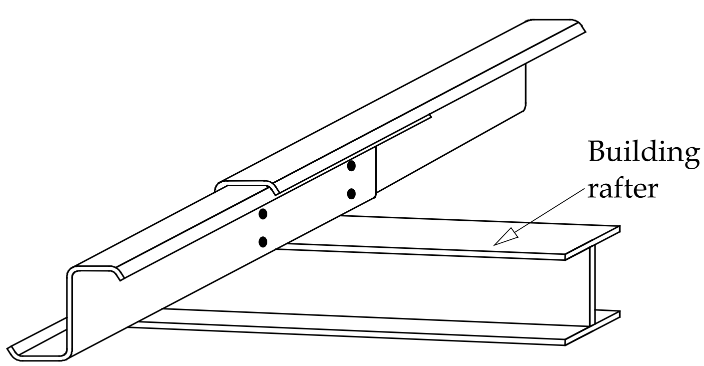

(b) Lapped Z-Purlins

Figure 1.2-1 Purlin Continuity Laps

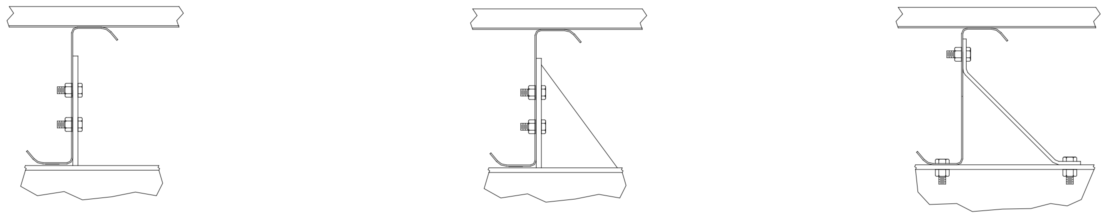

(a) Web Plate **(b) Stiffened Web Plate** **(c) Diagonal Bent Plate**

Figure 1.2-2 Purlin-to-Rafter Connections

Discrete braces may be installed to provide restraint in lieu of continuous bracing for cases where the continuous bracing provided by the panels is not sufficient or design by the Base Test Method is not possible. For a discrete braced system, the purlins are designed as unbraced beams between brace locations. These braces may be horizontal angles capable of resisting compression or tension, angle X-braces, threaded rods, or proprietary devices. Examples of discrete braces, both lateral and torsional, are shown in Figure 1.3-1. Lateral bracing forces that accumulate either in lateral braces or the diaphragm must be anchored to the primary lateral force resisting system. External anchorage is not needed for torsional braces, because torsional braces prevent the twist of the members.

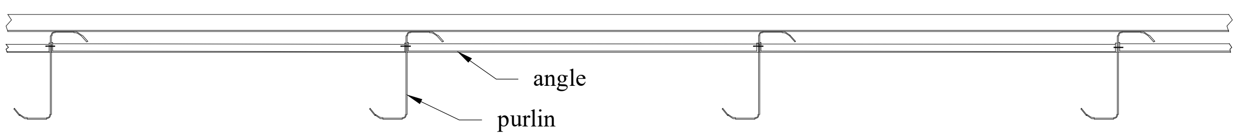

(a) Lateral Brace

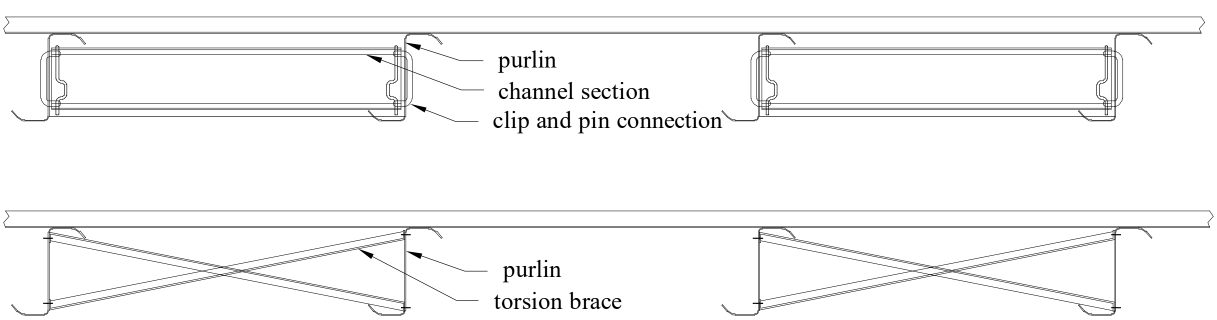

(b) Torsional Braces

Figure 1.3-1 Examples of Discrete Braces for Purlin Stability

1.4 System Anchorage

Whether lateral and/or torsional restraint is provided continuously by the panels or by discrete braces along the length of the purlin, the forces that are generated in those braces will accumulate and must be transferred to other force resisting systems. The elements that collect and transfer these forces to the primary roof structure are called the system anchorage. The system anchorage restrains the overall lateral (uphill or downhill) movement of the system at the top flange of the purlins. In the absence of system anchorage, on a low slope roof, a system of Z-sections will translate and rotate “uphill” towards the ridge because of the inclined principle axes and eccentricity of applied loads respectively. On roofs with a steeper slope, downslope forces begin to dominate, pushing the system of Z-sections at their top flange “downhill” towards the eave. C-sections, because of the eccentricity of the applied loads relative to the shear center, under gravity loads will rotate in the direction of the top flange. As roof slope increases, like with Z-sections, the downslope force will dominate pushing the system of C-section purlins towards the eave.

Most commonly, system anchorage devices are attached to purlin webs near the top flange and are directly or indirectly connected to the primary structural framing. Along the purlin span, system anchorage is provided symmetrically either at the support location or at discrete locations along the length. System anchorage is most common at the purlin supports because the force can be directly transferred to the primary structural framing. When located at the supports, the anchorage devices (anti-roll clips) typically consist of either a web plate, a multi-piece welded assembly that is attached to the purlin web and to the top flange of the rafter, or a diagonal bent clip as shown in Figure 1.2-2.

For anchorage along the purlin span, lateral restraint is most commonly applied near the third points. Anchorage at the midpoint is permitted but is less desirable as tests by Ellifritt, Sputo, and Haynes (1992) have shown that a midpoint brace may have a negative impact on the flexural strength of the purlin. The details of the anchorage along the span of the purlin are similar to those for lateral braces described above. Anchorage braces and lateral braces may be the same. However, special detailing considerations need to be addressed with preferred details varying greatly.

An alternative to interior anchorage braces is a system with lateral anchorage provided at the support locations and torsional braces applied at or near the third points of the purlin. Torsion moments generated in these torsional braces are balanced in adjacent purlins and therefore do not require external anchorage.

The intent of this Design Guide is to provide a comprehensive review of C- or Z-section purlin cold-formed steel roof framing systems with emphasis on the design of the system anchorage. All design provisions are from the 2016 edition of the American Iron and Steel Institute *North American Specification for the Design of Cold-Formed Steel Structural Members,* AISI S100-16 (AISI, 2016), referred to hereafter as AISI S100. Chapter 2 is an overview of the design methods for cold-formed purlin supported roof systems. The design of continuous purlin lines is discussed in Chapter 3, along with ASD and LRFD example calculations. LSD is not used in this design guide. The diaphragm requirements are discussed in Chapter 4. Chapter 5 is devoted to the procedures available to determine system anchorage requirements. The system anchorage requirements in AISI S100 are presented first with an extensive set of ASD and LRFD examples. Alternative methods to determine the anchorage requirements include the AISI S100 simplified solution, the AISI S100 matrix-based solution and the component stiffness method solutions. In addition to the calculation procedures, recommendations are made for frame element stiffness modelling and finite element modelling of roof systems to determine the anchorage requirements. Anchorage configurations, applications, and the analysis procedures in order of increasing complexity are listed in Table 1-1, with references to the applicable sections of this Design Guide. Chapter 6 discusses the additional topics of design considerations with standing seam panels on steel joists and concentrated loads from roof top units or hanging equipment.

Table 1-1 Anchorage Analysis Procedures

Anchorage Configuration	Application	Simplified Solution (5.5.1) (c)	Main Spec. Procedure (5.2)	Matrix Solution (5.5.2)	Component Stiffness Solution (5.5.4)	Frame Element Stiffness Model (5.5.5)	Finite Element Stiffness Model (5.5.6)
Lateral Bracing							
Supports, 1/3 Points or Midpoint	(a)	X	X	X	X	X	X
	(b)		X	X	X	X	X
				X		X	X
1/4 Points or 1/3 Points + Supports	(b)				X	X	X
						X	X
Arbitrary Locations						X	X
Torsional Bracing							
1/3 Points + Supports	(b)				X		X
Arbitrary Locations							X

(a) Uniform purlin spaces, uniform load, top flanges facing upslope and anchors evenly distributed

(b) Any "reversed" purlins evenly distributed

(c) Refers to section numbers in this Design Guide.

CHAPTER 2 DESIGN METHODS FOR PURLINS

Symbols and Definitions Used in Chapter 2

b	Flange width of the purlin (in.) (mm)
d	Depth of the purlin (in.) (mm)
C2	Coefficient for support restraint with standing seam panel from AISI S100 Table I6.4.1-1
C3	Coefficient for support restraint with standing seam panel from AISI S100 Table I6.4.1-1
F_y	Yield stress for design (psi) (MPa)
F_{yt}	Measured yield stress of tested purlin (psi) (MPa)
I_x	Moment of inertia of full unreduced section about major centroidal axis perpendicular to the web (in.^{4}) (mm^4)
I_{xy}	Product of inertia of full unreduced section about centroidal axes perpendicular and parallel to the web respectively (in.^{4}) (mm^4)
L	Span of the purlins tested, center to center of the supports (ft) (m)
M_n	Nominal flexural strength of a fully constrained beam, S_eF_y (lb-in.) (N-m)
$\overline{M}_{nt_{min}}$	Average flexural strength of the thinnest sections tested (lb-in.) (N-m)
$\overline{M}_{nt_{max}}$	Average flexural strength of the thickest sections tested (lb-in.) (N-m)
M_{nt}	Flexural strength of a tested purlin, $S_{et}F_{yt}$ (lb-in.) (N-m)
M_{ts}	Failure moment for the single span purlins tested, $w_{ts}L^2/8$ (lb-in.) (N-m)
p_d	Weight of the specimen (lb/ft^2) (N/m^2)
p_{ts}	Failure load of the single span system tested (lb/ft^2) (N/m^2)
P_L	Lateral anchorage force in accordance with Section I6.4.1 of the AISI S100
r	Correction factor
R	Reduction factor computed for nominal purlin properties
R_t	Modification factor from test, M_{ts}/M_{nt}
$R_{t_{min}}$	Mean minus one standard deviation of the reduction factors of the three thinnest purlins tested
$R_{t_{max}}$	Mean minus one standard deviation of the reduction factors of the three thickest purlins tested
s	Tributary width of the purlins tested (ft) (m)
S_e	Section modulus of the effective section (in.^{3}) (mm^3)
S_{et}	Section modulus of the effective section of the tested member using measured dimensions and the measured yield stress (in.^{3}) (mm^3)
t	Purlin thickness (in.) (mm)
t_i	Thickness of uncompressed glass fiber blanket insulation (in.) (mm)
w	Applied load (lb/ft^2) (N/m^2)
w_d	Dead weight of the panels and the purlin (lb/ft^2) (N/m^2)
w_{ts}	Failure load of the single span purlins tested (lb/ft) (N/m)
ϕ	Resistance factor

Ω Safety factor
σ_{max} One standard deviation of the R_t factors of the thickest purlin tested
σ_{min} One standard deviation of the R_t factors of the thinnest purlin tested

2.1 General

AISI S100 provides several design pathways for determining the strength of purlins in roof systems. The attachment of the panels to the exterior flange of a purlin affects the strength.

The strength of purlins with through-fastened panels subjected to gravity loads is not explicitly specified in AISI S100. However, the industry practice is to assume full lateral and torsional support for the purlin in the positive moment region. For uplift loading, through-fastened panels have a quantifiable impact on the strength of the purlins and therefore an empirically based method is utilized to determine their strength (R-factor Method).

Because standing seam systems are more variable than through-fastened systems and in general, provide less stability restraint, AISI S100 allows two methods for the design of purlins supporting standing seam systems. The first method is to test the purlin-panel system utilizing AISI S908, also known as the Base Test Method. The alternative approach is to ignore any restraining effects of the panels and design the purlins as a discrete braced system with intermediate braces along the span of the purlin.

Testing and rational engineering methods are permitted by AISI S100 for certain circumstances. For instance, in AISI S100 Section I6.2.1, Flexural Members Having One Flange Through-Fastened to Deck or Sheathing, it is stated that “if variables fall outside any of the above stated limits, the user shall perform full scale tests or apply a rational engineering analysis procedure.”

2.2 Purlins Supporting Through-Fastened Panels

2.2.1 Gravity Loading Assumptions

Although AISI S100 does not contain explicit provisions for purlins with one flange attached to metal panels subjected to gravity loads, industry practice assumes that the panels provide full lateral and torsional support to the compression flange in the positive moment region. Therefore, the limit state of global lateral-torsional buckling is eliminated, and the flexural strength is determined as the minimum of the local buckling strength and the distortional buckling flexural strength. The designer may use either the Direct Strength Method (DSM) or the Effective Width Method approach to calculate the strength. Utilizing the DSM, the local buckling strength is calculated according to Section F3.2.1 of AISI S100 and the distortional buckling strength is calculated according to Section F4.1. The traditional design approach calculates the local buckling strength using the Effective Width Method outlined in Section F3.1 and Appendix 1, and the distortional buckling strength per Section F4 and Appendix 2 Section 2.3.3.3. Alternatively, the local buckling strength may be calculated by Section F3.2 and Appendix 2 Section 2.3.3.2.

2.2.2 R-factor Method for Uplift Loading

The design procedure for purlins subject to uplift loading in AISI S100 Section I6.2.1, Flexural Members Having One Flange Through-Fastened to Deck or Sheathing, is based on the use of reduction factors (R-factors) to account for the flexural, torsional, or nonlinear distortional buckling behavior of purlins with through-fastened panels attached to the purlin tension flange. The local buckling behaviour of the purlin is largely independent of any system effects and therefore must be incorporated into the strength of the purlin. The R-factors are based on tests performed on simple span and continuous span systems using both C- and Z-sections. All tests were conducted without intermediate bracing.

The R-factor design method simply involves applying a reduction factor (R) to the nominal flexural strength considering local buckling only, $M_{n\ell}$, as determined by AISI S100 Section F3 with $F_n = F_y$ or $M_{ne} = M_y$.

$$M_n = RM_{n\ell o} \qquad \text{(AISI S100 Eq. I6.2.1-1)}$$

with R = values from AISI S100 Table I6.2.1-1 for simple span C- and Z-sections.

The restraint provided to the purlin is dependent on the behavior of the panel-to-purlin connection, and the rotational stiffness of the connection is dependent on purlin thickness, panel thickness, fastener type and location, and insulation. Therefore, the reduction factors only apply for the range of sections, lap lengths, panel configurations, and fasteners tested as set out in AISI S100 Section I6.2.1. For continuous span purlins, compressed glass fiber blanket insulation of thickness between zero and 6 in. does not measurably affect the purlin strength. The effect is greater for simple span purlins requiring that the reduction factor (R) be further reduced by the correction factor, r, where

$$r = 1.00 - 0.01t_i \qquad \text{(AISI S100 Eq. I6.2.1-2)}$$

and t_i is the thickness of uncompressed glass fiber insulation in inches.

The resulting available strength moment ($\phi_b M_n$) or (M_n/Ω_b) is compared with the maximum bending moment in the span determined from an elastic analysis. The resistance factor (ϕ_b) is 0.90 and the safety factor (Ω_b) is 1.67.

The AISI S100 R-factor design method does not apply to the region of a continuous beam between an inflection point and a support nor to cantilever beams. For these cases, the design must explicitly consider lateral-torsional buckling.

If the section geometry, lap length, panel configuration, fastener or combinations thereof are outside the Section I6.2.1 limits, full-scale tests or a rational engineering analysis may be used to determine the design strength. However, according to Section I6.2.1, for continuous purlin and girt systems in which adjacent bay span lengths vary by more than 20 percent, the R values for the adjacent bays shall be taken from the simple-span values in Table I6.2.1-1.

2.3 Purlins Supporting Standing Seam Panel Systems

The lateral and torsional restraint provided by standing seam panels and clips depends on the panel profile and clip details. Lateral restraint is provided by both friction in the clip and drape or hugging of the panels. Because of the wide range of panel profiles and clip details, it is difficult to accurately quantify with a calculation procedure the effects of this restraint on the flexural strength of a purlin. As a result, the designer may either ignore any strength benefits provided by the panels and design the purlin as a discrete braced system according to AISI S100 C2.2.1, or test the purlin-panel system utilizing AISI S908.

2.3.1 Discrete Braced Analysis

As discussed above, the increased strength that results from the lateral and torsion restraint provided by the standing seam panels may be conservatively ignored. To enhance the strength of the purlin, braces are provided at intermediate locations along the span of the purlin and the purlin is analyzed as a discrete braced system. The discrete braces should be designed to inhibit lateral displacement and torsional rotation of the purlin. As such, the braces constrain the purlin to bend in the plane of the web and thus the purlin will have a distribution of stresses in the cross section that follow closely the constrained or simple bending stress distribution.

The flexural strength of the purlin is the minimum of the lateral-torsional buckling strength, the local buckling strength or the distortional buckling strength. The lateral-torsional buckling strength is calculated according to AISI S100 Section F2 between brace points, the local buckling strength is calculated according to Section F3 using either the Effective Width Method (Section F3.1) or DSM (Section F3.2). Alternatively, the local buckling strength can be calculated by an elastic buckling analysis according to Appendix 2 Section 2.3.3.2. The distortional buckling strength is calculated according to Section F4 with distortional buckling moment determined by Section 2.3.3.3. When determining the distortional buckling strength of the purlin, the rotational restraint provided by the panels, k_ϕ, may be incorporated into the strength determination.

It is recommended that at least two symmetrically located braces within the middle third of the span be provided to effectively brace the purlin. For the endspan, the location of the braces should account for asymmetric support conditions. Full scale tests of a simple span purlin with a single brace at mid-span have shown that the purlin may have less strength than that predicted by AISI S100 as a result of the concentration of stresses at the mid-span brace.

The forces generated in lateral discrete braces must be resisted by external anchors. The magnitude of these brace forces, P_{L1}, at the top flange, P_{L2}, at the bottom flange, are calculated according to Section C2.2.1 of AISI S100. No stiffness requirements are provided for discrete lateral braces but the generally accepted lateral deflection limit of the purlin is the span length, L, divided by 360 (L/360). Note that the lateral deflection limit for torsional braces is L/180 according to AISI S100 Section I6.4.2.

Section I6.4.1 of AISI S100 states that brace forces may be determined according to I6.4.1 for C- section or Z-sections, if designed according to Chapter F, Section I6.1 or I6.2, and having through-fastened or standing seam panels attached to the top flanges. The provisions of I6.4.1 rely on the diaphragm to redistribute forces, which inherently changes the distribution of forces acting on the member. Therefore, unless analysis incorporating the panel effects is performed, best practices dictate that if the strength of the purlin is determined according to Chapter F without considering the redistribution of forces by the diaphragm, then so too, the forces in the braces should be determined by Section C2.2.1, which ignores the contribution of the diaphragm to redistribute forces.

2.3.2 Testing-Based Design

Because of the variability of lateral and torsion restraint provided by standing seam systems, and the difficulty of accurately predicting flexural strength by analytical methods alone, a testing-based design method, also known as the Base Test Method, was developed to determine the strength of purlins in standing seam systems. This method uses separate sets of simple span, two purlin line tests to establish the nominal moment strength of the positive moment regions of gravity loaded systems and the negative moment regions of uplift loaded systems. The results are then used to predict the strength of multi-span, multi-line systems for either gravity or wind uplift loadings. The method is not intended to determine or verify bracing strength, anchorage strength, or diaphragm strength. However, other AISI test standards exist that provide methods to determine anchorage strength (AISI S912, *Test Standard for Determining the Strength of a Roof Panel-to-Purlin-to-Anchorage Device Connection* (AISI, 2017e)) and diaphragm strength (AISI S907, *Test Standard for Determining the Strength and Stiffness of Cold-Formed Steel Diaphragms by the Cantilever Test Method* (AISI, 2017c)).

The nominal moment strength of the positive moment regions for gravity loading or the negative moment regions for uplift loading is to be determined using Section I6.2.2 of AISI S100 Appendix A for roof systems in the United States and Mexico.

$$M_n = RM_{n\ell o} \qquad \text{(AISI S100 Eq. I6.2.2-1)}$$

with R = the reduction factor determined in accordance with AISI S908. The nominal flexural strength considering local buckling only, $M_{n\ell o}$, is determined from AISI S100 Section F3 with $F_n = F_y$ or $M_{ne} = M_y$. The resistance factor (ϕ_b) for LRFD design is 0.90 and the factor of safety (Ω_b) for ASD design is 1.67. For roof systems in Canada, Section I6.2.2 of AISI S100 Appendix B requires discrete braces. Therefore, designs relying on the standing seam panel as the only bracing are not recognized.

To determine the relationship for R, six tests are required for each gravity or uplift load case and for each combination of panel profile, clip configuration, purlin profile, and lateral bracing layout. A purlin profile is defined as a set of purlins with the same depth, flange width, and edge stiffener angle, but with varying thickness and edge stiffener length. Three of the tests are conducted using the thinnest material and three using the thickest material used by the manufacturer for the purlin profile. All components used in the tests must be nominally identical to those used in the actual systems.

Results from the six tests are then used in AISI S908 Equation 8 to determine an R-factor relationship

$$R = \left(\frac{R_{t_{max}} - R_{t_{min}}}{\overline{M}_{nt_{max}} - \overline{M}_{nt_{min}}} \right)(M_n - \overline{M}_{nt_{min}}) + R_{t_{min}} < 1.0 \qquad \text{(AISI S908 Eq. 8)}$$

where

$R_{t_{max}}$ = Mean minus one standard deviation of the reduction factors of the three thickest purlins tested

$R_{t_{min}}$ = Mean minus one standard deviation of the reduction factors of the three thinnest purlins tested

$\overline{M}_{nt_{max}}$ = Average flexural strength of the thickest sections tested

$\overline{M}_{nt_{min}}$ = Average flexural strength of the thinnest sections tested

The reduction factor for each test (R_t) is computed from

$$R_t = M_{ts} / M_{nt} \qquad \text{(AISI S908 Eq. 7)}$$

Reported reduction factor values are generally between 0.40 and 0.98 for both gravity and uplift loading depending on the panel profile and clip details. Gravity loading tends to increase purlin rotation as a result of second order torsion that is caused by the lateral deflection of the system as shown in Figure 2.3-1(a). For uplift loading, second order torsion is somewhat counteracted by the eccentricity of the load transferred through the top flange, resulting in smaller rotations, as shown in Figure 2.3-1(b). For some standing seam Z-purlin systems, sufficient torsional restraint is provided by the panel/clip connection, so that a larger reduction factor may be obtained for uplift loading than for gravity loading.

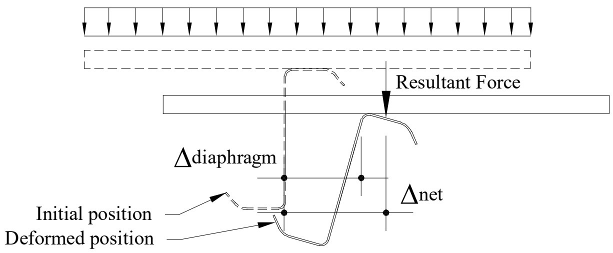

(a) Gravity Loading

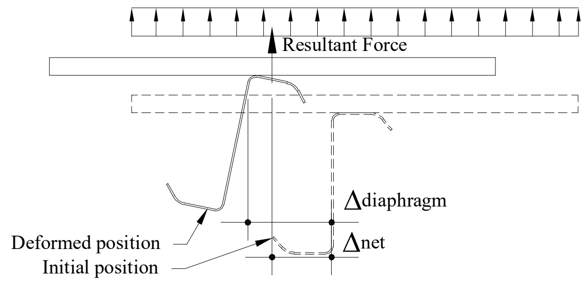

(b) Uplift Loading

Figure 2.3-1 Purlin Rotation due to Gravity and Uplift Loading

The AISI S908 testing-based design method allows purlins to be tested either with purlin flanges pointed in the same direction (the most common as-built configuration with purlin top flanges facing toward the building ridge), or with purlin flanges opposing. The as-built configuration must match the tested configuration, that is if the system is tested with flanges opposing, each alternating purlin must face in opposing directions in the as-built structure. If purlins are tested with flanges in the same direction, in the as-built structure, it is permitted to orient some purlins in the opposite direction (downslope) provided that the majority of purlins face upslope. The results of the testing must be evaluated differently according to whether purlin flanges are oriented in the same direction or opposing.

Purlin Flanges Oriented in the Same Direction

When the testing is performed with purlin flanges facing in the same direction, the tendency of the purlins to deflect laterally and roll places demand on the diaphragm and purlin-panel connection and induces second order forces. The test configuration with purlin flanges in the same direction is therefore the most realistic representation of the typical as-built conditions.

The maximum single span moment (M_{nt}) at mid-span is calculated using the uniformly distributed loading at failure determined from

$$w_{ts} = (p_{ts} + p_d)\ s + 2P_L(d/B) \qquad \text{(AISI S908 Eq. 1)}$$

where

$$P_L = 0.5\left(\frac{C2}{1000}\frac{I_{xy}L}{I_x d} + C3\frac{0.25bt}{d^2}\right)(p_{ts} + p_d)s \qquad \text{(AISI S908 Eq. 2)}$$

The additional uniformly distributed force, $2P_L(d/B)$, in AISI S908 Equation 1 is the downward force that is induced on the eave purlin necessary to balance the overturning moment on the system as shown in Figure 2.3-2. The overturning moment on the system is created because the anchorage force is applied at the top flange and is resisted at the bottom flange of the purlin at the support. The expression $2P_L(d/B)$ is applied only to Z-sections under gravity loading when the purlin flanges are facing in the same direction, but is not to be included when discrete point braces are used and the braces are restrained from lateral movement. In addition, the expression $2P_L(d/B)$ is not to be applied unless the downslope (eave side) purlin is the first to fail or if testing is performed for the uplift condition.

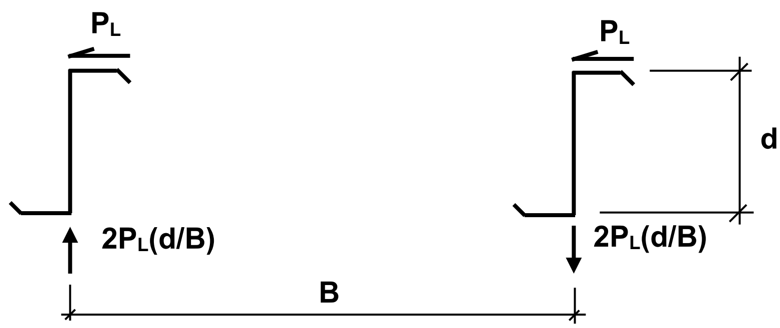

Figure. 2.3-2 Test Load Adjustment Factor

Purlin Flanges Oriented in Opposing Directions

When a specimen is tested with purlin flanges opposed, the lateral forces generated by the purlins are counterbalanced and the demand on the diaphragm and any second order effects are eliminated. Testing with the purlin flanges opposed is akin to a system with virtually infinite diaphragm stiffness and it can be shown that it will always produce significantly higher R-factors as compared to testing with the purlins facing in the same direction. The method does demonstrate the effectiveness of the panel/clip torsional resistance for the purlin. It also demonstrates the ability of the connection between the purlin and the panels to transmit lateral forces. If purlins are tested in the opposed position, then the roof system must be constructed with the purlins opposed. To determine the maximum failure moment from the test, because the lateral forces are balanced, the additional term $2P_L(d/B)$ must be eliminated from AISI S908 Equation 1 when purlin flanges are opposed.

The AISI S908 procedure requires that the tests be conducted using a test chamber capable of supporting a positive or negative internal pressure differential. Figure 2.3-3 shows a typical chamber.

Construction of a test setup must match that of the field erection instructions of the standing seam roof system manufacturer. The lateral bracing provided in the test must match the constructed lateral bracing. Tests can be conducted with:

1. Anti-roll devices at the ends of both purlins (supports restraint).
2. Anti-roll devices at the ends of only one of the purlins (supports restraint).
3. Intermediate lateral braces at interior locations along the length of the purlins (third point or mid-point brace).
4. Anti-roll devices at the ends of one or both purlins in combination with torsional braces at intermediate locations along the span (paired torsion brace).
5. A combination of anti-roll devices at the ends of one or both purlins in combination with lateral braces at interior locations (supports plus third point or mid-point brace).

If anti-roll devices are installed at the rafter support of each purlin in the test, then anti-roll devices must be provided at every purlin support location in the actual roof. Likewise, if intermediate lateral support is provided in the test, that support configuration is required in the actual roof. These intermediate lateral braces should be installed in the test such that the braces do not inhibit vertical deflection. If anti-roll devices are used at the ends of only one purlin in the test, the unrestrained purlin can be considered a “field” purlin if there is no positive connection between the two purlins. Positive connections can consist of angles, straps, and fasteners through the standing seam panels that directly transfer forces from the field purlin to the anti-roll device. These field purlins need not necessarily have anti-roll devices at every other purlin line assuming the following:

- The purlin in the test specimen that fails is the purlin without the anti-roll devices.
- The designer establishes that the number of anti-roll devices used in the as-built system has the ability to resist the anchorage forces calculated per AISI S100 Section I6.4.1.

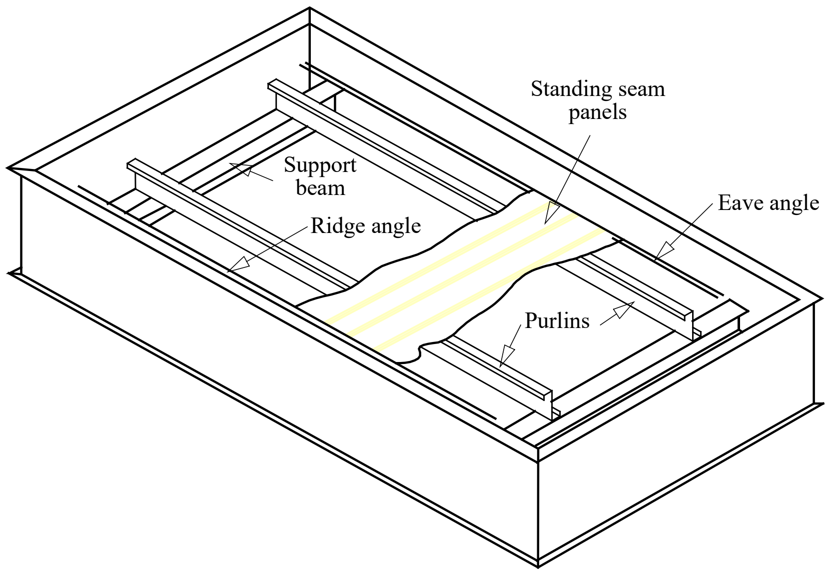

Figure 2.3-3 AISI S908 Test Chamber

Other Comments on the use of the AISI S908

- The test only provides an R-value for the moment capacity of the purlins. For sloped roof systems, there is the additional effect of down-slope forces. These forces, in addition to asymmetric bending and torsion, must be accounted for in the bracing requirements for the purlin system using either Sections C2.2.1 or I6.4.1, or in the roof diaphragm.
- Discrete bracing can be placed in the purlins as part of the system without anchoring these braces, as long as one tests and supplies the same condition.
- The test requires the longest purlin to be tested. The deviation in length should not be more than ten percent of the length tested.
- If bracing is used in the test, the number of braces used cannot be reduced for any purlin system unless additional tests are conducted.
- If the tests are conducted with the ends of both members restrained from moving horizontally (i.e., no field purlins), then the eave strut in the constructed system must be prevented from moving horizontally at its ends. Calculations or tests must be provided that the eave anchorage system has the capability to resist the anchorage forces for all of the purlins relying on the eave condition. It must also be demonstrated that the system is able to transfer the anchorage force to the eave strut anchorage points.
- The test was developed to incorporate limit states other than yielding. The tested purlins should have a steel yield at least equal to the design yield of the purlins. If not, then those other limit states may not be adequately captured.

Example 2.1. The R-value relationship for a set of gravity loading AISI S908 test data is to be determined. The tests were conducted using Z-sections with nominal thicknesses of 0.060 in. and 0.095 in. and a nominal yield stress of 55 ksi. The span length was 22 ft 9 in. and intermediate lateral braces were installed at the third points. In the following, the total supported load (w_{ts}) was equal to the sum of the applied load (w) and the weight of the panels and purlins (w_d). The maximum applied moment was M_{ts}. The moment M_{nt} was calculated using an effective section modulus, S_{et}, determined using the measured thickness, t, and the measured yield stress, F_{yt}. The reduction factor for each test, R_t, was from AISI S908 Equation 7. The test loadings and reduction factor data are summarized in Tables 2-1 and 2-2.

Table 2-1 Summary of Test Loadings

Test Number	Max. Applied Load w (lb/ft)	Deck Weight (lb/ft)	Purlin Weight (lb/ft)	w_d (lb/ft)	Total Load, w_{ts} (lb/ft)	M_{ts} (kip-in.)
1	91.8	4.0	3.10	7.10	98.9	76.8
2	86.3	4.0	3.14	7.14	93.4	72.5
3	81.8	4.0	3.10	7.10	88.9	69.0
4	186.5	4.0	5.05	9.05	195.6	151.9
5	189.1	4.0	5.01	9.01	198.1	153.8
6	184.5	4.0	4.91	8.91	193.4	150.1

Table 2-2 Reduction Factor Data

Test Number	t (in.)	S_{et} (in.)	F_{yt} (ksi)	$M_{nt}=S_{et}F_{yt}$ (kip-in.)	M_{ts} (kip-in.)	R_t
1	0.059	1.88	60.0	112.8	76.8	0.681
2	0.059	1.90	59.2	112.5	72.5	0.644
3	0.060	1.92	57.3	110.0	69.0	0.627
Average				111.8		0.651
4	0.097	3.38	68.4	231.2	151.9	0.657
5	0.096	3.38	67.1	226.8	153.8	0.678
6	0.097	3.30	66.5	219.5	150.1	0.684
Average				225.8		0.673

Using the test data,

σ_{max} = one standard deviation of the modification factors of the thickest purlins tested = 0.0142

σ_{min} = one standard deviation of the modification factors of the thinnest purlins tested = 0.0276

$$R_{t_{min}} = 0.651 - 0.0276 = 0.623$$

$$R_{t_{max}} = 0.673 - 0.0142 = 0.659$$

$$\overline{M}nt_{min} = 111.8\,\text{kip} - \text{in}$$

$$\overline{M}nt_{max} = 225.8\,\text{kip} - \text{in}$$

Reduction Factor Relation

Using AISI S908 Equation 8:

$$R = \left(\frac{R_{t_{max}} - R_{t_{min}}}{\overline{M}nt_{max} - \overline{M}nt_{min}}\right)(M_n - \overline{M}nt_{min}) + R_{t_{min}} < 1.0 \qquad \text{(AISI S908 Eq. 8)}$$

$$= \left(\frac{0.659 - 0.623}{225.8 - 111.8}\right)(M_n - 111.8) + 0.624 \leq 1.0$$

$$= \left(3.16 \times 10^{-4}\right)(M_n - 111.8) + 0.624 \leq 1.0$$

The variation of R with purlin strength for the standing seam roof system tested is shown in Figure 2.3-4. Figure 2.3-4 shows the R-value line with slope upward to the right. For some standing seam roof systems, the line will slope downward to the right.

Application

For a purlin having the same nominal depth, flange width, edge stiffener slope, and material specification as those used in the above and with a nominal flexural strength $M_n = S_eF_y$ = 135 kip-in., the reduction factor is

R = 0.316 (135-111.8)/1000 + 0.623 = 0.630

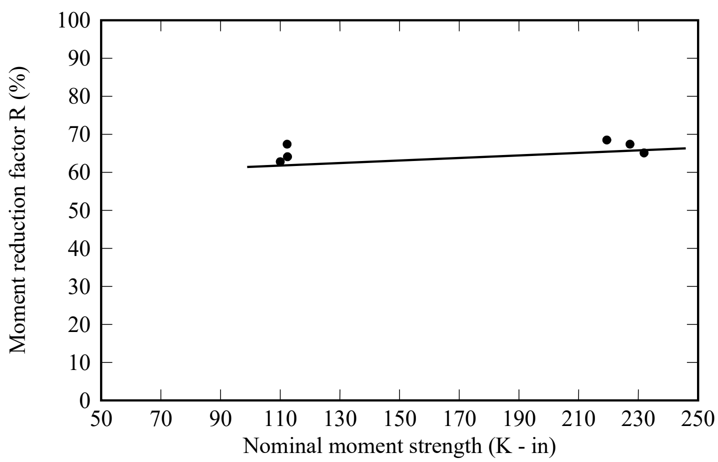

Figure 2.3-4 Reduction Factor versus Nominal Moment Strength

The positive moment design strength is then:
LRFD:

ϕ_b = 0.90

ϕM_n = $\phi_b R S_e F_y$ = 0.90 x 0.630 x135 = 76.5 kip-in.

ASD:

Ω_b = 1.67

M = RS_eF_y/Ω_b = 0.630 x 135/1.67 = 50.9 kip-in.

2.3.3 Procedure to Minimize Required Tests

AISI S908 requires that a set of six tests must be conducted for each combination of purlin profile, panel profile, clip type, intermediate bracing configuration, and loading. This requirement can result in a large number of tests for a given manufacturer. For instance, if a manufacturer produces

- a Z-purlin profile with two flange widths,
- a standing seam panel profile with two thicknesses, and
- three clip types (low sliding, high sliding, and low fixed),

the required number of tests is 72 (2 flange widths x 2 panel thicknesses x 3 clips x 6 tests).

Trout and Murray (2000) found for a specific purlin depth, the components that have the greatest effect on the standing seam roof system strength are the purlin flange width, clip type, and roof panel thickness. By comparing the strength reduction factors obtained from tests using various roof components, the following trends were found:

- Flange Width: Tests using purlins with a narrow flange width resulted in lower strengths for both thin and thick purlins of the same nominal cross-section.
- Clip Type: A single clip type produced the lowest results when compared to the other clips.
- Panel Thickness: Roof panel thickness had no effect on the strength of systems constructed with 10 in. deep purlins but did affect the strength when 8 in. deep purlins were used.

Although none of the roof components can be completely eliminated from a test matrix, by using trend relationships an acceptable test protocol has been developed for reducing the number of tests required.

Assuming a manufacturer has three clip types, two flange widths for each purlin type of one depth, and two nominally identical standing seam panel profiles rolled in two thicknesses, the following procedure will result in an R-value relationship (AISI S908 Equation 8) for all combinations with relatively few tests. This procedure assumes that the combination of one panel thickness, one clip type, and the purlin cross-section with the narrower flange width results in the lowest R-value for all other combinations of parameters. The procedure is:

- The clip type, which is thought to result in the lowest R_t-value is selected. For illustration, type C3 (tall sliding) is assumed.
- Using this clip type, the thinner panel, and the purlin with the narrow flange width, two tests are conducted for one depth purlin of the same nominal cross-section: One test is conducted with the thinnest purlin and one test with the thickest purlin in the inventory.
- With the R_t-values from the two tests, a trend line is found as shown in Figure 2.3-5. Depending on the details of the system, the trend line can have either positive or negative slope as shown.

- To verify the choice of clip, two additional tests are conducted using the purlin thickness that resulted in the lower R_t-value, one with each of the other two clip types C1 and C2. In Figure 2.3-5, the thinner purlin controls for the solid trend line and the thicker purlin controls for the dashed trend line.
- If the original clip type does result in the lowest R_t-value, as shown in Figure 2.3-6, the choice of clip type is verified.
- If the original clip does not result in the lowest R_t-value, a test using the clip with the lowest R_t-value and the other purlin thickness is conducted. Figure 2.3-7 shows the resulting data, assuming clip type C2 is the controlling clip type.

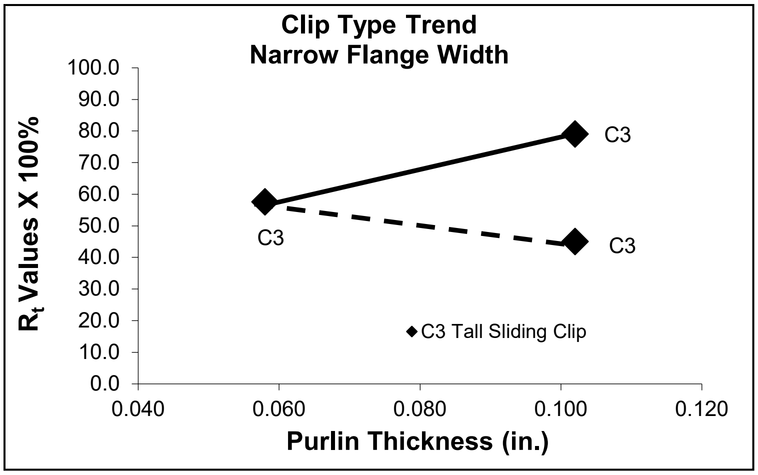

Figure 2.3-5 Possible Clip Type Trend Relationships

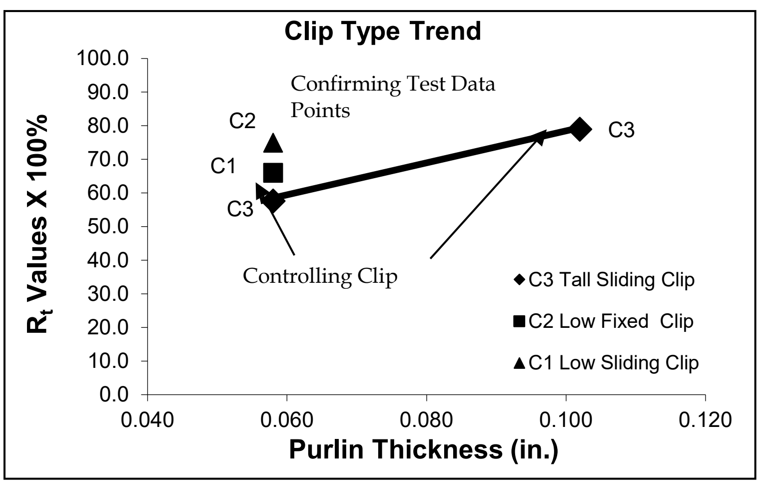

Figure 2.3-6 Confirmation of Initial Choice of Clip Type

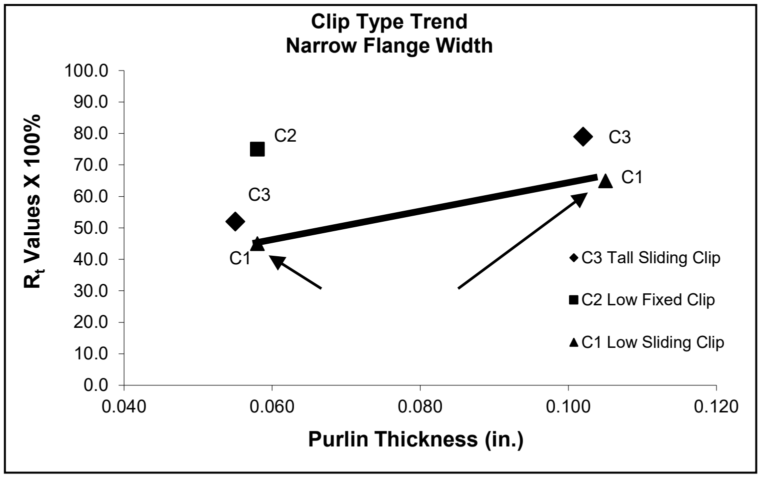

Figure 2.3-7 Confirmation of Clip Type

- Knowing the controlling clip type, two additional tests are required to validate the choice of panel thickness: one test is conducted using the controlling clip-type, the thinner purlin, and the other panel thickness; the other test is conducted using the controlling clip-type, the thicker purlin thickness and the other panel thickness.
- Using the combination of clip-type and panel thickness that resulted in the lowest R_t-value for the two purlin thicknesses, the remaining four tests are then conducted and the R-value relationship is developed. Figure 2.3-8 shows the completed test sequence and the final R-value line.

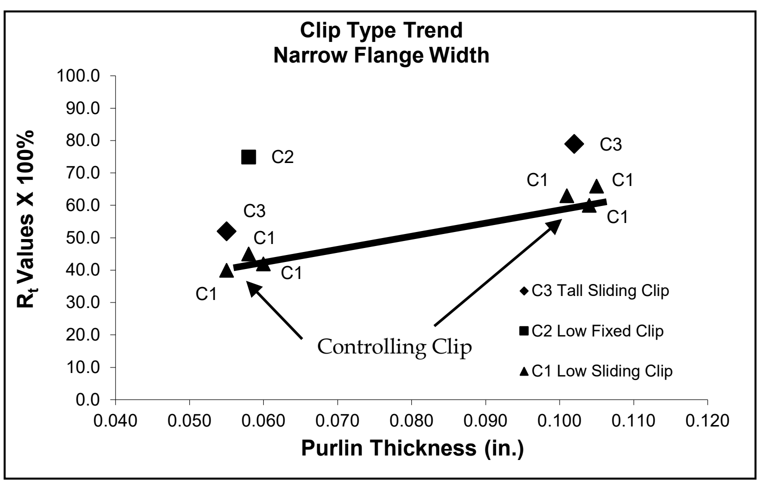

Figure 2.3-8 Final Results

Using the reduction procedure and assuming only one purlin depth and one purlin cross-section, the minimum required number of tests, for an inventory with three clip types, two flange widths, and two panel thicknesses is:

- Two tests with the initial clip type assumption to determine the slope of the trend line (one thin and one thick purlin).
- Two tests to confirm the initial clip-type selection (two remaining clip types).
- One test to determine the panel thickness trend (with controlling clip type).
- Four tests required to meet the requirements of AISI S908.

That is, 2 + 2 + 1 + 4 or 9 tests. Thus, the required number of tests for the loading condition (gravity or uplift) being considered is reduced from 72 tests (from above) to 9 tests in the best-case scenario. The worst-case scenario requires 14 tests.

Example 2.2. This example demonstrates the above procedure using actual test data. The following components were used in the tests:

- Three clip types: low sliding clip (C1), low fixed clip (C2), and tall sliding clip (C3).
- 8 in. deep Z-purlins with two thicknesses, thinnest and thickest in the inventory.
- Two flange widths: 2-1/2 in. and 3-1/2 in.
- 22 ga and 24 ga standing seam roof panel thicknesses having nominally identical profiles.

It was initially assumed that the tall sliding clip, C3, controls, and the initial two tests were conducted using the thinnest and thickest 8 in. deep Z-purlins with a 2-1/2 in. flange width (narrow flange) and the 22 ga roof panel. The results of these tests are shown in Figure 2.3-9. The thinner purlin gives the lower R_t-value of 0.571 (57.1 percent).

Based on these results, tests were conducted using the other two clip types, low sliding clip, C1, and low fixed clip, C2, and tested using the thinner purlin thickness, with all other roof components remaining nominally the same. The resulting R_t-values for the tests are shown in Figure 2.3-10. The R_t-values obtained were 60.2 percent (C1) and 61.4 percent (C2), confirming that the tall sliding clip controls. If the original clip selection did not result in the lowest R_t-value, a test using the clip with the lowest R_t-value and the other purlin thickness would be conducted.

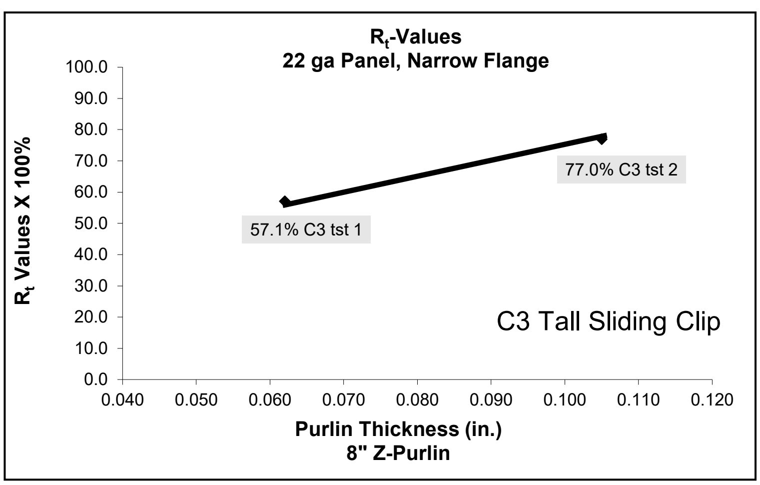

Figure 2.3-9 Initial test with Assumed Controlling Clip Type

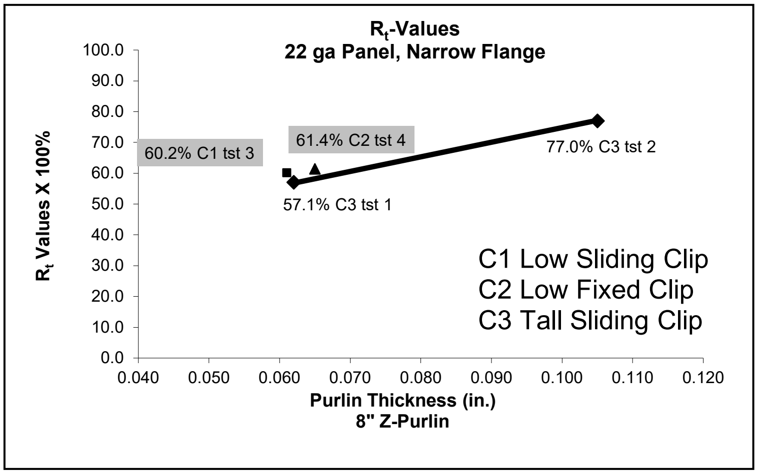

Figure 2.3-10 Controlling Clip Type Verification

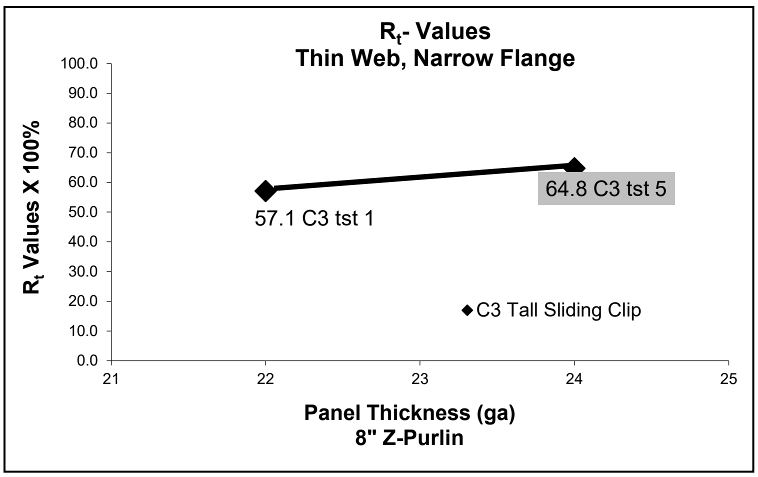

Figure 2.3-11 Roof Panel Trend Verification

After finding the controlling clip type and purlin thickness that results in the lowest R_t-value, the next step was to validate the panel thickness assumption. To do this, a test constructed using the same clip type and purlin thickness with the other roof panel thickness was conducted. From Figure 2.3-11, the tall sliding clip, C3, and the thinner purlin resulted in the lowest R_t-value. Therefore, a test was conducted using the same clip type and purlin thickness but with 24 ga deck material. The resulting R_t-value is 64.8 percent, which is greater than the R_t-value of 57.1 percent when the 22 ga roof panel was used as shown in Figure 2.3-11. Thus, the remaining tests were conducted using the 22 ga panel.

Knowing the combination of clip-type and panel thickness, which results in the lowest R_t-value for the two-purlin thicknesses, four additional tests were needed to satisfy the requirements of AISI S908. Figure 2.3-12 shows the results of the completed test sequence.

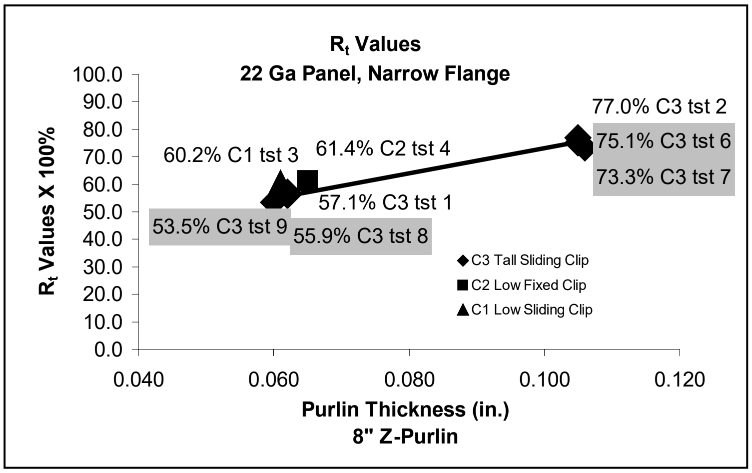

Figure 2.3-12 Final Verification

From the test data generated, the expression for the reduction factor (AISI S908 Equation 8) is developed as follows. From data in Table 2-3,

$$R_{t_{min}} = 0.555 - 0.018 = 0.537$$

$$R_{t_{max}} = 0.751 - 0.019 = 0.732$$

Table 2-3 Summary of Gravity Loading Test Results

Test No.	Purlin Thickness (in.)	R_t-value	$M_{nt}=S_tF_y$ (kip-in.)
1	0.062	0.571	110.5
8	0.062	0.559	118.3
9	0.060	0.535	116.3
Average		0.555	115.0
Standard Deviation		0.018	
2	0.105	0.770	215.3
6	0.105	0.751	218.3
7	0.106	0.733	219.7
Average		0.751	217.8
Standard Deviation		0.019	

$$\overline{M}_{nt_{min}} = 115.0\,\text{kip}-\text{in}$$

$$\overline{M}_{nt_{max}} = 217.8\,\text{kip}-\text{in}$$

Thus, the reduction factor equation, in terms of the nominal flexural strength of the section, M_n, for the tested purlins is:

$$R = \left(\frac{R_{t_{max}} - R_{t_{min}}}{\overline{M}_{nt_{max}} - \overline{M}_{nt_{min}}} \right)(M_n - \overline{M}_{nt_{min}}) + R_{t_{min}} < 1.0 \qquad \text{(AISI S908 Eq. 8)}$$

$$= \left(\frac{0.732 - 0.537}{217.8 - 115.0} \right)\left(M_n - 115.0\right) + 0.537 \leq 1.0$$

$$= 1.897(M_n - 115.0)/1000 + 0.537 \leq 1.0$$

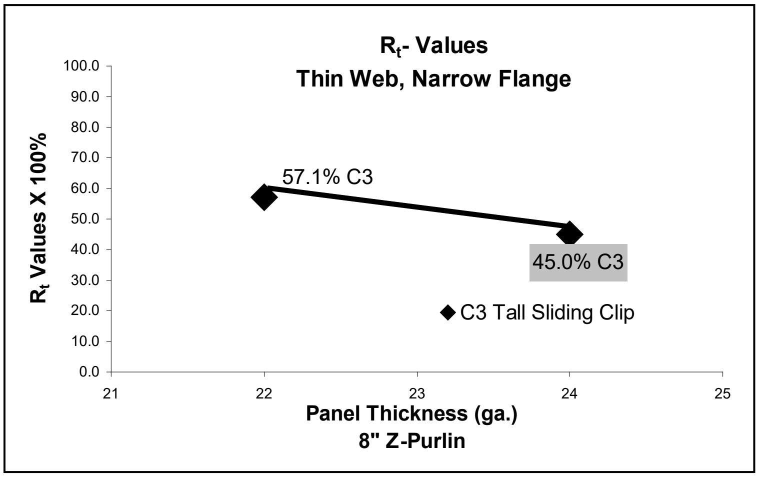

Figure 2.3.13 Roof Panel Thickness Trend

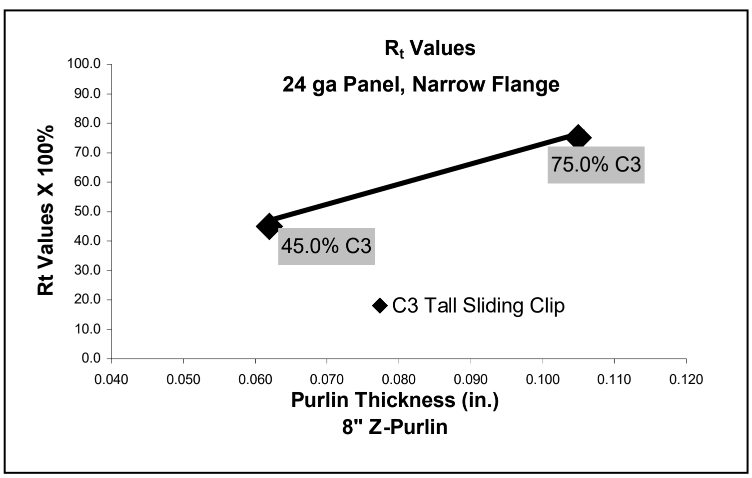

Figure 2.3-14 Determination of Panel Thickness Trend

If the initial choice of roof panel thickness did not result in the lowest R_t-value, as shown in Figure 2.3-11, three additional tests would be required to determine the controlling combination. For example, suppose that the use of a 24 ga panel resulted in an R_t-value of 45 percent, as shown in Figure 2.3-13. A controlling purlin thickness, with the now controlling panel thickness, would need to be determined. A test would be constructed using the same clip type and the now controlling panel thickness with the thicker purlin. With the R_t-values from the two tests a trend line would be found as shown in Figure 2.3-14. The thinner purlin gives the lower R_t-value of 45.0 percent, meaning the thinner purlin is the controlling purlin thickness for the roof system constructed with the 24 ga roof panel.

To verify the controlling clip, two additional tests would be conducted using the purlin thickness that resulted in the lower R_t-value, one with each of the other two clip types (C1 and C2). These two data points would be plotted and used to verify that the initial controlling clip type continues to give the lowest R_t-value. The resulting R_t-values for the test with the low fixed and low sliding clip are shown in Figure 2.3-15. The R_t-values obtained were 55.0 percent and 65.0 percent, confirming that the tall sliding clip controls.

Knowing the combination of clip type and purlin thickness that result in the lowest R_t-value for the 24 ga roof panel, the remaining four tests required by AISI S908 would be conducted, and the R-value relationship, AISI S908 Equation 8, would be developed as shown above. For this testing scenario, the required number of tests increases from 9 to 11, but is less than the 72 tests required by the original test procedure.

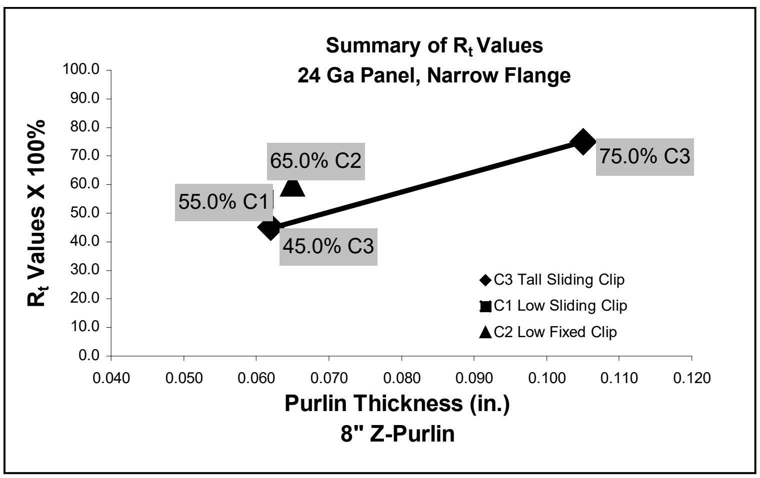

Figure 2.3-15 Controlling Clip Type Verification

CHAPTER 3 CONTINUOUS PURLIN DESIGN

Symbols and Definitions Used in Chapter 3

A_w Area of web (in.^{2}) (mm^2)
b Flange width (in.) (mm)
C Coefficient from AISI S100 Tables G5-2 and G5-3
C_b Bending coefficient dependent on moment gradient
C_h Web slenderness coefficient from AISI S100 Tables G5-2 and G5-3
C_N Bearing length coefficient from AISI S100 Tables G5-2 and G5-3
C_R Inside bend radius coefficient from AISI S100 Tables G5-2 and G5-3
C_w Torsional warping constant of cross-section
D Dead load (lb/ft^2) (N/m^2)
d Depth of section (in.) (mm)
E Modulus of elasticity of steel, 29,500,000 psi (203,000 MPa)
F_n Nominal global flexural stress (ksi) (MPa)
F_d Elastic distortional buckling stress (ksi) (MPa)
F_e Elastic buckling stress (ksi) (MPa)
F_v Nominal shear stress (ksi) (MPa)
F_y Yield stress (ksi) (MPa)
G Shear modulus of steel, 11,300 ksi (78,000 MPa)
h Depth of flat portion of web measured along plane (in.) (mm)
I_x Moment of inertia of full unreduced section about major centroidal axis perpendicular to the web (in.^{4}) (mm^4)
I_{xy} Product of inertia of the full unreduced section about centroidal axes parallel and perpendicular to the web (in.^{4}) (mm^4)
I_y Moment of inertia of full unreduced section about minor centroidal axis parallel to the web (in.^{4}) (mm^4)
I_{yc} Moment of inertia of compression portion of section about centroidal axis of entire section parallel to web, using full unreduced section
k_v Shear buckling coefficient
K_y Effective length factor for buckling about y-axis
L Span length (ft) (m)
L_r Roof live load (lb/ft^2) (N/m^2)
L_y Unbraced length of compression member for bending about y-axis (ft) (m)
M Required allowable flexural strength, ASD (lb-in.) (N-m)
M Required flexural strength at, or immediately adjacent to, the point of application of the concentrated load or reaction, P (lb-in.) (N-m)
$\overline{M}$ Required flexural strength [factored moment] (lb-in.) (N-m)
M_D Dead load bending moment (lb-in.) (N-m)
M_{Lr} Roof live load bending moment (lb-in.) (N-m)
M_n Nominal flexural strength [resistance] (lb-in.) (N-m)
M_{ne} Nominal flexural strength [resistance] for yielding and global (lateral-torsional) buckling (lb-in.) (N-m)
$M_{n\ell o}$ Nominal strength considering only local buckling from AISI S100 Section F3 (lb-in.) (N-m)

M_u	Required flexural strength for LRFD (lb-in.) (N-m)
M_w	Wind load bending moment (lb-in.) (N-m)
M_y	Member yield moment (lb-in.) (N-m)
m	Distance from the shear center to the mid-plane of the web (in.) (mm)
N	Actual length of bearing (in.) (mm)
P	Required allowable strength for concentrated load or reaction in presence of bending moment (lb) (N)
$\overline{P}$	Required strength for concentrated load or reaction in presence of bending moment
P_D	Dead load reaction (lb) (N)
P_n	Sum of nominal strength for concentrated load or reaction of each purlin at support in absence of bending moment determined in accordance with AISI S100 Section G5 (lb) (N)
R	Reduction factor determined in accordance with AISI S908
R	Inside bend radius (in.) (mm)
S_e	Effective section modulus calculated at extreme fiber compressive stress of F_n determined in accordance with AISI S100 Sections F3.1.1 and F3.1.3 (in.^{3}) (mm^3)
S_{et}	Effective section modulus calculated at extreme fiber tension stress of F_y (in.^{3}) (mm^3)
S_f	Elastic section modulus of full unreduced section relative to extreme compression fiber (in.^{3}) (mm^3)
t	Base steel thickness of any element or section (in.) (mm)
V	Required allowable shear strength for ASD (lb) (N)
$\overline{V}$	Required shear strength (lb) (N)
V_D	Shear force due to dead load (lb) (N)
V_{Lr}	Shear force due to roof live load (lb) (N)
V_n	Nominal shear strength (lb) (N)
V_u	Required shear strength for LRFD (lb) (N)
θ	Angle between web and bearing surface > 45° but no more than 90°
θ	Angle between vertical and plane of web of Z-section
μ	Poisson's ratio for steel, 0.3
ϕ_b	Resistance factor for bending strength
ϕ_v	Resistance factor for shear strength
ϕ_w	Resistance factor for web crippling strength
Ω_b	Safety factor for bending strength
Ω_v	Safety factor for shear strength
Ω_w	Safety factor for web crippling strength

3.1 General Design Considerations

3.1.1 Design and Analysis Considerations

Because most Z-purlins are essentially point symmetric and the applied loading is generally not parallel to a principal axis, the response to both gravity and wind uplift loading is complex. The problem is somewhat less complex for continuous C-purlins since bending is about the principal axes. Design is further complicated when standing seam roof panels, which may provide only partial lateral and/or torsional restraint, are used. In addition to AISI S100 provisions, a number of design and analysis considerations are needed. Commonly used considerations are:

1. Constrained bending, that is bending is about an axis perpendicular to the web.
2. Full lateral support is provided by through-fastened roof panels in the positive moment regions.
3. Partial lateral support is provided by standing seam roof panels in the positive moment regions, or the purlins are laterally unrestrained between intermediate braces. For the former, the AISI S908, also known as the base test method, is used to determine the level of restraint. For the latter, AISI S100 lateral-torsional buckling equations are used to determine the purlin strength.
4. An inflection point is a brace point.
5. For analysis, the purlin line is either considered prismatic, e.g., ignoring the increased stiffness because of the two cross-sections within the lap, or the purlin line is considered non-prismatic, e.g. considering the increased stiffness within the lap.
6. Use of vertical short-slotted holes, which facilitate erection of the purlin lines, for the bolted lap web-to-web connection does not affect the strength of continuous purlin lines.
7. The critical location for checking combined bending and shear is immediately adjacent to the end of the lap in the single purlin.

Constrained Bending Approximation

Constrained bending implies that bending is about an axis perpendicular to the Z-purlin web and that there is no purlin movement perpendicular to the web. That is, all movement is constrained in a plane parallel to the web. Since a Z-purlin is point symmetric and because the applied load vector is not generally parallel to a principal axis of the purlin, the purlin tends to move out of the plane of the web and rotate. Constrained bending therefore is not the actual behavior. However, it is a universally used assumption and its appropriateness is implied in AISI S100. For instance, the nominal global buckling strength equations for Z-sections in AISI S100 Section F2.1.3 applies to Z-section bending about the centroidal x-axis that is perpendicular to the web. All of the analyses referred to in this Section are based on the constrained bending assumption.

Panel Lateral Restraint Approximation

It is also assumed that through-fastened roof panels provide full restraint support to the purlin in the positive moment region. It is obvious that this assumption does not apply equally to standing seam roof systems. The degree of restraint provided depends on the panel profile, seaming method, and clip details. The restraint provided by the standing seam system consists of panel drape (or hugging) and clip friction or lockup. Lower values are obtained when “snap-together” (e.g., no field seaming) panels or two-piece (or sliding) clips are used. Higher values are obtained when field seamed panels and fixed clips are used. However, exceptions apply to both of these general statements.

AISI S100 Appendix A Section I6.2.2 Flexural Members Having One Flange Fastened to a Standing Seam Roof System allows the designer to determine the design strength of C- and Z-purlins using (1) the theoretical lateral-torsional buckling strength equations in AISI S100 Section F2, or (2) by testing according to AISI S908 as described in Section 2.3 of this Design Guide. AISI S908 indirectly establishes the lateral-torsional restraint provided by a standing seam panel/clip/bracing combination.

If intermediate braces are not used, a lateral-torsional buckling analysis will predict an equivalent R-value in the range 0.12 to 0.20 for typical depth-to-span ratios. The corresponding R-value obtained from AISI S908 will tend to be three to five times larger, which clearly shows the beneficial effects of panel drape and clip restraint. If intermediate bracing is used, R-values obtained from AISI S908 will sometimes be less than that predicted by a lateral-torsional analysis with the unbraced length equal to the distance between intermediate brace locations. The latter results are somewhat counterintuitive in that panel/clip restraint is not considered in the analytical solution, yet the resulting strength is greater than the experimentally determined value. Possible explanations for this anomaly are that the intermediate brace anchorage in the testing is not as rigid as assumed in the AISI S100 equations, or stress concentrations at the braces contribute to the failure mechanism. Also, AISI S100 Commentary Section F2.1(b) states that for Z-sections, "A conservative design approach is used in the Specification, in which the elastic buckling stress is taken to be one-half of that for I-members."

Prismatic / Non-prismatic Bending Approximation

One of two analysis assumptions are commonly made by designers of multiple span, lapped, purlin lines: (1) prismatic (uniform) moment of inertia or (2) non-prismatic (non-uniform) moment of inertia. For the prismatic assumption, the additional stiffness caused by the increased moment of inertia within the lap is ignored. For the non-prismatic assumption, the additional stiffness is accounted for by using the sum of the moments of inertia of the purlins forming the lap. Larger positive (mid-span) moments and smaller negative (end-region) moments result when the first assumption is used with gravity loading. The reverse is true for the second assumption. For uplift loading the same conclusions apply except that positive and negative moment locations are reversed. It follows then that the prismatic assumption is more conservative if the controlling strength location is within the span (the positive moment region) and that the non-prismatic assumption is more conservative if the controlling strength location is at the supports, i.e., within or near the lap (the negative moment region).

Since the purlins are not continuously connected within the lap, full continuity will not be achieved, the degree of fixity is difficult to determine experimentally. However, experimental evidence indicates that the non-prismatic assumption is the more accurate approach (Murray and Elhouar, 1994).

Inflection Point as Brace Point

For many years it has been generally accepted that an inflection point is a brace point in a Z-purlin line; however, it is not so stated in AISI S100. The American Institute of Steel Construction (AISC) *Specification for Structural Steel Buildings* (AISC, 2016) states that an inflection point is not a brace point. However, the inflection point has also been considered a brace point with C_b taken as 1.75 (CCFSS, 1992).

Because C- and Z-purlins tend to rotate or move in opposite directions on each side of an inflection point, tests were conducted by Bryant and Murray (2000) to determine if an inflection point can be safely assumed to behave as a brace point in continuous, gravity loaded, C- and Z-purlin lines of both through-fastened and standing seam roof systems. In the study, instrumentation was used to verify the actual location of the inflection point and the lateral movement of the bottom flange of the purlins on each side of the inflection point, as well as near the maximum moment location in an end span. The results were compared to movement predicted by finite element models of two of the tests. Both the experimental and analytical results showed that although lateral movement did occur at the inflection point, the movement was considerably less than at other locations along the purlins. The bottom flanges on both sides of the inflection point moved in the same direction and double curvature was not apparent from either the experimental or finite element results. The lateral movement in the tests using lapped C-purlins was larger than the movement in the Z-purlin tests, but was still relatively small.

The predicted and experimental controlling limit state for the three tests using through-fastened roof panels was shear plus bending failure immediately outside the lap in the end test bay. The experiment failure loads were compared to predicted values using provisions of AISI S100 and assuming (1) the inflection point is not a brace point, (2) the inflection point is a brace point, and (3) the negative moment region strength is equal to the effective yield moment, the lessor of S_eF_n and $S_{et}F_y$. All three analysis assumptions resulted in predicted failure loads less than the experimental failure loads: up to 23% for assumption (1), up to 11% for assumption (2), and approximately 8% for assumption (3). However, the bottom flange of a continuous purlin line moves laterally in the same direction on both sides of an inflection point, but the movement is relatively small. It is difficult to draw definite conclusions from this data. However, it appears that assuming full lateral-torsional restraint at the inflection point for through-fastened roof systems is conservative.

Vertical Slotted Holes at Lap

The web-to-web connection in lapped Z-purlin lines is generally made with two 1/2 in. diameter structural bolts approximately 1 1/2 in. from the end of the purlin as shown in Figure 1.2-1. To facilitate erection, vertical slotted web holes are generally used, which may allow slip in the lap invalidating the continuous purlin assumption. Murray and Elhouar (1994) analyzed 24 continuous span tests where vertical slotted holes were used in the lap connections. They found no indication in the data that the use of slots in the web connections of lapped purlins has any effect on the flexural strength of the purlins.

Critical Location for Combined Bending and Shear

The moment gradient between the inflection point and rafter support of continuous purlin lines is steep. As a result, the location where combined bending and shear is checked can be critical. The industry practice is to assume the critical location is immediately outside of the lapped portions of continuous Z-purlin systems, that is, in the single purlin, as opposed to at the web bolt line. The rationale for the assumption is that for cold-formed Z-purlins, the limit state of combined bending and shear is actually web buckling. Near the end of the lap and especially at the web-to-web bolt line, out of plane movement is restricted by the non-stressed purlin section, thus buckling cannot occur at this location. Figure 3.1-1 verifies this contention. The corresponding assumption for C-purlin systems is that the shear plus bending limit state occurs at the web-to-web vertical bolt line.

Figure 3.1-1 Photograph of Failed Purlin at End of Lap

3.1.2 Purlin Bracing

While the attachment of panels to the top flange of a purlin provides partial lateral-torsional resistance, additional braces are typically applied. These additional braces may provide lateral restraint, torsional restraint, or combined lateral-torsional restraint. When braces are utilized in conjunction with the lateral-torsional restraint provided by the panels, the braces are referred to as anchorage devices and designed according to AISI S100 Section I6.4. These anchorage devices work in conjunction with the panels and transfer forces out of the purlin-panel system to the primary structural system.

In cases where it is difficult to define the lateral and/or torsional restraint provided by the panels, as in many standing seam systems, the restraint provided by the panels can be conservatively ignored. Intermediate braces that resist lateral and/or torsional movements, referred to as discrete braces, are applied along the length. The forces generated in these braces are calculated according to AISI S100 Section C2.2.1 and must be transferred through the bracing system to the primary structural system. In cases where the lateral restraint provided by the panels is known, torsional only braces can be used. For the design of torsion braces, refer to Section 5.5.4.4.

Unbraced Purlins

Purlins that are unbraced between support locations are rarely encountered in purlin systems. If such a condition should occur, the member's global, local, and distortional buckling flexural strength is to be determined by AISI S100 Chapter F. For the unbraced condition, global buckling will often control. In a continuous purlin system, the global buckling flexural strength is checked for the unbraced length between inflection points. The moment gradient bending, C_b, is greater than unity but can conservatively be used as unity.

In the region of an intermediate support, that is the negative moment region of a continuous span purlin, the flexural capacity is computed for the unbraced length between the inflection point and the end of the lap with C_b either calculated using AISI S100 Eq. F2.1.1-2 or conservatively taken as 1.67. In the lapped region, the purlins are considered to be sufficiently braced against global and distortional buckling, so the flexural capacity is determined by the local buckling strength.

Anchorage of Purlin Bracing

The load carrying capacity of purlin systems attached to roof panels is dependent on the ability of the roof panels to torsionally and laterally restrain the purlins. The torsional restraint is provided by the bending strength and stiffness of the panels and the clip/fastener assembly which connects the roof system to the purlins. Lateral restraint is provided by the diaphragm capacity of the panels and any discrete point bracing designed into the system.

The torsional restraint is self-contained in the panels; however, brace forces and diaphragm forces accumulate and must be transferred to other structural elements, i.e., rigid frames, vertical bracing, etc.

Purlins having their compression flange attached to through-fastened panels are designed as laterally supported members. Forces which are developed in the bracing system and the panels must be calculated and anchored in accordance with AISI S100 Section I6.4.

In Section I6.4.1, equations to predict the anchorage forces are provided. The equations depend on the location and type of lateral bracing system. The cases included are:

1. Bracing at purlin supports
2. Third point bracing, and
3. Mid-span bracing.

The anchorage forces calculated in Section I6.4.1 of the AISI S100 are contingent upon the roof diaphragm having sufficient stiffness to limit the lateral deflection between braces to the span length/360. If the lateral deflection limit is not satisfied, additional braces along the span are required.

AISI S100 Section I6.4.2 allows an alternative bracing method where restraints at the frame lines are used in conjunction with pairs of braces along the span of the purlin that only provide torsional restraint to the purlins (do not restrict lateral movement). When using this type of system, the lateral deflection limit is relaxed to the span length/180. The anchorage forces and the forces in the braces may be calculated according to the component stiffness method presented in Chapter 5.

AISI S100 Section I6.4.1 also allows the use of rational analysis to determine anchorage forces provided the analysis meets the specified requirements. Several alternate rational analysis procedures (component stiffness method, frame stiffness model, and shell finite element model) are presented in Chapter 5.

Designers using interior bracing systems often anchor the bracing by balancing the bracing forces across the building ridge (Figure 3.1-2). This procedure requires that the structure have equal slopes, equal loading and equal lengths on each side of the ridge, in order for the bracing forces to be balanced. If these equalities do not exist then bracing members must be added to resist the unbalanced forces, or a proper number of purlins have their flanges facing one another to eliminate the unbalanced forces. The component of force perpendicular to the roof slope must also be considered at the ridge when this anchorage system is used.

For single sloped buildings or for buildings where the discrete braces cannot be anchored across the ridge, the bracing forces must be transferred to an anchor location. Rigid frame lines or braced frame lines are generally selected as anchorage points. To transfer the forces out of the discrete braces to these anchorage locations horizontal trusses are generally installed in the plane of the roof.

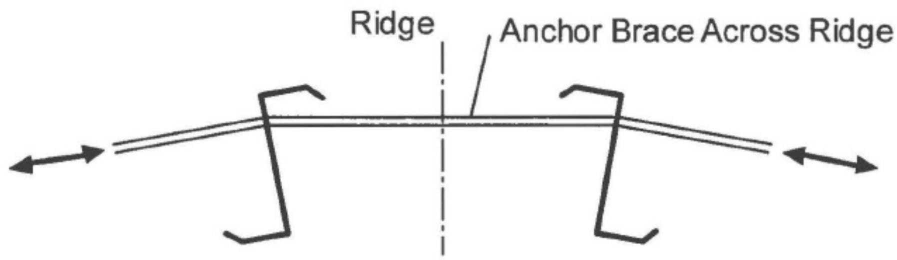

Figure 3.1-2 Anchor Force Transferred Across Ridge

Use of a system that incorporates only the standing seam panel roof diaphragm may be used. The diaphragm is anchored at discrete points along the rafter or at the building eave with an antiroll anchorage device as shown in Figure 3.1-3. The primary advantage of this system over discrete point bracing systems is that fewer parts need to be handled during erection. In addition, this system does not require modification for single slope buildings and does not require alteration for the inequalities mentioned above.

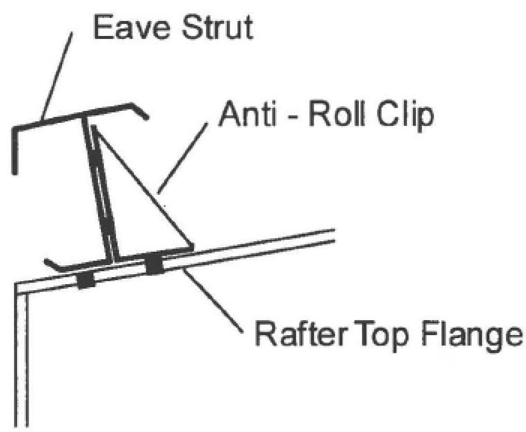

Figure 3.1-3 Diaphragm Anchorage at Eave

No matter what anchorage system is used the designer must prove by calculation or tests that the diaphragm can deliver the accumulated purlin anchorage forces into the anchorage points.

3.2 Design Limit States for Continuous Systems

3.2.1 Design Overview

The initial selection of purlins is often according to the flexural strength in the interior of the purlin span for either gravity or uplift loading. The flexural strength of the purlin in this region depends significantly on the extent to which the panels stabilize the purlin. Through-fastened systems provide more consistent and predictable restraint than highly variable standing seam systems and the strength can be calculated directly. Because of the large variations in standing seam systems, the flexural strength along the interior of the span must be determined by tests according to AISI S908 as discussed in Chapter 2. If test information is not available for a particular system, the system must be designed with discrete braces with the purlin considered unbraced between the braces. Because the flexural strength along the interior of the span is often the most important factor in the design of the purlin, the design process is typically divided into three design tracks: *through-fastened systems, standing seam systems per AISI S908, and discrete braced systems*. Once the flexural strength has been established along the interior of the span, many of the design limit states (shear, web crippling, etc.) are the same for each design track.

3.2.1.1 Through-Fastened Systems

Although AISI S100 does not contain explicit provisions for the positive moment region of purlins with one flange fastened to metal panels subjected to gravity loads, industry practice assumes that when fastened to the compression flange the panels provide full lateral and torsional support. Therefore, the limit state of global lateral-torsional buckling is eliminated and the flexural strength is determined as the minimum of the local buckling and distortional buckling flexural strengths.

For uplift loading, along the interior of the span, the compression flange is not attached to panels and therefore is only partially restrained against global buckling. A reduction factor (R-factor), as specified in AISI S100 Section I6.2.1, is applied to account for the reduced flexural strength. Reduction factors are based on tests that have captured the impacts of the partial panel restraint on global and distortional buckling. Local buckling strength must still be calculated.

Because the through-fastened system relies on the panels for strength and stability, the designer must ensure that the panels have adequate strength and stiffness and provide a pathway to transfer the forces from the panels to primary structure. These forces are commonly referred to as anchorage forces and are determined according to AISI S100 Section I6.4.1. Anchorage forces are only evaluated for gravity loads. Methods to evaluate the strength and stiffness of the diaphragm are discussed in Chapter 4.

3.2.1.2 Standing Seam Systems

Whereas the panels in through-fastened systems provides full lateral restraint to the top flange, and predictable and consistent lateral restraint through the stiffness of the panel connection to the top flange, the restraint provided by standing seam systems is typically less and can vary between manufacturers. As a result, it is much more difficult to analytically predict the contribution of the standing seam panel to the flexural strength of the purlin. Consequently, to design a standing seam purlin system, the designer must either rely on the flexural strength determined by AISI S908 or ignore the contribution of the panels and analyze the system as discrete braced.

If the purlin system is designed according to AISI S100 Section I6.2.2, which utilizes strength reduction factors determined by AISI S908, the system must meet the requirements for the anchorage of bracing in Section I6.4. The designer must demonstrate the manner in which the required forces are delivered to the anchorage system, i.e., determine how the load in the diaphragm accumulates at an anchorage device(s). See AISI S912 for the appropriate test procedure. If the system is designed as a discrete braced system, neglecting any restraint provided by the panels, the system must meet the bracing requirements of AISI S100 Section C2.2.1. A few important points to remember are:

1. If the test is conducted with anchorage devices at each purlin, the actual roof system must be built with anchorage devices at each purlin.
2. The requirements of AISI S100 Section I6.4 are less onerous than those of Section C2.2.1, and can only be used if the following conditions are satisfied:

a. Purlins are fastened to the deck or panels at the top flanges or covered with standing seam roof panels,

b. Panels have sufficient diaphragm strength to transfer the anchorage forces from the purlin to the anchorage points, and

c. The purlin top flange lateral displacements with respect to the reaction points do not exceed the span length divided by 360 (L/360) under service loads.

If the strength or deflection requirements are not met, then the bracing system must be designed using AISI S100 Section C2.2.1.

3. For standing seam roof systems, tests must be conducted to determine the capability of the roof panels and its connection to the anchorage device to transfer gravity load bracing forces to the anchor. A test procedure is outlined in AISI S912. For cases where the roof panels are through-fastened at the location of the anchorage device, the adequacy of the connection from panels to purlin to anchor can be calculated directly.

3.2.1.3 Design Using AISI S908

The following steps must be taken to design purlins subjected to gravity loading if the strength is based on using AISI S908, according to AISI S100 Section I6.2.2.

1. Conduct the base tests in accordance with AISI S908 to determine the strength reduction factors, R, for gravity and uplift cases. Discussion on the interpretation of test results is provided in Chapter 2.
2. Select the proper size purlins to provide the required moment capacity. The nominal strength of a purlin is determined in AISI S100 Appendix A Section I6.2.2, $M_n = RM_{n\ell o}$, where $M_{n\ell o}$ is the nominal strength considering only local buckling from Section F3.
3. Design the anchorage system in accordance with AISI S100 Section I6.4.1. If the diaphragm system meets the stiffness requirement of span length divided by 360 (L/360), under service loads, and if the diaphragm demand is at an acceptable level relative to the tested strength, provide the proper anchorage for the diaphragm system and any intermediate braces (if intermediate braces are part of the purlin bracing system).
4. Demonstrate that the anchorage forces which accumulate in the roof panels can be adequately transferred from the panels into the anchorage device. For through-fastened roof systems calculations may suffice; however, for standing seam systems, AISI S912 must be used.
5. If the diaphragm stiffness requirements per item 3 are *not* met, the contributions of the standing seam system must be ignored, and the system must be designed as a discrete based system with brace forces meeting the requirements of AISI S100 Section C2.2.1.
6. Testing is typically performed on simple span systems and therefore indicates the flexural capacity of the system at or near mid-span. For continuous span systems, the flexural strength must be checked between the inflection point and the end of the lap and in the lapped region over the supports. In the region between the inflection point and the end of the lap, the compression flange is considered unbraced and therefore can be calculated in accordance with Chapter F. In the region over the support, the sections are considered to be fully braced against the global buckling and, again, can be calculated in accordance with Sections F3 and F4.
7. Shear strength, combined shear and bending, web crippling and combined web crippling and buckling must be checked. Figure 3.2-6 summarizes the shear and web crippling limit states and the locations along the continuous span in which each limit state is checked.

For cases where the purlin is subjected to uplift loading, additional tests must be performed reflecting this loading condition. Typically, uplift loading will result in smaller R values than for gravity loaded systems. Determination of the nominal flexural strength near mid-span is the same as for gravity loaded systems where the nominal strength is the local buckling strength reduced by the R-factor from the uplift tests, or $M_n = RM_{n\ell o}$. The flexural strength may need to be checked in the region between the inflection point and the end of the lap and the lapped section over the support if the net uplift loads exceed the gravity loads.

Shear strength must be checked only if the net uplift exceeds the gravity forces. Web crippling is not a limit state since the connection to the primary structural system is in tension. System anchorage requirements are required only for gravity loading, and no additional anchorage or diaphragm checks are required for uplift loading.

Figure 3.2-5 summarizes the limit states for uplift loading.

3.2.1.4 Design with Discrete Bracing

If a standing seam system does not satisfy the minimum diaphragm requirements discussed in Chapter 4 or if AISI S908 test data is unavailable, the system must be designed as a discrete braced system. In this case, the contribution of the panels to the strength of the system is ignored for most limit states and the purlins are designed as unbraced between brace points. When investigating the distortional buckling strength according to AISI S100 Section F4, if the rotational stiffness of the connection between the purlin and panels is known, it can be incorporated into the distortional buckling strength, otherwise it is conservative to ignore. The predicted strength when analyzed as a discrete braced purlin system will typically be less than a comparable system tested according to AISI S908.

This design method requires bracing of the purlins. AISI S100 provides two methods for the determination of brace forces. Section I6.4.1, provides a method for systems with panels attached to the top flange of the purlins. This method relies on the contribution of the diaphragm to redistribute brace forces. The other method, Section C2.2.1, ignores the contribution of the diaphragm, which typically result in larger brace forces than systems that rely on the diaphragm. Regardless of the method, a load path transferring these brace forces to the primary structure must be provided.

In discrete braced systems, the braces must restrain the purlin both laterally and torsionally. Most commonly, systems utilize braces at the frame lines and a pair of symmetric braces near the third points. Mid-point braces are generally avoided because it is believed that the brace introduces a stress concentration at the location of the maximum moment. Some tests have shown significantly reduced flexural capacities when mid-point braces are used.

As with systems designed according to AISI S100 Section I6.2.2, the flexural strength of discrete braced systems must be checked near the middle of the span, the region between the inflection point and the end of the lap, and at the lapped section over the supports. The flexural strength must be checked for both gravity loads and uplift loads. As long as the net uplift loads do not exceed the gravity loads, gravity loads will control. Shear strength and web crippling must also be checked.

3.2.2 Flexural Strength for Gravity Loading

For continuous purlin systems subjected to gravity loading, the flexural strength must be checked at (1) the positive moment region along the interior of the span, (2) the negative moment region between the inflection point and the end of the lap, and (3) the lapped purlin in the negative moment region over the support.

3.2.2.1 Flexural strength along interior of span

In the positive moment region between supports, the unsupported flange is in tension, while the other flange, which is connected to the roof panels, is in compression. The extent to which the panels restrain the compression flange varies between through-fastened and standing seam systems. Therefore, different methodologies are used to determine the flexural strength of the purlin.

Through-fastened systems

Along the interior of the span, the purlin compression flange is attached to panels, effectively bracing it against lateral-torsional buckling. Thus, considering the global buckling strength according to AISI S100 Section F2.1, the nominal flexural buckling stress, F_n, is equal to the yield stress, F_y, meaning that the cross-section will reach the yield strength before global buckling can occur. Because global buckling won't control, the flexural strength of the purlin is determined as the minimum of the local buckling and distortional buckling strengths. The local buckling strength may be calculated using either the Effective Width Method in Section F3.1 or the Direct Strength Method in AISI S100 Section F3.2. The distortional buckling strength is calculated according to Section F4. Including the rotational restraint provided by the panels will increase the distortional buckling strength or it can be conservatively ignored. For both local and distortional buckling, AISI S100 Appendix 2 permits any elastic buckling analysis that includes the relevant mechanics or provides analytical buckling analysis solutions.

The design of through-fastened systems subjected to gravity load is summarized in Figure 3.2-1.

Standing Seam Systems

For the flexural strength along the interior of the span for standing seam systems, AISI S100 Section I6.2.2 refers to Appendix A for provisions specific to United States and Mexico. The nominal flexural strength is the product of the nominal flexural strength with consideration of local buckling only, $M_{n\ell o}$, and the reduction factor determined according to AISI S908. The reduction factor incorporates both the effects of global lateral-torsional buckling and distortional buckling. The nominal local buckling strength is calculated either according to the Effective Width Method in Section F3.1 or the Direct Strength Method in Section F3.2.

The design of standing seam systems subjected to gravity load using AISI S908 is summarized in Figure 3.2-2.

Discrete Braced Systems

When results from AISI S908 testing is unavailable or if the standing seam panels do not provide adequate strength and stiffness, the system must be designed as discrete braced. The most common configuration is a pair of braces symmetrically placed near the third points of the span. The purlin is unbraced between these braces and the flexural strength is the minimum of the global buckling, distortional buckling or local buckling strength. Global buckling is calculated in AISI S100 Section F2.1.3 for Z-sections and F2.1.1 for C-sections with C_b conservatively taken as unity. The distortional buckling strength can include the rotational restraint provided by the panels if known or can be conservatively ignored.

Design of discrete braced systems subjected to gravity load is summarized in Figure 3.2-3.

3.2.2.2 Flexural strength between the inflection point and the end of the lap

The compression flange is considered unbraced between the inflection point and the end of the lap and the strength is the same for through-fastened, standing seam and discrete braced systems. The global buckling strength is calculated from AISI S100 Section F2 with the unbraced length being taken as the distance between the inflection point and the end of the lap and C_b conservatively approximated as 1.67. Distortional buckling is calculated from Section F4 without the inclusion of the rotational restraint from the panels. Local buckling is calculated from AISI S100 Section F3. Note that in the lapped region and at the supports, the purlins often fabricated with pre-punched holes. Because the holes are relatively small and isolated, they have little impact on the strength of the purlin per AISI S100 Section E3.2.2.

3.2.2.3 Flexural strength in the lapped region at the interior support

The compression flange is considered fully laterally braced and therefore local buckling is the controlling limit state. The strength of the lapped section is the sum of the individual strengths of the two purlins.

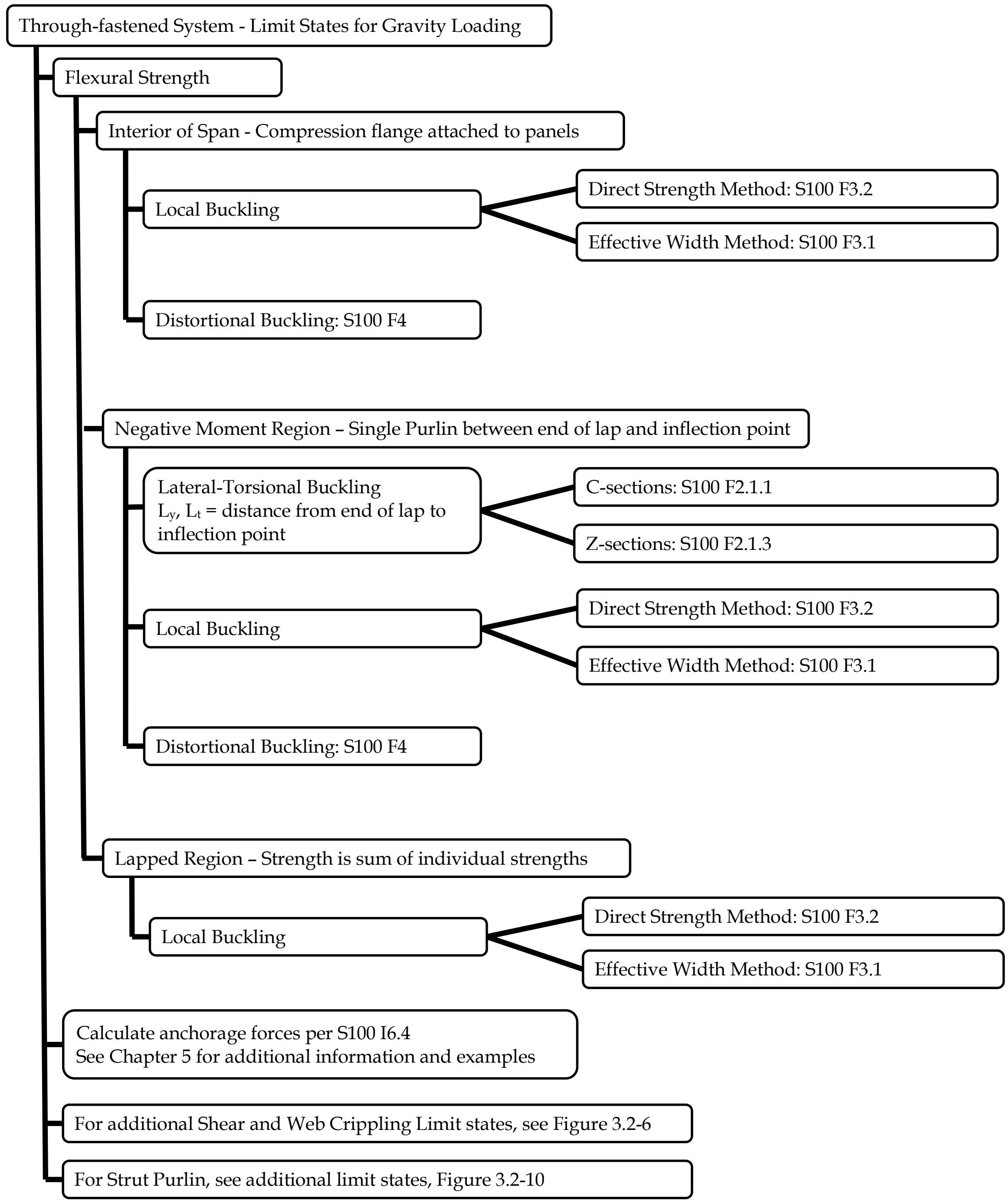

Figure 3.2-1 Through-Fastened System - Limit States for Gravity Loading

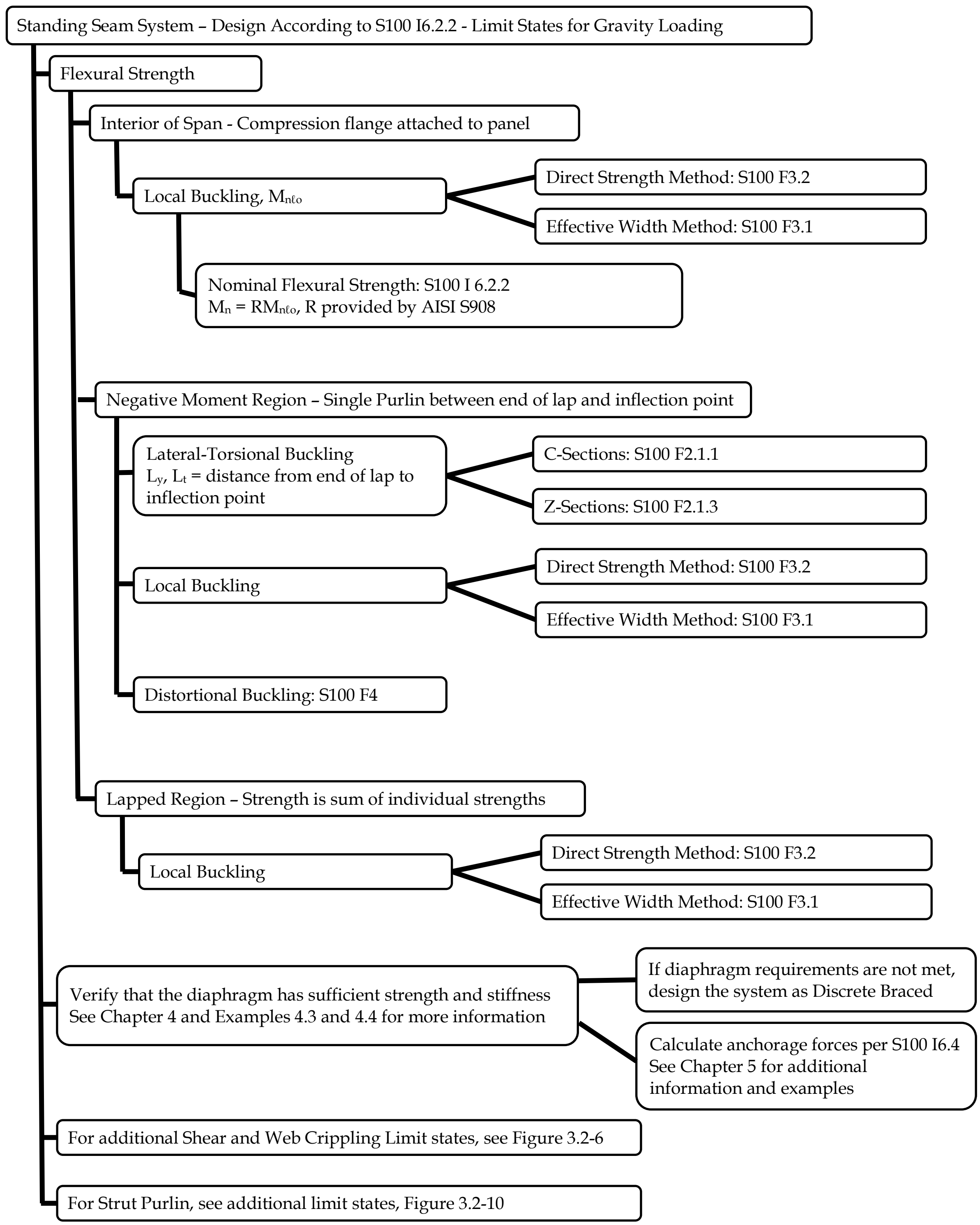

Figure 3.2-2 Standing Seam System - Limit States for Gravity Loading

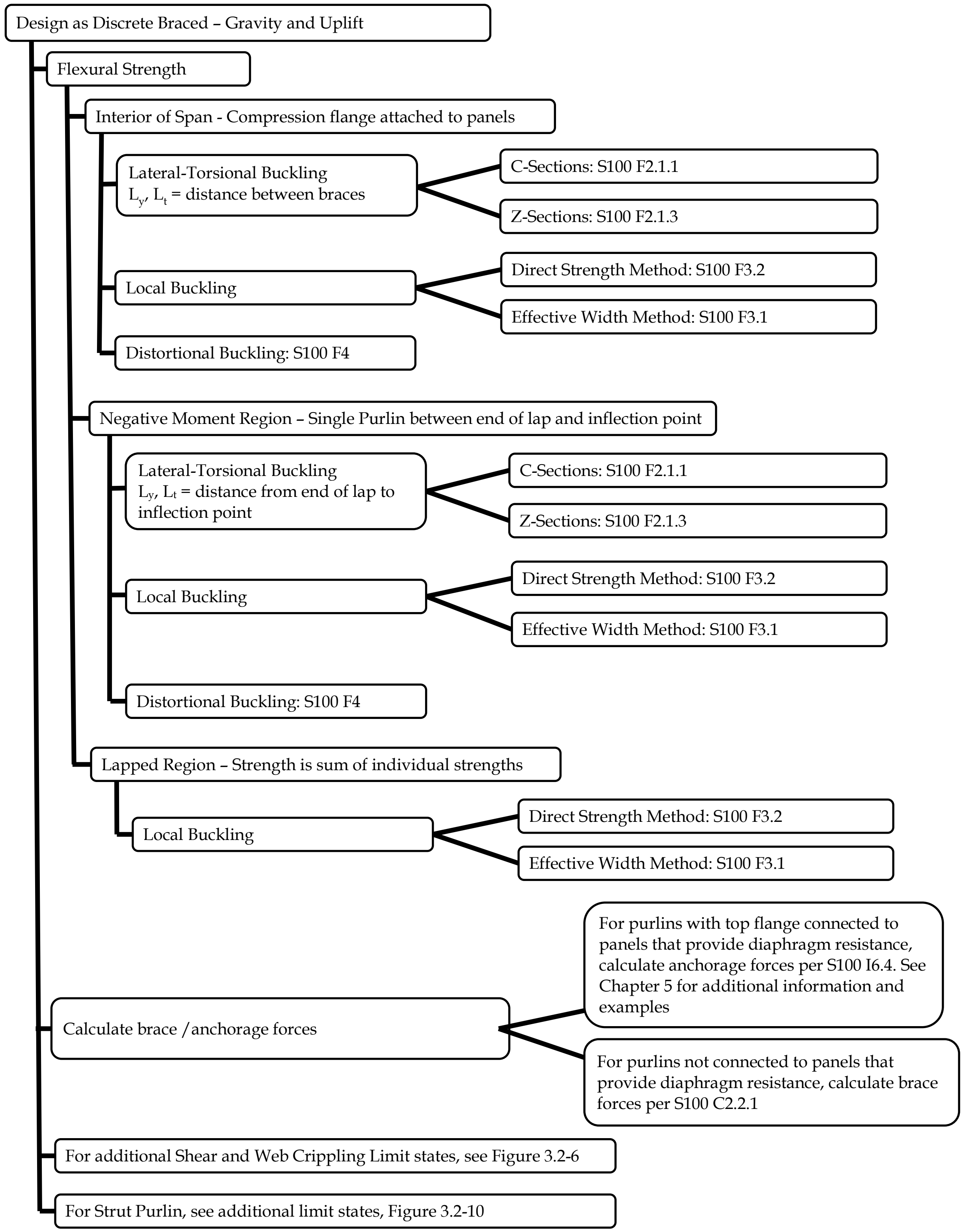

Figure 3.2-3 Discrete Braced System - Limit States for Gravity and Uplift Loading

3.2.3 Flexural Strength for Uplift Loading

For uplift loads, the critical location for flexural strength is near the mid-span in the negative moment region. The compression flange, although not directly attached to panels, is partially braced as a result of the rotational restraint provided by the panels on the tension side. Through-fastened systems, standing seam systems, and discrete braced systems are each treated differently as discussed below. In the region between the inflection point and the end of the lap, the compression flange is attached to panels, which provides an increased resistance to global and distortional buckling relative to the gravity load case. Unless the net uplift loading exceeds the gravity loading, the flexural strength does not need to be checked in the region between the end of the lap and the inflection point. Likewise, in the lapped region over the support where the purlin is considered fully braced, unless uplift loads exceed gravity loads, the strength under gravity loads will control. In cases where uplift loads exceed gravity loads, refer to the following sections.

Through-fastened Systems

In the negative moment region near the mid-span, the flexural strength of through-fastened systems is determined by Section I6.2.1. The panels partially restrain the lateral-torsional buckling of the section, but the strength is reduced relative to a fully laterally braced purlin. Therefore, a reduction factor, R, is applied according to the provisions of Section I6.2.1 to account for the reduced strength. This reduction factor is applied to the nominal local buckling strength, $M_{n\ell o}$, because the reduction factor accounts only for lateral-torsional buckling and distortional buckling. The provided R-factors were determined from tests with specimens that fit within the range of the fifteen conditions listed in Section I6.2.1. If the system does not satisfy the conditions listed, the system must either be tested or evaluated as a discrete braced system.

As discussed above, in the region between the inflection point and the end of the lap, the strength will be typically controlled by gravity loads unless the net uplift exceeds the gravity load or, in some situations, the uplift load is non-uniform. Under uplift loads, the compression flange in this region is attached to panels and it is considered fully braced against global buckling and the nominal strength is the minimum of the local and distortional buckling strengths.

Design of through-fastened systems subjected to uplift load is summarized in Figure 3.2-4.

Standing Seam Systems

AISI S100 provisions for standing seam systems subjected to uplift loading are found in Section I6.2.2 of Appendix A, which apply only to the United States and Mexico. Like the gravity systems, in the region near mid-span, the compression flange is partially restrained by the panels attached to the tension flange. Because of the variability of standing seam systems, the system must be tested according to AISI S908 in an uplift condition. The uplift condition will typically result in a lower reduction factor when compared to a comparable gravity system. AISI S908 testing captures the global and distortional buckling behavior. The nominal flexural strength is the product of the nominal local buckling strength and the reduction factor from the testing.

If gravity load strength checks are satisfied, the strength of the purlin between the inflection point and the end of the lap will typically be sufficient for the uplift condition. If the net uplift loads exceed the gravity loads or are non-uniform, the strength should be checked. The strength is the minimum of the global, distortional, and local buckling strengths. The compression flange is attached to panels and thus is partially restrained against global buckling. The global buckling strength can be conservatively approximated as the *maximum* of either the global buckling strength calculated with the reduction factor, R, from the AISI S908 gravity test or the global buckling strength with the compression flange unbraced between the inflection point and the end of the lap (same global buckling strength as calculated for gravity load). The distortional buckling strength in the region between the inflection point and the end of the lap can include the rotational restraint provided by the panels or conservatively ignore it.

The design of standing seam systems subjected to uplift load is summarized in Figure 3.2-5.

Discrete Braced Systems

For discrete braced systems, the purlin is unbraced between the braces. Like the gravity case, the flexural strength is the minimum of the global buckling, local buckling, and distortional buckling strength. The only difference between uplift and gravity loads occurs for the calculation of the distortional buckling strength. For the gravity load condition, the designer may choose to include the rotational restraint provided to the compression flange by the panels to calculate the distortional buckling strength along the interior of the span. Since for the uplift case the rotational restraint of the panels cannot be included, the strength will be less than the gravity case and the designer should check the region between the braces even if uplift loads are less than gravity loads. In the region between the inflection point and the end of the lap, the distortional buckling strength for uplift will be greater than the gravity case because in the case of uplift, the compression flange is attached to panels. Conservatively, the designer can ignore this increase in strength because the gravity load case will typically control the flexural strength in the region between the end of the lap and the inflection point.

The design of discrete braced systems subjected to uplift load is summarized in Figure 3.2-3.

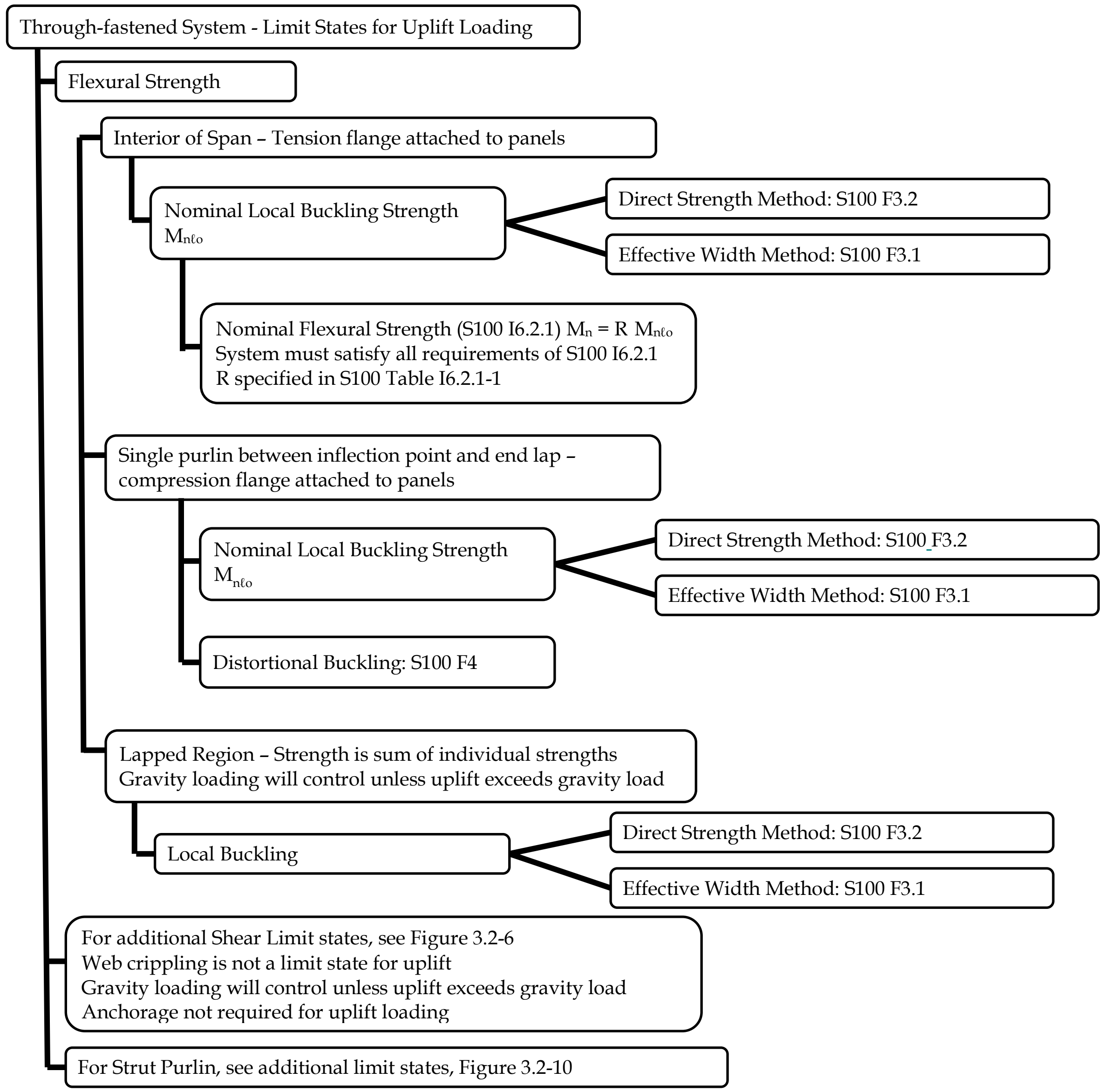

Figure 3.2-4 Through-Fastened System – Limit States for Uplift Loading

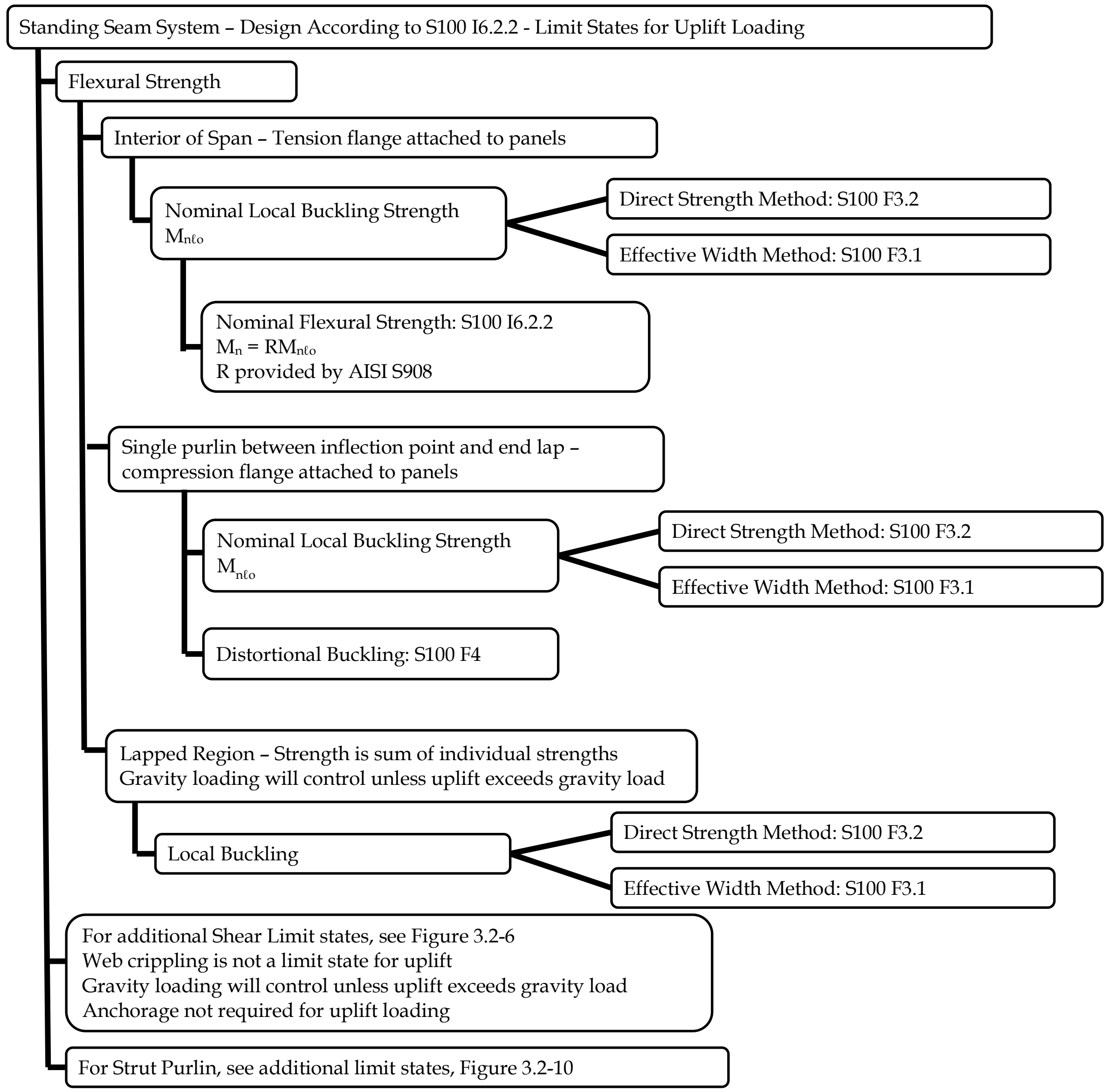

Figure 3.2-5 Standing Seam System – Limit States for Uplift Loading

3.2.4 Shear

The shear strength of a purlin web is defined by AISI S100 Section G2.1. Shear strength must be checked for the individual purlin beyond the lap and in the lapped region. Within the region of the lap, the shear strength is the sum of the individual strengths of the purlins.

3.2.5 Bending and Shear

The interaction of bending and shear must be considered by using AISI S100 Section H2. The bending capacity is typically based on the local buckling flexural strength per AISI S100 Section F3. Shear capacity is defined above. For continuous purlin systems the most critical location is generally at the end of the purlin laps.

3.2.6 Web Crippling

Web crippling is a design consideration for gravity loading conditions. At the free end of a purlin, for example at the end wall of a building, the purlin is subject to the end-one-flange loading condition. The web crippling capacity for this condition is defined by AISI S100 Section G5. The use of purlin web reinforcement or support clips can eliminate web crippling at the supports. Where purlins are lapped over an interior support, the web crippling strength is the sum of the individual web crippling strengths of the purlins. Coefficients for C-sections are found in Table G5-2, and coefficient for Z-sections are found in Table G5-3. Note that coefficients for built-up sections (Table G5-1) do not apply at the lap location. For uplift conditions, because the concentrated force at the support connection is in tension, web crippling does not need to be checked.

3.2.7 Web Crippling and Bending

At interior supports and overhangs of continuous span purlins, combined web crippling and bending must be evaluated unless purlin support clips are provided. AISI S100 Section H3 contains separate design provisions for single unreinforced webs, multiple unreinforced webs, such as back-to-back C-purlins, and nested Z-purlins. In the interaction equations, the flexural strength of the section is the local buckling strength determined from Section F3 and the web crippling strength determined from Section G5. The section strengths are additive when evaluating the interaction equation. The web crippling and bending case only needs to be calculated for the gravity case where the concentrated reaction is in compression.

3.2.8 Connections

AISI S100 Sections J2, J3, and J4 summarize the design rules for welded, bolted, and screw connections.

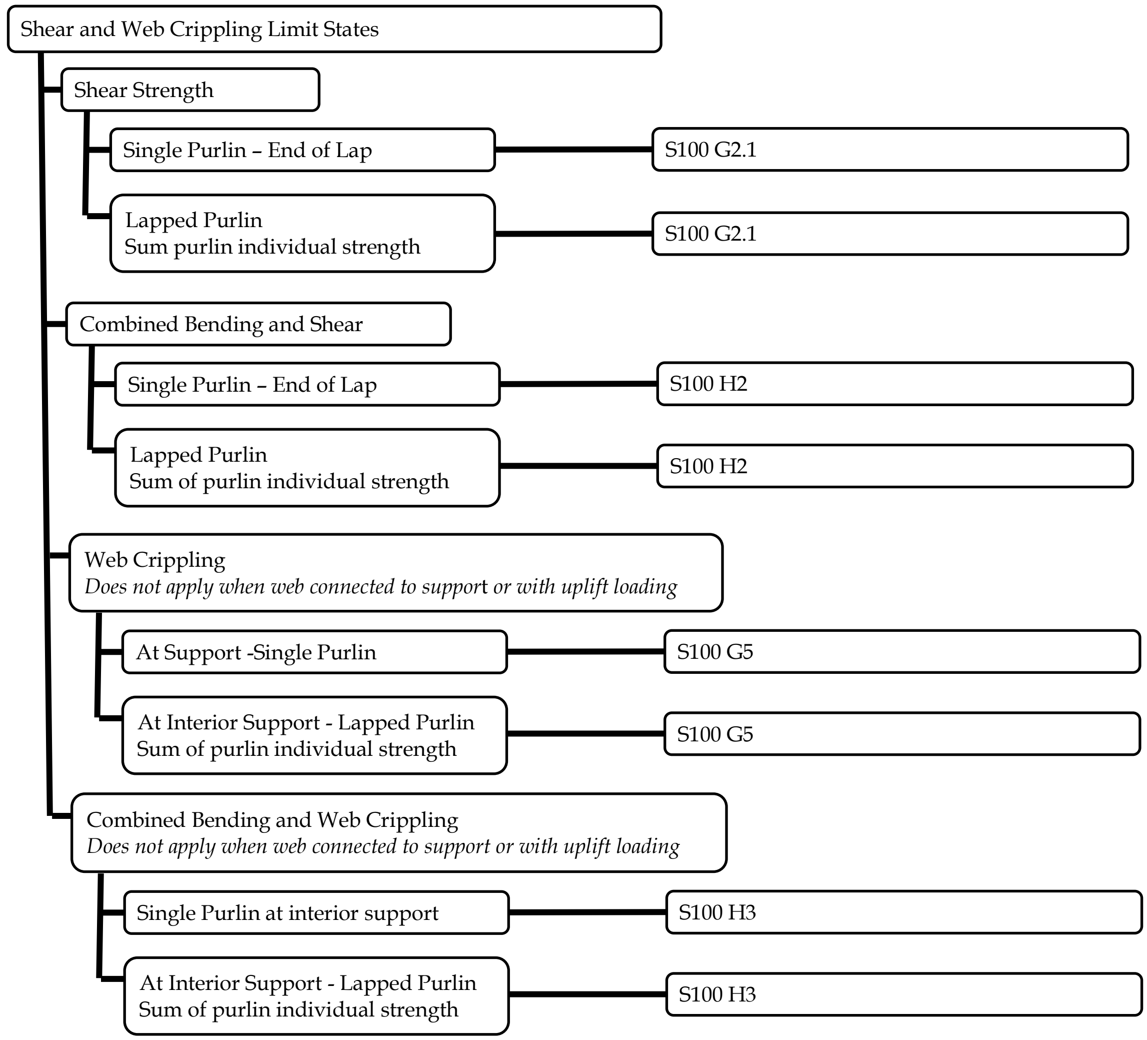

Figure 3.2-6 Shear and Web Crippling Limit States

3.2.9 Purlin Bracing

In purlin supported roof systems, the brace forces can be significant, so they are an important aspect to the design of the systems. The brace forces must be quantified with a pathway provided to transfer the forces to the primary structure. Through-fastened systems designed according to AISI S100 Section I6.2.1 and standing seam systems designed according to Section I6.2.2 partially rely on the restraint provided by the panels and the anchorage forces for these systems are determined according to Section I6.4. The brace forces in discrete braced systems which ignore any restraining contribution of the panels are determined according to Section C2.2.1.

3.2.9.1 Systems Relying on Panels For Stability

For through-fastened systems and standing seam systems that rely on the panels for stability, forces are generated in and transferred through the diaphragm. AISI S100 Section I6.4 provides provisions required to anchor the forces transferred through the diaphragm. In Section I6.4.1, an explicit method to calculate anchorage forces is provided as well as guidance on alternative methods of analysis. These methods are discussed extensively in Chapter 5 of this guide, with several examples provided.

3.2.9.2 AISI S100 Method for Discrete Brace Forces

The forces in the discrete braces are determined according to AISI S100 Section C2.2.1. The designer must provide a pathway to transfer these brace forces to the primary structure. The brace forces result from three load effects: unsymmetric bending resulting from rotated principal axes, downslope forces resulting from roof slope, and torsional moments.

The procedure to calculate the brace forces in Section C2.2.1 is a conservative procedure intended to envelop all bracing and load configurations. The brace forces are calculated as P_{L1} at the top flange and P_{L2} at the bottom flange. The positive directions for the forces are shown in Figure 3.2-7.

For uniformly distributed forces,

$$P_{L1} = 1.5\left[W_y K' - \frac{W_x}{2} + \frac{M_z}{d}\right] \quad \text{(AISI S100 Eq. C2.2.1-1)}$$

$$P_{L2} = 1.5\left[W_y K' - \frac{W_x}{2} - \frac{M_z}{d}\right] \quad \text{(AISI S100 Eq. C2.2.1-2)}$$

$$M_z = -W_x e_{sy} + W_y e_{sx} \quad \text{(Eq. 3.2-1)}$$

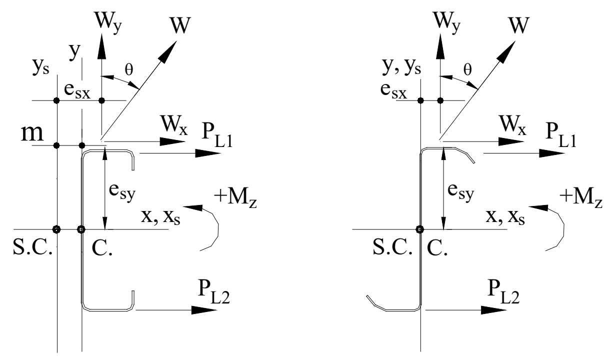

Figure 3.2-7 Nomenclature and Positive Directions for Discrete Braces

For concentrated loads,

$$P_{L1} = P_y K' - \frac{P_x}{2} + \frac{M_z}{d} \quad \text{(AISI S100 Eq. C2.2.1-6)}$$

$$P_{L2} = P_y K' - \frac{P_x}{2} - \frac{M_z}{d} \quad \text{(AISI S100 Eq. C2.2.1-7)}$$

$$M_z = -P_x e_{sy} + P_y e_{sx} \quad \text{(Eq. 3.2-2)}$$

where

$$K' = \frac{I_{xy}}{2I_x} \text{ for Z-sections} \quad \text{(AISI S100 Eq. C2.2.1-5)}$$

W_x, W_y = Components of design load (factored load) W parallel to the x- and y-axis respectively. W_x and W_y are positive if pointing in the positive x- and y-direction respectively.

W = Design load (factored load) applied within a distance of 0.5a each side of the brace

a = Longitudinal distance between centerline of braces

P_x, P_y = Components of design load (factored load) P parallel to the x- and y-axis respectively. P_x and P_y are positive if pointing in the positive x- and y-direction respectively.

P = Design concentrated load (factored load) applied within a distance of 0.3a each side of the brace plus 1.4(1-l/a) times each design concentrated load located between 0.3a and 1.0a from the brace.

l = Distance from concentrated load to the brace

When analyzing the distribution of forces throughout a system of purlins, there are two simplifications that can be employed. The first simplification is to quantify the brace forces at each purlin as a net horizontal force and moment. Using AISI S100 Eqs. C2.2.1-1 and C2.2.1-2, the net horizontal force, P_L is the sum of the forces at each flange, P_{L1} and P_{L2}.

$$P_L = P_{L1} + P_{L2} = 1.5\left(2W_y K' - W_x\right) \quad \text{(Eq. 3.2-3)}$$

The net moment, M_z is the difference between P_{L1} and P_{L2} multiplied by the depth of the purlin, d. M_z is typically calculated directly from Eqs. 3.2-1 and 3.2-2 although note that a factor of 1.5 must be applied to give an equivalent result for a uniformly applied load.

The second simplification is to subdivide the net horizontal force into the individual load effects; unsymmetric bending and downslope forces, because each load effect must be treated differently as the forces are distributed throughout the system. For example, Eq. 3.2-3 can be subdivided into the individual load effects

$$P_{L,unsym} = 1.5\left(2W_y K'\right) \quad \text{(Eq. 3.2-4)}$$

$$P_{L,down} = 1.5\left(-W_x\right) \quad \text{(Eq. 3.2-5)}$$

Note that the forces generated by unsymmetric bending result from forces applied along the y-axis (parallel to the web). Therefore, the net brace force (defined in the x-direction) must be zero. Eq. 3.2-4 provides the force for a brace along the span of the purlin (interior brace). At the support locations, the frame line, the brace forces must balance the forces from the interior brace. The downslope forces are real forces applied in the x-direction and therefore are distributed between interior braces and support braces according to the length of the purlin tributary to each brace. Similarly, the torsional moments are real moments and are similarly distributed according to the length tributary to the brace.

The brace forces, P_L, and brace moments, M_z, should be defined according to a global axis system (X axis in Figure 3.2-8). Typically, purlins are oriented with the top flanges facing upslope. P_L is positive when directed upslope and M_z is positive for a counterclockwise "roll" downslope. Care should be exercised in determining the direction of the brace forces for purlin flanges facing downslope.

3.2.9.3 Alternative Compatibility Method for Discrete Brace Forces

The equations provided in AISI S100 Section C2.2.1 are intended to envelop all brace configurations. In some cases, this can lead to an overly conservative approximation of the brace forces. In Seek (2016), a modified method was provided based on the same compatibility principles as the equations in Section C2.2.1. However, by using the coefficients provided in Tables 3-1 to 3-5, a much more accurate estimate of the brace forces may be realized. The brace forces at the top and bottom flange, P_{L1} and P_{L2} respectively, are calculated by

$$P_{L1} = \alpha C_1 U_y K' - C_2 \frac{U_x}{2} + \frac{M_z}{d} \quad \text{(Eq. 3.2-6)}$$

$$P_{L2} = \alpha C_1 U_y K' - C_2 \frac{U_x}{2} - \frac{M_z}{d} \quad \text{(Eq. 3.2-7)}$$

where

$$K' = \frac{I_{xy}}{2I_x} \quad \text{(Eq. 3.2-8, also AISI S100 C2.2.1-5)}$$

$$M_z = C_2\left(-U_x e_{sy} + \alpha U_y (e_{sx} - C_3 m)\right) + \alpha C_1 C_3 U_y m \quad \text{(Eq. 3.2-9)}$$

C_1, C_2 = Coefficients depending on the bracing configuration and load case defined in Tables 3-1 to 3-5

C_3 = 0 for interior braces

= 1 for braces at the support locations

U_x, U_y = Components of design load (factored load), U, in the x and y direction respectively (similar to W_x and W_y in Figure 3.2-8) and where U is defined according to the load cases in Tables 3-1 to 3-5

α = 1 for top flange facing upslope, -1 for top flange facing downslope

other variables are as shown in Figure 3.2-8

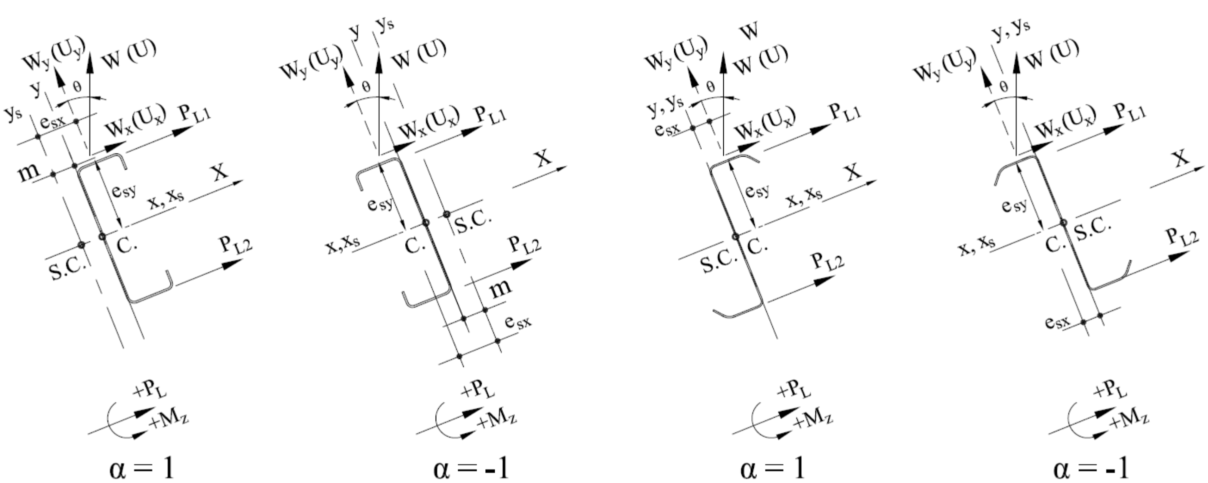

Figure 3.2-8 Positive Directions for Upslope and Downslope Facing Purlins

As described in Section 3.2.9.2, it is convenient to apply two simplifications when distributing the brace forces through a system of purlins. The first simplification is to define the brace forces as a net horizontal force, P_L and a net moment, M_z.

$$P_L = P_{L1} + P_{L2} = 2\alpha C_1 U_y K' - C_2 U_x \quad \text{(Eq. 3.2-10)}$$

The net moment, M_z is the difference between P_{L1} and P_{L2} multiplied by the depth of the purlin, d. M_z is typically calculated directly from Eq. 3.2-9.

The second simplification is to subdivide the net horizontal force into the individual load effects; unsymmetric bending and downslope forces, because each load effect must be treated differently as the forces are distributed throughout the system. For example, Eq. 3.2-3 can be subdivided into the individual load effects

$$P_{L,unsym} = 2\alpha C_1 U_y K' \quad \text{(Eq. 3.2-11)}$$

$$P_{L,down} = -C_2 U_x \quad \text{(Eq. 3.2-12)}$$

Note that the forces generated by unsymmetric bending result from forces applied along the y-axis (parallel to the web). Therefore, the net brace force (defined in the x-direction) must be zero and the brace forces along the span of the purlin (interior braces) are balanced by the braces at the support locations. This balance of forces is accounted through coefficient C_1, which is defined differently for the interior braces versus braces at the support locations. The downslope forces are real forces applied in the x-direction and therefore are distributed between interior braces and support braces according to displacement compatibility between the purlin and the brace. Similarly, the torsional moments are real moments and are similarly distributed according to displacement compatibility.

For analysis of a series of purlin lines, brace forces and moments should be considered in terms of global directions so that the brace forces can be summed as they accumulate. Typically, the top flange of a purlin faces upslope. A positive brace force, P_L, is directed upslope and a positive moment, M_z, rolls counterclockwise downslope. For purlins with the top flange facing downslope, some of the forces will be reversed. To facilitate the solution of brace forces in the global direction, that is positive brace forces directed upslope, the coefficient α is introduced. For purlins with the top flange facing upslope, α= 1 and for purlins with the top flange facing downslope, α = -1. The positive directions for force and eccentricity for upslope and downslope facing purlins are as shown in Figure 3.2-8.

Table 3-1. Equation Coefficients: Simple Span, Uniform Load Distribution, Single Brace

Load Case	Figure	Load, U[1]		Brace Location B1	Brace Location B2	Brace Location B3
1SB-U_1	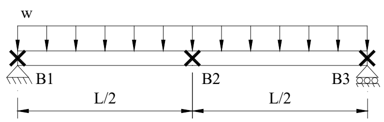	wL	C_1	-5/16	5/8	-5/16
			C_2	3/16	5/8	3/16
1SB-U_2 a < L/2 L/2 < (a+b)	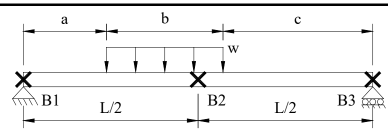	wb	C_1	$-\frac{1}{2}Y_{Ui}$	Y_{Ui}	$-\frac{1}{2}Y_{Ui}$
			C_2	$\frac{1}{2}\left(2-2\left(\frac{a}{L}\right)-\frac{b}{L}-Y_{Ui}\right)$	Y_{Ui}	$\frac{1}{2}\left(2\left(\frac{a}{L}\right)+\frac{b}{L}-Y_{Ui}\right)$
1SB-U_3 (a+b) < L/2	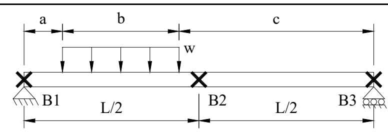			$Y_{U2}=\frac{L}{b}\left[\frac{b}{L}\left(\frac{18a+9b-2L}{2L}\right)+\frac{L-8a}{8L}+3\left(\frac{a}{L}\right)^2+\left(\frac{a}{L}\right)^4-\left(\frac{a+b}{L}\right)^3\left(\frac{4L-a-b}{L}\right)\right]$ $Y_{U3}=\frac{L}{b}\left[\frac{3b}{2L}\left(\frac{2a+b}{L}\right)+\left(\frac{a}{L}\right)^4-\left(\frac{a+b}{L}\right)^4\right]$		
1SB-U_4 L/2 < a	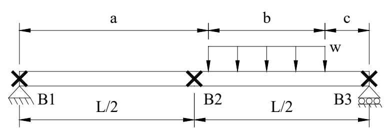			$Y_{U4}=\frac{L}{b}\left[\frac{b}{L}\left(\frac{18a+9b-2L}{2L}\right)+\left(4-\frac{a}{L}\right)\left(\frac{a}{L}\right)^3-\left(\frac{a+b}{L}\right)^3\left(\frac{4L-a-b}{L}\right)\right]$		
1UB-U_5 a < x x < (a+b)	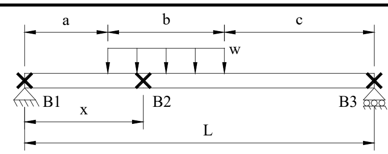	wb	C_1	$-\left(\frac{L-x}{L}\right)Y_{Ui}$	Y_{Ui}	$-\left(\frac{x}{L}\right)Y_{Ui}$
			C_2	$\frac{2a+b+2xY_{Ui}}{2L}$	Y_{Ui}	$\frac{2L-2a-b}{2L}+\left(\frac{x-L}{L}\right)Y_{Ui}$
1UB-U_6 x > (a+b)	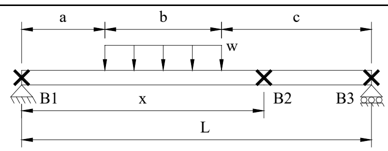			$Y_{U5}=\frac{L}{b}\left[\frac{1}{8}\left(\frac{x}{L-x}\right)^2-\frac{xb(2L-2a-b)}{4L(L-x)^2}+\frac{a(3a-2x)}{4(L-x)^2}+\frac{a^4}{8Lx^2(L-x)}+\frac{(a+b)^3(a+b-4L)}{8Lx(L-x)^2}+\frac{bL(2a+b)}{2x(L-x)^2}\right]$ $Y_{U6}=\frac{L}{b}\left[\frac{b}{L}\frac{(2a+b)(2L-x)}{4x(L-x)}+\frac{a^4-(a+b)^4}{8Lx^2(L-x)}\right]$		
1UB-U_7 x < a	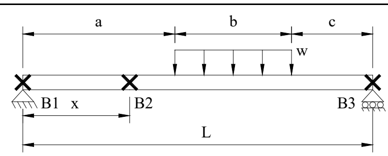			$Y_{U7}=\left[\frac{4bL^2(2a+b)+2bx^2(2a+b-2L)+a^3(4L-a)+(a+b)^3(a+b-4L)}{8bx(L-x)^2}\right]$		

[1]Note: according to the coordinate system shown in Figure 3.2-8, the downward load shown is negative

Table 3-2. Equation Coefficients: Simple Span, Concentrated Load, Single Brace

Load Case	Figure	Load, U[1]		Brace Location		
				B1	B2	B3
1SB-P_1	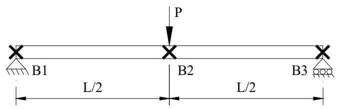	P	C_1	-1/2	1	-1/2
			C_2	0	1	0
1SB-P_2 a > L/2	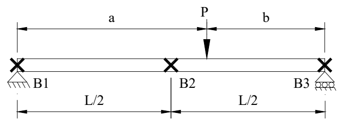		C_1	$-\left(\frac{3}{2}\left(\frac{b}{L}\right)-2\left(\frac{b}{L}\right)^3\right)$	$3\left(\frac{b}{L}\right)-4\left(\frac{b}{L}\right)^3$	$-\left(\frac{3}{2}\left(\frac{b}{L}\right)-2\left(\frac{b}{L}\right)^3\right)$
			C_2	$-\frac{1}{2}\left(\frac{b}{L}\right)+2\left(\frac{b}{L}\right)^3$	$3\left(\frac{b}{L}\right)-4\left(\frac{b}{L}\right)^3$	$1-\frac{5}{2}\left(\frac{b}{L}\right)+2\left(\frac{b}{L}\right)^3$
1SB-P_3 a < L/2	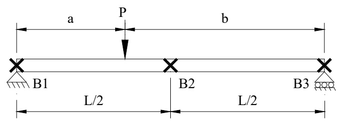		C_1	$-\left(\frac{3}{2}\left(\frac{a}{L}\right)-2\left(\frac{a}{L}\right)^3\right)$	$3\left(\frac{a}{L}\right)-4\left(\frac{a}{L}\right)^3$	$-\left(\frac{3}{2}\left(\frac{a}{L}\right)-2\left(\frac{a}{L}\right)^3\right)$
			C_2	$1-\frac{5}{2}\left(\frac{a}{L}\right)+2\left(\frac{a}{L}\right)^3$	$3\left(\frac{a}{L}\right)-4\left(\frac{a}{L}\right)^3$	$-\frac{1}{2}\left(\frac{a}{L}\right)+2\left(\frac{a}{L}\right)^3$
1UB-P_4 x = a	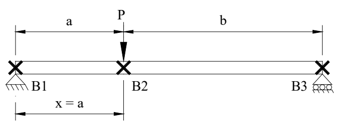		C_1	-b/L	1	-a/L
			C_2	0	1	0
1UB-P_5 x < a x < (a+b)	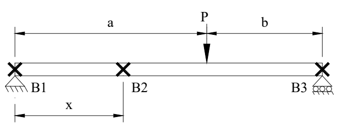		C_1	$-\frac{b(L-x)}{2Lx}\left(\frac{L^2-x^2-b^2}{(L-x)^2}\right)$	$\frac{b}{2x}\left(\frac{L^2-x^2-b^2}{(L-x)^2}\right)$	$-\frac{b}{2L}\left(\frac{L^2-x^2-b^2}{(L-x)^2}\right)$
			C_2	$\frac{b}{2L}\left(2-\frac{L-x}{x}\left(\frac{L^2-x^2-b^2}{(L-x)^2}\right)\right)$	$\frac{b}{2x}\left(\frac{L^2-x^2-b^2}{(L-x)^2}\right)$	$\frac{1}{2L}\left(2a-b\left(\frac{L^2-x^2-b^2}{(L-x)^2}\right)\right)$
1UB-P_6	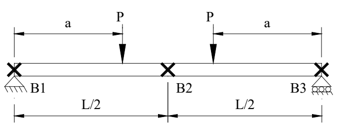		C_1	$-3\left(\frac{a}{L}\right)+4\left(\frac{a}{L}\right)^3$	$6\left(\frac{a}{L}\right)-8\left(\frac{a}{L}\right)^3$	$-3\left(\frac{a}{L}\right)+4\left(\frac{a}{L}\right)^3$
			C_2	$1-3\left(\frac{a}{L}\right)+4\left(\frac{a}{L}\right)^3$	$6\left(\frac{a}{L}\right)-8\left(\frac{a}{L}\right)^3$	$1-3\left(\frac{a}{L}\right)+4\left(\frac{a}{L}\right)^3$

[1]Note: according to the coordinate system shown in Figure 3.2-8, the downward load shown is negative.

Table 3-3 Equation Coefficients: Simple Span, Third Point Braces

<table>
<tr><th rowspan="2">Load Case</th><th rowspan="2">Figure</th><th rowspan="2">Load, U[1]</th><th></th><th colspan="4">Brace Location</th></tr>
<tr><th></th><th>B1</th><th>B2</th><th>B3</th><th>B4</th></tr>
<tr><td rowspan="2">3DB-U_1</td><td rowspan="2">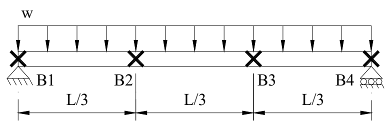</td><td rowspan="2">wL</td><td>C_1</td><td>-11/30</td><td>11/30</td><td>11/30</td><td>-11/30</td></tr>
<tr><td>C_2</td><td>4/30</td><td>11/30</td><td>11/30</td><td>4/30</td></tr>
<tr><td rowspan="3">3DB-P_1
a < L/3
L/2 <
(a+b)</td><td rowspan="3">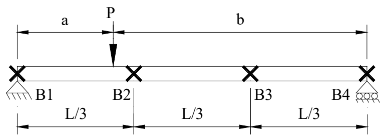</td><td rowspan="9">P</td><td>C_1</td><td>$-\frac{2}{3}Y_1-\frac{1}{3}Y_2$</td><td>$Y_1$</td><td>$Y_2$</td><td>$-\frac{1}{3}Y_1-\frac{2}{3}Y_2$</td></tr>
<tr><td>C_2</td><td>$\frac{b}{L}-\frac{2}{3}Y_1-\frac{1}{3}Y_2$</td><td>$Y_1$</td><td>$Y_2$</td><td>$\frac{a}{L}-\frac{1}{3}Y_1-\frac{2}{3}Y_2$</td></tr>
<tr><td colspan="5">$Y_1=\frac{3}{5}\left(\frac{a}{L}\right)\left[8-27\left(\frac{a}{L}\right)^2\right]$ $Y_2=\frac{3}{5}\left(\frac{a}{L}\right)\left[18\left(\frac{a}{L}\right)^2-2\right]$</td></tr>
<tr><td rowspan="3">3DB-P_2
a > L/3
a<2L/3</td><td rowspan="3">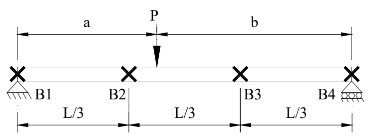</td><td>C_1</td><td>$-\frac{2}{3}Y_1-\frac{1}{3}Y_2$</td><td>$Y_1$</td><td>$Y_2$</td><td>$-\frac{1}{3}Y_1-\frac{2}{3}Y_2$</td></tr>
<tr><td>C_2</td><td>$\frac{b}{L}-\frac{2}{3}Y_1-\frac{1}{3}Y_2$</td><td>$Y_1$</td><td>$Y_2$</td><td>$\frac{a}{L}-\frac{1}{3}Y_1-\frac{2}{3}Y_2$</td></tr>
<tr><td colspan="5">$Y_1=\frac{3}{5}\left[\frac{64}{3}-40\frac{a}{L}+21\left(\frac{a}{L}\right)^3-24\left(\frac{b}{L}\right)^3\right]$ $Y_2=\frac{3}{5}\left[40\left(\frac{a}{L}\right)-\frac{56}{3}+21\left(\frac{b}{L}\right)^3-24\left(\frac{a}{L}\right)^3\right]$</td></tr>
<tr><td rowspan="3">3DB-P_3
a>2L/3</td><td rowspan="3">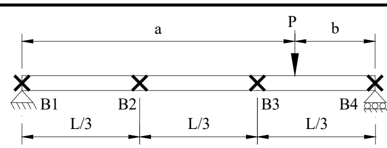</td><td>C_1</td><td>$-\frac{2}{3}Y_1-\frac{1}{3}Y_2$</td><td>$Y_1$</td><td>$Y_2$</td><td>$-\frac{1}{3}Y_1-\frac{2}{3}Y_2$</td></tr>
<tr><td>C_2</td><td>$\frac{b}{L}-\frac{2}{3}Y_1-\frac{1}{3}Y_2$</td><td>$Y_1$</td><td>$Y_2$</td><td>$\frac{a}{L}-\frac{1}{3}Y_1-\frac{2}{3}Y_2$</td></tr>
<tr><td colspan="5">$Y_1=\frac{3}{5}\left(\frac{b}{L}\right)\left[18\left(\frac{b}{L}\right)^2-2\right]$ $Y_2=\frac{3}{5}\left(\frac{b}{L}\right)\left[8-27\left(\frac{b}{L}\right)^2\right]$</td></tr>
</table>

[1]Note: according to the coordinate system shown in Figure 3.2-8, the downward load shown is negative.

Table 3-4. Equation Coefficients: Simple Span, Two Symmetric Braces

Load Case	Figure	Load, U[1]		Brace Location B1	B2	B3	B4
2SB-U$_1$	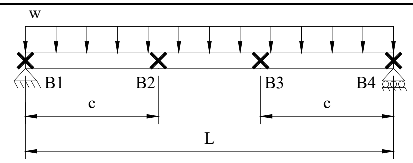	wL	C_1	-Y	$Y = \frac{11}{162}\frac{\left(L/c\right)^2}{\left(3-4\left(c/L\right)\right)}$	Y	-Y
			C_2	$\frac{1}{2} - Y$	Y	Y	$\frac{1}{2} - Y$
2SB-P$_1$ a < c	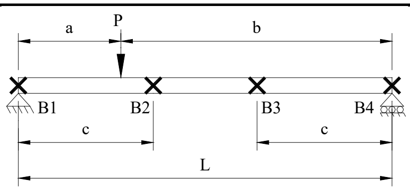	P	C_1	$Y_1\left(\frac{c}{L}-1\right) - Y_2\left(\frac{c}{L}\right)$	Y_1	Y_2	$Y_2\left(\frac{c}{L}-1\right) - Y_1\left(\frac{c}{L}\right)$
			C_2	$\left(1-\frac{a}{L}\right) + Y_1\left(\frac{c}{L}-1\right) - Y_2$	Y_1	Y_2	$\frac{a}{L} - Y_1\left(\frac{c}{L}\right) + Y_2\left(\frac{c}{L}-1\right)$
				$Y_1 = \frac{a}{c^2}\left[c - \frac{(a^2-c^2)(2L-3c)}{(3L-4c)(L-2c)}\right]$ $Y_2 = \frac{a}{c^2}\left[\frac{(a^2-c^2)(L-c)}{(3L-4c)(L-2c)}\right]$			
2SB-P$_2$ c < a a<(L-c)	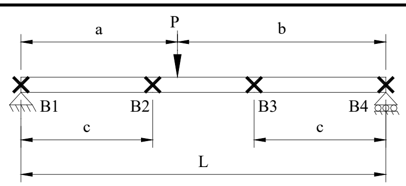		C_1	$Y_1\left(\frac{c}{L}-1\right) - Y_2\left(\frac{c}{L}\right)$	Y_1	Y_2	$Y_2\left(\frac{c}{L}-1\right) - Y_1\left(\frac{c}{L}\right)$
			C_2	$\left(1-\frac{a}{L}\right) + Y_1\left(\frac{c}{L}-1\right) - Y_2$	Y_1	Y_2	$\frac{a}{L} - Y_1\left(\frac{c}{L}\right) + Y_2\left(\frac{c}{L}-1\right)$
				$Y_1 = \frac{2(b)(L^2-b^2-c^2)(L-c)^2 - a(L^2-a^2-c^2)(L^2-2c^2)}{Lc(3L-4c)(L-2c)^2}$ $Y_2 = \frac{2(a)(L^2-b^2-c^2)(L-c)^2 - b(L^2-b^2-c^2)(L^2-2c^2)}{Lc(3L-4c)(L-2c)^2}$			
2SB-P$_3$ a>(L-c)	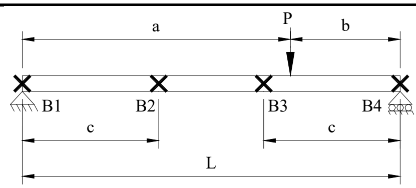		C_1	$Y_1\left(\frac{c}{L}-1\right) - Y_2\left(\frac{c}{L}\right)$	Y_1	Y_2	$Y_2\left(\frac{c}{L}-1\right) - Y_1\left(\frac{c}{L}\right)$
			C_2	$\left(1-\frac{a}{L}\right) + Y_1\left(\frac{c}{L}-1\right) - Y_2$	Y_1	Y_2	$\frac{a}{L} - Y_1\left(\frac{c}{L}\right) + Y_2\left(\frac{c}{L}-1\right)$
				$Y_1 = \frac{b}{c^2}\left[\frac{(b^2-c^2)(L-c)}{(3L-4c)(L-2c)}\right]$ $Y_2 = \frac{b}{c^2}\left[c - \frac{(b^2-c^2)(2L-3c)}{(3L-4c)(L-2c)}\right]$			

[1]Note: according to the coordinate system shown in Figure 3.2-8, the downward load shown is negative.

Table 3-5. Equation Coefficients: Multi-Span, Uniform Load

Load Case	Figure	Load, U[1]		Brace Location B1	B2	B3
1SB-EX-U	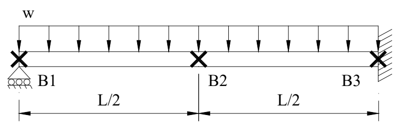	wL	C_1	-5/28	4/7	-11/28
			C_2	11/56	4/7	13/56
1SB-IN-U	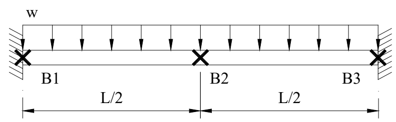		C_1	-1/4	1/2	-1/4
			C_2	1/4	1/2	1/4
1US-EX-U	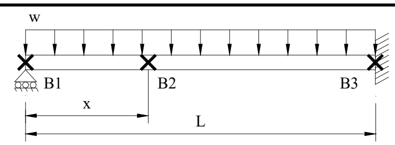		C_1	$-Y\left(\frac{(L-x)^2(2L+x)}{2L^3}\right)$	$Y=\frac{L^2}{4}\left[\frac{(L+2x)}{(L-x)(3L+x)x}\right]$	$-Y\left(\frac{(3L^2-x^2)^2x}{2L^3}\right)$
			C_2	$\frac{3}{8}-Y\left(\frac{(L-x)^2(L+2x)}{2L^3}\right)$	Y	$\frac{5}{8}-Y\left(\frac{(3L^2-x^2)^2x}{2L^3}\right)$
1US-IN-U	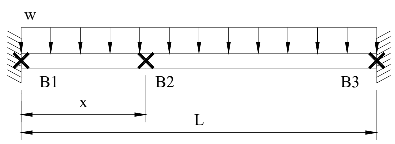		C_1	$-Y\left(\frac{(L-x)^2(L+2x)}{L^3}\right)$	$Y=\frac{L^2}{8x(L-x)}$	$-Y\left(\frac{x^2(3L-2x)}{L^3}\right)$
			C_2	$\frac{1}{2}-Y\left(\frac{(L-x)^2(L+2x)}{L^3}\right)$	Y	$\frac{1}{2}-Y\left(\frac{x^2(3L-2x)}{L^3}\right)$

Load Case	Figure	Load, U[1]		B1	B2	B3	B4
2SB-EX-U	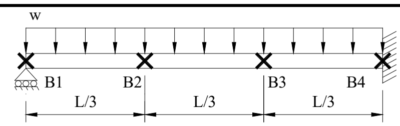	wL	C_1	$-\frac{342}{1404}$	$\frac{531}{1404}$	$\frac{450}{1404}$	$-\frac{639}{1404}$
			C_2	$\frac{184.5}{1404}$	$\frac{531}{1404}$	$\frac{450}{1404}$	$\frac{238.5}{1404}$
2SB-IN-U_1	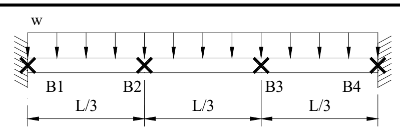		C_1	$-\frac{1}{3}$	$\frac{1}{3}$	$\frac{1}{3}$	$-\frac{1}{3}$
			C_2	$\frac{1}{6}$	$\frac{1}{3}$	$\frac{1}{3}$	$\frac{1}{6}$
2SB-IN-U_2	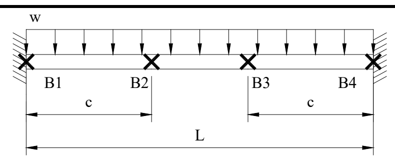		C_1	-Y	$Y=\frac{(L-c)^2}{4c(2L-3c)}$	Y	-Y
			C_2	$\frac{1}{2}-Y$	Y	Y	$\frac{1}{2}-Y$

[1]Note: according to the coordinate system shown in Figure 3.2-8, the downward load shown is negative

3.2.10 Purlins Subject to Axial Load – Strut Purlins

Strut purlins as a part of the horizontal roof truss bracing system are often subjected to a combination of axial forces and bending moments. In addition to the bending limit states discussed above, strut purlins must be analyzed first for resistance to axial load and then the interaction of axial load and bending. The design limit states for strut purlins are summarized in Figure 3.2-10.

3.2.10.1 Resistance to Axial Load Only

For resistance to axial load, strut purlins are analyzed for buckling about the major and minor orthogonal axes. For buckling about the major axis, systems with one flange attached to panels and discrete braced systems are essentially treated the same. For weak axis buckling, systems with one flange attached to panels are partially braced by the panels so special provisions for this system behavior are provided in AISI S100 Section I6. Discrete braced systems are analyzed for weak axis buckling between discrete braces.

Through-fastened systems

The determination of the axial strength for strut purlins supporting through-fastened roofs is found in the AISI S100 Section I6.2.3. For global buckling about the strong axis, Section I6.2.3(b) applies, which requires that the available strength be determined in accordance with Sections E2 and E3. For the global buckling strength in Section E2, the purlin is considered braced about its weak axis and the unbraced length for the strong axis is the distance between the laps with an effective length factor of one. Using the distance between the ends of the laps is conservative since it is usually slightly longer than the distance between inflection points. The interaction of global buckling and local buckling using either the Effective Width Method in Section E3.1 or the Direct Strength Method in Section E3.2 must also be considered.

For buckling about the weak axis, the rotational restraint provided by the connection between the purlin and the panels partially braces the free flange in the weak axis direction. Because of this partial restraint, the weak axis buckling strength of the strut purlin is less than that of a fully braced member but greater than that of an unbraced member. Parametric equations for the weak-axis buckling strength are provided in I6.2.3.(a). Local and distortional buckling strengths are implicitly included in the parametric equations. If the system does not satisfy the ten conditions listed Section I6.2.3, the strut purlin must be designed as discrete braced.

Standing Seam Systems

AISI S100 provisions to determine the axial compressive strength of a Z-section strut purlin with one flange attached to standing seam panels are found in Section I6.2.4 of Appendix A, which apply only to the United States and Mexico. Like through-fastened systems, standing seam systems must be analyzed for buckling about the strong and weak axis.

Strong axis buckling is calculated the same as for through-fastened systems. The global buckling strength is calculated according to AISI S100 Sections E2 with the weak axis considered fully braced and the strong axis unbraced between the laps with an effective length factor of one. The interaction between global buckling and local buckling is calculated either with the Effective Width Method as specified in Section E3.1 or the Direct Strength Method in E3.2.

For weak axis buckling, the standing seam panels partially brace the purlin. A parametric equation is provided in Appendix A Section I6.2.4 based on the reduction factor (R-factor) results of AISI S908 uplift tests for the system. Because the parametric equation was based on a series of tests, the system must satisfy the eight conditions specified in the Section. Otherwise, the system must be analyzed as discrete braced. Distortional buckling and local buckling are implicitly included in the parametric equation and therefore additional calculations of these strengths are not required.

Discrete Braced Systems

If the stabilizing contribution of the panels is ignored, the system must be designed as discrete braced. The strut purlin must be checked for buckling about the strong axis over its span length and buckling about the weak axis between braces.

Buckling about the strong axis is checked similar to systems with one flange attached to panels. Global buckling is calculated according to AISI S100 Section E2 with the weak axis considered fully braced, the strong axis unbraced between the end of the laps, and the effective length factor, k, equal to 1. The interaction between global buckling and local buckling is calculated by the Effective Width Method in Section E3.1 or the Direct Strength Method in Section E3.2.

For buckling about the weak axis, the strut purlin must be considered unbraced between discrete braces. For point-symmetric Z-sections, the global buckling strength is calculated according to AISI S100 Section E2.3 from the minimum of the torsional buckling stress, σ_t, from Section E2.2 and the weak axis flexural buckling stress, F_{cre}, from Section E2.1. For singly-symmetric C-sections, the global strength is calculated from the minimum of the weak axis buckling strength from Section E2.1 and the flexural-torsional buckling strength from E2.2. The designer must consider the interaction of global buckling and local buckling using the Effective Width Method in Section E3.1 or the Direct Strength Method of Section E3.2. Distortional buckling must also be considered and is calculated according to Section E4. The connection of panels to the purlin can provide some torsional resistance, k_ϕ, which can improve the distortional buckling strength. However, because the panels are only attached to one flange and the intervals between the connections at the clips can be large (16″ to 24″), the full stiffness of the connection may not be realized so it may be unconservative to include the full stiffness of the connection. The rotational stiffness of the connection can be conservatively taken as 0 in the calculations.

3.2.10.2 Interaction of Axial Load and Flexure

Strut purlins subjected to axial load are checked for the interaction of axial load and flexure according to the interaction equations of AISI S100 Section H1.2. Several load combinations are checked for the different moment conditions along the length of the purlin to determine the worst combined effect of axial load and bending.

The combination of axial load and bending generate the potential for member second order moments. Traditionally, member second order effects (P-δ) are calculated using the amplified first order analysis as part of the effective length method of Section C1.3. Alternatively, AISI S100 provides guidance to determine the second order effects from the Direct Analysis method using either a rigorous second order analysis from Section C1.1 or an amplified first order analysis from Section C1.2. Frame or story second order effects (P-Δ) are not considered in strut purlin systems.

When investigating the combined effects of axial load and bending, the designer must consider the additional moment introduced by the eccentricity of the force transfer from the strut purlin to the primary structure. The eccentric moment may be taken as P(d/2) as shown in Figure 3.2-9. However, if a flange brace or braces are located at the strut purlin location the rafter will not rotate, and the eccentric moment is virtually eliminated.

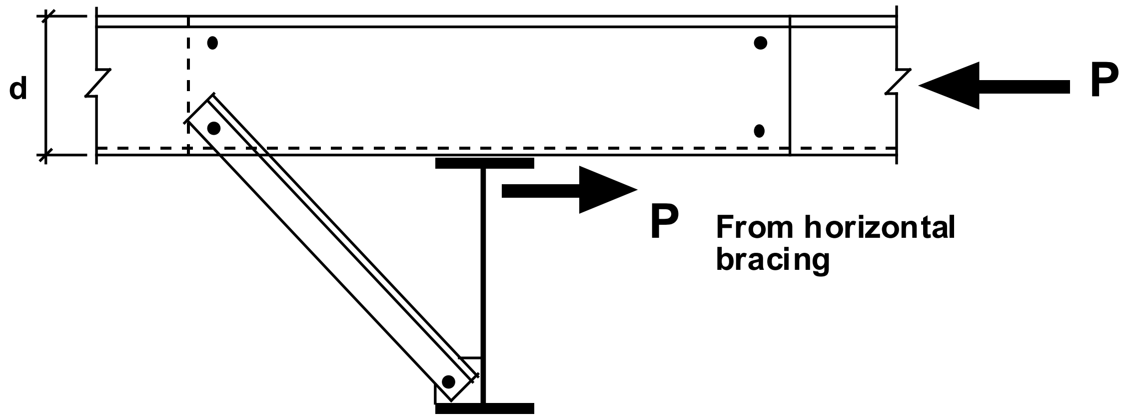

Figure 3.2-9 Strut Purlin with Flange Brace

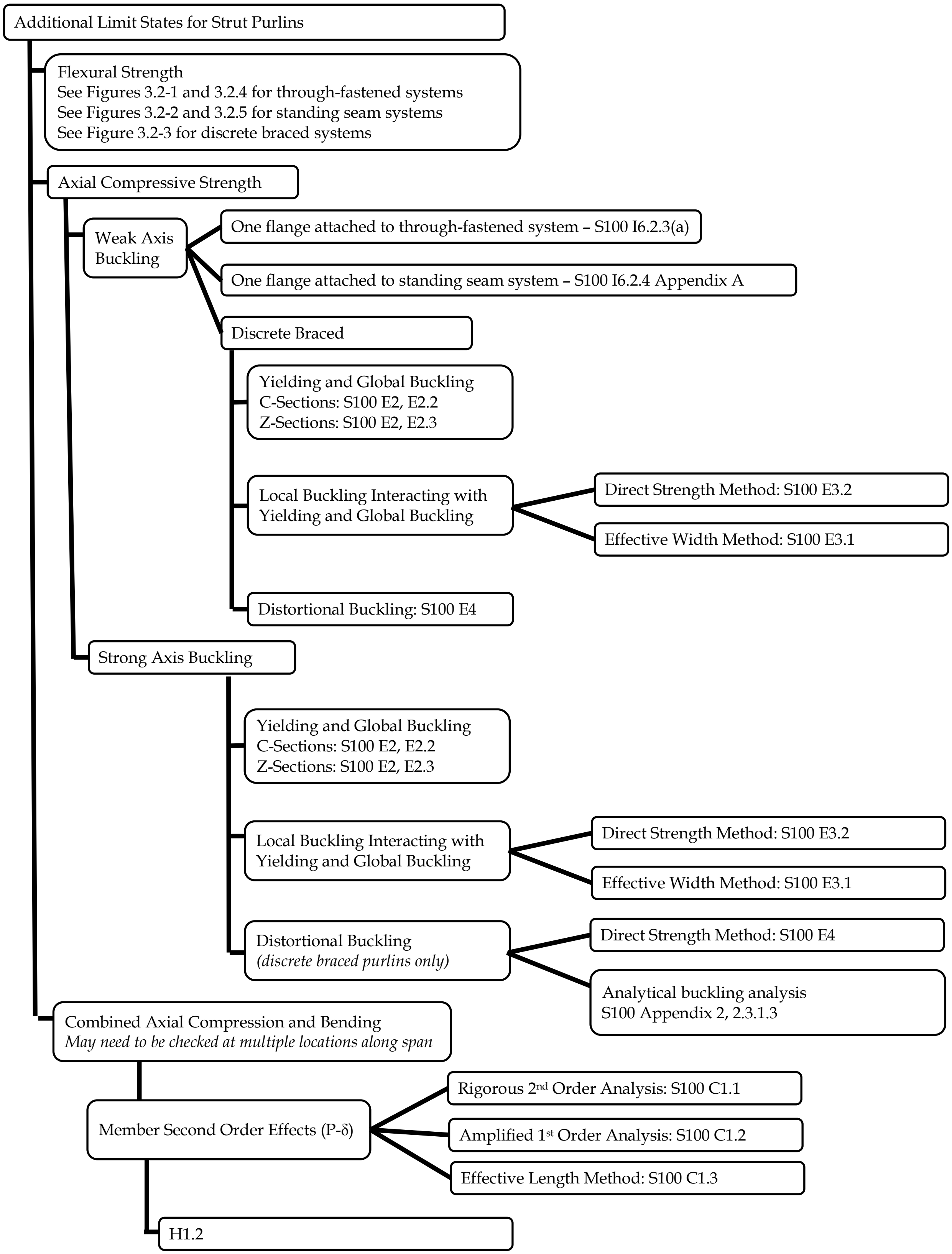

Figure 3.2-10 Limit States for Strut Purlins

3.3 Examples

3.3.1 Through-fastened Roof System Design Examples

3.3.1.1 Design Example: Four Span Continuous Z-Purlins Attached to Through-Fastened Panels (Gravity and Uplift Loads) -- ASD

Given

1. Four span Z-purlin system using laps at interior support points to create continuity.
2. Roof panels are attached with through-fasteners the entire length of the purlins.
3. Twelve purlin lines.
4. F_y = 55 ksi
5. Roof Slope = 0.5:12.
6. The top flange of each purlin is facing upslope except the purlin closest to the eave, which has its top flange facing downslope.
7. There are no discrete braces; anti-roll clips are provided at each support of every fourth purlin line.
8. Purlin flanges are bolted to a 1/4-in. thick support member with a bearing length of 5 in.
9. The rotational stiffness, k_ϕ, provided by the roof panels to the top flange of the purlins is 0.300 kip-in./rad/in.
10. The loads shown are parallel to the purlin webs.

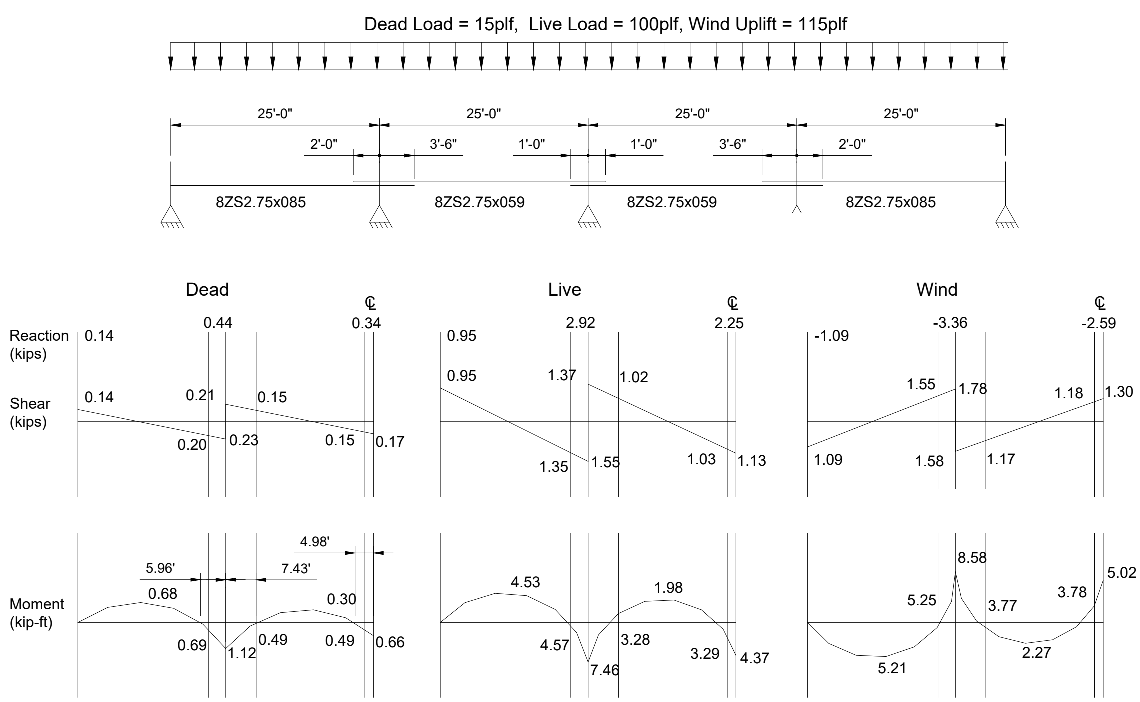

Notes: 1) Moments and forces are from unfactored nominal loads
2) Lap dimensions are shown to connection points of purlins

Figure 3.3-1 Shear and Moment Diagrams

Required

1. Check the design using ASD with ASCE/SEI 7-16 (ASCE, 2016) load combinations for
   (a) Gravity Loads
   (b) Uplift Loads
2. Compute the anchorage forces at the supports under gravity loads.

Solution

Note: The equations referenced in this example refer to AISI S100 equation numbers.

1. Assumptions for Analysis and Application of AISI S100 Provisions

AISI S100 does not define the methods of analysis to be used; these judgments are the responsibility of the designer. The following assumptions are considered good practice but are not intended to prohibit other approaches:

a. The purlins are connected within the lapped portions in a manner that achieves full continuity between the individual purlin members.

b. The continuous beam analysis to establish the shear and moment diagrams assumes continuous non-prismatic members between supports in which I_x within the lapped portions is the sum of the individual members. Gross values of I_x are used for the beam analysis.

c. The strength within the lapped portions is assumed to be the sum of the strengths of the individual members.

d. The attachment of the roof covering to the purlin provides continuous lateral support to the top flange.

e. For the calculation of the distortional buckling strength, the rotational restraint provided by the roof panels, k_ϕ, is included.

f. For gravity loads, the region at and near the interior supports is assumed to be not subject to lateral-torsional or distortional buckling between the support and the ends of the laps.

g. Under uniform gravity loading, the negative moment region between the end of the lap and the inflection point is assumed to have an unbraced length for lateral-torsional and distortional buckling equal to the distance from the end of the lap to the inflection point.

h. Since the loading, geometry and materials are symmetrical; only the first two spans are checked.

2. Section Properties

The following section properties are from AISI D100, *Cold-Formed Steel Design Manual* (AISI, 2017a) Table I-4 and Table II-4.

Interior Bays	End Bays
For: 8ZS2.75x059	For: 8ZS2.75x085
d = 8 in.	d = 8 in.
t = 0.059 in.	t = 0.085 in.
I_x = 8.69 in.^{4}	I_x = 12.40 in.^{4}
$S_f = S_{fy}$ = 2.17 in.^{3}	$S_f = S_{fy}$ = 3.11 in.^{3}
S_e = 1.82 in.^{3}	S_e = 2.84 in.^{3}
S_{et} = 1.82 in^3	S_{et} = 2.84 in.^{3}

I_y = 1.72 in.^{4} I_y = 2.51 in.^{4}

Both sections have inside bend radius, R = 0.1875 in. and flange width, b = 2.75 in.

3. Check Gravity Loads

3a. Strength for Bending Only (AISI S100 Chapter F)

Required Strength

ASD load combinations considered:

(1) D

(2) D + L_r

By inspection, D + L_r controls:

$M = M_D + M_{Lr}$

End Span, from left to right:

Maximum positive moment:	M = 0.68 + 4.53 = 5.21 kip-ft
Negative moment at end of right lap:	M = 0.69 + 4.57 = 5.26 kip-ft
Negative moment at support:	M = 1.12 + 7.46 = 8.58 kip-ft

Interior Span, from left to right:

Negative moment at end of left lap:	M = 0.49 + 3.28 = 3.77 kip-ft
Maximum positive moment:	M = 0.30 + 1.98 = 2.28 kip-ft
Negative moment at end of right lap:	M = 0.49 + 3.29 = 3.78 kip-ft
Negative moment at center support:	M = 0.66 + 4.37 = 5.03 kip-ft

Allowable Design Flexural Strength

Compute the lowest of the applicable flexural strengths from AISI S100 Sections F2.1 (yielding and global (lateral-torsional) buckling), F3 (local buckling interacting with yielding and global buckling), and F4 (distortional buckling).

End Span - At the location of maximum positive moment:

Calculate the allowable strength based on local buckling interacting with yielding and global buckling using the Effective Width Method in AISI S100 Section F3.1

The section is assumed to be fully braced against lateral-torsional buckling, but distortional buckling and local buckling strengths must be calculated. Because the section is sufficiently restrained against lateral-torsional buckling, the global flexural stress, $F_n = F_y$

$$M_n = M_{n\ell} = S_e F_n = (2.84)(55) = 156.2 \text{ kip-in.} \leq S_{et} F_y = (2.84)(55) = 156.2 \text{ kip-in.} \quad \text{(Eq. F3.1-1)}$$

$$\frac{M_n}{\Omega_b} = \frac{156.2}{1.67} = 93.5 \text{ kip-in.} = 7.79 \text{ kip-ft} \geq 5.26 \text{ kip-ft OK} \quad \text{(Eq. B3.2.1-2)}$$

Calculate the allowable distortional buckling strength per AISI S100 Section F4

The elastic distortional buckling stress, F_{crd}, is calculated in accordance with AISI S100 Appendix 2 Section 2.3.3.3. A conservative distortional buckling strength that ignores the restraint provided by the panels can be calculated using AISI S100 Commentary Appendix 2 Section 2.3.3.3 for members meeting the limitations of that section. In this case, the more accurate provisions of Appendix 2 Section 2.3.3.3 are used to take advantage of the stiffness provided by the roof panels.

The cross-section has a single web and a single edge–stiffened flange as required by Appendix 2 Section 2.3.3.3. Consider the contribution of the attached roof panel, which has a rotational stiffness, k_ϕ = 0.300 kip-in./rad./in. From AISI D100 Table II-9 for the 8ZS2.75x085

$k_{\phi fe}$ = 0.795 kip

$\tilde{k}_{\phi fg}$ = 0.0269 in.^{2}

$k_{\phi we}$ = 0.712 kip

$\tilde{k}_{\phi wg}$ = 0.00259 in.^{2}

Since there is no significant moment gradient in the vicinity of the maximum positive moment, use β = 1.0.

$$F_{crd} = \beta \frac{k_{\phi fe} + k_{\phi we} + k_\phi}{\tilde{k}_{\phi fg} + \tilde{k}_{\phi wg}} \quad \text{(Eq. 2.3.3.3-2)}$$

$$F_{crd} = (1.0)\frac{0.795 + 0.712 + 0.300}{0.0269 + 0.00259} = 61.3 \text{ ksi}$$

Calculate the allowable distortional buckling strength per AISI S100 Section F4.1

$$M_y = S_{fy}F_y \quad \text{(Eq. F4.1-4)}$$

$$= (3.11)(55) = 171 \text{ kip-in.}$$

$$M_{crd} = S_f F_{crd} \quad \text{(Eq. F4.1-5)}$$

$$= (3.11)(61.3) = 191 \text{ kip-in.}$$

$$\lambda_d = \sqrt{M_y / M_{crd}} \quad \text{(Eq. F4.1-3)}$$

$$= \sqrt{171/191} = 0.946 > 0.673 \text{ therefore,}$$

$$M_n = M_{nd} = \left(1 - 0.22\left(\frac{M_{crd}}{M_y}\right)^{0.5}\right)\left(\frac{M_{crd}}{M_y}\right)^{0.5} M_y$$

(Eq. F4.1-2)

$$= \left(1 - 0.22\left(\frac{1}{0.946}\right)\right)\left(\frac{1}{0.946}\right)(171) = 139 \text{ kip-in.}$$

$$\frac{M_n}{\Omega_b} = \frac{139}{1.67} = 83.1 \text{ kip-in.} = 6.92 \text{ kip-ft} \geq 5.21 \text{ kip-ft OK} \quad \text{(Eq. B3.2.1-2)}$$

End Span - In the region of negative moment between the end of the lap and the inflection point:

Calculate the allowable lateral-torsional buckling strength

Determine the allowable moment using the distance from the inflection point to the end of the lap as the unbraced length. Note, AISI 100 Section F2.1.3 allows use of either Eq. F2.1.3-1 or F2.1.3-2. Eq. F2.1.3-2 is generally conservative and is chosen for simplicity.

L_y= 5.96 - 2.00 = 3.96 ft = 47.5 in.

K_y = 1.0

$I_{yc} = \frac{I_y}{2} = \frac{2.51}{2} = 1.255 \text{ in.}^4$

C_b = 1.67 (Conservatively assumes linear moment diagram in this region).

$$F_{cre} = \frac{C_b \pi^2 E d I_{yc}}{2S_f (K_y L_y)^2} = \frac{(1.67)\pi^2(29500)(8.0)(1.255)}{(2)(3.11)((1.0)47.5)^2} = 347.9 \text{ ksi} \qquad \text{(Eq. F2.1.3-2)}$$

$2.78F_y = (2.78)(55) = 153$ ksi

Since $F_{cre} > 2.78F_y$, the section is not subject to lateral-torsional buckling and the global flexural stress, $F_n = F_y = 55$ ksi.

Calculate the allowable strength based on local buckling interacting with yielding and global buckling using the Effective Width Method in AISI S100 Section F3.1

$$M_n = M_{n\ell} = S_e F_n = (2.84)(55) = 156.2 \text{ kip-in.} \le S_{et} F_y = (2.84)(55) \qquad \text{(Eq. F3.1-1)}$$

$$\frac{M_n}{\Omega_b} = \frac{156.2}{1.67} = 93.5 \text{ kip-in.} = 7.79 \text{ kip-ft} \ge 5.26 \text{ kip-ft OK} \qquad \text{(Eq. B3.2.1-2)}$$

Calculate the allowable distortional buckling strength per AISI S100 Section F4

Calculate the elastic distortional buckling stress F_{crd}, for the negative moment region. Since the compression flange has no sheeting, there is no distortional restraint of the bottom flange, $k_\phi = 0$. Use the analytical solution procedure in Appendix 2 Section 2.3.3.3 of AISI S100 in lieu of the more conservative procedure from the Commentary accompanying Appendix 2 Section 2.3.3.3. From AISI D110 Table II-9 for 8ZS2.75x085

$k_{\phi fe} = 0.795$ kip

$\tilde{k}_{\phi fg} = 0.0269 \text{ in.}^2$

$k_{\phi we} = 0.712$ kip

$\tilde{k}_{\phi wg} = 0.00259 \text{ in.}^2$

$$F_{crd} = \beta \frac{k_{\phi fe} + k_{\phi we} + k_\phi}{\tilde{k}_{\phi fg} + \tilde{k}_{\phi wg}} \qquad \text{(Eq. 2.3.3.3-2)}$$

$$F_{crd}/\beta = \frac{0.795 + 0.712 + 0.0}{0.0269 + 0.00259} = 51.1 \text{ ksi}$$

Alternatively, F_d/β for the case where $k_\phi = 0$ may be taken from Table II-9 ($F_d/\beta = 51.1$ ksi)

From Table II-9

$L_{cr} = 21.7$ in.

The bottom flange is not restrained from rotation by the panel or other discrete bracing. Therefore, the unbraced length for distortional buckling, L_m, is taken as the distance between the end of the lap and the inflection point.

L_m = 47.5 in. (from above)

$L = \min(L_{cr}, L_m)$

$= \min(21.7, 47.5) = 21.7$ in.

The moments at the ends of the segment are:

$M_1 = 0.0$ kip-ft at the inflection point

M_2 = 5.26 kip-ft at the end of the lap

$$\beta = 1.0 \le 1 + 0.4\left(L / L_m\right)^{0.7}\left(1 - M_1 / M_2\right)^{0.7} \le 1.3 \qquad \text{(Eq. 2.3.3.3-3)}$$

$$= 1.0 \le 1 + 0.4\left(21.7 / 47.5\right)^{0.7}\left(1 - 0 / 5.26\right)^{0.7} \le 1.3$$

$= 1.0 \le 1.23 \le 1.3$ therefore, use β = 1.23

$$F_{crd} = \beta\left(F_{crd} / \beta\right)$$

$$F_{crd} = 1.23(51.1) = 62.9 \text{ ksi}$$

Calculate the allowable distortional buckling strength per AISI S100 Section F4.1

$$M_y = S_{fy}F_y \qquad \text{(Eq. F4.1-4)}$$

$$= (3.11)(55) = 171 \text{ kip-in.}$$

$$M_{crd} = S_f F_{crd} \qquad \text{(Eq. F4.1-5)}$$

$$= (3.11)(62.9) = 196 \text{ kip-in.}$$

$$\lambda_d = \sqrt{M_y / M_{crd}} \qquad \text{(Eq. F4.1-3)}$$

$= \sqrt{171 / 196}$ = 0.934 > 0.673 therefore,

$$M_n = M_{nd} = \left(1 - 0.22\left(\frac{M_{crd}}{M_y}\right)^{0.5}\right)\left(\frac{M_{crd}}{M_y}\right)^{0.5} M_y \qquad \text{(Eq. F4.1-2)}$$

= (1-0.22(1/0.934))(1/0.934)(171) = 140 kip-in.

$\frac{M_n}{\Omega_b} = \frac{140}{1.67}$ = 83.8 kip-in. = 7.0 kip-ft ≥ 5.26 kip-ft OK (Eq. B3.2.1-2)

End Span - In the lapped region over the support:

Calculate the allowable strength based on local buckling interacting with yielding and global buckling using the Effective Width Method in AISI S100 Section F3.1

In the lapped region at the support, the section is assumed to be sufficiently restrained against lateral-torsional buckling and distortional buckling. Because the section is sufficiently restrained against lateral-torsional buckling, the global flexural stress, $F_n = F_y$. The total strength is the sum of the individual strength of the two overlapped purlins.

For the end bay purlin, t = 0.085 in.
$M_n = M_{n\ell} = S_eF_n$ = (2.84)(55) = 156.2 kip-in. or 13.02 kip-ft ≤ $S_{et}F_y$ = (2.84)(55) (Eq. F3.1-1)

For the interior purlin, t = 0.059 in.
$M_n = M_{n\ell} = S_eF_n$ = (1.82)(55) = 100.1 kip-in. or 8.34 kip-ft ≤ $S_{et}F_y$ = (1.82)(55) (Eq. F3.1-1)

Combined strength of purlins

$\frac{M_n}{\Omega_b} = \frac{13.02 + 8.34}{1.67}$ = 12.79 kip-ft ≥ 8.58 kip-ft OK (Eq. B3.2.1-2)

Interior Span - In the region of negative moment between the end of the left lap and the inflection point:

Calculate the allowable lateral-torsional buckling strength

Determine the allowable moment using the distance from the inflection point to the end of the lap as the unbraced length. Note, AISI S100 Section F2.1.3 allows use of either Eq. F2.1.3-1 or F2.1.3-2. Eq. F2.1.3-2 is generally conservative and is chosen for simplicity.

L_y = 7.43 - 3.50 = 3.93 ft or 47.2 in.

K_y = 1.0

C_b =1.67 (conservatively assuming a linear moment diagram in this region).

$$I_{yc} = \frac{I_y}{2} = \frac{1.72}{2} = 0.86 \text{ in.}^4$$

$$F_{cre} = \frac{(1.67)\pi^2(29500)(8.0)(0.86)}{(2)(2.17)((1.0)47.2)^2} = 346 \text{ ksi} > (2.78)(55) = 153 \text{ ksi} \qquad \text{(Eq. F2.1.3-2)}$$

Since F_{cre} > 2.78F_y, the section is not subject to lateral-torsional buckling and the global flexural stress, $F_n = F_y$ = 55 ksi.

Calculate the allowable strength based on local buckling interacting with yielding and global buckling using the Effective Width Method in AISI S100 Section F3.1

$$M_n = M_{n\ell} = S_eF_n = (1.82)(55) = 100.1 \text{ kip-in.} \leq S_{et}F_y = (1.82)(55) \qquad \text{(Eq. F3.1-1)}$$

$$\frac{M_n}{\Omega_b} = \frac{100.1}{1.67} = 59.9 \text{ kip-in.} = 5.00 \text{ kip-f.} \geq 3.77 \text{ kip-ft} \quad \text{OK} \qquad \text{(Eq. B3.2.1-2)}$$

Calculate the allowable distortional buckling strength per AISI S100 Section F4

Since there is no distortional restraint of the bottom flange, take F_d/β from Table II-9 of AISI D100. From Table II-9 for the 8ZS2.75x059

F_d/β = 32.5 ksi

L_{cr} = 25.4 in.

The unbraced length for distortional buckling, L_m, is taken as the distance between the end of the lap and the inflection point.

L_m = 47.2 in. (from above)

L = min(L_{cr}, L_m)

= min(25.4, 47.2) = 25.4 in.

The moments at the ends of the segment are:

M_1 = 0.0 kip-ft at the inflection point

M_2 = 3.77 kip-ft at the end of the lap

$$\beta = 1.0 \leq 1 + 0.4(L/L_m)^{0.7}(1 - M_1/M_2)^{0.7} \leq 1.3 \qquad \text{(Eq. 2.3.3.3-3)}$$

$$= 1.0 \leq 1 + 0.4(25.4/47.2)^{0.7}(1 - 0/3.77)^{0.7} \leq 1.3$$

$$= 1.0 \leq 1.26 \leq 1.3 \text{ therefore, use } \beta = 1.26$$

$$F_{crd} = \beta(F_d/\beta)$$

F_{crd} = 1.26(32.5) = 41.0 ksi

Calculate the allowable distortional buckling strength per AISI S100 Section F4.1

$M_y = S_{fy}F_y$ (Eq. F4.1-4)

= (2.17)(55) = 119 kip-in.

$M_{crd} = S_f F_{crd}$ (Eq. F4.1-5)

= (2.17)(41.0) = 89.0 kip-in.

$\lambda_d = \sqrt{M_y / M_{crd}}$ (Eq. F4.1-3)

$= \sqrt{119 / 89.0}$ = 1.156 > 0.673 therefore,

$$M_n = \left(1 - 0.22\left(\frac{M_{crd}}{M_y}\right)^{0.5}\right)\left(\frac{M_{crd}}{M_y}\right)^{0.5} M_y \quad \text{(Eq. F4.1-2)}$$

= (1-0.22(1/1.16))(1/1.16)(119) = 83.1 kip-in.

$\frac{M_n}{\Omega_b} = \frac{83.1}{1.67}$ = 49.8 kip-in. = 4.15 kip-ft ≥ 3.77 kip-ft OK (Eq. B3.2.1-2)

Interior Span - At the location of maximum positive moment:

Calculate the allowable strength based on local buckling interacting with yielding and global buckling using the Effective Width Method in AISI S100 Section F3.1

The section is assumed to be fully braced against lateral-torsional buckling. Because the section is sufficiently restrained against lateral-torsional buckling, the global flexural stress, $F_n = F_y$

$M_n = M_{n\ell} = S_eF_n$ = (1.82)(55) = 100.1 kip-in. ≤ $S_{et}F_y$ = (1.82)(55) (Eq. F3.1-1)

$\frac{M_n}{\Omega_b} = \frac{100.1}{1.67}$ = 59.9 kip-in. = 5.00 kip-ft ≥ 2.28 kip-ft OK (Eq. B3.2.1-2)

Calculate the allowable distortional buckling strength per AISI S100 Section F4

The cross-section has a single web and a single edge–stiffened flange as required by Appendix 2, Section 2.3.3.3. Consider the contribution of the attached roof panel, which has a rotational stiffness, k_ϕ = 0.300 kip-in./rad./in. From AISI D100 Table II-9 for 8ZS2.75x059

$k_{\phi fe}$ = 0.250 kip

$\tilde{k}_{\phi fg}$ = 0.0134 in.^{2}

$k_{\phi we}$ = 0.230 kip

$\tilde{k}_{\phi wg}$ = 0.00132 in.^{2}

Since there is no significant moment gradient in the vicinity of the maximum positive moment, use β = 1.0.

$$F_{crd} = \beta \frac{k_{\phi fe} + k_{\phi we} + k_\phi}{\tilde{k}_{\phi fg} + \tilde{k}_{\phi wg}} \quad \text{(Eq. 2.3.3.3-2)}$$

$$F_{crd} = (1.0)\frac{0.250 + 0.230 + 0.300}{0.0134 + 0.00132} = 53.0 \text{ ksi}$$

Calculate the allowable distortional buckling strength per Section F4.1

$M_y = S_{fy}F_y$ (Eq. F4.1-4)

$= (2.17)(55) = 119$ kip-in.

$M_{crd} = S_f F_d$ (Eq. F4.1-5)

$= (2.17)(53.0) = 115$ kip-in.

$\lambda_d = \sqrt{M_y / M_{crd}}$ (Eq. F4.1-3)

$= \sqrt{119/115} = 1.017 > 0.673$ therefore,

$$M_n = \left(1 - 0.22\left(\frac{M_{crd}}{M_y}\right)^{0.5}\right)\left(\frac{M_{crd}}{M_y}\right)^{0.5} M_y \quad \text{(Eq. F4.1-2)}$$

$= (1\text{-}0.22(1/1.017))(1/1.017)(119) = 91.7$ kip-in.

$$\frac{M_n}{\Omega_b} = \frac{91.7}{1.67} = 54.9 \text{ kip-in.} = 4.58 \text{ kip-ft} \geq 2.28 \text{ kip-ft OK} \quad \text{(Eq. B3.2.1-2)}$$

Interior Span - In the region of negative moment between the end of the right lap and the inflection point:

Calculate the allowable lateral-torsional buckling strength

Determine the allowable moment using the distance from the inflection point to the end of the lap as the unbraced length with C_b =1.67

L_y= 4.98 - 1.00 = 3.98 ft or 47.8 in.

By inspection, the strength check for the right lap will be satisfied, since the unbraced length and the required strength is about the same as those at the left support. Therefore, the section is OK.

Interior Span - In the lapped region over the center support:

Calculate the allowable strength based on local buckling interacting with yielding and global buckling using the Effective Width Method in AISI S100 Section F3.1.

In the lapped region at the support, the section is assumed to be sufficiently restrained against lateral-torsional buckling and distortional buckling. Because the section is sufficiently restrained against lateral-torsional buckling, the global flexural stress, $F_n = F_y$. The total strength is the sum of the individual strength of the two overlapped purlins.

Combined strength of purlins

$$\frac{M_n}{\Omega_b} = \frac{8.34 + 8.34}{1.67} = 9.99 \text{ kip-ft} \geq 5.03 \text{ kip-ft OK} \quad \text{(Eq. B3.2.1-2)}$$

3b. Strength for Shear Only (AISI S100 Section G2.1)

Required Strength

By inspection, D + L_r controls:

$V = V_D + V_{Lr}$

End Span, from left to right:

At left support:	V = 0.14 + 0.95 = 1.09 kip
At end of right lap:	V = 0.20 + 1.35 = 1.55 kip
At first interior support:	V = 0.23 + 1.55 = 1.78 kip

Interior Span, from left to right:

At first interior support:	V = 0.21 + 1.37 = 1.58 kip
At end of left lap:	V = 0.15 + 1.02 = 1.17 kip
At end of right lap:	V = 0.15 + 1.03 = 1.18 kip
At center support:	V = 0.17 + 1.13 = 1.30 kip

Allowable Design Strength

End Span:

At the left support and right lap, t = 0.085 in. By inspection the end of the right lap controls.

The flat width of the web, h, is

$h = d - 2t - 2R = 8 - 2(0.085) - 2(0.1875) = 7.455$ in.

$k_v = 5.34$ for unreinforced webs

For t = 0.085 in. and h = 7.455 in., the elastic shear buckling stress is

$$F_{cr} = \frac{\pi^2 E k_v}{12(1-\mu^2)(h/t)^2} = \frac{\pi^2(29500)(5.34)}{12(1-0.3^2)(7.455/0.085)^2} = 18.51 \text{ ksi} \quad \text{(Eq. G2.3-2)}$$

$V_{cr} = A_w F_{cr} = (7.455)(0.085)(18.51) = 11.73$ kip (Eq. G2.3-1)

$V_y = 0.6A_w F_y = 0.6(7.455)(0.085)(55) = 20.91$ kip (Eq. G2.1-5)

$$\lambda_v = \sqrt{\frac{V_y}{V_{cr}}} = \sqrt{\frac{20.91}{11.73}} = 1.335 \quad \text{(Eq. G2.1-4)}$$

$\lambda_v > 1.227$

$V_n = V_{cr} = 11.73$ kip (Eq. G2.1-3a)

$$\frac{V_n}{\Omega_v} = \frac{11.73}{1.60} = 7.33 \text{ kip} \geq 1.55 \text{ kip} \quad \text{OK} \quad \text{(Eq. B3.2.1-2)}$$

At the first interior support, sum the strength of the two overlapped purlins:

The flat width of the web, h, is

$h = d - 2t - 2R = 8 - 2(0.059) - 2(0.1875) = 7.507$ in.

$k_v = 5.34$ for unreinforced webs

For t = 0.059 in. and h = 7.507 in.

$$F_{cr} = \frac{\pi^2 E k_v}{12(1-\mu^2)(h/t)^2} = \frac{\pi^2(29500)(5.34)}{12(1-0.3^2)(7.507/0.059)^2} = 8.79 \text{ ksi} \quad \text{(Eq. G2.3-2)}$$

$V_{cr} = A_w F_{cr} = (7.507)(0.059)(8.79) = 3.89$ kip (Eq. G2.3-1)

$V_y = 0.6A_w F_y = 0.6(7.507)(0.059)(55) = 14.62$ kip (Eq. G2.1-5)

$$\lambda_v = \sqrt{\frac{V_y}{V_{cr}}} = \sqrt{\frac{14.62}{3.89}} = 1.938 > 1.227 \quad \text{(Eq. G2.1-4)}$$

$V_n = V_{cr} = 3.89$ kip (Eq. G2.1-3a)

For the combined section:

$$\frac{V_n}{\Omega_v} = \frac{3.89 + 11.73}{1.60} = 9.76 \text{ kip} \geq 1.78 \text{ kip} \quad \text{OK} \qquad \text{(Eq. B3.2.1-2)}$$

Interior Span:

By inspection of the left and right laps, the right lap controls.

$$\frac{V_n}{\Omega_v} = \frac{3.89}{1.60} = 2.43 \text{ kip} \geq 1.18 \text{ kip} \quad \text{OK} \qquad \text{(Eq. B3.2.1-2)}$$

At the center support, sum the strength of the two overlapped purlins. For the combined section:

$$\frac{V_n}{\Omega_v} = \frac{3.89 + 3.89}{1.60} = 4.86 \text{ kip} \geq 1.30 \text{ kip} \quad \text{OK} \qquad \text{(Eq. B3.2.1-2)}$$

3c. Strength for Combined Bending and Shear (AISI S100 Section H2)

End Span:

$$\sqrt{\left(\frac{\overline{M}}{M_{a\ell o}}\right)^2 + \left(\frac{\overline{V}}{V_a}\right)^2} \leq 1.0 \qquad \text{(Eq. H2-1)}$$

where

$M_{a\ell o}$ = Available flexural strength for globally braced member at the initiation of yielding from AISI S100 Section F3 with $F_n = F_y$

$= \frac{M_n}{\Omega_b}$

V_a = Available shear strength when shear alone is considered in accordance with AISI S100 Sections G2 to G4

$= \frac{V_n}{\Omega_v}$

$\overline{M}$, $\overline{V}$ = Required flexural and shear strengths in accordance with ASD, LRFD, or LSD load combinations

Ω_b = 1.67

Ω_v = 1.60

At start of right lap, t = 0.085 in.

$$\sqrt{\left(\frac{(1.67)(5.26)}{13.02}\right)^2 + \left(\frac{(1.60)(1.55)}{11.73}\right)^2} = 0.71 \leq 1.0 \quad \text{OK}$$

At interior support,

$$\sqrt{\left(\frac{(1.67)(8.58)}{13.02 + 8.34}\right)^2 + \left(\frac{(1.60)(1.78)}{11.73 + 3.89}\right)^2} = 0.70 \leq 1.0 \quad \text{OK}$$

Interior Span:

At end of laps, t = 0.059 in. Right lap controls by inspection.

$$\sqrt{\left(\frac{(1.67)(3.78)}{8.34}\right)^2+\left(\frac{(1.60)(1.18)}{3.89}\right)^2} = 0.90 < 1.0 \quad \text{OK}$$

At center support,

$$\sqrt{\left(\frac{(1.67)(5.03)}{8.34+8.34}\right)^2+\left(\frac{(1.60)(1.30)}{3.89+3.89}\right)^2} = 0.57 \leq 1.0 \quad \text{OK}$$

3d. Web Crippling Strength (AISI S100 Section G5)

Required Strength

By inspection, D + L_r controls:

$P = P_D + P_{Lr}$

Supports, from left to right:

At left support:	P = 0.14 + 0.95 = 1.09 kip
At first interior support:	P = 0.44 + 2.92 = 3.36 kip
At center support:	P = 0.34 + 2.25 = 2.59 kip

Allowable Design Strength

The bearing length is 5 in.

At end supports use Eq. G5-1 of AISI S100.

$$P_n = Ct^2F_y \sin\theta\left(1-C_R\sqrt{\frac{R}{t}}\right)\left(1+C_N\sqrt{\frac{N}{t}}\right)\left(1-C_h\sqrt{\frac{h}{t}}\right) \quad \text{(Eq. G5-1)}$$

where

F_y = 55 ksi

θ = 90 degrees

R = 0.1875 in.

N = 5.0 in.

h = 7.455 in.

t = 0.085 in.

From AISI S100 Table G5-3, using the coefficients for the case of Fastened to Support/One-Flange Loading or Reaction/End

C = 4

C_R = 0.14

C_N = 0.35

C_h = 0.02

Ω_w = 1.75

Check Limits:

R/t = 0.1875/0.085 = 2.21 < 9 OK

h/t = 7.455/0.085 = 87.7 < 200 OK

N/t = 5.0/0.085 = 58.8 < 210 OK
N/h = 5.0/7.455 = 0.67 < 2.0 OK

$$P_n = (4)(0.085)^2(55)\sin 90\left(1-0.14\sqrt{\frac{0.1875}{0.085}}\right)\left(1+0.35\sqrt{\frac{5.0}{0.085}}\right)\left(1-0.02\sqrt{\frac{7.455}{0.085}}\right)$$

=3.77 kip

$$\frac{P_n}{\Omega_w} = \frac{3.77}{1.75} = 2.15 \text{ kip} \geq 1.09 \text{ kip} \quad \text{OK} \qquad \text{(Eq. B3.2.1-2)}$$

At interior supports use Eq. G5-1 of AISI S100. For webs consisting of two or more sheets, the nominal strength is calculated for each individual sheet and the results are added to obtain the nominal strength of the full section.

$$P_n = Ct^2F_y \sin\theta\left(1-C_R\sqrt{\frac{R}{t}}\right)\left(1+C_N\sqrt{\frac{N}{t}}\right)\left(1-C_h\sqrt{\frac{h}{t}}\right) \qquad \text{(Eq. G5-1)}$$

where

F_y = 55 ksi

θ = 90 degrees

R = 0.1875 in.

N = 5.0 in.

End Span	Interior Span
h = 7.455 in.	h = 7.507 in.
t = 0.085 in.	t = 0.059 in.

From AISI S100 Table G5-3, using the coefficients for the case of Fastened to Support/One-Flange Loading or Reaction/Interior

C = 13
C_R = 0.23
C_N = 0.14
C_h = 0.01
Ω_w = 1.65

Check Limits:

End Span		Interior Span	
R/t = 0.1875/0.085	= 2.21 < 5.5 OK	R/t = 0.1875/0.059	= 3.18 < 5.5 OK
h/t = 7.455/0.085	= 87.7 < 200 OK	h/t = 7.507/0.059	= 127 < 200 OK
N/t = 5.0/0.085	= 58.8 < 210 OK	N/t = 5.0/0.059	= 84.7 < 210 OK
N/h =5.0/7.455	= 0.67 < 2.0 OK	N/h= 5.0/7.507	= 0.67< 2.0 OK

End Span:

$$P_n = (13)(0.085)^2(55)\sin 90\left(1-0.23\sqrt{\frac{0.1875}{0.085}}\right)\left(1+0.14\sqrt{\frac{5.0}{0.085}}\right)\left(1-0.01\sqrt{\frac{7.455}{0.085}}\right)$$

= 6.39 kip

Interior Span:

$$P_n = (13)(0.059)^2(55)\sin 90\left(1-0.23\sqrt{\frac{0.1875}{0.059}}\right)\left(1+0.14\sqrt{\frac{5.0}{0.059}}\right)\left(1-0.01\sqrt{\frac{7.507}{0.059}}\right) \qquad \text{(Eq. G5-1)}$$

$= 2.98$ kip

At first interior support,

$$\frac{P_n}{\Omega_w} = \frac{6.39+2.98}{1.65} = 5.68 \text{ kip} \geq 3.36 \text{ kip} \quad \text{OK} \qquad \text{(Eq. B3.2.1-2)}$$

At center support,

$$\frac{P_n}{\Omega_w} = \frac{2.98+2.98}{1.65} = 3.61 \text{ kip} \geq 2.59 \text{ kip} \quad \text{OK} \qquad \text{(Eq. B3.2.1-2)}$$

3e. Combined Bending and Web Crippling (AISI S100 Section H3)

$$0.86\left(\frac{\overline{P}}{P_n}\right)+\left(\frac{\overline{M}}{M_{a\ell o}}\right) \leq \frac{1.65}{\Omega} \qquad \text{(Eq. H3-3a)}$$

where

$M_{n\ell o}$ = Sum of the Nominal Flexural Strength (resistance) of each purlin in the absence of axial load determined in accordance with AISI S100 Section F3 with $F_n = F_y$.

P_n = Sum of the Nominal Strength (resistance) for concentrated load or reaction in absence of bending moment of each purlin determined in accordance with AISI S100 Section G5.

Ω = 1.70

Ends of laps of each section are to be connected by a minimum of two 1/2 in. diameter A307 bolts through the web, the combined section is to be connected to the support by a minimum of two 1/2 in. diameter A307 bolts through the flanges, and the webs must be in contact. (Note: If the purlin webs are connected to a welded web plate as shown in Figure 1.2-2, the limit state of combined bending and web crippling does not apply.)

Check Limits:

$F_y = 55 \text{ ksi} \leq 70 \text{ ksi}$

$$\frac{t_{thick}}{t_{thin}} = \frac{0.085}{0.059} = 1.44 > 1.3 \quad \text{NG}$$

In this case, the strength of thicker purlin may be determined using a maximum thickness of (1.3)(0.059) = 0.077 or conservatively the strength of the thinner purlin. For this example, the strength of the combined section is conservatively determined as two times the strength of the thinner purlin.

End Span	Interior Span
R/t = 0.1875/0.085 = 2.21 < 5.5 OK	R/t = 0.1875/0.059 = 3.18 < 5.5 OK
h/t = 7.455/0.085 = 87.7 < 150 OK	h/t = 7.507/0.059 = 127 < 150 OK
N/t = 5.0/0.085 = 58.8 < 140 OK	N/t = 5.0/0.059 = 84.7 < 140 OK

$$0.86\left(\frac{3.36}{2.98+2.98}\right)+\left(\frac{8.58}{8.34+8.34}\right) = 1.00 \approx 1.65/1.70 = 0.97 \text{ OK}$$

At center support

$$0.86\left(\frac{2.59}{2.98+2.98}\right)+\left(\frac{5.03}{8.34+8.34}\right) = 0.68 < 1.65/1.70 = 0.97 \text{ OK}$$

4. Check Uplift Loads

4a. Strength for Bending Only (AISI S100 Section I6.2.1)

In the region where the tension flange is attached to the through-fastened deck or panels, the strength is checked by AISI S100 Section I6.2.1.

Required Strength

By inspection, $0.6M_D + M_W$ controls.

$M = (0.6M_D + 0.6M_w)$

End Span:

Moment near center of span: $M = (0.6)(0.68) - (0.6)(5.21) = -2.72$ kip-ft

Interior Span:

Moment near center of span: $M = (0.6)(0.30) - (0.6)(2.27) = -1.18$ kip-ft

Allowable Design Flexural Strength

Calculate the allowable flexural strength per AISI S100 Section I6.2.1 at the location of maximum negative moment

The section is partially restrained against lateral-torsional buckling and distortional buckling by the through-fastened panel. Assuming the fifteen conditions of AISI S100 Section I6.2.1 are met, the reduction in strength for continuous span Z-sections (R = 0.70) is obtained from AISI S100 Table I6.2.1-1.

$M_n = RM_{n\ell o}$

(Eq. I6.2.1-1)

$M_{n\ell o}$ = nominal flexural strength with consideration of local buckling only as determined from AISI S100 Section F3 with $F_n = F_y$.

R = 0.70 for both purlin thicknesses

End Span:

For t = 0.085 in.

Utilizing the Effective Width Method of AISI S100 Section F3.1

$M_{n\ell o} = S_eF_n = (2.84)(55) = 156.2$ kip-in. $= 13.02$ kip-ft $\leq S_{et}F_y = (2.84)(55)$ (Eq. F3.1-1)

$M_n = R\,M_{n\ell o} = (0.70)(13.02) = 9.11$ kip-ft (Eq. I6.2.1-1)

$\frac{M_n}{\Omega_b} = \frac{9.11}{1.67} = 5.46$ kip-ft > 2.72 kip-ft OK (Eq. B3.2.1-1)

Interior Span:

For t = 0.059 in.

M_n = (0.70)(1.82)(55) = 70.1 kip-in. or 5.84 kip-ft (Eq. I6.2.1-1)

$\frac{M_n}{\Omega_b} = \frac{5.84}{1.67}$ = 3.50 kip-ft > 1.18 kip-ft OK (Eq. B3.2.1-1)

4b. Other Comments

Since the magnitude of the shears, moments and reactions are approximately 65 percent of those of the gravity case, it can be concluded that the design satisfies the AISI S100 criteria for uplift.

5. System Anchorage

System anchorage is checked in the example provided in Section 5.4.3 for a standing seam system. The procedure is the same for through-fastened systems.

3.3.1.2 Design Example: Strut Purlin in Through-Fastened Roof System - ASD

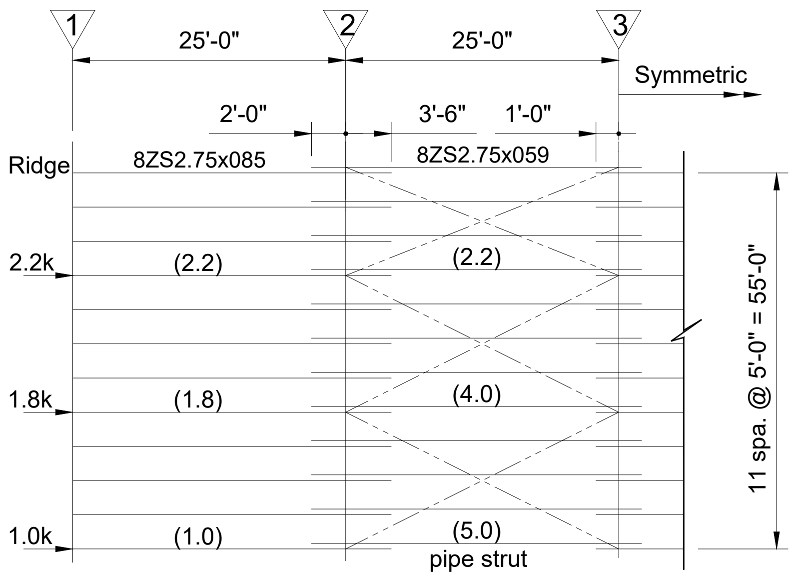

Figure 3.3-2 Applied Forces and Axial Force in Strut Purlins

Given

1. The four span continuous Z-purlin system with a through-fastened roof from Example 3.3.1.1.
2. The system has 12 purlin lines. The purlins at the first, fifth and ninth purlin lines are used as struts to transfer wind load from the end walls. The wind load transferred from each endwall column is shown in Figure 3.3-2. The force in each strut is shown in parenthesis with units of kips.
3. The maximum axial force from wind in the end span is 2.2 kip. The maximum axial force in the first interior span is 4.0 kip. At the eave of the building, a pipe strut is integrated into the vertical x-brace (therefore the axial force in the purlin is zero at the interior span at the eave).

Required

Using ASD with ASCE/SEI 7-16 (ASCE 2016) load combinations for endwall wind combined with (a) gravity loads and (b) uplift loads:

1. Check the strength of the strut purlin with respect to axial loads only.
2. Check the strength of the strut purlin with respect to combined axial load and bending. Note that the strength with respect to bending only is provided in Example 3.3.1.1.

Solution

Note: The equations referenced in this example refer to AISI S100 equation numbers.

1. Assumptions for Analysis and Application of the AISI S100 Provisions

AISI S100 does not define the methods of analysis to be used; these judgments are the responsibility of the designer. The following assumptions are considered good practice but are not intended to prohibit other approaches:

a. The attachment of the roof covering to the purlin provides continuous lateral support to the top flange.
b. Through-fastened at 12 in. o.c. with fasteners located at the center of the flange.
c. For the calculation of the distortional buckling strength, the rotational restraint provided by the roof panels, k_ϕ, is included.
d. Since the loading, geometry and materials are symmetrical; only the first two spans are checked.
e. Both flanges are restrained from lateral movement at the supports
f. Strut purlin forces are generated from wind loads parallel to the ridge. For wind loads parallel to the ridge, roof pressures can either be negative, resulting in a 115 lb/ft uplift or positive, resulting in 0 lb/ft. Consequently, strut forces should be considered both with maximum uplift moments as well as with gravity moments from live and dead load.

2. Section Properties

The following section properties are from AISI D100 Table I-4 and Table II-4.

Interior Bays	End Bays
For: 8ZS2.75x059	For: 8ZS2.75x085
d = 8 in.	d = 8 in.
t = 0.059 in.	t = 0.085 in.
$A = A_g = 0.881$ in.^{2}	$A = A_g = 1.27$ in.^{2}
$I_x = 8.69$ in.^{4}	$I_x = 12.40$ in.^{4}
$I_y = 1.72$ in.^{4}	$I_y = 2.51$ in.^{4}
$r_x = 3.14$ in.	$r_x = 3.13$ in.
$r_y = 1.40$ in.	$r_y = 1.41$ in.
$S_f = 2.17$ in.^{3}	$S_f = 3.11$ in.^{3}
$S_e = 1.82$ in.^{3}	$S_e = 2.84$ in.^{3}

Both sections have inside bend radius, R = 0.1875 in. and flange width, b = 2.75 in.

3. Check Required Strength

ASD load combinations considered:

(1) D+0.6W
(2) D + 0.75L_r + 0.75(0.6)W
(3) 0.6D+0.6W

Table 3-6 Axial Forces and Moments for ASD Load Combinations

Load Case	(1) D+0.6W	(2) D+0.75L_r+0.75(0.6)W	(3) 0.6D+0.6W
End Span			
P	0.6(2.2)=1.32	0.75(0.6)(2.2)=0.99	0.6(2.2)=1.32
M, Near Mid-span	0.68+0.6(0)=0.68	0.68+0.75(4.53)+0.75(0.6)(0) = 4.08	0.6(.68)-0.6(5.21)=-2.72
M, End of Right Lap	-0.69+0.6(0)= -0.69	-0.69-0.75(4.57)+0.75(0.6)(0) = -4.12	-0.6(.69)+0.6(5.25)= 2.74
Interior Span			
P	0.6(4.0)=2.4	0.75(0.6)(4.0)=1.8	0.6(4.0)=2.4
M, End of Right Lap	-0.49+0.6(0)= -0.49	-0.49-0.75(3.29)+0.75(0.6)(0) = -2.95	-0.6(.49)+0.6(3.78)= 1.97
M, Near Mid-span	0.30+0.6(0)=0.30	0.30+0.75(1.98)+0.75(0.6)(0) = 1.79	0.6(.30)-0.6(2.27)=-1.18
M, End of Left Lap	-0.49+0.6(0)= -0.49	-0.49-0.75(3.28)+0.75(0.6)(0) = -2.96	-0.6(.49)+0.6(3.77)= 1.97

Summary of required strength

End Span, from left to right:

Maximum axial force: P = 1.32 kip
Mid-span positive moment + Axial Force M = 4.08 kip-ft, P = 0.99 kip
Mid-span negative (uplift) moment + Axial Force M = -2.72 kip-ft, P = 1.32 kip
Negative Moment at end of right lap + Axial Force M = -4.12 kip-ft, P = 0.99 kip
Positive (uplift) Moment at end of right lap + Axial Force M = 2.74 kip-ft, P = 1.32 kip

Interior Span, from left to right:

Maximum axial force: P = 2.40 kip
Mid-span positive moment + Axial Force M = 1.79 kip-ft, P = 1.80 kip
Mid-span negative (uplift) moment + Axial Force M = -1.18 kip-ft, P = 2.40 kip
Note: moments at right and left lap nearly identical
Negative Moment at end of lap + Axial Force M = -2.96 kip-ft, P = 1.80 kip
Positive (uplift) Moment at end of lap + Axial Force M = 1.97 kip-ft, P = 2.40 kip

4. Check Allowable Design Strength

4a. Strength for Axial Load Only (AISI S100 Sections E2.1, E3, and I6.2.3)

Compute the lowest of the applicable axial strength limit states of local buckling interacting with yielding and global buckling (AISI S100 Sections E2.1 and E3) and flexural-torsional buckling strength (AISI Section S100 I6.2.3).

End Span:

Determine the strength from local buckling interacting with yielding and global buckling per AISI S100 Section E3, starting with the global flexural stress per AISI S100 Section E2.1

The strength check for flexural buckling about the x-axis assumes that the though-fastened deck sufficiently constrains the purlin to buckle about its x-axis without the introduction of flexural-torsional buckling. This check provides an upper bound for the axial strength.

$K = 1.0$

L = distance from end support to end-of-lap

= 23 ft = 276 in.

$$F_{cre} = \frac{\pi^2 E}{(KL/r_x)^2} \quad \text{(Eq. E2.1-1)}$$

$$= \frac{\pi^2(29500)}{((1.0)276/3.13)^2} = 37.4 \text{ ksi}$$

$$\lambda_c = \sqrt{\frac{F_y}{F_{cre}}} \quad \text{(Eq. E2-4)}$$

$$= \sqrt{\frac{55}{37.4}} = 1.21 < 1.50$$

$$F_n = \left(0.658^{\lambda_c^2}\right)F_y \quad \text{(Eq. E2-2)}$$

$$= \left(0.658^{(1.21)^2}\right)55 = 29.7 \text{ ksi}$$

$$P_{n\ell} = A_e F_n \le P_{ne} \quad \text{(Eq. E3.1-1)}$$

The effective area is calculated similar to Example I-10 in AISI D100. The flanges and flange stiffeners are fully effective and the web is subject to local buckling for f = 29.7 ksi.

A_e = 1.00 in.^{2}

$P_{n\ell}$ = (1.00)(29.7) = 29.7 kip < P_{ne}

Determine the flexural-torsional buckling strength about the weak axis per AISI S100 Section I6.2.3(a)

Note that per Section I6.2.3, consideration of distortional buckling may be excluded.

Check limits of applicability of AISI S100 Section I6.2.3

(1) $t = 0.085 \le 0.125$ OK

(2) $6 \le d = 8.00 \le 12$ OK

(3) Flanges are edge stiffened compression elements OK

(4) $70 \le d/t = 8.00/0.085 = 94.1 \le 170$ OK

(5) $2.8 \le d/b = 8.00/2.75 = 2.9 \le 5$ OK

(6) $16 \le \frac{\text{flat flange width}}{t} = \left(\frac{B-2(R+t)}{t}\right) = \left(\frac{2.75-2(0.1875+0.085)}{0.085}\right) = \left(\frac{2.350}{0.085}\right) = 27.6 \le 50$ OK

(7) Both flanges prevented from moving laterally at supports OK

(8) Fastener spacing ≤ 12 in. OK

Rotational stiffness is given as 0.300 kip-in./rad/in. By dividing this value by the purlin depth squared, it is converted to a rotational lateral stiffness for comparison to the limiting value, (0.300 kip-in./rad/in./(8 in.)^2 = 0.0047 kip/in./in.) > 0.0015 kip/in./in. OK

(9) F_y = 55 ksi ≥ 33 ksi OK

(10) Span Length = 25 ft ≤ 33 ft OK

All Conditions are satisfied

Compute P_n

$P_n = C_1C_2C_3AE/29500$ (Eq. I6.2.3-1)

α = 1 (units are inches)

$x = a/b$

$= 1.375/2.75 = 0.50$

$C_1 = 0.79x + 0.54$ (Eq. I6.2.3-2)

$= 0.79(0.50) + 0.54 = 0.94$

$C_2 = 1.17\alpha t + 0.93$ (Eq. I6.2.3-3)

$= 1.17(1)(0.085) + 0.93 = 1.03$

$C_3 = \alpha(2.5b-1.63d) + 22.8$ (Eq. I6.2.3-4)

$= 1(2.5(2.75)-1.63(8.00)) + 22.8 = 16.6$

$P_n = (0.935)(1.03)(16.6)(1.27)(29500)/29500$

$= 20.3$ kip

The axial strength is governed by the flexural-torsional buckling strength.

$$\frac{P_n}{\Omega} = \frac{20.3}{1.80} = 11.3 \text{ kip} > 1.32 \text{ kip OK} \quad \text{(Eq. B3.2.1-1)}$$

Interior Span:

Determine the strength from local buckling interacting with yielding and global buckling per AISI S100 Section E3, starting with the global flexural stress per AISI S100 Section E2.1

This strength check assumes that the though-fastened deck sufficiently constrains the purlin to buckle about its x-axis without the introduction of flexural-torsional buckling. This check provides an upper bound for the axial strength.

K = 1.0

L = distance between laps

= 25 – 3.5 – 1.0 = 20.5 ft = 246 in.

$$F_{cre} = \frac{\pi^2 E}{(KL/r_x)^2} \quad \text{(Eq. E2.1-1)}$$

$$= \frac{\pi^2(29500)}{((1.0)246/3.14)^2} = 47.4 \text{ ksi}$$

$$\lambda_c = \sqrt{\frac{F_y}{F_{cre}}} \quad \text{(Eq. E2-4)}$$

$$= \sqrt{\frac{55}{47.4}} = 1.08 < 1.50$$

$F_n = \left(0.658^{\lambda_c^2}\right)F_y$ (Eq. E2-2)

$= \left(0.658^{(1.08)^2}\right)55 = 33.8$ ksi

Determine the strength from local buckling interacting with yielding and global buckling from AISI S100 Section E3

$P_{n\ell} = A_eF_n < P_{ne}$ (Eq. E3.1-1)

The effective area is calculated similar to Example I-10 in AISI D100. The web, flanges and flange stiffeners are subject to local buckling for f = 33.8 ksi.

$A_e = 0.579$ in.^{2}

$P_{n\ell} = (0.579)(33.8) = 19.6$ kip $< P_{ne}$

Determine the flexural-torsional buckling strength about the weak axis per AISI S100 Section I6.2.3(a)

Note that per Section I6.2.3, consideration of distortional buckling may be excluded.
The section satisfies the ten limits of applicability in Section I6.2.3

Compute P_n

$P_n = C_1C_2C_3AE/29500$ (Eq. I6.2.3-1)

$\alpha = 1$ (units are inches)

$x = a/b$

$= 1.375/2.75 = 0.50$

$C_1 = 0.79x + 0.54$ (Eq. I6.2.3-2)

$= 0.79(0.50) + 0.54 = 0.935$

$C_2 = 1.17\alpha t + 0.93$ (Eq. I6.2.3-3)

$= 1.17(1)(0.059) + 0.93 = 1.00$

$C_3 = \alpha(2.5b-1.63d) +22.8$ (Eq. I6.2.3-4)

$= 1(2.5(2.75)-1.63(8.00) + 22.8 = 16.6$

$P_n = (0.935)(1.00)(16.6)(0.881)(29500)/29500$

$= 13.7$ kip

The axial strength is governed by the flexural-torsional buckling strength.

$\frac{P_n}{\Omega} = \frac{13.7}{1.80} = 7.61 \text{ kip} > 2.40 \text{ kip}$ OK (Eq. B3.2.1-1)

4b. Strength for Combined Compressive Axial Load and Bending (AISI S100 Section H1.2)

The combined strength must be evaluated near mid-span and at the end of the lap for both the end span and interior span for both gravity and uplift cases. Conservatively, the maximum force in the strut purlin (P = 1.32 kip for the end span, 2.40 for the interior span) is used to determine the effective area of the section and the second order effects for all bending cases. The design strength of the purlin subjected to bending only is taken from Example 3.3.1.1.

End Span – Near mid-span:

Determine the member second order effects (P-δ) using the amplified first-order elastic analysis of AISI S100 Section C1.2.1.1

The stiffness of the purlin is reduced by a factor of 0.90 per AISI S100 Section C1.1.1.3 and initial imperfections (defined in Section C1.1.1.2) are ignored as they are deemed to have a minimal impact on the second order effects on the strut purlin.

C_m = 1.0 (conservative for beam-columns with transverse loads in lieu of analysis)

L = 25 – 2 = 23 ft = 276 in.

K_x = 1.0

k_f = 0.90EI_x (stiffness of the structure is reduced by 0.90 per AISI S100 Section C1.1.1.3)

$$P_{eX} = \frac{\pi^2 k_f}{(K_x L_x)^2} \qquad \text{(Eq. C1.2.1.1-5)}$$

$$= \frac{\pi^2 (0.9)(29500)(12.40)}{((1.0)(276)^2} = 42.65 \text{ kip}$$

α = 1.60 for ASD

$$B_1 = C_m / \left(1 - \alpha \overline{P} / P_{ex}\right) \geq 1.0 \qquad \text{(Eq. C1.2.1.1-3)}$$

= (1.0)/(1-(1.60)(1.32)/42.65) = 1.05

Assume the flange braces are provided as shown in Figure 3.2-9 that prevent the rotation of the purlin and eliminate any additional moment resulting from the eccentricity of the axial force.

Use $\overline{M}_{nt}$ = M_x (flange braces preclude rafter rotation)

Calculate the combined effect of Compressive Axial Load and Bending per AISI S100 Section H1.2

$$\frac{\overline{P}}{P_a} + \frac{\overline{M}_x}{M_{ax}} + \frac{\overline{M}_y}{M_{ay}} \leq 1.0 \qquad \text{(Eq. H1.2-1)}$$

End Span – Gravity Loading near mid-span:

$\overline{M}_{nt}$ = M_x = 4.08 kip-ft

$$\overline{M}_x = B_1 \overline{M}_{nt} + B_2 \overline{M}_{\ell t} \qquad \text{(Eq. C1.2.1.1-1)}$$

= (1.05)(4.08) + B_2(0) = 4.28 kip-ft

$\overline{P}$ = 0.99 kip (Load Combination 2)

P_a = 11.3 kip (calculated in Part a)

M_{ax} = 6.92 kip-ft (calculated in Example 3.3.1.1)

$$\frac{0.99}{11.3} + \frac{4.28}{6.92} + 0 = 0.71 < 1.0 \text{ OK}$$

End Span – Uplift loading near mid-span:

When subjected to uplift loading, the required moment at the mid-span is less than the required moments for gravity loading. However, the design flexural strength is also less when subjected to uplift.

$\overline{M}_{nt}$ = M_x = -2.72 kip-ft

$\overline{M}_x = B_1\overline{M}_{nt} + B_2\overline{M}_{\ell t}$ (Eq. C1.2.1.1-1)

$\overline{M}_x$ = (1.05)(-2.72) + B_2(0) = -2.86 kip-ft

$\overline{P}$ = 1.32 kip (Load Combination 3)

P_a = 11.3 kip (calculated in Part a)

M_{ax} = 5.46 kip-ft (calculated in Example 3.3.1.1)

$$\frac{1.32}{11.3} + \frac{2.86}{5.46} + 0 = 0.52 < 1.0$$

End Span - At the end of the lap:

At the end of the lap, the axial strength of the section is the minimum of the column crushing strength (local buckling strength) and the distortional buckling strength. Conservatively, the axial strength determined above at the interior of the span can be used but the conservatism may be excessive. At the end of the lap, second order effects are considered to be negligible. Moment design strength is controlled by gravity load cases since the compression flange is not attached to panels.

Calculate axial strength (column crushing strength) considering local buckling using the effective width method from AISI S100 Section E3.1

$P_{n\ell} = A_eF_n \leq P_{ne}$ (Eq. E3.1-1)

A_e = 0.823 in.^{2} (calculated similar to AISI D100 Example I-10)

$F_n = F_y$ = 55 ksi for column crushing strength

$P_{n\ell}$ = (0.823)(55) = 45.3 kip

Calculate distortional buckling axial strength from AISI S100 Section E4.1

The purlin has one flange attached to panels, which provides rotational resistance to distortional buckling, but the other flange is free. Therefore, any rotational restraint provided by the panels is ignored. The distortional buckling unbraced length is considered to be the distance between the inflection point and the end of the lap, L_m = 47.5 in. When the distortional buckling length exceeds the distortional buckling half-wavelength, L_{cr}, the distortional buckling strength is determined according to AISI S100 Section E4.1. An example of determining the distortional buckling strength is provided in AISI D110. AISI D100 also provides distortional buckling strength values for common section. For this example, the distortional buckling strength will be taken directly from AISI D100 Table III-6.

L_{cr} = 24.0 in. < L_m = 47.5 in. (AISI D100 Table III-6)

Therefore,

P_{nd} = 39.0 kip (AISI D100 Table III-6)

The axial distortional buckling strength controls

$P_a = \frac{P_{nd}}{\Omega} = \frac{39.0}{1.80} = 21.7$ kip

$\overline{\mathbf{P}} = 0.99$ kip (Load Combination 2)

$\overline{M}_x = M_x = -4.12$ kip-ft (Load Combination 2)

$M_{ax} = 7.79$ kip-ft (calculated in Example 3.3.1.1)

$\frac{0.99}{21.7} + \frac{4.12}{7.79} + 0 = 0.57 < 1.0$ OK

Interior Span – Near mid-span:

Determine the member second order effects (P-δ) using the amplified first order elastic analysis of AISI S100 Section C1.2.1.1

The stiffness of the purlin is reduced by a factor of 0.90 per AISI S100 Section C1.1.1.3 and initial imperfections (defined in Section C1.1.1.2) are ignored as they are deemed to have a minimal impact on the second order effects on the strut purlin.

$C_m = 1.0$ (conservative for beam-columns with transverse loads in lieu of analysis)

$L = 25 – 3.50 – 1.00 = 20.5$ ft = 246 in.

$K_x = 1.0$

$k_f = 0.90EI_x$ (stiffness of the structure is reduced by 0.90 per AISI S100 Section C1.1.1.3)

$$P_{eX} = \frac{\pi^2 k_f}{(K_x L_x)^2} \quad \text{(Eq. C1.2.1.1-5)}$$

$$= \frac{\pi^2 (0.9)(29500)(8.69)}{((1.0)(246))^2} = 37.63 \text{ kip}$$

$\alpha = 1.60$ for ASD

$$B_1 = C_m / \left(1 - \alpha\overline{P} / P_{ex}\right) \geq 1.0 \quad \text{(Eq. C1.2.1.1-3)}$$

$= (1.0)/(1-(1.60)(2.40)/37.63) = 1.11$

Use $\overline{M}_{nt} = M_x$ (flange braces preclude rafter rotation)

Calculate the combined effect of Compressive Axial Load and Bending per AISI S100 Section H1.2

$$\frac{\overline{P}}{P_a} + \frac{\overline{M}_x}{M_{ax}} + \frac{\overline{M}_y}{M_{ay}} \leq 1.0 \quad \text{(Eq. H1.2-1)}$$

Interior Span - Gravity loading near mid-span:

$\overline{M}_{nt} = M_x = 1.79$ kip-ft

$\overline{M}_x = B_1\overline{M}_{nt} + B_2\overline{M}_{\ell t}$ (Eq. C1.2.1.1-1)

$= (1.11)(1.79) + B_2(0) = 1.99$ kip-ft

$M_{ax} = 4.58$ kip-ft (calculated in Example 3.3.1.1)

$P_a = 7.61$ kip (calculated in Part a)

$\overline{\mathbf{P}} = 1.80$ kip (Load Combination 2)

$$\frac{1.80}{7.61}+\frac{1.99}{4.58}+0=0.68<1.0\ \text{OK}$$

Interior Span – Uplift loading near mid-span:

When subjected to uplift loading, the required moment at the mid-span is less than that for gravity moments. However, the design flexural strength is also less when subjected to uplift.

$\overline{M}_{nt}$ = M_x = -1.18 kip-ft

$\overline{M}_x = B_1\overline{M}_{nt} + B_2\overline{M}_{\ell t}$ (Eq. C1.2.1.1-1)

$\overline{M}_x$ = (1.11)(-1.18) + B_2(0) = -1.31 kip-ft

M_{ax} = 3.50 kip-ft (calculated in Example 3.3.1.1)

P_a = 7.61 (calculated in Part a)

$\overline{P}$ = 2.40 kip (Load Combination 3)

$$\frac{2.40}{7.61}+\frac{1.31}{3.48}+0=0.69<1.0$$

Interior Span - At the end of the lap:

At the end of the lap, the axial strength of the section is the minimum of the column crushing strength (local buckling strength) and the distortional buckling strength. Conservatively, the axial strength determined above at the interior of the span can be used but the conservatism may be excessive. At the end of the lap, second order effects are considered to be negligible. Moment design strength is controlled by gravity load cases since the compression flange is not attached to panels.

Calculate axial strength (column crushing strength) considering local buckling using the effective width method from AISI S100 Section E3.1

$P_{n\ell} = A_eF_n \le P_{ne}$ (Eq. E3.1-1)

A_e = 0.472 in.^{2} (calculated similar to AISI D100 Ex I-10)

$F_n = F_y$ = 55 ksi for column crushing strength

P_a = (0.472)(55) = 26.0 kip

Calculate distortional buckling axial strength from AISI S100 Section E4.1

The purlin has one flange attached to panels, which provides rotational resistance to distortional buckling, but the other flange is free. Therefore, any rotational restraint provided by the panels is ignored. The distortional buckling unbraced length is the distance between the inflection point and the end of the lap, L_m = 47.8 in. When the distortional buckling length exceeds the distortional buckling half-wavelength, L_{cr}, the distortional buckling strength is determined according to AISI S100 Section E4.1. An example of determining the distortional buckling strength is provided in AISI D110. AISI D100 also provides distortional buckling strength values for common section. For this example, the distortional buckling strength will be taken directly from AISI D100 Table III-6.

L_{cr} = 28.1in. < L_m =47.8 in. (AISI D100 Table III-6)

Therefore,

P_{nd} = 21.7 kip (AISI D100 Table III-6)

The axial distortional buckling strength controls.

$$P_a = \frac{P_{nd}}{\Omega} = \frac{21.7}{1.80} = 12.1 \text{ kip}$$

$\overline{P}$ = 1.8 kip (Load Combination 2)

The moment at the end of the left lap is approximately equal to the moment at the end of the right lap. Only the right lap will be investigated.

$\overline{M}_x$ = -2.96 kip-ft (Load Combination 2)

The moment strength at the end of the left lap, as calculated in Example 3.3.1.1, is conservatively used for the strength at the end of the right lap.

M_{ax} = 4.15 kip-ft

$$\frac{1.8}{12.1} + \frac{2.96}{4.15} + 0 = 0.86 < 1.0 \text{ OK}$$

The strut-purlin satisfies all the axial force criteria as well as the combined axial force plus bending criteria.

3.3.2 Standing Seam Roof System Design Examples

3.3.2.1 Design Example: Four Span Continuous Z-Purlins Attached to Standing Seam Panels (Gravity and Uplift Loads) -- ASD

Given

1. Four span Z-purlin system using laps at interior support points to create continuity.
2. Roof covering is attached with standing seam panel clips along the entire length of the purlins.
3. Twelve purlin lines.
4. F_y = 55 ksi
5. Roof Slope = 0.5:12.
6. The top flange of each purlin is facing upslope except the purlin closest to the eave, which has its top flange facing downslope.
7. There are no discrete braces; anti-roll clips are provided at each support of every fourth purlin line.
8. Purlin flanges are bolted to a 1/4-in. thick support member with a bearing length of 5 in.
9. Tested R-values using AISI S908:
   For gravity loads:
   R = 0.85 for the 0.085 in. thick purlin
   R = 0.90 for the 0.059 in. thick purlin
   For uplift loads:
   R = 0.70 for the 0.085 in. thick purlin
   R = 0.70 for the 0.059 in. thick purlin
10. The loads shown are parallel to the purlin webs.

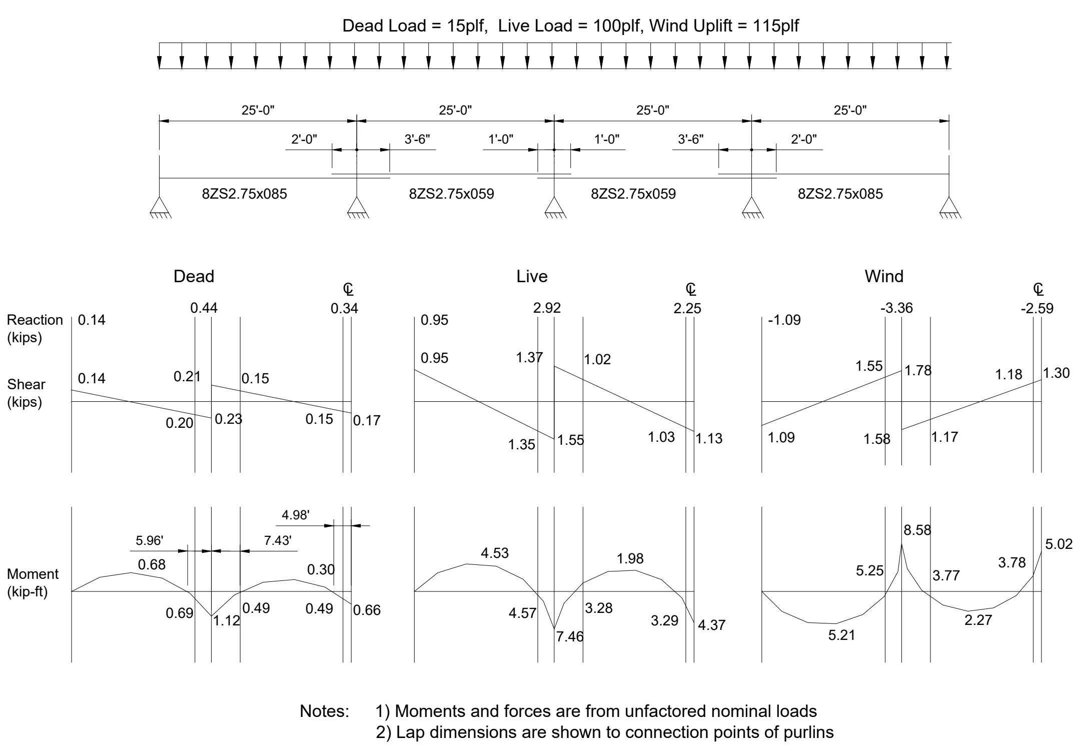

Figure 3.3-3 Shear and Moment Diagrams

Required

1. Check the design using ASD with ASCE/SEI 7-16 (ASCE 2016) load combinations for (a) Gravity Loads and (b) Uplift Loads.
2. Compute the anchorage forces at the supports under gravity loads.

Solution

Note: The equations referenced in this example refer to the AISI S100 equation numbers.

1. Assumptions for Analysis and Application of AISI S100 Provisions

AISI S100 does not define the methods of analysis to be used; these judgments are the responsibility of the designer. The following assumptions are considered good practice but are not intended to prohibit other approaches:

a. The purlins are connected within the lapped portions in a manner that achieves full continuity between the individual purlin members.

b. The continuous beam analysis to establish the shear and moment diagrams assumes continuous non-prismatic members between supports in which I_x within the lapped portions is the sum of the individual members. Gross values of I_x are used for the beam analysis.

c. The strength within the lapped portions is assumed to be the sum of the strengths of the individual members.

d. For gravity loads, the region at and near the interior supports is assumed to be not subject to lateral-torsional or distortional buckling between the support and the ends of the laps.

e. Under uniform gravity loading, the negative moment region between the end of the lap and the inflection point is assumed to have an unbraced length for lateral-torsional and distortional buckling equal to the distance from the end of the lap to the inflection point.

f. Since the loading, geometry and materials are symmetrical; only the first two spans are checked.

2. Section Properties

The following section properties are from AISI D100 Table I-4 and Table II-4.

Interior Bays	End Bays
For: 8ZS2.75x059	For: 8ZS2.75x085
d = 8 in.	d = 8 in.
t = 0.059 in.	t = 0.085 in.
I_x = 8.69 in.^{4}	I_x = 12.40 in.^{4}
$S_f = S_{fy}$ = 2.17 in.^{3}	$S_f = S_{fy}$ = 3.11 in.^{3}
S_e = 1.82 in.^{3}	S_e = 2.84 in.^{3}
I_y = 1.72 in.^{4}	I_y = 2.51 in.^{4}

Both sections have inside bend radius, R = 0.1875 in. and flange width, b = 2.75 in.

3. Check Gravity Loads

3a. Strength for Bending Only (AISI S100 Section I6.2.2)

Required Strength

ASD load combinations considered:

(1) D

(2) D + L_r

By inspection, D + L_r controls:

$M = M_D + M_{Lr}$

End Span, from left to right:

Maximum positive moment:	M = 0.68 + 4.53 = 5.21 kip-ft
Negative moment at end of right lap:	M = 0.69 + 4.57 = 5.26 kip-ft
Negative moment at support:	M = 1.12 + 7.46 = 8.58 kip-ft

Interior Span, from left to right:

Negative moment at end of left lap:	M = 0.49 + 3.28 = 3.77 kip-ft
Maximum positive moment:	M = 0.30 + 1.98 = 2.28 kip-ft
Negative moment at end of right lap:	M = 0.49 + 3.29 = 3.78 kip-ft
Negative moment at center support:	M = 0.66 + 4.37 = 5.03 kip-ft

Allowable Design Flexural Strength

End Span - At the location of maximum positive moment:

Calculate the allowable flexural strength per AISI S100 Section I6.2.2

The section is assumed to be partially restrained against lateral-torsional buckling and distortional buckling by the standing seam panel. The ability of the panel to restrain the purlin has been quantified by AISI S908 (R = 0.85).

$M_n = RM_{n\ell o}$ (Eq. I6.2.2-1)

$M_{n\ell o}$ = nominal flexural strength with consideration of local buckling only as determined from AISI S100 Section F3 with $F_n = F_y$.

Utilizing the Effective Width Method of AISI S100 Section F3.1

$M_{n\ell o} = S_eF_y = (2.84)(55) = 156.2$ kip-in. = 13.02 kip-ft (Eq. F3.1-1)

$M_n = R\,M_{n\ell o} = (0.85)(13.02) = 11.06$ kip-ft (Eq. I6.2.2-1)

$\frac{M_n}{\Omega_b} = \frac{11.06}{1.67} = 6.63 \text{ kip-ft} \geq 5.21 \text{ kip-ft}$ OK (Eq. B3.2.1-2)

End Span - In the region of negative moment between the end of the lap and the inflection point:

Determine the allowable moment per AISI S100 Section F2.1.3 using the distance from the inflection point to the end of the lap as the unbraced length

$L_y = 5.96 - 2.00 = 3.96$ ft = 47.5 in.

$K_y = 1.0$

$I_{yc} = \dfrac{I_y}{2} = \dfrac{2.51}{2} = 1.255\text{ in.}^4$

C_b = 1.67 (Conservatively assumes linear moment diagram in this region).

$$F_{cre} = \frac{C_b \pi^2 E d I_{yc}}{2S_f(K_y L_y)^2} = \frac{(1.67)\pi^2(29500)(8.0)(1.255)}{(2)(3.11)((1.0)47.5)^2} = 347.9\text{ ksi} \qquad \text{(Eq. F2.1.3-2)}$$

$2.78F_y = (2.78)(55) = 153$ ksi

Since $F_{cre} > 2.78F_y$, the section is not subject to lateral-torsional buckling and the global flexural stress, $F_n = F_y = 55$ ksi

Calculate the allowable strength based on local buckling interacting with yielding and global buckling using the effective width method in AISI S100 Section F3.1

$$M_n = M_{n\ell} = S_e F_n = (2.84)(55) = 156.2\text{ kip-in.} \le S_{et}F_y = (2.84)(55) \qquad \text{(Eq. F3.1-1)}$$

$$\frac{M_n}{\Omega_b} = \frac{156.2}{1.67} = 93.5\text{ kip-in.} = 7.79\text{ kip-ft} \ge 5.26\text{ kip-ft OK} \qquad \text{(Eq. B3.2.1-2)}$$

Calculate the allowable distortional buckling strength per Section F4

Calculate the elastic distortional buckling stress F_{crd}, for the negative moment region. Since the compression flange has no sheeting, there is no distortional restraint of the bottom flange, $k_\phi = 0$. Use the analytical solution procedure in Appendix 2 Section 2.3.3.3 of AISI S100 in lieu of the more conservative procedure from the Commentary accompanying Appendix 2 Section 2.3.3.3. From AISI D100 Table II-9 for the 8ZS2.75x085

$k_{\phi fe} = 0.795$ kip

$\tilde{k}_{\phi fg} = 0.0269\text{ in.}^2$

$k_{\phi we} = 0.712$ kip

$\tilde{k}_{\phi wg} = 0.00259\text{ in.}^2$

$$F_{crd} = \beta \frac{k_{\phi fe} + k_{\phi we} + k_\phi}{\tilde{k}_{\phi fg} + \tilde{k}_{\phi wg}} \qquad \text{(Eq. 2.3.3.3-2)}$$

$$F_{crd}/\beta = \frac{0.795 + 0.712 + 0.0}{0.0269 + 0.00259} = 51.1\text{ ksi}$$

Alternatively, F_d/β for the case where k_ϕ=0 may be taken from Table II-9 (F_d/β = 51.1 ksi). From Table II-9

L_{cr} = 21.7 in.

The bottom flange is not restrained from rotation by the panel or other discrete bracing. Therefore, the unbraced length for distortional buckling, L_m, is taken as the distance between the end of the lap and the inflection point.

L_m = 47.5 in. (from above)

$L = \min(L_{cr}, L_m)$

$= \min(21.7, 47.5) = 21.7$ in.

The moments at the ends of the segment are:

M_1 = 0.0 kip-ft at the inflection point

M_2 = 5.26 kip-ft at the end of the lap

$$\beta = 1.0 \le 1 + 0.4\left(L / L_m\right)^{0.7}\left(1 - M_1 / M_2\right)^{0.7} \le 1.3 \qquad \text{(Eq. 2.3.3.3-3)}$$

$$= 1.0 \le 1 + 0.4\left(21.7 / 47.5\right)^{0.7}\left(1 - 0 / 5.26\right)^{0.7} \le 1.3$$

$$= 1.0 \le 1.23 \le 1.3 \text{ therefore, use } \beta = 1.23$$

$$F_{crd} = \beta\left(F_{crd} / \beta\right)$$

$$F_{crd} = 1.23(51.1) = 62.9 \text{ ksi}$$

Calculate the allowable distortional buckling strength per AISI S100 Section F4.1

$$M_y = S_{fy}F_y \qquad \text{(Eq. F4.1-4)}$$

$$= (3.11)(55) = 171 \text{ kip-in.}$$

$$M_{crd} = S_f F_{crd} \qquad \text{(Eq. F4.1-5)}$$

$$= (3.11)(62.9) = 196 \text{ kip-in.}$$

$$\lambda_d = \sqrt{M_y / M_{crd}} \qquad \text{(Eq. F4.1-3)}$$

$$= \sqrt{171/196} = 0.934 > 0.673 \text{ therefore,}$$

$$M_n = M_{nd} = \left(1 - 0.22\left(\frac{M_{crd}}{M_y}\right)^{0.5}\right)\left(\frac{M_{crd}}{M_y}\right)^{0.5} M_y \qquad \text{(Eq. F4.1-2)}$$

$$= (1\text{-}0.22(1/0.934))(1/0.934)(171) = 140 \text{ kip-in.}$$

$$\frac{M_n}{\Omega_b} = \frac{140}{1.67} = 83.8 \text{ kip-in.} = 7.0 \text{ kip-ft} \ge 5.26 \text{ kip-ft} \quad \text{OK} \qquad \text{(Eq. B3.2.1-2)}$$

End Span - In the lapped region over the support:

Calculate the allowable strength based on local buckling interacting with yielding and global buckling using the effective width method in AISI S100 Section F3.1

In the lapped region at the support, the section is assumed to be sufficiently restrained against lateral-torsional buckling and distortional buckling. Because the section is sufficiently restrained against lateral-torsional buckling, the global flexural stress, $F_n = F_y$. The total strength is the sum of the individual strength of the two overlapped purlins.

For the end span purlin, t = 0.085 in.

$$M_n = M_{n\ell} = S_e F_y = (2.84)(55) = 156.2 \text{ kip-in. or } 13.02 \text{ kip-ft} \le S_{et}F_y = (2.84)(55) \qquad \text{(Eq. F3.1-1)}$$

For the interior purlin, t = 0.059 in.

$$M_n = M_{n\ell} = S_e F_y = (1.82)(55) = 100.1 \text{ kip-in. or } 8.34 \text{ kip-ft} \le S_{et}F_y = (1.82)(55) \qquad \text{(Eq. F3.1-1)}$$

Combined strength of purlins

$$\frac{M_n}{\Omega_b} = \frac{13.02 + 8.34}{1.67} = 12.79 \text{ kip-ft} \ge 8.58 \text{ kip-ft} \quad \text{OK} \qquad \text{(Eq. B3.2.1-2)}$$

Interior Span - In the region of negative moment between the end of the left lap and the inflection point:

Calculate the allowable lateral-torsional buckling strength per AISI S100 Section F2.1.3

Determine the allowable moment using the distance from the inflection point to the end of the lap as the unbraced length. Note, AISI S100 Section F2.1.3 allows use of either Eq. F2.1.3-1 or F2.1.3-2. Eq. F2.1.3-2 is generally conservative and is chosen for simplicity.

L_y = 7.43 - 3.50 = 3.93 ft or 47.2 in.

K_y = 1.0

C_b =1.67 (conservatively assuming a linear moment diagram in this region)

$I_{yc} = \frac{I_y}{2} = \frac{1.72}{2} = 0.86 \text{ in.}^4$

$$F_{cre} = \frac{(1.67)\pi^2(29500)(8.0)(0.86)}{(2)(2.17)((1.0)47.2)^2} = 346 \text{ ksi} > (2.78)(55) = 153 \text{ ksi} \quad \text{(Eq. F2.1.3-2)}$$

Since $F_{cre} > 2.78F_y$, the section is not subject to lateral-torsional buckling and the global flexural stress, $F_n = F_y = 55$ ksi.

Calculate the allowable strength based on local buckling interacting with yielding and global buckling using the effective width method in AISI S100 Section F3.1

$$M_n = M_{n\ell} = S_eF_n = (1.82)(55) = 100.1 \text{ kip-in.} \le S_{et}F_y = (1.82)(55) \quad \text{(Eq. F3.1-1)}$$

$$\frac{M_n}{\Omega_b} = \frac{100.1}{1.67} = 59.9 \text{ kip-in.} = 5.00 \text{ kip-ft} \ge 3.77 \text{ kip-ft} \quad \text{OK} \quad \text{(Eq. B3.2.1-2)}$$

Calculate the allowable distortional buckling strength per AISI S100 Section F4

Since there is no distortional restraint of the bottom flange, take F_d/β from AISI D100 Table II-9. From Table II-9 for the 8ZS2.75x059

F_d/β = 32.5 ksi

L_{cr} = 25.4 in.

The unbraced length for distortional buckling, L_m, is taken as the distance between the end of the lap and the inflection point.

L_m = 47.2 in. (from above)

$L = \min(L_{cr}, L_m)$

$= \min(25.4, 47.2) = 25.4$ in.

The moments at the ends of the segment are:

M_1 = 0.0 kip-ft at the inflection point

M_2 = 3.77 kip-ft at the end of the lap

$$\beta = 1.0 \le 1 + 0.4(L/L_m)^{0.7}(1 - M_1/M_2)^{0.7} \le 1.3 \quad \text{(Eq. 2.3.3.3-3)}$$

$$= 1.0 \le 1 + 0.4(25.4/47.2)^{0.7}(1 - 0/3.77)^{0.7} \le 1.3$$

$= 1.0 \le 1.26 \le 1.3$ therefore, use $\beta = 1.26$

$F_{crd} = \beta(F_{crd}/\beta)$

F_{crd} = 1.26(32.5) = 41.0 ksi

Calculate the allowable distortional buckling strength per AISI S100 Section F4.1

$M_y = S_{fy}F_y$ (Eq. F4.1-4)

$= (2.17)(55) = 119$ kip-in.

$M_{crd} = S_f F_d$ (Eq. F4.1-5)

$= (2.17)(41.0) = 89.0$ kip-in.

$\lambda_d = \sqrt{M_y / M_{crd}}$ (Eq. F4.1-3)

$= \sqrt{119 / 89.0} = 1.156 > 0.673$ therefore,

$$M_n = \left(1 - 0.22\left(\frac{M_{crd}}{M_y}\right)^{0.5}\right)\left(\frac{M_{crd}}{M_y}\right)^{0.5} M_y \quad \text{(Eq. F4.1-2)}$$

$= (1\text{-}0.22(1/1.16))(1/1.16)(119) = 83.1$ kip-in.

$\frac{M_n}{\Omega_b} = \frac{83.1}{1.67} = 49.8$ kip-in. = 4.15 kip-ft ≥ 3.77 kip-ft OK (Eq. B3.2.1-2)

Interior Span - At the location of maximum positive moment:

Calculate the allowable flexural strength per AISI S100 Section I6.2.2 Appendix A

At the location of maximum positive moment, the section is assumed to be partially restrained against lateral-torsional buckling and distortional buckling by the standing seam panel. The ability of the panel to restrain the purlin has been quantified by AISI S908 (R = 0.90).

$M_n = RM_{n\ell o}$ (Eq. I6.2.2-1)

$M_{n\ell o}$ = nominal flexural strength with consideration of local buckling only as determined from AISI S100 Section F3 with $F_n = F_y$.

Utilizing the Effective Width Method of AISI S100 Section F3.1

$M_{n\ell o} = S_e F_y = (1.82)(55) = 100.1$ kip-in. = 8.34 kip-ft (Eq.F3.1-1)t

$M_n = R\,M_{n\ell o} = (0.90)(8.34) = 7.51$ kip-ft (Eq. I6.2.2-1)

$\frac{M_n}{\Omega_b} = \frac{7.51}{1.67} = 4.49$ kip-ft ≥ 2.28 kip-ft OK (Eq. B3.2.1-2)

Interior Span - In the region of negative moment between the end of the right lap and the inflection point:

Determine the allowable moment using the distance from the inflection point to the end of the lap as the unbraced length.

L_y= 4.98 - 1.00 = 3.98 ft or 47.8 in.

By inspection, the strength check for the right lap will be satisfied, since the unbraced length and the required strength is about the same as those at the left support. Therefore the section is OK.

Interior Span - In the lapped region over the center support:

Calculate the allowable strength based on local buckling interacting with yielding and global buckling using the effective width method in AISI S100 Section F3.1

In the lapped region at the support, the section is assumed to be sufficiently restrained against lateral-torsional buckling and distortional buckling. Because the section is sufficiently restrained against lateral-torsional buckling, the global flexural stress, $F_n = F_y$. The total strength is the sum of the individual strength of the two overlapped purlins.

Combined strength of purlins

$$\frac{M_n}{\Omega_b} = \frac{8.34+8.34}{1.67} = 9.99 \text{ kip-ft} \geq 5.03 \text{ kip-ft} \quad \text{OK} \qquad \text{(Eq. B3.2.1-2)}$$

3b. Strength for Shear Only (AISI S100 Section G2.1)

Required Strength

By inspection, D + L_r controls:

$V = V_D + V_{Lr}$

End Span, from left to right:

At left support:	V = 0.14 + 0.95 = 1.09 kip
At end of right lap:	V = 0.20 + 1.35 = 1.55 kip
At first interior support:	V = 0.23 + 1.55 = 1.78 kip

Interior Span, from left to right:

At first interior support:	V = 0.21 + 1.37 = 1.58 kip
At end of left lap:	V = 0.15 + 1.02 = 1.17 kip
At end of right lap:	V = 0.15 + 1.03 = 1.18 kip
At center support:	V = 0.17 + 1.13 = 1.30 kip

Allowable Design Strength

End Span:

At the left support and right lap, t = 0.085 in. By inspection the end of the right lap controls.

For t = 0.085 in. and the flat depth of the web, h = 7.455 in., the elastic shear buckling stress is

$$F_{cr} = \frac{\pi^2 E k_v}{12(1-\mu^2)(h/t)^2} = \frac{\pi^2(29500)(5.34)}{12(1-0.3^2)(7.455/0.085)^2} = 18.51 \text{ ksi} \qquad \text{(Eq. G2.3-2)}$$

where k_v = 5.34 for unreinforced webs

$V_{cr} = A_w F_{cr} = (7.455)(0.085)(18.51) = 11.73$ kip (Eq. G2.3-1)

$V_y = 0.6 A_w F_y = 0.6(7.455)(0.085)(55) = 20.91$ kip (Eq. G2.1-5)

$$\lambda_v = \sqrt{\frac{V_y}{V_{cr}}} = \sqrt{\frac{20.91}{11.73}} = 1.335 \qquad \text{(Eq. G2.1-4)}$$

$\lambda_v > 1.227$

$V_n = V_{cr} = 11.73$ kip (Eq. G2.1-3a)

$$\frac{V_n}{\Omega_v} = \frac{11.73}{1.60} = 7.33 \text{ kip} \geq 1.55 \text{ kip} \quad \text{OK} \qquad \text{(Eq. B3.2.1-2)}$$

At the first interior support, sum the strength of the two overlapped purlins:

For t = 0.059 in. and the flat depth of the web, h = 7.507 in., the elastic shear buckling stress is

$$F_{cr} = \frac{\pi^2(29500)(5.34)}{12(1-0.3^2)(7.507/0.059)^2} = 8.79 \text{ ksi}$$

where k_v = 5.34 for unreinforced webs

V_{cr} = (7.507)(0.059)(8.79) = 3.89 kip

V_y = 0.6(7.507)(0.059)(55) = 14.62 kip

$$\lambda_v = \sqrt{\frac{14.62}{3.89}} = 1.938 > 1.227$$

$V_n = V_{cr}$ = 3.89 kip (Eq. G2.1-3a)

For the combined section:

$$\frac{V_n}{\Omega_v} = \frac{11.73+3.89}{1.60} = 9.76\text{kip} \geq 1.78 \text{ kip} \quad \text{OK} \qquad \text{(Eq. B3.2.1-2)}$$

Interior Span:

By inspection of the left and right laps, the right lap controls.

$$\frac{V_n}{\Omega_v} = \frac{3.89}{1.60} = 2.43 \text{ kip} \geq 1.18 \text{ kip} \quad \text{OK} \qquad \text{(Eq. B3.2.1-2)}$$

At the center support, sum the strength of the two overlapped purlins. For the combined section:

$$\frac{V_n}{\Omega_v} = \frac{3.89+3.89}{1.60} = 4.86 \text{ kip} \geq 1.30 \text{ kip} \quad \text{OK} \qquad \text{(Eq. B3.2.1-2)}$$

3c. Strength for Combined Bending and Shear (AISI S100 Section H2)

End Span:

$$\sqrt{\left(\frac{\overline{M}}{M_{a\ell o}}\right)^2 + \left(\frac{\overline{V}}{V_a}\right)^2} \leq 1.0 \qquad \text{(Eq. H2-1)}$$

where

$M_{a\ell o}$ = Available flexural strength for globally braced members from AISI S100 Section F3 with $F_n = F_y$

$= \frac{M_n}{\Omega_b}$

V_a = Available shear strength when shear alone is considered in accordance with AISI S100 Sections G2 to G4

$= \frac{V_n}{\Omega_v}$

$\overline{M}$, $\overline{V}$ = Required flexural and shear strengths in accordance with ASD, LRFD, or LSD load combinations

Ω_b = 1.67

Ω_v = 1.60

At start of right lap, t = 0.085 in.

$$\sqrt{\left(\frac{(1.67)(5.26)}{13.02}\right)^2+\left(\frac{(1.60)(1.55)}{11.73}\right)^2} = 0.71 \le 1.0 \quad \text{OK}$$

At first interior support,

$$\sqrt{\left(\frac{(1.67)(8.58)}{13.02+8.34}\right)^2+\left(\frac{(1.60)(1.78)}{11.73+3.89}\right)^2} = 0.70 \le 1.0 \quad \text{OK}$$

Interior Span:

At end of laps, t = 0.059 in. Right lap controls by inspection.

$$\sqrt{\left(\frac{(1.67)(3.78)}{8.34}\right)^2+\left(\frac{(1.60)(1.18)}{3.89}\right)^2} = 0.90 < 1.0 \quad \text{OK}$$

At center support,

$$\sqrt{\left(\frac{(1.67)(5.03)}{8.34+8.34}\right)^2+\left(\frac{(1.60)(1.30)}{3.89+3.89}\right)^2} = 0.57 \le 1.0 \quad \text{OK}$$

3d. Web Crippling Strength (AISI S100 Section G5)

Required Strength

By inspection, D + L_r controls:

$P = P_D + P_{Lr}$

Supports, from left to right:

At left support: P = 0.14 + 0.95 = 1.09 kip

At first interior support: P = 0.44 + 2.92 = 3.36 kip

At center support: P = 0.34 + 2.25 = 2.59 kip

Allowable Design Strength

The bearing length is 5 in.

At end supports use Eq. G5-1 of AISI S100.

$$P_n = Ct^2F_y \sin\theta\left(1-C_R\sqrt{\frac{R}{t}}\right)\left(1+C_N\sqrt{\frac{N}{t}}\right)\left(1-C_h\sqrt{\frac{h}{t}}\right) \quad \text{(Eq. G5-1)}$$

where

F_y = 55 ksi

θ = 90 degrees

R = 0.1875 in.

N = 5.0 in.
h = 7.455 in.
t = 0.085 in.

From AISI S100 Table G5-3, using the coefficients for the case of Fastened to Support/One-Flange Loading or Reaction/End

C = 4
C_R = 0.14
C_N = 0.35
C_h = 0.02
Ω_w = 1.75

Check limits:

R/t = 0.1875/0.085 = 2.21 < 9 OK
h/t = 7.455/0.085 = 87.7 < 200 OK
N/t = 5.0/0.085 = 58.8 < 210 OK
N/h = 5.0/7.455 = 0.67 < 2.0 OK

$$P_n = (4)(0.085)^2(55)\sin 90\left(1-0.14\sqrt{\frac{0.1875}{0.085}}\right)\left(1+0.35\sqrt{\frac{5.0}{0.085}}\right)\left(1-0.02\sqrt{\frac{7.455}{0.085}}\right) = 3.77 \text{ kip}$$

$$\frac{P_n}{\Omega_w} = \frac{3.77}{1.75} = 2.15 \text{ kip} \geq 1.09 \text{ kip} \quad \text{OK} \qquad \text{(Eq. B3.2.1-2)}$$

At interior supports use Eq. G5-1 of AISI S100. For webs consisting of two or more sheets, the nominal strength is calculated for each individual sheet and the results are added to obtain the nominal strength of the full section.

$$P_n = Ct^2F_y\sin\theta\left(1-C_R\sqrt{\frac{R}{t}}\right)\left(1+C_N\sqrt{\frac{N}{t}}\right)\left(1-C_h\sqrt{\frac{h}{t}}\right) \qquad \text{(Eq. G5-1)}$$

where

F_y = 55 ksi
θ = 90 degrees
R = 0.1875 in.
N = 5.0 in.

End span:	Interior Span
h = 7.455 in.	h = 7.507 in.
t = 0.085 in.	t = 0.059 in.

From Table G5-3, using the coefficients for the case of Fastened to Support/One-Flange Loading or Reaction/Interior

C = 13
C_R = 0.23
C_N = 0.14
C_h = 0.01
Ω_w = 1.65

Check limits:

End Span	Interior Span
R/t = 0.1875/0.085 = 2.21 < 5.5 OK	R/t = 0.1875/0.059 = 3.18 < 5.5 OK
h/t = 7.455/0.085 = 87.7 < 200 OK	h/t = 7.507/0.059 = 127 < 200 OK
N/t = 5.0/0.085 = 58.8 < 210 OK	N/t = 5.0/0.059 = 84.7 < 210 OK
N/h =5.0/7.455 = 0.67 < 2.0 OK	N/h= 5.0/7.507 = 0.67< 2.0 OK

End Span:

$$P_n = (13)(0.085)^2(55)\sin 90\left(1-0.23\sqrt{\frac{0.1875}{0.085}}\right)\left(1+0.14\sqrt{\frac{5.0}{0.085}}\right)\left(1-0.01\sqrt{\frac{7.455}{0.085}}\right) = 6.39 \text{ kip}$$

For t = 0.059 in.

$$P_n = (13)(0.059)^2(55)\sin 90\left(1-0.23\sqrt{\frac{0.1875}{0.059}}\right)\left(1+0.14\sqrt{\frac{5.0}{0.059}}\right)\left(1-0.01\sqrt{\frac{7.507}{0.059}}\right) = 2.98 \text{ kip}$$

At first interior support,

$$\frac{P_n}{\Omega_w} = \frac{6.39+2.98}{1.65} = 5.68 \text{ kip} \geq 3.36 \text{ kip} \quad \text{OK} \qquad \text{(Eq. B3.2.1-2)}$$

At center support,

$$\frac{P_n}{\Omega_w} = \frac{2.98+2.98}{1.65} = 3.61 \text{ kip} \geq 2.59 \text{ kip} \quad \text{OK} \qquad \text{(Eq. B3.2.1-2)}$$

3e. Combined Bending and Web Crippling (AISI S100 Section H3)

$$0.86\left(\frac{\overline{P}}{P_n}\right)+\left(\frac{\overline{M}}{M_{n\ell o}}\right) \leq \frac{1.65}{\Omega} \qquad \text{(Eq. H3-3a)}$$

where

$M_{n\ell o}$ = Sum of the Nominal Flexural Strength (resistance) of each purlin in the absence of axial load determined in accordance with AISI S100 Section F3 with $F_n = F_y$.

P_n = Sum of the Nominal Strength (resistance) of each purlin in the absence of bending moment for concentrated load or reaction determined in accordance with AISI S100 Section G5.

Ω = 1.70

Ends of laps of each section are to be connected by a minimum of two 1/2 in. diameter A307 bolts through the web, the combined section is to be connected to the support by a minimum of two 1/2 in. diameter A307 bolts through the flanges, and the webs must be in contact. (Note: If the purlin webs are connected to a welded web plate as shown in Figure 1.2-2, the limit state of combined bending and web crippling does not apply.)

Check limits at first interior support:

$F_y = 55 \text{ ksi} \leq 70 \text{ ksi}$

$$\frac{t_{thick}}{t_{thin}} = \frac{0.085}{0.059} = 1.44 > 1.3 \text{ NG}$$

In this case, the strength of thicker purlin may be determined using a maximum thickness of (1.3)(0.059) = 0.077 or conservatively the strength of the thinner purlin. For this example, the strength of the combined section is conservatively determined as two times the strength of the thinner purlin.

End Span	Interior Span
R/t = 0.1875/0.085 = 2.21 < 5.5 OK	R/t = 0.1875/0.059 = 3.18 < 5.5 OK
h/t = 7.455/0.085 = 87.7 < 150 OK	h/t = 7.507/0.059 = 127 < 150 OK
N/t = 5.0/0.085 = 58.8 < 140 OK	N/t = 5.0/0.059 = 84.7 < 140 OK

At first interior support

$$0.86\left(\frac{3.36}{2.98+2.98}\right)+\left(\frac{8.58}{8.34+8.34}\right)=1.00\approx 1.65/1.70=0.97\ \text{OK}$$

At center support

$$0.86\left(\frac{2.59}{2.98+2.98}\right)+\left(\frac{5.03}{8.34+8.34}\right)=0.68<1.65/1.70=0.97\ \text{OK}$$

4. Check Uplift Loads

4a. Strength for Bending Only (AISI S100 Section I6.2.2 Appendix A)

In the region where the tension flange is attached to the standing seam panels, the strength is checked by AISI S100 Section I6.2.2 Appendix A.

Required Strength

By inspection, $0.6M_D + 0.6M_W$ controls.

$M = 0.6M_D + 0.6M_W$

End Span:

Moment near center of span: $M = (0.6)(0.68) - (0.6)(5.21) = -2.72$ kip-ft

Interior Span:

Moment near center of span: $M = (0.6)(0.30) - (0.6)(2.27) = -1.18$ kip-ft

Allowable Design Strength

Calculate the allowable flexural strength per AISI S100 Section I6.2.2 Appendix A at the location of maximum negative moment

The section is assumed to be partially restrained against lateral-torsional buckling and distortional buckling by the standing seam panel. The ability of the panel to restrain the purlin has been quantified by AISI S908.

$M_n = RM_{n\ell o}$ (Eq. I6.2.2-1)

$M_{n\ell o}$ = nominal flexural strength with consideration of local buckling only as determined from F3 with $F_n = F_y$.

R = 0.70 for both purlin thicknesses

End Span:

For t = 0.085 in.

Utilizing the Effective Width Method of AISI S100 Section F3.1

$M_{n\ell o} = S_eF_y$ = (2.84)(55) = 156.2 kip-in. = 13.02 kip-ft ≤ $S_{et}F_y$ = (2.84)(55) (Eq. F3.1-1)

M_n = R $M_{n\ell o}$ = (0.70)(13.02) = 9.11 kip-ft (Eq. I6.2.2-1)

$\frac{M_n}{\Omega_b} = \frac{9.11}{1.67}$ = 5.46 kip-ft > 2.72 kip-ft OK (Eq. B3.2.1-1)

Interior Span:

For t = 0.059 in.

$M_{n\ell o} = S_eF_y$ = (1.82)(55) = 100.1 kip-in. = 8.34 kip-ft ≤ $S_{et}F_y$ = (1.82)(55) (Eq. F3.1-1)

M_n = R $M_{n\ell o}$ = (0.70)(8.34) = 5.84 kip-ft (Eq. I6.2.2-1)

$\frac{M_n}{\Omega_b} = \frac{5.84}{1.67}$ = 3.50 kip-ft > 1.18 kip-ft OK (Eq. B3.2.1-1)

4b. Other Comments

Because the magnitude of the shears, moments and reactions in the other regions are less than those under the gravity case and the compression flange in all other regions is braced by the panels, it can be concluded that the design satisfies the AISI 100 criteria for uplift.

5. System Anchorage

System anchorage is checked in the example provided in Section 5.4.3.

3.3.2.2 Design Example: Four Span Continuous C-Purlins Attached to Standing Seam Panels (Gravity and Uplift Loads) -- LRFD

Given

1. Four span C-purlin system using laps at interior support points to create continuity.
2. Roof covering is attached with standing seam panel clips along the entire length of the purlins.
3. Ten purlin lines.
4. F_y = 55 ksi
5. Roof Slope = 0.25:12.
6. Purlins are lapped back-to-back over interior supports but all face in the same direction in a given bay. The purlins in the left end bay face downslope.
7. There are no discrete braces; anti-roll clips are provided at each support of every fourth purlin line.
8. Purlin flanges are bolted to a 1/4-in. thick support member with a bearing length of 5 in.
9. Tested R-values using AISI S908:

   For gravity loads:

   R = 0.90 for the 0.070 in. thick purlin

   R = 0.95 for the 0.059 in. thick purlin

   For uplift load:

   R = 0.75 for the 0.070 in. thick purlin

   R = 0.75 for the 0.059 in. thick purlin
10. The loads shown are parallel to the purlin webs.

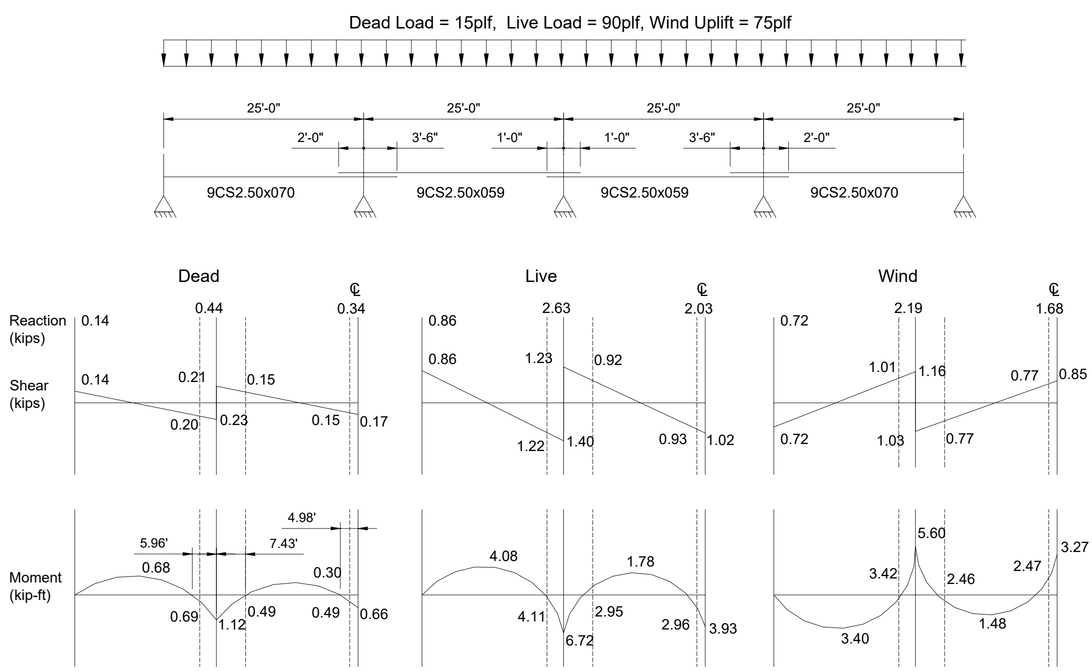

Notes: 1) Moments and forces are from unfactored nominal loads
2) Lap dimensions are shown to connection points of purlins

Figure 3.3-4 Shear and Moment Diagrams

Required

Check the design using LRFD with the ASCE/SEI 7-16 (ASCE 2016) load combinations for:
(a) Gravity Loads
(b) Uplift Loads

Solution

Note: The equations referenced in this example refer to the AISI S100 equation numbers.

1. Assumptions for Analysis and Application of the AISI S100 Provisions

AISI S100 does not define the methods of analysis to be used; these judgments are the responsibility of the designer. The following assumptions are considered good practice but are not intended to prohibit other approaches:

a. The purlins are connected within the lapped portions in a manner that achieves full continuity between the individual purlin members.
b. The continuous beam analysis to establish the shear and moment diagrams assumes continuous non-prismatic members between supports in which I_x within the lapped portions is the sum of the individual members. Gross values of I_x are used for the beam analysis.
c. The strength within the lapped portions is assumed to be the sum of the strengths of the individual members.
d. For gravity loads, the region at and near the interior supports is assumed to be not subject to lateral-torsional or distortional buckling between the support and the ends of the laps.
e. Under uniform gravity loading, the negative moment region between the end of the lap and the inflection point is assumed to have an unbraced length for lateral-torsional and distortional buckling equal to the distance from the end of the lap to the inflection point.
f. Since the loading, geometry and materials are symmetrical; only the first two spans are checked.

2. Section Properties

The following section properties are from AISI D100 Table I-1 and Table II-1.

<u>Interior Bays</u>	<u>End Bays</u>
For: 9CS2.5x059	For: 9CS2.5x070
$A = 0.881$ in.^{2}	$A = 1.05$ in.^{2}
$d = 9$ in.	$d = 9$ in.
$t = 0.059$ in.	$t = 0.070$ in.
$I_x = 10.3$ in.^{4}	$I_x = 12.20$ in.^{4}
$S_f = S_{fy} = 2.29$ in.^{3}	$S_f = S_{fy} = 2.71$ in.^{3}
$S_e = 1.89$ in.^{3}	$S_e = 2.47$ in.^{3}
$I_y = 0.698$ in.^{4}	$I_y = 0.828$ in.^{4}
$r_x = 3.42$ in.	$r_x = 3.41$ in.
$r_y = 0.890$ in.	$r_y = 0.890$ in.
$r_o = 3.90$ in.	$r_o = 3.90$ in.

Both sections have inside bend radius, R = 0.1875 in. and flange width, b = 2.50 in.

3. Check Gravity Loads

3a. Strength for Bending Only (AISI S100 Chapter F and Section I6.2.2)

Required Strength

LRFD load combinations considered

(1) 1.4D

(2) 1.2D + 1.6 L_r

By inspection, 1.2D + 1.6 L_r controls:

$M_u = 1.2M_D + 1.6M_{Lr}$

End Span, from left to right:

Maximum positive moment:	M_u = (1.2)(0.68) + (1.6)(4.08) = 7.34 kip-ft
Negative moment at end of right lap:	M_u = (1.2)(0.69) + (1.6)(4.11) = 7.40 kip-ft
Negative moment at support:	M_u = (1.2)(1.12) + (1.6)(6.72) = 12.10 kip-ft

Interior Span, from left to right:

Negative moment at end of left lap:	M_u = (1.2)(0.49) + (1.6)(2.95) = 5.31 kip-ft
Maximum positive moment:	M_u = (1.2)(0.30) + (1.6)(1.78) = 3.21 kip-ft
Negative moment at end of right lap:	M_u = (1.2)(0.49) + (1.6)(2.96) = 5.32 kip-ft
Negative moment at center support:	M_u = (1.2)(0.66) + (1.6)(3.93) = 7.08 kip-ft

Design Flexural Strength

End Span - At the location of maximum positive moment region:

Calculate the design flexural strength per AISI S100 Section I6.2.2 Appendix A

At the location of maximum positive moment, the section is assumed to be partially restrained against lateral-torsional buckling and distortional buckling by the standing seam panel. The ability of the panel to restrain the purlin has been quantified by AISI S908 (R = 0.90).

$M_n = RM_{n\ell o}$ (Eq. I6.2.2-1)

$M_{n\ell o}$ = nominal flexural strength with consideration of local buckling only as determined from F3 with $F_n = F_y$.

Utilizing the Effective Width Method of AISI S100 Section F3.1

$M_{n\ell o} = S_eF_y = (2.47)(55) = 135.9$ kip-in. = 11.32 kip-ft $\le S_{et}F_y = (2.47)(55)$ (Eq. F3.1-1)

$M_n = R\, M_{n\ell o} = (0.90)(11.32) = 10.19$ kip-ft (Eq. I6.2.2-1)

$\phi_b M_n = (0.90)(10.19) = 9.17$ kip-ft > 7.34 kip-ft OK (Eq. B3.2.1-2)

End Span - In the region of negative moment between the end of the lap and the inflection point:

Determine the allowable moment per AISI S100 Section F2.1.1 using the distance from the inflection point to the end of the lap as the unbraced length.

$r_o = \sqrt{r_x^2 + r_y^2 + r_o^2} = \sqrt{(3.41)^2 + (0.89)^2 + (3.90)^2} = 5.26$ in. (Eq. F2.1.1-3)

$L_y = L_t = 5.96 - 2.00 = 3.96$ ft = 47.5 in.

$K_y = K_t = 1.0$

$I_{yc} = \frac{I_y}{2} = \frac{0.828}{2} = 0.414 \text{ in.}^4$

$$\sigma_{ey} = \frac{\pi^2 E}{(K_y L_y / r_y)^2} = \frac{\pi^2 (29,500)}{(1.0(47.5)/0.89)^2} = 102 \text{ ksi} \quad \text{(Eq. F2.1.1-4)}$$

$$\sigma_t = \frac{1}{Ar_o}\left[GJ + \frac{\pi^2 EC_w}{(K_t L_t)^2}\right]$$

$$= \frac{1}{(1.05)(3.90)}\left[(11,300)(0.00171) + \frac{\pi^2 (29,500)(14.2)}{(1.0(47.5))^2}\right] = 452 \text{ ksi} \quad \text{(Eq. F2.1.1-5)}$$

$C_b = 1.67$ (Conservatively assumes linear moment diagram in this region).

$$F_{cre} = \frac{C_b r_o A}{S_f}\sqrt{\sigma_{ey}\sigma_t} = \frac{(1.67)(3.90)(1.05)}{2.71}\sqrt{(102)(452)} = 542 \text{ ksi} \quad \text{(Eq. F2.1.1-1)}$$

$2.78F_y = (2.78)(55) = 153 \text{ ksi} < F_{cre}$ (542 ksi)

Because $F_{cre} > 2.78F_y$ the section is not subject to lateral-torsional buckling and the global flexural stress, $F_n = F_y = 55$ ksi

Calculate the allowable strength based on local buckling interacting with yielding and global buckling using the effective width method in AISI S100 Section F3.1

$M_n = M_{n\ell} = S_e F_n = (2.47)(55) = 135.9 \text{ kip-in.} \leq S_{et} F_y = (2.47)(55)$ (Eq. F3.1-1)

$\phi_b M_n = (0.90)(135.9) = 122.3 \text{ kip-in.} = 10.19 \text{ kip-ft} \geq 7.40 \text{ kip-ft}$ (Eq.B3.2.2-2)

Calculate the design distortional buckling strength per AISI S100 Section F4

Calculate the elastic distortional buckling stress F_{crd}, for the negative moment region. Since the compression flange has no sheeting, there is no distortional restraint of the bottom flange, $k_\phi = 0$. Use the analytical solution procedure in Appendix 2 Section 2.3.3.3 of AISI S100 in lieu of the more conservative procedure from the Commentary accompanying Appendix 2 Section 2.3.3.3. From AISI D100 Table II-7 for the 9CS2.5x070

$k_{\phi fe} = 0.378$ kip

$\tilde{k}_{\phi fg} = 0.0118 \text{ in.}^2$

$k_{\phi we} = 0.354$ kip

$\tilde{k}_{\phi wg} = 0.00245 \text{ in.}^2$

$$F_{crd} = \beta \frac{k_{\phi fe} + k_{\phi we} + k_\phi}{\tilde{k}_{\phi fg} + \tilde{k}_{\phi wg}} \quad \text{(Eq. 2.3.3.3-2)}$$

$$F_{crd}/\beta = \frac{0.378 + 0.354 + 0.0}{0.0118 + 0.00245} = 51.4 \text{ ksi}$$

Alternatively, for the case where k_ϕ=0, Table II-7 may be used for values of F_{crd}/β, and L_{cr}:

F_{crd}/β = 51.3 ksi

L_{cr} = 24.1 in.

The bottom flange is not restrained from rotation by the panel or other discrete bracing. Therefore, the unbraced length for distortional buckling, L_m, is taken as the distance between the end of the lap and the inflection point.

L_m = 47.5 in. (from above)

$L = \min(L_{cr}, L_m)$

$= \min(24.1, 47.5) = 24.1$ in.

The moments at the ends of the unbraced length are:

M_1 = 0.0 kip-ft at the inflection point

M_2 = 7.40 kip-ft at the end of the lap

$$\beta = 1.0 \le 1 + 0.4(L/L_m)^{0.7}(1 - M_1/M_2)^{0.7} \le 1.3 \quad \text{(Eq. 2.3.3.3-3)}$$

$$= 1.0 \le 1 + 0.4(24.1/47.5)^{0.7}(1 - 0/7.40)^{0.7} \le 1.3$$

$$= 1.0 \le 1.25 \le 1.3 \text{ therefore, use } \beta = 1.25$$

$$F_{crd} = \beta(F_{crd}/\beta)$$

$$F_{crd} = 1.25(51.4) = 64.3 \text{ ksi}$$

Calculate the allowable distortional buckling strength per AISI S100 Section F4.1

$$M_y = S_{fy}F_y \quad \text{(Eq. F4.1-4)}$$

$$= (2.71)(55) = 149 \text{ kip-in.}$$

$$M_{crd} = S_f F_{crd} \quad \text{(Eq. F4.1-5)}$$

$$= (2.71)(64.3) = 174 \text{ kip-in.}$$

$$\lambda_d = \sqrt{M_y / M_{crd}} \quad \text{(Eq. F4.1-3)}$$

$$= \sqrt{149/174} = 0.925 > 0.673 \text{ therefore,}$$

$$M_n = M_{nd} = \left(1 - 0.22\left(\frac{M_{crd}}{M_y}\right)^{0.5}\right)\left(\frac{M_{crd}}{M_y}\right)^{0.5} M_y \quad \text{(Eq. F4.1-2)}$$

$$= (1-0.22(1/0.925))(1/0.925)(149) = 123 \text{ kip-in.}$$

$$\phi_b M_n = (0.90)(123) = 110.7 \text{ kip-in.} = 9.23 \text{ kip-ft} \ge 7.40 \text{ kip-ft} \quad \text{OK} \quad \text{(Eq. B3.2.2-2)}$$

End Span - In the lapped region over the support:

Calculate the design strength based on local buckling interacting with yielding and global buckling using the effective width method in AISI S100 Section F3.1

In the lapped region at the support, the section is assumed to be sufficiently restrained against lateral-torsional buckling and distortional buckling. Because the section is sufficiently restrained against lateral-torsional buckling, the global flexural stress, $F_n = F_y$. The total strength is the sum of the individual strength of the two overlapped purlins.

For the end bay purlin, t = 0.070 in.

$M_n = M_{n\ell} = S_eF_y$ = (2.47)(55) = 135.9 kip-in. or 11.32 kip-ft ≤ $S_{et}F_y$ = (2.47)(55) (Eq. F3.1-1)

For the interior purlin, t = 0.059 in.

$M_n = M_{n\ell} = S_eF_y$ = (1.89)(55) = 104.0 kip-in. or 8.66 kip-ft ≤ $S_{et}F_y$ = (1.89)(55) (Eq. F3.1-1)

Combined strength of purlins

ϕ_bM_n = (0.90)(11.32+8.66) = 18.0 kip-ft > 12.10 kip-ft OK (Eq. B3.2.2-2)

Interior Span - In the region of negative moment between the end of the left lap and the inflection point:

Calculate the allowable lateral-torsional buckling strength per AISI S100 Section F2.1.1

Determine the allowable moment using the distance from the inflection point to the end of the lap as the unbraced length.

$$r_o = \sqrt{r_x^2 + r_y^2 + r_o^2} = \sqrt{(3.42)^2 + (0.89)^2 + (3.90)^2} = 5.26 \text{ in.} \qquad \text{(Eq. F2.1.1-3)}$$

$L_y = L_t$ = 7.43 - 3.50 = 3.93 ft or 47.2 in.

$K_y = K_t$ = 1.0

C_b =1.67 (conservatively assuming a linear moment diagram in this region).

$$I_{yc} = \frac{I_y}{2} = \frac{0.698}{2} = 0.349 \text{ in.}^4$$

$$\sigma_{ey} = \frac{\pi^2 E}{(K_yL_y/r_y)^2} = \frac{\pi^2(29{,}500)}{(1.0(47.2)/0.89)^2} = 104 \text{ ksi} \qquad \text{(Eq. F2.1.1-4)}$$

$$\sigma_t = \frac{1}{Ar_o}\left[GJ + \frac{\pi^2 EC_w}{(K_tL_t)^2}\right]$$

$$= \frac{1}{(0.881)(3.90)}\left[(11{,}300)(0.00102) + \frac{\pi^2(29{,}500)(11.9)}{(1.0(47.2))^2}\right] = 456 \text{ ksi} \qquad \text{(Eq. F2.1.1-5)}$$

$$F_{cre} = \frac{C_br_oA}{S_f}\sqrt{\sigma_{ey}\sigma_t} = \frac{(1.67)(3.90)(0.881)}{2.29}\sqrt{(104)(456)} = 546 \text{ ksi} \qquad \text{(Eq. F2.1.1-1)}$$

Because $F_{cre} > 2.78F_y$, the section is not subject to lateral-torsional buckling and the global flexural buckling stress, $F_n = F_y$ = 55 ksi.

Calculate the design strength based on local buckling interacting with yielding and global buckling using the effective width method in AISI S100 Section F3.1

$M_n = M_{n\ell} = S_eF_n$ = (1.89)(55) = 104.0 kip-in. ≤ $S_{et}F_y$ = (1.89)(55) (Eq. F3.1-1)

ϕ_bM_n = (0.90)(104.0) = 93.6 kip-in. = 7.80 kip-ft > 5.31 kip-ft OK (Eq. B3.2.2-2)

Calculate the allowable distortional buckling strength per Section F4

Since there is no distortional restraint of the bottom flange, take F_{crd}/β from AISI D100 Table II-7 for the 9CS2.5x059

F_{crd} / β = 41.2 ksi

L_{cr} = 25.8 in.

The unbraced length for distortional buckling, L_m, is taken as the distance between the end of the lap and the inflection point.

L_m = 47.2 in. (from above)

L = min(L_{cr}, L_m)

= min(25.8, 47.2) = 25.8 in.

The moments at the ends of the unbraced length are:

M_1 = 0.0 kip-ft at the inflection point

M_2 = 5.31 kip-ft at the end of the lap

$$\beta = 1.0 \le 1 + 0.4\left(L / L_m\right)^{0.7}\left(1 - M_1 / M_2\right)^{0.7} \le 1.3 \quad \text{(Eq. 2.3.3.3-3)}$$

$$= 1.0 \le 1 + 0.4\left(25.8 / 47.2\right)^{0.7}\left(1 - 0 / 5.31\right)^{0.7} \le 1.3$$

$= 1.0 \le 1.26 \le 1.3$ therefore, use β = 1.26

$$F_{crd} = \beta\left(F_{crd} / \beta\right)$$

F_{crd} = 1.26(41.2) = 51.9 ksi

Calculate the distortional buckling design strength per Section F4.1

$M_y = S_{fy}F_y$ (Eq. F4.1-4)

= (2.29)(55) = 126 kip-in.

$M_y = S_{fy}F_y$ (Eq. F4.1-5)

= (2.29)(51.9) = 118.9 kip-in.

$$\lambda_d = \sqrt{M_y / M_{crd}} \quad \text{(Eq. F4.1-3)}$$

$= \sqrt{126 / 118.9}$ = 1.029 > 0.673 therefore,

$$M_n = \left(1 - 0.22\left(\frac{M_{crd}}{M_y}\right)^{0.5}\right)\left(\frac{M_{crd}}{M_y}\right)^{0.5} M_y \quad \text{(Eq. F4.1-2)}$$

= (1-0.22(1/1.029))(1/1.029)(126) = 96.3 kip-in.

$\phi_b M_n$ = (0.90)(96.3) = 86.7 kip-in. = 7.22 kip-ft > 5.31 kip-ft OK (Eq. B3.2.2-2)

Interior Span - At the location of maximum positive moment:

Calculate the flexural design strength per AISI S100 Section I6.2.2 Appendix A

At the location of maximum positive moment, the section is assumed to be partially restrained against lateral-torsional buckling and distortional buckling by the standing seam panel. The ability of the panel to restrain the purlin has been quantified by AISI S908 (R = 0.95).

M_n = $RM_{n\ell o}$
(Eq. I6.2.2-1)

$M_{n\ell o}$ = nominal flexural strength with consideration of local buckling only as determined from AISI S100 Section F3 with $F_n = F_y$.

Utilizing the Effective Width Method of AISI S100 Section F3.1

$M_{n\ell o} = S_eF_y$ = (1.89)(55) = 104.0 kip-in. = 8.66 kip-ft ≤ $S_{et}F_y$ = (1.89)(55) (Eq. F3.1-1)
M_n = R $M_{n\ell o}$ = (0.95)(8.66) = 8.23 kip-ft (Eq. I6.2.2-1)
ϕ_bM_n = (0.90)(8.23) = 7.41 kip-ft > 5.31 kip-ft OK (Eq. B3.2.2-2)

Interior Span - In the region of negative moment between the end of the right lap and the inflection point:

Calculate the allowable lateral-torsional buckling strength per AISI S100 Section F2.1.3

Determine the allowable moment using the distance from the inflection point to the end of the lap as the unbraced length.

L_y= 4.98 - 1.00 = 3.98 ft or 47.8 in.
K_y = 1.0
C_b =1.67 (conservatively assuming a linear moment diagram in this region).

By inspection, the strength check for the right lap will be satisfied, since the unbraced length and the required strength is about the same as those at the left support. Therefore the section is OK

Interior Span - In the lapped region over the center support:

Calculate the design strength based on local buckling interacting with yielding and global buckling using the effective width method in AISI S100 Section F3.1

In the lapped region at the support, the section is assumed to be sufficiently restrained against lateral-torsional buckling and distortional buckling. Because the section is sufficiently restrained against lateral-torsional buckling, the global flexural stress, $F_n = F_y$. The total strength is the sum of the individual strength of the two overlapped purlins.

Combined strength of purlins

ϕ_bM_n = (0.90)(8.66+8.66) = 15.59 kip-ft > 7.08 kip-ft OK (Eq. B3.2.2-2)

3b. Strength for Shear Only (AISI S100 Section G2.1)

Required Strength

By inspection, 1.2 D + 1.6 L_r controls:

V = $V_D + V_{Lr}$

End Span, from left to right:

At left support: V_u = (1.2)(0.14) + (1.6)(0.86) = 1.54 kip
At end of right lap: V_u = (1.2)(0.20) + (1.6)(1.22) = 2.19 kip
At first interior support: V_u = (1.2)(0.23) + (1.6)(1.40) = 2.52 kip

Interior Span, from left to right:

At first interior support:	$V_u = (1.2)(0.21) + (1.6)(1.23) = 2.22$ kip
At end of left lap:	$V_u = (1.2)(0.15) + (1.6)(0.92) = 1.65$ kip
At end of right lap:	$V_u = (1.2)(0.15) + (1.6)(0.93) = 1.67$ kip
At center support:	$V_u = (1.2)(0.17) + (1.6)(1.02) = 1.84$ kip

Design Strength

End Span:

At the left support and right lap, t = 0.070 in. By inspection the end of the right lap controls.

For t = 0.070 in. and the flat depth of the web, h = 8.485 in., the elastic shear buckling stress is

$$F_{cr} = \frac{\pi^2 E k_v}{12(1-\mu^2)(h/t)^2} = \frac{\pi^2(29500)(5.34)}{12(1-0.3^2)(8.485/0.070)^2} = 9.69 \text{ ksi} \quad \text{(Eq. G2.3-2)}$$

where k_v = 5.34 for unreinforced webs

$V_{cr} = A_w F_{cr} = (8.485)(0.070)(9.69) = 5.76$ kip (Eq. G2.3-1)

$V_y = 0.6A_w F_y = 0.6(8.485)(0.070)(55) = 19.60$ kip (Eq. G2.1-5)

$$\lambda_v = \sqrt{\frac{V_y}{V_{cr}}} = \sqrt{\frac{19.60}{5.76}} = 1.845 \quad \text{(Eq. G2.1-4)}$$

$\lambda_v > 1.227$

$V_n = V_{cr} = 5.76$ kip (Eq. G2.1-3a)

$\phi_v V_n = (0.95)(5.76) = 5.47 \text{ kip} \geq 2.19$ kip OK (Eq. B3.2.2-2)

At the first interior support, sum the strength of the two overlapped purlins:

For t = 0.059 in. and the flat depth of the web, h = 8.507 in., the elastic shear buckling stress is

$$F_{cr} = \frac{\pi^2(29500)(5.34)}{12\left(1-0.3^2\right)(8.507/0.059)^2} = 6.85 \text{ ksi}$$

where k_v = 5.34 for unreinforced webs

$V_{cr} = (8.507)(0.059)(6.85) = 3.44$ kip

$V_y = 0.6(8.507)(0.059)(55) = 16.56$ kip

$$\lambda_v = \sqrt{\frac{16.56}{3.44}} = 2.194 > 1.227$$

$V_n = V_{cr} = 3.44$ kip

For the combined section:

$\phi_v V_n = (0.95)(5.76 + 3.44) = 8.74 \text{ kip} \geq 2.52$ kip OK (Eq. B3.2.2-2)

Interior span:

By inspection of the left and right laps, the right lap controls.

$\phi_v V_n = (0.95)(3.44) = 3.27 \text{ kip} \geq 1.67$ kip OK (Eq. B3.2.2-2)

At the center support, sum the strength of the two overlapped purlins. For the combined section:

$\phi_v V_n = (0.95)(3.44 + 3.44) = 6.54 \text{ kip} \geq 1.84$ kip OK (Eq. B3.2.2-2)

3c. Strength for Combined Bending and Shear (AISI S100 Section H2)

End Span:

$$\sqrt{\left(\frac{\overline{M}}{M_{a\ell o}}\right)^2 + \left(\frac{\overline{V}}{V_a}\right)^2} \leq 1.0 \qquad \text{(Eq. H2-1)}$$

where

$M_{a\ell o}$ = Available flexural strength for globally braced members from AISI S100 Section F3 with $F_n = F_y$

= $\phi_b M_n$

V_a = Available shear strength when shear alone is considered in accordance with AISI S100 Sections G2 to G4

= $\phi_v V_n$

$\overline{M}$, $\overline{V}$ = Required strength in accordance with ASD, LRFD, or LSD load combinations

$\phi_b = 0.90$

$\phi_v = 0.95$

At start of right lap, t = 0.070 in.

$$\sqrt{\left(\frac{(7.40)}{(0.90)(11.32)}\right)^2 + \left(\frac{(2.19)}{(0.95)(5.76)}\right)^2} = 0.83 \leq 1.0 \quad \text{OK}$$

At first interior support,

$$\sqrt{\left(\frac{(12.10)}{(0.90)(11.32+8.66)}\right)^2 + \left(\frac{(2.52)}{(0.95)(5.76+3.44)}\right)^2} = 0.73 \leq 1.0 \quad \text{OK}$$

Interior Span:

At end of laps, t = 0.059 in. Right lap controls by inspection.

$$\sqrt{\left(\frac{(5.32)}{(0.90)(8.66)}\right)^2 + \left(\frac{(1.67)}{(0.95)(3.44)}\right)^2} = 0.85 \leq 1.0 \quad \text{OK}$$

At center support,

$$\sqrt{\left(\frac{(7.08)}{(0.90)(8.66+8.66)}\right)^2 + \left(\frac{(1.84)}{(0.95)(3.44+3.44)}\right)^2} = 0.53 \leq 1.0 \quad \text{OK}$$

3d. Web Crippling Strength (AISI S100 Section G5)

Required Strength

By inspection, $1.2D + 1.6L_r$ controls:

$P_u = 1.2P_D + 1.6P_{Lr}$

Supports, from left to right:

At left support: P_u = (1.2)(0.14) + (1.6)(0.86) = 1.54 kip
At first interior support: P_u = (1.2)(0.44) + (1.6)(2.63) = 4.74 kip
At center support: P_u = (1.2)(0.34) + (1.6)(2.03) = 3.66 kip

Design Strength

The bearing length is 5 in.

At end supports use Eq. G5-1 of AISI S100.

$$P_n = Ct^2F_y \sin\theta\left(1 - C_R\sqrt{\frac{R}{t}}\right)\left(1 + C_N\sqrt{\frac{N}{t}}\right)\left(1 - C_h\sqrt{\frac{h}{t}}\right) \qquad \text{(Eq. G5-1)}$$

where

F_y = 55 ksi
θ = 90 degrees
R = 0.1875 in.
N = 5.0 in.
h = 8.485 in.
t = 0.070 in.

From AISI S100 Table G5-2, using the coefficients for the case of Fastened to Support/One-Flange Loading or Reaction/End

C = 4
C_R = 0.14
C_N = 0.35
C_h = 0.02
ϕ_w = 0.85

Check Limits:

R/t = 0.1875/0.070 = 2.68< 9 OK
h/t = 8.485/0.070 = 121 < 200 OK
N/t = 5.0/0.070 = 71.4 < 210 OK
N/h = 5.0/8.485 = 0.59 < 2.0 OK

$$P_n = (4)(0.070)^2(55)\sin 90\left(1 - 0.14\sqrt{\frac{0.1875}{0.070}}\right)\left(1 + 0.35\sqrt{\frac{5.0}{0.070}}\right)\left(1 - 0.02\sqrt{\frac{8.485}{0.070}}\right) = 2.56 \text{ kip}$$

$\phi_w P_n$ = (0.85)(2.56) = 2.18 kip ≥ 1.54 kip OK (Eq. B3.2.2-2)

At interior supports use Eq. G5-1 of AISI S100. For webs consisting of two or more sheets, the nominal strength is calculated for each individual sheet and the results are added to obtain the nominal strength of the full section.

$$P_n = Ct^2F_y \sin\theta\left(1 - C_R\sqrt{\frac{R}{t}}\right)\left(1 + C_N\sqrt{\frac{N}{t}}\right)\left(1 - C_h\sqrt{\frac{h}{t}}\right) \qquad \text{(Eq. G5-1)}$$

where

F_y = 55 ksi
θ = 90 degrees
R = 0.1875 in.
N = 5.0 in.

End Span	Interior Span
h = 8.485 in.	h = 8.507 in.
t = 0.070 in.	t = 0.059 in.

From AISI S100 Table G5-2, using the coefficients for the case of Fastened to Support/One-Flange Loading or Reaction/Interior

$C = 13$
$C_R = 0.23$
$C_N = 0.14$
$C_h = 0.01$
$\phi_w = 0.90$

Check Limits:

End Span	Interior Span
R/t = 0.1875/0.070 = 2.68 < 5 OK	R/t = 0.1875/0.059 = 3.18 < 5 OK
h/t = 8.485/0.070 = 121 < 200 OK	h/t = 8.507/0.059 = 144 < 200 OK
N/t = 5.0/0.070 = 71.4 < 210 OK	N/t = 5.0/0.059 = 84.7 < 210 OK
N/h = 5.0/8.485 = 0.59 < 2.0 OK	N/h = 5.0/8.507 = 0.59 < 2.0 OK

End Span:

$$P_n = (13)(0.070)^2(55)\sin 90\left(1-0.23\sqrt{\frac{0.1875}{0.070}}\right)\left(1+0.14\sqrt{\frac{5.0}{0.070}}\right)\left(1-0.01\sqrt{\frac{8.485}{0.070}}\right) = 4.24 \text{ kip}$$

Interior Span:

$$P_n = (13)(0.059)^2(55)\sin 90\left(1-0.23\sqrt{\frac{0.1875}{0.059}}\right)\left(1+0.14\sqrt{\frac{5.0}{0.059}}\right)\left(1-0.01\sqrt{\frac{8.507}{0.059}}\right) = 2.96 \text{ kip}$$

At first interior support,

$\phi_w P_n$ = (0.90)(4.24+2.96) = 6.48 kip > 4.74 kip OK (Eq. B3.2.2-2)

At center support,

$\phi_w P_n$ = (0.90)(2.96+2.96) = 5.33 kip > 3.66 kip OK (Eq. B3.2.2-2)

3e. Combined Bending and Web Crippling (AISI S100 Section H3)

$$0.88\left(\frac{\overline{P}}{P_n}\right)+\left(\frac{\overline{M}}{M_{n\ell o}}\right) \le 1.46\phi \text{ for 2 C-sections back-to-back}$$ (Eq. H3-2b)

where

$M_{n\ell o}$ = Sum of the nominal flexural strength (resistance) of each purlin in the absence of axial load determined in accordance with AISI S100 Section F3 with $F_n = F_y$.

P_n = Sum of the nominal strength (resistance) of each purlin in the absence of bending moment for concentrated load or reaction determined in accordance with AISI S100 Section G5.

$\phi = 0.90$

Ends of laps of each section are to be connected by a minimum of two 1/2 in. diameter A307 bolts through the web, the combined section is to be connected to the support by a minimum of two 1/2 in. diameter A307 bolts through the flanges, and the webs must be in contact. (Note: If the purlin webs are connected to a welded web plate as shown in Figure 1.2-2, the limit state of combined bending and web crippling does not apply.)

At the first interior support,

$$0.88\left(\frac{4.74}{4.24+2.96}\right)+\left(\frac{12.10}{11.32+8.66}\right) = 1.18 \le (1.46)(0.90) = 1.31 \text{ OK}$$

At center support

$$0.88\left(\frac{3.66}{2.96+2.96}\right)+\left(\frac{7.08}{8.66+8.66}\right) = 0.95 < (1.46)(0.90) = 1.31 \text{ OK}$$

4. Check Uplift Loads

4a. Strength for Bending Only (AISI S100 Section I6.2.2 Appendix A)

Required Strength

By inspection, $0.9M_D + 1.6M_W$ controls.

$M_u = 0.9M_D + 1.6M_w$

End Span:

Moment near center of span: $M_u = (0.9)(0.68)+(1.6)(-3.40) = -4.83$ kip-ft

Interior Span:

Moment near center of span: $M_u = (0.9)(0.30)+(1.6)(-1.48) = -2.10$ kip-ft

Design Strength

Calculate the design flexural strength per AISI S100 Section I6.2.2 Appendix A at the location of maximum negative moment

The section is assumed to be partially restrained against lateral-torsional buckling and distortional buckling by the standing seam panel. The ability of the panel to restrain the purlin has been quantified by AISI S908.

$M_n = RM_{n\ell o}$ (Eq. I6.2.2-1)

R = 0.75 for both purlin thicknesses

End Span:

For t = 0.070 in.

Utilizing the Effective Width Method of AISI S100 Section F3.1

$M_{n\ell o} = S_e F_y = (2.47)(55) = 135.9$ kip-in. = 11.32 kip-ft

$M_n = R\, M_{n\ell o} = (0.75)(11.32) = 8.49$ kip-ft (Eq. I6.2.2-1)

$\phi_b M_n = (0.90)(8.49) = 7.64$ kip-ft > 4.83 kip-ft OK (Eq. B3.2.2-2)

Interior Span:

For t = 0.059 in.

$M_{n\ell o} = S_e F_y = (1.89)(55) = 104.0$ kip-in. = 8.66 kip-ft

$M_n = R\, M_{n\ell o} = (0.75)(8.66) = 6.50$ kip-ft (Eq. I6.2.2-1)

$\phi_b M_n = (0.90)(6.50) = 5.85$ kip-ft > 2.10 kip-ft OK (Eq. B3.2.2-2)

4b. Other Comments

Since the magnitude of the shears, moments and reactions are less than those under the gravity case and the compression flange in all other regions is braced by the panels, it can be concluded that the design satisfies the AISI 100 criteria for uplift.

3.3.2.3 Design Example: Strut Purlin in Standing Seam Roof System - LRFD

Given

1. The four span continuous Z-purlin system with a standing seam roof from Example 3.3.2.1 with the axial forces in the strut purlins from Example 3.3.1.2.
2. Strength Reduction factors from Example 3.3.2.1.
   For Gravity Loads
   R = 0.85 for the 0.085 in. thick purlin
   R = 0.90 for the 0.059 in. thick purlin
   For Uplift Loads
   R = 0.70 for the 0.085 in. thick purlin
   R = 0.70 for the 0.059 in. thick purlin

Required

Using LRFD with ASCE/SEI 7-16 (ASCE 2016) load combinations for endwall wind combined with (a) gravity loads and (b) uplift loads:

1. Check the strength of the strut purlin with respect to axial loads only.
2. Check the strength of the strut purlin with respect to combined axial load and bending. Note that the strength with respect to bending only is provided in Example 3.3.2.1.

Solution

Strut purlins in standing seam systems are analyzed the same way as through-fastened systems with one exception. For standing seam systems, the weak axis flexural buckling strength is calculated according to AISI S100 Section I6.2.4 Appendix A. Consequently, reference is made to Example 3.3.2.1 for all limit states except for weak axis flexural buckling.

Note: The equations referenced in this example refer to AISI S100 equation numbers.

1. Assumptions for Analysis and Application of the AISI S100 Provisions

AISI S100 does not define the methods of analysis to be used; these judgments are the responsibility of the designer. The following assumptions are considered good practice but are not intended to prohibit other approaches:

a. The attachment of the roof panels to the purlin provides partial lateral support to the top flange.
b. Standing seam panels are fastened to the purlin with sliding clips at 24 in. intervals.
c. For the calculation of the distortional buckling strength, the rotational restraint provided by the roof panels, k_ϕ, is included.
d. Since the loading, geometry and materials are symmetrical; only the first two spans are checked.
e. Both flanges are restrained from lateral movement at the supports.
f. Strut purlin forces are generated from wind loads parallel to the ridge. For wind loads parallel to the ridge, roof pressures can either be negative, resulting in a 115 lb/ft uplift or positive, resulting in 0 lb/ft. Consequently, strut forces should be considered both with maximum uplift moments as well as with gravity moments from live and dead load.

g. Flange braces are used to eliminate any additional moment introduced into the purlin resulting from the eccentric axial force transfer to the primary structure.

2. Section Properties

See Example 3.3.1.2.

3. Check Required Strength

LRFD load combinations considered:

(1) $1.2D + 1.0W + 0.5L_r$
(2) $1.2D + 1.6L_r + 0.5W$
(3) $0.9D+1.0W$

These load combinations are summarized in Table 3-7. The controlling load cases are shaded. For load combinations (1) and (2), because they are dominated by gravity load, wind load is conservatively not included in the calculation of maximum moment.

Table 3-7 Axial Forces and Moments for LRFD Load Combinations (1), (2), and (3)

Load Case	(1) $1.2D+1.0W+0.5L_r$	(2) $1.2D+1.6L_r+0.5W$	(3) $0.9D+1.0W$
End Span			
P	1.0(2.2)=2.2	0.5(2.2)=1.1	1.0(2.2)=2.2
M, Near Mid-span	1.2(0.68)+0.5(4.53) =3.08	1.2(0.68)+1.6(4.53) = 8.06	0.9(.68)-1.0(5.21)=-4.60
M, End of Right Lap	-(1.2)0.69-0.5(4.57) =-3.11	-1.2(0.69)-1.6(4.57)=-8.14	-0.9(.69)+1.0(5.25)=4.63
Interior Span			
P	1.0(4.0)=4.0	0.5(4.0)=2.0	1.0(4.0)=4.0
M, End of Right Lap	-1.2(0.49)-0.5(3.28) =-2.23	-1.2(0.49)-1.6(3.28)=-5.84	-0.9(.49)+1.0(3.77)=3.33
M, Near Mid-span	1.2(0.30)+0.5(1.98) =1.35	1.2(0.30)+1.6(1.98)= 3.53	0.9(.30)-1.0(2.27)=-2.00
M, End of Left Lap	-1.2(0.49)-0.5(3.29) =-2.23	-1.2(0.49)-1.6(3.29)=-5.85	-0.9(.49)+1.0(3.78)=3.34

Summary of required strength

End Span, left to right:

Maximum axial force:	P = 2.2 kip
Mid-span positive moment + Axial Force	M = 3.08 kip-ft, P = 2.2 kip
	M = 8.06 kip-ft, P = 1.1 kip
Mid-span negative (uplift) moment + Axial Force	M = -4.6 kip-ft, P = 2.2 kip
Negative Moment at end of right lap + Axial Force	M = -3.11 kip-ft, P = 2.2 kip
	M = -8.14 kip-ft, P = 1.1 kip
Positive (uplift) Moment at end of right lap + Axial Force	M = 4.63 kip-ft, P = 2.2 kip

Interior Span, left to right:

Maximum axial force:	P = 4.0 kip
Mid-span positive moment + Axial Force	M = 1.35 kip-ft, P = 4.0 kip
	M = 3.53 kip-ft, P = 2.0 kip
Mid-span negative (uplift) moment + Axial Force	M = -2.00 kip-ft, P = 4.0 kip
Note: moments at right and left lap nearly identical	
Negative Moment at end of lap + Axial Force	M = -2.23 kip-ft, P = 4.0 kip
	M = -5.85 kip-ft, P = 2.0 kip
Positive (uplift) Moment at end of lap + Axial Force	M = 3.34 kip-ft, P = 4.0 kip

4. Check Allowable Design Strength

4a. Strength for Axial Load Only (AISI S100 Chapter E)

End Span:

Calculate flexural buckling strength about the x-axis per AISI S100 Sections E2 and E3

From Example 3.3.1.2, the axial strength from flexural buckling interacting with local buckling:

$P_{n\ell} = (1.00)(29.8) = 29.8 \text{ kip} < P_{ne}$

Calculate flexural-torsional buckling strength about the weak axis per AISI S100 Section I6.2.4(a) Appendix A

Note that per Section I6.2.4(a) Appendix A, consideration of distortional buckling may be excluded.

Check limits of applicability of Section I6.2.4(a) Appendix A

(1) 0.054 in. ≤ t = 0.085 in. ≤ 0.125 in. OK
(2) 6 in. ≤ d = 8.00 in. ≤ 12 in. OK
(3) Flanges are edge-stiffened compression elements
(4) 70 ≤ d/t (8.00/0.085 = 94.1) ≤ 170 OK
(5) 2.8 ≤ d/b = 8.00/2.75 = 2.9 ≤ 5 OK
(6) $16 \le \dfrac{\text{flat flange width}}{t} = \dfrac{2.350}{0.085} = 27.6 \le 50$ OK
(7) Both flanges prevented from moving laterally at supports OK
(8) F_y (55 ksi) ≤ 70 ksi OK

All Conditions are satisfied.

Compute P_n:

$$P_n = k_{af} R F_y A \qquad \text{(Eq. I6.2.4-1)}$$

90 < d/t = 94.1 ≤ 130

$$k_{af} = 0.72 - \frac{d}{250t} \qquad \text{(Eq. I6.2.4-2)}$$

$$= 0.72 - \frac{8.00}{250(0.085)} = 0.34$$

R = 0.70 from the AISI S908 uplift testing

$P_n = (0.34)(0.70)(55)(1.27)$

= 16.6 kip

The axial strength is governed by the flexural-torsional buckling strength.

ϕP_n= 0.85(16.6) = 14.1 kip > 2.2 kip OK (Eq. B3.2.2-1)

Interior Span

Calculate flexural buckling strength about the x-axis per AISI S100 Sections E2 and E3

From Example 3.3.1.2, the axial strength from local buckling interacting with yielding and global buckling:

$P_{n\ell}$ = (0.579)(33.8) = 19.6 kip < P_{ne}

Calculate flexural-torsional buckling strength about the weak axis per AISI S100 Section I6.2.4(a) Appendix A

Note that per Section I6.2.4(a) Appendix A, consideration of distortional buckling may be excluded.

The section satisfies the eight limits of applicability of Section I6.2.4(a) Appendix A.

Compute P_n:

P_n = $k_{af}RF_yA$

(Eq. I6.2.4-1)

d/t = 8.00/0.059 = 136 > 130

k_{af} = 0.20

R = 0.70 from the AISI S908 uplift testing

P_n = (0.20)(0.70)(55)(0.881) = 6.8 kip

The axial strength is governed by the flexural-torsional buckling strength

ϕP_n= 0.85(6.8) = 5.8 kip > 4.0 kip OK (Eq. B3.2.2-1)

4b. Strength for Combined Compressive Axial Load and Bending (AISI S100 Section H1.2)

The combined strength must be evaluated near mid-span and at the end of the lap for both the end span and interior span for both gravity and uplift cases. The strength for combined bending and axial load at the end of the lap was evaluated for a through-fastened system in Example 3.3.1.2. Those results are unchanged for a standing seam system. However, at the interior of the span, the axial strength of the standing seam system is different and the combined effects must be re-checked.

The axial forces in the purlins are higher for load cases 1 and 3. Conservatively, the second order effects and the effective area of the strut are calculated based on the higher axial load combinations, load cases 1 and 3, and used for load case 2. The design strength of the purlin subjected to bending only is taken from Example 3.3.2.1. Second order effects are calculated in Example 3.3.1.2

End Span – Near mid-span:

Member second order moment amplifier (use conservatively for all load cases)

B_1 = 1.05 (from Example 3.3.1.2)

Use $\overline{M}_{nt}$ = M_x (flange braces preclude rafter rotation)

Calculate the combined effect of compressive axial load and bending per AISI S100 Section H1.2

$$\frac{\overline{P}}{P_a} + \frac{\overline{M}_x}{M_{ax}} + \frac{\overline{M}_y}{M_{ay}} \leq 1.0 \qquad \text{(Eq. H1.2-1)}$$

Gravity loading near mid-span

Load Case 1: M = 3.08 ft-kip P = 2.2 kip

$\overline{M}_{nt}$ = M_x = 3.08 kip-ft

$\overline{M}_x = B_1\overline{M}_{nt} + B_2\overline{M}_{\ell t}$ (Eq. C1.2.1.1-1)

= (1.05)(3.08) + B_2 (0) = 3.23 kip-ft

$\overline{P}$ = 2.2 kip (Load Combination 1)

P_a = 14.1 kip (calculated in Part a)

M_{ax} = (0.9)(11.06) = 9.95 kip-ft (calculated in Example 3.3.2.1)

$$\frac{2.2}{14.1} + \frac{3.23}{9.95} + 0 = 0.48 < 1.0 \text{ OK}$$

Load Case 2: M = 8.06 ft-kip P = 1.1 kip

$\overline{M}_{nt}$ = M_x = 8.06 kip-ft

$\overline{M}_x = B_1\overline{M}_{nt} + B_2\overline{M}_{\ell t}$ (Eq. C1.2.1.1-1)

= (1.05)(8.06) + B_2 (0) = 8.46 kip-ft

$\overline{P}$ = 1.1 kip (Load Combination 2)

P_a = 14.1 kip (calculated in Part a)

M_{ax} = (0.9)(11.06) = 9.95 kip-ft (calculated in Example 3.3.2.1)

$$\frac{1.1}{14.1} + \frac{8.46}{9.95} + 0 = 0.93 < 1.0 \text{ OK}$$

Uplift loading near mid-span

When subjected to uplift loading, the required moment at the mid-span is less than that for gravity moments. However, the design flexural strength is also less when subjected to uplift.

$\overline{M}_{nt}$ = M_x = -4.60 kip-ft

$\overline{M}_x = B_1\overline{M}_{nt} + B_2\overline{M}_{\ell t}$ (Eq. C1.2.1.1-1)

$\overline{M}_x$ = (1.05)(-4.60) + B_2 (0) = -4.83 kip-ft

$\overline{P}$ = 2.2 kip (Load Combination 3)

P_a = 14.1 kip (calculated in Part a)

M_{ax} = (0.9)(9.11) = 8.20 kip-ft (calculated in Example 3.3.2.1)

$$\frac{2.2}{14.13} + \frac{4.83}{8.2} + 0 = 0.74 < 1.0 \text{ OK}$$

Interior Span – Near mid-span:

Member second order moment amplifier (use conservatively for all load cases)

B_1 = 1.11 (from Ex 3.3.1.2)

Use $\overline{M}_{nt}$ = M_x (flange braces preclude rafter rotation)

Calculate the combined effect of compressive axial load and bending per AISI S100 Section H1.2

$$\frac{\overline{P}}{P_a} + \frac{\overline{M}_x}{M_{ax}} + \frac{\overline{M}_y}{M_{ay}} \le 1.0 \qquad \text{(Eq. H1.2-1)}$$

Gravity loading near mid-span

Load Case 1: M = 1.35 kip-ft, P = 4.0 kip

$\overline{M}_{nt}$ = M_x = 1.35 kip-ft

$\overline{M}_x = B_1\overline{M}_{nt} + B_2\overline{M}_{\ell t}$ (Eq. C1.2.1.1-1)

= (1.11)(1.35) + B_2 (0) = 1.50 kip-ft

$\overline{P}$ = 4.0 kip (Load Combination 1)

P_a = 5.8 kip (calculated in Part a)

M_{ax} = (0.9)(7.51) = 6.76 kip-ft (calculated in Example 3.3.2.1)

$$\frac{4.0}{5.80} + \frac{1.50}{6.76} + 0 = 0.91 < 1.0 \text{ OK}$$

Load Case 2: M = 3.53 kip-ft, P = 2.0 kip

$\overline{M}_{nt}$ = M_x = 3.53 kip-ft

$\overline{M}_x = B_1\overline{M}_{nt} + B_2\overline{M}_{\ell t}$ (Eq. C1.2.1.1-1)

= (1.11)(3.53) + B_2(0) = 3.92 kip-ft

$\overline{P}$ = 2.0 kip (Load Combination 2)

P_a = 5.8 kip (calculated in Part a)

M_{ax} = (0.9)(7.51) = 6.76 kip-ft (calculated in Example 3.3.2.1)

$$\frac{2.0}{5.80} + \frac{3.92}{6.76} + 0 = 0.92 < 1.0 \text{ OK}$$

Uplift loading near mid-span

When subjected to uplift loading, the required moment at the mid-span is less than that for gravity moments. However, the design flexural strength is also less when subjected to uplift.

$\overline{M}_{nt}$ = M_x = -2.00 kip-ft

$\overline{M}_x = B_1\overline{M}_{nt} + B_2\overline{M}_{\ell t}$ (Eq. C1.2.1.1-1)

$\overline{M}_x$ = (1.11)(-2.00) + B_2(0) = -2.22 kip-ft

$\overline{P}$ = 4.0 kip (Load Combination 3)

P_a = 5.8 kip (calculated in Part a)

M_{ax} = (0.9)(5.84) = 5.26 kip-ft (calculated in Example 3.3.2.1)

$$\frac{4.0}{5.80}+\frac{2.22}{5.25}+0=1.11>1.0 \text{ NG}$$

To satisfy the combined axial force and bending for the uplift condition, a larger member must be chosen for the interior span.

4c. Other Comments

The axial strength combined with bending must be checked at the ends of the laps for the single purlin. These conditions were checked in Example 3.3.1.2. At the location of the end of the lap, there is no difference in the procedure to calculate strength between the standing seam system of this example and the through-fastened system of Example 3.3.1.2. Since the combined axial force and bending strength exceeded the required strength in Example 3.3.1.2, the strength is sufficient here as well.

3.3.3 Discrete Braced System Design Examples

3.3.3.1 Design Example: Four Span Continuous Z-Purlins Attached to Standing Seam Panels – Discrete Braced System (Gravity and Uplift Loads) -- ASD

Given

1. Four span Z-purlin system using laps at interior support points to create continuity.
2. Roof covering is attached with standing seam panel clips along the entire length of the purlins. The connection between the purlins and the panel provides a rotational stiffness of 0.21 kip-in./rad/in.
3. Twelve purlin lines.
4. F_y = 55 ksi
5. Roof slope = 0.5:12.
6. The top flange of each purlin is facing upslope except the purlin closest to the eave, which has its top flange facing downslope.
7. Discrete braces that prevent lateral movement and torsional rotation are provided at each third point of each purlin.
8. Welded web plates 1/4-in. thick x 5 in. wide x 7.5 in. tall are provided at each support location.
9. The loads shown are parallel to the purlin webs.

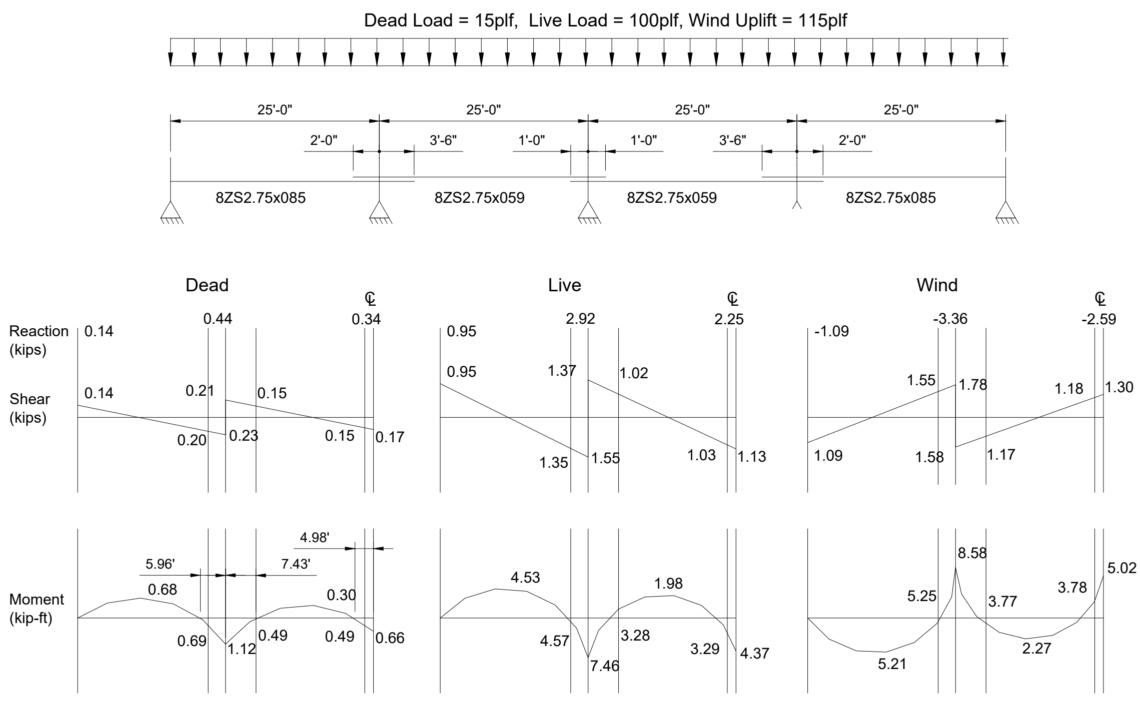

Notes: 1) Moments and forces are from unfactored nominal loads
2) Lap dimensions are shown to connection points of purlins

Figure 3.3-5 Shear and Moment Diagrams

Required

1. Check the design using ASD with ASCE/SEI 7-16 (ASCE 2016) load combinations for Gravity Loads.
2. Check the design using ASD with ASCE/SEI 7-16 (ASCE 2016) load combinations for Wind Uplift Loads.

Solution

Note: The equations referenced in this example refer to AISI S100 equation numbers.

1. Assumptions for Analysis and Application of the AISI S100 Provisions

AISI S100 does not define the methods of analysis to be used; these judgments are the responsibility of the designer. The following assumptions are considered good practice but are not intended to prohibit other approaches:

a. The standing seam roof system is designed as discrete braced. The restraining effects of the panels on global buckling are ignored although they are considered for distortional buckling.
b. The purlins are connected within the lapped portions in a manner that achieves full continuity between the individual purlin members.
c. The continuous beam analysis to establish the shear and moment diagrams assumes continuous non-prismatic members between supports in which I_x within the lapped portions is the sum of the individual members. Gross values of I_x are used for the beam analysis.
d. The strength within the lapped portions is assumed to be the sum of the strengths of the individual members.
e. For gravity loads, the region at and near the interior supports is assumed to be not subject to lateral-torsional or distortional buckling between the support and the ends of the laps.
f. Under uniform gravity loading, the negative moment region between the end of the lap and the inflection point is assumed to have an unbraced length for lateral-torsional and distortional buckling equal to the distance from the end of the lap to the inflection point.
g. Since the loading, geometry and materials are symmetrical; only the first two spans are checked.

2. Section Properties

The following section properties are from AISI D100 Table I-4 and Table II-4.

<u>Interior Bays</u>	<u>End Bays</u>
For: 8ZS2.75x059	For: 8ZS2.75x085
d = 8 in.	d = 8 in.
t = 0.059 in.	t = 0.085 in.
I_x = 8.69 in.^{4}	I_x = 12.40 in.^{4}
$S_f = S_{fy}$ = 2.17 in.^{3}	$S_f = S_{fy}$ = 3.11 in.^{3}
S_e = 1.82 in.^{3}	S_e = 2.84 in.^{3}
I_y = 1.72 in.^{4}	I_y = 2.51 in.^{4}

Both sections have inside bend radius, R = 0.1875 in. and flange width, b = 2.75 in.

3. Check Gravity Loads

3a. Strength for Bending Only (AISI S100 Chapter F)

Required Strength

ASD load combinations considered:

(1) D

(2) D + L_r

By inspection, D + L_r controls:

$M = M_D + M_{Lr}$

End Span, from left to right:

Maximum positive moment:	M = 0.68 + 4.53 = 5.21 kip-ft
Negative moment at end of right lap:	M = 0.69 + 4.57 = 5.26 kip-ft
Negative moment at support:	M = 1.12 + 7.46 = 8.58 kip-ft

Interior span, from left to right:

Negative moment at end of left lap:	M = 0.49 + 3.28 = 3.77 kip-ft
Maximum positive moment:	M = 0.30 + 1.98 = 2.28 kip-ft
Negative moment at end of right lap:	M = 0.49 + 3.29 = 3.78 kip-ft
Negative moment at center support:	M = 0.66 + 4.37 = 5.03 kip-ft

Allowable Design Flexural Strength

End Span - At the location of maximum positive moment:

The allowable flexural strength is the minimum of the global buckling, local buckling and the distortional buckling strength.

Calculate the allowable global buckling strength per AISI S100 Section F2.1

$L_y = 25/3 = 8.33$ ft = 100 in.

$I_{yc} = \frac{I_y}{2} = \frac{2.51}{2} = 1.255 \text{ in.}^4$

$K_y = 1.0$

$C_b \approx 1.0$ (Moment is approximately uniform.)

$$F_{cre} = \frac{C_b \pi^2 E d I_{yc}}{2S_f(K_y L_y)^2} = \frac{(1.0)\pi^2(29500)(8.0)(1.255)}{(2)(3.11)((1.0)100)^2} = 47.0 \text{ ksi} \quad \text{(Eq. F2.1.3-2)}$$

$0.56F_y = (0.56)(55) = 30.8$ ksi

$2.78F_y = (2.78)(55) = 153$ ksi

For $2.78F_y > F_{cre} > 0.56F_y$, use Eq. F2.1-2

$$F_n = \frac{10}{9}F_y\left(1 - \frac{10F_y}{36F_{cre}}\right) \quad \text{(Eq. F2.1-2)}$$

$$= \frac{10}{9}(55)\left(1 - \frac{10(55)}{36(47.0)}\right) = 41.2 \text{ ksi}$$

$M_{ne} = S_f F_n$ (Eq. F2.1-1)

$= (3.11)(41.2) = 128$ kip-in. = 10.7 kip-ft

$\frac{M_n}{\Omega_b} = \frac{128}{1.67} = 76.6$ kip-in. = 6.39 kip-ft ≥ 5.21 kip-ft OK (Eq. B3.2.1-2)

Calculate the allowable strength based on local buckling interacting with yielding and global buckling using the effective width method in AISI S100 Section F3.1

The stress at which global buckling will occur is $F_n = 41.2$ ksi. The effective section modulus of the shape should be calculated at this stress level as shown in AISI D100 Example I-10. At the stress level $F_n = 41.2$ ksi, the section is found to be fully effective, i.e. $S_e = S_f = 3.11$ in.^{3}. Note that the effective section modulus calculated at $F_y = 55$ ksi for the 8ZS2.75x085 is tabulated in AISI D100 Table II-4 ($S_e = 2.84$ in.^{3}). Conservatively, this effective section modulus calculated at a higher stress level may be used. Using the fully effective section modulus, the strength for local buckling interacting with global buckling is

$M_n = M_{n\ell} = S_e F_n = (3.11)(41.2) = 128.1$ kip-in. $\leq S_{et} F_y = (3.11)(41.2)$ (Eq. F3.1-1)

$\frac{M_n}{\Omega_b} = \frac{128.1}{1.67} = 76.7$ kip-in. = 6.39 kip-ft ≥ 5.21 kip-ft OK (Eq. B3.2.1-2)

Calculate the allowable distortional buckling strength per AISI S100 Section F4

Calculate the elastic distortional buckling stress F_{crd}. The distortional buckling rotational restraint provided by the panels, $k_\phi = 0.21$ kip-in./rad/in. Conservatively, this rotational restraint can be ignored. Use the analytical solution procedure in Appendix 2 Section 2.3.3.3 of AISI S100 in lieu of the more conservative procedure from the Commentary accompanying Appendix 2 Section 2.3.3.3. From AISI D100 Table II-9 for the 8ZS2.75x085

$k_{\phi fe} = 0.795$ kip

$\tilde{k}_{\phi fg} = 0.0269$ in.^{2}

$k_{\phi we} = 0.712$ kip

$\tilde{k}_{\phi wg} = 0.00259$ in.^{2}

$k_\phi = 0.210$ kip-in./rad/in.

$$F_{crd} = \beta \frac{k_{\phi fe} + k_{\phi we} + k_\phi}{\tilde{k}_{\phi fg} + \tilde{k}_{\phi wg}} \quad \text{(Eq. 2.3.3.3-2)}$$

$$F_{crd}/\beta = \frac{0.795 + 0.712 + 0.210}{0.0269 + 0.00259} = 58.2 \text{ ksi}$$

Because there is virtually no moment gradient, $\beta = 1.0$

$F_{crd} = \beta\left(F_{crd}/\beta\right)$

$F_{crd} = 1.0(58.2) = 58.2$ ksi

Calculate the allowable distortional buckling strength per AISI S100 Section F4.1

$M_y = S_{fy} F_y$ (Eq. F4.1-4)

$= (3.11)(55) = 171$ kip-in.

$M_{crd} = S_f F_{crd}$ (Eq. F4.1-5)

$= (3.11)(58.2) = 181$ kip-in.

$\lambda_d = \sqrt{M_y / M_{crd}}$ (Eq. F4.1-3)

$= \sqrt{171/181} = 0.972 > 0.673$ therefore,

$$M_n = M_{nd} = \left(1 - 0.22\left(\frac{M_{crd}}{M_y}\right)^{0.5}\right)\left(\frac{M_{crd}}{M_y}\right)^{0.5} M_y \quad \text{(Eq. F4.1-2)}$$

$= (1\text{-}0.22(1/0.972))(1/0.972)(171) = 136$ kip-in.

$\frac{M_n}{\Omega_b} = \frac{136}{1.67} = 81.5$ kip-in. $= 6.79$ kip-ft ≥ 5.21 kip-ft OK (Eq. B3.2.1-2)

End Span - In the region of negative moment between the end of the lap and the inflection point:

Note that the unbraced segment between the interior third point brace and the inflection point is deemed OK by inspection because it has a shorter unbraced length, lower maximum moment magnitude, and there is a significant moment gradient.

Calculate the allowable lateral-torsional buckling strength per AISI S100 Section F2.1.3

Determine the allowable moment using the distance from the inflection point to the lap as the unbraced length.

$L_y = 5.96 - 2.00 = 3.96$ ft $= 47.5$ in.

$K_y = 1.0$

$I_{yc} = \frac{I_y}{2} = \frac{2.51}{2} = 1.255$ in.^{4}

$C_b = 1.67$ (Conservatively assumes linear moment diagram in this region).

$$F_{cre} = \frac{C_b \pi^2 E d I_{yc}}{2S_f (K_y L_y)^2} = \frac{(1.67)\pi^2 (29500)(8.0)(1.255)}{(2)(3.11)((1.0)47.5)^2} = 347.9 \text{ ksi} \quad \text{(Eq. F2.1.3-2)}$$

$2.78F_y = (2.78)(55) = 153$ ksi

Since $F_{cre} > 2.78F_y$, the section is not subject to lateral-torsional buckling and the global flexural stress, $F_n = F_y = 55$ ksi.

Calculate the allowable strength based on local buckling interacting with yielding and global buckling using the effective width method in AISI S100 Section F3.1

$M_n = M_{n\ell} = S_e F_n = (2.84)(55) = 156.2$ kip-in. $\leq S_{et} F_y = (2.84)(55)$ (Eq. F3.1-1)

$\frac{M_n}{\Omega_b} = \frac{156.2}{1.67} = 93.5$ kip-in. $= 7.79$ kip-ft ≥ 5.26 kip-ft OK (Eq. B3.2.1-2)

Calculate the allowable distortional buckling strength per AISI S100 Section F4

Calculate the elastic distortional buckling stress F_{crd}, for the negative moment region. Since the compression flange has no sheeting, there is no distortional restraint of the bottom flange,

$k_\phi = 0$. Use the analytical solution procedure in Appendix 2 Section 2.3.3.3 of AISI S100 in lieu of the more conservative procedure from the Commentary accompanying Appendix 2 Section 2.3.3.3. From AISI D100 Table II-9 for the 8ZS2.75x085

$k_{\phi fe} = 0.795$ kip

$\tilde{k}_{\phi fg} = 0.0269$ in.^{2}

$k_{\phi we} = 0.712$ kip

$\tilde{k}_{\phi wg} = 0.00259$ in.^{2}

$$F_{crd} = \beta \frac{k_{\phi fe} + k_{\phi we} + k_\phi}{\tilde{k}_{\phi fg} + \tilde{k}_{\phi wg}} \qquad \text{(Eq. 2.3.3.3-2)}$$

$$F_{crd}/\beta = \frac{0.795 + 0.712 + 0.0}{0.0269 + 0.00259} = 51.1 \text{ ksi}$$

Alternatively, F_d/β for the case where k_ϕ=0 may be taken from Table II-9 (F_d/β = 51.1 ksi)

From Table II-9

$L_{cr} = 21.7$ in.

The bottom flange is not restrained from rotation by the panel or other discrete bracing. Therefore, the unbraced length for distortional buckling, L_m, is taken as the distance between the end of the lap and the inflection point.

L_m = 47.5 in. (from above)

$L = \min(L_{cr}, L_m)$

$= \min(21.7, 47.5) = 21.7$ in.

The moments at the ends of the segment are:

M_1 = 0.0 kip-ft at the inflection point

M_2 = 5.26 kip-ft at the end of the lap

$$\beta = 1.0 \le 1 + 0.4\left(L/L_m\right)^{0.7}\left(1 - M_1/M_2\right)^{0.7} \le 1.3 \qquad \text{(Eq. 2.3.3.3-3)}$$

$$= 1.0 \le 1 + 0.4\left(21.7/47.5\right)^{0.7}\left(1 - 0/5.26\right)^{0.7} \le 1.3$$

$= 1.0 \le 1.23 \le 1.3$ therefore, use $\beta = 1.23$

$F_{crd} = \beta\left(F_{crd}/\beta\right) = 1.23(51.1) = 62.9$ ksi

Calculate the allowable distortional buckling strength per Section F4.1

$M_y = S_{fy}F_y$ (Eq. F4.1-4)

$= (3.11)(55) = 171$ kip-in.

$M_{crd} = S_f F_{crd}$ (Eq. F4.1-5)

$= (3.11)(62.9) = 196$ kip-in.

$\lambda_d = \sqrt{M_y/M_{crd}}$ (Eq. F4.1-3)

$= \sqrt{171/196} = 0.934 > 0.673$ therefore,

$$M_n = M_{nd} = \left(1 - 0.22\left(\frac{M_{crd}}{M_y}\right)^{0.5}\right)\left(\frac{M_{crd}}{M_y}\right)^{0.5} M_y \qquad \text{(Eq. F4.1-2)}$$

$= (1\text{-}0.22(1/0.934))(1/0.934)(171) = 140$ kip-in

$$\frac{M_n}{\Omega_b} = \frac{140}{1.67} = 83.8 \text{ kip-in.} = 7.0 \text{ kip-ft} \geq 5.26 \text{ kip-ft OK} \qquad \text{(Eq. B3.2.1-2)}$$

End Span - In the lapped region over the support:

Calculate the allowable strength based on local buckling interacting with yielding and global buckling using the effective width method in AISI S100 Section F3.1.

In the lapped region at the support, the section is assumed to be sufficiently restrained against lateral-torsional buckling and distortional buckling. Because the section is sufficiently restrained against lateral-torsional buckling, the global flexural stress, $F_n = F_y$. The total strength is the sum of the individual strength of the two overlapped purlins.

For the end bay purlin, t = 0.085 in.

$M_n = M_{n\ell} = S_eF_y = (2.84)(55) = 156.2$ kip-in. or 13.02 kip-ft $\leq S_{et}F_y = (2.84)(55)$ (Eq. F3.1-1)

For the interior purlin, t = 0.059 in.

$M_n = M_{n\ell} = S_eF_y = (1.82)(55) = 101.1$ kip-in. or 8.34 kip-ft $\leq S_{et}F_y = (1.82)(55)$ (Eq. F3.1-1)

Combined strength of purlins

$$\frac{M_n}{\Omega_b} = \frac{13.02 + 8.34}{1.67} = 12.79 \text{ kip-ft} \geq 8.58 \text{ kip-ft OK} \qquad \text{(Eq. B3.2.1-2)}$$

Interior Span - In the region of negative moment between the end of the left lap and the inflection point:

Note that the unbraced segment between the interior third point brace and the inflection point is deemed OK by inspection because it has a shorter unbraced length, lower maximum moment magnitude, and there is a significant moment gradient.

Calculate the allowable lateral-torsional buckling strength per AISI S100 Section F2.1.3

Determine the allowable moment using the distance from the inflection point to the end of the lap as the unbraced length. Note, AISI 100 Section F2.1.3 allows use of either Eq. F2.1.3-1 or F2.1.3-2. Eq. F2.1.3-2 is generally conservative and is chosen for simplicity.

L_y = 7.43 - 3.50 = 3.93 ft or 47.2 in.
K_y = 1.0

C_b =1.67 (conservatively assuming a linear moment diagram in this region)

$$I_{yc} = \frac{I_y}{2} = \frac{1.72}{2} = 0.86 \text{ in.}^4$$

$$F_{cre} = \frac{(1.67)\pi^2(29500)(8.0)(0.86)}{(2)(2.17)((1.0)47.2)^2} = 346 \text{ ksi} > (2.78)(55) = 153 \text{ ksi} \qquad \text{(Eq. F2.1.3-2)}$$

Since F_{cre} > $2.78F_y$, the section is not subject to lateral-torsional buckling and the global flexural stress, $F_n = F_y = 55$ ksi.

Calculate the allowable strength based on local buckling interacting with yielding and global buckling using the effective width method in AISI S100 Section F3.1

$M_n = M_{n\ell} = S_eF_n = (1.82)(55) = 100.1$ kip-in. $\leq S_{et}F_y = (1.82)(55)$ (Eq. F3.1-1)

$\frac{M_n}{\Omega_b} = \frac{100.1}{1.67} = 59.9$ kip-in = 5.00 kip-ft ≥ 3.77 kip-ft OK (Eq. B3.2.1-2)

Calculate the allowable distortional buckling strength per AISI S100 Section F4

Since there is no distortional restraint of the bottom flange, take F_d/β from AISI D100 Table II-9 for the 8ZS2.75x059

$F_d/\beta = 32.5$ ksi

$L_{cr} = 25.4$ in.

The unbraced length for distortional buckling, L_m, is taken as the distance between the end of the lap and the inflection point.

L_m = 47.2 in. (from above)

$L = \min(L_{cr}, L_m)$

$= \min(25.4, 47.2) = 25.4$ in.

The moments at the ends of the segment are:

M_1 = 0.0 kip-ft at the inflection point

M_2 = 3.77 kip-ft at the end of the lap

$\beta = 1.0 \leq 1 + 0.4\left(L / L_m\right)^{0.7}\left(1 - M_1 / M_2\right)^{0.7} \leq 1.3$ (Eq. 2.3.3.3-3)

$= 1.0 \leq 1 + 0.4\left(25.4 / 47.2\right)^{0.7}\left(1 - 0 / 3.77\right)^{0.7} \leq 1.3$

$= 1.0 \leq 1.26 \leq 1.3$ therefore, use $\beta = 1.26$

$F_{crd} = \beta\left(F_d / \beta\right)$

$F_{crd} = 1.26(32.5) = 41.0$ ksi

Calculate the allowable distortional buckling strength per Section F4.1

$M_y = S_{fy}F_y$ (Eq. F4.1-4)

$= (2.17)(55) = 119$ kip-in.

$M_{crd} = S_fF_{crd}$

(Eq. F4.1-5)

$= (2.17)(41.0) = 89.0$ kip-in.

$\lambda_d = \sqrt{M_y / M_{crd}}$ (Eq. F4.1-3)

$= \sqrt{119 / 89.0} = 1.156 > 0.673$ therefore,

$$M_n = \left(1 - 0.22\left(\frac{M_{crd}}{M_y}\right)^{0.5}\right)\left(\frac{M_{crd}}{M_y}\right)^{0.5} M_y \quad \text{(Eq. F4.1-2)}$$

$$= \left(1 - 0.22\left(\frac{1}{1.16}\right)\right)\left(\frac{1}{1.16}\right)(119) = 83.1 \text{ kip-in.}$$

$$\frac{M_n}{\Omega_b} = \frac{83.1}{1.67} = 49.8 \text{ kip-in.} = 4.15 \text{ kip-ft} \geq 3.77 \text{ kip-ft OK} \qquad \text{(Eq. B3.2.1-2)}$$

Interior Span - At the location of maximum positive moment:

The allowable flexural strength is the minimum of the global buckling, local buckling and the distortional buckling strength.

Calculate the allowable global buckling strength per AISI S100 Section F2.1

L_y= 25/3 = 8.33 ft = 100 in.

$$I_{yc} = \frac{I_y}{2} = \frac{1.72}{2} = 0.86 \text{ in.}^4$$

K_y = 1.0

$C_b \approx$ 1.0 (Moment is approximately uniform).

$$F_{cre} = \frac{C_b \pi^2 E d I_{yc}}{2S_f (K_y L_y)^2} = \frac{(1.0)\pi^2(29500)(8.0)(0.86)}{(2)(2.17)((1.0)100)^2} = 46.2 \text{ ksi} \qquad \text{(Eq. F2.1.3-2)}$$

$0.56F_y$ = (0.56)(55) = 30.8 ksi

$2.78F_y$ = (2.78)(55) = 153 ksi

For $2.78F_y > F_{cre} > 0.56F_y$, use Eq. F2.1-2

$$F_n = \frac{10}{9}F_y\left(1 - \frac{10F_y}{36F_{cre}}\right) \qquad \text{(Eq. F2.1-2)}$$

$$= \frac{10}{9}(55)\left(1 - \frac{10(55)}{36(46.2)}\right) = 40.9 \text{ ksi}$$

$M_{ne} = S_f F_n$ (Eq. F2.1-1)

= (2.17)(40.9) = 88.8 kip-in.

$$\frac{M_n}{\Omega_b} = \frac{88.8}{1.67} = 53.2 \text{ kip-in.} = 4.43 \text{ kip-ft} \geq 2.28 \text{ kip-ft OK} \qquad \text{(Eq. B3.2.1-2)}$$

Calculate the allowable strength based on local buckling interacting with yielding and global buckling using the effective width method in AISI S100 Section F3.1

The stress at which global buckling will occur is F_n = 40.9 ksi. The effective section modulus of the shape should be calculated at this stress level as shown in AISI D100 Example I-10. At the stress level F_n = 40.8 ksi, the effective section modulus S_e = 2.00 in.^{3}. Note that the effective section modulus calculated at F_y = 55 ksi for the 8ZS2.75X059 is tabulated in AISI D100 Table II-4 (S_e = 1.81). Conservatively, this effective section modulus calculated at a higher stress level may be used. Using the fully effective section modulus, the strength for local buckling interacting with global buckling is

$M_n = M_{n\ell} = S_e F_n$ = (2.00)(40.9) = 81.8 kip-in. $\leq S_{et}F_y$ =(2.00)(40.9) (Eq. F3.1-1)

$\frac{M_n}{\Omega_b} = \frac{81.8}{1.67}$ = 49.0 kip-in. = 4.08 kip-ft ≥ 2.28 kip-ft OK (Eq. B3.2.1-2)

Calculate the allowable distortional buckling strength per AISI S100 Section F4.1

Calculate the elastic distortional buckling stress F_d. The rotational restraint provided by the panels, k_ϕ = 0.21 kip-in./rad/in, can improve the distortional buckling strength, but it can be conservatively ignored. Use the analytical solution procedure in Appendix 2 Section 2.3.3.3 of AISI S100 in lieu of the more conservative procedure from the Commentary accompanying Appendix 2 Section 2.3.3.3. From AISI D100 Table II-9 for the 8ZS2.75x059

$k_{\phi fe}$ = 0.250 kip

$\tilde{k}_{\phi fg}$ = 0.0134 in.^{2}

$k_{\phi we}$ = 0.230 kip

$\tilde{k}_{\phi wg}$ = 0.00132 in.^{2}

k_ϕ = 0.21 kip-in./rad/in.

$$F_{crd} = \beta \frac{k_{\phi fe} + k_{\phi we} + k_\phi}{\tilde{k}_{\phi fg} + \tilde{k}_{\phi wg}} \quad \text{(Eq. 2.3.3.3-2)}$$

$$F_{crd}/\beta = \frac{0.250 + 0.230 + 0.210}{0.0134 + 0.00132} = 46.9 \text{ ksi}$$

Because there is virtually no moment gradient, β = 1.0

$$F_{crd} = \beta\left(F_{crd}/\beta\right)$$

$$F_{crd} = 1.0(46.9) = 46.9 \text{ ksi}$$

Calculate the allowable distortional buckling strength per AISI S100 Section F4.1

$M_y = S_{fy}F_y$ (Eq. F4.1-4)

= (2.17)(55) = 119 kip-in.

$M_{crd} = S_f F_{crd}$ (Eq. F4.1-5)

= (2.17)(46.9) = 102 kip-in.

$\lambda_d = \sqrt{M_y / M_{crd}}$ (Eq. F4.1-3)

= $\sqrt{119/102}$ = 1.080 > 0.673 therefore,

$$M_n = \left(1 - 0.22\left(\frac{M_{crd}}{M_y}\right)^{0.5}\right)\left(\frac{M_{crd}}{M_y}\right)^{0.5} M_y \quad \text{(Eq. F4.1-2)}$$

= (1-0.22(1/1.080))(1/1.080)(119) = 87.7 kip-in.

$\frac{M_n}{\Omega_b} = \frac{87.7}{1.67}$ = 5256 kip-in. = 4.38 kip-ft ≥ 2.28 kip-ft OK (Eq. B3.2.1-2)

Interior Span - In the lapped region over the center support:

Calculate the allowable strength based on local buckling interacting with yielding and global buckling using the effective width method in AISI S100 Section F3.1

In the lapped region at the support, the section is assumed to be sufficiently restrained against lateral-torsional buckling and distortional buckling. Because the section is sufficiently restrained against lateral-torsional buckling, the global flexural stress, $F_n = F_y$. The total strength is the sum of the individual strength of the two overlapped purlins.

Combined strength of purlins

$$\frac{M_n}{\Omega_b} = \frac{8.34 + 8.34}{1.67} = 9.99 \text{ kip-ft} \geq 5.03 \text{ kip-ft} \quad \text{OK} \qquad \text{(Eq. B3.2.1-2)}$$

3b. Strength for Shear Only (AISI S100 Section G2.1)

The shear strength is the same as calculated in Examples 3.3.1.1 and 3.3.2.1

3c. Strength for Combined Bending and Shear (AISI S100 Section H2)

The strength for combined bending and shear is calculated the same as in Examples 3.3.1.1 and 3.3.1.2.

3d. Web Crippling Strength (AISI S100 Section G5)

At each support location, the purlins are attached by a welded web plate (welded web plate provides discrete brace at the support location. The welded web plate eliminates the possibility of web crippling and therefore does not need to be checked.

3e. Combined Bending and Web Crippling (AISI S100 Section H3)

Connection through welded web plate at each support location eliminates the possibility of web crippling.

4. Check Uplift Loads

4a. Strength for Bending Only (AISI S100 Chapter F)

When designing with discrete braces, the influence of the panels is ignored except when calculating distortional buckling strength. In the positive moment regions, because the net uplift forces are less than the gravity forces, global buckling and local buckling interacting with global buckling are OK by inspection. Because the influence of the panels rotationally restraining the compression flange was included in the calculation of the distortional buckling strength under gravity loads, the distortional buckling strength must be re-calculated for uplift loads. In the negative moment regions for gravity loads, the panels do not contribute to the strength. Therefore, the available strength in the negative moment regions calculated for gravity loads is conservative for uplift loads.

Required Strength

By inspection, $0.6M_D + 0.6M_W$ controls.

$M = 0.6M_D + 0.6M_w$

End Span:

Moment near center of span: $M = [(0.6)(0.68) - (0.6)(5.21)] = -2.72$ kip-ft

Interior Span:

Moment near center of span: $M = [(0.6)(0.30) - (0.6)(2.27)] = -1.18$ kip-ft

Allowable Design Flexural Strength:

End Span:

Calculate the allowable distortional buckling strength near the middle of the end span per AISI S100 Section F4

Since there is no distortional restraint of the bottom flange, take F_d/β from AISI D100 Table II-9 for the 8ZS2.75x085

F_d/β = 51.1 ksi

Because there is virtually no moment gradient, β = 1.0

$F_{crd} = \beta\left(F_d / \beta\right)$

F_{crd} = 1.0(51.1) = 51.1 ksi

Calculate the allowable distortional buckling strength per AISI S100 Section F4.1

$M_y = S_{fy}F_y$ (Eq. F4.1-4)

= (3.11)(55) = 171 kip-in.

$M_{crd} = S_fF_{crd}$

(Eq. F4.1-5)

= (3.11)(51.1) = 159 kip-in.

$\lambda_d = \sqrt{M_y / M_{crd}}$ (Eq. F4.1-3)

= $\sqrt{171/159}$ = 1.037 > 0.673 therefore,

$$M_n = M_{nd} = \left(1 - 0.22\left(\frac{M_{crd}}{M_y}\right)^{0.5}\right)\left(\frac{M_{crd}}{M_y}\right)^{0.5} M_y \quad \text{(Eq. F4.1-2)}$$

= (1-0.22(1/1.037))(1/1.037)(171) = 130 kip-in.

$\frac{M_n}{\Omega_b} = \frac{130}{1.67}$ = 77.8 kip-in. = 6.49 kip-ft ≥ 2.72 kip-ft OK (Eq. B3.2.1-2)

Interior Span:

Calculate the allowable distortional buckling strength near the middle of the interior span per AISI S100 Section F4

Since there is no distortional restraint of the bottom flange, take F_d/β from AISI D100 Table II-9 for the 8ZS2.75x059

F_d/β = 32.5 ksi

Because there is virtually no moment gradient, β = 1.0

$F_{crd} = \beta\left(F_d / \beta\right)$

F_{crd} = 1.0(32.5) = 32.5 ksi

Calculate the allowable distortional buckling strength per AISI S100 Section F4.1

$M_y = S_{fy}F_y$ (Eq. F4.1-4)

= (2.17)(55) = 119 kip-in.

$M_{crd} = S_fF_{crd}$ (Eq. F4.1-5)

= (2.17)(32.5) = 70.5 kip-in.

$$\lambda_d = \sqrt{M_y / M_{crd}} \quad \text{(Eq. F4.1-3)}$$

$$= \sqrt{119 / 70.5} = 1.299 > 0.673 \text{ therefore,}$$

$$M_n = \left(1 - 0.22\left(\frac{M_{crd}}{M_y}\right)^{0.5}\right)\left(\frac{M_{crd}}{M_y}\right)^{0.5} M_y \quad \text{(Eq. F4.1-2)}$$

$$= (1\text{-}0.22(1/1.299))(1/1.299)(119) = 76.0 \text{ kip-in.}$$

$$\frac{M_n}{\Omega_b} = \frac{76.0}{1.67} = 45.5 \text{ kip-in.} = 3.79 \text{ kip-ft} \geq 1.18 \text{ kip-ft OK} \quad \text{(Eq. B3.2.1-2)}$$

4b. Other Comments

Since the magnitude of the shears, moments and reactions are approximately 65 percent of those of the gravity case, it can be concluded that the design satisfies the AISI S100 criteria for uplift.

5. Calculate Brace Forces

Forces in the discrete braces are calculated according to the envelope method from AISI S100 Section C2.2.1 in Example 3.3.3.2 and according to the displacement compatibility method in Example 3.3.3.3.

3.3.3.2 Design Example: Discrete Brace Forces for Four Span Continuous Z-Purlin System (ASD) – AISI S100 Envelope Method

Given

The system of purlins analyzed for the strength limit states in Example 3.3.3.1

Required

Calculate the brace forces according to the envelope method in AISI S100 Section C2.2.1

Solution

At the support locations, discrete bracing is provided by a welded web plate as shown in Figure 3.3-6. At the third points along the span, bracing is provided by a channel with a moment connection to the web of the purlin as shown in Figure 3.3-7. The brace forces will be resolved as a net axial force and a moment. Brace forces are calculated in each span. For a brace at an interior support, the net brace force is the sum of the brace forces from each span.

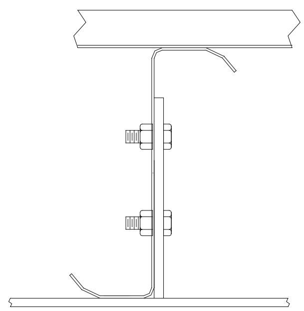

Figure 3.3-6 Welded Web Plate

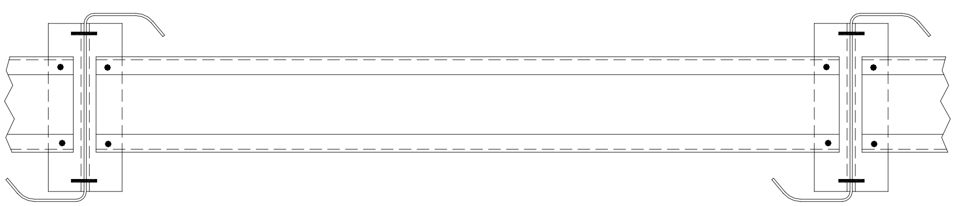

Figure 3.3-7 Third Point Discrete Braces

The ASD load combination that will result in the largest brace forces is:

$D + L_r$

The uniformly applied force,

$w = 15 \text{ lb/ft} + 100 \text{ lb/ft} = 115 \text{ lb/ft}$

For the slope 0.5:12

$\theta = 2.39°$

Using the positive directions shown in Figure 3.2-7, the components of distributed force w_x, w_y are

w_y = -(115)cos(2.39) = -114.9 lb/ft
w_x = -(115)sin(2.39) = -4.80 lb/ft

The eccentricity of the applied load on the top flange is typically assumed to be 1/3 of the flange width

e_{sx} = 2.75/3 = 0.917 in.

The centerline distance between braces

a = 8.33 ft = 100 in.

For an interior brace on a typical field purlin

W_y = -(8.33)(114.9) = -957 lb
W_x = -(8.33)(4.80) = -40.0 lb

For the ridge purlin, which is assumed to have half the tributary width of the typical field purlin

W_y = -479 lb
W_x = -20.0 lb

For the eave purlin which has its top flange facing downslope

W_y = -479 lb
W_x = -20.0 lb

Note that the above design loads are for the interior third point braces. For the braces at the exterior support location, the design load will be half of the adjacent third point forces because the tributary width at the support is half of the width of the third point brace. At an interior support, the design force equals the sum of force from each span adjacent to the support.

End Span - Unsymmetric Bending

The unsymmetric bending factor

$K' = I_{xy}/(2I_x)$ = 4.11/((2)(12.40)) = 0.166 (AISI S100 Eq. C2.2.1-5)

where I_{xy} is from AISI D110 Table I-4.

For the interior braces, the total brace force for unsymmetric bending at both flanges is

$P_{unsym,int} = P_1 + P_2 = 2(1.5(W_yK'))$ = 2(1.5(-957)(0.166)) = -477 lb (Eq. 3.2-3)

The braces at the support location must balance the interior brace force from unsymmetric bending. From symmetry,

$P_{unsym,spt}$ = -(-477) = 477 lb

The unsymmetric bending forces at the eave and ridge purlin are half the field purlin. Because the eave purlin has its top flanges facing downslope, the brace forces will be directed in the opposite direction of the field and ridge purlins.

End Span - Downslope Forces

The net downslope brace force is the sum of the brace forces at the flanges. At the interior brace

$P_{down,int} = P_1 + P_2 = (-1.5(W_x/2)+(-1.5(W_x/2)= (-1.5(-40/2)+ (-1.5(-40/2) = 60$ lb (Eq. 3.2-3)

At the exterior support location, the brace force is half that of the interior brace

$P_{down,spt} = 60/2 = 30$ lb

The downslope brace forces in the eave and ridge purlin are half of the field purlin because the tributary width is half that of a field purlin.

End Span - Overturning Moment

The couple created by the difference between P_1 and P_2 at the interior brace for a field purlin is

$M_{z,int} = 1.5(-W_x e_{sy} + W_y e_{sx}) = 1.5(-(-40)(8.00/2) + (-957)(0.917)) = -1078$ lb-in. (Eq. 3.2-1)

Note that in the above calculation, a factor of 1.5 is applied from Eq. C2.2.1-1/C.2.2.1-2) to give an equivalent result.

At the ridge purlin interior brace, the moment will be half that of a field purlin.

$M_{z,int\ ridge} = -1077/2 = -539$ kip-in.

At the eave purlin interior brace, the downslope moment is in the same direction as the overturning moment.

$M_{z,int\ eave} = 1.5(-(-20)(8.00/2) - (-479)(0.917)) = 779$ kip-in. (Eq. 3.2-1)

Note that in the above calculation, a factor of 1.5 is applied from Eq. C2.2.1-1/C.2.2.1-2) to give an equivalent result.

For a field purlin at the support location, the overturning moment is half the moment at the interior brace

$M_{z,spt} = -1077/2 = -539$ kip-in.

For a ridge purlin at the support location, the overturning moment is half that of a field purlin.

$M_{z,spt\ ridge} = -539/2 = -270$ kip-in.

For an eave purlin at the support location, the downslope moment is in the same direction as the overturning moment. The overturning moment is half that of the eave third point brace.

$M_{z,spt\ eave} = 779/2 = 390$ kip-in.

The analysis results for the end span are summarized in Table 3-8.

Interior Span - Unsymmetric Bending, Downslope Forces, and Overturning Moment

The interior span is analyzed using the same procedure as the end span, although the calculations are not shown. The analysis results are summarized in Table 3-8.

Table 3-8 Brace Forces Generated by Each Purlin

		End Span				Interior Span			
		Support	3rd Point	Support, Left Side	Support, Net	Support, Right Side	3rd Point	Support, Left Side	Support, Net
Field Purlin	$P_{unsymmetric}$, lb	477	-477	477	948	471	-471	471	942
	$P_{downslope}$, lb	30	60	30	60	30	60	30	60
	P_L, lb	507	-417	507	1008	501	-417	501	1002
	M_z, lb-in.	-539	-1077	-539	-1078	-539	-1077	-539	-1078
Ridge Purlin	$P_{unsymmetric}$, lb	239	-239	239	474	235	-235	235	470
	$P_{downslope}$, lb	15	30	15	30	15	30	15	30
	P_L, lb	254	-209	254	504	250	-205	250	500
	M_z, lb-in.	-270	-539	-270	-540	-270	-539	-270	-540
Eave Purlin	$P_{unsymmetric}$, lb	-239	239	-239	-474	-235	235	-235	-470
	$P_{downslope}$, lb	15	30	15	30	15	30	15	30
	P_L, lb	-224	269	-224	-444	-220	265	-220	-440
	M_z, lb-in.	390	779	390	780	390	779	390	780
Total P_L			-4110				-4110		

Force Exerted on Welded Web Plate

The net force on a brace at an interior support location is the sum of the brace forces on each side. The most heavily loaded brace occurs at the first interior frame line for a field purlin. The net horizontal force on the welded web plate applied at the mid-height of the purlin is

P_L = 507 + 501 = 1008 lb

The net torsional moment is

M_z = -539 -539 = -1078 lb-in.

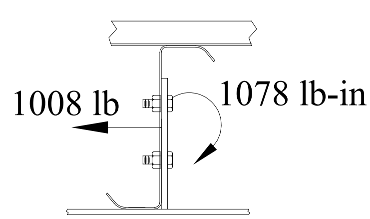

Figure 3.3-8 Forces on Web Plate

Collection of Forces and Moments at Third Point Braces

End moments are generated at each end of the braces. These moments are balanced by a couple from the end shears as shown in Figure 3.3-9. An imbalance of moments can induce an additional downward (or upward) force in the plane of the web. If the bracing member is essentially continuous through the connections, the bracing will distribute minor imbalances through the system. If there are large imbalances, or if there are discontinuities in the bracing member, the end shears at the bracing members can be significant and should be investigated for the impact on the additional flexural demand placed on the purlins.

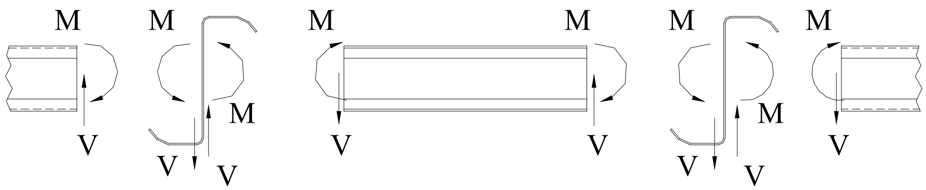

Figure 3.3-9 Balance of Moment for Interior Brace

The axial forces are transferred to the primary structure through a truss as shown in Figure 3.3-11. The axial force in the horizontal braces collects from the ridge to the eave as shown in Figure 3.3-10. The designer must consider this collection of forces in the design of the connections of the braces to each purlin. The net force transferred to the truss at each third point is

P_L = -209 + 10(-417) + 269 = -4110 lb

The distribution of the forces in the eave truss is shown in Figure 3.3-11. Note that the eave member must be designed as a strut purlin because of the axial force introduced to the member. At the first field purlin from the eave, there is a tension force introduced into this purlin between the third point braces, which also needs to be considered in the design of this purlin.

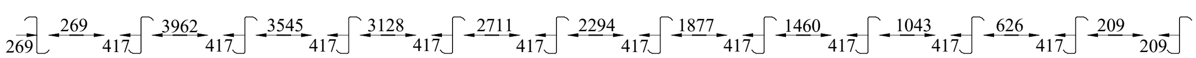

Figure 3.3-10 Collection of Brace Axial Forces

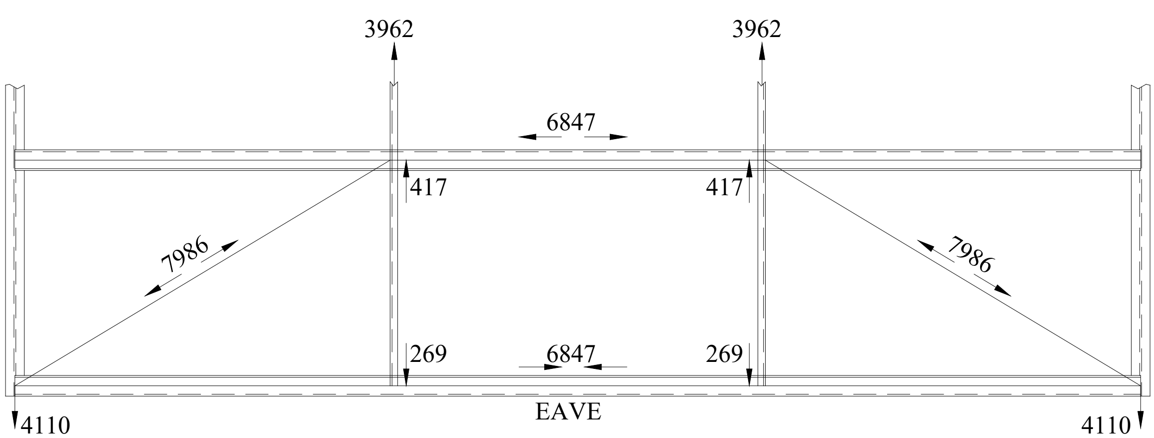

Figure 3.3-11 Eave Truss to Transfer Brace Forces

3.3.3.3 Design Example: Discrete Brace Forces for Four Span Continuous Z-Purlin System (ASD) – Displacement Compatibility Method

Given

The system of purlins analyzed for the strength limit states in Example 3.3.3.1

Required

Calculate the brace forces according to the displacement compatibility method in Section 3.2.9.3 of this guide.

Solution

Similar to the previous example, the brace forces will be resolved as a net axial force and an overturning moment. Combining equations (Eq. 3.2-6) and (Eq. 3.2-7), the net axial force is

$$P_L = P_{L1}+P_{L2} = 2\alpha C_1 U_y K' - C_2 U_x \qquad \text{(Eq. 3.2-10)}$$

The design load, U, is defined in Table 3-5. For the uniformly distributed load, U = wL.

Since both the end span and interior span are the same length, for the typical field purlin

$U = (-115)(25) = -2875$ lb

$U_y = (-2875)\cos(2.39) = -2872$ lb

$U_x = (-2875)\sin(2.39) = -120$ lb

The eccentricity of the applied load on the top flange is again assumed to be 1/3 the flange width

$e_{sx} = 2.75/3 = 0.917$ in.

and

$e_{sy} = d/2 = 8.00/2 = 4$ in.

For Z-sections since the shear center is located at the centroid, m = 0.

End Span

The unsymmetric bending factor is

$K' = I_{xy}/(2I_x) = 4.11/((2)(12.40)) = 0.166$ (AISI S100 Eq. C2.2.1-5; also Eq. 3.2-8)

The braces will be analyzed from the end support to the first interior support. The pertinent portion of Table 3-5 is repeated here to provide the coefficients.

		B1	B2	B3	B4
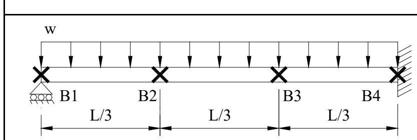	C_1	$-\frac{342}{1404}$	$\frac{531}{1404}$	$\frac{450}{1404}$	$-\frac{639}{1404}$
	C_2	$\frac{184.5}{1404}$	$\frac{531}{1404}$	$\frac{450}{1404}$	$\frac{238.5}{1404}$

The brace at the end support location corresponds with brace B1 from the charts (C_1 = -342/1404, C_2 = 184.5/1404, and C_3 =1).

The net axial force at the brace marked as B1 in the above figure is the sum of the forces at the top and bottom flanges.

$P_L = P_{L1} + P_{L2} = 2\alpha C_1 U_y K' - C_2 U_x$ (Eq. 3.2-10)

$= 2(1)\left(\frac{-342}{1404}\right)(-2872)(0.166) - \left(\frac{184.5}{1404}\right)(-120)$

$= 248$ lb

The moment at the brace location B1 is

$M_z = C_2\left(-U_x e_{sy} + \alpha U_y(e_{sx} - C_3 m)\right) + \alpha C_1 C_3 U_y m$ (Eq. 3.2-9)

$= \frac{184.5}{1404}\left(-(-120)(4) + (1)(-2872)(0.917 - 0)\right) + 0$

$= -283$ lb-in.

At the first interior third point brace location (B2), the coefficients are (C_1 = 531/1404, C_2 = 531/1404, and C_3 = 1).

The net axial force at the brace is the sum of the forces at the top and bottom flanges.

$P_L = 2\left(\frac{531}{1404}\right)(-2872)(0.166) - \left(\frac{531}{1404}\right)(-120)$

$= -315$ lb

The moment at the brace is

$M_z = \frac{531}{1404}\left(-(-120)(4) + (-2872)(0.917 - 0)\right) + 0$

$= -815$ lb-in.

The second interior third point brace (B3) and the brace at the frame line (B4) are calculated similarly. For the second interior third point, with $C_1 = C_2$ = 450/1404

P_L = -267 lb

M_z = -690 lb-in.

For the brace at the frame line, with C_1 = -639/1404, C_2 = 238.5/1404, and C_3 = 1.

P_L = 454 lb

M_z = -366 lb-in.

For the ridge purlin, because the tributary area is half that of a field purlin, the brace forces will be half that of a field purlin. The brace forces are summarized in Table 3-9.

The eave purlin has half the tributary width of a field purlin and the top flange pointed downslope (α = -1).

At the end support location, the net brace force is

$P_L = P_{L1} + P_{L2} = 2\alpha C_1 U_y K' - C_2 U_x$ (Eq. 3.2-10)

$= 2(-1)\left(\frac{-342}{1404}\right)(-1436)(0.166) - \left(\frac{184.5}{1404}\right)(-60)$

$= -108$ lb

and the moment at the brace is

$M_z = C_2\left(-U_x e_{sy} + \alpha U_y(e_{sx} - C_3 m)\right) + \alpha C_1 C_3 U_y m$ (Eq. 3.2-9)

$= \frac{184.5}{1404}\left(-(-60)(4) + (-1)(-1436)(0.917 - 0)\right) + 0$

$= 205$ lb-in.

The remaining brace locations on the end span are calculated similarly and are tabulated in Table 3-9.

Interior Span

For the interior span, the coefficients C_1 and C_2 are again provided in Table 3-5. The pertinent portion of the Table 3-5 is again recreated here.

		B1	B2	B3	B4
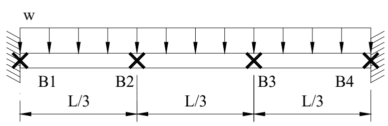	C_1	$-\frac{1}{3}$	$\frac{1}{3}$	$\frac{1}{3}$	$-\frac{1}{3}$
	C_2	$\frac{1}{6}$	$\frac{1}{3}$	$\frac{1}{3}$	$\frac{1}{6}$

Using these coefficients for the interior span, the brace forces are calculated in the same manner as the end span and are tabulated in Table 3-9. At the first interior support location, the effect on the welded web plate at each purlin line is the sum of the forces and moments from each adjacent span. Likewise, at the middle support, since the system is symmetric, the net force is twice the force applied from one side. The net force at each support location is tabulated in Table 3-9. Because the third point braces are restrained by a truss at the eave, the brace forces accumulate in the third point braces moving from the ridge to the eave (see previous example). The total third point brace forces that must be restrained at the eave are tabulated in Table 3-9.

Table 3-9 Brace Forces Generated at Each Purlin and Total Brace Force

		End Span					Interior Span				
		Support	3rd Point, 1st Int.	3rd Point, 2nd Int.	Support Left Side	Support Net	Support Right Side	3rd Point, 1st Int.	3rd Point, 2nd Int.	Support Left Side	Support Net
Field Purlin	P_L, lb	248	-315	-267	454	792	338	-278	-278	337	676
	M_z, lb-in.	-283	-815	-690	-366	-725	-359	-718	-718	-359	-718
Ridge Purlin	P_L, lb	124	-157	-133	227	396	169	-139	-139	169	338
	M_z, lb-in.	-142	-407	-345	-183	-363	-180	-359	-359	-180	-360
Eave Purlin	P_L, lb	-108	203	172	-207	-356	-149	179	179	-149	-298
	M_z, lb-in.	205	589	499	264	523	259	519	519	259	518
Total P_L			-3104	-2631				-2740	-2740		

Comments

Note that the brace forces and moments using the alternate displacement compatibility method, summarized in Table 3-9 are approximately 20% to 50% less than the forces and moments using equations in AISI S100, summarized in Table 3-8, for this particular bracing configuration. The AISI S100 equations are a simplified method intended to envelop all bracing configurations and will typically result in conservative results. The compatibility method is a more accurate representation of the actual brace forces.

3.3.3.4 Example: Strut Purlin in Standing Seam Roof System with Discrete Braces - ASD

Given

1. The four span continuous Z-purlin system with a standing seam roof and third point discrete braces from Example 3.3.3.1 with the axial forces in the strut purlins from Example 3.3.3.1.2.

Required

Using ASD with ASCE/SEI 7-10 (ASCE 2010) load combinations for axial wind combined with (a) gravity loads and (b) uplift loads

1. Check the strength with respect to axial loads only
2. Check the strength with respect to combined axial load and bending. Note that the strength with respect to bending only is provided in Example 3.3.3.1.

Solution

Note: The equations referenced in this example refer to the AISI S100 equation numbers.

1. Assumptions and Design Values for Analysis and Application of AISI S100 Provisions

AISI S100 does not define the methods of analysis to be used; these judgments are the responsibility of the designer. The following assumptions are considered good practice but are not intended to prohibit other approaches:

a. The standing seam roof system is designed as discrete braced. The restraining effects of the panels on global buckling are ignored although they are considered for distortional buckling.

b. Standing seam panels are fastened to the purlin with sliding clips at 24 in. intervals.

c. Panel has a rotational stiffness of 0.21 kip-in./rad/in. determined by tests in accordance with AISI S901.

d. Since the loading, geometry and materials are symmetrical; only the first two spans are checked.

e. Both flanges are restrained from lateral movement at the supports

f. Strut purlin forces are generated from wind loads parallel to the ridge. For wind loads parallel to the ridge, roof pressures can either be negative, resulting in a 115 lb/ft uplift or positive, resulting in 0 lb/ft. Consequently, strut forces should be considered both with maximum uplift moments as well as with gravity moments from live and dead load.

g. Flange braces are used to eliminate any additional moment introduced into the purlin resulting from the eccentric axial force transfer to the primary structure.

2. Section Properties

The following section properties are from AISI D100 Table I-4 and Table II-4.

Interior Bays
For: 8ZS2.75x059
d = 8 in.
t = 0.059 in.
A_g = 0.881 in.^{2}
I_x = 8.69 in.^{4}
I_y = 1.72 in.^{4}
r_x = 3.14 in.
r_y = 1.40 in.
S_f = 2.17 in.^{3}
S_e = 1.82 in.^{3}
J = 0.00102 in.^{4}
C_w = 19.3 in.^{6}

End Bays
For: 8ZS2.75x085
d = 8 in.
t = 0.085 in.
A_g = 1.27 in.^{2}
I_x = 12.40 in.^{4}
I_y = 2.51 in.^{4}
r_x = 3.13 in.
r_y = 1.41 in.
S_f = 3.11 in.^{3}
S_e = 2.84 in.^{3}
J = 0.00306 in.^{4}
C_w = 28.0 in.^{6}

Both sections have inside bend radius, R = 0.1875 in. and flange width, b = 2.75 in.

3. Required Strength

ASD load combinations considered:

(1) $D + 0.75L_r + 0.75(0.6)W$
(2) $0.6D+0.6W$

Table 3-10 Axial Forces and Moments for ASD Load Combination

Load Case	(1) $D+0.75L_r+0.75(0.6)W$	(2) $0.6D+0.6W$
End Span		
P	0.75(0.6)(2.2)=0.99	0.6(2.2)=1.32
M, Near Mid-span	0.68+0.75(4.53)+0.75(0.6)(0) = 4.08	0.6(.68)-0.6(5.21)=-2.72
M, End of Right Lap	-0.69-0.75(4.57)+0.75(0.6)(0) = -4.12	-0.6(.69)+0.6(5.25)= 2.74
Interior Span		
P	0.75(0.6)(4.0)=1.8	0.6(4.0)=2.4
M, End of Right Lap	-0.49-0.75(3.28)+0.75(0.6)(0) = -2.95	-0.6(.49)+0.6(3.77)= 1.97
M, Near Mid-span	0.30+0.75(1.98)+0.75(0.6)(0) = 1.79	0.6(.30)-0.6(2.27)=-1.18
M, End of Left Lap	-0.49-0.75(3.29)+(0.75(0.6)(0) = -2.96	-0.6(.49)+0.6(3.78)= 1.97

Shaded cells represent the maximum load effects.

Summary of required strength

End Span:

Maximum axial force: P = 1.32 kip
Mid-span positive moment + Axial Force M = 4.08 kip-ft, P = 0.99 kip
Mid-span negative (uplift) moment + Axial Force M = -2.72 kip-ft, P = 1.32 kip
Negative Moment at end of right lap + Axial Force M = -4.12 kip-ft, P = 0.99 kip

Positive (uplift) Moment at end of right lap + Axial Force M = 2.74 kip-ft, P = 1.32 kip

Interior Span:

Maximum axial force: P = 2.40 kip
Mid-span positive moment + Axial Force M = 1.79 kip-ft, P = 1.80 kip
Mid-span negative (uplift) moment + Axial Force M = -1.18 kip-ft, P = 2.40 kip
Note: moments at right and left lap nearly identical
Negative Moment at end of lap + Axial Force M = -2.96 kip-ft, P = 1.80 kip
Positive (uplift) Moment at end of lap + Axial Force M = 1.97 kip-ft, P = 2.40 kip

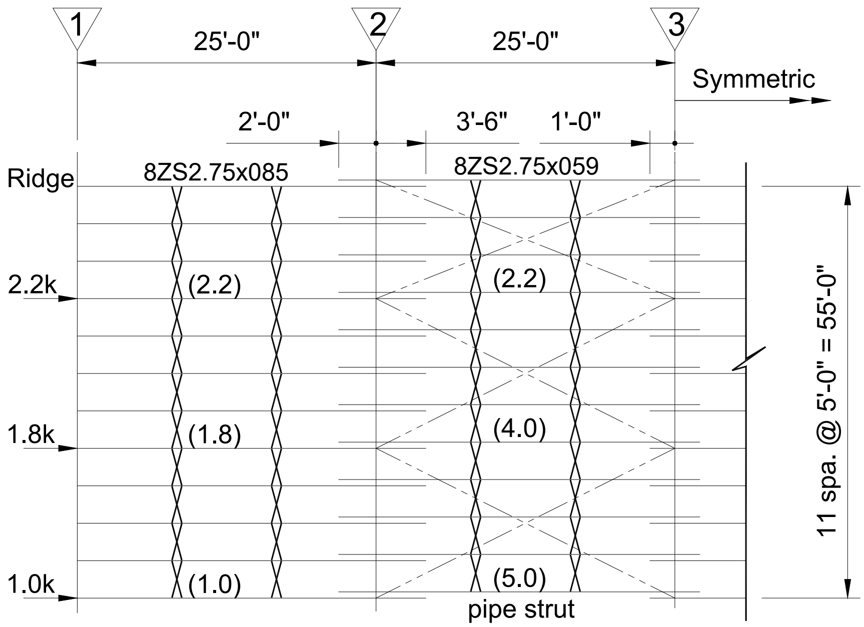

Figure 3.3-12 Applied Forces and Axial Force in Strut Purlins

3a. Strength for Axial Load Only (AISI S100 Chapter E)

End Span:

The purlin must be checked for global buckling about both the x- and y-axes. For buckling about the x-axis, the effective length, KL, is the distance from the end support to the interior lap. For buckling about the y-axis, the unbraced length is the distance between braces. Similarly, the section is unrestrained against torsion over the length between the braces. As a result, according to AISI S100 Section E2.3, for the point symmetric Z-sections, the elastic critical stress is the minimum of the flexural buckling stress and the torsional buckling stress.

Determine the global flexural buckling stress per AISI S100 Section E2.1

$K_x = K_y = K_t = 1.0$

$L_x = 25 \text{ ft} - 2 \text{ ft} = 23 \text{ ft} = 276 \text{ in.}$

$L_y = L_t = 8.33 \text{ ft} = 100 \text{ in.}$

$$\frac{K_x L_x}{r_x} = \frac{(1.0)276}{3.13} = 88.2$$

$$\frac{K_yL_y}{r_y} = \frac{(1.0)100}{1.41} = 70.9$$

Because $\frac{K_xL_x}{r_x} > \frac{K_yL_y}{r_y}$ flexural buckling about the x-axis will control

$$F_{cre} = \frac{\pi^2 E}{(K_xL_x / r_x)^2} \quad \text{(Eq. E2.1-1)}$$

$$= \frac{\pi^2 (29500)}{(88.2)^2} = 37.4 \text{ ksi}$$

Determine the torsional buckling stress per AISI S100 Section E2.2

$$r_o = \sqrt{r_x^2 + r_y^2 + x_o^2} \quad \text{(Eq. E2.2-4)}$$

$$= \sqrt{3.13^2 + 1.41^2 + 0} = 3.43 \text{ in.}$$

$$\sigma_t = \frac{1}{Ar_o^2}\left[GJ + \frac{\pi^2 EC_w}{(K_tL_t)^2}\right] \quad \text{(Eq. E2.2-5)}$$

$$= \frac{1}{1.27(3.43)^2}\left[11300(0.00306) + \frac{\pi^2 (29500)(28.0)}{((1.0)100)^2}\right]$$

$$= 56.9 \text{ ksi}$$

Since the flexural buckling stress, F_{cre} = 37.4 ksi, is less than the torsional buckling stress, σ_t, flexural buckling will control.

$$\lambda_c = \sqrt{\frac{F_y}{F_{cre}}} \quad \text{(Eq. E2-4)}$$

$$= \sqrt{\frac{55}{37.4}} = 1.21 < 1.50$$

$$F_n = \left(0.658^{\lambda_c^2}\right)F_y \quad \text{(Eq. E2-2)}$$

$$= \left(0.658^{(1.21)^2}\right)55 = 29.8 \text{ ksi}$$

Determine the strength from local buckling interacting with yielding and global buckling per AISI S100 Section E3

$$P_{n\ell} = A_eF_n < P_{ne} \quad \text{(Eq. E3.1-1)}$$

The effective area is calculated similar to Example I-10 in AISI D100. The flanges and flange stiffeners are fully effective and the web is subject to local buckling for f = 29.8 ksi.

A_e = 1.00 in.^{2}

$P_{n\ell}$ = (1.00)(29.8) = 29.8 kip $\leq P_{ne}$

$$\frac{P_n}{\Omega_c} = \frac{29.8}{1.80} = 16.6 \text{ kip} \geq 1.32 \text{ kip OK} \qquad \text{(Eq. B3.2.1-2)}$$

Calculate the allowable distortional buckling strength per AISI S100 Section E4

Calculate the elastic distortional buckling stress F_{crd}. Use the analytical solution procedure in Appendix 2 Section 2.3.3.3 of AISI S100 in lieu of the more conservative procedure from the Commentary accompanying Appendix 2 Section 2.3.3.3. The connection of the standing seam panels does provide some rotational restraint to the purlin. The torsional stiffness of this connection is quantified by k_ϕ = 0.21 kip-in./rad/in. Because this restraint is applied to only one flange at intervals of the clip spacing (typically 16 in. or 24 in) the resistance that it contributes to the distortional buckling strength is may be less Therefore, the distortional buckling restraint provided by the panels is conservatively ignored in calculating the distortional buckling strength for axial loads. Other distotional buckling properties for the 8ZS2.75x085 can be determined from AISI D100 Table II-9.

$k_{\phi fe}$ = 0.795 kip

$\tilde{k}_{\phi fg}$ = 0.0269 in.^{2}

$k_{\phi we}$ = 0.712 kip

$\tilde{k}_{\phi wg}$ = 0.00259 in.^{2}

k_ϕ = 0 kip-in./rad/in. (conservative to ignore partial contribution from panels)

$$F_{crd} = \frac{k_{\phi fe} + k_{\phi we} + k_\phi}{\tilde{k}_{\phi fg} + \tilde{k}_{\phi wg}} \qquad \text{(Eq. 2.3.1.3-2)}$$

$$F_{crd} = \frac{0.795 + 0.712 + 0}{0.0269 + 0.00259} = 51.1 \text{ ksi}$$

The elastic distortional buckling load, P_{crd}, is calculated

$$P_{crd} = A_g F_{crd} \qquad \text{(Eq. 2.3.1.3-1)}$$

$$= (1.27)(51.1) = 64.9 \text{ kip}$$

Calculate the allowable distortional buckling strength per AISI S100 Section E4.1

$$P_y = A_g F_y = (1.27)(55) = 69.9 \text{ kip} \qquad \text{(Eq. E4.1-4)}$$

$$\lambda_d = \sqrt{P_y / P_{crd}} \qquad \text{(Eq. E4.1-3)}$$

$$= \sqrt{69.9/64.9} = 1.038 > 0.561 \text{ therefore,}$$

$$P_{nd} = \left(1 - 0.25\left(\frac{P_{crd}}{P_y}\right)^{0.6}\right)\left(\frac{P_{crd}}{P_y}\right)^{0.6} P_y \qquad \text{(Eq. E4.1-2)}$$

$$= \left(1 - 0.25\left(\frac{64.9}{69.9}\right)^{0.6}\right)\left(\frac{64.9}{69.9}\right)^{0.6}(69.9) = 50.9 \text{ kip}$$

$$\frac{P_n}{\Omega_c} = \frac{50.9}{1.80} = 28.3 \text{ kip} \geq 1.32 \text{ kip OK} \qquad \text{(Eq. B3.2.1-2)}$$

Interior Span:

Determine the global flexural buckling stress per AISI S100 Section E2.1

$K_x = K_y = K_t = 1.0$

L_x = 25 ft – 3.5 ft – 1 ft = 20.5 ft = 246 in.

$L_y = L_t$ = 8.33 ft = 100 in.

$$\frac{K_x L_x}{r_x} = \frac{(1.0)246}{3.14} = 78.3$$

$$\frac{K_y L_y}{r_y} = \frac{(1.0)100}{1.40} = 71.4$$

Since $\frac{K_x L_x}{r_x} > \frac{K_y L_y}{r_y}$ flexural buckling about the x-axis will control

$$F_{cre} = \frac{\pi^2 (29500)}{(78.3)^2} = 47.5 \text{ ksi}$$

Determine the torsional buckling stress per AISI S100 Section E2.2

$$r_o = \sqrt{3.14^2 + 1.40^2 + 0} = 3.44 \text{ in.}$$

$$\sigma_t = \frac{1}{0.881(3.44)^2}\left[11300(0.00102) + \frac{\pi^2(29500)(19.3)}{((1.0)100)^2}\right]$$

= 55.0 ksi

Since the flexural buckling stress, F_{cre} = 47.5 ksi, is less than the torsional buckling stress, σ_t, flexural buckling will control.

$$\lambda_c = \sqrt{\frac{55}{47.5}} = 1.08 < 1.50$$

$$F_n = \left(0.658^{(1.08)^2}\right)55 = 33.8 \text{ ksi}$$

Determine the strength from local buckling interacting with yielding and global buckling per AISI S100 Section E3

$P_{n\ell} = A_e F_n \le P_{ne}$ (Eq. E3.1-1)

The effective area is calculated similar to Example I-10 in AISI D100. The web, flanges and flange stiffeners are subject to local buckling for f = 33.8 ksi.

A_e = 0.579 in.^{2}

$P_{n\ell}$ = (0.579)(33.8) = 19.6 k < P_{ne}

$$\frac{P_n}{\Omega_c} = \frac{19.6}{1.80} = 10.9 \text{ kip} \ge 2.40 \text{ kip OK}$$ (Eq. B3.2.1-2)

Calculate the allowable distortional buckling strength per Section E4.1

From AISI D100 Table II-9 for the 8ZS2.75x059

$k_{\phi fe}$ = 0.250 kip

$\tilde{k}_{\phi fg}$ = 0.0134 in.^{2}

$k_{\phi we}$ = 0.230 kip

$\tilde{k}_{\phi wg}$ = 0.00132 in.^{2}

k_{ϕ} = 0 kip-in./rad/in. (conservative to ignore partial contribution from panels)

$$F_{crd} = \frac{k_{\phi fe} + k_{\phi we} + k_{\phi}}{\tilde{k}_{\phi fg} + \tilde{k}_{\phi wg}} \qquad \text{(Eq. 2.3.1.3-2)}$$

$$F_{crd} = \frac{0.250 + 0.230 + 0}{0.0134 + 0.00132} = 32.6 \text{ ksi}$$

The elastic distortional buckling load, P_{crd}, is calculated

$$P_{crd} = A_g F_{crd} \qquad \text{(Eq. 2.3.1.3-1)}$$

$$= (0.881)(32.6) = 28.7 \text{ kip}$$

Calculate the allowable distortional buckling strength per AISI S100 Section E4.1

$$P_y = A_g F_y = (0.881)(55) = 48.5 \text{ kip}$$

$$\lambda_d = \sqrt{P_y / P_{crd}} \qquad \text{(Eq. E4.1-3)}$$

$$= \sqrt{48.5 / 28.7} = 1.300 > 0.561 \text{ therefore,}$$

$$P_{nd} = \left(1 - 0.25\left(\frac{P_{crd}}{P_y}\right)^{0.6}\right)\left(\frac{P_{crd}}{P_y}\right)^{0.6} P_y \qquad \text{(Eq. E4.1-2)}$$

$$= \left(1 - 0.25\left(\frac{28.7}{48.5}\right)^{0.6}\right)\left(\frac{28.7}{48.5}\right)^{0.6}(48.5) = 28.9 \text{ kip}$$

$$\frac{P_n}{\Omega_c} = \frac{28.9}{1.80} = 16.1 \text{ kip} \geq 2.40 \text{ kip OK} \qquad \text{(Eq. B3.2.1-2)}$$

3b. Strength for Combined Compressive Axial Load and Bending (AISI S100 Section H1.2)

The combined strength must be evaluated near mid-span and at the end of the lap for both the end span and interior span for both gravity and uplift cases. The strength for combined bending and axial load at the end of the lap was evaluated for a through-fastened system in Example 3.3.1.2. Those results are unchanged for this system with discrete braces because the bottom flange is in flexural compression and is unrestrained in both cases. However, at the interior of the span, the flexural and axial strength of the discrete braced system are different than the through-fastened system and the combined effects must be checked.

The axial forces in the purlin are higher for load combination 2. Conservatively, the second order effects and the effective area of the strut are calculated based on the higher axial load combination 2, and used for load combination 1. The design strength of the purlin subjected to bending only is taken from Example 3.3.3.1. Second order effects are calculated in Example 3.3.1.2

End Span – Near mid-span:

Member second order moment amplifier (use conservatively for all load cases)

B_1 = 1.05 (from Example 3.3.1.2)

Use $\overline{M}_{nt} = M_x$ (flange braces preclude rafter rotation)

Calculate the combined effect of compressive axial load and bending per AISI S100 Section H1.2

$$\frac{\overline{P}}{P_a} + \frac{\overline{M}_x}{M_{ax}} + \frac{\overline{M}_y}{M_{ay}} \le 1.0 \quad \text{(Eq. H1.2-1)}$$

Gravity loading near mid-span

Conservatively use the largest axial load, P = 1.32 kip from load combination 2, with the largest moment, M_x = 4.08 ft-kip from load combination 1

$\overline{M}_{nt} = M_x = 4.08$ kip-ft

$\overline{M}_x = B_1\overline{M}_{nt} + B_2\overline{M}_{\ell t}$ (Eq. C1.2.1.1-1)

$= (1.05)(4.08) + B_2(0) = 4.28$ kip-ft

$\overline{P} = P = 1.32$ kip

P_a = 16.6 kip (from Part a)

M_{ax} = 6.39 kip-ft (From Example 3.3.3.1)

$$\frac{1.32}{16.6} + \frac{4.08}{6.39} + 0 = 0.72 < 1.0 \text{ OK}$$

Uplift loading near mid-span

The flexural distortional buckling strength under gravity loads calculated in Example 3.3.3.1 included the contribution of the rotational restraint provided by the panels. For uplift loading, since the bottom flange is in compression near the mid-span, this contribution to the strength must be eliminated. In Example 3.3.3.1, the distortional buckling flexural strength for uplift loading, M_{nd}/Ω_b = 6.48 kip-ft. Because the distortional buckling strength exceeds the combined global/local flexural strength, the combined global/local flexural strength will control and is the same as for gravity load, $M_{n\ell}/\Omega_b$ = 6.39 kip-ft. Because the required flexural strength for uplift loading is less than that for gravity loading, and the combined axial/flexural strength exceeded the required strength for gravity loading, the required strength for uplift loading is sufficient by inspection.

Interior Span – Near mid-span:

Member second order moment amplifier (use conservatively for all load cases)

B_1 = 1.11 (from Example 3.3.1.2)

Use $\overline{M}_{nt} = M_x$ (flange braces preclude rafter rotation)

Calculate the combined effect of compressive axial load and bending per AISI S100 H1.2

$$\frac{\overline{P}}{P_a}+\frac{\overline{M}_x}{M_{ax}}+\frac{\overline{M}_y}{M_{ay}}\le 1.0 \qquad \text{(Eq. H1.2-1)}$$

Gravity loading near mid-span

Conservatively use the largest axial load, P = 2.40 kip from load combination 2, with the largest moment, M_x = 1.79 kip-ft from load combination 1

$\overline{M}_{nt}$ = M_x = 1.79 kip-ft

$\overline{M}_x$ = $B_1\overline{M}_{nt} + B_2\overline{M}_{\ell t}$ (Eq. C1.2.1.1-1)

= (1.11)(1.79) + B_2(0) = 1.99 kip-ft

$\overline{P}$ = P = 2.40 kip

P_a = 10.9 kip (from Part a)

M_{ax} = 4.08 kip-ft (from Example 3.3.3.1)

$$\frac{2.40}{10.9}+\frac{1.99}{4.08}+0=0.71<1.0 \text{ OK} \qquad \text{(Eq. H1.2-1)}$$

Uplift loading near mid-span

The flexural distortional buckling strength under gravity loads calculated in Example 3.3.3.1 included the contribution of the rotational restraint provided by the panels. For uplift loading, since the bottom flange is in compression near the mid-span, this contribution to the strength must be eliminated. For the interior span, the distortional buckling flexural strength controls so the combined bending and axial load effects must be checked.

$\overline{M}_{nt}$ = M_x = -1.18 kip-ft

$\overline{M}_x$ = $B_1\overline{M}_{nt} + B_2\overline{M}_{\ell t}$ (Eq. C1.2.1.1-1)

$\overline{M}_x$ = (1.11)(-1.18) + B_2(0) = -1.31 kip-ft (Eq. C1.2.1.1-1)

$\overline{P}$ = P = 2.40 kip

P_a = 10.9 kip (from Part a)

M_{ax} = 3.81 kip-ft (from Example 3.3.3.1)

$$\frac{2.40}{10.9}+\frac{1.31}{3.81}+0=0.56<1.0 \text{ OK}$$

3c. Other Comments

The axial strength combined with bending must be checked at the ends of the laps for the single purlin. These conditions were checked in Example 3.3.1.1. At the location of the end of the lap, there is no difference in the procedure to calculate strength between the discrete braced system of this example and the through-fastened system of Example 3.3.1.2. Since the combined axial force and bending strength exceeded the required strength in Example 3.3.1.2, the strength is sufficient here as well.

CHAPTER 4 DIAPHRAGM REQUIREMENTS

Symbols and Definitions Used in Chapter 4

a Depth of diaphragm in AISI S907 (ft) (m)
b Width of diaphragm in AISI S907 (ft) (m)
C_e Stiffness contribution from panel end restraint (lb) (N)
C_1 to C_3 Bending Coefficients used in Eq. 4.1-11
d′ Depth of diaphragm (in.) (mm)
E Modulus of elasticity of steel (29,500,000 psi) (203,000 MPa)
G′ Total shear stiffness of the diaphragm including panel end restraints (lb/in.) (N/m)
G_1 Average diaphragm stiffness from AISI S907 without panel end restraints (lb/in.) (N/m)
G_2 Average diaphragm stiffness from AISI S907 with panel end restraints (lb/in.) (N/m)
I_{my} Modified moment of inertia of full unreduced section about minor centroidal axis (in.^{4}) (mm^4)
I_x Moment of inertia of the full unreduced section about major centroidal axis perpendicular to the web (in.^{4}) (mm^4)
I_{xy} Product of inertia of the full unreduced section about major and minor centroidal axes perpendicular and parallel to the web respectively (in.^{4}) (mm^4)
I_y Moment of inertia of the full unreduced section about minor centroidal axis parallel to the web (in.^{4}) (mm^4)
K_e Shear stiffness of the panel end restraint (lb/in.) (N/m)
K_n Shear stiffness of the diaphragm without panel end restraint (lb/in.) (N/m)
L Span length (ft) (m)
m Distance from shear center to mid-plane of web (in.) (mm)
N_p Total number of purlins in a bay
P_1 Average test load for AISI S907 without panel end restraints (lb) (N)
P_2 Average test load for AISI S907 with panel end restraints (lb) (N)
$P_{0.65}$ 65% of ultimate test load from AISI S907 (lb) (N)
P_L Lateral force resisted by the anchorage system (lb) (N)
P_N Nominal test load for determining the rotational stiffness of the connection between the purlin and the panels (lb) (N)
Q_e Nominal strength of panel end restraint (lb) (N)
S_e Nominal shear strength of panel end restraint per foot of diaphragm depth (lb/ft) (N/m)
S_n Nominal diaphragm shear strength without panel end restraint (lb/ft) (N/m)
S_{nt} Nominal diaphragm shear strength including panel end restraint (lb/ft) (N/m)
v Shear force per foot length in diaphragm (lb/ft) (N/m)
w Total uniform load for all purlin lines in a bay (lb/ft) (N/m)
w_{diaph} Distributed in-plane load on roof diaphragm ((lb/ft) (N/m)
α Coefficient for purlin orientations
Δ_s In-plane deflection of diaphragm at service load level (in.) (mm)
γ Ratio of lateral anchorage force to the applied gravity load

η	Number of upslope facing purlins minus number of downslope facing purlins
σ_{diaph}	Proportion of gravity load transferred to diaphragm force as a result of unsymmetric bending
θ	Roof slope (degrees)
ϕ	Resistance factor
Ω	Safety factor

4.1 Determining Diaphragm Requirements for Use with AISI Section I6.4.1

In purlin supported roof systems, the panels provide lateral support to the purlins through diaphragm action. To ensure that the panels provide sufficient restraint to resist global buckling and limit geometric second order effects, lateral displacement limits are specified in Section I6.4.1 of AISI S100. If the diaphragm has sufficient stiffness to satisfy the lateral displacement limits, then the anchorage forces can be determined using the anchorage equations in Section I6.4.1 or other methods of rational analysis. In addition, the load path of forces through the panel system to the anchorage devices must be evaluated to ensure that the system has adequate strength to resist the forces. If the diaphragm system does not satisfy the stiffness criteria, then a discrete point bracing system should be designed in accordance with Section C2.2.1 of AISI S100.

Through-fastened metal panel systems, in general, have sufficient strength and stiffness to satisfy most applications related to purlin supported roof systems. Standing seam systems, while providing better performance as a weather barrier, will typically be much more flexible than a through-fastened system. When a diaphragm fails to meet the stiffness criteria, the majority of diaphragm stiffness loss in standing seam systems comes from seam slip and clip flexibility. In many cases, the connections at the end of a panel run will inhibit panel slip and thus increase the strength and stiffness. These connections can include an eave connection where the panels are through-fastened to an eave member, or a connection at the end of a panel that includes end closures stiffened by a back-up plate. In general, these connections that inhibit seam slip are referred to as "panel end restraints."

The effect of the panel end restraint can be determined from diaphragm tests, such as the tests outlined in AISI S907. The benefit of the panel end restraint can lead to unconservative assumptions relative to the diaphragm strength and stiffness if the results are not evaluated properly. In the absence of panel end restraints, the strength and stiffness of the diaphragm is constant per unit depth of the diaphragm. On the other hand, the strength and stiffness of a panel end restraint is constant and therefore will effectively have a greater impact on these structural properties of a shallow diaphragm than a deep one. For example, if the AISI S907 method is used to determine the strength and stiffness properties of a shallow diaphragm, and the values obtained from the test are then used to predict the structural properties of a deeper diaphragm, the effects of the panel end restraint on the strength and stiffness will be overstated. Stating this in another way, assuming that a particular roof system has no ability to resist seam slip; then, the total stiffness is derived solely from the fasteners in the panel end restraint. The resistance per unit length of the diaphragm decreases if the depth (length perpendicular to purlin span) increases and the width remains constant.

Throughout the remainder of the chapter, methodologies to evaluate both the strength and the stiffness of the diaphragm are presented. The methods presented to evaluate the strength demands on the diaphragm are generally conservative. This is consistent with observed behavior of actual roof systems where failures from insufficient diaphragm strength have not been observed.

4.1.1 Establishing Diaphragm Strength and Stiffness

The strength and stiffness of any size diaphragm with end restraints can be obtained by first obtaining the strength and stiffness of the diaphragm alone (i.e., multiplying test values by the physical dimensions of the actual diaphragm) and then adding the strength and stiffness of the end restraint (Fisher and Nunnery, 1996).

Thus, the diaphragm shear strength can be represented as:

$S_{nt} = S_n + S_e$ (Eq. 4.1-1)

where,

S_{nt} = Nominal diaphragm shear strength including panel end restraint

S_n = Nominal diaphragm shear strength without panel end restraint

S_e = Nominal shear strength of the panel end restraint

The stiffness of the system can be represented similarly as:

$G' = K_n + K_e$ (Eq. 4.1-2)

where,

G' = Total shear stiffness of the diaphragm including panel end restraint

K_n = Shear stiffness of the diaphragm without panel end restraint

K_e = Shear stiffness of the panel end restraint

To obtain S_n, S_e, K_n and K_e tests must be conducted as illustrated in Figures 4.1-1 and 4.1-2.

Shown in Figure 4.1-1 is the test arrangement that should be used to determine the nominal diaphragm shear strength and diaphragm stiffness without panel end restraints. The test should be conducted following AISI S907, *Test Standard for Cantilever Test Method for Cold Formed Steel Diaphragms* (AISI, 2017). The test load is delivered into the panels through a member at the panel ends parallel to the load. This member is connected to the panels using only the system's purlin-panel clips. A similar member is connected between the diaphragm reaction points at the opposite end of the panels. Members simulating typical interior purlins are positioned at an appropriate spacing within the assembly again connected to the panels with purlin-panel clips. Along the remaining two sides, edge members are provided. These edge members can be attached to the test panels with self-drilling fasteners. Care must be taken to ensure that the attachment of the edge members to the test panels does not create an end restraint condition. The shear strength of the diaphragm without panel end restraints is

$S_n = P_1/b$ (Eq. 4.1-3)

Shown in Figure 4.1-2 is the test arrangement for determining the diaphragm properties of the panels and the contribution from the attached panel end restraints. The construction of the test assembly is identical to that shown in Figure 4.1-1, except for the inclusion of the assembly that makes up the panel end restraints. This assembly can either be an eave member to which the panels are through-fastened or a panel end closure that inhibits seam movement. The panel end assembly is typically included along both panel ends in the assembly to eliminate the panel warping effects along the ends of the panels. It is generally accepted in the industry that the warping and seam slip, if not prevented, would unrealistically reduce the strength and stiffness of the panel end restraints in the test. However, when an eave member is included along both panel ends in the test arrangement, then the strength and stiffness effects of a single panel end restraint are doubled.

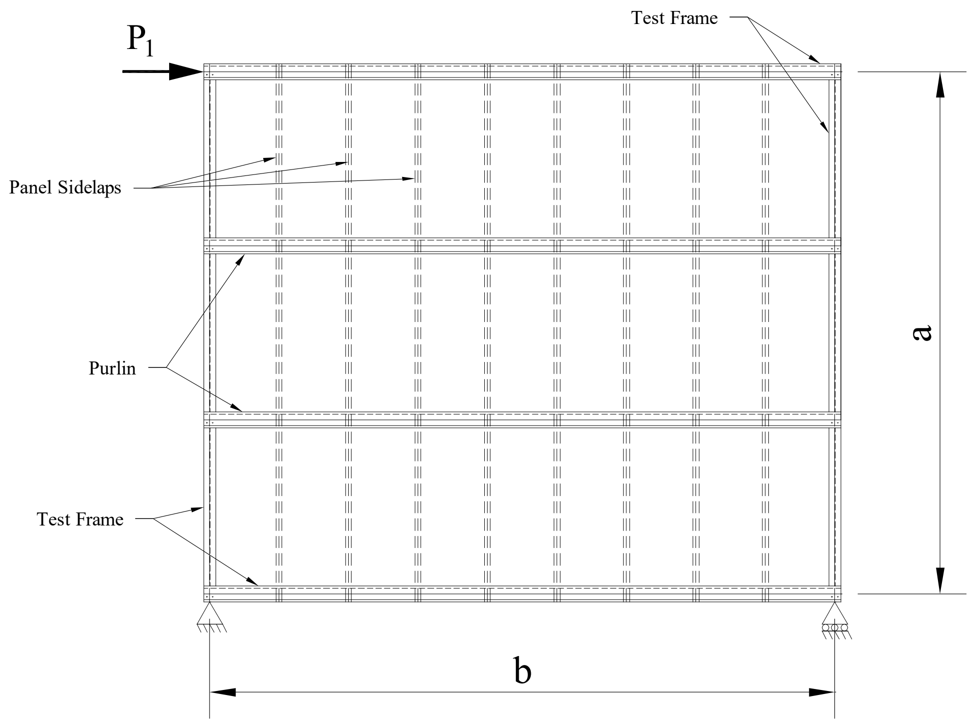

Figure 4.1-1 AISI S907 Test Assembly without Panel End Restraints

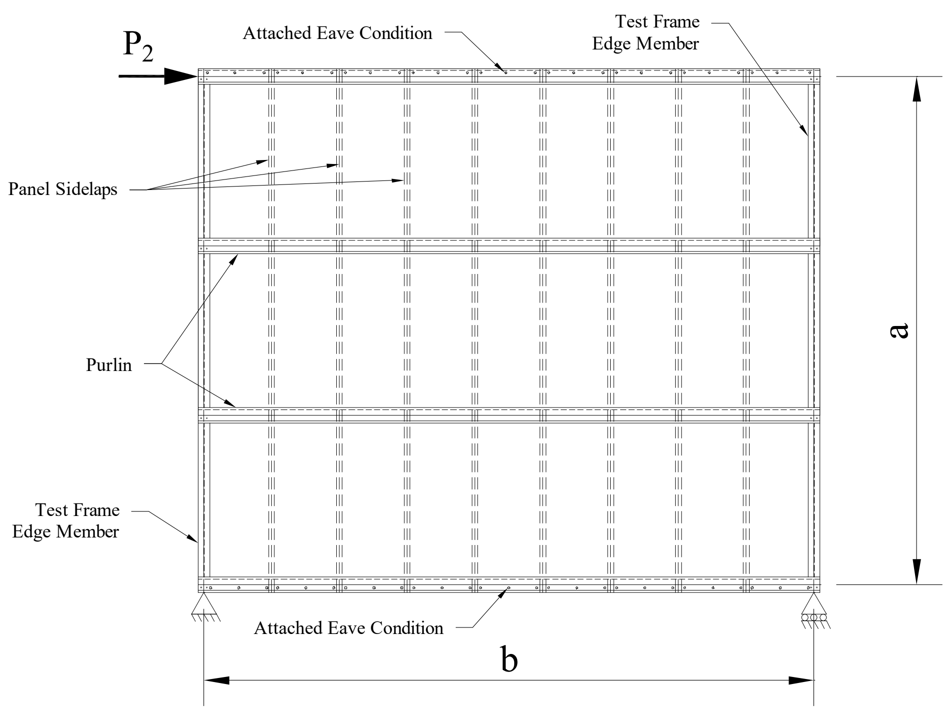

Figure 4.1-2 AISI S907 Test Assembly with Panel End Restraints

The strength and stiffness contribution of the panel end restraint can be determined by subtracting the test load P_1 obtained from the tests using the arrangement in Figure 4.1-1 from the test load P_2 using the arrangement shown in Figure 4.1-2 and dividing by two. The resulting value is the additional strength or stiffness provided by a single end restraint.

Strength Contribution from the Panel End Restraints:

Based on the diaphragm tests shown in Figures 4.1-1 and 4.1-2, the shear strength per foot, S_e, furnished by the attachment of the standing seam panels to the eave member can be determined from the equation:

$$S_e = (P_2 - P_1)/2b \quad \text{(Eq. 4.1-4)}$$

The strength furnished by the eave attachment can be determined by modeling the diaphragm as a series of cantilever shear walls as shown in Figure 4.1-3.

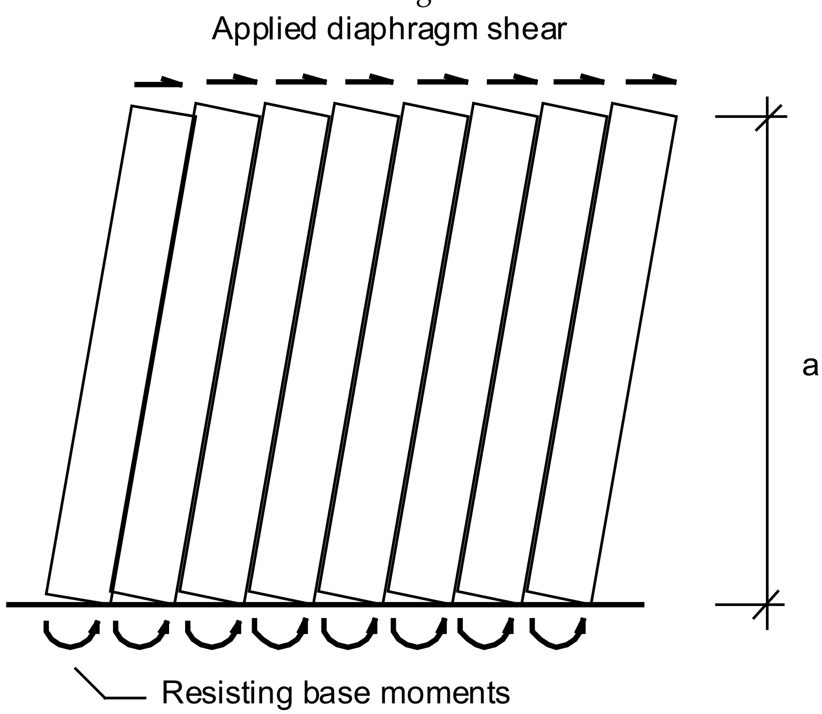

Figure 4.1-3 Panel End Restraint Resistance (End Restraint at One End)

The panel end restraint resists the panel shear through the development of a resisting moment derived from the moment capacity of the panel-fastener-eave member connection. The shear strength furnished by an individual panel equals the base moment resistance divided by the distance from the base to the line of action of the shear force. The eave attachment contribution to the resisting shear per foot is Q_e/a where Q_e is a constant for the panel representing the panel end restraint moment resistance, and a is the depth of the test assembly. From AISI S907:

$$Q_e = (S_e)(a) \quad \text{(Eq. 4.1-5)}$$

For any diaphragm, the total diaphragm strength per foot can be obtained from the equation:

$$S_{nt} = S_n + Q_e/d' \quad \text{(Eq. 4.1-6)}$$

where, d′ is the depth of the diaphragm.

These diaphragm strengths must be multiplied by the appropriate safety and resistance factors and compared to the required strength. Safety and resistance factors for diaphragm strength are found in Table B1.1 of AISI S310, *North American Standard for the Design of Profiled Steel Diaphragm Panels* (AISI, 2020), which is reproduced in Table 4-1. Safety and resistance factors are dependent upon the failure mechanism in the test (connection failure vs. panel buckling) and the load type.

Table 4-1 Safety Factors and Resistance Factors for Diaphragms (AISI D310-20 Table B1.1)

Load Type or Combinations Including	Connection Type	Limit State					
		Connection-Related			Stability-Related		
		Ω_d (*ASD*)	ϕ_d (*LRFD*)	ϕ_d (*LSD*)	Ω_d (*ASD*)	ϕ_d (*LRFD*)	ϕ_d (*LSD*)
Wind	Welds	2.15	0.75	0.60	2.00	0.80	0.75
	Screws	2.00	0.80	0.75			
Earthquake and All Others	Welds	3.00	0.55	0.40			
	Screws	2.30	0.70	0.55			

Stiffness Contribution from the Eave Connection:

From the AISI S907 tests, when panel end restraints are used at both panel ends, the stiffness, K_e, furnished by each panel end restraint equals:

$$K_e = (G_2 - G_1)/2 \qquad \text{(Eq. 4.1-7)}$$

where G_2 and G_1 are the average diaphragm shear stiffnesses calculated from the tests with and without panel end restraints, respectively. Since the deformation from the panel end restraint occurs almost totally at the eave attachment (Figure 4.1-4), with the remainder of the panel being rigid, K_e can be expressed as a constant C_e divided by the height of the panel, a, used in the tests. Rearranging to solve for C_e,

$$C_e = (K_e)(a) \qquad \text{(Eq. 4.1-8)}$$

For any depth diaphragm, the added stiffness of the panel end attachments can be determined by dividing the constant C_e by the depth of the diaphragm, d′. The total stiffness of the diaphragm is the sum of the stiffness of the diaphragm without panel end restraints plus the effective stiffness of the panel end restraints for the given diaphragm depth:

$$G' = K_n + C_e/d' \qquad \text{(Eq. 4.1-9)}$$

where, d′ is the depth of the diaphragm. The use of S_e and G' are further described in Example 4.2.

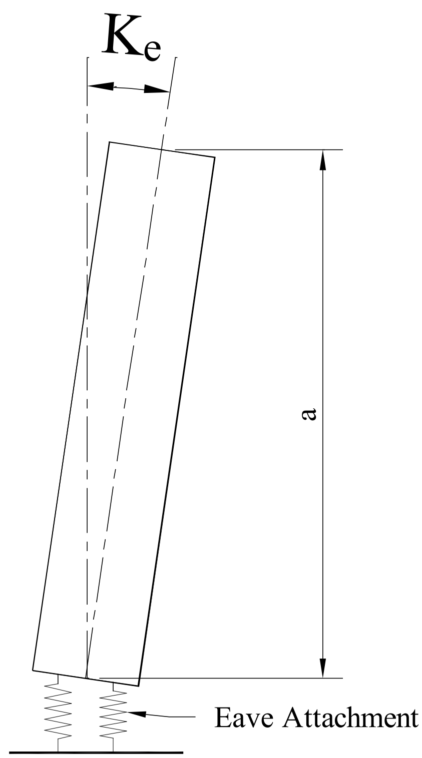

Figure 4.1-4 Diaphragm Stiffness per Unit Length

4.1.2 Evaluation of Diaphragm Strength and Stiffness

If the anchorage equations in Section I6.4.1 of AISI S100 are intended to be used for bracing a particular purlin system, then AISI S100 requires that the lateral deflection of the top flange of the purlin braced by the panels not exceed the span length divided by 360 under nominal loads (specified loads). Diaphragm deflections are evaluated from shear deflection equations using the tested diaphragm shear stiffness G'. Traditionally G' has been established using the secant modulus at 0.4 times the maximum test load. Because load deflection curves for diaphragms are normally non-linear, using the secant modulus established at $0.4P_u$ per the AISI S907 procedure may overestimate the stiffness of the diaphragm. For systems where there are large diaphragm demands, i.e., thicker purlins with long spans, using a G' determined at $0.65P_u$, which typically results in a lower stiffness, may be appropriate.

To calculate the deflection between brace locations, the in-plane force in the diaphragm, w_{diaph}, is approximated to be uniform. This in-plane force is a function of the unsymmetric bending for point symmetric Z-sections, torsion in both Z- and C-sections, and the downslope forces on a sloped roof. The displacement of the diaphragm varies for each bracing configuration.

When a system is braced laterally only at the support locations, the maximum deflection is at mid-span and the maximum shear force occurs at the supports. When the system has a lateral brace at an interior location only, i.e., mid-point or third point brace, maximum deflections will occur at the frame line and the maximum in-plane shear force may occur at either the brace location or the frame line. In the case of support braces combined with interior braces, deflection should be calculated at an interior brace location. The maximum in-plane shear force could occur at either the support location or interior brace location. Each of these bracing configurations is described in more detail in the following sections.

Diaphragm In-plane Force for Z-sections

Most commonly, Z-sections are oriented with the top flange facing upslope. As a result of unsymmetric bending, a Z-section will deflect laterally upslope resulting in an upslope force in the diaphragm. As the slope of a roof increases, the downslope component of the gravity load counteracts the upslope unsymmetric bending component. The balance point for most Z-sections is at a slope between 1:12 and 2:12. At steeper slopes, the force in the diaphragm is downslope and results in a downslope translation.

Two equations are provided below to calculate the in-plane force in a diaphragm for Z-sections. Eq. 4.1-10 assumes a rigid diaphragm and will closely predict the in-plane diaphragm force for through-fastened systems and will typically provide a conservative estimate for more flexible standing seam systems. Eq. 4.1-11 accounts for the diaphragm flexibility and will better predict the in-plane diaphragm force for standing seam systems. A more detailed calculation for the in-plane diaphragm force that includes the torsional flexibility of the connection between the purlin and the panels is provided as part of the framework for the component stiffness method in Section 5.5.4. Note that this design approach is not addressed in AISI S100.

For a Z-section that is restrained by a rigid diaphragm, the in-plane force in the diaphragm, w_{diaph}, is

$$w_{diaph} = w\left(\alpha \frac{I_{xy}}{I_x}\cos\theta - \sin\theta\right) \qquad \text{(Eq. 4.1-10)}$$

where,

w = Total uniform load for all purlin lines in a bay
= w_u or w_a for strength requirements from LRFD or ASD load combination respectively
= $w_{service}$, service load combination for deflection criteria

α = +1 for top flange facing in the uphill direction, and

α = -1 for top flange facing in the downhill direction

I_{xy} = Product of inertia of full unreduced section about major and minor centroidal axes perpendicular and parallel to the web respectively

I_x = Moment of inertia of full unreduced section about major centroidal axis perpendicular to the web

θ = Roof slope

For through-fastened systems, which typically have large diaphragm stiffness values (G' > 2000 lb/in.), the in-plane force in the diaphragm will closely match that of Eq. 4.1-10. The unsymmetric bending component of the in-plane diaphragm force (I_{xy}/I_x) is affected by the stiffness of the diaphragm as well as the torsional flexibility of the connection between the purlin and the panels.

The term σ_{diaph} is introduced to represent the unsymmetric bending portion of the in-plane diaphragm force including the flexibility of the diaphragm. The total in-plane force in the diaphragm including diaphragm flexibility is

$$w_{diaph} = w(\alpha\sigma_{diaph} - \sin\theta) \qquad \text{(Eq. 4.1-11)}$$

where

$$\sigma_{diaph} = \frac{C_1 \frac{\left(\frac{I_{xy}}{I_x}\cos\theta\right)L^4}{EI_{my}} + C_2 \frac{\alpha \cdot N_p \cdot L^2 \sin\theta}{G'd'}}{C_1 \frac{L^4}{EI_{my}} + C_3 \frac{\alpha \cdot \eta \cdot L^2}{G'd'}} \qquad \text{(Eq. 4.1-12)}$$

And

$$I_{my} = \frac{I_x I_y - I_{xy}^2}{I_x} \qquad \text{(Eq. 4.1-13)}$$

N_p = Total number of purlins in a bay

η = Number of upslope facing purlins minus number of downslope facing purlins

C_1, C_2, and C_3 = Coefficients as shown in Table 4-2

Table 4-2 Coefficients C_1, C_2, and C_3

		Supports Supports + 1/3 Torsion	Midpoint	1/3 Point
C_1	Simple Span	5/384	5/384	11/972
	End Span Outside 1/2 Span	1/185	1/185	5/972
	End Span Inside 1/2 Span	1/185	1/185	7/1944
	Multi-span Interior Span	1/384	1/384	1/486
C_2		1/8	-1/8	-1/18
C_3		1/8	1/8	1/9

For a rigid diaphragm, the value of G′ is large, causing the second terms in the numerator and denominator of Eq. 4.1-11 to approach zero. As a result, Eq. 4.1-11 simplifies to $\sigma_{diaph} = I_{xy} \cos\theta/I_x$.

When including the diaphragm flexibility, the in-plane diaphragm force, w_{diaph}, will vary from the rigid diaphragm values. For a purlin with its top flange facing upslope and anchored at the supports, the direction of its translation is dependent on the roof slope for a given non-rigid diaphragm stiffness (< 2,000 lb/in.). On a low slope roof, the mid-span of the purlin translates upslope (+x-axis) as cacluated by Eq. 4.1-16 and as shown in Figure 4.1-5. Corresponding to this upslope translation, the result of Eq. 4.1-11 is such that $\sigma_{diaph} < I_{xy} \cos\theta/I_x$. As the slope of the roof increases, the mid-span of the purlin translates downslope (-x-axis), and $\sigma_{diaph} > I_{xy} \cos\theta/I_x$. Figure 4.1-6 shows the unsymmetric bending force, σ_{diaph}, relative to the diaphragm stiffness for an 8ZS2.75x085 spanning 25 ft- 0 in. for both a flat roof and 6:12 slope roof. The value for a rigid diaphragm with no slope (I_{xy}/I_x) is shown for reference.

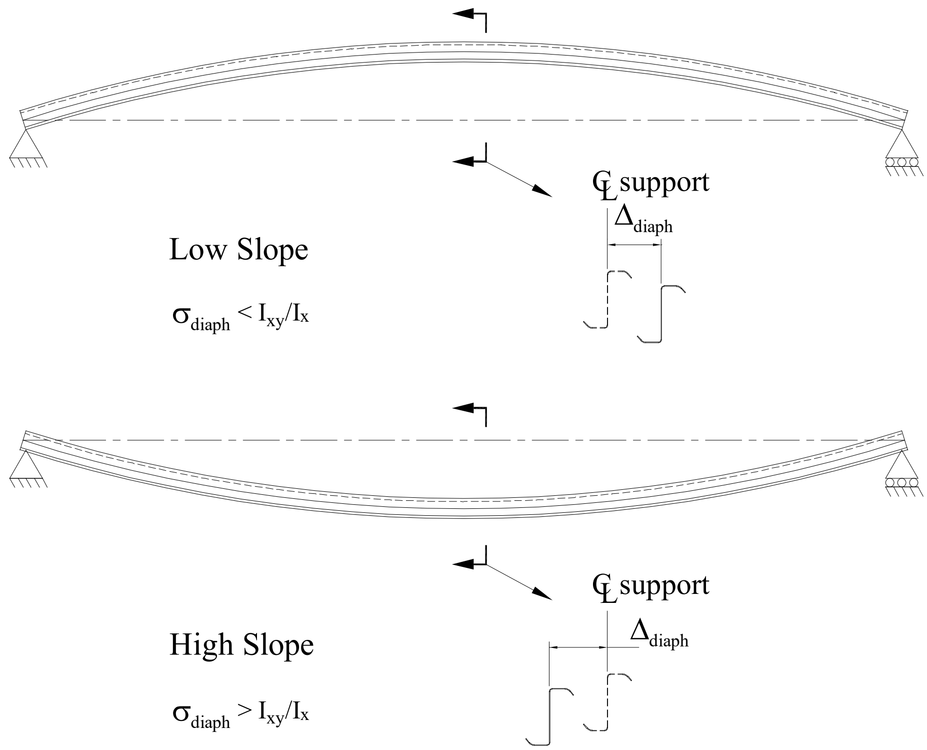

Figure 4.1-5 Effect of Diaphragm Displacement on σ_{diaph} for Supports Restraint

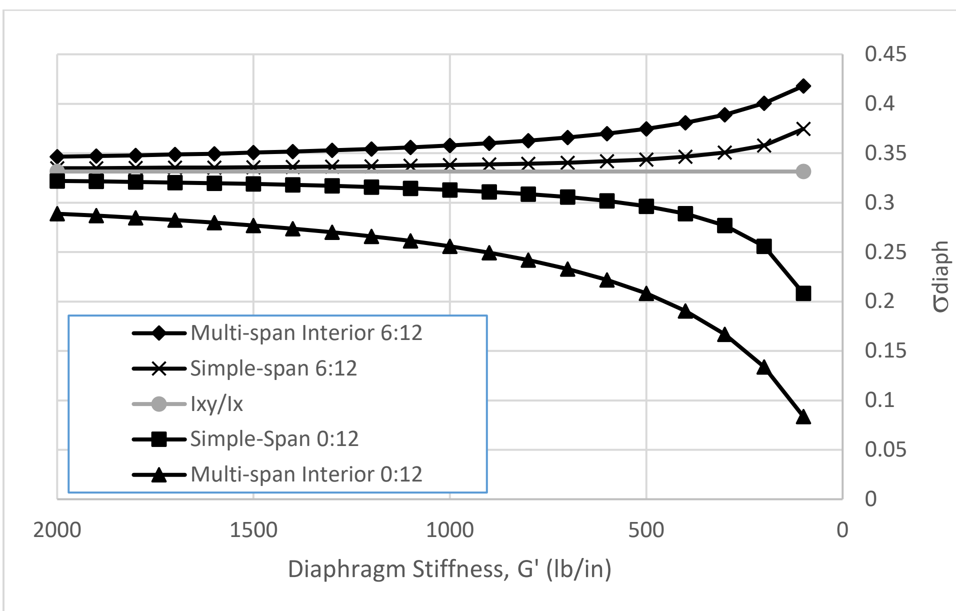

Figure 4.1-6 Unsymmetric Bending Force, σ_{diaph}, vs. Diaphragm Stiffness

For an interior restraint configuration, the Z-section is considered fixed at the restraint location and the top flange will translate laterally at the frame lines. On a low slope roof, the top flange of the purlin at the frame line will translate downslope. Looking at the deflected shape as shown in Figure 4.1-7, the mid-span is displaced in the positive x-direction relative to the ends.

The unsymmetric bending component of the in-plane diaphragm force is less than the rigid diaphragm value. As the roof slope increases, the downslope component of the force causes additional deflection at the frame lines further reducing the unsymmetric bending force.

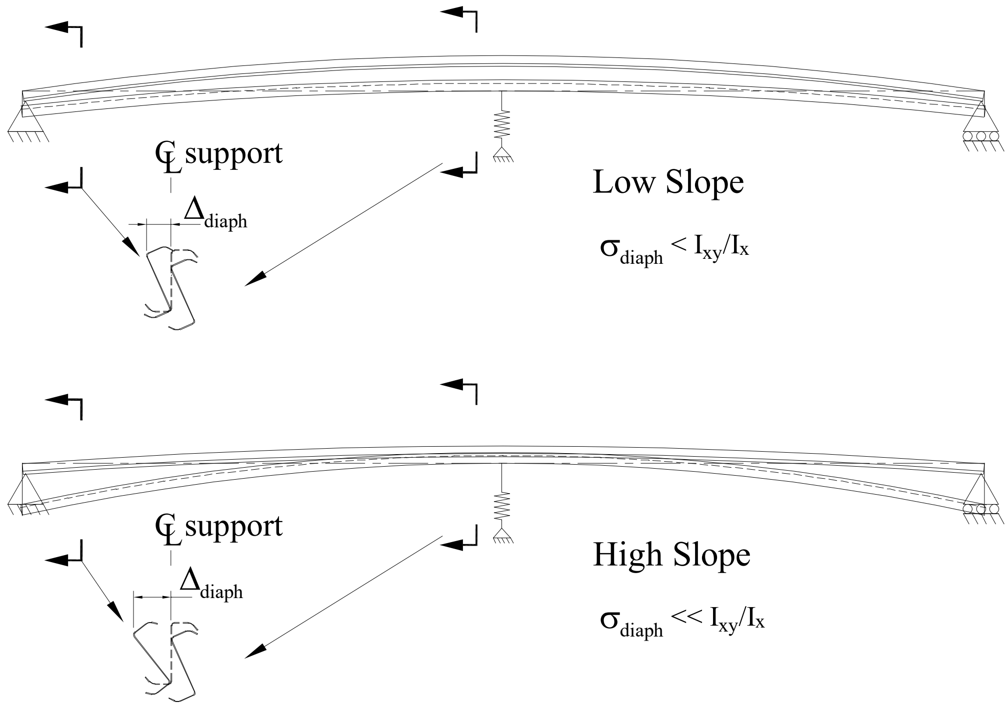

Figure 4.1-7 Effect of Diaphragm Displacement on σ_{diaph} for Interior Anchorage

By including diaphragm flexibility, a more realistic force in the diaphragm is realized for standing seam systems that typically have a lower stiffness and strength than through-fastened systems. For a more detailed prediction of the in-plane diaphragm forces, see Section 5.5.4.1 for the component stiffness method. The component stiffness method, in addition to diaphragm flexibility, includes torsional flexibility in the connection between the purlin and the panel. For most systems, this flexibility has a small effect on the in-plane diaphragm force and is conservative to ignore.

Diaphragm In-plane Force for C-sections

For Z-sections, the unsymmetric bending of the point symmetric section is a major component of the in-plane diaphragm force. C-sections, which are singly symmetric are not subject to unsymmetric bending deformations. However, the eccentric shear center of the C-section causes torsion of the section that is resisted by diaphragm action in the panels. The in-plane force in the panels resulting from this torsion has traditionally been approximated as 5% of the applied force parallel to the web of the C-section. Using this approximation, the total in-plane force in the diaphragm, including the downslope component of the applied gravity load is

$$w_{diaph} = w(\alpha 0.05\cos\theta - \sin\theta) \quad \text{(Eq. 4.1-14)}$$

Where w, α, and θ are as defined above.

For a low slope roof with C-section flanges facing upslope, the in-plane diaphragm force is small, and the corresponding upslope diaphragm deflection is small. As the slope increases, the in-plane diaphragm force and corresponding deformation quickly shifts downslope.

For a more detailed analysis of the in-plane diaphragm forces that includes flexibility of the diaphragm and the connection between the purlin and the panels, see the component stiffness method in Section 5.5.4.

System Requirements

For system designs where the purlins rely on the diaphragm for stability, the diaphragm must satisfy stiffness and strength requirements. Equations for the maximum diaphragm shear force and maximum deflection are provided below for each anchorage configuration.

For diaphragm stiffness requirements, load combinations at a service load level are used. If the panels are relied upon to provide lateral restraint for the purlins and anchorage forces are determined by AISI S100, the panels must be checked for stiffness. The stiffness of the diaphragm must be sufficient to limit the lateral deflection of purlins between brace points to L/360 for most anchorage configurations as outlined in AISI S100 Section 16.4.1, and L/180 for supports plus torsion braces per Section 1.6.4.2. Because the flexural deflection in a diaphragm is normally small relative to the shear deflection, the flexural deflection is typically ignored.

For panel strength demands, AISI S100 Section I6.4.1 requires that the load path of the stabilizing forces in the diaphragm through the panels and connections to the purlins be checked. The strength of the diaphragm can be determined from the results of tests performed according to AISI S907 and the strength of the panel-to-purlin-to-anchorage device connection can be determined from tests performed according to AISI S912 (AISI 2017e). The maximum shear demands on the diaphragm and connections can be calculated by the equations outlined in the following sections. Note that the shear demands on the diaphragm calculated below are generally conservative. Recent research (Seek, 2022) has shown that when the nonlinear behavior of a standing seam diaphragm is considered, the shear reversals near anchorage devices are more gradual and the peak shear forces at the brace locations can be significantly reduced. Additionally, industry experience shows that the diaphragm strength limit state for purlin bracing and anchorage rarely controls.

Supports (Frame Line) Anchorage

With a supports (frame line) anchorage condition, the purlin supporting the diaphragm is supported vertically and laterally at the support locations. The distribution of shear force follows that of a beam with a uniformly distributed load as shown in Figure 4.1-8. The figure shows the distribution of diaphragm forces separated according to (a) unsymmetric bending, (b) downslope forces and (c) the unsymmetric and downslope forces combined. Maximum shear forces in the diaphragm occur adjacent to the frame lines. The shear force per unit length along the depth of the diaphragm is

$$v = \frac{w_{diaph} L}{2d'} \qquad \text{(Eq. 4.1-15)}$$

Maximum deflection occurs at mid-span. The deflection will be upslope for low slope roofs and downslope for high slope roofs. The deflection is

$$\Delta_s = \frac{w_{diaph} L^2}{8G'd'} \qquad \text{(Eq. 4.1-16)}$$

The above equations are also valid for anchorage at the frame lines used in conjunction with third point torsion restraints.

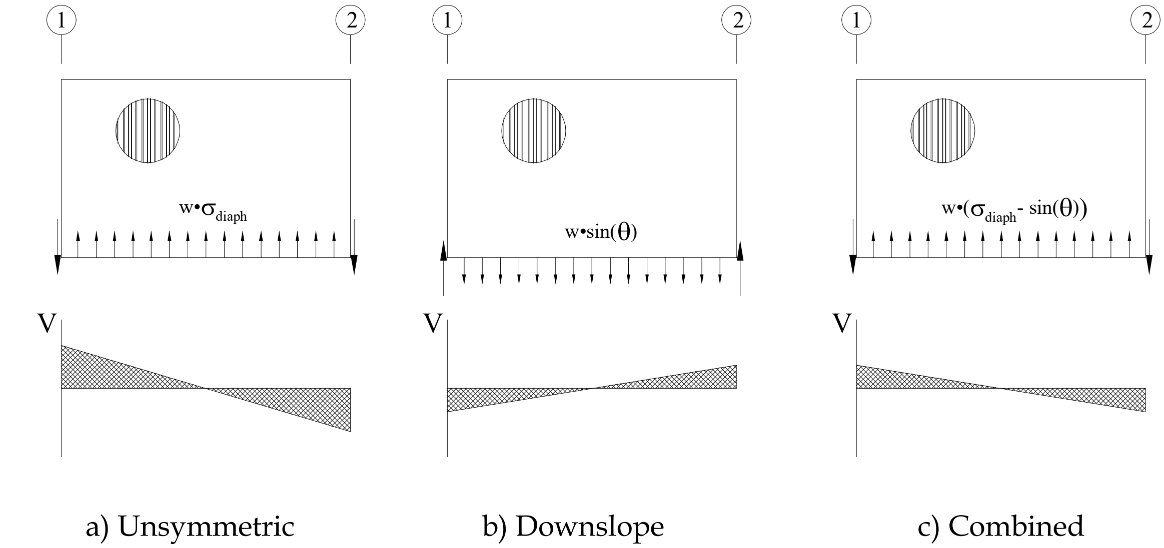

Figure 4.1-8 Diaphragm Shear Distribution – Supports Anchorage

Mid-point Anchorage

The maximum shear force and maximum diaphragm deflection for an interior anchorage configuration is complicated because the purlin is supported vertically at the frame line and laterally along its span. Figure 4.1-9 shows the distribution of diaphragm forces separated according to (a) unsymmetric bending, (b) downslope forces and (c) the unsymmetric and downslope forces combined. Maximum shear force in the diaphragm can occur at the frame line but more commonly will occur adjacent to the mid-point brace. Both locations should be checked.

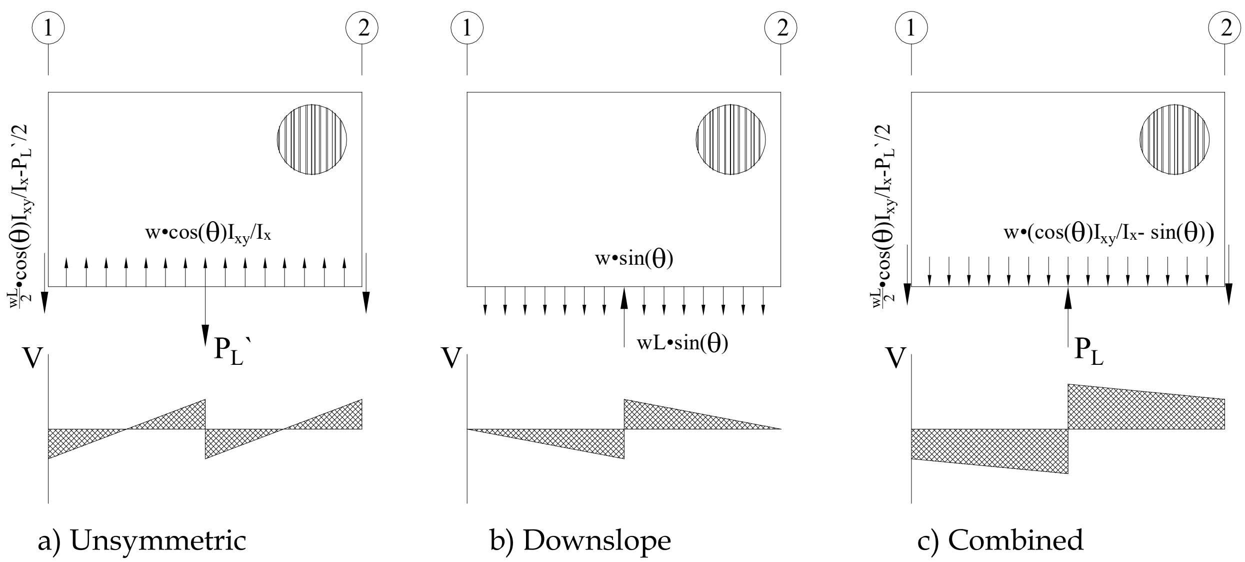

Figure 4.1-9 Diaphragm Shear Distribution – Mid-point Anchorage

The shear force per unit length at the frame line location is

$$v = \frac{P_L - w_{diaph} L}{2d'} \qquad \text{(Eq. 4.1-17)}$$

The shear force per unit length adjacent to the mid-point brace is

$$v = \frac{P_L}{2d'} \qquad \text{(Eq. 4.1-18)}$$

where

P_L = mid-point anchorage force calculated from Section 5.4 or 5.5.4.

The maximum in-plane diaphragm deflection will occur at the frame line and will typically be downslope for Z-sections with their top flanges facing upslope. C-sections will deflect upslope for low slope roofs but the deflection quickly reverses to downslope as roof slope increases. The deflection of the diaphragm at the frame line is

$$\Delta_s = \frac{P_L L}{4G'd'} - \frac{w_{diaph} L^2}{8G'd'} \qquad \text{(Eq. 4.1-19)}$$

Note that for high slope roofs, P_L will be negative.

Third Point Anchorage

The diaphragm in a third point anchorage configuration will behave similar to a mid-point configuration. Maximum shear force in the diaphragm may occur either adjacent to the frame line or adjacent to either side of the third point anchor. Figure 4.1-10 shows the distribution of shear forces for a) unsymmetric bending, b) downslope forces and c) the combined shear force.

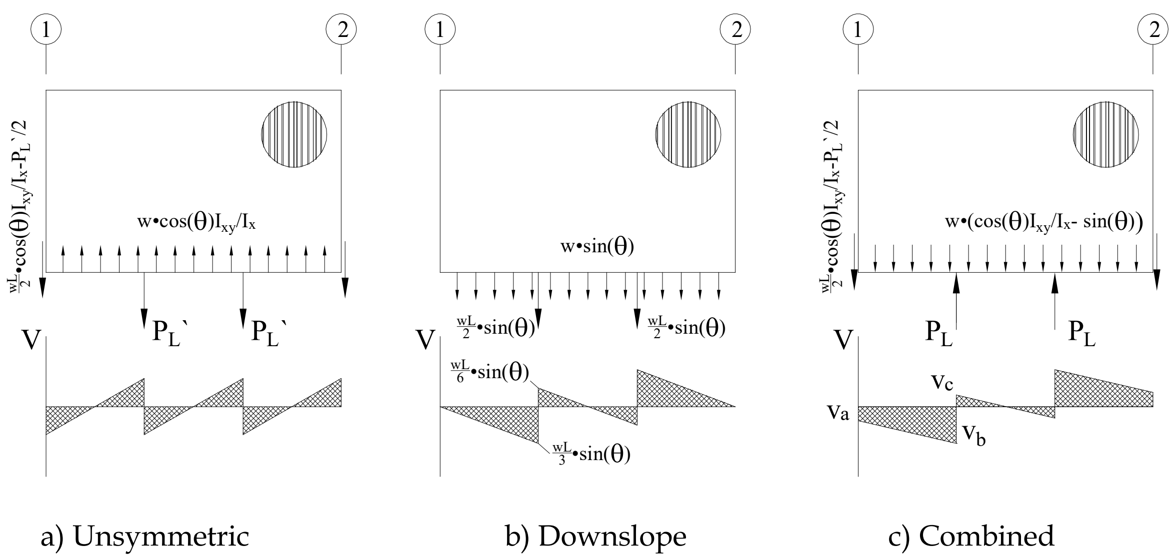

Figure 4.1-10 Diaphragm Shear Distribution – Third Point Anchorage

The shear force per unit length at the frame line location is

$$v_a = \frac{2P_L - w_{diaph}L}{2d'} \qquad \text{(Eq. 4.1-20)}$$

The shear force per unit length at third point (side nearest frame line) is

$$v_b = \frac{6P_L - w_{diaph}L}{6d'} \qquad \text{(Eq. 4.1-21)}$$

The shear force per unit length at the third point (side nearest mid-span) is

$$v_c = \frac{w_{diaph}L}{6d'} \qquad \text{(Eq. 4.1-22)}$$

Maximum deflections will typically occur at the frame line and will primarily be directed downslope for both low slope and high slope roofs. Diaphragm displacement between the third points is small relative to the displacement at the frame lines and will not control.

The in-plane diaphragm displacement at the frame line is

$$\Delta_s = \frac{P_L L}{3G'd'} - \frac{w_{diaph}L^2}{9G'd'} \qquad \text{(Eq. 4.1-23)}$$

4.2 Example Diaphragm Calculations Using AISI S907

Determine the strength and stiffness of a standing seam diaphragm from a test performed according to AISI S907. The tests were conducted using the configuration shown in Figure 4.2-1. The first series of tests were performed *without* panel end restraints and the second series of tests were conducted *with* panel end restraints. The test results are summarized in Tables 4-3 and 4-4. The panel end restraints consisted of a typical eave connection with the panel through-fastened to the eave member and a ridge closure with a back-up plate at the ridge.

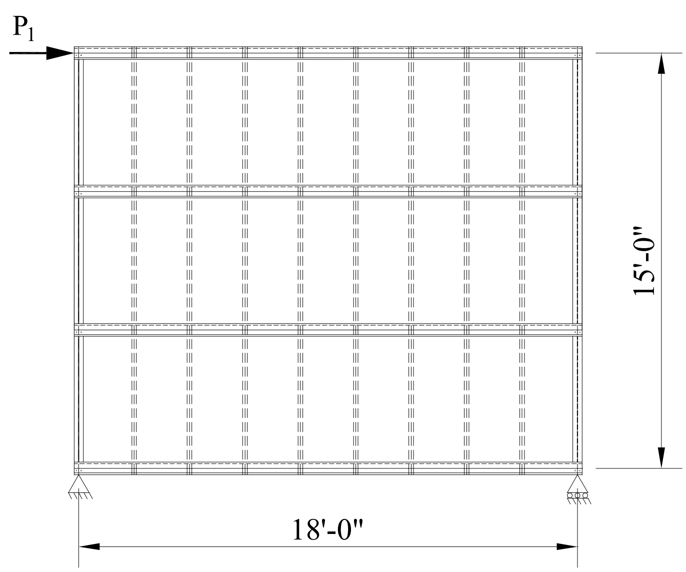

Figure 4.2-1 Diaphragm Test Arrangement

Table 4-3 Tests without Panel End Restraints

Test	P_n (lb)	$P_{0.65}$ (lb)	Δ (in.)	S_n (lb/ft)	G′ (lb/in.)
1	1580	1027	3.25	88	263
2	1540	1001	3.19	86	261
Average	1560			87	262

Table 4-4 Test with Panel End Restraints

Test	P_n (lb)	$P_{0.65}$ (lb)	Δ (in.)	G′ (lb/in.)
1	5110	3322	2.44	1134
2	5020	3263	2.39	1138
Average	5065			1136

From the test results:

The strength of the panels without end restraints is

$$S_n = \frac{P_1}{b} = \frac{1560}{18} = 87\ \text{lb}/\text{ft} \qquad \text{(Eq. 4.1-3)}$$

The strength of the panel end restraints per unit length of the test diaphragm is

$$S_e = \frac{(P_2 - P_1)}{b} = \frac{(5065 - 1560)}{18} = 195\ \text{lb}/\text{ft} \qquad \text{(Eq. 4.1-4)}$$

The constant strength of the panel end restraints is

$$Q_e = S_e a = (195)(15) = 2925\ \text{lb} \qquad \text{(Eq. 4.1-5)}$$

The total strength of the diaphragm is

$$S_{nt} = S_n + \frac{Q_e}{d'} = 87\ \text{plf} + \frac{2925\ \text{lb}}{d'} \qquad \text{(Eq. 4.1-6)}$$

The diaphragm shear stiffness without panel end restraints is

$K_n = G'_1 = 262$ lb/in.

The contribution of the panel end restraints to the diaphragm stiffness is

$$K_e = G'_2 - G'_1 = 1136 - 262 = 874\ \text{lb}/\text{in} \qquad \text{(Eq. 4.1-7)}$$

The constant stiffness of the panel end restraints is

$$C_e = K_e a = (874)(15) = 13{,}110\ \text{lb-ft}/\text{in} \qquad \text{(Eq. 4.1-8)}$$

The total stiffness of the diaphragm is

$$G' = K_n + \frac{C_e}{d'} = 262\ \text{lb}/\text{in} + \frac{13{,}110\ \text{lb-ft}/\text{in}}{d'} \qquad \text{(Eq. 4.1-9)}$$

where d′ is the depth of the diaphragm in feet

Results Summary

The standing seam diaphragm, excluding the panel end restraints, has a strength S_n = 87 lb/ft and a stiffness K_n = 262 lb/in. The eave and ridge connections provide additional shear strength Q_e = 2925 lb. and additional stiffness of C_e = 13,110 lb-ft/in. For an LRFD evaluation, resistance factors must be applied. For an ASD evaluation, safety factors must be applied.

4.3 Example Diaphragm Calculations to Determine Purlin Stability (Diaphragm Flexibility Excluded) - ASD

Using ASD, determine if the strength and the stiffness of the diaphragm from the example provided in Section 4.2 is adequate for the system of purlins that is analyzed for anchorage forces in the example provided in Section 5.4.3. Use the conservative approximation of the in-plane diaphragm force neglecting diaphragm flexibility (Eq. 4.1-10).

Solution

In the example from Section 5.4.3, the eave purlin (Purlin 1) is oriented with the top flange facing downslope. The remainder of the purlins (Purlins 2 to 12) are oriented upslope. For the exterior span purlins (8ZS2.75x085), the uniform force in the diaphragm at each purlin is

Purlin 1: $w_{diaph,1} = (23)(2.5)\left((-1)\frac{4.11}{12.4}\cos(2.39) - \sin(2.39)\right) = -21.44 \text{ lb/ft}$

Purlin 12: $w_{diaph,12} = (23)(2.5)\left((1)\frac{4.11}{12.4}\cos(2.39) - \sin(2.39)\right) = 16.64 \text{ lb/ft}$

Purlin 2-11: $w_{diaph,2-11} = (23)(5)\left((1)\frac{4.11}{12.4}\cos(2.39) - \sin(2.39)\right) = 33.29 \text{ lb/ft}$

The total force in the diaphragm is

$w_{diaph} = -21.44 + 16.64 + 10(33.29) = 328 \text{ lb/ft}$

A similar calculation is performed for the interior span purlins (8ZS2.75x059) resulting in a uniform force, w_{diaph} = 328 lb/ft. Because the in-plane diaphragm forces in each bay are approximately the same and all other parameters are the same, only the exterior bay will be evaluated.

Evaluate Diaphragm Shear Strength

The maximum factored shear force per unit length in the diaphragm is

$$v = \frac{w_{diaph} L}{2d'} = \frac{(328)(25)}{2(55)} = 75 \text{ lb/ft} \quad \text{(Eq. 4.1-15)}$$

From Example 4.2, the strength of the diaphragm excluding the eave attachments is S_n = 87 lb/ft and the added strength of the eave attachment is Q_e = 2925 lb. Applying a conservative safety factor, Ω_d = 2.5, the total strength of the diaphragm including the strength of the eave attachments is

$$\frac{S_{nt}}{\Omega_d} = \frac{S_n + Q_e/d'}{\Omega_d} = \frac{87 + 2925/55}{2.5} = 56 \text{ lb/ft} \quad \text{(Eq. 4.1-6)}$$

The predicted required strength of the diaphragm (75 lb/ft) is greater than the allowable design strength (56 lb/ft). Note, this method to predict the required strength is generally conservative.

Evaluate Diaphragm Deflection

The stiffness of the diaphragm is

$$G' = K_n + \frac{C_e}{d'} = 262\ \text{lb}/\text{in} + \frac{13{,}110\ \text{lb}-\text{ft}/\text{in}}{55\ \text{ft}} = 500\ \text{lb}/\text{in} \qquad \text{(Eq. 4.1-9)}$$

The maximum in-plane deflection of the diaphragm is

$$\Delta_s = \frac{w_{diaph} L^2}{8G'd'} = \frac{(328)(25)^2}{8(500)(55)} = 0.93\ \text{in} > L/360 = 0.83\ \text{in} \quad \text{NG} \qquad \text{(Eq. 4.1-16)}$$

Another way to evaluate the diaphragm stiffness is to solve for the minimum stiffness that will meet the L/360 deflection limit. That is,

$$G' \geq \frac{(45)\, w_{diaph} L}{d'} = \frac{(45)(328)(25)}{(55)}\left(\frac{1\ \text{ft}}{12\ \text{in}}\right) = 559\ \text{lb}/\text{in} \quad \text{NG}$$

Therefore, provided that the diaphragm has a stiffness greater than 559 lb/in., it will satisfy the L/360 deflection criteria. Since the provided diaphragm has a stiffness of 500 lb/in., it does not satisfy the maximum lateral deflection requirement.

Results Summary

When the conservative approximation neglecting diaphragm flexibility was used, the diaphragm does not have adequate strength to satisfy the shear strength requirement, nor does it have adequate stiffness to satisfy the L/360 lateral deflection limit. The next example evaluates the diaphragm by including diaphragm flexibility.

4.4 Example Diaphragm Calculations to Determine Purlin Stability (Diaphragm Flexibility included) - ASD

Using ASD, determine if the strength and stiffness of the diaphragm from Example 4.2 is adequate for the system of purlins that is analyzed for anchorage forces in Section 5.4.3. Include diaphragm flexibility to determine the in-plane diaphragm force.

Solution

The in-plane force in the diaphragm is

$$w_{\text{diaph}} = w\left(\alpha\sigma_{diaph} - \sin\theta\right) \quad \text{(Eq. 4.1-11)}$$

In the Section 5.4.3 example, because the eave purlin (Purlin 1) is oriented with the top flange facing downslope, σ_{diaph} must be calculated separately from the remainder of the purlins (Purlins 2 to 12) that are oriented upslope. Exterior span purlins (8ZS2.75x085) must be calculated separately from the interior span purlins (8ZS2.75x059).

The total number of purlins in the bay, n_p = 12. The net number of purlins facing upslope, η = 11 – 1 = 10.

First analyzing the exterior bay, the modified moment of inertia about the y-axis is

$$I_{my} = \frac{I_x I_y - I_{xy}^2}{I_x} = \frac{(12.40)(2.51) - 4.11^2}{12.40} = 1.15\,\text{in}^4$$

From the previous example, G' = 500 lb/in. From Table 4-2, the C_1 = 1/185, C_2 = 1/8, and C_3 = 1/8.

For Purlin 1, facing downslope,

$$\sigma_{diaph} = \frac{C_1 \dfrac{\left(\dfrac{I_{xy}}{I_x}\cos\theta\right)L^4}{EI_{my}} + C_2 \dfrac{\alpha \cdot N_p \cdot L^2 \sin\theta}{G'd'}}{C_1 \dfrac{L^4}{EI_{my}} + C_3 \dfrac{\alpha \cdot \eta \cdot L^2}{G'd'}} \quad \text{(Eq. 4.1-12)}$$

$$\sigma_{\text{diaph,1}} = \frac{\dfrac{1}{185} \cdot \dfrac{\left(\dfrac{4.11}{12.40}\cos(2.39)\right)(300)^4}{(29.5\times10^6)(1.15)} + \dfrac{(-1)(12)(300)^2 \sin(2.39)}{8(500)(660)}}{\dfrac{1}{185}\dfrac{(300)^4}{(29.5\times10^6)(1.15)} + \dfrac{(-1)(10)(300)^2}{8(500)(660)}} = 0.432$$

Note that since Purlin 1 is oriented downslope but the deformation of the diaphragm is upslope, the unsymmetric bending force is larger than that in a rigid diaphragm.

For Purlins 2 to 12, facing upslope,

$$\sigma_{\text{diaph},2-12}=\frac{\frac{1}{185}\cdot\frac{\left(\frac{4.11}{12.40}\cos(2.39)\right)(300)^4}{(29.5\times10^6)(1.15)}+\frac{(1)(12)(300)^2\sin(2.39)}{8(500)(660)}}{\frac{1}{185}\frac{(300)^4}{(29.5\times10^6)(1.15)}+\frac{(1)(10)(300)^2}{8(500)(660)}}=0.272$$

The uniform force in the diaphragm at each purlin is

Purlin 1: $w_{\text{diaph},1} = (23)(2.5)((-1)\ (0.432) - \sin(2.39)) = -27.24$ lb/ft

Purlin 12: $w_{\text{diaph},12} = (23)(2.5)((1)(0.272) - \sin(2.39)) = 13.24$ lb/ft

Purlin 2-11: $w_{\text{diaph},2-11} = (23)(5)((1)\ (0.272) - \sin(2.39)) = 26.48$ lb/ft

The total force in the diaphragm is

$w_{\text{diaph}} = -27.24 + 13.24 + 10(26.48) = 251$ lb/ft

With all other conditions equal, the in-plane diaphragm forces for an interior span will typically be less than an exterior span as a result of continuity. Calculations are provided below as verification. For the interior span purlins (8ZS2.75x059)

$$I_{my}=0.785\text{in}^4$$

For Purlin 1, facing downslope, with C_1 = 1/384, C_2 = 1/8, and C_3 = 1/8

$$\sigma_{\text{diaph},1}=0.494$$

For Purlins 2-12, facing upslope,

$$\sigma_{\text{diaph},2-12}=0.252$$

The uniform force in the diaphragm at each purlin is

Purlin 1: $w_{\text{diaph},1} = (23)(2.5)((-1)\ (0.494) - \sin(2.39)) = -30.80$ lb/ft

Purlin 12: $w_{\text{diaph},12} = (23)(2.5)((1)(0.252) - \sin(2.39)) = 12.09$ lb/ft

Purlin 2-11: $w_{\text{diaph},2-11} = (23)(5)((1)\ (0.252) - \sin(2.39)) = 24.18$ lb/ft

The total force in the diaphragm is

$w_{\text{diaph}} = -30.80 + 12.09 + 10(24.18) = 223$ lb/ft

The above analysis confirms that the in-plane diaphragm force in the interior spans is less than the exterior spans (by approximately 12%), therefore the exterior spans will control the strength and stiffness analysis.

Evaluate Diaphragm Shear Strength

The maximum factored shear force per unit length in the diaphragm in the exterior span is

$$v=\frac{w_{\text{diaph}}L}{2d'}=\frac{(257)(25)}{2(55)}=57\text{ plf} \quad \text{(Eq. 4.1-14)}$$

The strength of the diaphragm from the previous example is

$$\frac{S_{nt}}{\Omega_d} = \frac{1}{2.5}\left(87 + \frac{2925}{55}\right) = 56 \text{ lb / ft} \approx v = 57 \text{ lb / ft} \text{ Say OK} \quad \text{(Eq. 4.1-5)}$$

The diaphragm has adequate strength. Note, this method to predict the required strength results in a smaller value than the previous example although it is still considered a conservative approximation.

Evaluate Diaphragm Deflection

From Example 4.3, the stiffness of the diaphragm is

G′ = 500 lb/in.

The maximum in-plane deflection of the diaphragm is

$$\Delta_s = \frac{w_{diaph} L^2}{8G'd'} = \frac{(251)(25)^2}{8(500)(55)} = 0.71 \text{ in} < L/360 = 0.83 \text{ in} \quad \text{OK} \quad \text{(Eq. 4.1-16)}$$

The diaphragm has adequate stiffness to satisfy the diaphragm in-plane deflection criteria.

Results Summary

By including the diaphragm flexibility in the calculations to determine the in-plane diaphragm force, the force in the diaphragm is approximately 30% less than the force predicted using the conservative approximation of the previous example. This more refined analysis shows that with the reduced in-plane force in the diaphragm, the diaphragm has adequate strength and stiffness to satisfy requirements.

4.5 Example Diaphragm Calculations to Determine Purlin Stability (Diaphragm Flexibility Excluded) - Interior Anchorage - LRFD

Using LRFD, determine the maximum shear force and deflection of the diaphragm from the example provided in Section 5.4.1. The purlins are simple span with restraints at 1/3 points. The diaphragm is a through-fastened diaphragm with G′ = 9000 lb/in. (essentially rigid). The force in the anchorage device, P_L = 432 lb.

Solution

The in-plane force in the diaphragm at service load levels is

$$w_{diaph} = w\left(\alpha \frac{I_{xy}}{I_x}\cos\theta - \sin\theta\right) = \left(\frac{44}{1.5}\right)(15)\left((1)\frac{8.41}{28.4}\cos(1.194) - \sin(1.194)\right) = 121 \text{ plf}$$

(Eq. 4.1-10)

The factored in-plane force in the diaphragm is

$w_{diaph,u}$ = (121)(1.5) = 182 lb/ft

The maximum shear force must be checked at the frame line and each side of the brace.

At the frame line:

$$v_u = \frac{P_L}{d'} - \frac{w_{diaph} L}{2d'} = \frac{432}{15} - \frac{(182)(20)}{2(15)} = \text{-92.5 lb/ft} \quad \text{(Eq. 4.1-20)}$$

At the outside edge of the third point anchor

$$v_u = \frac{P_L}{d'} - \frac{w_{diaph} L}{6d'} = \frac{432}{15} - \frac{(182)(20)}{6(15)} = -11.6 \text{ lb/ft} \qquad \text{(Eq. 4.1-21)}$$

At the inside edge of the third point anchor

$$v_u = \frac{w_{diaph} L}{6d'} = \frac{(182)(20)}{6(15)} = 40.4 \text{ lb/ft} \qquad \text{(Eq. 4.1-22)}$$

Therefore, the maximum factored shear force in the diaphragm occurs at the frame lines and has a magnitude of 92.6 lb/ft.

The deflection of the diaphragm is calculated at the frame lines at service load levels.

$$\Delta_S = \frac{P_L L}{3G'd'} - \frac{(w_{diaph})L^2}{9G'd'} = \frac{\left(\frac{432}{1.5}\right)(20)}{3(9000)(15)} - \frac{121(20)^2}{9(9000)(15)} = 0.014\text{-}0.040\text{=-}0.026 \text{ in.} \qquad \text{(Eq. 4.1-23)}$$

The deflection is compared to the limit of L/360 where L is the distance between lines of anchorage (1/3 of the span length).

$$\frac{L}{360} = \frac{\frac{1}{3}(20\text{ft})(12\ \text{in}/\text{ft})}{360} = 0.22\text{in} >> 0.026\text{in}.$$

Note, in the example in Section 5.4.1, the deflection of the diaphragm is approximated as a cantilever from the third point to the support location. The approximation of a cantilever generally gives good correlation although slightly unconservative relative to the more refined calculation presented here. However, because interior anchorage configurations are so effective in limiting lateral deflection, the lateral deflection limits are typically very small and won't control the design.

CHAPTER 5 SYSTEM ANCHORAGE REQUIREMENTS

Symbols and Definitions used in Chapter 5

Note: Other variables in this Chapter have been defined as they are introduced.

A	Full unreduced cross-sectional area of the member (in.^{2}) (mm^2)
A_p	Gross cross-sectional area of the roof panel per unit width(in.^{2}) (mm^2)
a	Torsional constant $\sqrt{\frac{EC_w}{GJ}}$
B	In-plane depth of the diaphragm (ft) (m)
B	Width of the roof plane (ft) (m)
Bay	Total width of the diaphragm perpendicular to the span (ft) (m)
b	Width of C- or Z-section top flange (in.) (mm)
b_{pl}	Width of the anti-roll clip or web plate (in.) (mm)
C_w	Torsional warping constant of the cross-section (in.^{6}) (mm^6)
C1 to C6	Coefficients tabulated in AISI S100 Tables I6.4.1-1 to I6.4.1-3
C1	Flexural deflection constant
D	Dead load (lb/ft^2) (N/m^2)
d	Depth of the C- or Z-section (in.) (mm)
$d_{p_{i,j}}$	Distance along the roof slope between the ith purlin line and the jth anchorage device
$d_{p_{o,j}}$	Distance along the roof slope between the ridge and the jth anchorage device
$d_{p_{i,o}}$	Distance along the roof slope between the ith purlin line and the ridge
E	Modulus of elasticity (29,500,000 psi) (203,000 MPa)
G	Shear modulus (11,300,00 psi) (78,000 MPa)
G′	Diaphragm shear stiffness. Ratio of shear per foot to the deflection per unit width of diaphragm assembly (lb/in.) (N/m)
h	Height of applied restraint measured from the base of the purlin parallel to the web (in.) (mm)
I_{my}	Modified moment of inertia of full unreduced section about minor centroidal axis (in.^{4}) (mm^4)
I_x	Moment of inertia of the full unreduced section about major centroidal axis perpendicular to the web (in.^{4}) (mm^4)
I_{xy}	Product of inertia of the full unreduced section about major and minor centroidal axes perpendicular and parallel to the web respectively (in.^{4}) (mm^4)
I_y	Moment of inertia of the full unreduced section about minor centroidal axis parallel to the web (in.^{4}) (mm^4)
I_{panel}	Gross moment of inertia of the panel (in.^{4}) (mm^4)
i	Index of each purlin line
J	Saint-Venant torsion constant (in.^{4}) (mm^4)
j	Index for each anchorage device
K_{3rd}	Total stiffness of the anchorage at the third points (lb/in.) (N/m)
K_a	Lateral stiffness of anchorage device (lb/in.) (N/m)
K_{a_req}	Required lateral stiffness of the anchorage device (lb/in.) (N/m)
K_{config}	Stiffness of the purlin web above the anchorage device (lb/in.) (N/m)

K_{D_k} Stiffness of the spring modeling connection between purlin k and k+1 based on the axial stiffness of the roof panels (lb/in.) (N/m)
K_{device} Stiffness of the anchorage device at a height along the web of a purlin where restraint is applied (lb/in.) (N/m)
$K_{eff_{i,j}}$ Effective lateral stiffness of the jth anchorage device with respect to the ith purlin (lb/in.) (N/m)
K_{rafter} Rotational stiffness of the purlin-to-rafter connection (lb-in./in.) (N-m/m)
K_{req} Required stiffness (lb/in.) (N/m)
K_{rest} Stiffness of externally applied restraint (lb/in.) (N/m)
K_{spt} Combined anchorage device and rafter stiffness at the frame line (lb/in.) (N/m)
K_{sys} Lateral stiffness of the roof system, neglecting the anchorage devices (lb/in.) (N/m)
K^*_{sys} Lateral stiffness of the spring modeling inherent restraint at one purlin (lb/in.) (N/m)
K_{total} Total stiffness of the system at anchorage device (lb/in.) (N/m)
K_{total_i} Effective lateral stiffness of all elements resisting the force P_i (lb/in.) (N/m)
K_{panel} Rotational stiffenss provided by the panels (lb-in./in.) (N-m/m)
K_{trib} Combined anchorage and rafter stiffness at the frame line tributary to each half-span (lb/in.) (N/m)
k Index for each purlin spacing
k_{conn} Rotational stiffness of the connection between the purlin and panels per unit length along the span of the purlin (lb-in./ft) (N-m/m)
k_{mclip} Combined rotational stiffness of panels and connection between the purlin and panels per unit length along the span of the purlin (lb-in./ft) (N-m/m)
L Span of the purlin (ft) (m)
L_B Purlin segment length for test for determining the rotational stiffness of the connection between the purlin and the panels (ft) (m)
L_{diaph} Span of the diaphragm between the lines of anchorage
m Horizontal distance from the shear center of the C-section to the mid-plane of web (m = 0 for Z-sections) (in.) (mm)
M_{3rd} Moment in the third point torsional brace (lb-in.) (N-m)
M_{local} Moment developed in the panels due to the cross-sectional deformation of the purlin (lb-in.) (N-m)
M_{rafter} Resisting moment developed in the connection between the rafter and the purlin due to the lateral movement of the top flange relative to the base (lb-in.) (N-m)
M_{panel} Resisting moment developed in the panels along the span of the purlin due to the lateral movement of the top flange relative to the base (lb-in.) (N-m)
$M_{torsion}$ Moment developed in the panels due to twist of the purlin relative to the panels (lb-in.) (N-m)
N_a Number of anchorage devices along a line of anchorage
$n_{downslope}$ Number of purlins with flanges facing downslope in a bay
N_p Number of purlin lines on the roof slope
$n_{upslope}$ Number of purlins with flanges facing upslope in a bay
P_h Anchorage force per anchorage device at the height of the restraint (lb) (N)

P_i Lateral force introduced into the system at the ith purlin (lb) (N)
P_L Lateral force resisted by the anchorage system (lb) (N)
P_{L_j} Lateral force to be resisted by the jth anchorage device (lb) (N)
P_{L-s} Lateral force to be resisted by each anchorage device (lb) (N)
P_N Nominal test load for determining the rotational stiffness of the connection between the purlin and the panels (lb) (N)
P_{sc} Shear force in the connection between the purlin and the panels at the anchorage device location (lb) (N)
q Design load in the plane of the web (lb/ft^2) (N/m^2)
q_{drift} Design drift snow load (lb/ft^2) (N/m^2)
R_{local} Coefficient to account for the purlin cross-sectional deformations
R_{sys} Reduction factor to account for the panel system effects
S Typical purlin spacing (ft) (m)
S Snow load (lb/ft^2) (N/m^2)
S_k Distance between purlin k+1 and k (ft) (m)
span Span of the panels between the adjacent purlins (ft) (m)
t Base steel thickness of the purlin (in.) (mm)
t_e Base steel thickness of the eave member (in.) (mm)
t_{lap} Equivalent thickness of the purlins at the lap (in.) (mm)
t_{pl} Thickness of the web bolted rafter plate (in.) (mm)
Width Tributary width of the diaphragm (perpendicular to the purlin span) per purlin (in.) (mm)
W_{pi} Total required vertical load supported by the ith purlin in a single bay (lb) (N)
W_s Total required vertical load supported by all purlins in a single bay (lb) (N)
w Uniform loading on the purlin (lb/ft) (N/m)
w_{diaph} Distributed in-plane load on the roof diaphragm (lb/ft^2) (N/m^2)
w_i Required distributed gravity load supported by the ith purlin per unit length (lb/ft) (N/m)
w_{rest} Uniform diaphragm restraint force provided by the panels (lb/ft) (N/m)
α Coefficient for purlin direction
β Torsional constant for a beam subjected to uniform torsion (rad)
β_{3rd} Torsional constant for a beam subjected to a concentrated torque at third points (rad/lb/in.) (rad/N/m)
δ Coefficient for determining the load eccentricity on the purlin top flange (1/3)
Δ_a Allowable deflection of the purlin along the line of anchorage (in.) (mm)
Δ_{config} Deflection of the web of the purlin relative to the height of the restraint at the anchorage location (in.) (mm)
Δ_{device} Deflection of the anchorage device at the anchorage location (in.) (mm)
Δ_{diaph} In-plane deflection of the roof diaphragm (in.) (mm)
Δ_{rest} Lateral deflection of the top flange of purlin at restraint (in.) (mm)
Δ_S Simplified approximation of the purlin deflection along the line of anchorage (in.) (mm)
γ Ratio of the lateral anchorage force to the applied gravity load

η Number of upslope facing purlins minus the number of downslope facing purlins ($n_{upslope}$ - $n_{downslope}$)
κ Torsional constant for a beam subjected to a parabolically varying torsion ($rad \cdot in.^2$) ($rad \cdot mm^2$)
σ Proportion of the uniformly applied vertical force transferred to a uniform restraint force in the panels
θ Angle between the vertical and the plane of the purlin web (degrees)
τ Torsional constant for a beam subjected to uniform torsion with uniformly distributed rotational springs resistance (rad/lb) (rad/N)
Φ Rotation of the Z purlin at the mid-span without torsional resistance (rad)
Φ_{local} Rotation of the flange relative to the web due to cross section deformation (rad)
Φ_{net} Net rotation of the Z purlin at the mid-span with torsional restraint from the panels (rad)
$\Phi_{Mtorsion}$ Rotation of the purlin at the mid-span due to the torsional restraint from the panels (rad)
ϕ Resistance factor
Ω Safety factor

5.1 Introduction

The design of purlins, as presented in AISI S100 and illustrated in the previous chapters of this Design Guide, neglects any torsional stresses in the members due to loading that is oblique to the principal axes or eccentric to the shear center. Typically, in metal building roof systems, the roof panels provide sufficient lateral and some torsional restraint to the purlins to justify the use of the provisions within AISI S100. The lateral support provided to the purlins produces lateral forces perpendicular to the web of the purlins. These lateral forces accumulate as a shear force across the roof diaphragm that must be transferred from the plane of the panels into the primary lateral resistance system, or to a point where it is counteracted by an opposing force.

This Chapter presents background information on the research that led to the development of the provisions presented in AISI S100, as well as guidance on the application of the provisions to several commonly encountered special conditions. These special procedures are introduced and illustrated with examples. Also, both a simplified and a more thorough solution procedure are presented.

In metal building roofs, the anchorage force is commonly transferred to the main frames through a connection between the purlin and the rafter that restrains torsional rotation of the purlin at the rafter, typically referred to as an anti-roll anchorage device. This anchorage technique requires few additional parts and does not rely on the presence of counteracting forces. Additionally, lateral braces may be provided at discrete locations along a purlin span. These discrete braces must either be arranged so the anchorage forces counteract or they must provide a continuous load pathway to the building's lateral load resisting system. Resisting the anchorage forces with opposing forces is frequently not practical due to asymmetric geometry or loading, such as unbalanced snow loads. The transfer of the anchorage forces from the lines of anchorage to the lateral load resisting system can be accomplished through the addition of diagonal bracing or by connecting the braces to a collector element, such as a spandrel beam. During the development of the latest anchorage provisions, it was found that the flexibility of these collector elements can greatly influence the forces and displacements within the system anchorage.

It is important to recognize that a typical metal building structure consists of several interrelated load resisting systems, and that the same mechanisms that provide lateral support to the purlins under flexural loads will also resist lateral movement under other loading conditions. For example, the thermal movement of the roof panels relative to the primary framing below will create differential movement between the top and bottom flanges of the purlins. The forces that develop in the system due to this movement can be avoided by concentrating the lateral resistance at a single location and allowing the roof to expand away from this point. However, due to the flexibility of the roof system, this may not provide adequate support for the purlins most remote from this anchorage device. Another approach is to provide several points of anchorage distributed throughout the roof plane, each with enough stiffness to adequately support the purlins, but also flexible enough to allow the roof system to expand and contract under thermal changes without generating excessive lateral forces. Also, in metal building roof systems, it is common to rely on the diaphragm action of the roof panels to transfer the longitudinal wind and seismic loads on the building to the sidewalls. Depending on the details used, this diaphragm shear may also be transferred through other secondary framing members and must also be addressed.

An alternative method is to use torsional braces to directly resist the torsional moments developed within the roof system. These will typically take the form of diaphragm members, such as cold formed channels, that connect to the purlin webs. When these braces are used, the roof system may deflect significantly in the plane of the roof panels, but because the purlins cannot rotate, they still achieve their full design strength.

5.2 Development of Design Provisions

The provisions presented in AISI S100 Section I6.4, Roof System Bracing and Anchorage, draw heavily on the testing performed at Virginia Tech by Lee and Murray (2001), and Seek and Murray (2004a), as well as the experience of the members of the AISI Task Group on Anchorage and Bracing. The knowledge base upon which the provisions are built was expanded by the analytical work of Sears (2007), Seek (2007), Sears and Murray (2007), and Seek and Murray (2007), which culminated in the development of the design provisions and analysis models presented in AISI S100 and in this Design Guide.

5.2.1 Provisions of AISI S100 Section I6.4.1 Anchorage of Bracing for Purlin Roof Systems under Gravity Load with Top Flange Connected to Metal Sheathing

The provisions presented in AISI S100 Section I6.4.1 have two parts: a semi-empirical force calculation starting with Eq. I6.4.1-1 and a simplified relative stiffness analysis starting with Eq. I6.4.1-7. The provisions replicate the results of the 3D computer stiffness model presented in Section 5.5.5 of this Design Guide. The computer model was developed and validated using the results of laboratory testing, and allowed for the analysis of systems that were not tested. A large matrix of test models was analyzed and the results were used to develop the provisions in the AISI S100.

Modeling Basics

In both the computer model and the manual calculation procedure, uniform roof loads are resolved as line loads at each purlin based on the tributary area. In the physical roof system these loads are transferred from the panels, referred to as sheathing in AISI S100, to the purlin through bearing on the top flange. This bearing produces an uneven force distribution across the width of the purlin flange that is not well defined. It was found during the development of the computer stiffness model, that the effects of this eccentric load can be approximated by applying the line load at a distance equal to one-fourth of the flange width from the mid-plane of the purlin web.

The anchorage devices are represented by spring restraints at the top of the anchored purlins. The stiffness of the springs must be quantified by testing or detailed analysis. When establishing both the strength and stiffness of the anchorage devices it is important to recognize that the AISI S100 provisions assume the anchorage device is connected at the purlin-to-panel interface. Since most anchorage devices will connect to the purlin web, the appropriate adjustments must be made to the results of the tests or analyses to yield values for an equivalent anchorage at the purlin-to-panel interface.

In the computer stiffness model, the purlin-to-rafter and the purlin-to-panel connections are modeled as rotational springs. For the manual calculation procedure there is no need to quantify the stiffness of these springs, as this spring stiffness is not explicitly used.

Model Simplifications

Since the intent of these design provisions is to address the lateral behavior, the design model is simplified to a one-dimensional system with only lateral degrees of freedom. The lateral effect of the gravity load is found from the semi-empirical equation for P_i, the lateral force introduced into the system at the ith purlin,

$$P_i = C1 \cdot W_{p_i} \cdot \left[\left(\frac{C2}{1000} \cdot \frac{I_{xy} L}{I_x d} + C3 \cdot \frac{(m + 0.25b)t}{d^2} \right) \alpha \cdot \cos\theta - C4 \cdot \sin\theta \right] \qquad \text{(AISI S100 Eq. I6.4.1-2)}$$

This equation includes three primary parts, where the first represents the effect of the load being applied oblique to the principal axes, the second models the load application eccentric to the shear center while the third applies the downslope component of the applied load. The form of this equation was derived from a combination of basic mechanics and statistical analysis of the results of the computer stiffness model. The force, P_i, represents the anchorage force at a given purlin if every purlin is anchored with a rigid anchorage device.

In this one-dimensional model, the rotational degrees of freedom are not included, so the rotational restraint provided at the purlin-to-panel connections must be replaced with equivalent lateral restraints. The mechanisms involved that contribute to the behavior of this spring are the rotation of the connections and the out of plane bending of the purlin web. It was found, through statistical analysis of the computer stiffness model results, that the stiffness of these lateral springs is found from

$$K^*_{sys} = \frac{C5}{1000} \cdot \frac{ELt^2}{d^2} \qquad \text{(Eq. 5.2.1-1)}$$

The purlins are linked together by the roof panels, which will carry an axial load. The behavior of the panels is modeled as axial springs with a stiffness of

$$K_{D_k} = \frac{C6 \cdot LA_p E}{S_k} \qquad \text{(Eq. 5.2.1-2)}$$

At this point the model can be solved with matrix methods. The applicable solution is presented in Section 5.5.2.

However, there was a desire to simplify the procedure so that it is practical to carry out the calculations with basic algebraic calculations. The model was simplified slightly by grouping the stiffness of all the K^*_{sys} springs into one, globally acting, spring with a stiffness of

$$K_{sys} = \frac{C5}{1000} \cdot N_p \cdot \frac{ELt^2}{d^2} \qquad \text{(AISI S100 Eq. I6.4.1-6)}$$

This may be done without substantially affecting the results because the stiffness of the K_{sys} springs is relatively small compared to the axial behavior of the roof panels and the panels behave approximately as a rigid strut.

The forces in the multi-degree-of-freedom system may be found without the use of matrix methods by considering each purlin separately and the elements of the model that contribute to its stability. At each purlin, the force, P_i, is distributed to each of the anchorage devices and to the K_{sys} spring, based on the relative stiffness of each of the elements. Since the anchorage devices are in series with the axial behavior of the roof panels, the stiffness of the anchorage devices is effectively reduced due to the axial flexibility of the panels. This reduced stiffness is found from

$$K_{eff_{i,j}} = \left[\frac{1}{K_a} + \frac{d_{p_{i,j}}}{C6 \cdot LA_p E} \right]^{-1}$$ (AISI S100 Eq. I6.4.1-4)

With the stiffness of each supporting element defined, the force, P_i, is distributed to each of these elements based upon their relative stiffness.

This pseudo-single-degree-of-freedom procedure provides nearly the same force, P_L, as the matrix solution. However, the procedure does not provide the lateral displacements of the purlins. To develop an estimate of the lateral deflections, two special cases were considered.

1) For a roof system with anchorage only at one purlin line, the deflection at the anchorage device is the anchorage force divided by the device stiffness, P_L/K_a. The deflection at other purlins is larger due to the flexibility of the panels. This increase mimics the decrease in the value of K_{eff} and indicates that the stiffness reduction included in K_{eff} should be included in the deflection calculation.
2) For a roof system with an anchorage device at every purlin, the deflection at each purlin is again the anchorage force divided by the device stiffness, P_L/K_a. Multiplying the numerator and denominator by the number of purlins, N_p, produces an equivalent expression, $N_pP_L/(N_PK_a)$. If the system stiffness is neglected, and the purlins are uniformly spaced, the anchorage force is simply P_i and the numerator of the previous expression is equal to the sum of all P_i terms. If the flexibility of the panels is neglected, K_{eff} equals K_a, and the denominator becomes the summation of K_{eff}, or K_{total}. Making these substitutions results in $\Delta_i = sum(P_i)/K_{total}$.

This approximation works well when anchorage devices are relatively stiff and reasonably spaced. As the distance between anchorage points increases, the approximation will tend to over-predict the displacement.

For the anchorage devices to perform properly they must possess adequate strength and stiffness. Based on the observations of past purlin tests by members of the AISI Task Group on Anchorage and Bracing, a lateral displacement limit of the purlin depth divided by 20 has been established as the critical point where an anchorage device becomes ineffective and the purlin is at risk of a global stability failure. For convenience, this displacement limit has been reformulated as a critical stiffness limit for use in AISI S100.

For multi-span systems with anchorage at the supports, the anchorage force is transferred partially from each of the adjacent bays. If these two bays have different span lengths or purlin sizes, the following procedure is used to average the effect from each bay.

1) The forces, P_i, are calculated independently using the properties of each of the two bays separately. The resulting force is then averaged for each purlin line.
2) The system stiffness, K_{sys}, is calculated by evaluating the equation with L, t, and d taken as the average of the values from the two bays.
3) The effective lateral stiffness of the anchorage device, K_{eff}, is calculated using the average of the two span lengths.

This procedure is illustrated in the example provided in Section 5.4.3.

For multi-span systems with restraints at 1/3 points or midpoints, analysis of computer stiffness models has shown that the anchorage forces can be reasonably estimated by calculating an average force in a manner similar to that outlined above for restraints at the supports, except the procedure considers three bays: the current bay and one to each side of the current bay.

During the verification of the model and the calibration of the coefficients in the calculation procedure, significant scatter was observed in the results at the end anchorage in multi-span systems. This is most likely due to the difference in the lateral stiffness of the purlins at the end frame line and the first interior frame line and how this affects the distribution of the forces between the first few lines of anchorage. To account for this scatter and to minimize the chance of calculating significantly unconservative forces, the provisions require that the line of anchorage nearest the end of a multi-span system be designed for the larger of the forces calculated for the line of anchorage, and 80% of the value found using the coefficients C2, C3 and C4 for the typical interior case.

5.2.2 Provisions of AISI S100 Section I6.4.2 Alternate Lateral and Stability Bracing for Purlin Roof Systems

The provisions of AISI S100 Section I6.4.2 are intended to apply to torsional braces along the span of a C- or Z-section that only resist torsion of the purlin and do not resist the lateral movement of the section. When used in conjunction with anti-roll devices at the frame lines, the torsional braces are effective in stabilizing the purlin even as it is permitted to move laterally. For this reason, a more relaxed requirement for the lateral displacement of the C-section or Z-section at mid-span is permitted.

Analysis of torsional braces can be first order because if the lateral deflection criteria are met, second order effects should be minimal and easily absorbed by the torsional braces. An analysis of torsional braces should consider the forces generated due to the eccentricity of the applied loads and the effects of the interaction of the lateral restraining forces in the panels with the purlin. Analysis should also include the effects the torsional braces have on the lateral restraints applied at the frame line. The component stiffness method presented in detail in Section 5.5.4 of this Design Guide provides a method for evaluating torsional braces at one-third points. Torsional braces may also be evaluated using the finite element analysis models outlined in Section 5.5.6.

5.3 Applications of the AISI S100 Provisions

The provisions of AISI S100 Section I6.4 provide design criteria and analysis procedures for the required restraint of purlin systems so that the torsional stresses in the members are negligible and the purlin design provisions in AISI S100 Section I6.2 may be utilized. The provisions of AISI S100 Section I6.4.1 are applicable to restraint systems that resist the movement of purlins within the plane of the roof panels, thus indirectly minimizing the member torsion. AISI S100 Section I6.4.2 provides general guidance for the design of systems where lateral displacements are not restrained, but the torsional moments are resisted directly by braces attached to the purlins.

ASD vs. LRFD

Since the procedures are used to calculate forces and/or moments within the bracing systems rather than the resistance provided by an anchorage device, they are equally applicable to ASD and LRFD design methodologies. The only distinction required is the use of nominal loads for ASD and factored loads for LRFD when calculating the force distributed to the anchorage devices. However, for the stability check within the provisions an adjustment is required. The displacement limit of d/20 in AISI S100 was established based on the observations of tests. Therefore, the limit is based on the deflection under ultimate loads. However, in this formulation no adjustment has been made in either equation for the likely variability in the provided stiffness. To make this adjustment a resistance factor, ϕ, or the safety factor, Ω, is included in the deflection and/or minimum stiffness limits.

Load Cases and Pattern Loading

It is generally accepted that the lateral effects in metal building roof systems are only of concern for downward loading on the roof, due to the destabilizing effect of the top flange gravity loading. Generally, the anchorage force and stiffness requirements need only be checked under the controlling gravity load combination, typically a combination of dead load and roof live or snow load. Since the lateral effects are primarily induced by the application of the load, and not the flexural behavior of the purlin, the effects of pattern loading only need to be considered when the forces tend to counteract, such as back-to-back C-sections with restraints at the supports.

5.3.1 Discrete Bracing

When lateral restraints resist the movement of the purlins within the plane of the roof panels and transfer the resulting force to an element of the lateral load resisting system, the provisions of AISI S100 Section I6.4.1 provide a means of predicting the forces in the anchorage devices and verifying stability of the purlin system. As presented in AISI S100, the provisions address the requirements for the majority of metal building roof systems. Various conditions exist where the applicability of the provisions is not perfectly clear. The following provides the authors' recommendations for applying the provisions to several of these conditions.

Non-Uniform Loading

The general presentation of the AISI S100 provisions is based on the application of uniform loads. The provisions can be directly applied to systems where the gravity load varies from the eave to ridge (for example, snow drift at the high side) by using the appropriate line load, W_p, at each purlin. However, when the loads vary along the length of the purlin (e.g., snow drift at the end wall) a special approach is needed.

In the AISI S100 procedure the force W_p is equal to wL, or twice the simple span end reaction. When the load is non-uniform the force W_p should be taken as twice the end reaction of a simple span beam with the same bay span and loading as the purlin under consideration.

Cantilevers

For purlin spans that cantilever over an end support, the value of W_p when analyzing the line of anchorage nearest the cantilevered end is taken as twice the end reaction for a simple span beam with the same back span, cantilever and loading. Also, the value of L used to calculate K_{sys} and K_{eff} is the back span length. At other lines of anchorage, the effect of the cantilever is neglected. This procedure is illustrated in the example provided in Section 5.4.5.

Flush Mounted Purlins

Where purlins are flush mounted to the web of the supporting rafter, each connection must be designed to resist the moment caused by the force P_i applied at the purlin-to-panel interface. This moment will typically be equal to $P_i(d/2)$.

Purlin-to-Rafter Connections

The provisions in AISI S100 are based on tests of purlins where the bottom flanges were bolted directly to the rafter flange. However, it is also common for purlins to be attached through the web plates that are welded or bolted to the rafter as shown in Figure 1.2-2.

If all purlins are connected with identical web plates, the attachment may simply be designed for the force P_i as described above for flush mounted purlins. If the typical connection does not provide adequate strength or stiffness, then selected locations may be stiffened. For this condition, it is recommended that the provisions be applied by either treating the stiffened connections as anchorage points and assuming the behavior of the other purlins is the same as that for the flange bolted condition, or by treating all of the connections as anchorage points with the appropriate stiffness values, K_a, used at each purlin. In this second condition K_{sys} should be conservatively taken as zero, otherwise some of the system stiffness would be counted twice.

Lines of Anchorage Not at Exact 1/3 Points

Where two lines of anchorage are installed at points somewhere between the 1/3 points and the midpoint, the anchorage devices should conservatively be designed for the larger of the forces found for 1/3 point restraints or half the value for midpoint restraints. Using two lines of anchorage outboard of the 1/3 points is not recommended.

Non-Parallel Rafters

In cases where building rafters are not parallel (hips, valleys, skewed end walls etc.) the force P_i is to be calculated using the appropriate span length for each purlin. The values of K_{sys} and K_{eff} may be calculated using the average purlin span.

Eave Struts

When the deflection and rotation of the building eave member is continuously supported by the wall system, the member may be neglected in the anchorage calculations. However, if this is not the case (open sidewall) the eave member needs to be considered.

Opposing Purlins

For low sloped roofs, where the anchorage force is positive, a portion of the purlins can be turned with the top flange facing downslope to counteract the tendency of the roof system to displace upslope. To model this condition, the term α in AISI S100 Eq. I6.4.1-2 is taken as +1 for those purlins that face upslope and -1 for those that face downslope. If the reversed purlins are not evenly distributed throughout the roof plane, the AISI S100 provisions will not adequately address the minimum stiffness requirements. If the reversed purlins are grouped into one area, the matrix solution presented in Section 5.5.2 of this Design Guide is recommended to more completely address the displacement of the purlins.

Diaphragm Load

To ensure that the roof panels provide adequate support to the purlins to justify the design of the purlins without considering torsional stresses, AISI S100 limits the lateral deflection of the diaphragm to L/360, at service level loads. AISI S100 is silent as to the force to be used for this check, and the work by Sears and Murray (2007), upon which the AISI S100 provisions are based, did not directly address this requirement. However, the component stiffness method (Seek and Murray 2006) does provide a method to check this displacement. By starting with the provisions of the component stiffness method, and identifying those terms that have the greatest influence on the diaphragm load, it can be shown that the line load applied to the diaphragm is very reasonably approximated as follows.

$$w_{diaph} = \sum \left[w \left(\frac{I_{xy}}{I_x} \alpha \cos\theta - \sin\theta \right) \right]_i \qquad \text{(Eq. 5.3.1-1)}$$

With this value the diaphragm deflection for all span conditions is approximated by

$$\Delta_{diaph} = \frac{w_{diaph} L^2}{8G'B} \qquad \text{(Eq. 5.3.1-2)}$$

5.3.2 Torsional Bracing

Torsional bracing (Figure 1.3-1(b)) can be evaluated using the methodology described in (Seek and Avci 2021). The components of gravity load normal and parallel to the plane of panels on a sloped roof cause torsional moments on a purlin that must be resisted by the torsional restraints. Diaphragm forces generated in the panels as a purlin is loaded and deflects laterally produce additional torsional moments. It is typically assumed that torsional restraints completely restrict rotation of the purlin at the restraint because most torsional restraints, if properly connected near the top and bottom flanges, possess considerably more stiffness than the torsional stiffness of a cold-formed purlin. However, the behavior of these systems is very sensitive to the connection details, and typically the behavior of these systems should be verified by tests. The magnitude of the moments at the internal torsional restraints affects the lateral forces anchored at each frame line.

Systems of purlins with torsional braces can be evaluated in pairs. At each end of the torsional brace, a moment is generated. Equilibrium of the brace is maintained through the development of opposing shear forces at each end of the brace applying uplift forces to one purlin and downward forces to the other. These forces should be considered when evaluating the flexural strength of the purlin.

5.4 Examples – AISI S100 Provisions

In the following examples, which are based on AISI S100 provisions, equation numbers referenced are from S100 and AISI D100, *Cold-Formed Steel Design Manual (*AISI, 2017).

5.4.1 Example: Single Bay Z-Purlin Attached to Through-Fastened Panels with One-Third Points Anchorage at Low Eave Purlin - LRFD

Determine the anchorage force, using LRFD, for a single bay roof with four parallel 10ZS3.25x105 purlin lines spaced at 5 ft - 0 in. on center, top purlin flange facing in up-slope direction, a slope of 1/4 in. per ft, and a factored uniform load of 44 psf. The roof system is a through-fastened panel with a cross-sectional area of 0.18 in.^{2}/ft and shear stiffness of 9000 lb/in. The system is anchored at one-third points of the low eave purlin, and the anchorage devices have a stiffness of 15 kip/in.

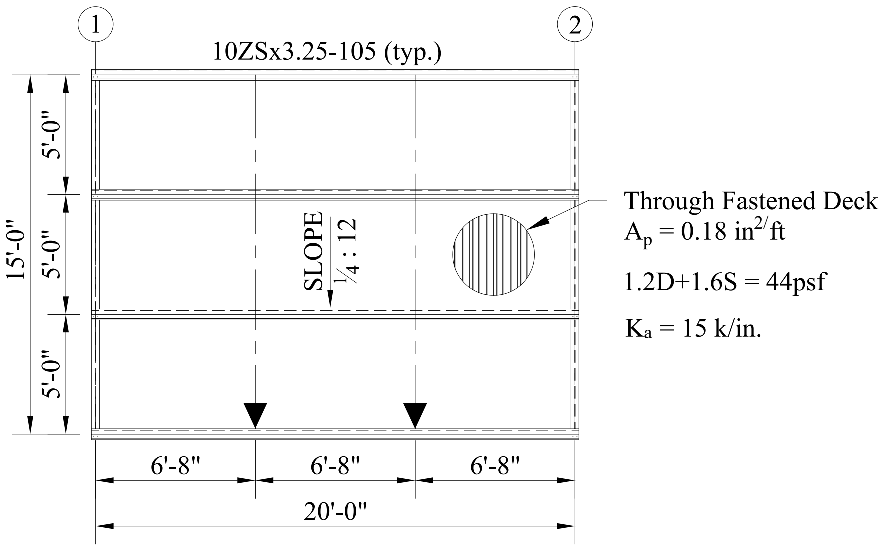

System Configuration

N_p = 4

N_a = 1

K_a = 15 kip/in.

A_p = 0.18 in.^{2}/ft

G′ = 9000 lb/in.

θ = arctan(0.25/12) = 1.194 degrees

B = 15 ft/cos (1.194 degrees)

10ZS3.25x105 Purlin Properties from AISI D100 Table I-4

d = 10 in.

b = 3.25 in.

t = 0.105 in.

I_x = 28.4 in.^{4}

I_{xy} = 8.41 in.^{4}

Coefficients from AISI S100 Table I6.4.1-3

C1 = 0.5
C2 = 7.8
C3 = 42
C4 = 0.98
C5 = 0.39
C6 = 0.40

Purlin 1 is the eave (anchored) purlin and Purlin 4 is the ridge purlin.
The gravity load tributary to each purlin is:

$$W_{p_1} = W_{p_4} = (2.5)(44)(20) = 2200\text{ lb}$$

$$W_{p_2} = W_{p_3} = (5)(44)(20) = 4400\text{ lb}$$

To verify whether the diaphragm provides the required stiffness, the diaphragm deflection is checked. Since this check is performed at the service load level, the loads found above are divided by 1.5 to adjust the forces to approximately the unfactored level.

$$w_{diaph} = \sum \left[\frac{W_p}{L} \left(\frac{I_{xy}}{I_x} \cos\theta - \sin\theta \right) \right]_i \qquad \text{(Eq. 5.3.1-1)}$$

$$= \left[2\,\frac{(2200+4400)/1.5}{20} \left(\frac{8.41}{28.4} \cos(1.194) - \sin(1.194) \right) \right] = 121.1\text{ plf}$$

With this value the in-plane diaphragm deflection at each frame line is found by treating one-third of the span as a cantilever.

$$\Delta_{diaph} = \frac{w_{diaph} {L_{diaph}}^2}{2G'B} \qquad \text{(Eq. 5.3.1-2)}$$

$$= \frac{(121.1)(20/3)^2}{2(9000)(^{15}/_{\cos(1.194)})} = 0.020\text{ in} < L/360 = (20\text{x}12/3)/360 = 0.22\text{ in} \quad \text{OK}$$

The in-plane deflection at the midpoint of the bay is one fourth of this value.

AISI S100 Eq. I6.4.1-2 is used to calculate the lateral load introduced into the system at each purlin:

$$P_i = C1 \cdot W_{p_i} \cdot \left[\left(\frac{C2}{1000} \cdot \frac{I_{xy}L}{I_x d} + C3 \cdot \frac{(m+0.25b)t}{d^2} \right) \alpha \cdot \cos\theta - C4 \cdot \sin\theta \right] \qquad \text{(AISI S100 Eq. I6.4.1-2)}$$

$$P_1 = P_4 = 0.5(2200) \left[\left(\frac{7.8}{1000} \frac{(8.41)(20\text{x}12)}{(28.4)(10)} + 42\,\frac{(0+0.25(3.25))(0.105)}{10^2} \right) (1)\cos(1.194) - (0.98)\sin(1.194) \right]$$

$$= 78\text{ lb}$$

Then P_2 and P_3 is found by scaling the result by the W_p terms,

$$P_2 = P_3 = 78\,\frac{4400}{2200} = 156\text{ lb}$$

The system stiffness is found from AISI S100 Eq. I6.4.1-6:

$$K_{sys} = \frac{C5}{1000} \cdot N_p \frac{ELt^2}{d^2} \qquad \text{(AISI S100 Eq. I6.4.1-6)}$$

$$= \frac{0.39}{1000} \cdot (4) \frac{(29500)(20x12)(0.105^2)}{10^2} = 1.22 \, {}^{kip}\!/_{in}$$

The effective stiffness of the anchorage device, relative to each purlin is found from AISI S100 Eq. I6.4.1-4,

$$K_{eff(i,j)} = \left[\frac{1}{K_a} + \frac{d_{p_{i,j}}}{C6 \cdot LA_p E} \right]^{-1} \qquad \text{(AISI S100 Eq. I6.4.1-4)}$$

$$K_{eff(1,1)} = \left[\frac{1}{15} + 0 \right]^{-1} = 15 \, {}^{kip}\!/_{in}$$

$$K_{eff(2,1)} = \left[\frac{1}{15} + \frac{5x12 / \cos(1.194)}{0.40(20x12)(0.18/12)(29500)} \right]^{-1} = 14.69 \, {}^{kip}\!/_{in}$$

$$K_{eff(3,1)} = \left[\frac{1}{15} + \frac{(10x12) / \cos(1.194)}{0.40(20x12)(0.18/12)(29500)} \right]^{-1} = 14.39 \, {}^{kip}\!/_{in}$$

$$K_{eff(4,1)} = \left[\frac{1}{15} + \frac{(15x12) / \cos(1.194)}{0.40(20x12)(0.18/12)(29500)} \right]^{-1} = 14.10 \, {}^{kip}\!/_{in}$$

The total stiffness at each purlin is calculated from the results above and AISI S100 Eq. I6.4.1-5.

$$K_{total(i)} = \sum_{j=1}^{N_a} \left(K_{eff_{i,j}} \right) + K_{sys} \qquad \text{(AISI S100 Eq. I6.4.1-5)}$$

$$K_{total(1)} = 15 + 1.22 = 16.22 \, {}^{kip}\!/_{in}$$

$$K_{total(2)} = 14.69 + 1.22 = 15.91 \, {}^{kip}\!/_{in}$$

$$K_{total(3)} = 14.39 + 1.22 = 15.61 \, {}^{kip}\!/_{in}$$

$$K_{total(4)} = 14.10 + 1.22 = 15.32 \, {}^{kip}\!/_{in}$$

The smallest of these stiffness values, which is the stiffness provided to the most remote purlin, is compared to the required minimum stiffness according to AISI S100 Eq. I6.4.1-7

$$K_{total} > K_{req} \qquad \text{(AISI S100 Eq. I6.4.1-7)}$$

where

$$K_{req} = \frac{1}{\phi}\frac{20 \cdot \left|\sum_{i=1}^{N_p} P_i\right|}{d} \qquad \text{(AISI S100 Eq. I6.4.1-8b)}$$

$$= \frac{1}{0.75} \cdot \frac{20(2 \cdot 0.078 + 2 \cdot 0.156)}{10} = 1.25 \,{}^{kip}\!/_{in} < K_{total(4)} = 15.32 \,{}^{kip}\!/_{in} \quad \text{OK}$$

Finally, the force at the anchorage device is found from the AISI S100 Eq. I6.4.1-1,

$$P_L = \sum_{i=1}^{N_p}\left(P_i \frac{K_{eff_{i,j}}}{K_{total_i}}\right) \qquad \text{(AISI S100 Eq. I6.4.1-1)}$$

$$= 78\frac{15}{16.22} + 156\frac{14.69}{15.91} + 156\frac{14.39}{15.61} + 78\frac{14.10}{15.32} = 432 \text{ lb}$$

5.4.2 Example: Single Bay Z-Purlin Attached to Through-Fastened Panels with One-Third Points Anchorage at Low and Ridge Purlins - LRFD

Repeat the example from Section 5.4.1, but add anchorage devices to the ridge purlin.

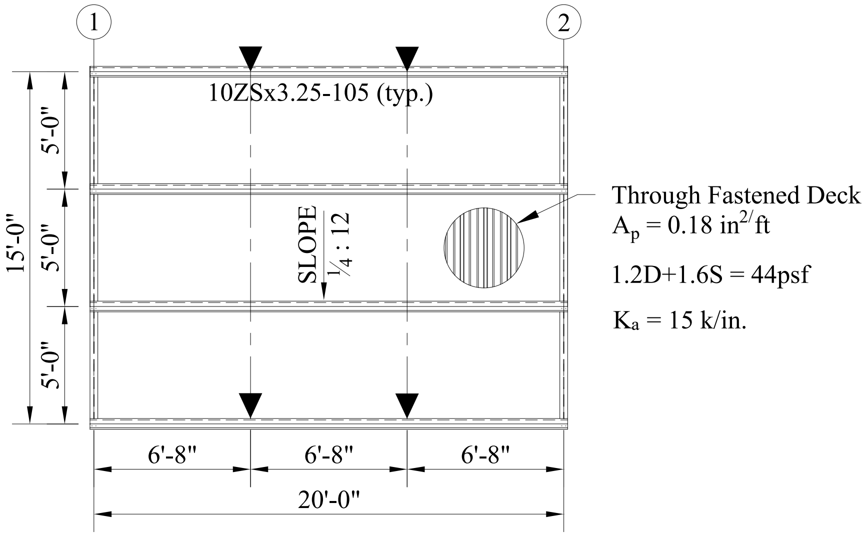

The following values from the example in Section 5.4.1 are also applicable to this example:

$P_1 = P_4 = 78$ lb
$P_2 = P_3 = 156$ lb
$K_{sys} = 1.22$ kip/in.
$K_{req} = 1.25$ kip/in.
$K_{eff(1,1)} = 15$ kip/in.
$K_{eff(2,1)} = 14.69$ kip/in.
$K_{eff(3,1)} = 14.39$ kip/in.
$K_{eff(4,1)} = 14.10$ kip/in.

By inspection the effective stiffness values for the second anchorage device are simply the reverse of those for the first anchorage device.

$K_{eff(1,2)} = 14.10$ kip/in.
$K_{eff(2,2)} = 14.39$ kip/in.
$K_{eff(3,2)} = 14.69$ kip/in.
$K_{eff(4,2)} = 15$ kip/in.

The total stiffness at each purlin is calculated from the results above and the AISI S100 Eq. I6.4.1-5,

$$K_{total_i} = \sum_{j=1}^{N_a}\left(K_{eff_{i,j}}\right) + K_{sys} \qquad \text{(AISI S100 Eq. I6.4.1-5)}$$

$$K_{totat(1)} = 15 + 14.10 + 1.22 = 30.32 \,{}^{kip}\!/_{in}$$

$$K_{total(2)} = 14.69 + 14.39 + 1.22 = 30.30 \, {}^{kip}\!/_{in}$$

$$K_{total(3)} = 14.39 + 14.69 + 1.22 = 30.30 \, {}^{kip}\!/_{in}$$

$$K_{total(4)} = 14.10 + 15 + 1.22 = 30.32 \, {}^{kip}\!/_{in}$$

The smallest of these stiffness values is compared to the required minimum stiffness, K_{req}, according to AISI S100 Eq. I6.4.1-7. Eq. I6.4.1-8b yields the same value of K_{req} as in Section 5.4.1.

$K_{total} > K_{req}$ (AISI S100 Eq. I6.4.1-7)

where

K_{req} = 1.25 kip/in. < $K_{total(2)}$ = 30.30 kip/in. OK

Finally the anchorage force is found from the AISI S100 Eq. I6.4.1-1.

$$P_{L_j} = \sum_{i=1}^{N_p} \left(P_i \frac{K_{eff_{i,j}}}{K_{total_i}} \right) \quad \text{(AISI S100 Eq. I6.4.1-1)}$$

$$P_{L_1} = 78 \frac{15}{30.32} + 156 \frac{14.69}{30.30} + 156 \frac{14.39}{30.30} + 78 \frac{14.10}{30.32} = 225 \text{ lb}$$

$$P_{L_2} = 78 \frac{14.10}{30.32} + 156 \frac{14.39}{30.30} + 156 \frac{14.69}{30.30} + 78 \frac{15}{30.32} = 225 \text{ lb}$$

Note that the anchorage forces from this example are slightly greater than half of that found from the example in Section 5.4.1. This occurs because as additional stiffness is introduced into the system, less force is taken by the “system effect”.

5.4.3 Example: Four Span Continuous Z-Purlin Attached to Standing Seam Panels - ASD

Evaluate the anchorage system for the four continuous spans, standing seam roof system shown. The system consists of twelve parallel Z-purlin lines, with the first purlin reversed (top flange facing downslope) and anchorage devices at the support points of the first, fifth, and ninth purlins. The anchorage devices provide a lateral stiffness of 40 kip/in. The standing seam roof panels have a cross-sectional area of 0.20 in.^{2}/ft and a shear stiffness value of 1200 lb/in. The roof slope is 1/2 in. per ft and the dead plus snow service level roof load is 23 psf.

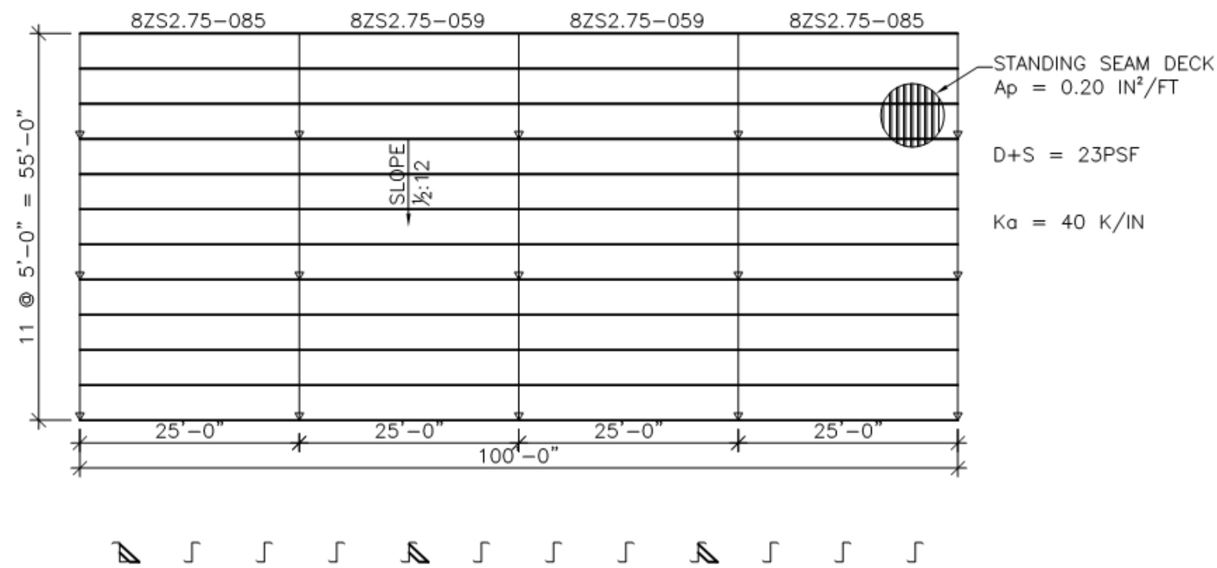

System Properties

N_p = 12

N_a = 3

K_a = 40 kip/in.

A_p = 0.20 in.^{2}/ft

G′ = 1200 lb/in.

θ = arctan(0.5/12) = 2.39 degrees

Purlin Properties from AISI D100 Table I-4

	End Bays	Interior Bays
	8ZS2.75x085	8ZS2.75x059
d	= 8 in.	8 in.
b	= 2.75 in.	2.75 in.
t	= 0.085 in.	0.059 in.
I_x	= 12.40 in.^{4}	8.69 in.^{4}
I_{xy}	= 4.11 in.^{4}	2.85 in.^{4}
I_y	= 2.51 in.^{4}	1.72 in.^{4}

Coefficients from AISI S100 Table I6.4.1-1

		Frame Line 1	Frame Line 2	Frame Line 3
C1	=	0.5	1.0	1.0
C2	=	13	1.7	4.3
C3	=	11	69	55
C4	=	0.35	0.77	0.71
C5	=	2.4	1.6	1.4
C6	=	0.25	0.13	0.17

Purlin Layout and Loading

Purlin Number, i	1	2	3	4	5	6	7	8	9	10	11	12
Location (ft)	0	5	10	15	20	25	30	35	40	45	50	55
Dist From Anch A (ft)	0.00	5.00	10.01	15.01	20.02	25.02	30.03	35.03	40.03	45.04	50.04	55.05
Dist From Anch B (ft)	20.02	15.01	10.01	5.00	0.00	5.00	10.01	15.01	20.02	25.02	30.03	35.03
Dist From Anch C (ft)	40.03	35.03	30.03	25.02	20.02	15.01	10.01	5.00	0.00	5.00	10.01	15.01

Purlin Number, i	1	2	3	4	5	6	7	8	9	10	11	12
Tributary Width (ft)	2.5	5	5	5	5	5	5	5	5	5	5	2.5
W_{pi} (lb)	1438	2875	2875	2875	2875	2875	2875	2875	2875	2875	2875	1438
Purlin Orientation, α	-1	1	1	1	1	1	1	1	1	1	1	1

Frame Line 1 Calculations

Find the system stiffness from AISI S100 Eq. I6.4.1-6

$$K_{sys} = \frac{C5}{1000} \cdot N_p \frac{ELt^2}{d^2} \qquad \text{(AISI S100 Eq. I6.4.1-6)}$$

$$= \frac{2.4}{1000} \cdot (12) \frac{(29500)(25x12)(0.085^2)}{8^2} = 28.77\ \mathrm{kip/in}$$

The effective stiffness values for each anchorage device, with respect to each purlin, are calculated from AISI S100 Eq. I6.4.1-4.

$$K_{eff_{i,j}} = \left[\frac{1}{K_a} + \frac{d_{p_{i,j}}}{C6 \cdot LA_pE}\right]^{-1} \qquad \text{(AISI S100 Eq. I6.4.1-4)}$$

$$= \left[\frac{1}{40} + \frac{d_{p_{i,j}}}{0.25(25x12)(0.20/12)(29500)}\right]^{-1}$$

Purlin Number, i	1	2	3	4	5	6	7	8	9	10	11	12
$K_{eff,A}$ (kip/in.)	40.0	37.6	35.4	33.5	31.7	30.2	28.8	27.5	26.3	25.2	24.2	23.3
$K_{eff,B}$ (kip/in.)	31.7	33.5	35.4	37.6	40.0	37.6	35.4	33.5	31.7	30.2	28.8	27.5
$K_{eff,C}$ (kip/in.)	26.3	27.5	28.8	30.2	31.7	33.5	35.4	37.6	40.0	37.6	35.4	33.5
Sum (kip/in.)	98.0	98.5	99.5	101.2	103.5	101.2	99.5	98.5	98.0	92.9	88.4	84.2
K_{total}=Sum+K_{sys} (kip/in.)	126.8	127.3	128.3	130.0	132.2	130.0	128.3	127.3	126.8	121.7	117.1	113.0

Force distribution factors (DF) are calculated by finding the stiffness ratio, K_{eff} divided by the corresponding K_{total}, which are found in AISI S100 Eq. I6.4.1-1.

Purlin Number	1	2	3	4	5	6	7	8	9	10	11	12
DF A	0.315	0.295	0.276	0.257	0.240	0.232	0.224	0.216	0.207	0.207	0.207	0.206
DF B	0.250	0.263	0.276	0.289	0.302	0.289	0.276	0.263	0.250	0.248	0.246	0.243
DF C	0.207	0.216	0.224	0.232	0.240	0.257	0.276	0.295	0.315	0.309	0.302	0.296

The individual purlin forces are calculated from AISI S100 Eq. I6.4.1-2

$$P_i = C1 \cdot W_{p_i} \cdot \left[\left(\frac{C2}{1000} \cdot \frac{I_{xy}L}{I_x d} + C3 \cdot \frac{(m+0.25b)t}{d^2} \right) \alpha \cdot \cos\theta - C4 \cdot \sin\theta \right] \quad \text{(AISI S100 Eq. I6.4.1-2)}$$

$$P_1 = 0.5(1438)\left[\left(\frac{13}{1000} \frac{(4.11)(25x12)}{(12.40)(8)} + 11 \cdot \frac{(0+0.25(2.75))(0.085)}{8^2} \right)(-1)\cos(2.39) - (0.35)\sin(2.39) \right] = -133.7 \text{ lb}$$

$$P_2 \text{ to } P_{11} = 0.5(2875)\left[\left(\frac{13}{1000} \frac{(4.11)(25x12)}{(12.40)(8)} + 11 \cdot \frac{(0+0.25(2.75))(0.085)}{8^2} \right)(1)\cos(2.39) - (0.35)\sin(2.39) \right] = 225.6 \text{ lb}$$

$$P_{12} = P_2 / 2 = 112.8 \text{ lb}$$

These values must not be taken as less than 80% of that found using "All Other Locations" coefficients.

$$P_1 = (0.80)0.5(1438)\left[\left(\frac{4.3}{1000} \frac{(4.11)(25x12)}{(12.40)(8)} + 55 \cdot \frac{(0+0.25(2.75))(0.085)}{8^2} \right)(-1)\cos(2.39) - (0.71)\sin(2.39) \right] = -76.6 \text{ lb}$$

$$P_2 \text{ to } P_{11} = (0.80)0.5(2875)\left[\left(\frac{4.3}{1000} \frac{(4.11)(25x12)}{(12.40)(8)} + 55 \cdot \frac{(0+0.25(2.75))(0.085)}{8^2} \right)(1)\cos(2.39) - (0.71)\sin(2.39) \right] = 85.1 \text{ lb}$$

$$P_{12} = P_2 / 2 = 42.6 \text{ lb}$$

These forces are then distributed to each anchorage device with the distribution factors found above.

Purlin Number, i	1	2	3	4	5	6	7	8	9	10	11	12
P_i (lb)	-133.7	225.6	225.6	225.6	225.6	225.6	225.6	225.6	225.6	225.6	225.6	112.8
P_i to Anch A (lb)	-42.2	66.6	62.2	58.1	54.1	52.4	50.6	48.7	46.8	46.7	46.6	23.3
P_i to Anch B (lb)	-33.5	59.3	62.2	65.2	68.2	65.2	62.2	59.3	56.4	55.9	55.4	27.4
P_i to Anch C (lb)	-27.7	48.7	50.6	52.4	54.1	58.1	62.2	66.6	71.2	69.6	68.1	33.4

Then taking the summation across each row yields the final anchorage forces.

P_{LA} (lb)	514
P_{LB} (lb)	603
P_{LC} (lb)	607

The smallest stiffness of the system is checked using AISI S100 Eq. I6.4.1-8a

$$K_{total} \geq K_{req} \qquad \text{(AISI S100 Eq. I6.4.1-7)}$$

$$K_{req} = \Omega \frac{20 \cdot \left| \sum_{i=1}^{N_p} P_i \right|}{d} \qquad \text{(AISI S100 Eq. I6.4.1-8a)}$$

$$= 2.0 \frac{20(-0.1337 + 10 \cdot 0.2256 + 0.1128)}{8} = 11.2 \,{}^{kip}\!/_{in} < K_{total(12)} = 113 \,{}^{kip}\!/_{in} \quad \text{OK}$$

Frame Line 2 Calculations

The system stiffness is found from

$$K_{sys} = \frac{C5}{1000} \cdot N_p \frac{ELt^2}{d^2} \qquad \text{(AISI S100 Eq. I6.4.1-6)}$$

$$= \frac{1.6}{1000} \cdot (12) \frac{(29500)(25x12)((0.085 + 0.059)/2)^2}{8^2} = 13.76 \,{}^{kip}\!/_{in}$$

The effective stiffness values and distribution factors for each anchorage device, with respect to each purlin, are calculated from AISI S100 Eq. I6.4.1-4

$$K_{eff_{i,j}} = \left[\frac{1}{K_a} + \frac{d_{p_{i,j}}}{C6 \cdot LA_p E} \right]^{-1} \qquad \text{(AISI S100 Eq. I6.4.1-4)}$$

$$= \left[\frac{1}{40} + \frac{d_{p_{i,j}}}{0.13(25x12)(0.20/12)(29500)} \right]^{-1}$$

Purlin Number, i	1	2	3	4	5	6	7	8	9	10	11	12
$K_{eff,A}$ (kip/in.)	40.0	35.5	32.0	29.1	26.6	24.6	22.8	21.3	20.0	18.8	17.8	16.8
$K_{eff,B}$ (kip/in.)	26.6	29.1	32.0	35.5	40.0	35.5	32.0	29.1	26.6	24.6	22.8	21.3
$K_{eff,C}$ (kip/in.)	20.0	21.3	22.8	24.6	26.6	29.1	32.0	35.5	40.0	35.5	32.0	29.1
Sum (kip/in.)	86.6	85.9	86.8	89.2	93.3	89.2	86.8	85.9	86.6	78.9	72.6	67.2
K_{total}=Sum+K_{sys} (kip/in.)	100.4	99.7	100.6	103.0	107.1	103.0	100.6	99.7	100.4	92.7	86.3	81.0
DF A	0.398	0.357	0.318	0.282	0.249	0.239	0.227	0.214	0.199	0.203	0.206	0.208
DF B	0.265	0.292	0.318	0.345	0.374	0.345	0.318	0.292	0.265	0.265	0.264	0.263
DF C	0.199	0.214	0.227	0.239	0.249	0.282	0.318	0.357	0.398	0.383	0.370	0.359

The individual purlin forces are calculated from AISI S100 Eq. I6.4.1-2 using the properties of the first bay, then the interior bay and the resulting forces are averaged.

$$P_i = C1 \cdot W_{p_i} \cdot \left[\left(\frac{C2}{1000} \cdot \frac{I_{xy}L}{I_x d} + C3 \cdot \frac{(m+0.25b)t}{d^2} \right) \alpha \cdot \cos\theta - C4 \cdot \sin\theta \right] \qquad \text{(AISI S100 Eq. I6.4.1-2)}$$

$$P_{1-Left} = 1.0(1438)\left[\left(\frac{1.7}{1000}\frac{(4.11)(25x12)}{(12.40)(8)} + 69 \cdot \frac{(0+0.25(2.75))(0.085)}{8^2}\right)(-1)\cos(2.39) - (0.77)\sin(2.39)\right] = -166.9 \text{ lb}$$

$$P_{2-Left} = 1.0(2875)\left[\left(\frac{1.7}{1000}\frac{(4.11)(25x12)}{(12.40)(8)} + 69 \cdot \frac{(0+0.25(2.75))(0.085)}{8^2}\right)(1)\cos(2.39) - (0.77)\sin(2.39)\right] = 149.5 \text{ lb}$$

$$P_{12-Left} = P_2 \,/\, 2 = 74.8 \text{ lb}$$

$$P_{1-Right} = 1.0(1438)\left[\left(\frac{1.7}{1000}\frac{(2.85)(25x12)}{(8.69)(8)} + 69 \cdot \frac{(0+0.25(2.75))(0.059)}{8^2}\right)(-1)\cos(2.39) - (0.77)\sin(2.39)\right] = -138.9 \text{ lb}$$

$$P_{2-Right} = 1.0(2875)\left[\left(\frac{1.7}{1000}\frac{(2.85)(25x12)}{(8.69)(8)} + 69 \cdot \frac{(0+0.25(2.75))(0.059)}{8^2}\right)(1)\cos(2.39) - (0.77)\sin(2.39)\right] = 93.5 \text{ lb}$$

$$P_{12-Right} = P_2 \,/\, 2 = 46.8 \text{ lb}$$

These forces are then distributed to each anchorage device with the distribution factors found above.

Purlin Number, i	1	2	3	4	5	6	7	8	9	10	11	12
P_i Left (lb)	-166.9	149.5	149.5	149.5	149.5	149.5	149.5	149.5	149.5	149.5	149.5	74.8
P_i Right (lb)	-138.9	93.5	93.5	93.5	93.5	93.5	93.5	93.5	93.5	93.5	93.5	46.8
P_i (lb)	-152.9	121.5	121.5	121.5	121.5	121.5	121.5	121.5	121.5	121.5	121.5	60.8

Force to Anch A (lb)	-60.9	43.3	38.6	34.3	30.2	29.0	27.6	26.0	24.2	24.6	25.0	12.6
Force to Anch B (lb)	-40.6	35.4	38.6	41.9	45.4	41.9	38.6	35.4	32.3	32.2	32.1	16.0
Force to Anch C (lb)	-30.4	26.0	27.6	29.0	30.2	34.3	38.6	43.3	48.4	46.6	45.0	21.8

P_{LA} (lb)	255
P_{LB} (lb)	349
P_{LC} (lb)	361

The smallest stiffness of the system is checked using AISI S100 Eq. I6.4.1-8a.

$$K_{total} \geq K_{req} \qquad \text{(AISI S100 Eq. I6.4.1-7)}$$

$$K_{req} = \Omega \frac{20 \cdot \left| \sum_{i=1}^{N_p} P_i \right|}{d} \qquad \text{(AISI S100 Eq. I6.3.1-8a)}$$

$$= 2.0 \frac{20(-0.1529 + 10 \cdot 0.1215 + 0.0608)}{8} = 5.6 \,{}^{kip}\!/_{in} < K_{total(12)} = 83 \,{}^{kip}\!/_{in} \quad \text{OK}$$

Frame Line 3 Calculations

The forces along Frame Line 3 are found by applying the procedure using the properties of the interior bays. For brevity, the calculations are presented only in tabular form.

$$K_{sys} = 8.09 \, {}^{kip}\!/_{in}$$

Purlin Number, i	1	2		3	4	5	6	7	8	9	10	11	12
$K_{eff,A}$ (kip/in.)	40.0	36.5		33.6	31.1	28.9	27.0	25.4	23.9	22.6	21.5	20.4	19.5
$K_{eff,B}$ (kip/in.)	28.9	31.1		33.6	36.5	40.0	36.5	33.6	31.1	28.9	27.0	25.4	23.9
$K_{eff,C}$ (kip/in.)	22.6	23.9		25.4	27.0	28.9	31.1	33.6	36.5	40.0	36.5	33.6	31.1
Sum (kip/in.)	91.6	91.5		92.5	94.6	97.8	94.6	92.5	91.5	91.6	85.0	79.4	74.5
K_{total}=Sum+K_{sys} (kip/in.)	99.7	99.6		100.6	102.7	105.9	102.7	100.6	99.6	99.7	93.1	87.5	82.6
DF A	0.401	0.366		0.334	0.303	0.273	0.263	0.252	0.240	0.227	0.231	0.234	0.236
DF B	0.290	0.312		0.334	0.355	0.378	0.355	0.334	0.312	0.290	0.290	0.290	0.290
DF C	0.227	0.240		0.252	0.263	0.273	0.303	0.334	0.366	0.401	0.392	0.384	0.376
P_i (lb)	-168.5	167.1		167.1	167.1	167.1	167.1	167.1	167.1	167.1	167.1	167.1	83.5
Force to Anch A (lb)	-67.6	61.2		55.7	50.5	45.6	44.0	42.2	40.2	38.0	38.5	39.0	19.7
Force to Anch B (lb)	-48.9	52.1		55.7	59.4	63.1	59.4	55.7	52.1	48.5	48.5	48.5	24.2
Force to Anch B (lb)	-38.3	40.2		42.2	44.0	45.6	50.5	55.7	61.2	67.1	65.5	64.1	31.4

P_{LA} (lb)	407
P_{LB} (lb)	518
P_{LC} (lb)	529

$$K_{req} = 7.9 \, {}^{kip}\!/_{in} < 82.6 \, {}^{kip}\!/_{in} \quad \text{OK}$$

Finally the diaphragm deflection is checked. Since the loads and spans are the same for all bays, the bay with the largest I_{xy}/I_x ratio will control. If all other dimensions are equal, this will be the thicker purlin.

$$w_{diaph} = \sum \left[\frac{W_p}{L} \left(\frac{I_{xy}}{I_x} \alpha \cos\theta - \sin\theta \right) \right]_i \qquad \text{(Eq. 5.3.1-1)}$$

$$= \left[\frac{1438}{25} \left(\frac{4.11}{12.40} (-1) \cos(2.39) - \sin(2.39) \right) + \frac{10(2875)(1) + 1438}{25} \left(\frac{4.11}{12.40} (1) \cos(2.39) - \sin(2.39) \right) \right] = 328 \text{ plf}$$

With this value the diaphragm deflection is found from,

$$\Delta_{diaph} = \frac{w_{diaph} L^2_{diaph}}{8G'B} \qquad \text{(Eq. 5.3.1-2)}$$

$$= \frac{(328)(25)^2}{8(1200)({}^{55}\!/_{\cos(2.39)})} = 0.388\text{in} < L/360 = (25\text{x}12)/360 = 0.83\text{in} \quad \text{OK}$$

5.4.4 Example: Three Span Continuous C-Purlins Supporting Standing Seam Panels - LRFD

Evaluate the interior frame lines of the three span, standing seam roof system shown and determine whether anchorage devices are needed. The system consists of seven parallel lines of C-shaped purlins. The purlins in the end bays are oriented with the flanges facing upslope, while the center bay has flanges facing downslope, except the low eave members, which are simple span and all three bays are oriented with flanges facing upslope. No external anchorage devices are provided at the interior frame lines. The standing seam panels have a cross-sectional area of 0.33 in.^{2}/ft and the roof slope is 1 in./ft. The purlins are 8C2.5x070. The roof load consists of a uniform dead load (panel and purlin self weight) of 3 psf and roof snow load of 21 psf. Use LRFD.

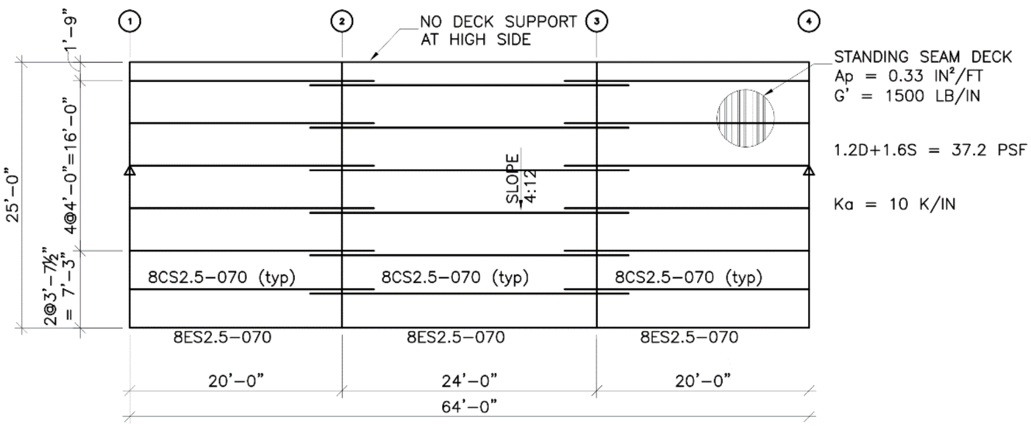

System Properties

N_p = 7

A_p = 0.33 in.^{2}/ft

θ = arctan(1/12) = 4.76 degrees

q = 1.2D+1.6S = 1.2(3)+1.6(21)=37.2 psf

Purlin Properties from AISI D100 Table I-1

d = 8 in.

b = 2.5 in.

t = 0.070 in.

m = 1.09 in.

I_{xy} = 0.0 in.^{4}

Coefficients from AISI S100 Table I6.4.1-1 for first interior frame line

C1 = 1.0

C2 = 1.7

C3 = 69

C4 = 0.77

C5 = 1.6

C6 = 0.13

The system stiffness is found from AISI S100 Eq. I6.4.1-6:

$$K_{sys} = \frac{C5}{1000} \cdot N_p \frac{ELt^2}{d^2} \qquad \text{(AISI S100 Eq. I6.4.1-6)}$$

$$= \frac{1.6}{1000} \cdot (7) \frac{(29500)((20+24)/2)(12)(0.070^2)}{8^2} = 6.68 \,\text{kip/in}$$

The purlin arrangement and tributary widths are as follows where purlins are numbered from the low eave and only the first interior frame line is considered. Note that since snow load is the dominant force, the tributary widths are based on the projected horizontal distances.

Purlin Number, i	1	2	3	4	5	6	7
Location (ft)	0	3.625	7.25	11.25	15.25	19.25	23.25
α End Bay	1.00	1.00	1.00	1.00	1.00	1.00	1.00
α Interior Bay	1.00	-1.00	-1.00	-1.00	-1.00	-1.00	-1.00
Tributary Width (ft)	1.8125	3.625	3.8125	4.0	4.0	4.0	3.75

AISI S100 Eq. I6.4.1-2 is used to calculate the load introduced into the system at each purlin. All terms except W_{pi} are dependent only on the purlin section and span, not the load or location within the roof plane. By recognizing this, a purlin load ratio, $\gamma = P_i/W_{pi}$, can be calculated for each purlin section.

Purlin Load Ratios:

$$\gamma = C1\left[\left(\frac{C2}{1000} \cdot \frac{I_{xy}L}{I_x d} + C3 \cdot \frac{(m+0.25b)t}{d^2}\right)\alpha \cdot \cos\theta - C4 \cdot \sin\theta\right] \qquad \text{(AISI S100 Eq. I6.4.1-2)}$$

$$\gamma_{(\alpha=1)} = 1.0\left[\left(0 + 69 \cdot \frac{(1.09+0.25(2.5))(0.070)}{8^2}\right)(1)\cos(4.76) - 0.77 \cdot \sin(4.76)\right] = 0.0650$$

$$\gamma_{(\alpha=-1)} = 1.0\left[\left(0 + 69 \cdot \frac{(1.09+0.25(2.5))(0.070)}{8^2}\right)(-1)\cos(4.76) - 0.77 \cdot \sin(4.76)\right] = -0.1929$$

The total lateral force each purlin introduces to the system is calculated on the left and right side for the frame line, P_i Left and P_i Right. The net force lateral force each purlin introduces, P_i, is half the sum of the forces on each side. Since the loads will be partially counteracting at the frame lines, the three possible cases for pattern snow loading must be considered.

Load Case 1: Full Snow on End Bay, Half on Interior Bay

Purlin Number, i	1	2	3	4	5	6	7
W_{pi} Left (lb)	1348.5	2697.0	2836.5	2976.0	2976.0	2976.0	2790.0
P_i Left (lb)	87.7	175.4	184.5	193.5	193.5	193.5	181.5
W_{pi} Right (lb)	887.4	1774.8	1866.6	1958.4	1958.4	1958.4	1836.0
P_i Right (lb)	57.7	-342.4	-360.1	-377.8	-377.8	-377.8	-354.2
P_i (lb)	72.7	-83.5	-87.8	-92.1	-92.1	-92.1	-86.4

K_{req}	1.54
K_{req}/K_{sys}	23%

Load Case 2: Full Snow on Interior Bay, Half on End Bay

Purlin Number, i	1	2	3	4	5	6	7
W_{pi} Left (lb)	739.5	1479.0	1555.5	1632.0	1632.0	1632.0	1530.0
P_i Left (lb)	48.1	96.2	101.2	106.1	106.1	106.1	99.5
W_{pi} Right (lb)	1618.2	3236.4	3403.8	3571.2	3571.2	3571.2	3348.0
P_i Right (lb)	105.2	-624.4	-656.7	-689.0	-689.0	-689.0	-645.9
P_i (lb)	76.7	-264.1	-277.8	-291.4	-291.4	-291.4	-273.2

K_{req}	5.38
K_{req}/K_{sys}	80%

Load Case 3: Full Snow on Both Bays

Purlin Number, i	1	2	3	4	5	6	7
W_{pi} Left (lb)	1348.5	2697.0	2836.5	2976.0	2976.0	2976.0	2790.0
P_i Left (lb)	87.7	175.4	184.5	193.5	193.5	193.5	181.5
W_{pi} Right (lb)	1618.2	3236.4	3403.8	3571.2	3571.2	3571.2	3348.0
P_i Right (lb)	105.2	-624.4	-656.7	-689.0	-689.0	-689.0	-645.9
P_i (lb)	96.5	-224.5	-236.1	-247.7	-247.7	-247.7	-232.2

K_{req}	4.47
K_{req}/K_{sys}	67%

The required stiffness is calculated by AISI S100 Eq. I6.3.1-4 using the sum of lateral forces, P_i, for each load case. Since for all load cases K_{sys} is greater than K_{req}, these calculations indicate that the system is adequate without the addition of discrete points of anchorage. It must also be shown that each purlin-to-rafter connection is capable of resisting the lateral force P_i; in this case the maximum P_i is 291.4 lb. Also, it should be noted that there remains a significant amount of uncertainty in the behavior of purlin anchorage systems, especially in terms of lateral stiffness and displacements. Therefore this technique of eliminating external anchorage requirements should be used with caution.

5.4.5 Example: Cantilever Z-Purlin System - ASD

Evaluate the roof system with the snow drift and end cantilevers shown. The system consists of seven parallel purlin lines on each side of the ridge, but no continuity is provided between the opposing slopes. The purlins have a 19 ft main span with 1 ft left cantilever (frame setback) and a 5 ft right overhang (gable overhang). Anchorage devices are provided at the supports of the 4th and 7th purlin lines. The roof system consists of standing seam panels with a cross-sectional area of 0.38 in.^{2}/ft at a slope of 4 in./ft. The purlins are 10ZS2.75x085 and the eave struts are 10ES2.5x105. The roof loading consists of a uniform dead load of 2 psf, a uniform snow load of 13.6 psf, and a snow drift against the adjacent structure. The snow drift load tapers from 47 psf over a distance of 11 ft – 10 3/16 in. Use ASD.

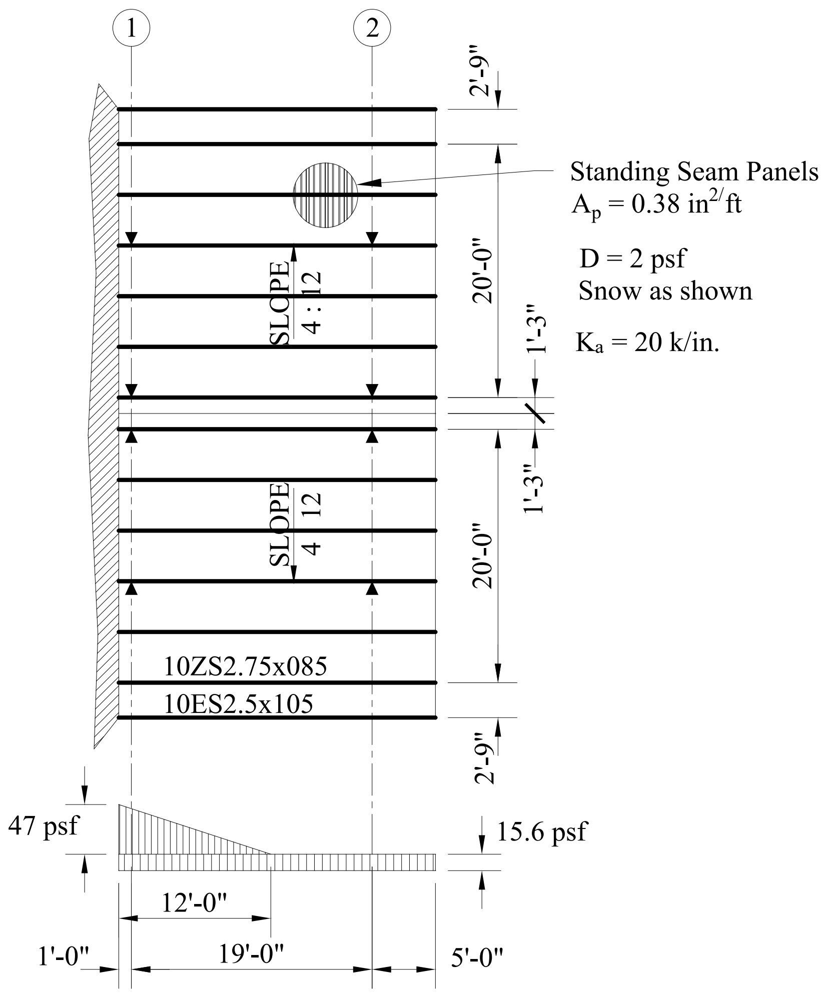

System Properties

N_p = 7

N_a = 2

K_a = 20 kip/in.

A_p = 0.38 in.^{2}/ft

θ = arctan(4/12) = 18.43 degrees

Purlin Properties from AISI D100 Table I-4

d = 10 in.
b = 2.75 in.
t = 0.085 in.
I_x = 21.0 in.^{4}
I_{xy} = 5.20 in.^{4}
m = 0 in.

Eave Strut Properties (similar to 10CS2.5x105 in AISI D100 Table I-1)

d = 10 in.
b = 2.5 in.
t = 0.105 in.
I_x = 23.3 in.^{4}
I_{xy} = 0.098 in.^{4}
m = 1.56 in.

Coefficients from AISI S100 Table I6.4.1-1 for a simple span, which is used to approximate the propped cantilever condition.

C1 = 0.5
C2 = 8.3
C3 = 28
C4 = 0.61
C5 = 0.29
C6 = 0.051

To calculate the system stiffness, AISI S100 Eq. I6.4.1-6 is modified slightly to account for the difference in thickness of the members, six purlins (0.085 in.) and one eave strut (0.105 in.). Also, L is taken as the length of the main span without the cantilevers.

$$K_{sys} = \frac{C5}{1000} \cdot N_p \cdot \frac{ELt^2}{d^2} \qquad \text{(AISI S100 Eq. I6.4.1-6)}$$

$$K_{sys} = \frac{0.29(29500)(19x12)}{1000(10^2)} \cdot \left[(6)(0.085)^2 + (1)(0.105)^2\right] = 1.06 \text{kip/in} \qquad \text{(Modified Eq. I6.4.1-6)}$$

The effective stiffness of each anchorage device, relative to each purlin is calculated from AISI S100 Eq. I6.4.1-4. The equation is evaluated in the table below for each combination of purlin and anchorage device. The only changing variable is the distance between the purlin and the anchorage device, $d_{p(i,j)}$. Also in this table is the total stiffness supporting each purlin, $K_{total(i)}$.

$$K_{eff_{i,j}} = \left[\frac{1}{K_a} + \frac{d_{p_{i,j}}}{C6 \cdot LA_pE}\right]^{-1} \qquad \text{(AISI S100 Eq. I6.4.1-4)}$$

$$K_{total_i} = \sum_{j=1}^{N_a}\left(K_{eff_{i,j}}\right) + K_{sys} \qquad \text{(AISI S100 Eq. I6.4.1-5)}$$

Purlin Number, i	1	2	3	4	5	6	7
Location (ft)	0	2.75	6.75	10.75	14.75	18.75	22.75
Dist From Anch A (ft)	11.33	8.43	4.22	0.00	4.22	8.43	12.65
Dist From Anch B (ft)	23.98	21.08	16.86	12.65	8.43	4.22	0.00

$K_{eff,A}$ (kip/in.)	16.0	16.86	18.30	20.00	18.30	16.86	15.63
$K_{eff,B}$ (kip/in.)	13.07	13.64	14.57	15.63	16.86	18.30	20.00
Sum (kip/in.)	29.07	30.50	32.87	35.63	35.15	35.15	35.63
K_{total}=Sum+K_{sys} (kip/in.)	30.1	31.6	33.9	36.7	36.2	36.2	36.7

With these values the stiffness ratio in AISI S100 Eq. I6.4.1-1 is evaluated to find a distribution factor representing the portion of the load introduced at each purlin that is distributed to each anchorage device. The sum of the distribution factors at each purlin is less than unity due to the portion of the load that is resisted by the system effect.

Purlin Number, i	1	2	3	4	5	6	7
DF A	0.531	0.534	0.539	0.545	0.505	0.466	0.426
DF B	0.434	0.432	0.429	0.426	0.466	0.505	0.545

To address the effects of the snow drift and the cantilever, the load on each frame is calculated taking into account the snow drift and the adjacent cantilever, but neglecting the other cantilever.

By taking moments about Frame Line 2, the load on Frame Line 1 is:

$$R_1 = \frac{0.5(47)(11.85)\left(20 - {}^{11.85}\!/_{3}\right) + 15.6(20)(10)}{19} = 399.4\ {}^{lb}\!/_{ft}$$

For the load on Frame Line 2 the snow drift is truncated at Frame Line 1.

$$q_{drift} = 47\frac{10.85}{11.85} = 43.03\,\text{psf}$$

Then taking moments about Frame Line 1 yields the load on Frame Line 2 of:

$$R_2 = \frac{0.5(43.03)(10.85)\left({}^{10.85}\!/_{3}\right) + 15.6(24)(12)}{19} = 280.9\ {}^{lb}\!/_{ft}$$

AISI S100 Eq. I6.4.1-2 is used to calculate the load introduced into the system at each purlin. All terms except W_{pi} are dependent only on the purlin section and span, not the load or location within the roof plane. By recognizing this, a purlin load ratio, $\gamma_i = P_i/W_{pi}$, can be calculated for each purlin section.

Purlin Load Ratios:

$$\gamma = C1\left[\left(\frac{C2}{1000}\cdot\frac{I_{xy}L}{I_x d} + C3\cdot\frac{(m+0.25b)t}{d^2}\right)\alpha\cdot\cos\theta - C4\cdot\sin\theta\right] \qquad \text{(From AISI S100 Eq. I6.4.1-2)}$$

$$\gamma_p = 0.5\left[\left(\frac{8.3}{1000}\cdot\frac{(5.20)(19x12)}{(21.0)(10)}+28\cdot\frac{\left(0+0.25(2.75)\right)(0.085)}{10^2}\right)1\cdot\cos(18.43)-0.61\cdot\sin(18.43)\right]$$
$$=-0.0665$$

$$\gamma_e = 0.5\left[\left(\frac{8.3}{1000}\cdot\frac{(0.098)(19x12)}{(23.3)(10)}+28\cdot\frac{(1.56+0.25(2.5))(0.105)}{10^2}\right)1\cdot\cos(18.43)-0.61\cdot\sin(18.43)\right]=-0.0656$$

These load ratios are then multiplied by the force W_p, which due to the cantilevers and non-uniform load, is taken as two times the frame loads above times the tributary width at each purlin. Then the forces P_i are multiplied by the distribution factors found above to find the force distributed to each anchorage device.

For anchorage along Frame Line 1:

Purlin Number, i	1	2	3	4	5	6	7
Tributary Width (ft)	1.375	3.375	4	4	4	4	3.25
Load Factor, γ_i	-0.0656	-0.0665	-0.0665	-0.0665	-0.0665	-0.0665	-0.0665

W_{p1} (lb)	1098.5	2696.3	3195.6	3195.6	3195.6	3195.6	2596.4
P_1 (lb)	-72.1	-179.2	-212.4	-212.4	-212.4	-212.4	-172.6

Load to Anch A (lb)	-38.3	-95.7	-114.5	-115.8	-107.3	-98.9	-73.5
Load to Anch B (lb)	-31.3	-77.5	-91.2	-90.5	-98.9	-107.3	-94.1
Load to System Effect (lb)	-2.5	-6.0	-6.6	-6.1	-6.2	-6.2	-5.0

For anchorage along Frame Line 2:

Purlin Number, i	1	2	3	4	5	6	7
W_{p2} (lb)	772.5	1896.1	2247.2	2247.2	2247.2	2247.2	1825.8
P_2 (lb)	-50.7	-126.0	-149.3	-149.3	-149.3	-149.3	-121.3

Load to Anch A (lb)	-26.9	-67.3	-80.5	-81.4	-75.5	-69.5	-51.7
Load to Anch B (lb)	-22.0	-54.5	-64.1	-63.6	-69.5	-75.5	-66.1
Load to System Effect (lb)	-1.8	-4.2	-4.7	-4.3	-4.4	-4.4	-3.5

The summation in AISI S100 Eq. I6.4.1-1 is carried out by taking the sum of the values in the rows in the tables above. This yields the anchorage force at each purlin. The portion of the force carried by the system effect is also calculated in a similar fashion.

	FL 1	FL 2
P_{LA} (lb)	-644	-453
P_{LB} (lb)	-591	-415
P_L System (lb)	-39	-27
Sum	-1273	-895

The "Sum" values in the table above are the total of all the anchorage forces along each frame line, and are equivalent to the sum of the P_i values. These values are used in AISI S100 Eq. I6.4.1-8a for the calculation of the required minimum effective stiffness, and then compared to the total stiffness provided, K_{total}, according to AISI S100 Eq. I6.4.1-7 ($K_{total} \geq K_{req}$).

$$K_{req} = \Omega \cdot \frac{20 \cdot \left| \sum_{i=1}^{N_p} P_i \right|}{d} \qquad \text{(AISI S100 Eq. I6.4.1-8a)}$$

$$= 2.0 \frac{20(1.271)}{10} = 5.09 \, {}^{kip}\!/_{in} < K_{total(1)} = 30.1 \, {}^{kip}\!/_{in} \quad \text{OK}$$

Because the forces along Frame Line 1 are significantly greater than the forces along Frame Line 2, the required stiffness will be greater along Frame Line 1, and thus control the design. Therefore, calculations for Frame Line 2 are not necessary. If calculations were necessary for Frame Line 2, the calculations would be similar to the calculations for Frame Line 1.

5.4.6 Example: Single Span Z-Purlin Attached to Through-Fastened Panels with One-Third Points Anchorage - ASD

The system shown consists of 17 parallel purlin lines on each side of the ridge, and continuity is provided between the opposing slopes. Anchorage devices are provided at the one-third points at the 3rd and 10th purlin lines on each side of the ridge and have a lateral stiffness of 10 kip/in. The through-fastened roof panel system has a cross-sectional area of 0.21 in.^{2}/ft and the roof slope of 1/2 in./ft. The purlins are 10ZS2.75x085 and the eave strut purlins are 10ZS2.5x105. Evaluate the anchorage system for a dead load of 4 psf and the effects of a 30 psf ground snow load.

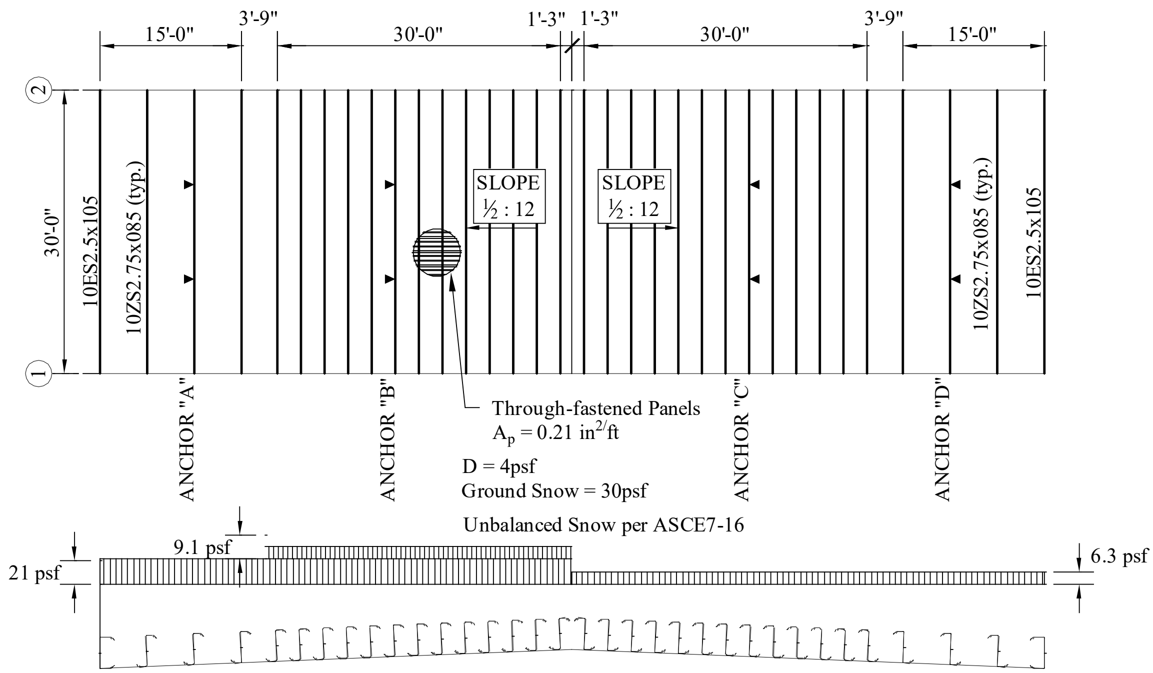

System Properties

N_{p1} = N_{p2} =17

N_a = 4

K_a = 10 kip/in.

A_p = 0.21 in.^{2}/ft

θ = arctan(0.5/12) = 2.39 degrees

Purlin Properties from AISI D100 Table I-4

d = 10 in.

b = 2.75 in.

t = 0.085 in.

I_x = 21.0 in.^{4}

I_{xy} = 5.20 in.^{4}

m = 0

Eave Strut Properties (similar to 10CS2.5x105 in AISI D100 Table I-1)

d = 10 in.
b = 2.5 in.
t = 0.105 in.
I_x = 23.3 in.^{4}
I_{xy} = 0.098 in.^{4}
m = 1.56 in.

Coefficients from AISI S100 Table I6.4.1-3

C1 = 0.5
C2 = 7.8
C3 = 42
C4 = 0.98
C5 = 0.39
C6 = 0.40

To calculate the system stiffness, AISI S100 Eq. I6.4.1-6 is modified to account for the difference in thickness of the eave strut and the typical purlins and the reduced effectiveness of elements on the far side of the ridge, which is addressed by the bracketed part of the equation containing the cosine term.

$$K_{sys} = \frac{C5}{1000} \cdot \left[\left(N_{p1} - 1\right)\left(\frac{ELt^2}{d^2}\right) + \left(\frac{ELt_e^2}{d^2}\right) \right] \cdot \left[1 + (\cos(2\theta))^2\right] \quad \text{(Eq. 5.4.6-1)}$$

$$= \frac{0.39}{1000} \cdot \left[\left(\frac{(29500)(30 \times 12)}{10^2}\right)\left((17-1)0.085^2 + 0.105^2\right) \right] \cdot \left[1 + \left(\cos\left(2(2.39)\right)\right)^2\right] = 10.45\,{}^{kip}/_{in}$$

The effective stiffness of each anchorage device, relative to each purlin is calculated from AISI S100 Eq. I6.4.1-5. The equation is evaluated in the table below for each combination of purlin and anchorage device. The only changing variable is the distance between the purlin and the anchorage device, $d_{p(i,j)}$. Also in this table is the total stiffness supporting each purlin, $K_{total(i)}$.

If purlin "i" and anchorage device "j" are on the same side of the ridge, then:

$$K_{eff_{i,j}} = \left[\frac{1}{K_a} + \frac{d_{p_{i,j}}}{C6 \cdot LA_pE}\right]^{-1} \quad \text{(AISI S100 Eq. I6.4.1-4)}$$

If purlin "i" and anchorage device "j" are on the opposite sides of the ridge, then:

$$K_{eff_{i,j}} = \left[\left(\frac{1}{K_a} + \frac{d_{p_{o,j}}}{C6 \cdot LA_pE}\right)\frac{1}{\cos^2(2\theta)} + \frac{d_{p_{i,o}}}{C6 \cdot LA_pE}\right]^{-1} \quad \text{(Eq. 5.4.6-2)}$$

Where $d_{po,j}$ is the distance from the ridge to the anchorage device, and $d_{pi,o}$ is the distance from the purlin to the ridge. Note in the above equation, the additional cosine term accounts for the reduced effectiveness of elements on the far side of the ridge.

$$K_{total_i} = \sum_{j=1}^{N_a}\left(K_{eff_{i,j}}\right) + K_{sys} \quad \text{(AISI S100 Eq. I6.4.1-5)}$$

Purlin Number, i	1	2	3	4	5	6	7	8	9	10	11	12	13	14	15	16	17
Location (ft)	0	5	10	15	18.75	21.25	23.75	26.25	28.75	31.25	33.75	36.25	38.75	41.25	43.75	46.25	48.75
Dist From Anch A (ft)	10.01	5.00	0.00	5.00	8.76	11.26	13.76	16.26	18.77	21.27	23.77	26.27	28.77	31.28	33.78	36.28	38.78
Dist From Anch B (ft)	31.28	26.27	21.27	16.26	12.51	10.01	7.51	5.00	2.50	0.00	2.50	5.00	7.51	10.01	12.51	15.01	17.52
Dist From Anch C (ft	68.81	63.81	58.80	53.80	50.04	47.54	45.04	42.54	40.03	37.53	35.03	32.53	30.03	27.52	25.02	22.52	20.02
Dist From Anch D (ft)	90.08	85.07	80.07	75.07	71.31	68.81	66.31	63.81	61.30	58.80	56.30	53.80	51.29	48.79	46.29	43.79	41.29
Alpha, α	1.00	1.00	1.00	1.00	1.00	1.00	1.00	1.00	1.00	1.00	1.00	1.00	1.00	1.00	1.00	1.00	1.00
$K_{eff,A}$ (kip/in.)	9.84	9.92	10.00	9.92	9.86	9.82	9.78	9.74	9.71	9.67	9.63	9.59	9.56	9.52	9.48	9.45	9.41
$K_{eff,B}$ (kip/in.)	9.52	9.59	9.67	9.74	9.80	9.84	9.88	9.92	9.96	10.00	9.96	9.92	9.88	9.84	9.80	9.76	9.73
$K_{eff,C}$ (kip/in.)	8.99	9.05	9.12	9.19	9.24	9.27	9.31	9.34	9.38	9.41	9.45	9.49	9.52	9.56	9.60	9.63	9.67
$K_{eff,D}$ (kip/in.)	8.72	8.78	8.84	8.90	8.95	8.99	9.02	9.05	9.08	9.12	9.15	9.19	9.22	9.25	9.29	9.32	9.36
Sum (kip/in.)	37.1	37.3	37.6	37.8	37.9	37.9	38.0	38.1	38.1	38.2	38.2	38.2	38.2	38.2	38.2	38.2	38.2
K_{total}=Sum+K_{sys} (kip/in.)	47.5	47.8	48.1	48.2	48.3	48.4	48.4	48.5	48.6	48.7	48.6	48.6	48.6	48.6	48.6	48.6	48.6

Purlin Number, i	18	19	20	21	22	23	24	25	26	27	28	29	30	31	32	33	34
Location (ft)	51.25	53.75	56.25	58.75	61.25	63.75	66.25	68.75	71.25	73.75	76.25	78.75	81.25	85	90	95	100
Dist From Anch A (ft)	41.29	43.79	46.29	48.79	51.29	53.80	56.30	58.80	61.30	63.81	66.31	68.81	71.31	75.07	80.07	85.07	90.08
Dist From Anch B (ft)	20.02	22.52	25.02	27.52	30.03	32.53	35.03	37.53	40.03	42.54	45.04	47.54	50.04	53.80	58.80	63.81	68.81
Dist From Anch C (ft	17.52	15.01	12.51	10.01	7.51	5.00	2.50	0.00	2.50	5.00	7.51	10.01	12.51	16.26	21.27	26.27	31.28
Dist From Anch D (ft)	38.78	36.28	33.78	31.28	28.77	26.27	23.77	21.27	18.77	16.26	13.76	11.26	8.76	5.00	0.00	5.00	10.01
Alpha, α	1.00	1.00	1.00	1.00	1.00	1.00	1.00	1.00	1.00	1.00	1.00	1.00	1.00	1.00	1.00	1.00	1.00
$K_{eff,A}$ (kip/in.)	9.36	9.32	9.29	9.25	9.22	9.19	9.15	9.12	9.08	9.05	9.02	8.99	8.95	8.90	8.84	8.78	8.72
$K_{eff,B}$ (kip/in.)	9.67	9.63	9.60	9.56	9.52	9.49	9.45	9.41	9.38	9.34	9.31	9.27	9.24	9.19	9.12	9.05	8.99
$K_{eff,C}$ (kip/in.)	9.73	9.76	9.80	9.84	9.88	9.92	9.96	10.00	9.96	9.92	9.88	9.84	9.80	9.74	9.67	9.59	9.52
$K_{eff,D}$ (kip/in.)	9.41	9.45	9.48	9.52	9.56	9.59	9.63	9.67	9.71	9.74	9.78	9.82	9.86	9.92	10.00	9.92	9.84
Sum (kip/in.)	38.2	38.2	38.2	38.2	38.2	38.2	38.2	38.2	38.1	38.1	38.0	37.9	37.9	37.8	37.6	37.3	37.1
K_{total}=Sum+K_{sys} (kip/in.)	48.6	48.6	48.6	48.6	48.6	48.6	48.6	48.7	48.6	48.5	48.4	48.4	48.3	48.2	48.1	47.8	47.5

With these values the stiffness ratio in AISI S100 Eq. I6.4.1-1 is evaluated to find a distribution factor representing the portion of the load introduced at each purlin that is distributed to each anchorage device.

Purlin Number, i	1	2	3	4	5	6	7	8	9	10	11	12	13	14	15	16	17
DF A	0.207	0.208	0.208	0.206	0.204	0.203	0.202	0.201	0.200	0.199	0.198	0.197	0.197	0.196	0.195	0.194	0.194
DF B	0.200	0.201	0.201	0.202	0.203	0.203	0.204	0.204	0.205	0.206	0.205	0.204	0.203	0.202	0.202	0.201	0.200
DF C	0.189	0.189	0.190	0.191	0.191	0.192	0.192	0.193	0.193	0.193	0.194	0.195	0.196	0.197	0.197	0.198	0.199
DF D	0.183	0.184	0.184	0.185	0.185	0.186	0.186	0.187	0.187	0.187	0.188	0.189	0.190	0.190	0.191	0.192	0.193
DF Sys	0.220	0.219	0.217	0.217	0.216	0.216	0.216	0.215	0.215	0.215	0.215	0.215	0.215	0.215	0.215	0.215	0.215

Purlin Number	18	19	20	21	22	23	24	25	26	27	28	29	30	31	32	33	34
DF A	0.193	0.192	0.191	0.190	0.190	0.189	0.188	0.187	0.187	0.187	0.186	0.186	0.185	0.185	0.184	0.184	0.183
DF B	0.199	0.198	0.197	0.197	0.196	0.195	0.194	0.193	0.193	0.193	0.192	0.192	0.191	0.191	0.190	0.189	0.189
DF C	0.200	0.201	0.202	0.202	0.203	0.204	0.205	0.206	0.205	0.204	0.204	0.203	0.203	0.202	0.201	0.201	0.200
DF D	0.194	0.194	0.195	0.196	0.197	0.197	0.198	0.199	0.200	0.201	0.202	0.203	0.204	0.206	0.208	0.208	0.207
DF Sys	0.215	0.215	0.215	0.215	0.215	0.215	0.215	0.215	0.215	0.215	0.215	0.216	0.216	0.216	0.217	0.217	0.219

AISI S100 Eq. I6.4.1-2 is used to calculate the load introduced into the system at each purlin. All terms except W_{pi} are dependent only on the purlin section and span, not the load or location within the roof plane. By recognizing this, a purlin load ratio, $\gamma = P_i/W_{pi}$, can be calculated for each purlin section.

Purlin Load Ratios:

$$\gamma = C1\left[\left(\frac{C2}{1000}\cdot\frac{I_{xy}L}{I_x d}+C3\cdot\frac{(m+0.25b)t}{d^2}\right)\alpha\cdot\cos\theta - C4\cdot\sin\theta\right] \quad \text{(AISI S100 Eq. I6.4.1-2)}$$

$$\gamma_p = 0.5\left[\left(\frac{7.8}{1000}\cdot\frac{(5.20)(30x12)}{(21.0)(10)}+42\cdot\frac{\left(0+0.25(2.75)\right)(0.085)}{10^2}\right)1\cdot\cos(2.39)-0.98\cdot\sin(2.39)\right]=0.0266$$

$$\gamma_e = 0.5\left[\left(\frac{7.8}{1000}\cdot\frac{(0.098)(30x12)}{(23.3)(10)}+42\cdot\frac{(1.56+0.25(2.5))(0.105)}{10^2}\right)1\cdot\cos(2.39)-0.98\cdot\sin(2.39)\right]=0.0283$$

These load factors are then multiplied by the force W_{pi}. Then the forces P_i are multiplied by the distribution factors found in the above table to determine the force distributed to each anchorage device. For Purlins 18 to 34, the force P_i is determined by multiplying the product of $\gamma_i \cdot W_{pi}$ by (-1) to account for the change in roof slope on the opposite side of the ridge from Purlins 1 to 17.

Purlin Number, i	1	2	3	4	5	6	7	8	9	10	11	12	13	14	15	16	17
Tributary Width (ft)	2.5	5	5	4.375	3.125	2.5	2.5	2.5	2.5	2.5	2.5	2.5	2.5	2.5	2.5	2.5	2.5
Load Factor	0.0282	0.0208	0.0208	0.0208	0.0208	0.0208	0.0208	0.0208	0.0208	0.0208	0.0208	0.0208	0.0208	0.0208	0.0208	0.0208	0.0208
W_{pi} (lb)	1875	3750	3750	3281	3368	2558	2558	2558	2558	2558	2558	2558	2558	2558	2558	2558	2558
P_i(lb)	53.1	99.7	99.7	87.3	89.6	68.0	68.0	68.0	68.0	68.0	68.0	68.0	68.0	68.0	68.0	68.0	68.0
Load to Anch A (lb)	11.0	20.7	20.7	18.0	18.3	13.8	13.7	13.7	13.6	13.5	13.5	13.4	13.4	13.3	13.3	13.2	13.2
Load to Anch B (lb)	10.6	20.0	20.1	17.6	18.2	13.8	13.9	13.9	13.9	14.0	13.9	13.9	13.8	13.8	13.7	13.7	13.6
Load to Anch C (lb)	10.0	18.9	18.9	16.6	17.1	13.0	13.1	13.1	13.1	13.2	13.2	13.3	13.3	13.4	13.4	13.5	13.5
Load to Anch D (lb)	9.7	18.3	18.3	16.1	16.6	12.6	12.7	12.7	12.7	12.7	12.8	12.8	12.9	12.9	13.0	13.0	13.1
Load to System Effect (lb)	11.7	21.8	21.7	18.9	19.4	14.7	14.7	14.7	14.6	14.6	14.6	14.6	14.6	14.6	14.6	14.6	14.6
Purlin Number, i	18	19	20	21	22	23	24	25	26	27	28	29	30	31	32	33	34
Tributary Width (ft)	2.5	2.5	2.5	2.5	2.5	2.5	2.5	2.5	2.5	2.5	2.5	2.5	3.125	4.375	5	5	2.5
Load Factor	0.0208	0.0208	0.0208	0.0208	0.0208	0.0208	0.0208	0.0208	0.0208	0.0208	0.0208	0.0208	0.0208	0.0208	0.0208	0.0208	0.0282
W_{pi} (lb)	773	773	773	773	773	773	773	773	773	773	773	773	966	1352	1545	1545	773
P_i (lb)	-20.5	-20.5	-20.5	-20.5	-20.5	-20.5	-20.5	-20.5	-20.5	-20.5	-20.5	-20.5	-25.7	-36.0	-41.1	-41.1	-21.9
Load to Anch A (lb)	-4.0	-3.9	-3.9	-3.9	-3.9	-3.9	-3.9	-3.9	-3.8	-3.8	-3.8	-3.8	-4.8	-6.6	-7.6	-7.5	-4.0
Load to Anch B (lb)	-4.1	-4.1	-4.1	-4.0	-4.0	-4.0	-4.0	-4.0	-4.0	-4.0	-3.9	-3.9	-4.9	-6.9	-7.8	-7.8	-4.1
Load to Anch C (lb)	-4.1	-4.1	-4.1	-4.2	-4.2	-4.2	-4.2	-4.2	-4.2	-4.2	-4.2	-4.2	-5.2	-7.3	-8.3	-8.2	-4.4
Load to Anch D (lb)	-4.0	-4.0	-4.0	-4.0	-4.0	-4.1	-4.1	-4.1	-4.1	-4.1	-4.1	-4.2	-5.2	-7.4	-8.5	-8.5	-4.5
Load to System Effect (lb)	-4.4	-4.4	-4.4	-4.4	-4.4	-4.4	-4.4	-4.4	-4.4	-4.4	-4.4	-4.4	-5.6	-7.8	-8.9	-9.0	-4.8

The summation in AISI S100 Eq. I6.4.1-1 is carried out by taking the sum of the values in the rows in the tables above. This yields the anchorage force at each purlin. Also, the portion of the force carried by the system effect is calculated in a similar fashion.

P_{LA} (lb)	173
P_{LB} (lb)	173
P_{LC} (lb)	157
P_{LD} (lb)	150
P_L System (lb)	180
Sum	833

The resulting forces indicate that the entire roof system translates in the upwind direction (to the right in the figure above). With anchorage points at one-third points it is common that the anchorage system can only resist forces in one direction. If this is the case, then the anchorage points on the windward side of the roof (C&D) will be ineffective. Therefore, the system would need to be reanalyzed neglecting the ineffective anchorage devices. For this analysis, most of the values above are still applicable. The total stiffness is computed neglecting the two ineffective anchorage devices, and different distribution factors are calculated and applied to the purlin forces.

Purlin Number	1	2	3	4	5	6	7	8	9	10	11	12	13	14	15	16	17
$K_{eff,A}$ (kip/in.)	9.84	9.92	10.00	9.92	9.86	9.82	9.78	9.74	9.71	9.67	9.63	9.59	9.56	9.52	9.48	9.45	9.41
$K_{eff,B}$ (kip/in.)	9.52	9.59	9.67	9.74	9.80	9.84	9.88	9.92	9.96	10.00	9.96	9.92	9.88	9.84	9.80	9.76	9.73
Sum (kip/in.)	19.4	19.5	19.7	19.7	19.7	19.7	19.7	19.7	19.7	19.7	19.6	19.5	19.4	19.4	19.3	19.2	19.1
K_{total}=Sum+K_{sys} (kip/in.)	29.8	30.0	30.1	30.1	30.1	30.1	30.1	30.1	30.1	30.1	30.0	30.0	29.9	29.8	29.7	29.7	29.6
DF A	0.330	0.331	0.332	0.329	0.327	0.326	0.325	0.324	0.322	0.321	0.321	0.320	0.320	0.319	0.319	0.318	0.318
DF B	0.319	0.320	0.321	0.324	0.325	0.327	0.328	0.329	0.331	0.332	0.332	0.331	0.331	0.330	0.330	0.329	0.329
DF Sys	0.351	0.349	0.347	0.347	0.347	0.347	0.347	0.347	0.347	0.347	0.348	0.349	0.350	0.351	0.351	0.352	0.353
Load to Anch A (lb)	17.5	33.0	33.1	28.7	29.3	22.2	22.1	22.0	21.9	21.8	21.8	21.8	21.7	21.7	21.7	21.7	21.6
Load to Anch B (lb)	17.0	31.9	32.0	28.2	29.2	22.2	22.3	22.4	22.5	22.6	22.6	22.5	22.5	22.5	22.4	22.4	22.4
Load to System Effect (lb)	18.6	34.8	34.6	30.3	31.1	23.6	23.6	23.6	23.6	23.6	23.7	23.7	23.8	23.8	23.9	24.0	24.0

Purlin Number	18	19	20	21	22	23	24	25	26	27	28	29	30	31	32	33	34
$K_{eff,A}$ (kip/in.)	9.36	9.32	9.29	9.25	9.22	9.19	9.15	9.12	9.08	9.05	9.02	8.99	8.95	8.90	8.84	8.78	8.72
$K_{eff,B}$ (kip/in.)	9.67	9.63	9.60	9.56	9.52	9.49	9.45	9.41	9.38	9.34	9.31	9.27	9.24	9.19	9.12	9.05	8.99
Sum (kip/in.)	19.0	19.0	18.9	18.8	18.7	18.7	18.6	18.5	18.5	18.4	18.3	18.3	18.2	18.1	18.0	17.8	17.7
K_{total}=Sum+K_{sys} (kip/in.)	29.5	29.4	29.3	29.3	29.2	29.1	29.1	29.0	28.9	28.8	28.8	28.7	28.6	28.5	28.4	28.3	28.2
DF A	0.317	0.317	0.317	0.316	0.316	0.315	0.315	0.315	0.314	0.314	0.313	0.313	0.313	0.312	0.311	0.310	0.310
DF B	0.328	0.328	0.327	0.327	0.326	0.326	0.325	0.325	0.324	0.324	0.323	0.323	0.322	0.322	0.321	0.320	0.319
DF Sys	0.355	0.355	0.356	0.357	0.358	0.359	0.360	0.361	0.362	0.362	0.363	0.364	0.365	0.366	0.368	0.370	0.371
Load to Anch A (lb)	-6.5	-6.5	-6.5	-6.5	-6.5	-6.5	-6.5	-6.5	-6.5	-6.4	-6.4	-6.4	-8.0	-11.2	-12.8	-12.8	-6.8
Load to Anch B (lb)	-6.7	-6.7	-6.7	-6.7	-6.7	-6.7	-6.7	-6.7	-6.7	-6.7	-6.6	-6.6	-8.3	-11.6	-13.2	-13.2	-7.0
Load to System Effect (lb)	-7.3	-7.3	-7.3	-7.3	-7.4	-7.4	-7.4	-7.4	-7.4	-7.4	-7.5	-7.5	-9.4	-13.2	-15.1	-15.2	-8.1

P_{LA} (lb)	275
P_{LB} (lb)	274
P_L System (lb)	285
Sum	833

The simplified model that forms the basis for the minimum stiffness requirement in AISI S100 Eq. I6.4.1-8 does not correctly represent a system where large groups of purlins have opposing flanges. This can be seen in the special case of a flat roof where all purlin top flanges are oriented toward the centerline. AISI S100 Eq. I6.4.1-8 would yield a required stiffness of zero (also implying zero lateral displacement) since the forces P_i cancel out.

For this example, the stiffness requirement can be conservatively evaluated by taking only the leeward side of the roof. The minimum total stiffness occurs at Purlin 17, which is compared to the required stiffness.

$$K_{req} = \Omega \cdot \frac{20\left|\sum_{i=1}^{N_p} P_i\right|}{d} \qquad \text{(AISI S100 Eq. I6.4.1-8a)}$$

$$= 2.0\frac{20(1.246)}{10} = 4.98\,\text{kip}/\text{in} < K_{total(17)} = 29.6\,\text{kip}/\text{in} \quad \text{OK}$$

5.5 Alternate Solution Procedures

AISI S100 allows for rational analysis to predict anchorage forces that can be used in lieu of the prediction method outlined in Section I6.4.1. In the following sections, five alternative analysis procedures are presented. Section 5.5.1 presents a method based on AISI S100 that is simplified to approximate the roof system with uniformly distributed purlins and forces. In Section 5.5.2, the AISI S100 anchorage method is formulated into a matrix framework. The component stiffness method, which provides a detailed analysis of the interaction of the components of the roof system and allows for analysis of additional anchorage configurations is presented in Section 5.5.4. In Section 5.5.5, guidance is provided to analyze anchorage forces using frame elements in a structural software package. Section 5.5.6 provides guidance on analyzing anchorage forces using a shell finite element model.

5.5.1 AISI S100 Simplified Procedure

The solution procedure in AISI S100 can be conservatively simplified if the roof system under consideration has nominally uniform purlin spaces, uniform loads, approximately uniformly distributed anchorage devices, and the majority of the purlin top flanges face upslope. For this simplification the total load supported by all the purlins within a bay is found.

$$W_s = qLB \qquad \text{(Eq. 5.5.1-1)}$$

The approximate and conservative anchorage force, $P_{L\text{-}s}$, is then found from a modified form of AISI S100 Eq. I6.4.1-2:

$$P_{L-s} = C1 \cdot \left[\left(\frac{C2}{1000} \cdot \frac{I_{xy}L}{I_x d} + C3 \cdot \frac{(m+0.25b)t}{d^2}\right)\cos\theta - C4 \cdot \sin\theta\right]\frac{W_s}{N_a} \qquad \text{(Eq. 5.5.1-2)}$$

Or the equation may be simplified even further and more conservatively to:

$$P_{L-s} = C1 \cdot \left[\left(\frac{I_{xy}}{2I_x} + \frac{(m+0.25b)}{d}\right)\cos\theta\right]\frac{W_s}{N_a} > C1 \cdot (\sin\theta)\frac{W_s}{N_a} \qquad \text{(Eq. 5.5.1-3)}$$

For the stiffness requirement, one may either compare the estimated purlin deflection to the allowable deflection, or the minimum required anchorage device stiffness to the actual stiffness. The purlin deflection is conservatively estimated from

$$\Delta_S = P_{L-s}\left[\frac{1}{K_a} + \frac{(N_p - N_a)S}{C6 \cdot LA_pE}\right] \quad \text{(Eq. 5.5.1-4)}$$

The resulting estimated deflection is then compared to the allowable deflection

$$\Delta_a = \frac{d}{\Omega \cdot 20} \text{ or } \phi\frac{d}{20} \quad \text{(Eq. I6.4.1-9)}$$

Alternatively, the required anchorage device stiffness, K_a, can be found from one of the following

$$K_{a\_req} = \frac{20 \cdot C6 \cdot LA_pEP_{L-s}}{\frac{1}{\Omega}C6 \cdot LA_pEd - 20P_{L-s}S(N_p - N_a)}\text{, for ASD} \quad \text{(Eq. 5.5.1-5a)}$$

$$K_{a\_req} = \frac{20 \cdot C6 \cdot LA_pEP_{L-s}}{\phi C6 \cdot LA_pEd - 20P_{L-s}S(N_p - N_a)}\text{, for LRFD or LSD} \quad \text{(Eq. 5.5.1-5b)}$$

Unlike AISI S100 Eq. I6.4.1-8, this yields the required anchorage stiffness directly, not the required total effective stiffness. The solution of this equation can result in negative values, meaning that the stiffness criteria, as evaluated with the simplified procedure, cannot be satisfied with the current number of anchorage devices. It is noted that this stiffness evaluation can be very conservative, especially for large roof systems.

5.5.2 Matrix-Based Solution

The design procedure presented in AISI S100 utilizes a relative stiffness technique to distribute anchorage forces. To develop the manual procedure, the stiffness analysis was simplified slightly and presented in a revised, single-degree-of-freedom format. The same underlying stiffness model can also be solved using matrix methods. This allows for the direct calculation of the displacements and potentially a better evaluation of the minimum stiffness requirements.

To formulate the stiffness model, the forces P_i are applied to nodes representing each purlin. Linear springs connect each adjacent node and model the axial behavior of the roof panels. The stiffness of these springs is related to K_{eff} and is found from

$$K_{D_k} = \frac{C6 \cdot LA_pE}{S_k} \quad \text{(Eq. 5.5.2-1)}$$

where k varies from one to the number of purlin spaces and S_k is the panel span between purlin k and k+1. To simplify the calculations in the manual procedure, the stiffness of all the purlins in the absence of the anchorage devices was collected into a single term K_{sys}. For the matrix solution K_{sys} is found for each purlin individually and applied as a spring support at the corresponding node. The stiffness of the spring is found by removing the number of purlins, N_p, from AISI S100 Eq. I6.4.1-6, yielding

$$K^{*}_{sys} = \frac{C5}{1000} \cdot \frac{ELt^2}{d^2} \qquad \text{(Eq. 5.5.2-2)}$$

The resulting one-dimensional model can be solved with a relatively simple system of equations as shown in the following example in Section 5.5.3.

5.5.3 Example: Example from Section 5.4.3 Using the Simplified Method and Matrix-Based Solution

Re-solve the Frame Line 3 case from the example in Section 5.4.3 using the simplified method and the matrix-based solution. Note the diaphragm deflection check is the same as that shown in Section 5.4.3.

Simplified Method

$$W_s = qLB \qquad \text{(Eq. 5.5.1-1)}$$

$$W_s = (23\text{psf})(55\text{ft})(25\text{ft}) = 31,625\,\text{lb}$$

$$P_{L-s} = C1 \cdot \left[\left(\frac{C2}{1000} \cdot \frac{I_{xy}L}{I_x d} + C3 \cdot \frac{(m+0.25b)t}{d^2}\right)\cos\theta - C4 \cdot \sin\theta\right]\frac{W_s}{N_a} \qquad \text{(Eq. 5.5.1-2)}$$

$$P_{L-s} = 1.0 \cdot \left[\left(\frac{4.3}{1000}\frac{(2.85)(25x12)}{(8.69)(8)} + 55 \cdot \frac{(0+0.25(2.75))(0.059)}{8^2}\right)\cos(2.39) - 0.71\sin(2.39)\right]\frac{31,625}{3} = 612\,\text{lb}$$

$$S = 5\text{ft}$$

$$\Delta_S = P_{L-s}\left[\frac{1}{K_a} + \frac{(N_p - N_a)S}{C6 \cdot LA_pE}\right] \qquad \text{(Eq. 5.5.1-3)}$$

$$= 0.612\left[\frac{1}{40} + \frac{(12-3)(5x12)}{0.17(25x12)(0.20/12)(29500)}\right] = 0.028\text{ in}$$

$$\Delta_a = \frac{d}{\Omega \cdot 20} \qquad \text{(AISI S100 Eq. I6.4.1-9a)}$$

$$= \frac{8}{2(20)} = 0.2\,\text{in}$$

$$K_{a\_req} = \frac{20 \cdot C6 \cdot LA_pEP_{L-s}}{\frac{1}{\Omega}C6 \cdot LA_pEd - 20P_{L-s}S(N_p - N_a)} \qquad \text{(Eq. 5.5.1-5a)}$$

$$= \frac{20(0.17)(25x12)(0.2/12)(29500)(0.612)}{\frac{1}{2.0}(0.17)(25x12)(0.2/12)(29500)(8) - 20(0.612)(5x12)(12-3)} = 3.28\,{}^{\text{kip}}\!/_{\text{in}}$$

Matrix Solution

$$K_{Dk} = \frac{C6 \cdot LA_pE}{S_k} \qquad \text{(Eq. 5.5.2-1)}$$

$$K_{Dk} = \frac{0.17(25x12)(0.20/12)(29500)}{(5x12)/\cos(2.39)} = 417.6\,{}^{\text{kip}}\!/_{\text{in}}$$

$$K^*_{sys} = \frac{C5}{1000} \cdot \frac{ELt^2}{d^2} \qquad \text{(Eq. 5.5.2-2)}$$

$$K^*_{sys} = \frac{1.4}{1000} \cdot \frac{(29500)(25x12)(0.059^2)}{8^2} = 0.674\,{}^{\text{kip}}\!/_{\text{in}}$$

Stiffness Matrix Representing the Axial Stiffness of the Roof Panels:

$$K_1 = \begin{bmatrix}
418 & -418 & 0 & 0 & 0 & 0 & 0 & 0 & 0 & 0 & 0 & 0 \\
-418 & 836 & -418 & 0 & 0 & 0 & 0 & 0 & 0 & 0 & 0 & 0 \\
0 & -418 & 836 & -418 & 0 & 0 & 0 & 0 & 0 & 0 & 0 & 0 \\
0 & 0 & -418 & 836 & -418 & 0 & 0 & 0 & 0 & 0 & 0 & 0 \\
0 & 0 & 0 & -418 & 836 & -418 & 0 & 0 & 0 & 0 & 0 & 0 \\
0 & 0 & 0 & 0 & -418 & 836 & -418 & 0 & 0 & 0 & 0 & 0 \\
0 & 0 & 0 & 0 & 0 & -418 & 836 & -418 & 0 & 0 & 0 & 0 \\
0 & 0 & 0 & 0 & 0 & 0 & -418 & 836 & -418 & 0 & 0 & 0 \\
0 & 0 & 0 & 0 & 0 & 0 & 0 & -418 & 836 & -418 & 0 & 0 \\
0 & 0 & 0 & 0 & 0 & 0 & 0 & 0 & -418 & 836 & -418 & 0 \\
0 & 0 & 0 & 0 & 0 & 0 & 0 & 0 & 0 & -418 & 836 & -418 \\
0 & 0 & 0 & 0 & 0 & 0 & 0 & 0 & 0 & 0 & -418 & 418
\end{bmatrix}$$

Stiffness Matrix Representing System Effect:

$$K_2 = \begin{bmatrix}
0.674 & 0 & 0 & 0 & 0 & 0 & 0 & 0 & 0 & 0 & 0 & 0 \\
0 & 0.674 & 0 & 0 & 0 & 0 & 0 & 0 & 0 & 0 & 0 & 0 \\
0 & 0 & 0.674 & 0 & 0 & 0 & 0 & 0 & 0 & 0 & 0 & 0 \\
0 & 0 & 0 & 0.674 & 0 & 0 & 0 & 0 & 0 & 0 & 0 & 0 \\
0 & 0 & 0 & 0 & 0.674 & 0 & 0 & 0 & 0 & 0 & 0 & 0 \\
0 & 0 & 0 & 0 & 0 & 0.674 & 0 & 0 & 0 & 0 & 0 & 0 \\
0 & 0 & 0 & 0 & 0 & 0 & 0.674 & 0 & 0 & 0 & 0 & 0 \\
0 & 0 & 0 & 0 & 0 & 0 & 0 & 0.674 & 0 & 0 & 0 & 0 \\
0 & 0 & 0 & 0 & 0 & 0 & 0 & 0 & 0.674 & 0 & 0 & 0 \\
0 & 0 & 0 & 0 & 0 & 0 & 0 & 0 & 0 & 0.674 & 0 & 0 \\
0 & 0 & 0 & 0 & 0 & 0 & 0 & 0 & 0 & 0 & 0.674 & 0 \\
0 & 0 & 0 & 0 & 0 & 0 & 0 & 0 & 0 & 0 & 0 & 0.674
\end{bmatrix}$$

Stiffness Matrix Representing Anchorage Devices:

$$K_3 = \begin{bmatrix}
40 & 0 & 0 & 0 & 0 & 0 & 0 & 0 & 0 & 0 & 0 & 0 \\
0 & 0 & 0 & 0 & 0 & 0 & 0 & 0 & 0 & 0 & 0 & 0 \\
0 & 0 & 0 & 0 & 0 & 0 & 0 & 0 & 0 & 0 & 0 & 0 \\
0 & 0 & 0 & 0 & 0 & 0 & 0 & 0 & 0 & 0 & 0 & 0 \\
0 & 0 & 0 & 0 & 40 & 0 & 0 & 0 & 0 & 0 & 0 & 0 \\
0 & 0 & 0 & 0 & 0 & 0 & 0 & 0 & 0 & 0 & 0 & 0 \\
0 & 0 & 0 & 0 & 0 & 0 & 0 & 0 & 0 & 0 & 0 & 0 \\
0 & 0 & 0 & 0 & 0 & 0 & 0 & 0 & 0 & 0 & 0 & 0 \\
0 & 0 & 0 & 0 & 0 & 0 & 0 & 0 & 40 & 0 & 0 & 0 \\
0 & 0 & 0 & 0 & 0 & 0 & 0 & 0 & 0 & 0 & 0 & 0 \\
0 & 0 & 0 & 0 & 0 & 0 & 0 & 0 & 0 & 0 & 0 & 0 \\
0 & 0 & 0 & 0 & 0 & 0 & 0 & 0 & 0 & 0 & 0 & 0
\end{bmatrix}$$

Complete Stiffness Matrix, $K=K_1+K_2+K_3$:

$$K = \begin{bmatrix}
459 & -418 & 0 & 0 & 0 & 0 & 0 & 0 & 0 & 0 & 0 & 0 \\
-418 & 836 & -418 & 0 & 0 & 0 & 0 & 0 & 0 & 0 & 0 & 0 \\
0 & -418 & 836 & -418 & 0 & 0 & 0 & 0 & 0 & 0 & 0 & 0 \\
0 & 0 & -418 & 836 & -418 & 0 & 0 & 0 & 0 & 0 & 0 & 0 \\
0 & 0 & 0 & -418 & 876 & -418 & 0 & 0 & 0 & 0 & 0 & 0 \\
0 & 0 & 0 & 0 & -418 & 836 & -418 & 0 & 0 & 0 & 0 & 0 \\
0 & 0 & 0 & 0 & 0 & -418 & 836 & -418 & 0 & 0 & 0 & 0 \\
0 & 0 & 0 & 0 & 0 & 0 & -418 & 836 & -418 & 0 & 0 & 0 \\
0 & 0 & 0 & 0 & 0 & 0 & 0 & -418 & 876 & -418 & 0 & 0 \\
0 & 0 & 0 & 0 & 0 & 0 & 0 & 0 & -418 & 836 & -418 & 0 \\
0 & 0 & 0 & 0 & 0 & 0 & 0 & 0 & 0 & -418 & 836 & -418 \\
0 & 0 & 0 & 0 & 0 & 0 & 0 & 0 & 0 & 0 & -418 & 419
\end{bmatrix}$$

Applied Force Vector, calculated from AISI S100 Eq. I6.4.1-2:

P = {-169 167 167 167 167 167 167 167 167 167 167 83} lb

Solve for Nodal Displacements:

$\Delta = K^{-1}P =$ {9.63 10.97 11.92 12.50 12.70 13.73 14.39 14.67 14.57 15.49 16.04 16.21} x 10^{-3} in. (Eq. 5.5.3-1)

Solve for Anchorage Forces:

$P_L = K_3 \Delta =$ {384 0 0 0 508 0 0 0 583 0 0 0} lb (Eq. 5.5.3-2)

Comparison of Methods

The anchorage forces from the three solution methods are compared in the table below. It can be seen that the AISI S100 method and the matrix solution method provide similar results. As discussed above the Simplified Procedure provides conservative forces as long as the anchorage devices are evenly distributed along the roof slope.

Method	P_{LA}, lb	P_{LB}, lb	P_{LC}, lb
AISI S100	407	518	529
Simplified Procedure	612	612	612
Matrix Based Method	385	508	583

5.5.4 Component Stiffness Method

The component stiffness method is an alternative manual calculation procedure to Section I6.4.1 in AISI S100. The two procedures are based on the same principal – forces generated by a system of purlins are distributed to the external anchorage devices according to relative stiffness. In each procedure, however, the forces generated by the system of purlins and the distribution of the forces are calculated differently. The component stiffness method can be used to determine anchorage forces for supports, third points, midpoints, supports plus third point torsional brace and supports plus third point lateral bracing configurations.

The roof system is divided into three types of "components": the external restraint, the connection between the purlin and rafter, and the connection between the panels and purlin. The roof system is treated as a single degree of freedom system and the contributions of each component are related by stiffness. The stiffness of each of the components is defined as the force or moment developed in the component per unit lateral displacement of the top flange at the restraint.

A three step process is used to determine the magnitude of the anchorage force using the component stiffness method. First, the magnitude of the overturning force, P_i, generated by each purlin as the purlin transfers the gravity loads from the panels to the frame lines is determined. Calculations of the overturning force consider the eccentricity of the applied loads and the effects of the resistance provided by the panels. Next, the resistance of the system to the overturning forces is determined. The anchorage device provides most of the resistance to the overturning forces, however the system of purlins has some inherent resistance to the overturning forces in the connection between the purlin and the frame line and the connection between the purlin and panels. The stiffness of each "component" of the system, the anchorage device, the purlin-rafter connection and the purlin-panel connection, is calculated. In the third step, the stiffness of each "component" is compared to determine the distribution of the overturning force between the anchorage device, the purlin-rafter connection and the purlin-panel connection. The anchorage force, P_L, is the magnitude of the overturning force distributed to each anchorage device.

5.5.4.1 Component Stiffness Method - General

The basis for the component stiffness method is discussed in the following section. Solutions to different bracing configurations are discussed in Section 5.5.4.4 and equations specific to the different bracing configurations are presented in Section 5.5.4.6.

Generation of Overturning Moments. The component stiffness method is based upon the free body diagrams shown in Figures 5.5-1(a) and 5.5-2(a). Figure 5.5-1(a) displays the overturning forces and moments developed in the roof system and Figure 5.5-2(a) shows the forces restraining the system. The gravity load applied to the top flange of the purlin as shown in Figure 5.5-1(a) is divided into a normal component, $w \cdot L \cdot \cos\theta$, perpendicular to the plane of the panels and a downslope component, $w \cdot L \cdot \sin\theta$, in the plane of the panels, where w is the uniformly applied gravity load along the span of the purlin, L is the span of the purlin and θ is the angle of the roof plane relative to the horizontal. The normal component of the gravity load is approximated to act at some eccentricity, δb, along the top flange of the purlin.

As the gravity loads are applied, lateral deformation of the purlin is restrained through the development of diaphragm forces in the panels. Moments are developed in the connection between the purlin and the panels as the panels resist the torsion of the purlin and the local rotation of the top flange of the purlin. Twisting of the purlin results from the gravity load being applied eccentrically to the shear center of the purlin and the eccentricity of the diaphragm restraint provided by the panels. The panels resist the torsional rotations through the development of moment, $M_{torsion}$. Additional moments in the panels, M_{local}, are developed by the resistance of the panels to cross-sectional deformation of the purlin. The forces and moments shown in Figure 5.5-1(a) have a net overturning effect on the purlin about its base at the rafter location, $P_i \cdot d$, shown in Figure 5.5-1(b) .

$$\sum M_{Base} = P_i d = wL(\delta b \cos\theta - d \sin\theta) + M_{torsion} + M_{local} \qquad \text{(Eq. 5.5.4-1)}$$

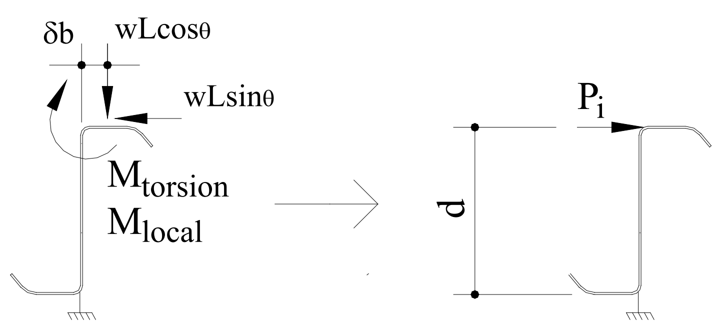

(a) Forces Generated **(b) Net Overturning**

Figure 5.5-1 Free Body Diagram of Forces Generated

The overturning moment due to the normal component of gravity load, the torsional moment and the local bending moment are all a function of the eccentricity of the gravity load, δb.

Ghazanfari and Murray (1983) proposed that the normal component of the gravity load acts at an eccentricity of δb = b/3. Comparison of the component stiffness method to test results by Lee and Murray (2001) and Seek and Murray (2004) show good correlation for an eccentricity of one third of the flange width so it is recommended that this value be used. Generally, for a low slope roof (roof slope less than 1:12), it is typically conservative to overestimate eccentricity while for steeper slope roofs, underestimating eccentricity is conservative.

Resistance to Overturning Moments. Figure 5.5-2(a) shows the resistance of the system of purlins to these overturning moments. The majority of the resistance is provided by the external anchorage, P_L. However, an anchorage device has a finite stiffness, and as the anchorage device permits displacement of the top flange, additional resistance is provided by the inherent lateral stiffness of the system, "system effects". As the top of the purlin moves laterally relative to the base, the purlin rotates about the longitudinal axis relative to the panel and a resisting moment is developed in the panel, M_{panel}. Similarly, the connection between the rafter and the purlin resists the rotation of the purlin through the development of a moment at the connection. Summing moments about the base of the purlin, the anchorage force, P_L, at the top of the purlin is

$$P_L = P_i + \frac{M_{shtg} + M_{rafter}}{d} \quad \text{(Eq. 5.5.4-2)}$$

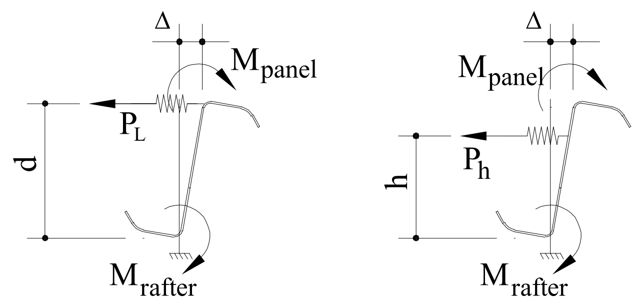

(a) Anchorage At Top Flange **(b) Anchorage at Web**

Figure 5.5-2 Free Body Diagram of Resisting Forces

Note that in Figure 5.5-2, P_i, P_L, M_{panel}, and M_{rafter}, and Δ are shown in the positive direction. For a positive applied force, P_i, the anchorage force, P_L, and the lateral displacement will be positive while the resisting moments of the panels and rafter, M_{panel}, and M_{rafter} respectively, will be negative.

The forces resisted by each "component", the external anchorage device, the panels, and the connection of the purlin to the rafter, are directly related to the displacement of the top flange at the anchorage device. The component stiffness method defines the stiffness of each of these components as the force or moment generated in the component per unit displacement of the top flange of the purlin at the anchorage device location. Therefore, the anchorage stiffness, K_{rest}, is the force in the anchorage device at the top flange of the panels relative to the displacement of the top flange at the anchorage device location. The panel stiffness, K_{panel}, is the moment generated in the connection between the purlin and the panels per unit displacement of the purlin top flange at the anchorage device location. Similarly, the rafter stiffness, K_{rafter}, is the moment generated at the rafter location per unit displacement of the top flange at the anchorage device location. By defining the stiffness of each of the components relative to the displacement of the top flange of the purlin at the anchorage device, the purlin is treated as a single degree of freedom system. The force resisted by the anchorage device is the product of the net overturning forces in the system and the relative stiffness of the anchorage device to the total stiffness of the system, or

$$P_L = P_i \cdot \frac{K_{rest}}{K_{rest} + K_{panel} + K_{rafter}} \qquad \text{(Eq. 5.5.4-3)}$$

Locating the anchorage device below the top flange of the purlin will reduce the anchorage device stiffness because of the additional flexibility introduced through the bending of the web and will increase the anchorage force because of the reduced moment arm, h, as shown in Figure 5.5-2(b). The reduced stiffness is accounted for in equations for the anchorage device stiffness. The increase in the anchorage force is calculated as

$$P_h = P_L \cdot \frac{d}{h} \qquad \text{(Eq. 5.5.4-4)}$$

Note the difference between the moments developed in the panels. The torsional moment, $M_{torsion}$, and the local bending moment, M_{local}, are generated along the span of the purlin as the top flange of the purlin is rigidly restrained at the anchorage device location. Therefore, the torsional moment and local bending moment are considered part of the overturning forces that must be restrained and are embedded in the overturning force equation, P_i. As the flexibility of the anchorage device allows lateral displacement of the top flange, the panel moment, M_{panel} is developed to resist this lateral movement. It is dependent upon the lateral displacement of the top flange at the anchorage device and therefore is considered part of the stiffness of the system.

Torsional Moment-General. The panels connected to the top flange of the purlin resist the torsional rotation of the purlin. The torsional moment is the moment that is applied to the purlin as a result of the resistance provided by the panel. To determine the torsional moment, the purlin, subjected to a uniform gravity load, is rigidly restrained at the top flange at the anchorage device location. The lateral deflection and rotation of the purlin along its span is restrained by the panels through the development of shear forces in the diaphragm and moments due to the torsional resistance of the panels. Compatibility between the displaced shape of the purlin and the panels is used to determine the restraining forces in the panels. Because the displaced shape of the purlin is dependent upon the anchorage device location, an individual set of equations must be derived for each anchorage device configuration. To illustrate how the torsional moment and diaphragm forces are determined, the two quantities will be derived for both a Z-section and a C-section with support anchorage.

Torsional Moment – Z-sections. To determine the interacting forces between the purlin and the panel for a purlin with anchorage devices at its supports, compatibility of the displaced shape is determined at the mid-span of a single span Z-section. The Z-section is restrained laterally at the top and bottom flanges at the frame line and subjected to external gravity loads applied to the top flange. In the absence of panels and neglecting second order effects, as the component of the gravity load normal to the plane of the panels, $w \cdot L \cdot \cos\theta$, acts at an eccentricity, δb, on the top flange of the Z-section, as shown in Figure 5.5-1(a), the Z-section will deflect laterally ($\Delta_{x,cen}$) and twist clockwise about its longitudinal axis ($\Delta_{x,torsion}$) as shown in Figure 5.5-3. Panels attached to the top flange of the Z-section resist this deformation through the development of a uniform horizontal force along the length of the Z-section, w_{rest}, as shown in Figure 5.5-4. Application of this uniform force to the top flange of the Z-section results in a restoring lateral deflection

($\Delta_{x,restoring,center}$) and a counterclockwise twist of the Z-section ($\Delta_{x,restoring,torsion}$). The uniform restraint force in the panels, w_{rest}, and the downslope component of the gravity load, $w \cdot L \cdot \sin\theta$, result in additional deformation of the top flange of the Z-section at mid-span due to the diaphragm flexibility of the panels. Equating the unrestrained displacements to the restoring displacements, the uniform restraint force in the plane of the diaphragm is determined by

$$w_{rest} = w \cdot \sigma \qquad \text{(Eq. 5.5.4-5)}$$

where

$$\sigma = \frac{\dfrac{5\left(\dfrac{I_{xy}}{I_x}\cos\theta\right)L^4}{384EI_{my}} + \dfrac{[(\delta b + m)\cos\theta]d}{2}\tau + \dfrac{L^2 \sin\theta}{8G'Width}}{\dfrac{5L^4}{384EI_{my}} + \dfrac{d^2}{4}\tau + \dfrac{L^2}{8G'Width}} \qquad \text{(Eq. 5.5.4-6)}$$

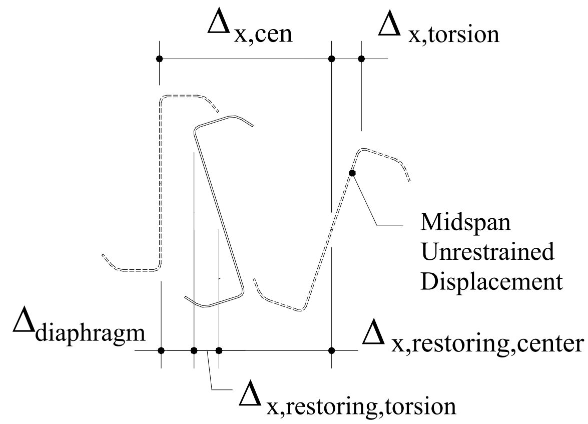

Figure 5.5-3 Mid-span Displacement Compatibility

For definitions of the terms used in Eq. 5.5.4-6 refer to the nomenclature in the beginning of this chapter. The distance from the shear center to the center of the web, m, is zero for Z-sections. The term σ is used for convenience of calculation and is the proportion of the uniformly applied vertical force, w, transferred to a uniform restraint force in the plane of the panels, w_{rest}. This proportion can typically be approximated as $\sigma \approx I_{xy}/I_x$ for Z-sections. As the combined torsional stiffness of the Z-section and panels increases, the second terms in the numerator and denominator will approach zero. Similarly, as the diaphragm stiffness increases, the third terms in the numerator and denominator will approach zero. Therefore, for a perfectly rigid diaphragm and torsionally rigid Z-section-panel connection, constrained bending is achieved and σ will reduce to I_{xy}/I_x. For low-slope roofs, reducing the diaphragm stiffness will reduce the uniform restraint force in the panels which will result in $\sigma < I_{xy}/I_x$. For roofs with steeper slopes (typically greater than a 1:12 slope) reducing the diaphragm stiffness will increase the uniform restraint force in the panels relative to the rigid case, or $\sigma > I_{xy}/I_x$. Unlike with the diaphragm stiffness, no simple trend was observed with respect to the torsional stiffness of the Z-section but in general, the torsional stiffness has a small effect on σ.

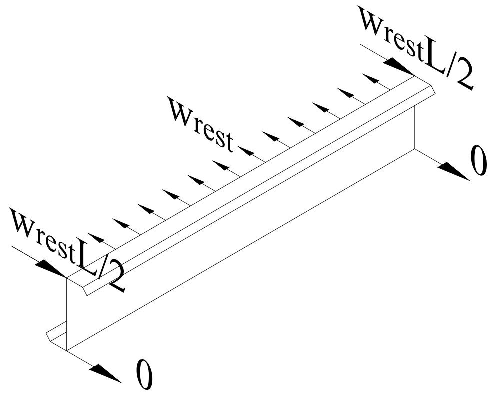

Figure 5.5-4 Uniform Restraint Force in Panels

Once the uniform restraint force in the panels has been determined, the mid-span torsional rotation of the Z-section and corresponding moment generated in the panels is determined. For a Z-section with anchorage at the supports, the rotation of a Z-section about its longitudinal axis is restricted at its ends and increases to maximum at mid-span, Φ, as shown in Figure 5.5-5(a). The variation of the torsional rotation is approximately parabolic along the length of the Z-section. The connection between the panels and the Z-section resists this torsion through the development of a moment along the length of the Z-section, $M_{torsion}$, as shown in Figure 5.5-5(b). The moment in the panels is proportional to the rotation of the Z-section about its longitudinal axis. The stiffness of the connection between the panels and the Z-section, k_{mclip}, is defined as the moment developed in the connection per unit rotation of the Z-section per unit length along the span. The moment caused by the resistance of the panels results in an additional torsional rotation of the Z-section, $\Phi_{Mtorsion}$, as shown in Figure 5.5-5(b). The net torsional rotation of the Z-section at mid-span, Φ_{net}, is the sum of the rotation caused by the eccentrically applied gravity load, the rotation caused by the uniform lateral resistance of the panels at the top flange, and the rotation due to the panel moment, or

$$\Phi_{net} = \left(w\left(\left(\delta b + m \right) \cos\theta \right) - w_{rest} \frac{d}{2} \right) \frac{a^2 \beta}{GJ} - \Phi_{net} \cdot k_{mclip} \left(\frac{\kappa}{GJ} \right) \quad \text{(Eq. 5.5.4-7)}$$

which is simplified to yield

$$\Phi_{net} = w\left(\left(\delta b + m \right) \cos\theta - \sigma \frac{d}{2} \right) \tau \quad \text{(Eq. 5.5.4-8)}$$

where

$$\tau = \frac{\dfrac{a^2 \beta}{GJ}}{1 + k_{mclip} \dfrac{\kappa}{GJ}} \quad \text{(Eq. 5.5.4-9)}$$

The net torsional rotation of the Z-section from Eq. 5.5.4-8 at mid-span is the peak rotation in the parabolic distribution. Relating the moment in the panels to the rotation by $M=\Phi_{net} \cdot k_{mclip}$ and integrating along the length of the Z-section, the total moment in the connection between the panels and Z-section generated along the length of the Z-section is

$$M_{torsion} = \tfrac{2}{3} k_{mclip} \cdot wL\left(\sigma \frac{d}{2} - ((\delta b)\cos\theta)\right)\tau \qquad \text{(Eq. 5.5.4-10a)}$$

As the Z-section is oriented in Figure 5.5-5, with the top flange facing to the right, the positive direction for the torsional rotation and the torsional moment is clockwise. Therefore, as the Z-section undergoes positive torsion, a negative moment is developed in the panels.

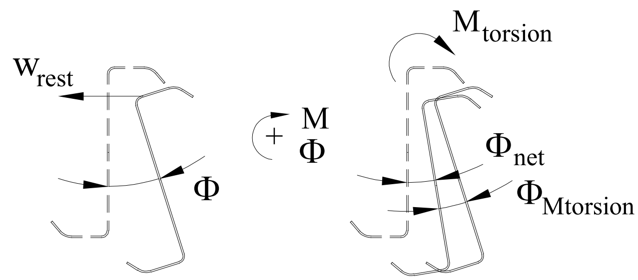

(a) Rotation without Torsional Resistance (b) Net Rotation with Torsional Resistance

Figure 5.5-5 Rotation of Z-Section at Mid-Span

Torsional Moment – C-sections. For determining anchorage forces, Z-sections and C-sections have two main differences. First, Z-sections have principal axes that are oblique to the centroidal axes while, for a C-section, the principal axes correspond with the centroidal axes. A C-section does not deflect laterally when subjected to loads in the plane of the web as a Z-section does. As a result, the uniform restraint force in the panels is much less for a C-section than for a similar configuration with a Z-section. Secondly, the shear center of a C-section is located at some distance, m, from the web while for a Z-section, m = 0. Because of this additional eccentricity, torsion of the C-section plays a larger role in the development of the torsional moment.

Like for a Z-section, the first step in determining the anchorage forces for a C-section is to calculate the uniform restraint force in the panels. For a single span C-section with supports anchorage, Eq. 5.4.4-6 is used to calculate the uniform restraint force in the panels. In the numerator of the equation to calculate the uniform restraint force, the term including I_{xy} is eliminated and the eccentricity of the shear center, m, is included in the torsional term. The equation reduces to

$$\sigma = \frac{\dfrac{((\delta b + m)\cos\theta)d}{2}\tau + \dfrac{L^2 \sin\theta}{8G'Width}}{\dfrac{5L^4}{384EI_{my}} + \dfrac{d^2}{4}\tau + \dfrac{L^2}{8G'Width}} \qquad \text{(Eq. 5.5.4-11)}$$

The uniform restraint force along the length of the purlin is small and will typically be on the order of 1% to 5% of the applied uniform load.

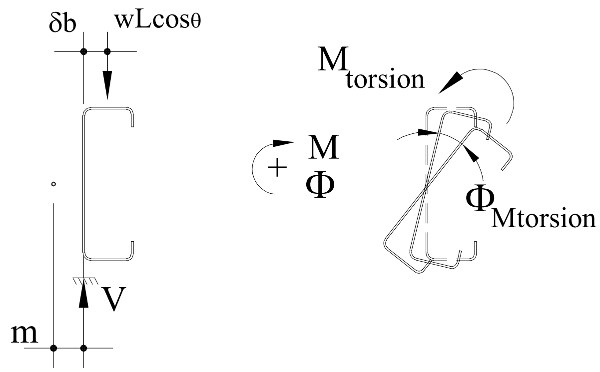

(a) Moment due to Applied Gravity Load **(b) Torsional Moment**

Figure 5.5-6 Moments Acting on C-Section

Because the uniform restraint force in the panels is relatively small, the torsion of the C-section is dominated by the overturning caused by the component of gravity load normal to the panels (refer to Figure 5.5-6). This torsion results in a positive (clockwise) rotation of the C-section about its longitudinal axis. The panels resist this positive rotation with the development of a negative torsional moment. Therefore, the torsional moment for C-sections is similar to that for Z-sections, determined by Eq. 5.5.4-10a. For C-sections, considering the shear center locations, the torsional moment, $M_{torsion}$, can be expressed as

$$M_{torsion} = \tfrac{2}{3} k_{mclip} \cdot wL\left(\sigma \frac{d}{2} - \left(\left(\delta b + m\right)\cos\theta\right)\right)\tau \qquad \text{(Eq. 5.5.4-10b)}$$

It is important to note that the vertical reaction at the base of the section is assumed to act in the plane of the web (refer to Figure 5.5-6(a)). Thus, for a C-section, the overturning moment due to the normal component of the gravity load ($wL\cdot\delta b\cos\theta$) is independent of the location of the shear center. The location of the shear center only affects the torsion of the C-section along its span (and the corresponding torsional moment). As a result, for a flat slope roof, the negative torsional moment can exceed the positive gravity moment, resulting in a negative net overturning moment.

Local Bending Moment. The equations for the torsional moment assume that plane sections always remain plane. Because purlins are manufactured from relatively thin material, the purlin cross section can deform without fully transferring the moments predicted in the torsion moment equations (Eqs. 5.5.4-10a and 5.5.4-10b). This additional deformation is approximated by the model shown in Figure 5.5-7. As the component of the gravity load normal to the plane of the panels acts eccentrically on the top flange of the purlin, the flange deflects causing a local rotation of the purlin relative to the panels. Due to the rotational resistance of the connection between the purlin and the panels, a moment is developed in the panels. The magnitude of this moment, referred to as the local bending moment, is

$$M_{local} = -wL \cdot \delta b \cos\theta \cdot \frac{k_{mclip}}{k_{mclip} + \dfrac{Et^3}{3d}} \qquad \text{(Eq. 5.5.4-12)}$$

In the component stiffness method, the local bending moment is incorporated into the equations as a reduction factor, R_{local}, where

$$R_{local} = \frac{k_{mclip}}{k_{mclip} + \frac{Et^3}{3d}} \quad \text{(Eq. 5.5.4-13)}$$

The overturning force due to the eccentricity of the normal component of the gravity load is reduced by a factor of (1-R_{local}). The user is to be cautioned with units when using Eq. 5.5.4-13. The units of k_{mclip} are typically specified in lb-in./rad/ft. The second term in the numerator will need to be multiplied by a factor of 12 in./ft to obtain consistent units.

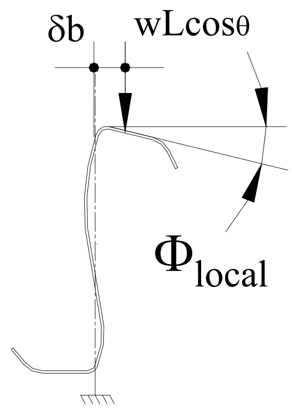

Figure 5.5-7 Local Deformation of Z-Section

5.5.4.2 Stiffness of Components

Anchorage Stiffness. For the purposes of determining stiffness, anchorage configurations are divided into two categories: support and interior. A support anchorage is applied along the frame line while an interior anchorage is applied along the interior of the span.

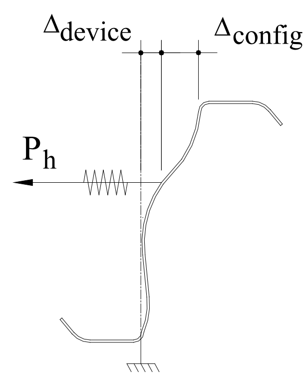

Figure 5.5-8 Combined Displacement of Device and Configuration

Anchorage Stiffness – Support Anchorage Configuration. The stiffness of each anchorage is defined as the force developed at the top flange of the purlin at the anchorage per unit displacement of the top flange at the anchorage location. As shown in Figure 5.5-8, the lateral deflection at the anchorage is the combination of the deflection of the anchorage device, Δ_{device}, and the deflection of the web of the purlin relative to the height the applied restraint, Δ_{config}. The total stiffness at the anchorage, K_{rest}, provided in Eq. 5.5.4-14 is the combination of the stiffness of the device at the height at which the restraint is applied, K_{device}, and the stiffness of the purlin web as the force is transferred from the top flange of the purlin to the anchorage device, K_{config}. The net stiffness of the anchorage, K_{rest}, is defined as the anchorage force at the top flange of the purlin per unit displacement of the top flange.

$$K_{rest} = \frac{\left(\frac{h}{d}\right)^2 K_{device} \cdot K_{config}}{\frac{h}{d} K_{device} + K_{config}} \qquad \text{(Eq. 5.5.4-14)}$$

For a support anchorage, the stiffness of the device is generally very high relative to the configuration stiffness. The device stiffness will typically have a negligible effect on the overall anchorage stiffness and can be considered rigid in many cases. For determination of the anchorage force, this approximation will be conservative, although the predicted deformation of the system will be unconservative.

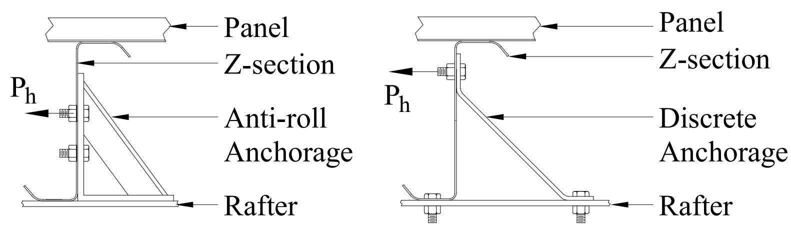

(a) Anti-roll Anchorage Device **(b) Discrete Anchorage Device**

Figure 5.5-9 Support Anchorage Configurations

Support anchorage devices are divided into two categories – discrete and anti-roll anchorage devices. A discrete anchorage device provides lateral resistance at a discrete location along the height of the purlin as shown in Figure 5.5-9(b) while an anti-roll anchorage device clamps to the web of the purlin at multiple locations along the depth as shown in Figure 5.5-9(a). The anti-roll anchorage device prevents deformation of the purlin web below the anchorage location while a discrete anchorage device permits some deformation, resulting in a variation in stiffness. An equation to predict the stiffness of each type of configuration is provided due to this variation in stiffness.

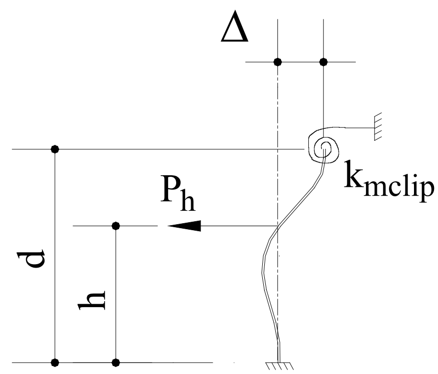

Figure 5.5-10 Stiffness Model – Discrete Anchorage Device

The equation to predict the configuration stiffness of a discrete anchorage configuration is based on a two-dimensional beam model bent about the thickness of the web as shown in Figure 5.5-10. To account for the third dimension, the effective width of the web and the panel, the representative equation was calibrated to the results of finite element models as described by Seek and Murray (2004). The resulting configuration stiffness for a discrete anchorage is

$$K_{config} = \frac{\frac{1}{15} d \cdot (3Et^3)}{h(d-h)^2} \left[\frac{\frac{1}{15} d \cdot 2Et^3 (3d-h) + \frac{L}{80} \cdot k_{mclip} \cdot d(3d-2h)}{\frac{1}{15} d \cdot Et^3 (4d-h) + \frac{L}{80} \cdot k_{mclip} \cdot d(d-h)} \right] \qquad \text{(Eq. 5.5.4-15)}$$

where d is the depth of the section, h is the height of the applied restraint, L is the span length of the purlin and k_{mclip} is the rotational stiffness of the connection between the purlin and the panel.

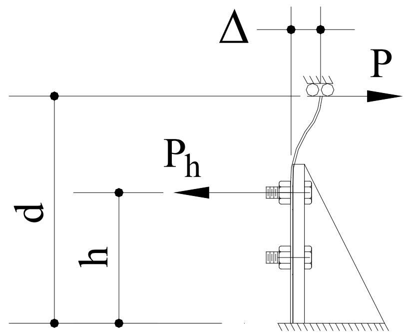

Figure 5.5-11 Stiffness Model – Anti-Roll Anchorage Device

For an anti-roll anchorage device, the configuration stiffness is based upon the two-dimensional line element model shown in Figure 5.5-11. The model assumes that restraint is applied at the top row of bolts and the web of the purlin is rotationally fixed at this point. The effective width of the web is assumed to be the width of the anti-roll clip, b_{pl} and the top of the purlin is assumed to be fixed to the panels. The configuration stiffness equation given by Eq. 5.5.4-16 is the familiar formula for a fixed-fixed cantilever beam multiplied by d/h to transfer the stiffness to the restraint height, h.

$$K_{config} = \frac{Eb_{pl} t^3}{(d-h)^3} \left(\frac{d}{h} \right) \qquad \text{(Eq. 5.5.4-16)}$$

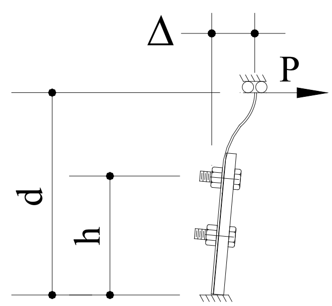

Figure 5.5-12 Stiffness Model – Rafter Plate

A type of anti-roll anchorage device is a single web plate. The device stiffness and the configuration stiffness of the web plate is calculated directly by modeling the web plate and purlin web as a two-dimensional cantilever beam model as shown in Figure 5.5-12. The beam, modeled as a prismatic section, has a width equal to the width of the web plate. For a distance from the top of rafter elevation to the top row of bolts, the beam has a thickness equal to that of the web plate. Above the top row of bolts the beam model has the thickness equal to the purlin web thickness. The model incorporates both the device and configuration stiffness, and the resulting net stiffness of the anchorage for a web bolted rafter plate is

$$K_{rest} = \frac{E \cdot b_{pl} \cdot t_{pl}{}^{3} \cdot t^{3}\left(t^{3}h + t_{pl}^{3}\left(d-h\right)\right)}{\left(t^{3}h^{2} - t_{pl}^{3}\left(d-h\right)^{2}\right)^{2} + 4t^{3}t_{pl}{}^{3}d^{2}h\left(d-h\right)} \qquad \text{(Eq. 5.5.4-17)}$$

The provided equations for the configuration stiffness for a discrete anchorage device will typically overestimate the stiffness of the configuration, which will lead to a conservative approximation of the anchorage force but may underestimate the amount of deflection in the system. Conversely, for an anti-roll anchorage device, the provided equation will typically underestimate the stiffness which will result in an overestimation of the deformation at the anchorage location. Most anti-roll anchorage devices have substantial strength and the design of such systems will typically be deflection controlled. Because no testing or finite element modeling was performed with anti-roll anchorage devices, it is conservative to underestimate the stiffness of the anti-roll anchorage device.

Anchorage Stiffness – Interior Anchorage Configuration. Interior anchorage configurations should be attached as close as possible to the top flange of the purlin to minimize the deformation of the purlin web as the anchorage force is transferred out of the panels and into the anchorage device. Flexibility therefore is introduced only through the deformation of the anchorage. From Eq. 5.5.4-14, the configuration stiffness is considered infinite and the net anchorage stiffness reduces to

$$K_{rest} = \left(\frac{h}{d}\right)^{2} K_{device} \qquad \text{(Eq. 5.5.4-18)}$$

Stiffness of System. The system of purlins has an inherent resistance to lateral forces through the connection of the purlin to the rafter and through the connection of the panels to the purlin, referred to as the rafter stiffness, K_{rafter} and panel stiffness, K_{panel}, respectively. For determining both anchorage forces and the deformation of the system, it is conservative to underestimate the rafter stiffness and the panel stiffness. A low estimate of the rafter stiffness and the panel stiffness will result in the prediction of a larger anchorage force than actual and will result in a larger displacement. For simplicity, the rafter stiffness and the panel stiffness can conservatively be eliminated. However, the contribution of the panels and the rafter connection to the resistance of overturning forces can be significant and economically advantageous to include.

Stiffness of System – Rafter Stiffness. The connection of the purlin to the rafter provides resistance to overturning forces through the development of a moment at the base of the purlin. The rafter stiffness is defined as the moment generated at the base of the purlin per unit lateral displacement of the top flange of the purlin. Two basic connection configurations are considered, a flange-bolted connection, shown in Figure 5.5-13(a) and a web bolted rafter plate connection, shown in Figure 5.5-13(b). In a flange-bolted configuration, the bottom flange of the purlin is through-bolted to the top flange of the rafter with two bolts. The clamping action of the bolts permits the development of a moment, M_{rafter}, of the base of the purlin as the top flange of the purlin moves laterally. The stiffness of a flange bolted connection, derived from a two-dimensional beam element model and calibrated to the results of finite element models as described in Seek and Murray (2006), is

$$K_{rafter} = 0.45\frac{Et^3}{2d} \qquad \text{(Eq. 5.5.4-19)}$$

where E is the modulus of elasticity of the purlin, t is the thickness of the purlin and d is the depth of the purlin.

(a) Flange Bolted **(b) Web Plate Bolted**

Figure 5.5-13 Typical Rafter to Purlin Connections

The second rafter connection configuration considered is a web bolted rafter plate. In this connection configuration, a plate, typically welded to the rafter, is bolted to the web of the purlin. Like the flange bolted connection, as the top flange of the purlin moves laterally, a moment is generated at the base of the purlin to resist this movement. Because of the added stiffness of the rafter plate, the web-bolted rafter plate configuration has considerably more stiffness than the flange bolted configuration. The rafter stiffness for a web plate shown in Eq. 5.5.4-20 is the same as Eq. 5.5.4-17 for a supports restraint except the stiffness is multiplied by the depth of the purlin, d, to convert it to moment at the base of the purlin per unit displacement of the top of the purlin.

$$K_{rafter} = \frac{E \cdot b_{pl} \cdot t_{pl}{}^3 \cdot t^3\left(t^3 h + t_{pl}^3(d-h)\right) \cdot d}{\left(t^3 h^2 - t_{pl}^3 (d-h)^2\right)^2 + 4t^3 t_{pl}{}^3 d^2 h(d-h)} \qquad \text{(Eq. 5.5.4-20)}$$

It is important not to count the stiffness of a rafter plate twice when using the component stiffness method. When considered a restraint, the stiffness of the rafter plate should only be considered in the restraint stiffness. When the rafter plate is considered a typical rafter connection and used in conjunction with stiffer anti-roll anchorage devices, the stiffness of the rafter plate should be considered part of the rafter stiffness.

Stiffness of System – Panel Stiffness. The second inherent contribution of the system to the lateral resistance comes from the connection between the purlin and the panels. As the top flange of the purlin moves laterally, the purlin is approximated to rotate about its base as shown in Figure 5.5-14. As the purlin rotates relative to the plane of the panels, a moment is developed in the connection between the purlin and the panels. The rotation of the purlin about its base is approximated to be uniform and thus generates a uniform moment in the connection between the purlin and panels along the length of the purlin. As the uniform moment is applied to the purlin, additional torsional rotations are generated in the purlin. These torsional rotations are approximated to vary parabolically along the length of the purlin and are accounted for by the $(1\text{-}2/3k_{mclip}\tau)$ term in Eq. 5.5.4-21. The theoretical equation for the panel stiffness was further modified through comparison of the equation to the results of finite element models as described in Seek and Murray (2004; 2006). The resulting equation for the stiffness of the panel considering the full purlin span is

$$K_{panel} = \frac{k_{mclip}L}{d}\left(\frac{\frac{1}{4}Et^3}{0.38k_{mclip}d + 0.71\frac{Et^3}{4}}\right)\left(1 - \tfrac{2}{3}k_{mclip}\tau\right) \quad \text{(Eq. 5.5.4-21)}$$

Where L is the purlin span, d is the depth of the purlin, t is the thickness of the purlin, k_{mclip} is the rotational stiffness of the connection between the purlin and the panels and τ is the torsional term defined by Eq. 5.5.4-9.

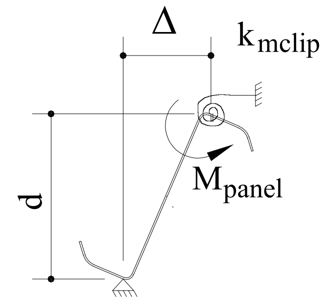

Figure 5.5-14 Panel Moment Stiffness

5.5.4.3 Anchorage Effectiveness

System Deformation. Lateral deflection should be checked at the anchorage location as excessive deformation undermines the intent of anchorage system to prevent overturning of the purlin. In the event that adequate stiffness is not provided to limit deflection, the stiffness of the anchorage can be increased by adding anchorage devices or increasing the stiffness of the existing anchorage devices. Lateral deflection also should be checked at the extremes of the system to ensure that the diaphragm has sufficient stiffness to transfer the forces along the length of the purlin to the restraints. The lateral deflection of the top flange of the purlin at the anchorage location can be approximated by

$$\Delta_{rest} = \frac{P_L}{K_{rest}} \quad \text{(Eq. 5.5.4-22)}$$

In general, as a purlin is allowed to deflect laterally, the calculated anchorage force decreases. The method does not account for any second order effects, therefore displacements should be minimized, particularly at the anchorage location. AISI S100 limits the lateral displacement of the top flange of the purlin, Δ_{tf}, calculated at factored load levels for LRFD and at nominal load levels for ASD to a deflection

$$\Delta_{tf} \le \frac{1}{\Omega}\frac{d}{20} \quad \text{(ASD)} \quad \text{(AISI S100 Eq. I6.4.1-9a)}$$

$$\Delta_{tf} \le \phi\frac{d}{20} \quad \text{(LRFD)} \quad \text{(AISI S100 Eq. I6.4.1-9b)}$$

With a flexible diaphragm, lateral deflection of the purlin at mid-span relative to the anchorage location is expected. For a support anchorage and support plus third points torsion anchorage configuration, the lateral displacement of the diaphragm at the mid-span of the purlin relative to the anchorage location is

$$\Delta_{diaph} = \sum_{N_p} \left(w(\alpha\sigma - \sin\theta)\right)_i \frac{L^2}{8G'Bay} \quad \text{(Eq. 5.5.4-23)}$$

For a third points configuration, the deformation of the diaphragm at the frame line relative to the third points is

$$\Delta_{diaph} = \sum_{N_p} \left(-w\left(\alpha\sigma - \sin\theta \frac{\sum K_{rest}}{K_{total}}\right)\right)_i \frac{L^2}{9G'Bay} + \frac{\sum P_L L}{3G'Bay} \quad \text{(Eq. 5.5.4-24)}$$

For a midpoint anchorage device configuration, the diaphragm displacement at the frame line relative to the midpoint is

$$\Delta_{diaph} = \sum_{N_p} \left(-w\left(\alpha\sigma - \sin\theta \frac{\sum K_{rest}}{K_{total}}\right)\right)_i \frac{L^2}{8G'Bay} + \frac{\sum P_L L}{4G'Bay} \quad \text{(Eq. 5.5.4-25)}$$

In the above equations, a positive deflection indicates upslope translation.

Shear Force Transfer from Panels to Purlin. An important consideration is the shear force transfer from the panels to the purlin at the anchorage device location, P_{sc}. This force can be significant and must be transferred over a small width of panel in the region of the anchorage device. For configurations with anchorage devices at the frame lines, the magnitude of the shear force transferred from the panels to the purlin is calculated by

$$P_{sc} = P_L + \frac{wL}{2}(0.9\sigma\alpha - \sin\theta) - P_i \quad \text{(Eq. 5.5.4-26)}$$

For a midpoint or third point configuration, the shear force between the purlin and the panels may be conservatively approximated as the anchorage force. A reduction in this force can typically be achieved using Eq. 5.5.4.27.

$$P_{sc} = P_L + \frac{wL}{20}\left(-0.9\sigma + \frac{\delta b \cos\theta}{d}\right)\alpha \quad \text{(Eq. 5.5.4-27)}$$

5.5.4.4 Anchorage Configurations

The component stiffness method has been applied to five anchorage configurations: supports, third points, midpoint, supports plus third points torsion braces, and support plus third points lateral anchorage devices. In the following section, a brief summary of each configuration is given. A summary of equations applicable to each configuration is given in Section 5.5.4.6.

To determine anchorage forces for all configurations except midpoints, roof systems are evaluated per half-span (from the frame line to the center of the span). A single span system has two half-spans but because of symmetry, only one half-span must be evaluated. In multiple span systems, each half-span must be evaluated separately although symmetry and repetition are used wherever possible. For midpoint configurations, each span is evaluated individually.

The overturning force, P_i, for each purlin must be determined. Fundamental to the overturning force is the uniform restraint force, $w_{rest} = w \cdot \sigma$, in the panels due to diaphragm action in the panels. Both P_i and σ must be calculated for each purlin in the half-span. For repetitive members, w_{rest} and P_i will be proportional to the applied load and only need to be recalculated for varying cross sections and orientations.

After the overturning forces are determined, they are distributed according to the relative stiffness of each of the components. The net stiffness at each anchorage device is calculated and the total stiffness at an anchorage location is the sum of the individual stiffness of each anchorage device. The stiffness of the system is the inherent resistance of the system to lateral movement. Each purlin contributes a rafter and panel stiffness to the system stiffness. The panel stiffness for the half-bay is one half the stiffness of the full span. The rafter stiffness is dependent upon the connection between the rafter and the purlin at the frame line. The total stiffness is the sum of the anchorage stiffness and the system stiffness. The force in each component is the sum of all the overturning forces in the half-span multiplied by the stiffness of the component relative to the total stiffness of the half-span.

Support Anchorage. A support anchorage configuration is the most common anchorage configuration and is fortunately the simplest. As the purlin is supported vertically and anchored laterally at the frame lines, maximum vertical and lateral displacements as well as torsional rotations occur at the mid-span (or close to the mid-span for the end span of a multi-span system) relative to a fixed location at the frame lines.

Support Anchorage – Single Span System. A single span system is evaluated for the half-span from the frame line to the center of the span. The uniform restraint force in the panels, σ (Eq. 5.5.4-51) and the overturning force, P_i (Eq. 5.5.4-49), are calculated for each purlin in the bay. Note that for repetitive members, the overturning force is proportional to the applied load which simplifies calculations. The total overturning force is the sum of the overturning forces for each individual purlin. The total stiffness, K_{total} (Eq. 5.5.4-48), is the sum of the stiffness of each half-span: all the anchorage devices along the frame line, K_{rest} (Eqs. 5.5.4-30 and 5.5.4-33), the rafter stiffness of all the purlins without anchorage devices, K_{Rafter} (Eqs. 5.5.4-35 and 5.5.4-36), and the panel stiffness of each purlin in the bay, K_{panel} (Eq. 5.5.4-37). The anchorage force at each anchorage device location at the top of the purlin, P_L (Eq. 5.5.4-46), is determined by multiplying the total overturning force by the ratio of the stiffness of the anchorage device to the total stiffness of the half-span. If the anchorage device provides restraint at a height below the top of the purlin, the force at the anchorage height, P_h, is calculated by (Eq. 5.5.4-47).

Support Anchorage – Multiple Span Systems. Multiple span systems are categorized whether it is an exterior or interior frame line. The exterior frame line for a multiple span system is treated similar to a single span system. The total force is the sum of the overturning forces for each purlin, P_i (Eq. 5.5.4-49), for the half-span adjacent to the exterior frame line. The total stiffness, K_{total} (Eq. 5.5.4-48), is the sum of the anchorage device stiffness along the exterior frame line, all the anchorage devices along the frame line, K_{rest} (Eqs. 5.5.4-30 and 5.5.4-33), the rafter stiffness of the purlins without anchorage devices along the exterior frame line, K_{Rafter} (Eqs. 5.5.4-35 and 5.5.4-36), and the panel stiffness of each purlin in the bay, K_{panel} (Eq. 5.5.4-37), of the half-span adjacent to the exterior frame line. The anchorage force at each anchorage device location at the top of the purlin, P_L (Eq. 5.5.4-46), is the total overturning force multiplied by the ratio of the stiffness of the anchorage device to the total stiffness of the half-span adjacent to the exterior frame line.

At an interior frame line, the anchorage force must consider the effects of both half-spans adjacent to the frame line. The overturning forces, P_i (Eq. 5.5.4-49), must be determined for both half-spans adjacent to the frame line while taking into account the torsional and flexural differences whether the adjoining bay is a typical interior or end bay. The total overturning force along the frame line is the sum of the overturning forces for all purlins along the frame line for both half-spans adjacent to the frame line. The total stiffness, K_{total} (Eq. 5.5.4-48), is the sum of the stiffness of all the anchorage devices along the frame line, K_{rest} (Eqs. 5.5.4-30 and 5.5.4-33), the rafter stiffness of all the purlins without anchorage devices, K_{Rafter} (Eqs. 5.5.4.35 and 5.5.4-36), and the panel stiffness of each purlin in the bay, K_{panel} (Eq. 5.5.4-37), of each purlin for both half-spans adjacent to the frame line. The anchorage force at each anchorage location at the top of the purlin, P_L (Eq. 5.5.4-46), is the total overturning force multiplied by the ratio of the stiffness of the anchorage device to the total stiffness.

Support Anchorage - Deflection and Panel Connection Shear. Lateral deflection of the top flange of the purlin at the frame lines is checked to ensure that the anchorage device has sufficient stiffness. The lateral deflection of the mid-span of the purlin relative to the frame line, Δ_{diaph} (Eq. 5.5.4-53), is checked from the lateral deflection of the diaphragm. The mid-span diaphragm lateral deflection is compared to the AISI S100 limits.

For a support anchorage configuration, the force transfer between the panels and purlin, P_{sc} (Eq. 5.5.4-54), is significant along the frame lines. The connection between the purlin and the panels should be checked at each anchorage device. For an exterior frame line, the force in the connection between the panels and the purlin includes the anchorage force and the uniform restraint force in the panels for half the span. At an interior frame line, it is important to include the restraint force in the panels from both half-spans adjacent to the interior frame line.

Third Point Anchorage. For both single and multiple span systems, each half-span between the centerline of the span and the frame line is analyzed independently. The total stiffness, K_{total} (Eq. 5.5.4-57) is the sum of the stiffness of all third point anchorage devices, K_{rest} (Eq. 5.5.4-34), and the panel stiffness (K_{panel} Eq. 5.5.4-37) of all the purlins in the half-span. The stiffness of the rafter connection is assumed to be small and is ignored in the development of equations for third point anchorage. If the connection between the rafter and purlin has considerable stiffness such as a welded web plate, the bracing configuration should be considered as support plus third point anchorage configuration. For single span and multiple span interior systems, the anchorage force at both third points will be equal. For the end span of multiple span system, the third point force for each half-span must be calculated separately. The forces are then summed and distributed to both third points in the end span according to the relative stiffness of each anchorage device.

The lateral deflection of the system must be checked at the third points, Δ_{rest} (Eq. 5.5.4-61) and along the frame lines, Δ_{diaph} (Eq. 5.5.4-62). At the anchorage points, the lateral deflection is compared to the $\phi d/20$ (LRFD) or $d/(20\Omega)$ (ASD) limits specified in AISI S100. The difference in the lateral deflection between the third points and the frame lines is compared to the L/360 limit in AISI S100. For a low slope roof, it is common to get a negative (downslope) deflection of the top flange of the purlin at the frame line.

Midpoint Anchorage. For a midpoint anchorage configuration, overturning forces for each purlin, P_i (Eq. 5.5.4-67), are determined for a full span. The total stiffness, K_{total} (Eq. 5.5.4-66) is the sum of the stiffness of all midpoint anchorage devices along the line of anchorage, K_{rest} (Eq. 5.5.4-34), and the panel stiffness, K_{panel} (Eq. 5.5.4-37), of all the purlins in the bay. Like for a third point configuration, the stiffness of the rafter connection is assumed to be small (as for a flange bolted configuration) and is ignored. For a rafter connection that has considerable stiffness (as with a web plate) the equations provided are invalid.

The lateral deflection of the system must be checked at the midpoints, Δ_{rest} (Eq. 5.5.4-70) and along the frame lines, Δ_{diaph} (Eq. 5.5.4-71). At the anchorage device locations, the lateral deflection is compared to the $\phi d/20$ (LRFD) or $d/(20\Omega)$ (ASD) limits specified in AISI S100. The difference in the lateral deflection between the midpoint and the frame lines is compared to the L/360 limit in AISI S100. For a low slope roof, it is common to get a negative (downslope) deflection of the top flange of the purlin at the frame line.

Support Plus Third Point Torsion Restraints. For a support plus third point torsion restraint configuration, lateral anchorage is provided along the frame lines and torsional restraints that resist rotation of the purlin are connected at third points between pairs of purlins. The behavior of a third point plus torsional restraint configuration is similar to that of a support anchorage configuration. For a support anchorage configuration, as the purlin twists, moments are developed in the panels to resist this torsion. For a third point torsional restraint, the torsional restraints resist the twisting through the development of moments at each end of the torsional brace. The braces are considered to have a much greater torsional stiffness than the panels, so all of the torsion is resisted by the third point braces. This approximation will lead to conservative anchorage forces.

Some moment is developed in the panels near the frame lines as the support anchorage devices allow the top flange of the purlin to move laterally, causing rotation of the purlin. The inherent stiffness of the system, therefore, is a combination of this moment in the panels near the frame lines and the moments developed in the third point torsion braces. These system effects are included in the calculation of the moments at the third point torsion braces, M_{3rd}, and the overturning forces at the frame line, P_i, so there is no need to further reduce the anchorage forces for system effects.

The system of purlins is evaluated per half-span from the frame line to the centerline of the span. The first thing that must be determined is the stiffness along the frame line tributary to the half-span analyzed, K_{trib}. Because the panel stiffness is embedded in the equations, the total stiffness of the system, K_{total} (Eq. 5.5.4-76), is the sum of the stiffness of all the anchors and the connections of the purlin to the rafter for all purlins not directly restrained along the frame line. At an interior frame line, the tributary stiffness to each of the half-spans adjacent to the frame line is half of the total stiffness. At an exterior frame line or for a single span system, the tributary stiffness is the total stiffness along the frame line. Next, for each purlin along the length of the bay, the uniform restraint force is calculated. Once the uniform restraint force is calculated, the moment in the third point torsion brace, M_{3rd} (Eq. 5.5.4-73), and the overturning force at the frame line, P_i (Eq. 5.5.4-77), is calculated for each purlin. The anchorage force at the top of the purlin at each anchorage device along the frame line, P_L (Eq. 5.5.4-74) is determined by summing the overturning forces for all purlins and multiplying by the ratio of the anchorage device stiffness to the total stiffness along the frame line.

Lateral deflection of the system is checked at the frame lines, Δ_{rest} (Eq. 5.5.4-81) and at the mid-span of the bay, Δ_{diaph} (Eq. 5.5.4-82). The lateral deflection of the top flange at the frame line is limited to $\phi d/20$ (LRFD) or $d/(20\Omega)$ (ASD) as specified in AISI S100 Section I6.4.2. The mid-span lateral deflection is calculated from the deformation of the diaphragm from the uniform restraint force in the panels. For an end span in a multiple span system, the average uniform restraint force for each half-span in the end bay is used to determine the lateral deflection of the diaphragm. The mid-span lateral deflection is compared to the L/180 limit specified in AISI S100 Section I6.4.2. This limit is less stringent than the limit for other restraint configurations because AISI S100 recognizes that as the purlins deflect laterally, torsional rotation is limited by the torsional restraints allowing the purlins to maintain their strength. Second order overturning moments are also easily absorbed by the torsional braces.

Like a support anchorage configuration, the force in the connection between the panels and purlin, P_{sc} (Eq. 5.5.4-83), is critical along the frame lines. At an exterior frame line at an anchor, P_{sc} includes the anchorage force and the uniform restraint force from the half-span. At an interior frame line, P_{sc} includes the anchorage force and the uniform restraint force in the panels for both spans adjacent to the frame line.

Support Plus Third Point Lateral Anchorage. The support plus third point lateral anchorage configuration is solved in a slightly different manner than the other anchorage configurations. Because the system is restrained at the frame lines and at the interior of the bay, both the third point anchorage and the diaphragm restrain movement of the purlin relative to the frame lines. The distribution of anchorage forces between the third points and supports is a function of the relative stiffness of the restraints to the stiffness of the diaphragm. For a stiff diaphragm and flexible restraints, most of the mid-span lateral deflection of the purlin is restrained by diaphragm action in the panels and a large uniform restraint force is developed in the panels. Most of the overturning force is resisted by the anchorage devices along the frame line. As the stiffness of the diaphragm decreases relative to the stiffness of the restraints, the uniform restraint force in the panels decreases and more of the overturning force is resisted by the third point anchorages. The net restraint force, the sum of forces between the supports and third point anchorages, will remain relatively constant as the relative stiffness between the diaphragm and anchorages changes. Only the distribution of forces between the third points and supports changes significantly.

The first step is to calculate the stiffness of the anchors at each anchorage location. At the frame line, the total stiffness, K_{spt} (Eq. 5.5.4-88) is the sum of the anchorage stiffness, $(K_{rest})_{spt}$ (Eqs. 5.5.4-30 and 5.5.4-33), and the stiffness of the purlin to rafter connection, K_{rafter} (Eqs. 5.5.4-35 and 5.5.4-36), for the purlins not directly connected to an anchorage device. For an interior frame line, the tributary stiffness, K_{trib}, to each half-span adjacent to the frame line is half the total stiffness at the frame line. At an exterior frame line or in a single span configuration, the tributary stiffness to the half-span adjacent to the frame line is the total stiffness. The total stiffness at the third point, K_{3rd} (Eq. 5.5.4-87) is the sum of the stiffness of all the anchorages along the line of anchorage $(K_{rest})_{3rd}$ (Eq. 5.5.4-34).

The equation for the uniform restraint force in the panels for a support plus third point configuration is based on the equation for a third point configuration with additional factors applied to account for the stiffness of the anchorage devices, local bending effects and system effects. The uniform restraint force in the panels for a support plus third point lateral anchorage configuration should always be less than the same system with a third point only anchorage configuration.

The system of purlins is divided into half-spans. For each purlin, the ratio of the uniform restraint force in the panels to the uniformly applied load, σ (Eq. 5.5.4-93), is calculated. The overturning forces at the third point, $(P_{3rd})_i$ (Eq. 5.5.4-89), and the frame line, $(P_{spt})_i$ (Eq. 5.5.4-90) are calculated directly for each purlin. Purlin system effects are included in the calculation for $(P_{3rd})_i$ and $(P_{spt})_i$. The anchorage force for each anchorage device at the top of the purlin, $(P_L)_{3rd}$ (Eq. 5.4.4-84) or ($(P_L)_{spt}$ Eq. 5.5.4-85) is the sum of all the overturning forces at that location, ($(P_{spt})_i$ or $(P_{3rd})_i$), multiplied by the ratio of the stiffness of the individual anchorage device, (K_{rest}), to the total stiffness at the location, (K_{spt} or K_{3rd}).

For support plus third point lateral anchorage configuration, lateral deflections tend to be small. Lateral deflection, Δ_{rest} (Eq. 5.5.4-104), is checked at the frame line and third points and is compared to the allowable anchorage deflection, $\phi d/20$ (LRFD) or $d/(20\Omega)$ (ASD), as specified in

AISI S100. Because there is little diaphragm deflection between the third points, the deflection of the interior of the span is approximated as the deflection at the third points. The difference between the third point and support deflection at service load levels is compared to the limit of L/360 in AISI S100.

Forces in the connection between the purlin and the panels at the anchorage location, P_{sc}, are calculated the same as for a support anchorage configuration for anchorage devices along the frame line (Eq. 5.5.4-105) and for a third point configuration for the anchorage at the third points (Eq. 5.5.4-106). Because the uniform restraint force in the panels is typically less for a support plus third point configuration relative to a support only configuration, the uniform restraint force along the frame line will typically be less for a support plus third point configuration than a similar system with supports only anchorage devices. Conversely, the force in the connection between the panels and purlin will typically be larger at the third points in a support plus third point configuration than a similar system with only third point restraints.

5.5.4.5 Tests to Determine Stiffness of Components

Anchorage Device Stiffness. The anchorage device stiffness at the frame line may also be determined by a simple test procedure with the apparatus shown in Figure 5.5-15. The apparatus consists of a segment of purlin approximately 2 ft long anchored in the manner representing the typical anchorage device connection. For a typical through-fastened rib style panel, a total of 3 fasteners at 12 in. intervals should be used to connect the purlin to the panels, with the center fastener located directly over the centerline of the restraint. For a standing seam profile deck, the seam of the deck with a single clip should be centered directly over the restraint. The stiffness of the panel connection is affected by the presence of insulation so if insulation is to be incorporated into the actual roof system, it should be included in the test as well. Displacement should be recorded as close as possible to the top flange of the purlin, Δ_1, and if it is desirable to capture the relative slip between the Z-section and the panels, the deflection of the panels, Δ_2, should be recorded as well. The panels are permitted to move laterally but prevented from moving vertically at a distance of span/2 from the purlin where "span" is the purlin spacing.

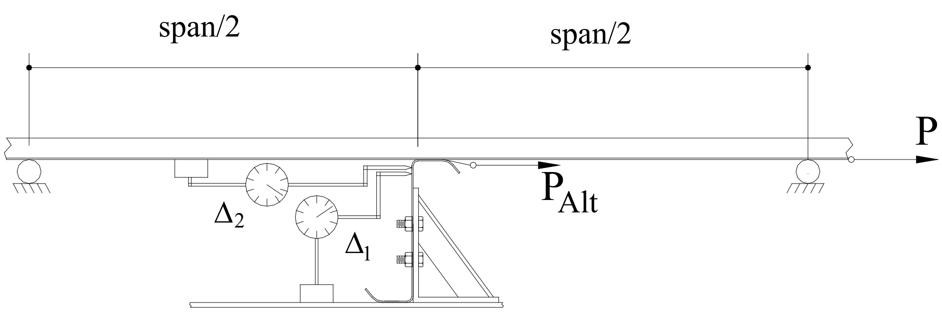

Figure 5.5-15 Test to Determine Stiffness of Support Anchorage Device

Horizontal load, P, is applied through the panels parallel to the original plane of the panels. Applying the load through the panels provides verification of the strength of the panel-to-purlin connection as well. Alternatively, the horizontal load, P_{Alt}, can be applied directly to the top flange of the purlin if the connection between the purlin and the panels possesses considerable slip. The restraint stiffness is defined as the load applied at the top flange, P, per unit displacement at the top flange, Δ_1. For a non-linear relationship between displacement and applied load, a criterion for determining the nominal stiffness similar to that in test standard AISI S901, *Rotational Lateral Test Method for Beam-to-Panel Assemblies,* should be used. This test procedure captures the net restraint stiffness, that is, the combined effect of the device stiffness and the configuration stiffness. The component stiffness method does not make accommodations for slip between the Z-section and the panels. If excessive slip between the Z-section and panels is observed through this test procedure, some mechanism for transferring forces through the system of Z-sections should be considered.

Stiffness of Purlin – Panel Connection. The rotational stiffness of the connection between the purlin and the panels, k_{mclip}, is defined as the moment generated per unit rotation of the purlin per unit length of the purlin. This moment is developed as a result of prying action. For a through-fastened system, the connection is made with a single screw placed near a rib of the panels and into the top flange of the purlin. As the purlin rotates, a compressive force is developed between the panels and the tip of the flange, and tension is developed in the fastener. The stiffness of the connection is a function of many factors: the purlin thickness, flange width and spacing, the panel thickness and moment of inertia, the fastener spacing, position of the fastener relative to the web of the purlin and relative to the panel rib and the presence of insulation.

For a standing seam clip, as the purlin rotates, compression is developed in the shoulders of the clip and tension is developed in the tab as it pulls from the seam. Because it is connected directly to the seam it can possess considerable stiffness. For a standing seam system, the stiffness of the panel-to-purlin connection is a function of the clip material and geometry, the "tightness" of the clip tab in the panel seam, the purlin thickness and the presence of insulation.

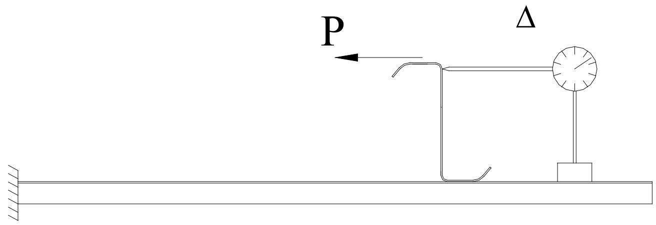

Figure 5.5-16 Test Set-up for Determining Stiffness of Panel Z-Section Connection

With so many factors involved, the stiffness of the connection between the purlin and the panels, k_{mclip}, cannot easily be determined analytically but can be readily determined by test. The test procedure is outlined in the test standard AISI S901, *Rotational Lateral Test Method for Beam-to-Panel Assemblies.* The basic test assembly is shown in Figure 5.5-16. A panel segment with a span representative of the purlin spacing in a roof system is attached to a segment of purlin and a load is applied to the free flange of the purlin. As the lateral load, P, is applied to the free flange of the purlin, the lateral displacement, Δ, of the free flange is measured. By relating the displacement to the applied load the rotational-lateral stiffness is determined. Some modifications to the results of the test procedure are required to determine the rotational stiffness of the panel-to-purlin connection, k_{mclip}.

The displacement of the free flange measured according to AISI S901 is the combined displacement of the flexure in the web of the purlin and the rotation of the panel-to-purlin connection. Provided the apparatus is set up as prescribed in AISI S901, additional deformation due to flexure of the panels is eliminated. To determine the panel-to-purlin connection stiffness, k_{mclip}, the displacement due to the flexibility of the purlin web must be eliminated as described by Heinz (1994). The displacement of the web is approximated from theory by treating the purlin web as a fixed-free cantilever beam element, and the resulting stiffness of the connection between the panels and the purlin is

$$k_{conn} = \frac{P_N d^2}{L_B}\left(12 \,{}^{in.}\!/_{ft}\right)\left(\frac{1}{\Delta_N - \dfrac{P_N d^3}{3EL_B t^3}}\right) \qquad \text{(Eq. 5.5.4-28)}$$

where P_N is the nominal test load (lb), Δ_N is the nominal test displacement (in.), L_B is the purlin length (in.), d is the depth of the purlin (in.), and t is the thickness of the purlin (in.). The units of k_{conn} will be lb-in./rad/ft. Eq. 5.5.4-28 thus provides the stiffness of the connection between the purlin and the panels in terms of the moment per unit displacement of the free flange per unit length of the purlin. The net rotational stiffness, k_{mclip}, must also include the rotational flexibility of the panels spanning between purlin lines. This flexibility, derived from theory, is added to the flexibility of the panel-to-purlin connection and the net stiffness of the purlin-panel connection is

$$k_{mclip} = \frac{12E \cdot I_{panel} \cdot k_{conn}}{span\left(12 \,{}^{in}\!/_{ft}\right) \cdot k_{conn} + 12E \cdot I_{panel}} \qquad \text{(Eq. 5.5.4-29)}$$

where I_{panel} is the gross moment of inertia of the panel (in^4/ft); and span is the distance between the centerline of each span of the panels (ft).

5.5.4.6 Equation Summary

Summary of Stiffness Equations

Restraint Stiffness – Support Anchorage

$$K_{rest} = \frac{\left(\frac{h}{d}\right)^2 K_{device} \cdot K_{config}}{\frac{h}{d} K_{device} + K_{config}} \qquad \text{(Eq. 5.5.4-30)}$$

Discrete Brace

$$K_{config} = \frac{\frac{1}{15} d(3Et^3)}{h(d-h)^2}\left[\frac{\frac{1}{15} d \cdot 2Et^3(3d-h) + \frac{L}{80} k_{mclip} \cdot d(3d-2h)}{\frac{1}{15} d \cdot Et^3(4d-h) + \frac{L}{80} k_{mclip} \cdot d(d-h)}\right] \qquad \text{(Eq. 5.5.4-31)}$$

Anti-roll Clip

$$K_{config} = \frac{Eb_{pl}t^3}{(d-h)^3}\left(\frac{d}{h}\right) \qquad \text{(Eq. 5.5.4-32)}$$

Total Stiffness of a rafter welded web plate

$$K_{rest} = \frac{E \cdot b_{pl} \cdot t_{pl}{}^3 \cdot t^3 \left(t^3 h + t_{pl}^3 (d-h)\right)}{\left(t^3 h^2 - t_{pl}^3 (d-h)^2\right)^2 + 4t^3 t_{pl}{}^3 d^2 h (d-h)} \qquad \text{(Eq. 5.5.4-33)}$$

Restraint Stiffness – Interior Restraint

$$K_{rest} = \left(\frac{h}{d}\right)^2 K_{device} \qquad \text{(Eq. 5.5.4-34)}$$

Rafter Stiffness

Web Bolted to Rafter Clip

$$K_{rafter} = \frac{E \cdot b_{pl} \cdot t_{pl}{}^3 \cdot t^3 \left(t^3 h + t_{pl}^3 (d-h)\right) \cdot d}{\left(t^3 h^2 - t_{pl}^3 (d-h)^2\right)^2 + 4t^3 t_{pl}{}^3 d^2 h (d-h)} \qquad \text{(Eq. 5.5.4-35)}$$

Flange Bolted

$$K_{Rafter} = 0.45 \frac{Et^3}{2d} \qquad \text{(Eq. 5.5.4-36)}$$

Panel Stiffness

$$K_{panel} = \frac{k_{mclip} L}{d}\left(\frac{\frac{1}{4} Et^3}{0.38 k_{mclip} d + 0.71 \frac{Et^3}{4}}\right)\left(1 - \frac{2}{3} k_{mclip} \tau\right) \qquad \text{(Eq. 5.5.4-37)}$$

Summary of Torsion Equations

$$a = \sqrt{\frac{EC_W}{GJ}} \qquad \text{(Eq. 5.5.4-38)}$$

$$\tau = \frac{\dfrac{a^2\beta}{GJ}}{1 + k_{mclip}\dfrac{\kappa}{GJ}} \qquad \text{(Eq. 5.5.4-39)}$$

Single span and multi-span end bay half-span adjacent to exterior frame line (Warping "Free") from Seaburg and Carter (1997).

$$\beta = \frac{L^2}{8a^2} + \frac{1}{\cosh\left(\dfrac{L}{2a}\right)} - 1 \qquad \text{(Eq. 5.5.4-40)}$$

$$\kappa = \frac{8a^4}{L^2}\left(\frac{\cosh\left(\dfrac{L}{2a}\right) - 1}{\cosh\left(\dfrac{L}{2a}\right)}\right) + \frac{5L^2}{48} - a^2 \qquad \text{(Eq. 5.5.4-41)}$$

$$\beta_{3rd} = \frac{L}{GJ}\left(\frac{1}{3} - \frac{a}{L}\frac{\sinh\left(\dfrac{L}{3a}\right)}{\cosh\left(\dfrac{L}{2a}\right)}\right) \qquad \text{(Eq. 5.5.4-42)}$$

Multi-span interior and multi-span end bay half-span adjacent to interior frame line (Warping "Fixed") from Seaburg and Carter (1997)

$$\beta = \frac{L^2}{8a^2} + \frac{L}{2a}\frac{1 - \cosh\left(\dfrac{L}{2a}\right)}{\sinh\left(\dfrac{L}{2a}\right)} \qquad \text{(Eq. 5.5.4-43)}$$

$$\kappa = \left(\frac{aL}{3} - \frac{4a^3}{L}\right)\left(\frac{1 - \cosh\left(\dfrac{L}{2a}\right)}{\sinh\left(\dfrac{L}{2a}\right)}\right) + \frac{5L^2}{48} - a^2 \qquad \text{(Eq. 5.5.4-44)}$$

$$\beta_{3rd} = \frac{L}{GJ}\left(\frac{1}{3} + \frac{a}{L}\left(\frac{\left(1 - \cosh\left(\dfrac{L}{3a}\right)\right)\left(1 - \cosh\left(\dfrac{L}{2a}\right)\right)}{\sinh\left(\dfrac{L}{2a}\right)} - \sinh\left(\dfrac{L}{3a}\right)\right)\right) \qquad \text{(Eq. 5.5.4-45)}$$

Supports Anchorage Configuration

Anchorage force per anchorage device

$$P_L = \sum_{N_p} P_i \cdot \frac{K_{rest}}{K_{total}} \quad \text{(force at top of purlin)} \qquad \text{(Eq. 5.5.4-46)}$$

$$P_h = P_L \frac{d}{h} \quad \text{(force at height of anchorage)} \qquad \text{(Eq. 5.5.4-47)}$$

where

$$K_{total} = \sum_{N_a} K_{rest} + \frac{\sum_{N_p} K_{panel} + \sum_{N_p - N_a} K_{rafter}}{d} \qquad \text{(Eq. 5.5.4-48)}$$

Total overturning force generated per purlin per half-span

$$P_i = \frac{wL}{2d} \cdot \left[\left(\delta b \cos\theta \left(1 - R_{local}\right) + \tfrac{2}{3} k_{mclip} \tau \left(\sigma \frac{d}{2} - \left(\delta b + m\right) \cos\theta \right) \right) \alpha - d \sin\theta \right] \qquad \text{(Eq. 5.5.4-49)}$$

$$R_{local} = \frac{k_{mclip}}{k_{mclip} + \dfrac{Et^3}{3d}} \qquad \text{(Eq. 5.5.4-50)}$$

$$\sigma = \frac{C1 \dfrac{\left(\dfrac{I_{xy}}{I_x} \cos\theta \right) L^4}{EI_{my}} + \dfrac{\left(\left(\delta b + m\right) \cos\theta \right) d}{2} \tau + \dfrac{\alpha \cdot N_p \cdot L^2 \sin\theta}{8G'Bay}}{C1 \dfrac{L^4}{EI_{my}} + \dfrac{d^2}{4} \tau + \dfrac{\alpha \cdot \eta \cdot L^2}{8G'Bay}} \qquad \text{(Eq. 5.5.4-51)}$$

where C1 = 5/384 Single Span
= 1/185 Multi-Span End Bay
= 1/384 Multi-Span Interior

Single Span

Total stiffness is the sum of the restraints at the frame line, sum of the rafter stiffness at the frame line and the sum of half the panel stiffness for all purlins in the bay. The total force generated by the system is the sum of P_i for all purlins in the bay.

Multi-Span for Half-Span Adjacent to Exterior Frame Line

Total stiffness is the sum of the restraints at the exterior frame line, sum of the rafter stiffness at the exterior frame line and half the sum of the panel stiffness for all purlins in the end bay. The total force generated by the system is the sum of P_i for all purlins in the half bay closest to the exterior frame line.

Multi-Span Interior

Total stiffness is the sum of the restraints at the interior frame line, sum of the rafter stiffness at the frame line, and half the sum of panel stiffness for all purlins in each bay adjacent to the frame line. The total force generated by the system is the sum of P_i for all purlins in each half bay adjacent to the frame line.

Lateral deflection of the top flange of the purlin at the restraint.

$$\Delta_{rest} = \frac{P_L}{K_{rest}} \quad \text{(Eq. 5.5.4-52)}$$

In-plane deflection of the roof diaphragm at the mid-span relative to the restraint

$$\Delta_{diaph} = \sum_{N_p} \left(w(\alpha\sigma - \sin\theta)\right)_i \frac{L^2}{8G'Bay} \quad \text{(Eq. 5.5.4-53)}$$

Shear force in the connection between the purlin and the panels at the anchorage location

$$P_{sc} = P_L + \frac{wL}{2}\left(0.9\sigma\alpha - \sin\theta\right) - P_i \quad \text{(Eq. 5.5.4-54)}$$

Third Point Anchorage

Anchorage force per anchorage device

$$P_L = \sum_{N_p} P_i \cdot \frac{K_{rest}}{K_{total}} \text{ (force at top of purlin)} \quad \text{(Eq. 5.5.4-55)}$$

$$P_h = P_L \frac{d}{h} \text{ (force at height of anchorage)} \quad \text{(Eq. 5.5.4-56)}$$

where

$$K_{total} = \sum K_{rest} + \frac{\sum K_{panel}}{d} \quad \text{(Eq. 5.5.4-57)}$$

Total overturning force generated per purlin per half-span

$$P_i = \frac{wL}{2d} \cdot \left[\begin{aligned} &\left(\delta b \cos\theta \left(1 - R_{local}\right) + \tfrac{2}{3} k_{mclip} \tau \left(\sigma \frac{d}{2} - \left(\delta b + m\right)\cos\theta \right)\right)\alpha - d\sin\theta \\ &+ \frac{L^2 k_{mclip}}{3G'Bay \cdot d}\left(1 - \tfrac{2}{3} k_{mclip}\tau\right)\left(\frac{\eta\sigma}{3} + \frac{N_p \sin\theta}{6} - \frac{\eta \cdot \delta b \cos\theta}{2d}\right) \end{aligned} \right] \quad \text{(Eq. 5.5.4-58)}$$

$$R_{local} = \frac{k_{mclip}}{k_{mclip} + \dfrac{Et^3}{3d}} \quad \text{(Eq. 5.5.4-59)}$$

$$\sigma = \frac{C1 \dfrac{\left(\dfrac{I_{xy}}{I_x}\cos\theta\right)L^4}{EI_{my}} + \dfrac{\left(\left(\delta b + m\right)\cos\theta\right)d}{2}\tau - \dfrac{\alpha \cdot N_p \cdot L^2 \sin\theta}{18G'Bay}}{C1 \dfrac{L^4}{EI_{my}} + \dfrac{d^2}{4}\tau + \dfrac{\alpha \cdot \eta \cdot L^2}{9G'Bay}} \quad \text{(Eq. 5.5.4-60)}$$

where C1 = 11/972 Single Span
= 5/972 Multi-Span End Bay – outer half-span
= 7/1944 Multi-Span End Bay – inner half-span
= 1/486 Multi-Span Interior

Distribution of Forces - All Conditions (Single and Multiple Span)

Total stiffness is the sum of the restraints along the third point and half the sum of the panel stiffness for all purlins in the bay. The total force generated by the system is the sum of P_i for each half-span for all purlins in the bay.

Lateral deflection of the top flange of the purlin at the restraint.

$$\Delta_{rest} = \frac{P_L}{K_{rest}}$$ (Eq. 5.5.4-61)

In-plane deflection of the roof diaphragm at the frame lines relative to the restraint

$$\Delta_{diaph} = \sum_{N_p}\left(-w\left(\alpha\sigma - \sin\theta\frac{\sum K_{rest}}{K_{total}}\right)\right)_i \frac{L^2}{9G'Bay} + \frac{\sum P_L L}{3G'Bay} \quad \text{(Eq. 5.5.4-62)}$$

Shear force in the connection between the purlin and the panels at the anchorage location

$$P_{sc} = P_L + \frac{wL}{20}\left(-0.9\sigma + \frac{\delta b\cos\theta}{d}\right)\alpha \quad \text{(Eq. 5.5.4-63)}$$

Midpoint Point Anchorage

Anchorage force per anchorage device

$$P_L = \sum_{N_p} P_i \cdot \frac{K_{rest}}{K_{total}} \text{ (force at top of purlin)} \quad \text{(Eq. 5.5.4-64)}$$

$$P_h = P_L\frac{d}{h} \text{ (force at height of anchorage)} \quad \text{(Eq. 5.5.4-65)}$$

where

$$K_{total} = \sum K_{rest} + \frac{\sum K_{panel}}{d} \quad \text{(Eq. 5.5.4-66)}$$

Total overturning force generated per purlin per span

$$P_i = \frac{wL}{d}\cdot\left[\begin{array}{l}\left(\delta b\cos\theta(1-R_{local}) + \tfrac{2}{3}k_{mclip}\tau\left(\sigma\frac{d}{2} - (\delta b + m)\cos\theta\right)\right)\alpha - d\sin\theta \\ + \frac{L^2 k_{mclip}}{4G'Bay\cdot d}\left(1 - \tfrac{2}{3}k_{mclip}\tau\right)\left(\frac{\eta\sigma}{2} + \frac{N_p\sin\theta}{2} - \frac{\eta\cdot\delta b\cos\theta}{d}\right)\end{array}\right] \quad \text{(Eq. 5.5.4-67)}$$

$$R_{local} = \frac{k_{mclip}}{k_{mclip} + \frac{Et^3}{3d}} \quad \text{(Eq. 5.5.4-68)}$$

$$\sigma = \frac{C1\dfrac{\left(\dfrac{I_{xy}}{I_x}\cos\theta\right)L^4}{EI_{my}} + \dfrac{((\delta b + m)\cos\theta)d}{2}\tau - \dfrac{\alpha \cdot N_p \cdot L^2 \sin\theta}{8G'Bay}}{C1\dfrac{L^4}{EI_{my}} + \dfrac{d^2}{4}\tau + \dfrac{\alpha \cdot \eta \cdot L^2}{8G'Bay}} \qquad \text{(Eq. 5.5.4-69)}$$

where C1 = 5/384 Single Span
= 1/185 Multi-Span End Bay
= 1/384 Multi-Span Interior

Distribution of Forces - All Conditions (Single and Multiple Span)

Total stiffness is the sum of the restraints along the midpoint and the sum of the panel stiffness for all purlins in the bay. The total force generated by the system is the sum of P_i for all purlins in the bay.

Lateral deflection of the top flange of the purlin at the restraint.

$$\Delta_{rest} = \frac{P_L}{K_{rest}} \qquad \text{(Eq. 5.5.4-70)}$$

In-plane deflection of the roof diaphragm at the frame lines relative to the restraint

$$\Delta_{diaph} = \sum_{N_p}\left(-w\left(\alpha\sigma - \sin\theta\frac{\sum K_{rest}}{K_{total}}\right)\right)_i \frac{L^2}{8G'Bay} + \frac{\sum P_L L}{4G'Bay} \qquad \text{(Eq. 5.5.4-71)}$$

Shear force in the connection between the purlin and the panels at the anchorage location

$$P_{sc} = P_L + \frac{wL}{20}\left(-0.9\sigma + \frac{\delta b\cos\theta}{d}\right)\alpha \qquad \text{(Eq. 5.5.4-72)}$$

Supports Plus Third Point Torsional Restraint

Moment in each third point torsion restraint

$$M_{3rd} = w\left(\alpha\left(\sigma\frac{d}{2} - (\delta b + m)\cos\theta\right)\frac{a^2\beta}{GJ}\left(d^2\frac{K_{trib}}{N_p} + \frac{L}{9}k_{mclip}\right) + \left(d\sin\theta - (\alpha)\delta b\cos\theta\left(1 - R_{local}\right)\right)\frac{L}{2}\right)\xi \qquad \text{(Eq. 5.5.4-73)}$$

Anchorage force per anchorage device along the frame line

$$P_L = \sum_{N_p} P_i \cdot \frac{K_{rest}}{K_{total}} \quad \text{(force at top of purlin)} \qquad \text{(Eq. 5.5.4-74)}$$

$$P_h = P_L\frac{d}{h} \quad \text{(force at height of anchorage)} \qquad \text{(Eq. 5.5.4-75)}$$

where

$$K_{total} = \sum_{N_a} K_{rest} + \frac{\sum_{N_p - N_a} K_{rafter}}{d} \quad \text{(Eq. 5.5.4-76)}$$

with

K_{trib} = C3 K_{total}

C3 = 1.0 single span and multi-span exterior frame line

= 0.5 multi-span interior frame line

Total overturning force generated per purlin

$$P_i = w\left(\alpha\left(\sigma\frac{d}{2} - (\delta b + m)\cos\theta\right)\frac{a^2\beta}{GJ} - \left(d\sin\theta - (\alpha)\delta b\cos\theta\left(1 - R_{local}\right)\right)\frac{\beta_{3rd}L}{2}\right)d \cdot \frac{K_{trib}}{N_p}\xi$$

(Eq. 5.5.4-77)

where

$$\xi = \frac{1}{1 + \left(d^2\frac{K_{trib}}{N_p} + \frac{L}{9}k_{mclip}\right)\beta_{3rd}} \quad \text{(Eq. 5.5.4-78)}$$

with

$$R_{local} = \frac{k_{mclip}}{k_{mclip} + \frac{Et^3}{3d}} \quad \text{(Eq. 5.5.4-79)}$$

$$\sigma = \frac{C1\frac{\left(\frac{I_{xy}}{I_x}\cos\theta\right)L^4}{EI_{my}} + \frac{\left((\delta b + m)\cos\theta\right)d}{2}\left(\frac{a^2\beta}{GJ} - \frac{L}{2}\cdot\beta_{3rd}\right)\xi + \frac{\alpha \cdot N_p \cdot L^2\sin\theta}{8G'Bay}}{C1\frac{L^4}{EI_{my}} + \frac{d^2}{4}\frac{a^2\beta}{GJ}\xi + \frac{\alpha \cdot \eta L^2}{8G'Bay}} \quad \text{(Eq. 5.5.4-80)}$$

where C1 = 5/384 Single Span

= 1/185 Multi-Span End Bay

= 1/384 Multi-Span Interior

Single Span

Total stiffness is the sum of the restraints at the frame line, sum of the rafter stiffness at the frame line, and the sum of half the panel stiffness for all purlins in the bay. The total force generated by the system is the sum of P_i for all purlins in the bay.

Multi-Span Half-Span Adjacent to Exterior Frame Line

Total stiffness is the sum of the restraints at the exterior frame line, sum of the rafter stiffness at the exterior frame line, and half the sum of the panel stiffness for purlins in end bay. The total force generated by the system is the sum of P_i for all purlins in the half bay closest to the exterior frame line.

Multi-Span Interior

Total stiffness is the sum of the restraints at the interior frame line, sum of the rafter stiffness at the frame line, and half the sum of the panel stiffness for purlins in each bay adjacent to the frame line. The total force generated by the system is the sum of P_i for all purlins in each half bay adjacent to the frame line.

Lateral deflection of the top flange of the purlin at the restraint.

$$\Delta_{rest} = \frac{P_L}{K_{rest}}$$

(Eq. 5.5.4-81)

In-plane deflection of the roof diaphragm at the mid-span relative to the restraint

$$\Delta_{diaph} = \sum_{N_p} \left(w(\alpha\sigma - \sin\theta)\right)_i \frac{L^2}{8G'Bay} \quad \text{(Eq. 5.5.4-82)}$$

Shear force in the connection between the purlin and the panels at the anchorage device

$$P_{sc} = P_L + \frac{wL}{2}\left(0.9\sigma\alpha - \sin\theta\right) - P_i \quad \text{(Eq. 5.5.4-83)}$$

Supports Plus Third Point Lateral Anchorage

Anchorage force per anchorage device

$$(P_L)_{3rd} = \sum_{N_p} (P_{3rd})_i \cdot \frac{K_{rest}}{K_{3rd}} \quad \text{(force at top of purlin at 3rd point anchorage)} \quad \text{(Eq. 5.5.4-84)}$$

$$(P_L)_{spt} = \sum_{N_p} \left(P_{spt}\right)_i \cdot \frac{K_{rest}}{K_{spt}} \quad \text{(force at top of purlin at frame line anchorage)} \quad \text{(Eq. 5.5.4-85)}$$

$$P_h = P_L \frac{d}{h} \quad \text{(force at height of anchorage)} \quad \text{(Eq. 5.5.4-86)}$$

where

$$K_{3rd} = \sum_{N_a} (K_{rest})_{3rd} \quad \text{(Eq. 5.5.4-87)}$$

$$K_{spt} = \left(\sum_{N_a} (K_{rest})_{spt} + \frac{\sum_{N_p - N_a} K_{rafter}}{d} \right) \quad \text{(Eq. 5.5.4-88)}$$

with

$(K_{rest})_{3rd}$ = stiffness of the anchorage at the purlin third point (lb/in.) (N/m)

$(K_{rest})_{spt}$ = stiffness of the anchorage at the frame line (lb/in.) (N/m)

K_{trib} = C3 K_{spt}

C3 = 1.0 single span and multi-span exterior frame line

= 0.5 multi-span interior frame line

Total overturning force generated per purlin per half-span distributed between third point and frame line anchorages

$$\left(P_{3rd}\right)_i = \frac{wL}{2}\cdot\left[\begin{array}{l}\left(\frac{\delta b\cos\theta}{d}\left(1-R_{local}\right)+\frac{2}{3}k_{mclip}\left(\frac{\sigma}{2}-\frac{(\delta b+m)}{d}\cos\theta\right)\tau\right)\left(\frac{2d^2K_{trib}}{2d^2K_{trib}+N_p k_{mclip}LR_{sys}}\right)\psi\alpha\\ +\frac{2K_{trib}\sigma L}{9G'Bay}\psi\alpha-\sin\theta D_{3rd}\end{array}\right]$$

(Eq. 5.5.4-89)

$$\left(P_{spt}\right)_i = \frac{wL}{2}\cdot\left[\begin{array}{l}\left(\frac{\delta b\cos\theta}{d}\left(1-R_{local}\right)+\frac{2}{3}k_{mclip}\left(\frac{\sigma}{2}-\frac{(\delta b+m)}{d}\cos\theta\right)\tau\right)\left(\frac{2d^2K_{trib}}{2d^2K_{trib}+N_p k_{mclip}LR_{sys}}\right)\alpha(1+F)\\ +\frac{2K_{trib}\sigma L}{9G'Bay}\alpha F-\sin\theta D_{spt}\end{array}\right]$$

(Eq. 5.5.4-90)

where

$$R_{sys} = \frac{1}{2}\left(\frac{\frac{Et^3}{4}}{0.38k_{mclip}d+0.71\frac{Et^3}{4}}\right)\left(1-\tfrac{2}{3}k_{mclip}\tau\right) \quad \text{(Eq. 5.5.4-91)}$$

$$R_{local} = \frac{k_{mclip}}{k_{mclip}+\frac{Et^3}{3d}} \quad \text{(Eq. 5.5.4-92)}$$

$$\sigma = \frac{C1\frac{\left(\frac{I_{xy}}{I_x}\cos\theta\right)L^4}{EI_{my}}+A\cdot\frac{((\delta b)\cos\theta)d}{2}\tau+B\cdot\frac{N_p\alpha L^2\sin\theta}{18G'Bay}}{C1\frac{L^4}{EI_{my}}+C\cdot\frac{d^2}{4}\tau+\frac{\eta\alpha L^2}{9G'Bay}\left(1+K_{trib}\psi\Gamma\right)} \quad \text{(Eq. 5.5.4-93)}$$

where C1 = 11/972 Single Span
= 5/972 Multi-Span End Bay– outer half-span
= 7/1944 Multi-Span End Bay – inner half-span
= 1/486 Multi-Span Interior

$$\psi = \frac{\left(3G'BayK_{3rd}\right)\left(1+k_{mclip}\frac{\kappa}{GJ}\right)\left(N_p k_{mclip}LR_{sys}+2d^2K_{trib}\right)}{X1+X2} \quad \text{(Eq. 5.5.4-94)}$$

$$X1 = \left(3G'BayK_{trib}+LK_{trib}K_{3rd}\right)\left(1+k_{mclip}\frac{\kappa}{GJ}\right)\left(N_p k_{mclip}LR_{sys}+2d^2K_{trib}\right) \quad \text{(Eq. 5.5.4-95)}$$

$$X2 = (3G'BayK_{3rd})(2d^2K_{trib})\left(1 + k_{mclip}\frac{\kappa}{GJ} - \frac{\beta_{3rd}}{4}\frac{2}{3}k_{mclip}L\right) \quad \text{(Eq. 5.5.4-96)}$$

$$\Gamma = \left(C2\frac{\alpha L^3}{EI_{my}} + \frac{\alpha\frac{d^2}{4}\beta_{3rd}}{\left(1 + k_{mclip}\frac{\kappa}{GJ}\right)} - \frac{N_p \cdot L}{3G'Bay}\right)\frac{1}{N_p} \quad \text{(Eq. 5.5.4-97)}$$

where C2 = 5/162 Single Span
= 65/4779 Multi-Span End Bay – outer half-span
= 91/8100 Multi-Span End Bay – inner half-span
= 1/162 Multi-Span Interior

$$A = \left(\frac{\delta b + m}{\delta b}\right) + \eta\alpha\frac{L}{d^2}\left(\frac{2}{3}k_{mclip}\left(\frac{\delta b + m}{\delta b}\right) - \frac{(1 - R_{Local})}{\tau}\right)\left(\frac{2d^2K_{trib}}{2d^2K_{trib} + N_p k_{mclip} LR_{sys}}\right)\Gamma\psi$$

(Eq. 5.5.4-98)

$$B = \frac{(2K_{trib} - K_{3rd})3G'Bay}{LK_{trib}K_{3rd} + 3G'Bay(K_{trib} + K_{3rd})} \quad \text{(Eq. 5.5.4-99)}$$

$$C = 1 + \alpha\eta\frac{\frac{2}{3}k_{mclip}L}{d^2}\left(\frac{2d^2K_{trib}}{2d^2K_{trib} + N_p k_{mclip} LR_{sys}}\right)\Gamma\psi \quad \text{(Eq. 5.5.4-100)}$$

$$D_{3rd} = \frac{K_{3rd}(9G'Bay + 2LK_{trib})}{3[LK_{trib}K_{3rd} + 3G'Bay(K_{trib} + K_{3rd})]}\left(\frac{2d^2(K_{trib} + K_{3rd})}{2d^2(K_{trib} + K_{3rd}) + N_p k_{mclip} LR_{sys}}\right)$$

(Eq. 5.5.4-101)

$$D_{Spt} = \frac{K_{trib}(9G'Bay + LK_{3rd})}{3[LK_{trib}K_{3rd} + 3G'Bay(K_{trib} + K_{3rd})]}\left(\frac{2d^2(K_{trib} + K_{3rd})}{2d^2(K_{trib} + K_{3rd}) + N_p k_{mclip} LR_{sys}}\right)$$

(Eq. 5.5.4-102)

$$F = \frac{\left(\frac{\beta_{3rd}}{4}\frac{2}{3}k_{mclip}L - \left(1 + k_{mclip}\frac{\kappa}{GJ}\right)\right)}{\left(1 + k_{mclip}\frac{\kappa}{GJ}\right)}\left(\frac{2d^2K_{trib}}{2d^2K_{trib} + N_p k_{mclip} LR_{sys}}\right)\psi \quad \text{(Eq. 5.5.4-103)}$$

Single Span

The total overturning force at each frame line is the sum of $(P_{spt})_i$ for the half-span adjacent to the frame line for all purlins in the bay. The total overturning force at each third point is the sum of $(P_{3rd})_i$ for the half-span containing the third point for all purlins in the bay. Overturning forces must be distributed to each anchorage (support or third point) according to its relative stiffness along that line of anchorage.

Multi-Span Half-Span Adjacent to Exterior Frame Line

The total overturning force at exterior frame line is the sum of $(P_{spt})_i$ for the half-span adjacent to the frame line for all purlins in the bay. The total overturning force at the exterior third point is the sum of $(P_{3rd})_i$ for the half-span containing the third point for all purlins in the bay. Overturning forces must be distributed to each anchorage (support or third point) according to its relative stiffness along that line of anchorage.

Multi-Span Interior

The total overturning force at the interior frame line is the sum of $(P_{spt})_i$ for each half-span adjacent to the frame line for all purlins in the bay. The total overturning force at either third point is the sum of $(P_{3rd})_i$ for the half-span containing the third point for all purlins in the bay. Overturning forces must be distributed to each anchorage (support or third point) according to its relative stiffness along that line of anchorage.

Lateral deflection of the top flange of the purlin at the restraint (frame line or third point anchorage).

$$\Delta_{rest} = \frac{P_L}{K_{rest}}$$

(Eq. 5.5.4-104)

Shear force in the connection between the purlin and the panels at the support anchorage location

$$P_{sc} = P_L + \frac{wL}{2}(0.9\sigma\alpha + \sin\theta) - P_i \qquad \text{(Eq. 5.5.4-105)}$$

Shear force in the connection between the purlin and the panels at third point anchorage location

$$P_{sc} = P_L + \frac{wL}{20}\left(-0.9\sigma + \frac{\delta b \cos\theta}{d}\right)\alpha \qquad \text{(Eq. 5.5.4-106)}$$

5.5.4.7 Z-Section Examples

Four examples using the component stiffness method to predict anchorage forces are provided based on the roof system from the continuous purlin design example in Section 3.2.3.2.1. The roof system has four 25 ft spans with purlins lapped over the interior supports. The purlins in the end bays are 8ZS2.75x085 and the interior bays are 8ZS2.75x059. There are a total of 12 purlin lines spaced at 5 ft-0 in. on center with the top flange of the purlin closest to the eave turned downslope while the top flanges of the remaining purlins face upslope. The roof slope is 1/2 in./ft and the gravity loads are 3 psf dead and 20 psf live. The roof covering is attached with standing seam panel clips along the entire length of the purlins. The panels have a diaphragm stiffness G′ = 1000 lb/in. and the rotational stiffness of the standing seam panel clips, k_{mclip} = 2500 lb-in./(rad-ft).

In the example in Section 5.5.4.7.1, the anchorage forces are calculated for the anti-roll anchorage devices applied along the frame line at every fourth purlin. In the example from Section 5.5.4.7.2, anti-roll anchorage devices are replaced by anchorage applied at the third points of each span. The example in Section 5.5.4.7.3 demonstrates anchorage forces for lateral restraint applied along the frame line in conjunction with torsional restraints applied at the third point of each purlin. In the example in Section 5.5.4.7.4, third point anchorage devices are combined with anchorage along the frame lines in the form of welded web plates (b_{pl} = 5 in.) attached to the rafters.

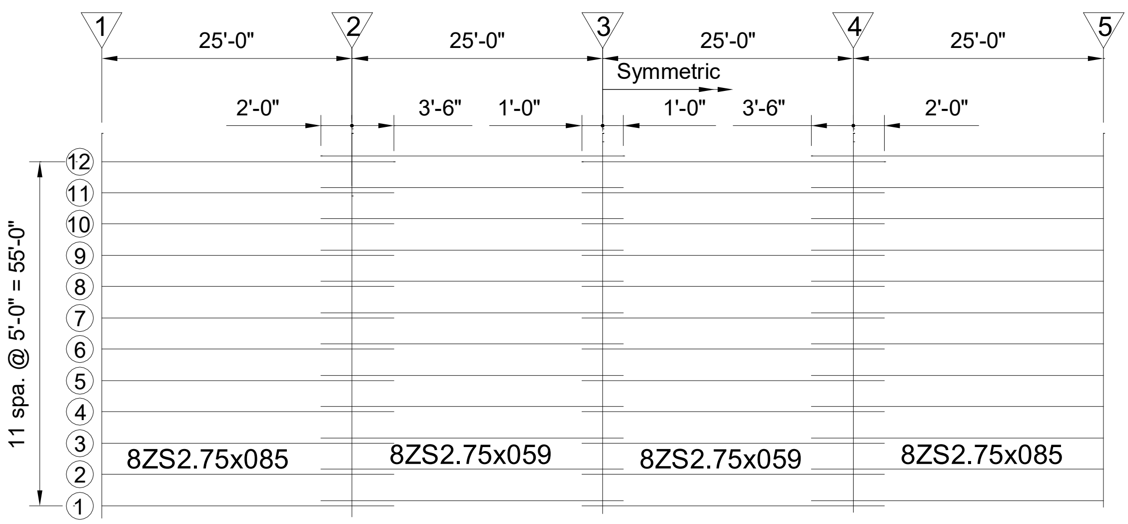

Figure 5.5-17 Roof Layout for Anchorage Examples

The following properties are used in each example.

System Properties

L	=	25 ft
Bay	=	55 ft
N_p	=	12
η	=	$n_{upslope} - n_{downslope} = 11 - 1 = 10$

Uniform load

Dead = 3 psf

Live = 20 psf

$w = (3 + 20)\text{psf} \cdot 5\text{ft} = 115\text{plf}$

Roof Slope, θ = 2.39 degrees (1/2:12)

G' = 1000 lb/in.

k_{mclip} = 2500 lb-in./rad/ft

E = 29500000 psi

G = 11300000 psi

Section Properties

The following sections properties are used for the two Z-sections:

INTERIOR BAYS	END BAYS
For: 8ZS2.75x059	For: 8ZS2.75x085
t = 0.059 in.	t = 0.085 in.
d = 8.0 in.	d = 8.0 in.
b = 2.75 in.	b = 2.75 in.
I_x = 8.69 in.^{4}	I_x = 12.40 in.^{4}
I_y = 1.72 in.^{4}	I_y = 2.51 in.^{4}
I_{xy} = 2.85 in.^{4}	I_{xy} = 4.11 in.^{4}
J = 0.00102 in.^{4}	J = 0.00306 in.^{4}
C_w = 19.3 in.^{6}	C_w = 28.0 in.^{6}
$I_{my} = \frac{I_x I_y - I_{xy}^2}{I_x}$ = 0.79 in.^{4}	$I_{my} = \frac{I_x I_y - I_{xy}^2}{I_x}$ = 1.15 in.^{4}

Purlin Torsional Properties

End span 8ZS2.75x085. Outside half-span approximated with both ends "warping free"

$$a = \sqrt{\frac{EC_W}{GJ}} = \sqrt{\frac{E \cdot 28.0\text{in}^6}{G \cdot 0.00306\text{in}^4}} = 154.6\text{ in} \qquad \text{(Eq. 5.5.4.-38)}$$

$$\beta = \frac{L^2}{8a^2} + \frac{1}{\cosh\left(\frac{L}{2a}\right)} - 1 = \frac{(300\text{ in})^2}{8 \cdot (154.6\text{ in})^2} + \frac{1}{\cosh\left(\frac{300\text{ in}}{2 \cdot 154.6\text{ in}}\right)} - 1 = 0.133\text{ rad} \qquad \text{(Eq. 5.5.4.-40)}$$

$$\kappa = \frac{8a^4}{L^2}\left(\frac{\cosh\left(\frac{L}{2a}\right) - 1}{\cosh\left(\frac{L}{2a}\right)}\right) + \frac{5L^2}{48} - a^2 \qquad \text{(Eq. 5.5.4-41)}$$

$$\kappa = \frac{8(154.6\text{in})^4}{(300\text{in})^2}\left(\frac{\cosh\left(\frac{300\text{in}}{2\cdot 154.6\text{in}}\right)-1}{\cosh\left(\frac{300\text{in}}{2\cdot 154.6\text{in}}\right)}\right)+\frac{5(300\text{in})^2}{48}-(154.6\text{in})^2 = 2597\ \text{rad}\cdot\text{in}^2$$

$$\tau = \frac{\frac{a^2\beta}{GJ}}{1+\frac{k_{mclip}}{GJ}\kappa} = \frac{\frac{(154.6\ \text{in})^2\cdot 0.133\text{rad}}{G\cdot 0.00306\text{in}^4}}{1+\frac{2500\ {}^{\text{lb}\cdot\text{in}}/_{\text{rad}\cdot\text{ft}}\left({}^{1\text{ft}}/_{12\text{in.}}\right)}{G\cdot 0.00306\text{in}^4}\cdot 2597\text{rad}\cdot\text{in}^2} = 0.0055\ \frac{\text{rad}}{\text{lb}} \qquad \text{(Eq. 5.5.4-39)}$$

$$\beta_{3rd} = \frac{L}{GJ}\left(\frac{1}{3}-\frac{a}{L}\frac{\sinh\left(\frac{L}{3a}\right)}{\cosh\left(\frac{L}{2a}\right)}\right) = \frac{(300\text{in})}{G\cdot 0.00306\text{in}^4}\left(\frac{1}{3}-\frac{154.6\ \text{in}}{300\text{in}}\frac{\sinh\left(\frac{300\text{in}}{3\cdot 154.6\ \text{in}}\right)}{\cosh\left(\frac{300\text{in}}{2\cdot 154.6\ \text{in}}\right)}\right) = 0.000839\ {}^{1}/_{\text{lb}\cdot\text{in}}$$

(Eq. 5.5.4-42)

End bay 8ZS2.75x085. Inside half-span approximated with both ends "warping fixed"

$$a = \sqrt{\frac{EC_W}{GJ}} = \sqrt{\frac{E\cdot 28.0\text{in}^6}{G\cdot 0.00306\text{in}^4}} = 154.6\ \text{in} \qquad \text{(Eq. 5.5.4-38)}$$

$$\beta = \frac{L^2}{8a^2}+\frac{L}{2a}\frac{1-\cosh\left(\frac{L}{2a}\right)}{\sinh\left(\frac{L}{2a}\right)} = \frac{(300\text{in})^2}{8\cdot(154.6\text{in})^2}+\frac{300\text{in}}{(2)(154.6\text{in})}\frac{1-\cosh\left(\frac{300\text{in}}{2\cdot 154.6\text{in}}\right)}{\sinh\left(\frac{300\text{in}}{2\cdot 154.6\text{in}}\right)} = 0.034\ \text{rad}$$

(Eq. 5.5.4-43)

$$\kappa = \left(\frac{aL}{3}-\frac{4a^3}{L}\right)\left(\frac{1-\cosh\left(\frac{L}{2a}\right)}{\sinh\left(\frac{L}{2a}\right)}\right)+\frac{5L^2}{48}-a^2 \qquad \text{(Eq. 5.5.4-44)}$$

$$\kappa = \left(\frac{(154.6\,\text{in})(300\,\text{in})}{3}-\frac{4(154.6\,\text{in})^3}{300\,\text{in}}\right)\left(\frac{1-\cosh\left(\frac{300\,\text{in}}{2(154.6\,\text{in})}\right)}{\sinh\left(\frac{300\,\text{in}}{2(154.6\,\text{in})}\right)}\right)+\frac{5(300\,\text{in})^2}{48}-(154.6\,\text{in})^2 = 699\ \text{rad}\cdot\text{in}^2$$

$$\tau = \frac{\frac{a^2\beta}{GJ}}{1+\frac{k_{mclip}}{GJ}\kappa} = \frac{\frac{(154.6\text{in})^2\cdot 0.034\text{rad}}{G\cdot 0.00306\text{in}^4}}{1+\frac{\left(2500\ {}^{\text{lb}\cdot\text{in}}/_{\text{rad}\cdot\text{ft}}\right)\left({}^{1\text{ft}}/_{12\text{in}}\right)}{G\cdot 0.00306\text{in}^4}\cdot 699\ \text{rad}\cdot\text{in}^2} = 0.0045\ \frac{\text{rad}}{\text{lb}} \qquad \text{(Eq. 5.5.4-39)}$$

$$\beta_{3rd} = \frac{L}{GJ}\left[\frac{1}{3}+\frac{a}{L}\left(\frac{\left(1-\cosh\left(\frac{L}{3a}\right)\right)\left(1-\cosh\left(\frac{L}{2a}\right)\right)}{\sinh\left(\frac{L}{2a}\right)}-\sinh\left(\frac{L}{3a}\right)\right)\right] \qquad \text{(Eq. 5.5.4-45)}$$

$$\beta_{3rd} = \frac{(300\text{in})}{G\cdot 0.00306\text{in}^4}\left[\frac{1}{3}+\frac{154.6\text{in}}{300\text{in}}\left(\frac{\left(1-\cosh\left(\frac{300\text{in}}{3\cdot 154.6\text{in}}\right)\right)\left(1-\cosh\left(\frac{300\text{in}}{2\cdot 154.6\text{in}}\right)\right)}{\sinh\left(\frac{300\text{in}}{2\cdot 154.6\text{in}}\right)} - \sinh\left(\frac{300\text{in}}{3\cdot 154.6\text{in}}\right)\right)\right] = 0.000230\ ^1\!/_{\text{lb}\cdot\text{in}}$$

Interior bay 8ZS2.75x059. Approximated with both ends "warping fixed"

$$a=\sqrt{\frac{EC_W}{GJ}}=\sqrt{\frac{E\cdot 19.3\text{in}^6}{G\cdot 0.00102\text{in}^4}}=222.3\text{ in} \qquad \text{(Eq. 5.5.4-38)}$$

$$\beta=\frac{L^2}{8a^2}+\frac{L}{2a}\frac{1-\cosh\left(\frac{L}{2a}\right)}{\sinh\left(\frac{L}{2a}\right)}=\frac{(300\text{in})^2}{8\cdot(222.3\text{in})^2}+\frac{300\text{in}}{(2)(222.3\text{in})}\frac{1-\cosh\left(\frac{300\text{in}}{2\cdot 222.3\text{in}}\right)}{\sinh\left(\frac{300\text{in}}{2\cdot 222.3\text{in}}\right)}=0.0083\text{ rad}$$

(Eq. 5.5.4-43)

$$\kappa=\left(\frac{aL}{3}-\frac{4a^3}{L}\right)\left(\frac{1-\cosh\left(\frac{L}{2a}\right)}{\sinh\left(\frac{L}{2a}\right)}\right)+\frac{5L^2}{48}-a^2 \qquad \text{(Eq. 5.5.4-44)}$$

$$\kappa=\left(\frac{(222.3\text{in})(300\text{ in})}{3}-\frac{4(222.3\text{ in})^3}{300\text{ in}}\right)\left(\frac{1-\cosh\left(\frac{300\text{ in}}{2(222.3\text{ in})}\right)}{\sinh\left(\frac{300\text{ in}}{2(222.3\text{ in})}\right)}\right)+\frac{5(300\text{ in})^2}{48}-(222.3\text{ in})^2=353.8\text{ rad}\cdot\text{in}^2$$

$$\tau=\frac{\frac{a^2\beta}{GJ}}{1+\frac{k_{mclip}}{GJ}\kappa}=\frac{\frac{(222.3\text{in})^2\cdot 0.0083\text{ rad}}{G\cdot 0.00102\text{in}^4}}{1+\frac{\left(2500\ ^{\text{lb}\cdot\text{in}}\!/_{\text{rad}\cdot\text{ft}}\right)\left(^{1\text{ft}}\!/_{12\text{in}}\right)}{G\cdot 0.00102\text{in}^4}\cdot 353.8\text{rad}\cdot\text{in}^2}=0.0048\frac{\text{rad}}{\text{lb}} \qquad \text{(Eq. 5.5.4-39)}$$

$$\beta_{3rd}=\frac{L}{GJ}\left[\frac{1}{3}+\frac{a}{L}\left(\frac{\left(1-\cosh\left(\frac{L}{3a}\right)\right)\left(1-\cosh\left(\frac{L}{2a}\right)\right)}{\sinh\left(\frac{L}{2a}\right)}-\sinh\left(\frac{L}{3a}\right)\right)\right] \qquad \text{(Eq. 5.5.4-45)}$$

$$\beta_{3rd} = \frac{(300\text{in})}{G\cdot 0.00102\text{in}^4}\left[\frac{1}{3}+\frac{222.3\text{in}}{300\text{in}}\left(\frac{\left(1-\cosh\left(\frac{300\text{in}}{3\cdot 222.3\text{in}}\right)\right)\left(1-\cosh\left(\frac{300\text{in}}{2\cdot 222.3\text{in}}\right)\right)}{\sinh\left(\frac{300\text{in}}{2\cdot 222.3\text{in}}\right)} - \sinh\left(\frac{300\text{in}}{3\cdot 222.3\text{in}}\right)\right)\right] = 0.00035\ ^1\!/_{\text{lb}\cdot\text{in}}$$

5.5.4.7.1 Example: Anchorage Forces for Anti-Roll Anchorage Device

Given

1. Using the system configuration shown at the beginning of section 5.5.4.7, there are no discrete bracing lines; anti-roll anchorage devices are provided at each support at every fourth purlin line (lines 1, 5 and 9 from the eave). Each anti-roll anchorage device is attached to the web of the Z-section with two rows of two 1/2 in. diameter A307 bolts. The bottom row of bolts is 3 in. from the bottom flange and the top row is 6 in. from the bottom flange. The stiffness of each anti-roll anchorage device, K_{device} = 40 kip/in. The width of the anti-roll anchorage device is b_{pl} = 5.0 in.
2. Purlin flanges are bolted to the support member with two 1/2 in. diameter A307 bolts through the bottom flange.

Required

1. Compute the anchorage forces along each frame line due to gravity loads.
2. Compute the lateral deflection of the top flange of the Z-section along each frame line and at the purlin mid-span.
3. Compute the shear force in the standing seam panel clips at each anchorage device.

Solution

Assumptions for Analysis

1. Since the loading, geometry and materials are symmetric, check the first two spans only.
2. Each restraint location is considered to have a single degree of freedom along the line of the anchorage. It is assumed that there is some mechanism to rigidly transfer forces from the remote purlins to the anchorage devices. The panels provide the mechanism to transfer the force as long as the connection between the purlin and the panels has sufficient strength and stiffness to transfer the force.
3. It is assumed that the total stiffness of the adjacent frame lines is approximately the same.

Procedure

1. Calculate the uniform restraint provided by the panels, w_{rest}, expressed as a proportion of the applied uniform load.

$$w_{rest} = w \cdot \sigma$$

where

$$\sigma = \frac{C1\dfrac{\left(\dfrac{I_{xy}}{I_x}\cos\theta\right)L^4}{EI_{my}} + \dfrac{\left((\delta b + m)\cos\theta\right)d}{2}\tau + \dfrac{\alpha \cdot N_p \cdot L^2 \sin\theta}{8G'Bay}}{C1\dfrac{L^4}{EI_{my}} + \dfrac{d^2}{4}\tau + \dfrac{\alpha \cdot \eta \cdot L^2}{8G'Bay}} \qquad \text{(Eq. 5.5.4-51)}$$

The uniform restraint force provided by the panels must be calculated separately for the upslope and downslope facing purlins.

a. End bay – half-span adjacent to Frame Line 1 (approximated as a simple-fixed beam with warping free ends).

Downslope facing purlin. C1 = 1/185 α = -1

$$\sigma = \frac{\dfrac{\left(\dfrac{4.11\text{in}^4}{12.40\text{in}^4}\cos(2.39°)\right)(300\text{in})^4}{185\cdot E\cdot 1.15\text{in}^4} + \dfrac{\left(\left(\frac{2.75\text{in}}{3}+0\right)\cos(2.39°)\right)8.0\text{in}}{2}0.0055\dfrac{\text{rad}}{\text{lb}} + \dfrac{(-1)(12)(300\text{in})^2\sin(2.39°)}{8\cdot\left(1000\,{}^{\text{lb}}\!/_{\text{in}}\right)(660\text{in})}}{\dfrac{(300\text{in})^4}{185\cdot E\cdot 1.15\text{in}^4} + \dfrac{(8.0\text{in})^2}{4}0.0055\dfrac{\text{rad}}{\text{lb}} + \dfrac{(-1)(10)(300\text{in})^2}{8\cdot\left(1000\,{}^{\text{lb}}\!/_{\text{in}}\right)(660\text{in})}}$$

$\sigma = 0.363$

Upslope facing purlin. All terms same as above except with α =1

$\sigma = 0.294$

b. End bay – half-span adjacent to Frame Line 2 (approximated as a simple-fixed beam with warping fixed ends).

Downslope facing purlin. C1 = 1/185 α = -1

$$\sigma = \frac{\dfrac{\left(\dfrac{4.11\text{in}^4}{12.40\text{in}^4}\cos(2.39°)\right)(300\text{in})^4}{185\cdot E\cdot 1.15\text{in}^4} + \dfrac{\left(\left(\frac{2.75\text{in}}{3}+0\right)\cos(2.39°)\right)8.0\text{in}}{2}0.0045\dfrac{\text{rad}}{\text{lb}} + \dfrac{(-1)(12)(300\text{in})^2\sin(2.39°)}{8\cdot\left(1000\,{}^{\text{lb}}\!/_{\text{in}}\right)(660\text{in})}}{\dfrac{(300\text{in})^4}{185\cdot E\cdot 1.15\text{in}^4} + \dfrac{(8.0\text{in})^2}{4}0.0045\dfrac{\text{rad}}{\text{lb}} + \dfrac{(-1)(10)(300\text{in})^2}{8\cdot\left(1000\,{}^{\text{lb}}\!/_{\text{in}}\right)(660\text{in})}}$$

$\sigma = 0.365$

Upslope facing purlin. All terms same as above except with α = 1

$\sigma = 0.295$

c. Interior bay - (approximated as a fixed-fixed beam with warping fixed ends)

Downslope facing purlin. C1 = 1/384 α = -1

$$\sigma = \frac{\dfrac{\left(\dfrac{2.85\text{in}^4}{8.69\text{in}^4}\cos(2.39°)\right)(300\text{in})^4}{384\cdot E\cdot 0.79\text{in}^4} + \dfrac{\left(\left(\frac{2.75\text{in}}{3}+0\right)\cos(2.39°)\right)8.0\text{in}}{2}0.0048\dfrac{\text{rad}}{\text{lb}} + \dfrac{(-1)(12)(300\text{in})^2\sin(2.39°)}{8\cdot\left(1000\,{}^{\text{lb}}\!/_{\text{in}}\right)(660\text{in})}}{\dfrac{(300\text{in})^4}{384\cdot E\cdot 0.79\text{in}^4} + \dfrac{(8.0\text{in})^2}{4}0.0048\dfrac{\text{rad}}{\text{lb}} + \dfrac{(-1)(10)(300\text{in})^2}{8\cdot\left(1000\,{}^{\text{lb}}\!/_{\text{in}}\right)(660\text{in})}}$$

$\sigma = 0.376$

Upslope facing purlin all terms same as above except with α =1

$\sigma = 0.28$

2. Calculate the overturning forces generated by each purlin.

a. End bay – half-span adjacent to Frame Line 1 (approximated as each end warping free)

Local deformation reduction factor

$$R_{local} = \frac{k_{mclip}}{k_{mclip} + \frac{Et^3}{3d}} = \frac{2500\,^{lb\cdot in}/_{rad\cdot ft}}{2500\,^{lb\cdot in}/_{rad\cdot ft} + \frac{E\cdot(0.085in)^3}{3\cdot 8.0in}\left(12\,^{in}/_{ft}\right)} = 0.216 \qquad \text{(Eq. 5.5.4-50)}$$

Purlin 1 w = 57.5 lb/ft α = -1

$$P_i = \frac{wL}{2d}\cdot\left[\left(\delta b\cos\theta\left(1-R_{local}\right) + \tfrac{2}{3}k_{mclip}\tau\left(\sigma\frac{d}{2} - \left(\delta b + m\right)\cos\theta\right)\right)\alpha - d\sin\theta\right] \qquad \text{(Eq. 5.5.4-49)}$$

$$P_1 = \frac{(57.5plf)(25ft)}{(2)(8.0in)}\cdot\left[\begin{array}{l}\left(\begin{array}{l}\frac{2.75in}{3}\cos(2.39°)(1-0.216) + \frac{2}{3}\left(2500\,^{lb\cdot in}/_{rad\cdot ft}\right)\left(^{1ft}/_{12in}\right)\left(0.0055\frac{rad}{lb}\right)\\ \left((0.363)\frac{8.0in}{2} - \left(\frac{2.75in}{3}+0\right)\cos(2.39°)\right)\end{array}\right)(-1)\\ -(8.0in)\sin(2.39°)\end{array}\right]$$

$$P_1 = -132\ \text{lb}$$

Purlins 2-11 w = 115 lb/ft α = 1

$$P_{2-11} = 106\ \text{lb}$$

Purlin 12 w = 57.5 lb/ft α = 1

$$P_{12} = 53\ \text{lb}$$

b. End bay – half-span adjacent to Frame Line 2 (approximated as each end warping fixed)

Local deformation reduction factor

$$R_{local} = 0.216$$

Purlin 1 w = 57.5 lb/ft α = -1

$$P_1 = \frac{(57.5plf)(25ft)}{2(8.0in).}\cdot\left[\begin{array}{l}\left(\begin{array}{l}\frac{2.75in}{3}\cos(2.39°)(1-0.216) + \frac{2}{3}\left(2500\,^{lb\cdot in}/_{rad\cdot ft}\right)\left(^{1ft}/_{12in}\right)\left(0.0045\frac{rad}{lb}\right)\\ \left((0.365)\frac{8.0in}{2} - \left(\frac{2.75in}{3}+0\right)\cos(2.39°)\right)\end{array}\right)(-1)\\ -(8.0in)\sin(2.39°)\end{array}\right]$$

$$P_1 = -125\ \text{lb}$$

Purlins 2-11 w = 115 lb/ft α = 1

$$P_{2-11} = 99\ \text{lb}$$

Purlin 12 w = 57.5 lb/ft α = 1

$$P_{12} = 49 \text{ lb}$$

c. Interior bay

Local deformation reduction factor

$$R_{local} = \frac{k_{mclip}}{k_{mclip} + \frac{Et^3}{3d}} = \frac{2500 \, {}^{lb\cdot in}/_{rad\cdot ft}}{2500 \, {}^{lb\cdot in}/_{rad\cdot ft} + \frac{E\cdot(0.059in)^3}{3\cdot 8.0in}\left(12 \, {}^{in}/_{ft}\right)} = 0.452 \qquad \text{(Eq. 5.5.4-50)}$$

Purlin 1 w = 57.5 lb/ft α = -1

$$P_1 = \frac{(57.5plf)(25ft)}{(2)(8.0in)} \cdot \left[\frac{\left(\frac{2.75in}{3}\cos(2.39°)(1-0.452) + \frac{2}{3}\left(2500 \, {}^{lb\cdot in}/_{rad\cdot ft}\right)\left({}^{1ft}/_{12in}\right)\left(0.0048\frac{1}{lb}\right)\right)}{\left(\left(0.376\right)\frac{8.0in}{2} - \left(\frac{2.75in}{3}+0\right)\cos(2.39°)\right)}(-1) - (8.0in)\sin(2.39°) \right]$$

$$P_1 = -110 \text{ lb}$$

Purlins 2-11 w = 115 lb/ft α = 1

$$P_{2-11} = 55 \text{ lb}$$

Purlin 12 w = 57.5 lb/ft α = 1

$$P_{12} = 27 \text{ lb}$$

3. Calculate the stiffness of the restraints.

The stiffness of each restraint device is

$$K_{device} = 40 \, {}^{kip}/_{in}$$

The net stiffness of the restraint must include the configuration stiffness which accounts for the flexibility of the web of the purlin between the top of the anchorage device and the top flange of the purlin.

a. Frame Line 1

Configuration stiffness

$$K_{config} = \frac{Eb_{pl}t^3}{(d-h)^3}\cdot\frac{d}{h} = \frac{E(5\,in)(0.085\,in)^3}{(8.0\,in - 6.0\,in)^3}\cdot\frac{8.0\,in}{6.0\,in} = 15.1 \, {}^{kip}/_{in} \qquad \text{(Eq. 5.5.4-32)}$$

Net restraint stiffness

$$K_{rest} = \frac{\left(\frac{h}{d}\right)^2 K_{device} K_{config}}{\frac{h}{d} K_{device} + K_{config}} = \frac{\left(\frac{6in}{8in}\right)^2 \left(40 \, {}^{kip}/_{in}\right)\left(15.1 \, {}^{kip}/_{in}\right)}{\frac{6in}{8in}\left(40 \, {}^{kip}/_{in}\right) + 15.1 \, {}^{kip}/_{in}} = 7.5 \, {}^{kip}/_{in} \qquad \text{(Eq. 5.5.4-30)}$$

b. Frame Line 2

To account for the purlins at the lap, the combined purlins are given an equivalent thickness.

$$t_{lap} = \sqrt[3]{t_1^3 + t_2^3} = \sqrt[3]{(0.085in)^3 + (0.059in)^3} = 0.094\,in$$

Configuration stiffness

$$K_{config} = \frac{Eb_{pl}t^3}{(d-h)^3} \cdot \frac{d}{h} = \frac{E(5in)(0.094in)^3}{(8in - 6in)^3} \cdot \frac{8in}{6in} = 20.1 \, {}^{kip}/_{in} \qquad \text{(Eq. 5.5.4-32)}$$

Net restraint stiffness

$$K_{rest} = 9.0 \, {}^{kip}/_{in}$$

c. Frame Line 3

Equivalent thickness at lap

$$t_{lap} = \sqrt[3]{t_2^3 + t_2^3} = \sqrt[3]{(0.059in)^3 + (0.059in)^3} = 0.074in$$

Configuration stiffness

$$K_{config} = \frac{Eb_{pl}t^3}{(d-h)^3} \cdot \frac{d}{h} = \frac{E(5in)(0.074in)^3}{(8in - 6in)^3} \cdot \frac{8in}{6in} = 10.1 \, {}^{kip}/_{in} \qquad \text{(Eq. 5.5.4-32)}$$

Net restraint Stiffness

$$K_{rest} = 5.7 \, {}^{kip}/_{in}$$

4. Calculate the stiffness of the system.

a. Calculate the stiffness of the panels.

$$K_{panel} = \frac{k_{mclip}L}{d}\left(\frac{\frac{Et^3}{4}}{0.38k_{mclip}d + 0.71\frac{Et^3}{4}}\right)\left(1 - {}^{2}/_{3}\, k_{mclip}\tau\right) \qquad \text{(Eq. 5.5.4-37)}$$

i. End bay. It is conservative to use the torsional coefficient, τ, for a warping free ends when evaluating the effect of the panels stiffness at both Frame Lines 1 and 2.

$$K_{panel} = \frac{2500\,{}^{lb\cdot in}\!/_{rad\cdot ft}\,25ft}{8.0in}\left(\frac{\frac{E(0.085in)^3}{4}}{(0.38)\left(2500\,{}^{lb\cdot in}\!/_{rad\cdot ft}\right)\left({}^{1ft}\!/_{12in}\right)(8.0in)+0.71\cdot\frac{E(0.085in)^3}{4}}\right)$$

$$\left(1-\left({}^{2}\!/_{3}\,2500\,{}^{lb\cdot in}\!/_{rad\cdot ft}\right)\left({}^{1ft}\!/_{12in}\right)\left(0.0055\frac{rad}{lb}\right)\right)$$

$$K_{panel} = 2117\,{}^{lb\cdot in}\!/_{in}$$

ii. Interior bay, t = 0.059 in. τ = 0.0048 rad/lb

$$K_{panel} = 2317\,{}^{lb\cdot in}\!/_{in}$$

b. Calculate the stiffness of the connection between the rafter and the Z-sections that are not at a restraint device (flange bolted connection)

$$K_{rafter} = 0.45\frac{Et^3}{2d} \qquad \text{(Eq. 5.5.4-36)}$$

Exterior Frame Line

$$K_{rafter} = 0.45\frac{E(0.085in)^3}{2\cdot 8in} = 510\,{}^{lb\cdot in}\!/_{in}$$

At the interior frame lines, the equivalent thickness of the laps is used.

First Interior Frame Line

$$K_{rafter} = 0.45\frac{E(0.094in)^3}{2\cdot 8in} = 680\,{}^{lb\cdot in}\!/_{in}$$

Second Interior Frame Line

$$K_{rafter} = 0.45\frac{E(0.074in)^3}{2\cdot 8in} = 341\,{}^{lb\cdot in}\!/_{in}$$

5. Calculate the total stiffness of the system attributed to each restraint location (frame line).

$$K_{total} = \sum_{N_a} K_{rest} + \frac{\sum_{N_p} K_{panel} + \sum_{N_p - N_a} K_{rafter}}{d} \qquad \text{(Eq. 5.5.4-48)}$$

a. At Frame Line 1, the stiffness includes three anchorage devices, the rafter stiffness of nine purlins flange bolted to the rafters and the panel stiffness of half of the end bay for twelve purlins.

$$K_{total} = 3\left(7.5\,{}^{kip}\!/_{in}\right) + 12\frac{2117\,{}^{lb\cdot in}\!/_{in}}{(2)(8in)} + 9\frac{510\,{}^{lb\cdot in}\!/_{in}}{8.0in} = 24.8\,{}^{kip}\!/_{in}$$

b. At Frame Line 2, the stiffness includes three anchorage devices, the rafter stiffness of nine purlins flange bolted to the rafters, and the panel stiffness of half of the end bay and half of the interior bay for twelve purlins.

$$K_{total} = 3\left(9.0\,{}^{kip}\!/_{in}\right) + 12\frac{2117\,{}^{lb\cdot in}\!/_{in}}{(2)(8in)\left(1000\,{}^{lb}\!/_{kip}\right)} + 12\frac{2317\,{}^{lb\cdot in}\!/_{in}}{(2)(8in)\left(1000\,{}^{lb}\!/_{kip}\right)} + 9\frac{680\,{}^{lb\cdot in}\!/_{in}}{(8.0in)\left(1000\,{}^{lb}\!/_{kip}\right)} = 31.1\,{}^{kip}\!/_{in}$$

c. At Frame Line 3, the stiffness includes three anchorage devices, the rafter stiffness of nine purlins flange bolted to the rafters, and two times the panel stiffness of half of the interior bay for twelve purlins

$$K_{total} = 3\left(5.7\,{}^{kip}\!/_{in}\right) + 9\frac{341\,{}^{lb\cdot in}\!/_{in}}{8.0in} + 12\frac{2317\,{}^{lb\cdot in}\!/_{in}}{8.0in} = 21.0\,{}^{kip}\!/_{in}$$

6. Distribute the overturning forces to each restraint.

a. Frame Line 1

The total load generated by the end bay half-span adjacent to Frame Line 1 is

$$\sum_{N_p} P_i = (P_1 + 10P_{2-11} + P_{12}) = (-132\text{ lb}) + 10(106\text{ lb}) + 53\text{ lb} = 981\text{ lb}$$

Distribution to each anchorage device along Frame Line 1

$$P_L = \sum_{N_p} P_i \cdot \frac{K_{rest}}{K_{total}} = (981\text{ lb})\frac{7.5\,{}^{kip}\!/_{in}}{24.8\,{}^{kip}\!/_{in}} = 297\text{ lb} \qquad \text{(Eq. 5.5.4-46)}$$

Anchorage force at the height of the restraint

$$P_h = P_L\frac{d}{h} = (297\text{ lb})\frac{8\text{ in}}{6\text{ in}} = 396\text{ lb} \qquad \text{(Eq. 5.5.4-47)}$$

b. Frame Line 2

The total load generated by each half-span adjacent to Frame Line 2 is

$$\sum_{N_p} P_i = (P_1 + 10P_{2-11} + P_{12})_{Left} + (P_1 + 10P_{2-11} + P_{12})_{Right}$$

$$\sum_{N_p} P_i = (-125\text{ lb}) + 10(99\text{ lb}) + (49\text{ lb}) + ((-110\text{ lb}) + 10(55\text{ lb}) + (27\text{ lb})) = 1375\text{ lb}$$

Distribution to each anchorage device along Frame Line 2

$$P_L = \sum_{N_p} P_i \cdot \frac{K_{rest}}{K_{total}} = (1375\text{ lb})\frac{9.0\,{}^{kip}\!/_{in}}{31.2\,{}^{kip}\!/_{in}} = 397\text{ lb} \qquad \text{(Eq. 5.5.4-46)}$$

Anchorage force at the height of the restraint

$$P_h = P_L\frac{d}{h} = (397\text{ lb})\frac{8\text{in}}{6\text{in}} = 529\text{ lb} \qquad \text{(Eq. 5.5.4-47)}$$

c. Frame Line 3

At Frame Line 3, it is assumed that half of the force generated at each bay adjacent to the frame line is distributed to the interior frame line.

$$\sum_{N_p} P_i = 2\left(\left(P_1 + 10P_{2-11} + P_{12}\right)_{Int}\right) = 2\left(\left(-110\text{ lb}\right) + 10\left(55\text{ lb}\right) + \left(27\text{ lb}\right)\right) = 934\text{ lb}$$

Distribution to each anchorage device along Frame Line 3

$$P_L = \sum_{N_p} P_i \cdot \frac{K_{rest}}{K_{total}} = \left(934\text{ lb}\right)\frac{5.7\,{}^{kip}/_{in}}{21.0\,{}^{kip}/_{in}} = 254\text{ lb} \quad \text{(Eq. 5.5.4-46)}$$

Anchorage force at the height of the restraint

$$P_h = P_L\frac{d}{h} = \left(254\text{ lb}\right)\frac{8\text{ in}}{6\text{ in}} = 339\text{ lb} \quad \text{(Eq. 5.5.4-47)}$$

7. Check the deflection of the system and compare to the limits specified in AISI S100 Section I6.4.1

a. Lateral deflection of the purlin top flange

Allowable deflection limit (ASD)

$$\Delta_{tf} \le \frac{1}{\Omega}\frac{d}{20} = \frac{1}{2.00}\frac{8\text{ in}}{20} = 0.20\text{ in} \quad \text{(AISI S100 Eq. I6.4.1-9a)}$$

Frame Line 1

$$\Delta_{rest} = \frac{P_L}{K_{rest}} = \frac{297\text{ lb}}{\left(7.5\,{}^{kip}/_{in}\right)\left(1000\,{}^{lb}/_{kip}\right)} = 0.040\text{ in} \le 0.20\text{ in} \quad \text{OK} \quad \text{(Eq. 5.5.4-52)}$$

Frame Line 2

$$\Delta_{rest} = \frac{P_L}{K_{rest}} = \frac{397\text{ lb}}{\left(9.0\,{}^{kip}/_{in}\right)\left(1000\,{}^{lb}/_{kip}\right)} = 0.044\text{ in} \le 0.20\text{ in} \quad \text{OK} \quad \text{(Eq. 5.5.4-52)}$$

Frame Line 3

$$\Delta_{rest} = \frac{P_L}{K_{rest}} = \frac{254\text{ lb}}{\left(5.7\,{}^{kip}/_{in}\right)\left(1000\,{}^{lb}/_{in}\right)} = 0.045\text{ in} \le 0.20\text{ in} \quad \text{OK} \quad \text{(Eq. 5.5.4.-52)}$$

b. Mid-span deflection of the diaphragm relative to the restraint

Allowable deflection limit

$$\Delta_{ms} \le \frac{L}{360} = \frac{25\text{ft}\left(12\,{}^{in}/_{ft}\right)}{360} = 0.83\text{ in}$$

$$\Delta_{diaph} = \sum_{N_p}\left(w\left(\alpha\sigma - \sin\theta\right)\right)_i \frac{L^2}{8G'Bay} \quad \text{(Eq. 5.5.4-53)}$$

End Bay

Use the average uniform diaphragm force between the two half-spans.

$$\overline{\sigma}_1 = \tfrac{1}{2}(0.363 + 0.365) = 0.364$$

$$\overline{\sigma}_{2-12} = \tfrac{1}{2}(0.294 + 0.295) = 0.295$$

$$\Delta_{diaph} = \left[57.5 \,\mathrm{lb/ft}\left((-1)0.364 - \sin(2.39°)\right) + \left[(10)(115 \,\mathrm{lb/ft}) + (1)(57.5 \,\mathrm{lb/ft})\right]\left((1)0.295 - \sin(2.39°)\right)\right]$$

$$\frac{(25\mathrm{ft})^2}{8(1000 \,\mathrm{lb/in})(55\mathrm{ft})} = 0.40 \text{ in}$$

$$\Delta_{diaph} = 0.40 \text{ in} \le 0.83 \text{ in} \quad \text{OK}$$

Interior Bay

$$\Delta_{diaph} = \left[57.5 \,\mathrm{lb/ft}\left((-1)0.376 - \sin(2.39°)\right) + \left[(10)(115 \,\mathrm{lb/ft}) + (1)(57.5 \,\mathrm{lb/ft})\right]\left((1)0.28 - \sin(2.39°)\right)\right]$$

$$\frac{(25\mathrm{ft})^2}{8(1000 \,\mathrm{lb/in})(55\mathrm{ft})} = 0.375 \text{ in}$$

$$\Delta_{diaph} = 0.375 \text{ in} \le 0.83 \text{ in} \quad \text{OK}$$

8. Calculate the shear force in the connection between the panels and the purlin at the anchorage device location.

$$P_{sc} = P_L + \frac{wL}{2}(0.9\sigma\alpha - \sin\theta) - P_i \qquad \text{(Eq. 5.5.4-54)}$$

Frame Line 1

Downslope Purlin 1

$$P_{sc} = 297 \text{ lb} + \frac{(57.5\text{plf})(25\text{ft})}{2}\left(0.9(0.363)(-1) - \sin(2.39°)\right) - (-132 \text{ lb}) = 163 \text{ lb}$$

Upslope Purlins 5 and 9

$$P_{sc} = 297 \text{ lb} + \frac{(115\text{plf})(25\text{ft})}{2}\left(0.9(0.294)(1) - \sin(2.39°)\right) - (106 \text{ lb}) = 512 \text{ lb}$$

Frame Line 2

Downslope Purlin 1

$$P_{sc} = 397 \text{ lb} + \frac{(57.5\text{plf})(25\text{ft})}{2}\left(0.9(0.365)(-1) - \sin(2.39°)\right) - (-125 \text{ lb})$$
$$+ \frac{(57.5\text{plf})(25\text{ft})}{2}\left(0.9(0.376)(-1) - \sin(2.39°)\right) - (-110 \text{ lb}) = 94 \text{ lb}$$

Upslope Purlins 5 and 9

$$P_{sc} = 397\text{ lb} + \frac{(115\text{ plf})(25\text{ft})}{2}\left(0.9(0.295)(1) - \sin(2.39°)\right) - (99\text{ lb}) + \frac{(115\text{ plf})(25\text{ ft})}{2}\left(0.9(0.280)(1) - \sin(2.39°)\right) - (55\text{ lb}) = 869\text{ lb}$$

Frame Line 3

Downslope Purlin 1

$$P_{sc} = 254\text{ lb} + 2\cdot\left[\frac{(57.5\text{plf})(25\text{ft})}{2}\left(0.9(0.376)(-1) - \sin(2.39°)\right) - (-110\text{ lb})\right] = -75\text{ lb}$$

Upslope Purlins 5 and 9

$$P_{sc} = 254\text{ lb} + 2\cdot\left[\frac{(115\text{plf})(25\text{ft})}{2}\left(0.9(0.280)(1) - \sin(2.39°)\right) - (55\text{ lb})\right] = 748\text{ lb}$$

5.5.4.7.2 Example: Third Point Anchorage

Given

1. From the previous example, the anchorage devices are replaced by third point anchorage devices along the eave of the system (at Purlin Line 1). Each third point brace is attached to the top flange and has a stiffness of 15 kip/in.
2. Purlin flanges are bolted to the support member with two 1/2 in. diameter A307 bolts through the bottom flange.

Required

1. Compute the anchorage forces at each third point restraint due to gravity loads.
2. Compute the lateral deflection of the top flange of the Z-section at each third point and along each frame line.
3. Compute the shear force in the standing seam panel clips at each anchorage device.

Solution

Assumptions for Analysis

a. Since the loading, geometry and materials are symmetric, check the first two spans only.
b. Each restraint location is considered to have a single degree of freedom along the run of purlins. It is assumed that there is some mechanism to rigidly transfer forces from the remote purlins to the anchorage device. The panels provide the mechanism to transfer the force as long as the connection between the purlin and the panels has sufficient strength and stiffness to transfer the force.
c. It is assumed that the total stiffness of the system in each bay is approximately the same.

Procedure

1. Calculate the uniform restraint provided by the panels, w_{rest}, expressed as a proportion of the applied uniform load.

$$w_{rest} = w \cdot \sigma$$

where

$$\sigma = \frac{C1\dfrac{\left(\dfrac{I_{xy}}{I_x}\cos\theta\right)L^4}{EI_{my}} + \dfrac{\left((\delta b + m)\cos\theta\right)d}{2}\tau - \dfrac{\alpha \cdot N_p \cdot L^2 \sin\theta}{18G'Bay}}{C1\dfrac{L^4}{EI_{my}} + \dfrac{d^2}{4}\tau + \dfrac{\alpha \cdot \eta \cdot L^2}{9G'Bay}} \qquad \text{(Eq. 5.5.4-60)}$$

The uniform restraint force provided by the panels must be calculated separately for the upslope and downslope facing purlins.

a. End bay – half-span adjacent to Frame Line 1 (approximated as a simple-fixed beam with warping free-fixed ends)

Lateral deflections are considered at each third point while torsion is considered at the mid-span for simplicity

Purlin 1 C1 = 5/972 α = -1

$$\sigma = \frac{\dfrac{5\left(\dfrac{4.11\text{in}^4}{12.40\,\text{in}^4}\cos(2.39°)\right)(300\text{in})^4}{972\cdot E\cdot 1.15\text{in}^4} + \dfrac{\left(\left(\frac{2.75\text{in}}{3}+0\right)\cos(2.39°)\right)8.0\text{in}}{2}0.0055\dfrac{\text{rad}}{\text{lb}} - \dfrac{(-1)(12)(300\text{in})^2\sin(2.39°)}{18\cdot\left(1000\,{}^{\text{lb}}\!/_{\text{in}}\right)(660\text{in})}}{\dfrac{5(300\text{in})^4}{972\cdot E\cdot 1.15\text{in}^4} + \dfrac{(8.0\text{in})^2}{4}0.0055\dfrac{\text{rad}}{\text{lb}} + \dfrac{(-1)(10)(300\text{in})^2}{9\cdot\left(1000\,{}^{\text{lb}}\!/_{\text{in}}\right)(660\text{in})}}$$

$\sigma = 0.370$

Purlins 2-12 same as above except with α = 1

$\sigma = 0.288$

b. End bay – half-span adjacent to Frame Line 2 (approximated as a simple-fixed beam with warping free-fixed ends).

Purlin 1 C1 = 7/1944 α = -1

$\sigma = 0.391$

Purlins 2-12 C1 = 7/1944 α = 1

$\sigma = 0.275$

c. Interior bay - (approximated as a fixed-fixed beam with warping fixed ends).

Purlin 1 C1 = 1/486 α = -1

$\sigma = 0.399$

Purlins 2-12 C1 = 1/486 α = 1

$\sigma = 0.263$

2. Calculate the overturning forces generated by each purlin.

a. End bay – half-span adjacent to Frame Line 1 (approximated as each end warping free)

R_{local} = 0.216 (from previous example)

Purlin 1 w = 57.5 lb/ft α = -1

$$P_i = \frac{wL}{2d}\cdot\left[\begin{aligned}&\left(\delta b\cos\theta\left(1-R_{local}\right)+\tfrac{2}{3}k_{mclip}\tau\left(\sigma\frac{d}{2}-(\delta b+m)\cos\theta\right)\right)\alpha - d\sin\theta\\ &+\frac{L^2k_{mclip}}{3G'Bay\cdot d}\left(1-{}^{2}\!/_{3}k_{mclip}\tau\right)\left(\frac{\eta\sigma}{3}+\frac{N_p\sin\theta}{6}-\frac{\eta\cdot\delta b\cos\theta}{2d}\right)\end{aligned}\right] \quad \text{(Eq. 5.5.4-58)}$$

$$P_1 = \frac{\left(57.5\,{}^{lb}\!/\!_{ft}\right)(25ft)}{(2)(8in)} \cdot \left[\begin{array}{l} \left(\frac{2.75in}{3}\cos(2.39°)(1-0.216) + \frac{2}{3}\left(2500\,{}^{lb\cdot in}\!/\!_{rad\cdot ft}\left({}^{1ft}\!/\!_{12in}\right)\right)\left(0.0055\frac{rad}{lb}\right)\left((0.370)\frac{8.0in}{2} - \left(\frac{2.75in}{3}+0\right)\cos(2.39°)\right)\right)(-1) \\ -(8.0in)\sin(2.4°) + \frac{(25ft)^2\,2500\,{}^{lb\cdot in}\!/\!_{rad\cdot ft}}{3\left(1000\,{}^{lb}\!/\!_{in}\right)(55ft)(10in)}\left(1 - {}^{2}\!/\!_{3}2500\,{}^{lb\cdot in}\!/\!_{rad\cdot ft}\left({}^{1ft}\!/\!_{12in}\right)\left(0.0055\frac{rad}{lb}\right)\right) \\ \left(\frac{(10)(0.370)}{3} + \frac{12\sin(2.39°)}{6} - \frac{(10)\left(\frac{2.75in}{3}\right)\cos(2.39°)}{(2)(8in)}\right) \end{array}\right]$$

$P_1 = -115\ lb$

Purlins 2-11 w = 115 lb/ft $\alpha = 1$

$P_{2-11} = 125\ lb$

Purlin 12

Since the load on Purlin 12 is half that of Purlins 2-11, the overturning force is half that of Purlins 2-12, or

$P_{12} = 63\ lb$

b. End bay – half-span adjacent to Frame Line 2

R_{local} = 0.216 (from previous example)

Purlin 1 w = 57.5 lb/ft α = -1

$P_1 = -98\ lb$

Purlins 2-11 w = 115 lb/ft $\alpha = 1$

$P_{2-11} = 124\ lb$

Purlin 12

$P_{12} = 62 \cdot lb$ (half of purlins 2-11)

c. Interior bay

R_{local} = 0.45 (from previous example)

Purlin 1 w = 57.5 lb/ft α = -1

$P_1 = -86\ lb$

Purlins 2-11 w = 115 lb/ft $\alpha = 1$

$P_{2-11} = 74\ lb$

Purlin 12

$P_{12} = 37\ lb$ (half of Purlins 2-11)

3. Calculate the stiffness of the restraints

   The stiffness of each restraint device is

   $$K_{device} = 15\,{}^{kip}\!/_{in}$$

The restraint is applied to the top of the Z-section and it is assumed that this connection is rigid, i.e., the configuration stiffness is essentially rigid. Therefore, the restraint stiffness becomes

$$K_{rest} = \left(\frac{h}{d}\right)^2 K_{device} = \left(\frac{8\,in}{8\,in}\right)^2 15\,{}^{kip}\!/_{in} = 15\,{}^{kip}\!/_{in} \qquad \text{(Eq. 5.5.4-34)}$$

4. Calculate the stiffness of the system.

a. Calculate the stiffness of the panels

   The panel stiffness is the same as was calculated in the previous example.

   End bay $K_{panel} = 2117\,{}^{lb\cdot in}\!/_{in}$

   Interior bay $K_{panel} = 2317\,{}^{lb\cdot in}\!/_{in}$

b. Calculate the stiffness of the connection between the rafter and the Z-sections (flange-bolted connection).

The connection between the rafter and the Z-section is a flange-bolted connection. Because the stiffness of this connection is relatively small, it is ignored for a third points restraint configuration. If the connection between the Z-section and rafter has significant stiffness, such as with a rafter web plate (welded plate), the restraint configuration must be considered a third points plus supports configuration (see the example in Section 5.5.7.4.4).

5. Calculate the total stiffness of the system attributed to each restraint location

$$K_{total} = \sum K_{rest} + \frac{\sum\left(K_{panel} + K_{rafter}\right)}{d} \qquad \text{(Eq. 5.5.4-57)}$$

a. End bay. The total stiffness attributed to each restraint is the stiffness of the restraint plus one half of the panel stiffness of the end bay for twelve purlins.

$$K_{total} = 15\,{}^{kip}\!/_{in} + \frac{(12)\left(2117\,{}^{lb\cdot in}\!/_{in} + 0\right)}{(2)(8in)\left({}^{1000\,lb}\!/_{kip}\right)} = 16.6\,{}^{kip}\!/_{in}$$

b. Interior bay. The total stiffness attributed to each restraint is the stiffness of the restraint plus one half of the panel stiffness of the interior bay for twelve purlins.

$$K_{total} = 15\,{}^{kip}\!/_{in} + \frac{(12)\left(2317\,{}^{lb\cdot in}\!/_{in} + 0\right)}{(2)(8in)\left({}^{1000\,lb}\!/_{kip}\right)} = 16.7\,{}^{kip}\!/_{in}$$

6. Distribute overturning forces to each restraint.

The total load generated by half the span (tributary to each restraint) is

$$\sum_{N_p} P_i = \left(P_1 + 10\,P_{2-11} + P_{12}\right)$$

a. End bay – half-span adjacent to Frame Line 1

$$\sum_{N_p} P_i = \left(-114\text{ lb}\right) + 10\left(125\text{ lb}\right) + \left(63\text{ lb}\right) = 1199\text{ lb}$$

Force in each anchorage device closest to Frame Line 1

$$P_L = \sum_{N_p} P_i \cdot \frac{K_{rest}}{K_{total}} = \left(1199\text{ lb}\right)\frac{15\,^{kip}\!/_{in}}{16.6\,^{kip}\!/_{in}} = 1083\text{ lb} \qquad \text{(Eq. 5.5.4-55)}$$

b. End bay – half-span adjacent to Frame Line 2

$$\sum_{N_p} P_i = \left(-98\text{ lb}\right) + 10\left(124\text{ lb}\right) + \left(62\text{ lb}\right) = 1204\text{ lb}$$

Force in each anchorage device closest to Frame Line 2

$$P_L = \sum_{N_p} P_i \cdot \frac{K_{rest}}{K_{total}} = \left(1204\text{ lb}\right)\frac{15\,^{kip}\!/_{in}}{16.6\,^{kip}\!/_{in}} = 1088\text{ lb}$$

c. Interior bay

$$\sum_{N_p} P_i = \left(-86\text{ lb}\right) + 10\left(74\text{ lb}\right) + \left(37\text{ lb}\right) = 691\text{ lb}$$

Force in each anchorage device

$$P_L = \sum_{N_p} P_i \cdot \frac{K_{rest}}{K_{total}} = \left(691\text{ lb}\right)\frac{15\,^{kip}\!/_{in}}{16.7\,^{kip}\!/_{in}} = 621\text{ lb}$$

7. Check the deflection of the system and compare to the limits specified in AISI S100 Section I6.4.1

a. Lateral displacement of purlin top flange at anchorage location

Allowable deflection limit (ASD)

$$\Delta_{tf} \le \frac{1}{\Omega}\frac{d}{20} = \frac{1}{2.00}\frac{8\text{ in}}{20} = 0.20\text{ in} \qquad \text{(AISI S100 Eq. I6.4.1-9a)}$$

End bay - third point adjacent to Frame Line 1

$$\Delta_{rest} = \frac{P_L}{K_{rest}} = \frac{1083\text{lb}}{15\,^{kip}\!/_{in}\left(1000\,^{lb}\!/_{kip}\right)} = 0.072\text{ in} \le 0.20\text{ in} \quad \text{OK} \qquad \text{(Eq. 5.5.4-61)}$$

End bay - third point adjacent to Frame Line 2

$$\Delta_{rest} = \frac{P_L}{K_{rest}} = \frac{1088\text{ lb}}{15\,{}^{kip}\!/_{in}\left(1000\,{}^{lb}\!/_{kip}\right)} = 0.073\text{ in} \le 0.20\text{ in} \quad \text{OK} \qquad \text{(Eq. 5.5.4-61)}$$

Interior third points

$$\Delta_{rest} = \frac{P_L}{K_{rest}} = \frac{691\text{ lb}}{15\,{}^{kip}\!/_{in}\left(1000\,{}^{lb}\!/_{kip}\right)} = 0.046\text{ in} \le 0.20\text{ in} \quad \text{OK} \qquad \text{(Eq. 5.5.4-61)}$$

b. Deflection of the diaphragm relative to the restraint (displacement along frame lines)

Allowable deflection limit

$$\Delta_{ms} \le \frac{L}{360} = \frac{25\text{ft}\,{}^{12in}\!/_{ft}}{360} = 0.83\text{ in}$$

$$\Delta_{diaph} = \sum_{N_p}\left(-w\left(\alpha\sigma - \sin\theta\frac{K_{rest}}{K_{total}}\right)\right)_i \frac{L^2}{9G'Bay} + \frac{\sum P_L L}{3G'Bay} \qquad \text{(Eq. 5.5.4-62)}$$

End bay – half-span adjacent to Frame Line 1

$$\Delta_{diaph} = \begin{bmatrix} -57.5\,{}^{lb}\!/_{ft}\left((-1)0.370 - \sin(2.39°)\dfrac{15\,{}^{kip}\!/_{in}}{16.6\,{}^{kip}\!/_{in}}\right) \\ -\left(10\left(115\,{}^{lb}\!/_{ft}\right) + 57.5\,{}^{lb}\!/_{ft}\right)\left((1)0.288 - \sin(2.39°)\dfrac{15\,{}^{kip}\!/_{in}}{16.6\,{}^{kip}\!/_{in}}\right) \end{bmatrix} \frac{(25\text{ft})^2}{9\left(1000\,{}^{lb}\!/_{in}\right)(55\text{ft})} +$$

$$+\frac{(1083\text{ lb})(25\text{ft})}{3(1000\text{lb}/\text{in})(55\text{ft})} = -0.25\text{ in}$$

$$\Delta_{diaph} = -0.25\text{ in} \le 0.83\text{ in} \quad \text{OK}$$

End bay – half-span adjacent to Frame Line 2

$$\Delta_{diaph} = -0.23\text{ in} \le 0.83\text{ in} \quad \text{OK}$$

Interior bay

$$\Delta_{diaph} = -0.28\text{ in} \le 0.83\text{ in} \quad \text{OK}$$

8. Calculate the shear force in the connection between the panels and the purlin at the anchorage device location.

$$P_{sc} = P_L + \frac{wL}{20}\left(-0.9\sigma + \frac{\delta b\cos\theta}{d}\right)\alpha \qquad \text{(Eq. 5.5.4-63)}$$

End bay - third point adjacent to Frame Line 1

$$P_{sc} = 1083\,\text{lb} + \frac{\left(57.5\,{}^{\text{lb}}\!/\!{}_{\text{ft}}\right)\left(25\text{ft}\right)}{20}\left(-0.9\left(0.370\right) + \frac{\left(2.75\text{in}\right)\cos\left(2.39°\right)}{\left(3\right)\left(8.0\text{in}\right)}\right)\left(-1\right) = 1098\,\text{lb}$$

End bay - third point adjacent to Frame Line 2

$$P_{sc} = 1088 + \frac{\left(57.5\,{}^{\text{lb}}\!/\!{}_{\text{ft}}\right)\left(25\text{ft}\right)}{20}\left(-0.9\left(0.391\right) + \frac{\left(2.75\text{in}\right)\cos\left(2.39°\right)}{\left(3\right)\left(8.0\text{in}\right)}\right)\left(-1\right) = 1105\,\text{lb}$$

Interior third points

$$P_{sc} = 621\,\text{lb} + \frac{\left(57.5\,{}^{\text{lb}}\!/\!{}_{\text{ft}}\right)\left(25\text{ft}\right)}{20}\left(-0.9\left(0.399\right) + \frac{\left(2.75\text{in}\right)\cos\left(2.39°\right)}{\left(3\right)\left(8.0\text{in}\right)}\right)\left(-1\right) = 639\,\text{lb}$$

5.5.4.7.3 Example: Supports Plus Third Point Torsional Bracing

Given

1. Four span continuous Z-section purlin system from the example introduced at the beginning of Section 5.5.4.7.
2. Torsional braces are applied at the third points of purlins. Each purlin is attached to rafters with rafter web plates (welded plates). Web plates are 1/4 in. thick by 5 in. wide (b_{pl}) by 7 in. tall. Web plates are attached to the web of the Z-sections with two rows of two 1/2 in. diameter A307 bolts. The bottom row of bolts is 3 in. from the bottom flange and the top row is 6 in. from the bottom flange.

Required

1. Compute the anchorage forces along each frame line due to gravity loads.
2. Compute the end moments of the torsional braces.
3. Compute the lateral deflection of the top flange of the Z-section along each frame line and at the purlin mid-span.
4. Compute the shear force in the standing seam panel clips at each anchorage device.

Solution

Assumptions for Analysis

a. Since the loading, geometry and materials are symmetrical, check the first two spans only.
b. For simplicity, each half-span of the continuous system of purlins is analyzed individually.
c. It is assumed that the stiffness of the adjacent frame lines is approximately the same, i.e., at an interior frame line, half of the total stiffness along the frame line is considered tributary to each adjacent bay.

Procedure

1. Calculate the restraint stiffness of the rafter web plates.

$$K_{rest} = \frac{E \cdot b_{pl} \cdot t_{pl}{}^3 \cdot t^3\left(t^3 h + t_{pl}^3 (d-h)\right)}{\left(t^3 h^2 - t_{pl}^3 (d-h)^2\right)^2 + 4t^3 t_{pl}{}^3 d^2 h (d-h)} \qquad \text{(Eq. 5.5.4-33)}$$

a. Frame Line 1

$$K_{rest} = \frac{E \cdot 5\text{in} \cdot (0.25\text{in})^3 (0.085\text{in})^3 \left((0.085\text{in})^3 6.0\text{in} + (0.25\text{in})^3 (8.0\text{in} - 6.0\text{in})\right)}{\left((0.085\text{in})^3 (6.0\text{in})^2 - (0.25\text{in})^3 (8.0\text{in} - 6.0\text{in})^2\right)^2 + 4(0.085\text{in})^3 (0.25\text{in})^3 (8.0\text{in})^2 6.0\text{in}(8.0\text{in} - 6.0\text{in})}$$

$$K_{rest} = 1589 \text{ lb/in}$$

Total stiffness along exterior frame line

$$K_{total} = \sum_{N_a} K_{rest} + \sum_{N_a - N_p} \frac{K_{rafter}}{d} = \frac{(12)\left(1589 \text{ lb/in}\right)}{1000 \text{ lb/kip}} + \frac{0}{8.0 \text{ in}} = 19.07 \text{ kip/in} \qquad \text{(Eq. 5.5.4-76)}$$

b. Frame Line 2

Equivalent purlin thickness at the lap

$$t_{lap} = \sqrt[3]{t_1^3 + t_2^3} = \sqrt[3]{(0.085in)^3 + (0.059in)^3} = 0.094in$$

$$K_{rest} = 1690\,{}^{lb}\!/_{in}$$

$$K_{total} = \sum_{N_a} K_{rest} + \sum_{N_a - N_p} \frac{K_{rafter}}{d} = \frac{(12)(1690\,{}^{lb}\!/_{in})}{1000\,lb/kip} + \frac{0}{8.0\,in} = 20.28\,{}^{kip}\!/_{in} \qquad \text{(Eq. 5.5.4-76)}$$

c. Frame Line 3

Equivalent purlin thickness at the lap

$$t_{lap} = \sqrt[3]{t_2^3 + t_2^3} = \sqrt[3]{(0.059in)^3 + (0.059in)^3} = 0.074in$$

$$K_{rest} = 1451\,{}^{lb}\!/_{in}$$

$$K_{total} = \sum_{N_a} K_{rest} + \sum_{N_a - N_p} \frac{K_{rafter}}{d} = \frac{(12)(1451\,{}^{lb}\!/_{in})}{1000\,lb/kip} + \frac{0}{8.0\,in} = 17.41\,{}^{kip}\!/_{in} \qquad \text{(Eq. 5.5.4-76)}$$

2. Calculate the moments generated in each third point torsional restraint and the overturning force along the frame line. Analyze each half-span individually.

a. End bay – half-span adjacent to Frame Line 1.

Calculate the uniform restraint provided by the panels, w_{rest}, expressed as a proportion of the applied uniform load.

$$w_{rest} = w \cdot \sigma$$

where

$$\sigma = \frac{C1\dfrac{\left(\dfrac{I_{xy}}{I_x}\cos\theta\right)L^4}{EI_{my}} + \dfrac{((\delta b + m)\cos\theta)d}{2}\left(\dfrac{a^2\beta}{GJ} - \dfrac{L}{2}\cdot\beta_{3rd}\right)\xi + \dfrac{(\alpha)(N_p)L^2\sin\theta}{8G'Bay}}{C1\dfrac{L^4}{EI_{my}} + \dfrac{d^2}{4}\dfrac{a^2\beta}{GJ}\xi + \dfrac{(\alpha)(\eta)L^2}{8G'Bay}} \qquad \text{(Eq. 5.5.4-80)}$$

The uniform restraint force provided by the panels must be calculated separately for the upslope and downslope facing purlins.

Exterior frame line

$K_{trib} = C_3 K_{total}$ = (1.0)(19.07 kip/in) = 19070 lb/in.

$$\xi = \frac{1}{1 + \left(d^2\dfrac{K_{trib}}{N_p} + \dfrac{L}{9}k_{mclip}\right)\beta_{3rd}} \qquad \text{(Eq. 5.5.4-78)}$$

$$\xi = \frac{1}{1+\left((8.0\text{in})^2 \frac{19070\,\text{lb/in}}{12} + \frac{25\,\text{ft}}{9} 2500\,\text{lb·in/rad·ft}\right) 0.000841\,\text{1/lb·in}} = 0.011$$

Purlin 1 (facing downslope) α= -1

$$\sigma = \frac{\begin{bmatrix} \frac{\left(\frac{4.11\text{in}^4}{12.40\,\text{in}^4}\cos(2.39°)\right)(300\text{in})^4}{185\cdot E\cdot 1.148\text{in}^4} + \frac{\left(\left(\frac{2.75\text{in}}{3}+0\right)\cos(2.39°)\right)8.0\text{in}}{2}\left(\frac{(154.6\text{in})^2\,0.132\text{rad}}{G\cdot 0.00306\text{in}^4} - \frac{300\text{in}\cdot 0.000841\,\text{1/lb·in}}{2}\right)0.011 \\ + \frac{(-1)(12)(300\text{in})^2\sin(2.39°)}{8\cdot(1000\,\text{lb/in})(660\text{in})} \end{bmatrix}}{\frac{(300\text{in})^4}{185\cdot E\cdot 1.148\text{in}^4} + \frac{(8.0\text{in})^2}{4\cdot\text{rad}}\left(\frac{(154.6\text{in})^2\,0.132\text{rad}}{G\cdot 0.00306\text{in}^4}\right)0.011 + \frac{(-1)(10)(300\text{in})^2}{8\cdot(1000\,\text{lb/in})(660\text{in})}}$$

σ = 0.367

Purlins 2-12 (facing upslope). Same as above except α=1

$\sigma = 0.294$

Calculate the moment generated at each torsional restraint.

$$M_{3rd} = w\left(\alpha\left(\sigma\frac{d}{2} - (\delta b + m)\cos\theta\right)\frac{a^2\beta}{GJ}\left(d^2\frac{K_{trib}}{N_p} + \frac{L}{9}k_{mclip}\right) + \left(d\sin\theta - (\alpha)\delta b\cos\theta(1-R_{local})\right)\frac{L}{2}\right)\xi$$

(Eq. 5.5.4-73)

where

$$R_{local} = \frac{k_{mclip}}{k_{mclip} + \frac{Et^3}{3d}} = \frac{2500\,\text{lb·in/rad·ft}}{2500\,\text{lb·in/rad·ft} + \frac{E\cdot(0.085\text{in})^3}{3\cdot 8.0\text{in}}\left(12\,\text{in/ft}\right)} = 0.216$$

(Eq. 5.5.4-79)

Purlin 1 (facing downslope). $\alpha = -1$ and $w = 57.5\,\text{lb/ft}$

$$M_{3rd} = 57.5\,\text{lb/ft}\begin{pmatrix} (-1)\left(0.367\frac{8.0\text{in}}{2} - \left(\frac{2.75\text{in}}{3}+0\right)\cos(2.39°)\right)\frac{(154.6\text{in})^2\,0.133\text{rad}}{G\cdot 0.00306\text{in}^4} \\ \left((8.0\text{in})^2\frac{19{,}070\,\text{lb/in}}{12} + \frac{25\text{ft}}{9}2500\,\text{lb·in/rad·ft}\right)\cdot\frac{1\text{ft}}{12\text{in}} \\ +\left(8.0\text{in}\cdot\sin(2.39°) - (-1)\frac{2.75\text{in}}{3}\cos(2.39°)(1-0.216)\right)\frac{25\text{ft}}{2} \end{pmatrix}0.011$$

$M_{3rd} = -282\text{ lb}\cdot\text{in}$

Calculate the overturning force at Frame Line 1.

$$P_i = w\left(\alpha\left(\sigma\frac{d}{2} - (\delta b + m)\cos\theta\right)\frac{a^2\beta}{GJ} - \left(d\sin\theta - (\alpha)\delta b\cos\theta(1-R_{local})\right)\frac{\beta_{3rd}L}{2}\right)d\cdot\frac{K_{trib}}{N_p}\xi$$

(Eq. 5.5.4-77)

$$P_i = 57.5\,{}^{lb}\!/_{ft}\left(\begin{array}{l}(-1)\left(0.367\dfrac{8.0in}{2}-\left(\frac{2.75in}{3}+0\right)\cos(2.39^\circ)\right)\dfrac{(154.6in)^2\,0.133rad}{G\cdot 0.00306in^4}\cdot\dfrac{1ft}{12in}\\ -\left(8.0\,in\cdot\sin(2.39^\circ)-(-1)\frac{2.75in}{3}\cos(2.39^\circ)(1-0.216)\right)\dfrac{0.000839\,{}^{1}\!/_{lb\cdot in}\cdot 25ft}{2}\end{array}\right)(8.0in)\left(\dfrac{19{,}070\,{}^{lb}\!/_{in}}{12}\right)(0.011)$$

$P_i = -123$ lb

Purlins 2-11 (facing upslope). Same as Purlin 1 except $\alpha = 1$, $w = 115\,{}^{lb}\!/_{ft}$, and $\sigma = 0.294$

$M_{3rd} = 268$ lb·in

$P_i = 97$ lb

Purlin 12 (facing upslope). Same as Purlins 2-11 except w = 57.5 lb/ft (half of Purlins 2-11)

$M_{3rd} = 134$lb·in

$P_i = 48$ lb

b. End bay – half-span adjacent to Frame Line 2

Same as previous section. Only half of the total stiffness along the interior frame line is considered tributary to each adjacent half-span.

$K_{trib} = C_3 K_{total} = 0.5\left(20.28\,{}^{kip}\!/_{in}\right) = 10.14\,{}^{kip}\!/_{in}$

$\xi = 0.067$

Purlin 1 (facing downslope). $\alpha = -1$ and w = 57.5 lb/ft

$\sigma = 0.363$

Purlins 2-12 (facing upslope). α= 1 and w = 115 lb/ft

$\sigma = 0.292$

Calculate the moment generated at each torsional restraint and overturning force at Frame Line 2, P_i.

Purlin 1 (facing downslope). $\alpha = -1$ and $w = 57.5$plf

$M_{3rd} = -194$ lb·in

$P_i = -105$ lb

Purlins 2-11 (facing upslope). Same as Purlin 1 except $\alpha = 1$ $w = 115$ plf $\sigma = 0.292$

$M_{3rd} = 190$ lb·in

$P_i = 82$ lb

Purlin 12 (facing upslope). Same as Purlins 2-11 except w = 57.5 lb/ft (half of Purlins 2-11)

$M_{3rd} = 95$ lb·in

$P_i = 41$ lb

c. Interior bay – half-span adjacent to Frame Line 2

Same as previous section. Only half of the total stiffness along the interior frame line is considered tributary to each adjacent half-span.

$$K_{trib} = C_3 K_{total} = 0.5\left(20.28\ ^{kip}\!/_{in}\right) = 10.14\ ^{kip}\!/_{in}$$

$$\xi = 0.045$$

Purlin 1 (facing downslope). α = -1 and w =57.5 lb/ft

$$\sigma = 0.375$$

Purlins 2-12 (facing upslope). α = 1 and w =115 lb/ft

$$\sigma = 0.275$$

Calculate the moment generated at each torsional restraint and overturning force at Frame Line 2, P_i.

Purlin 1 (facing downslope). $\alpha = -1$ and $w = 57.5\text{plf}$

$$M_{3rd} = -244\ \text{lb} \cdot \text{in}$$

$$P_i = -94\ \text{lb}$$

Upslope facing Purlins 2-11 (facing upslope). Same as Purlin 1 except $\alpha = 1 \quad w = 115\text{plf}$

$$\sigma = 0.275$$

$$M_{3rd} = 159\ \text{lb} \cdot \text{in}$$

$$P_i = 45\ \text{lb}$$

Purlin 12 (facing upslope). Same as Purlins 2-11 except w = 57.5 lb/ft (half of Purlins 2-11)

$$M_{3rd} = 80\ \text{lb} \cdot \text{in}$$

$$P_i = 22\ \text{lb}$$

d. Interior bay – half-span adjacent to Frame Line 3.

Same as previous section. Only half of the total stiffness along the interior frame line is considered tributary to each adjacent half-span.

$$K_{trib} = C_3 K_{total} = 0.5\left(17.41\ ^{kip}\!/_{in}\right) = 8.70\ ^{kip}\!/_{in}$$

$$\xi = 0.051$$

Purlin 1 (facing downslope). α = -1 and w =57.5 lb/ft

$$\sigma = 0.373$$

Purlins 2-12 (facing upslope). α=1 and w = 115 lb/ft.

$$\sigma = 0.273$$

Calculate the moment generated at each torsional restraint and overturning force at Frame Line 3, P_i.

Purlin 1 (facing downslope). $\alpha = -1$ and $w = 57.5\text{plf}$

$$M_{3rd} = -237 \text{ lb} \cdot \text{in}$$
$$P_i = -91 \text{ lb}$$

Purlins 2-11 (facing upslope). Same as Purlin 1 except $\alpha = 1$ $\quad w = 115\text{plf}$ $\quad \sigma = 0.274$

$$M_{3rd} = 152 \text{ lb} \cdot \text{in}$$
$$P_i = 43 \text{ lb}$$

Purlin 12 (facing upslope). Same as Purlins 2-12 except $w = 57.5$ plf (half of Purlins 2-11)

$$M_{3rd} = 76 \text{ lb} \cdot \text{in}$$
$$P_i = 22 \text{ lb}$$

3. Calculate the anchorage forces along each frame line.

   The forces, P_i, calculated above include system effects (the inherent stiffness of the system of purlins), therefore it is not necessary to reduce for system effects.

a. Frame line 1

   The total force generated along Frame Line 1 is the sum of forces at each purlin.

$$\sum_{N_p} P_i = P_1 + 10P_{2-11} + P_{12} = -123 \text{ lb} + (10)97 \text{ lb} + 48 \text{ lb} = 895 \text{ lb}$$

   The force along the frame line is distributed according to the relative stiffness of each restraint on the frame line.

$$P_L = \sum_{N_p} P_i \cdot \frac{K_{rest}}{K_{total}} = (895 \text{ lb}) \frac{1.59 \, {}^{kip}\!/_{in}}{19.07 \, {}^{kip}\!/_{in}} = 75 \text{ lb} \qquad \text{(Eq. 5.5.4-74)}$$

b. Frame Line 2

   The total force generated is the sum of forces at each purlin in each half-span adjacent to the frame line.

$$\sum_{N_p} P_i = (P_1 + 10P_{2-11} + P_{12})_{Left} + (P_1 + 10P_{2-11} + P_{12})_{Right}$$

$$\sum_{N_p} P_i = (-105 \text{ lb} + (10)82 \text{ lb} + 41 \text{ lb}) + (-94 \text{ lb} + (10)45 \text{ lb} + 22 \text{ lb}) = 1134 \text{ lb}$$

   The force along the frame line is distributed according to the relative stiffness of each restraint on the frame line.

$$P_L = \sum_{N_p} P_i \cdot \frac{K_{rest}}{K_{total}} = (1134 \text{ lb}) \frac{1.69 \, {}^{kip}\!/_{in}}{20.3 \, {}^{kip}\!/_{in}} = 94 \text{ lb} \qquad \text{(Eq. 5.5.4-74)}$$

c. Frame Line 3

Because the system is symmetric, the total force is two times the sum of the forces for one half bay.

$$\sum_{N_p} P_i = 2(P_1 + 10P_{2-11} + P_{12})$$

$$\sum_{N_p} P_i = 2(P_1 + 10P_{2-11} + P_{12}) = 2(-91\text{ lb} + (10)43\text{ lb} + 21\text{ lb}) = 720\text{ lb}$$

The force along the frame line is distributed according to the relative stiffness of each restraint on the frame line.

$$P_L = \sum_{N_p} P_i \cdot \frac{K_{rest}}{K_{total}} = (720\text{ lb})\frac{1.45\,{}^{kip}/_{in}}{17.40\,{}^{kip}/_{in}} = 60\text{ lb} \qquad \text{(Eq. 5.5.4.-4)}$$

Summary of purlin forces

	End Bay						Interior Bay					
	Adj. to Frame 1			Adj. to Frame 2			Adj. to Frame 2			Adj. to Frame 3		
Purlin	σ	P_i	M_{3rd}	σ	P_i	M_{3rd}	σ	P_i	M_{3rd}	σ	P_i	M_{3rd}
		(lb)	(lb-in)		(lb)	(lb-in)		(lb)	(lb-in)		(lb)	(lb-in)
1	0.367	-123	-282	.363	-105	-194	.375	-94	-244	.323	-91	-237
2-11	0.294	97	268	.292	82	190	.275	45	159	.273	43	152
12	0.294	48	134	.292	41	95	.275	22	80	.273	22	76
	ΣP_i = 895			ΣP_i = 756			ΣP_i = 378			ΣP_i = 360		
				Fr. 2 total P_i = 756+378 = 1134 lb						Fr. 3 total P_i=720 lb		

4. Check the deflection of the system and compare to the limits specified in AISI S100 Section I6.4.1

a. Lateral deflection of the purlin top flange

Allowable deflection limit (ASD)

$$\Delta_{tf} \le \frac{1}{\Omega}\frac{d}{20} = \frac{1}{2.00}\frac{8\text{ in}}{20} = 0.20\text{ in} \qquad \text{(AISI S100 Eq. I6.4.1-9a)}$$

Frame Line 1

$$\Delta_{rest} = \frac{P_L}{K_{rest}} = \frac{(75\text{ lb})}{\left(1.59\,{}^{kip}/_{in}\right)\left(1000\,{}^{lb}/_{kip}\right)} = 0.047\text{ in} \le 0.20\text{ in OK} \qquad \text{(Eq. 5.5.4-81)}$$

Frame Line 2

$$\Delta_{rest} = \frac{P_L}{K_{rest}} = \frac{(94\text{ lb})}{\left(1.69\,{}^{kip}/_{in}\right)\left(1000\,{}^{lb}/_{kip}\right)} = 0.056\text{ in} \le 0.20\text{ in OK} \qquad \text{(Eq. 5.5.4-81)}$$

Frame Line 3

$$\Delta_{rest} = \frac{P_L}{K_{rest}} = \frac{(60\text{ lb})}{\left(1.45\,{}^{kip}\!/\!_{in}\right)\left(1000\,{}^{lb}\!/\!_{kip}\right)} = 0.041\text{ in} \le 0.20\text{ in OK} \quad \text{(Eq. 5.5.4-81)}$$

b. Mid-span deflection of the diaphragm relative to the restraint

Allowable deflection limit

$$\Delta_{ms} \le \frac{L}{180} = \frac{25\text{ft}\left(12\text{in}/\text{ft}\right)}{180} = 1.67\text{in}$$

$$\Delta_{diaph} = \sum_{N_p} \left(w\left(\alpha\sigma - \sin\theta\right)\right)_i \frac{L^2}{8G'Bay} \quad \text{(Eq. 5.5.4-82)}$$

End Bay

The uniform restraint force for each half-span in the bay is averaged. Typically, there should not be a substantial difference between the two.

$$(\sigma_1)_{ave} = \tfrac{1}{2}(0.367 + 0.363) = 0.365$$

$$(\sigma_{2-12})_{ave} = \tfrac{1}{2}(0.294 + 0.292) = 0.293$$

$$\Delta_{diaph} = \left[57.5\text{plf}\left((-1)0.365 - \sin(2.39°)\right) + \left[(10)(115\text{plf}) + (1)(57.5\text{plf})\right]\left((1)0.293 - \sin(2.39°)\right)\right]$$

$$\frac{(25\text{ft})^2}{8\left(1000\,{}^{lb}\!/\!_{in}\right)(55\text{ft})} = 0.40\text{in}$$

$$\Delta_{diaph} = 0.40\text{in} \le 1.67\text{in} \quad \text{OK}$$

Interior bay

$$(\sigma_1)_{ave} = \tfrac{1}{2}(0.375 + 0.373) = 0.374$$

$$(\sigma_{2-12})_{ave} = \tfrac{1}{2}(0.274 + 0.275) = 0.275$$

$$\Delta_{diaph} = \left[57.5\text{plf}\left((-1)0.374 - \sin(2.39°)\right) + \left[(10)(115\text{plf}) + (1)(57.5\text{plf})\right]\left((1)0.275 - \sin(2.39°)\right)\right]$$

$$\frac{(25\text{ft})^2}{8\left(1000\,{}^{lb}\!/\!_{in}\right)(55\text{ft})} = 0.37\text{ in}$$

$$\Delta_{diaph} = 0.37\text{ in} \le 1.67\text{in} \quad \text{OK}$$

Summary of System Deflections

Deflections at Frame Line

Frame line 1 $\Delta_{rest} = 0.047\text{ in} \le 0.20\text{ in}$ OK

Frame line 2 $\Delta_{rest} = 0.056\text{ in} \le 0.20\text{ in}$ OK

Frame line 3 $\Delta_{rest} = 0.041\text{ in} \le 0.20\text{ in}$ OK

Deflections at Purlin Mid-span

End Bay $\Delta_{diaph} = 0.40\,\text{in} \le 1.67\,\text{in}$ OK

Interior Bay $\Delta_{diaph} = 0.37\,\text{in} \le 1.67\,\text{in}$ OK

5. Calculate the shear force in the connection between the panels and the purlin at the anchorage device location

$$P_{sc} = P_L + \left(\frac{wL}{2}(0.9\sigma\alpha - \sin\theta) - P_i\right) \qquad \text{(Eq. 5.5.4-83)}$$

a. Frame Line 1 – typical purlin

$$P_{sc} = 74\,\text{lb} + \frac{(115\text{plf})(25\text{ft})}{2}\left(0.9(0.294)(1) - \sin(2.39°)\right) - (96\text{lb}) = 298\,\text{lb}$$

b. Frame Line 2 – typical purlin

$$P_{sc} = 95 + \frac{(115\text{plf})(25\text{ft})}{2}\left(0.9(0.292)(1) - \sin(2.39°)\right) - 82\,\text{lb}$$
$$+ \frac{(115\text{plf})(25\text{ft})}{2}\left(0.9(0.275)(1) - \sin(2.39°)\right) - 45\,\text{lb} = 546\,\text{lb}$$

c. Frame Line 3 – typical purlin

$$P_{sc} = 63 + 2 \cdot \left[\frac{(115\text{plf})(25\text{ft})}{2}\left(0.9(0.274)(1) - \sin(2.39°)\right) - 43\,\text{lb}\right] = 566\,\text{lb}$$

5.5.4.7.4 Example: Supports Plus Third Point Lateral Anchorage

Given

1. Four span continuous Z-purlin system introduced at the beginning of Section 5.5.4.7.
2. Third point braces are applied at the third points of the eave purlin (Purlin 1). Each lateral brace is applied at the purlin top flange and has a stiffness of 15.0 kip/in.
3. Each purlin is attached to rafters with rafter web plates (welded plates). Web plates are 1/4 in. thick by 5 in. wide (b_{pl}) by 7 in. tall. Web plates are attached to the web of the Z-sections with two rows of two 1/2 in. diameter A307 bolts. The bottom row of bolts is 3 in. from the bottom flange and the top row is 6 in. from the bottom flange.

Required

1. Compute the anchorage forces along each frame line and each third point due to gravity loads.
2. Compute the lateral deflection of the top flange of the Z-section along each frame line and at the purlin third points.
3. Compute the shear force in the standing seam panel clips at the frame line for a typical upslope facing purlin and at the third points at the restrained purlin.

Solution

Assumptions for Analysis

a. Since the loading, geometry and materials are symmetrical, check the first two spans only.
b. For simplicity, each half-span of the continuous system of purlins is analyzed individually.
c. It is assumed that the stiffness of the adjacent frame lines is approximately the same, i.e., at an interior frame line, half of the total stiffness along the frame line is considered tributary to each adjacent bay.

Procedure

1. Calculate the restraint stiffness of the rafter web plates.

Calculations for rafter web plates are shown in Section 5.5.4.7.3

a. Frame Line 1

Stiffness of the web bolted plate connection $K_{rest} = (K_{rest})_{spt} = 1589$ lb/in.

Total stiffness along Frame Line 1

$$K_{spt} = \sum_{N_a}(K_{rest})_{spt} + \frac{\sum\limits_{N_p - N_a} K_{rafter}}{d} = (12)\frac{1589\ \text{lb/in}}{1000\ \text{lb/kip}} + \frac{0}{8.0\ \text{in}} = 19.07\ \text{kip/in} \qquad \text{(Eq. 5.5.4-88)}$$

b. Frame Line 2

Equivalent purlin thickness at the lap $t_{lap} = 0.094$ in

Stiffness of the web bolted plate connection $K_{rest} = (K_{rest})_{spt} = 1690$ lb/in.

Total stiffness along Frame Line 2

$$K_{spt} = \sum_{N_a}(K_{rest})_{spt} + \frac{\sum_{N_p-N_a} K_{rafter}}{d} = (12)\frac{1690\,{}^{lb}\!/_{in}}{1000\,{}^{lb}\!/_{kip}} + \frac{0}{8.0\,in} = 20.28\,{}^{kip}\!/_{in} \quad \text{(Eq. 5.5.4-88)}$$

c. Frame Line 3

Equivalent purlin thickness at the lap $t_{lap} = 0.074$ in

Stiffness of the web bolted plate connection $K_{rest} = 1451\,{}^{lb}\!/_{in}$

Total stiffness along Frame Line 3

$$K_{spt} = \sum_{N_a}(K_{rest})_{spt} + \frac{\sum_{N_p-N_a} K_{rafter}}{d} = (12)\frac{1451\,{}^{lb}\!/_{in}}{1000\,{}^{lb}\!/_{kip}} + \frac{0}{d} = 17.41\,{}^{kip}\!/_{in} \quad \text{(Eq. 5.5.4-88)}$$

2. Calculate the overturning forces and distribute between the third points and the frame lines.

a. End bay – half-span adjacent to Frame Line 1

$$K_{trib} = C3(K_{spt}) = 1.0\left(19.07\,{}^{kip}\!/_{in}\right) = 19.07\,{}^{kip}\!/_{in}$$

$$K_{3rd} = 15.0\,{}^{kip}\!/_{in}$$

Reduction factor to account for the panel system effects

$$R_{sys} = \frac{1}{2}\left(\frac{{}^{1}\!/_{4}Et^3}{0.38k_{mclip}d + 0.71\frac{Et^3}{4}}\right)\left(1 - {}^{2}\!/_{3}k_{mclip}\tau\right) \quad \text{(Eq. 5.5.4-91)}$$

$$R_{sys} = \frac{1}{2}\left(\frac{{}^{1}\!/_{4}E(0.085in)^3}{(0.38)\left(\frac{2500\,{}^{lb\cdot in}\!/_{rad\cdot ft}}{12\,{}^{in}\!/_{ft}}\right)(8.0\,in) + (0.71)\frac{E(0.085in)^3}{4}}\right)\left(1 - {}^{2}\!/_{3}\left(\frac{2500\,{}^{lb\cdot in}\!/_{rad\cdot ft}}{12\,{}^{in}\!/_{ft}}\right)\left(0.0055\,{}^{rad}\!/_{lb}\right)\right) = 0.139$$

Reduction factor to account for the local deformation

$$R_{local} = \frac{k_{mclip}}{k_{mclip} + \frac{Et^3}{3d}} = \frac{2500\,{}^{lb\cdot in}\!/_{rad\cdot ft}}{2500\,{}^{lb\cdot in}\!/_{rad\cdot ft} + \frac{E(0.085in)^3}{3(8.0in)}\left(12\,{}^{in}\!/_{ft}\right)} = 0.216 \quad \text{(Eq. 5.5.4-92)}$$

Calculate the uniform restraint force in the panels. $w_{rest} = w \cdot \sigma$

Purlin 1 (facing downslope). α = -1, C1 = 5/972, C2 = 65/4779 and w =57.5 lb/ft

$$\psi = \frac{(3G'BayK_{3rd})\left(1 + k_{mclip}\frac{\kappa}{GJ}\right)\left(N_p k_{mclip} L R_{sys} + 2d^2 K_{trib}\right)}{X1 + X2} \quad \text{(Eq. 5.5.4-94)}$$

where

$$X1 = \left(3G'BayK_{trib} + LK_{trib}K_{3rd}\right)\left(1 + k_{mclip}\frac{\kappa}{GJ}\right)\left(N_p k_{mclip} LR_{sys} + 2d^2 K_{trib}\right) \qquad \text{(Eq. 5.5.4-95)}$$

$$X2 = \left(3G'BayK_{3rd}\right)\left(2d^2 K_{trib}\right)\left(1 + k_{mclip}\frac{\kappa}{GJ} - \frac{\beta_{3rd}}{4}\frac{2}{3}k_{mclip}L\right) \qquad \text{(Eq. 5.5.4-96)}$$

$$X1 = \left[\begin{array}{l} \left[3\left(\frac{1000\,{}^{lb}/_{in}}{1000\,{}^{lb}/_{kip}}\right)(660in)\left(19.07\,{}^{kip}/_{in}\right) + (300in)\left(19.07\,{}^{kip}/_{in}\right)\left(15\,{}^{kip}/_{in}\right)\right] x \\ \left(1 + \frac{2500\,{}^{lb\cdot in}/_{rad\cdot ft}}{12\,{}^{in}/_{ft}}\frac{2582rad\cdot in^2}{G\cdot 0.00306in^4}\right)\times \\ \times\left((12)\left(\frac{2500\,{}^{lb\cdot in}/_{rad\cdot ft}}{\left(1000\,{}^{lb}/_{kip}\right)\left(12\,{}^{in}/_{ft}\right)}\right)(300in)(0.139) + (2)(8in)^2\left(19.07\,{}^{kip}/_{in}\right)\right) \end{array}\right] = 5.236\cdot 10^9\,kip^3$$

$$X2 = \left[\begin{array}{l} \left[3\left(\frac{1000\,{}^{lb}/_{in}}{1000\,{}^{lb}/_{kip}}\right)(660in)\left(15\,{}^{kip}/_{in}\right)\right]\left((2)(8in)^2\left(19.07\,{}^{kip}/_{in}\right)\right)\times \\ \times\left(1 + \frac{2500\,{}^{lb\cdot in}/_{rad\cdot ft}}{12\,{}^{in}/_{ft}}\frac{2582rad\cdot in^2}{G\left(0.00306in^4\right)} - \frac{0.000841\,{}^{rad}/_{lb\cdot in}}{4}\left(\frac{2}{3}\right)\left(2500\,{}^{lb\cdot in}/_{rad\cdot ft}\right)(25ft)\right) \end{array}\right] = 5.733x10^8\,kip^3$$

$$\psi = \frac{\left(3\left(\frac{1000\,{}^{lb}/_{in}}{1000\,{}^{lb}/_{kip}}\right)(660in)\left(15\,{}^{kip}/_{in}\right)\right)\left(1 + \frac{2500\,{}^{lb\cdot in}/_{rad\cdot ft}}{12\,{}^{in}/_{ft}}\frac{2582rad\cdot in^2}{G\cdot 0.00306in^4}\right)\left[\begin{array}{l}(12)\left(\frac{2500\,{}^{lb\cdot in}/_{rad\cdot ft}}{\left(1000\,{}^{lb}/_{in}\right)\left(12\,{}^{in}/_{ft}\right)}\right)(300in)(0.135) + \\ (2)(8.0in)^2\left(19.07\,{}^{kip}/_{in}\right)\end{array}\right]}{5.236\cdot 10^9\,kip^3 + 5.733\cdot 10^8\,kip^3} = 0.217$$

$$\Gamma = \left(C2\frac{\alpha L^3}{EI_{my}} + \frac{\alpha\frac{d^2}{4}\beta_{3rd}}{\left(1 + k_{mclip}\frac{\kappa}{GJ}\right)} - \frac{N_p\cdot L}{3G'Bay}\right)\frac{1}{N_p} \qquad \text{(Eq. 5.5.4-97)}$$

$$\Gamma = \left(\frac{65(-1)(300in)^3}{4779\cdot E\cdot 1.148in^4} + \frac{(-1)\frac{(8.0in)^2}{4}0.000841\,{}^{rad}/_{lb\cdot in}}{1 + \frac{2500\,{}^{lb\cdot in}/_{rad\cdot ft}}{12\,{}^{in}/_{ft}}\frac{2582rad\cdot in^2}{G\cdot 0.00306in^4}} - \frac{(12)25ft}{3\left(1000\,{}^{lb}/_{in}\right)(55ft)}\right)\cdot\frac{1}{12} = -0.00112\,{}^{in}/_{lb}$$

$$A = \left(\frac{\delta b + m}{\delta b}\right) + \eta\alpha\frac{L}{d^2}\left(\frac{2}{3}k_{mclip}\left(\frac{\delta b + m}{\delta b}\right) - \frac{\left(1 - R_{Local}\right)}{\tau}\right)\left(\frac{2d^2 K_{trib}}{2d^2 K_{trib} + N_p k_{mclip} LR_{sys}}\right)\Gamma\psi$$

(Eq. 5.5.4-98)

$$A = 1 + \left[(10)(-1)\frac{300\text{in}}{(8.0\text{in})^2}\left(\frac{2}{3}\left(\frac{2500\,{}^{\text{lb}\cdot\text{in}}/_{\text{rad}\cdot\text{ft}}}{12\,{}^{\text{in}}/_{\text{ft}}}\right)(1) - \frac{(1-0.216)}{0.0055\,{}^{\text{rad}}/_{\text{lb}}}\right) \times \left(\frac{2(8.0\text{in})^2\,19.07\,{}^{\text{kip}}/_{\text{in}}}{2(8.0\text{in})^2\,19.07\,{}^{\text{kip}}/_{\text{in}} + (12)\left(\frac{2500\,{}^{\text{lb}\cdot\text{in}}/_{\text{rad}\cdot\text{ft}}}{1000\,{}^{\text{lb}}/_{\text{kip}}}\right)(25\text{ft})(0.135)}\right)\cdot\left(-0.00112\,{}^{\text{in}}/_{\text{lb}}\right)(0.217) \right] = 0.960$$

$$B = \frac{(2K_{trib} - K_{3rd})3G'Bay}{LK_{trib}K_{3rd} + 3G'Bay(K_{trib} + K_{3rd})} \qquad \text{(Eq. 5.5.4-99)}$$

$$B = \frac{\left(2\cdot 19.07\,{}^{\text{kip}}/_{\text{in}} - 15\,{}^{\text{kip}}/_{\text{in}}\right)(3)\left(\frac{1000\,{}^{\text{lb}}/_{\text{in}}}{1000\,{}^{\text{lb}}/_{\text{kip}}}\right)(55\text{ft})}{25\text{ft}\left(19.07\,{}^{\text{kip}}/_{\text{in}}\right)\left(15\,{}^{\text{kip}}/_{\text{in}}\right) + 3\left(\frac{1000\,{}^{\text{lb}}/_{\text{in}}}{1000\,{}^{\text{lb}}/_{\text{kip}}}\right)(55\text{ft})\left(19.07\,{}^{\text{kip}}/_{\text{in}} + 15\,{}^{\text{kip}}/_{\text{in}}\right)} = 0.299$$

$$C = 1 + \alpha\eta\frac{\frac{2}{3}k_{mclip}L}{d^2}\left(\frac{2d^2K_{trib}}{2d^2K_{trib} + N_p k_{mclip} L R_{sys}}\right)\Gamma\psi \qquad \text{(Eq. 5.5.4-100)}$$

$$C = 1 + (10)(-1)\frac{\frac{2}{3}\left(\frac{2500\,{}^{\text{lb}\cdot\text{in}}/_{\text{rad}\cdot\text{ft}}}{12\,{}^{\text{in}}/_{\text{ft}}}\right)300\text{in}}{(8.0\text{in})^2}\left(\frac{2(8.0\text{in})^2\,19.07\,{}^{\text{kip}}/_{\text{in}}}{2(8.0\text{in})^2\,19.07\,{}^{\text{kip}}/_{\text{in}} + (12)\left(\frac{2500\,{}^{\text{lb}\cdot\text{in}}/_{\text{rad}\cdot\text{ft}}}{1000\,{}^{\text{lb}}/_{\text{kip}}}\right)(25\text{ft})(0.135)}\right)\text{x}$$

$$\text{x}\left(0.00112\,{}^{\text{in}}/_{\text{lb}}\right)(0.217)$$

$$C = 2.52$$

$$\sigma = \frac{C1\frac{\left(\frac{I_{xy}}{I_x}\cos\theta\right)L^4}{EI_{my}} + A\cdot\frac{((\delta b)\cos\theta)d}{2}\tau + B\cdot\frac{n_p\alpha L^2\sin\theta}{18G'Bay}}{C1\frac{L^4}{EI_{my}} + C\cdot\frac{d^2}{4}\tau + \frac{\eta\alpha L^2}{9G'Bay}(1 + K_{trib}\psi\Gamma)} \qquad \text{(Eq. 5.5.4-93)}$$

$$\sigma = \frac{\frac{5\left(\frac{4.11\text{in}^4}{12.40\text{in}^4}\cos(2.39°)\right)(300\text{in})^4}{972\cdot E\cdot 1.15\text{in}^4} + (0.960)\frac{\left(\frac{2.75\text{in}}{3}\cos(2.39°)\right)8.0\text{in}}{2\cdot\text{rad}}0.0055\frac{\text{rad}}{\text{lb}} + (0.299)\frac{(12)(-1)(300\text{in})^2\sin(2.39°)}{18\cdot\left(1000\,{}^{\text{lb}}/_{\text{in}}\right)(660\text{in})}}{\frac{5(300\text{in})^4}{972\cdot E\cdot 1.15\text{in}^4} + (2.52)\frac{(8.0\text{in})^2}{4\cdot\text{rad}}0.0055\frac{\text{rad}}{\text{lb}} + \frac{(10)(-1)(300\text{in})^2}{9\cdot\left(1000\,{}^{\text{lb}}/_{\text{in}}\right)(660\text{in})}\left(1 + \left(19.07\,{}^{\text{kip}}/_{\text{in}}\right)(0.217)\left(-0.00112\,{}^{\text{in}}/_{\text{lb}}\right)\left(1000\,{}^{\text{lb}}/_{\text{kip}}\right)\right)} = 0.212$$

$$w_{rest} = w\cdot\sigma = 57.5\,{}^{\text{lb}}/_{\text{ft}}(0.212) = 12.2\,{}^{\text{lb}}/_{\text{ft}}$$

Calculate the distribution of the downslope force between the third point and the frame line restraint

$$D_{3rd} = \frac{K_{3rd}(9G'Bay + 2LK_{trib})}{3[LK_{trib}K_{3rd} + 3G'Bay(K_{trib} + K_{3rd})]}\left(\frac{2d^2(K_{trib} + K_{3rd})}{2d^2(K_{trib} + K_{3rd}) + n_p k_{mclip} LR_{sys}}\right)$$

(Eq. 5.5.4-101)

$$D_{Spt} = \frac{K_{trib}(9G'Bay + LK_{3rd})}{3[LK_{trib}K_{3rd} + 3G'Bay(K_{trib} + K_{3rd})]}\left(\frac{2d^2(K_{trib} + K_{3rd})}{2d^2(K_{trib} + K_{3rd}) + N_p k_{mclip} LR_{sys}}\right)$$

(Eq. 5.5.4-102)

$$D_{3rd} = \left[\frac{15\,{}^{kip}/_{in}\left(9\left(\frac{1000\,{}^{lb}/_{in}}{1000\,{}^{lb}/_{kip}}\right)(55ft) + 2\left(19.07\,{}^{kip}/_{in}\right)25ft\right)}{3\left[(25ft)\left(19.07\,{}^{kip}/_{in}\right)\left(15\,{}^{kip}/_{in}\right) + 3\left(\frac{1000\,{}^{lb}/_{in}}{1000\,{}^{lb}/_{kip}}\right)(55ft)\left(19.07\,{}^{kip}/_{in} + 15\,{}^{kip}/_{in}\right)\right]} \times \left(\frac{2(8.0in)^2\left(19.07\,{}^{kip}/_{in} + 15\,{}^{kip}/_{in}\right)}{2(8.0in)^2\left(19.07\,{}^{kip}/_{in} + 15\,{}^{kip}/_{in}\right) + (12)\left(\frac{2500\,{}^{lb\cdot in}/_{rad\cdot ft}}{1000\,{}^{lb}/_{kip}}\right)(25ft)(0.135)}\right)\right] = 0.55$$

$$D_{spt} = \left[\frac{19.07\,{}^{kip}/_{in}\left(9\left(\frac{1000\,{}^{lb}/_{in}}{1000\,{}^{lb}/_{kip}}\right)(55ft) + \left(15\,{}^{kip}/_{in}\right)25ft\right)}{3\left[(25ft)\left(19.07\,{}^{kip}/_{in}\right)\left(15\,{}^{kip}/_{in}\right) + 3\left(\frac{1000\,{}^{lb}/_{in}}{1000\,{}^{lb}/_{kip}}\right)(55ft)\left(19.07\,{}^{kip}/_{in} + 15\,{}^{kip}/_{in}\right)\right]} \times \left(\frac{2(8.0in)^2\left(19.07\,{}^{kip}/_{in} + 15\,{}^{kip}/_{in}\right)}{2(8.0in)^2\left(19.07\,{}^{kip}/_{in} + 15\,{}^{kip}/_{in}\right) + (12)\left(\frac{2500\,{}^{lb\cdot in}/_{rad\cdot ft}}{1000\,{}^{lb}/_{kip}}\right)(25ft)(0.135)}\right)\right] = 0.42$$

$$(P_{3rd})_i = \frac{wL}{2}\cdot\left[\left(\frac{\delta b\cos\theta}{d}(1 - R_{local}) + \frac{2}{3}k_{mclip}\left(\frac{\sigma}{2} - \frac{(\delta b + m)}{d}\cos\theta\right)\tau\right)\left(\frac{2d^2K_{trib}}{2d^2K_{trib} + N_p k_{mclip} LR_{sys}}\right)\psi\alpha + \frac{2K_{trib}\sigma L}{9G'Bay}\psi\alpha - \sin\theta D_{3rd}\right]$$

(Eq. 5.5.4-89)

$$\left(P_{3rd}\right)_1=\frac{(57.5\text{plf})(25\text{ft})}{2}\cdot\left(\begin{array}{l}\left(\dfrac{\frac{2.75\text{in}}{3}\cos(2.39°)}{8.0\text{in}}(1-0.216)+\frac{2}{3}\dfrac{2500\,{}^{\text{lb}\cdot\text{in}}/_{\text{rad}\cdot\text{ft}}}{12\,{}^{\text{in}}/_{\text{ft}}}\left(\dfrac{0.212}{2}-\dfrac{\left(\frac{2.75\text{in}}{3}+0\right)\cos(2.39°)}{8.0\text{in}}\right)0.0055\,{}^{\text{rad}}/_{\text{lb}}\right)\times\\ \times\left(\dfrac{2(8.0\text{in})^2\left(19.07\,{}^{\text{kip}}/_{\text{in}}\right)}{2(8.0\text{in})^2\left(19.07\,{}^{\text{kip}}/_{\text{in}}\right)+(12)\left(\dfrac{2500\,{}^{\text{lb}\cdot\text{in}}/_{\text{rad}\cdot\text{ft}}}{1000\,{}^{\text{lb}}/_{\text{kip}}}\right)(25\text{ft})(0.135)}\right)(0.217)(-1)\\ +\dfrac{(2)\left(19.07\,{}^{\text{kip}}/_{\text{in}}\right)(0.212)(\cdot 25\text{ft})}{9\left(\dfrac{1000\,{}^{\text{lb}}/_{\text{in}}}{1000\,{}^{\text{lb}}/_{\text{kip}}}\right)(55\text{ft})}(-1)(0.217)-\sin(2.39°)(0.55)\end{array}\right)$$

$$\left(P_{3rd}\right)_1=-92.6\text{ lb}$$

$$F=\frac{\left(\frac{\beta_{3rd}}{4}\frac{2}{3}k_{mclip}L-\left(1+k_{mclip}\frac{\kappa}{GJ}\right)\right)}{\left(1+k_{mclip}\frac{\kappa}{GJ}\right)}\left(\frac{2d^2K_{trib}}{2d^2K_{trib}+N_pk_{mclip}LR_{sys}}\right)\psi \qquad \text{(Eq. 5.5.4-103)}$$

$$F=\left[\begin{array}{l}\left(\dfrac{\left(\frac{0.000841\,{}^{1}/_{\text{lb}\cdot\text{in}}}{4}\frac{2}{3}\left(2500\,{}^{\text{lb}\cdot\text{in}}/_{\text{rad}\cdot\text{ft}}\right)(25\text{ft})-\left(1+\frac{2500\,{}^{\text{lb}\cdot\text{in}}/_{\text{rad}\cdot\text{ft}}}{12\,{}^{\text{in}}/_{\text{ft}}}\frac{2582\text{rad}\cdot\text{in}^2}{G\cdot 0.00306\text{in}^4}\right)\right)}{\left(1+\frac{2500\,{}^{\text{lb}\cdot\text{in}}/_{\text{rad}\cdot\text{ft}}}{12\,{}^{\text{in}}/_{\text{ft}}}\frac{2582\text{rad}\cdot\text{in}^2}{G\cdot 0.00306\text{in}^4}\right)}\right)\times\\ \times\left(\dfrac{2(8.0\text{in})^2\left(19.07\,{}^{\text{kip}}/_{\text{in}}\right)}{2(8.0\text{in})^2\left(19.07\,{}^{\text{kip}}/_{\text{in}}\right)+(12)\left(\dfrac{2500\,{}^{\text{lb}\cdot\text{in}}/_{\text{rad}\cdot\text{ft}}}{1000\,{}^{\text{lb}}/_{\text{kip}}}\right)(25\text{ft})(0.135)}\right)(0.217)\end{array}\right]=-0.0989$$

$$\left(P_{spt}\right)_i=\frac{wL}{2}\cdot\left[\begin{array}{l}\left(\dfrac{\delta b\cos\theta}{d}(1-R_{local})+\frac{2}{3}k_{mclip}\left(\dfrac{\sigma}{2}-\dfrac{(\delta b+m)}{d}\cos\theta\right)\tau\right)\left(\dfrac{2d^2K_{trib}}{2d^2K_{trib}+N_pk_{mclip}LR_{sys}}\right)\alpha(1+F)\\ +\dfrac{2K_{trib}\sigma L}{9G'Bay}\alpha F-\sin\theta D_{spt}\end{array}\right]$$

(Eq. 5.5.4-90)

$$\left(P_{spt}\right)_1 = \frac{(57.5\text{plf})(25\text{ft})}{2}\cdot\left(\begin{array}{l}\left(\dfrac{\frac{2.75\text{in}}{3}\cos(2.39°)}{8.0\text{in}}(1-0.216)+\frac{2}{3}\dfrac{2500\,{}^{\text{lb·in}}\!/\!_{\text{rad·ft}}}{12\,{}^{\text{in}}\!/\!_{\text{ft}}}\left(\dfrac{0.212}{2}-\dfrac{\left(\frac{2.75\text{in}}{3}+0\right)\cos(2.39°)}{8.0\text{in}}\right)0.0055\,{}^{\text{rad}}\!/\!_{\text{lb}}\right)\times \\ \times\left(\dfrac{2(8.0\text{in})^2\left(19.07\,{}^{\text{kip}}\!/\!_{\text{in}}\right)}{2(8.0\text{in})^2\left(19.07\,{}^{\text{kip}}\!/\!_{\text{in}}\right)+(12)\left(\dfrac{2500\,{}^{\text{lb·in}}\!/\!_{\text{rad·ft}}}{1000\,{}^{\text{lb}}\!/\!_{\text{kip}}}\right)(25\text{ft})(0.135)}\right)(-1)(1+(-0.0989)) \\ +\dfrac{(-1)(2)\left(19.07\,{}^{\text{kip}}\!/\!_{\text{in}}\right)(0.179)(\cdot 25\text{ft})}{9\left(\dfrac{1000\,{}^{\text{lb}}\!/\!_{\text{in}}}{1000\,{}^{\text{lb}}\!/\!_{\text{kip}}}\right)(55\text{ft})}(-1)(-0.10)-\sin(2.39°)(0.42)\end{array}\right)$$

$\left(P_{spt}\right)_1 = -35.3\text{ lb}$

Purlins 2-11 (facing upslope) $\alpha = 1$ and w = 115 lb/ft

$\psi = 0.217$ (same as Purlin 1)

$\Gamma = 0.00082\,{}^{\text{in}}\!/\!_{\text{lb}}$

$A = 0.971$

$B = 0.299$ (same as Purlin 1)

$C = 2.11$

$\sigma = 0.206$

$D_{3rd} = 0.55$ (same as Purlin 1)

$D_{spt} = 0.42$ (same as Purlin 1)

Forces generated

$\left(P_{3rd}\right)_{2-11} = 115\text{ lb}$

$F = -0.10$ (same as Purlin 1)

$\left(P_{spt}\right)_{2-11} = 19\text{ lb}$

Purlin 12 (facing upslope). α = 1 and w =57.5 lb/ft. Since the uniform loading is half that of Purlins 2-11, the brace forces generated are half that for Purlins 2-11.

$\left(P_{3rd}\right)_{12} = 57\text{ lb}$

$\left(P_{spt}\right)_{12} = 9.5\text{ lb}$

b. End bay – half-span adjacent to Frame Line 2

Same as previous section. Only half of the stiffness along the interior frame line is considered tributary to each adjacent half-span.

$K_{trib} = C3\left(K_{spt}\right) = 0.5\left(20.28\,{}^{\text{kip}}\!/\!_{\text{in}}\right) = 10.14\,{}^{\text{kip}}\!/\!_{\text{in}}$

$K_{3rd} = 15.0 \,{}^{kip}\!/_{in}$

Reduction factor to account for the panel system effects

$R_{sys} = 0.221$

Reduction factor to account for local deformation.

$R_{local} = 0.216$ (same as previous)

Calculate the uniform restraint force in the panels. $w_{rest} = w \cdot \sigma$

Purlin 1 (facing downslope). α = -1, C1 = 7/1944, C2 = 91/8100 and w =57.5 lb/ft

$X1 = 4.975 \cdot 10^{17}\ lb^3$

$X2 = 1.081 \cdot 10^{17}\ lb^3$

$\psi = 0.373$

$\Gamma = -0.000955 \,{}^{in}\!/_{lb}$

$A = 0.477$

$B = 0.110$

$C = 3.06$

$\sigma = 0.198$

$w_{rest} = w \cdot \sigma = 57.5 \,{}^{lb}\!/_{ft} \cdot 0.198 = 11.4 \,{}^{lb}\!/_{ft}$

Calculate the distribution of the downslope force between the third point and the frame line restraint.

$D_{3rd} = 0.60$

$D_{spt} = 0.35$

$\left(P_{3rd}\right)_1 = -91\ lb$

$F = -0.179$

$\left(P_{spt}\right)_1 = -26\ lb$

Purlins 2-11 (facing upslope). $\alpha = 1$ and w = 115 lb/ft

$\psi = 0.373$ (same as Purlin 1)

$\Gamma = 0.000652 \,{}^{in}\!/_{lb}$

$A = 0.644$

$B = 0.108$ (same as Purlin 1)

$C = 2.40$

$\sigma = 0.190$

$w_{rest} = w \cdot \sigma = 115 \,{}^{lb}\!/_{ft} \cdot 0.190 = 21.9 \,{}^{lb}\!/_{ft}$

$D_{3rd} = 0.60$ (same as Purlin 1)

$D_{spt} = 0.35$ (same as Purlin 1)

Forces generated

$(P_{3rd})_{2-11} = 105\text{ lb}$

$F = -0.179$ (same as Purlin 1)

$(P_{spt})_{2-11} = 10.3\text{ lb}$

Purlin 12 (facing upslope). $\alpha = 1$ and w = 57.5 lb/ft. Since the uniform loading is half that of Purlins 2-11, the brace forces generated are half that for Purlins 2-11.

$(P_{3rd})_{12} = 52\text{ lb}$

$(P_{spt})_{12} = 5.2\text{ lb}$

c. Interior bay – half-span adjacent to Frame Line 2.

Half of the total stiffness along the interior frame line is considered tributary to each adjacent half-span.

$K_{trib} = 0.5(K_{spt}) = 0.5(20.28\ \text{kip/in}) = 10.14\ \text{kip/in}$

$K_{3rd} = 15.0\ \text{kip/in}$

Reduction factor to account for the panel system effects

$R_{sys} = 0.148$

Reduction factor to account for local deformation

$R_{local} = 0.452$

Calculate the uniform restraint force in the panels. $w_{rest} = w \cdot \sigma$

Purlin 1 (facing downslope). α = -1 and w =57.5 lb/ft

$X1 = 6.846 \cdot 10^{17}\ \text{lb}^3$

$X2 = 1.445 \cdot 10^{17}\ \text{lb}^3$

$\psi = 0.373$

$\Gamma = -0.000811\ \text{in/lb}$

$A = 1.323$

$B = 0.110$

$C = 2.81$

$\sigma = 0.207$

$w_{rest} = w \cdot \sigma = 57.5\,\text{plf} \cdot 0.207 = 11.9\,\text{plf}$

Calculate the distribution of the downslope force between the third point and frame line restraint.

$D_{3rd} = 0.61$

$D_{spt} = 0.36$

Forces generated

$(P_{3rd})_1 = -89 \text{ lb}$

$F = -0.174$

$(P_{spt})_1 = -14.6 \text{ lb}$

Purlins 2-11 (facing upslope). α = 1 and w =115 lb/ft

$\psi = 0.373$ (same as Purlin 1)
$\Gamma = 0.000508 \, {}^{in}\!/\!_{lb}$
$A = 1.202$
$B = 0.110$ (same as Purlin 1)
$C = 2.14$
$\sigma = 0.194$
$D_{3rd} = 0.61$ (same as Purlin 1)
$D_{spt} = 0.36$ (same as Purlin 1)

Forces generated

$(P_{3rd})_{2-11} = 95 \text{ lb}$
$F = -0.174$ (same as Purlin 1)
$(P_{spt})_{2-11} = -15.4 \text{ lb}$

Purlin 12 (facing upslope). α = 1 and w =57.5 lb/ft. Since the uniform loading is half that of Purlins 2-11, the brace forces generated are half that for Purlins 2-11.

$(P_{3rd})_{12} = 48 \text{ lb}$

$(P_{spt})_{12} = -7.7 \text{ lb}$

d. Interior bay – half-span adjacent to Frame Line 3.

The stiffness of the restraints along Frame Line 3 is slightly less than along Frame Line 2. In lieu of performing additional calculations, the restraint forces determined above can be conservatively used for the half-span adjacent to Frame Line 3.

Restraint Stiffness

$K_{trib} = 0.5(K_{spt}) = 0.5(17.41 \, {}^{kip}\!/\!_{in}) = 8.7 \, {}^{kip}\!/\!_{in}$

$K_{3rd} = 15.0 \, {}^{kip}\!/\!_{in}$

Purlin 1 (facing downslope). α = -1 and w =57.5 lb/ft

$(P_{3rd})_1 = -89 \text{ lb}$

$\left(P_{spt}\right)_1 = -14.6 \text{ lb}$

Purlins 2-11 (facing upslope). α = 1 and w =115 lb/ft

$\left(P_{3rd}\right)_{2-11} = 95 \text{ lb}$

$\left(P_{spt}\right)_{2-11} = -15.4 \text{ lb}$

Purlin 12 (facing upslope). α = 1 and w =57.5 lb/ft

$\left(P_{3rd}\right)_{12} = 48 \text{ lb}$

$\left(P_{spt}\right)_{12} = -7.7 \text{ lb}$

4. Calculate the anchorage forces along each frame line.

   The forces, P_i, calculated above include system effects (the inherent stiffness of the system of purlins), therefore it is not necessary to adjust for system effects.

a. Frame Line 1

   The total force generated along Frame Line 1 is the sum of forces at each purlin.

$$\sum_{N_p} P_i = P_1 + 10P_{2-11} + P_{12} = -35 \text{ lb} + (10)19 \text{ lb} + 9.5 \text{ lb} = 165 \text{ lb}$$

   The force along the frame line is distributed according to the relative stiffness of each restraint on the frame line.

$$\left(P_L\right)_{spt} = \sum_{N_p} P_i \cdot \frac{K_{rest}}{K_{spt}} = (165 \text{ lb}) \frac{1.59 \text{ kip/in}}{19.07 \text{ kip/in}} = 13.8 \text{ lb} \qquad \text{(Eq. 5.5.4-85)}$$

b. Frame Line 2

   The total force generated is the sum of forces at each purlin in each half-span adjacent to the frame line.

$$\sum_{N_p} P_i = \left(P_1 + 10P_{2-11} + P_{12}\right)_{Left} + \left(P_1 + 10P_{2-11} + P_{12}\right)_{Right}$$

$$\sum_{N_p} P_i = \left(-27 \text{ lb} + (10)10.3 \text{ lb} + 5.2 \text{ lb}\right) + \left(-14.6 \text{ lb} + (10)(-15.4 \text{ lb}) + (-7.7 \text{ lb})\right) = -94 \text{ lb}$$

   The force along the frame line is distributed according to the relative stiffness of each restraint on the frame line.

$$\left(P_L\right)_{spt} = \sum_{N_p} P_i \cdot \frac{K_{rest}}{K_{spt}} = (-94 \text{ lb}) \frac{1.69 \text{ kip/in}}{20.28 \text{ kip/in}} = -7.8 \text{ lb} \qquad \text{(Eq. 5.5.4-85)}$$

c. Frame Line 3

Because the system is symmetric, the total force is two times the sum of the forces for one half bay.

$$\sum_{N_p} P_i = 2\left(P_1 + 10P_{2-11} + P_{12}\right) = 2\left(-14.6\text{ lb} + (10)(-15.4\text{ lb}) + (-7.7\text{ lb})\right) = -353\text{ lb}$$

The force along the frame line is distributed according to the relative stiffness of each restraint on the frame line.

$$\left(P_L\right)_{spt} = \sum_{N_p} P_i \cdot \frac{K_{rest}}{K_{spt}} = \left(-353\text{ lb}\right)\frac{1.45\ ^{kip}\!/_{in}}{17.40\ ^{kip}\!/_{in}} = -29\text{ lb} \qquad \text{(Eq. 5.5.4-85)}$$

5. Calculate the forces at the third point anchorage devices.

   The forces generated in each span are averaged (assuming that both third points have approximately equivalent stiffness).

a. End bay

$$\sum_{N_p} P_i = \frac{1}{2}\left[\left(P_1 + 10P_{2-11} + P_{12}\right)_{outside} + \left(P_1 + 10P_{2-11} + P_{12}\right)_{inside}\right]$$

$$\sum_{N_p} P_i = \frac{1}{2}\left[\left(-93\text{ lb} + (10)115\text{ lb} + 57\text{ lb}\right) + \left(-91\text{ lb} + (10)105\text{ lb} + 52\text{ lb}\right)\right] = 1063\text{ lb}$$

$$\left(P_L\right)_{3rd} = \sum_{N_p} P_i \cdot \frac{K_{rest}}{K_{3rd}} = \left(1063\text{ lb}\right)\frac{15\ ^{kip}\!/_{in}}{15\ ^{kip}\!/_{in}} = 1063\text{ lb} \qquad \text{(Eq. 5.5.4-84)}$$

b. Interior bay

$$\sum_{N_p} P_i = \frac{1}{2}\left[2\cdot\left(P_1 + 10P_{2-11} + P_{12}\right) = 2\cdot\left(-89\text{ lb} + (10)(95\text{ lb}) + 48\text{ lb}\right)\right] = 909\text{ lb}$$

$$\left(P_L\right)_{3rd} = \sum_{N_p} P_i \cdot \frac{K_{rest}}{K_{3rd}} = \left(909\text{ lb}\right)\frac{15\ ^{kip}\!/_{in}}{15\ ^{kip}\!/_{in}} = 909\text{ lb} \qquad \text{(Eq. 5.5.4-84)}$$

6. Check the deflection of the system and compare to limits specified in AISI S100 Section I6.4.1

a. Lateral deflection of the purlin top flange at the frame line

   Allowable deflection limit (ASD)

$$\Delta_{tf} \le \frac{1}{\Omega}\frac{d}{20} = \frac{1}{2.00}\frac{8\text{in}}{20} = 0.20\text{in} \qquad \text{(AISI S100 Eq. I6.4.1-9a)}$$

   Frame Line 1

$$\Delta_{rest\_spt1} = \frac{P_L}{K_{rest}} = \frac{\left(13.8\cdot\text{lb}\right)}{1.59\ ^{kip}\!/_{in}} = 0.009\text{in} \le 0.20\text{in}\ \text{ OK} \qquad \text{(Eq. 5.5.4-104)}$$

   Frame Line 2

$$\Delta_{rest\_spt2} = \frac{P_L}{K_{rest}} = \frac{(-7.8\,lb)}{1.69\,{}^{kip}\!/_{in}} = -0.005in \le 0.20in \;\; OK \qquad \text{(Eq. 5.5.4-104)}$$

Frame Line 3

$$\Delta_{rest\_spt3} = \frac{P_L}{K_{rest}} = \frac{(-29\,lb)}{1.45\,{}^{kip}\!/_{in}} = -0.020\,in \le 0.20\;in \;\; OK \qquad \text{(Eq. 5.5.4-104)}$$

b. Deflection along the span is checked at the third point anchorage devices. Diaphragm deflection between the anchorage locations is typically minimal.

Allowable deflection limit (ASD)

$$\Delta_{ms} \le \frac{L}{360} = \frac{25ft\,{}^{12in}\!/_{ft}}{360} = 0.83\,in$$

End bay

$$\Delta_{3rdExt} = \frac{P_L}{K_{rest}} = \frac{(1063\;lb)}{15\,{}^{kip}\!/_{in}} = 0.071\;in \le 0.83\;in \;\;\; OK \qquad \text{(Eq. 5.5.4-104)}$$

Interior bay

$$\Delta_{3rdInt} = \frac{P_L}{K_{rest}} = \frac{(910\;lb)}{15\,{}^{kip}\!/_{in}} = 0.061\;in \le 0.83\;in \;\; OK \qquad \text{(Eq. 5.5.4-104)}$$

7. Calculate the shear force in the connection between the panels and purlin at the anchorage locations.

a. At the frame line

$$P_{sc} = P_L + \frac{wL}{2}(0.9\sigma\alpha - \sin\theta) - P_i \qquad \text{(Eq. 5.5.4-105)}$$

Frame Line 1 - typical purlin

$$P_{sc} = 13.8\;lb + \frac{(115\,plf)(25\,ft)}{2}\left(0.9(0.206)(1) - \sin(2.4°)\right) - (19\;lb) = 201\;lb$$

Frame Line 2 - typical purlin

$$P_{sc} = -7.8 + \frac{(115\;plf)(25\,ft)}{2}\left(0.9(0.190)(1) - \sin(2.4°)\right) - 10.3\;lb$$
$$+\frac{(115\,plf)(25\,ft)}{2}\left(0.9(0.194)(1) - \sin(2.4°)\right) - (-15.4) = 374\;lb$$

Frame Line 3 - typical purlin

$$P_{sc} = -29 + 2\cdot\left[\frac{(115\,plf)(25\,ft)}{2}\left(0.9(0.194)(1) - \sin(2.4°)\right) - (-15.4\;lb)\right] = 384\;lb$$

b. At third points

Using the larger value of σ from the two half-spans in the bay.

$$P_{sc} = P_L + \frac{wL}{20}\left(-0.9\sigma + \frac{\delta b \cos\theta}{d}\right)\alpha \qquad \text{(Eq. 5.5.4-106)}$$

Exterior third points

$$P_{sc} = 1063 + \frac{(57.5\,\text{plf})(25\,\text{ft})}{20}\left(-0.9(0.206) + \frac{(2.75\text{in})\cos(2.4°)}{(3)(8.0\text{in})}\right)(-1) = 1012\text{ lb}$$

Interior third points

$$P_{sc} = 909 + \frac{(57.5\,\text{plf})(25\,\text{ft})}{20}\left(-0.9(0.207) + \frac{(2.75\text{in})\cos(2.4°)}{(3)(8.0\text{in})}\right)(-1) = 857\text{ lb}$$

5.5.4.8 C-Section Example

An example using the component stiffness method to predict anchorage forces is provided based on the roof system from the continuous purlin design example in Section 3.3.2.2.

Given

1. The roof system has four 25 ft spans with purlins lapped over the interior supports. The purlins in the end bay are 9CS2.5x070 and the interior bays are 9CS2.5x059. There is a total of 12 purlin lines spaced at 5 ft-0 in. on center. To facilitate lapping of the purlins, webs of purlins in adjacent spans are placed back to back. Referring to the roof plan below in Figure 5.5.4-18, the top flanges of the purlins in the end bay on the left are facing downslope. The direction of the top flanges of the purlins alternate moving from left to right on the plan. Roof slope is 1/2 on 12(θ = 2.39°).
2. Gravity loads are 3 psf dead and 20 psf live.
3. The standing seam roofing system has a diaphragm stiffness of G′ = 2500 lb/in. and the rotational stiffness of the panel-to-purlin connection is k_{mclip} = 3600 lb-in./rad/ft.
4. There are no discrete bracing lines. Anti-roll clips are provided at each support at every fifth purlin line. Each anti-roll anchorage device is attached to the web of the C-section with two rows of two 1/2 in. diameter A307 bolts. The bottom row of bolts is 3 in. from the bottom flange and the top row is 7 in. from the bottom flange. The stiffness of each anti-roll anchorage device is K_{device} = 40 kip/in. The width of the anti-roll anchorage device is b_{pl} = 5.0 in.
5. Purlin flanges are bolted to the support member with two 1/2 in. diameter A307 bolts through the bottom flange.

Required

1. Compute the anchorage forces along each frame line due to gravity loads.
2. Compute the lateral deflection of the top flange of the C-section along each frame line and at the purlin mid-span.
3. Compute the shear force in the standing seam panel clips at each anchorage device.

Solution

Assumptions for Analysis

1. Because the direction of the top flanges of the C-sections alternates, symmetry cannot be used.
2. Each anchorage device location is considered to have a single degree of freedom along the line of the anchorage. It is assumed that there is some mechanism to rigidly transfer the forces from the remote purlins to the anchorage device. The panels provide the mechanism to transfer the force as long as the connection between the purlin and the panels has sufficient strength and stiffness.
3. It is assumed that the total stiffness of the adjacent frame lines is approximately the same.

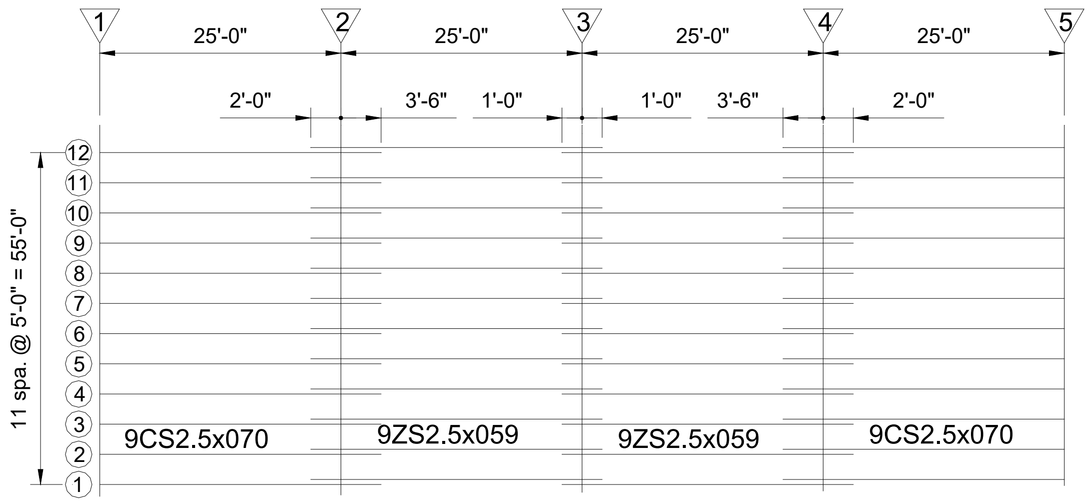

Figure 5.5.418 Roof Layout for C-Section Example

System Properties

L = 25 ft
Bay = 55 ft
Width = 55 ft/11 purlin spaces = 5 ft

Uniform load

Dead = 3 psf
Live = 20 psf
w = (3 psf + 20 psf)(5 ft) = 115 lb/ft

Roof Slope, θ = 2.39 degrees (1/2:12)
G′ = 2500 lb/in.
k_{mclip} = 3600 lb-in./rad/ft
E = 29,500,000 psi
G = 11,300,000 psi

Section Properties

The following sections properties are used for the two C-sections:

INTERIOR BAYS	END BAYS
For: 9CS2.5x059	For: 9CS2.5x070
t = 0.059 in.	t = 0.070 in.
d = 9.0 in.	d = 9.0 in.
b = 2.50 in.	b = 2.50 in.
I_x = 10.30 in.^{4}	I_x = 12.20 in.^{4}
I_y = 0.698 in.^{4}	I_y = 0.828 in.^{4}
I_{xy} = 0.0 in.^{4}	I_{xy} = 0.0 in.^{4}
m = 1.05 in.	m = 1.05 in.

$J = 0.00102 \text{ in.}^4$ $\quad$ $J = 0.00171 \text{ in.}^4$

$C_w = 11.9 \text{ in.}^6$ $\quad$ $C_w = 14.2 \text{ in.}^6$

$I_{my} = \dfrac{I_x I_y - I_{xy}^2}{I_x} = 0.698 \text{ in.4}$ $\quad$ $I_{my} = \dfrac{I_x I_y - I_{xy}^2}{I_x} = 0.828 \text{ in.}^4$

Purlin Torsional Properties

End bay 9CS2.5x070. Outside half-span approximated with both ends "warping free"

$$a = \sqrt{\frac{EC_W}{GJ}} = \sqrt{\frac{E \cdot 14.2\text{in}^6}{G \cdot 0.00171\text{in}^4}} = 147.2 \text{ in} \qquad \text{(Eq. 5.5.4-38)}$$

$$\beta = \frac{L^2}{8a^2} + \frac{1}{\cosh\left(\frac{L}{2a}\right)} - 1 = \frac{(300\text{in})^2}{8 \cdot (147.2\text{in})^2} + \frac{1}{\cosh\left(\frac{300\text{in}}{2 \cdot 147.2\text{in}}\right)} - 1 = 0.158 \text{ rad} \qquad \text{(Eq. 5.5.4-40)}$$

$$\kappa = \frac{8a^4}{L^2}\left(\frac{\cosh\left(\frac{L}{2a}\right) - 1}{\cosh\left(\frac{L}{2a}\right)}\right) + \frac{5L^2}{48} - a^2 \qquad \text{(Eq. 5.5.4-41)}$$

$$\kappa = \frac{8(147.2\text{in})^4}{(300\text{in})^2}\left(\frac{\cosh\left(\frac{300\text{in}}{2 \cdot 147.2\text{in}}\right) - 1}{\cosh\left(\frac{300\text{in}}{2 \cdot 147.2\text{in}}\right)}\right) + \frac{5(300\text{in})^2}{48} - (147.2\text{in})^2 = 2786 \,\text{rad} \cdot \text{in}^2$$

$$\tau = \frac{\frac{a^2\beta}{GJ}}{1 + \frac{k_{mclip}}{GJ}\kappa} = \frac{\frac{(147.2\text{in})^2 \cdot 0.158\text{rad}}{G \cdot 0.00171\text{in}^4}}{1 + \frac{3600\,{}^{\text{lb}\cdot\text{in}}/_{\text{rad}\cdot\text{ft}}}{G \cdot 0.00171\text{in}^4} \cdot 2786\text{rad} \cdot \text{in}^2} = 0.0040 \,\frac{\text{rad}}{\text{lb}} \qquad \text{(Eq. 5.5.4-39)}$$

End bay 9CS2.5x070. Inside half-span approximated with both ends "warping fixed"

$$a = \sqrt{\frac{EC_W}{GJ}} = \sqrt{\frac{E \cdot 14.2\text{in}^6}{G \cdot 0.00171\text{in}^4}} = 147.2 \text{ in} \qquad \text{(Eq. 5.5.4-38)}$$

$$\beta = \frac{L^2}{8a^2} + \frac{L}{2a}\,\frac{1 - \cosh\left(\frac{L}{2a}\right)}{\sinh\left(\frac{L}{2a}\right)} = \frac{(300\text{in})^2}{8 \cdot (147.2\text{in})^2} + \frac{300\text{in}}{(2)(147.2\text{in})}\,\frac{1 - \cosh\left(\frac{300\text{in}}{2 \cdot 147.2\text{in}}\right)}{\sinh\left(\frac{300\text{in}}{2 \cdot 147.2\text{in}}\right)} = 0.041 \text{ rad}$$

(Eq. 5.5.4-43)

$$\kappa = \left(\frac{aL}{3} - \frac{4a^3}{L}\right)\left(\frac{1 - \cosh\left(\frac{L}{2a}\right)}{\sinh\left(\frac{L}{2a}\right)}\right) + \frac{5L^2}{48} - a^2 \qquad \text{(Eq. 5.5.4-44)}$$

$$\kappa = \left(\frac{(147.2\text{in})(300\text{in})}{3} - \frac{4(147.2\text{in})^3}{300\text{in}}\right)\left(\frac{1-\cosh\left(\frac{300\text{in}}{2(147.2\text{in})}\right)}{\sinh\left(\frac{300\text{in}}{2(147.2\text{in})}\right)}\right) + \frac{5(300\text{in.})^2}{48} - (147.2\text{in})^2$$

$$\kappa = 764\ \text{rad}\cdot\text{in}^2$$

$$\tau = \frac{\frac{a^2\beta}{GJ}}{1+\frac{k_{mclip}}{GJ}\kappa} = \frac{\frac{(147.2\text{in})^2\cdot 0.041\text{rad}}{G\cdot 0.00171\text{in}^4}}{1+\frac{3600\ ^{\text{lb}\cdot\text{in}}/_{\text{rad}\cdot\text{ft}}}{G\cdot 0.00171\text{in}^4}\cdot 764\text{rad}\cdot\text{in}^2} = 0.0036\,\frac{\text{rad}}{\text{lb}} \qquad \text{(Eq. 5.5.4-39)}$$

Interior bay 9CS2.5x059. Approximated with both ends "warping fixed"

$$a = 174.5\ \text{in}$$

$$\beta = 0.021\ \text{rad}$$

$$\kappa = 559\ \text{rad}\cdot\text{in}^2$$

$$\tau = 0.0036\,\frac{\text{rad}}{\text{lb}}$$

Procedure

1. Calculate the uniform restraint provided by the panels, w_{rest}, expressed as a proportion of the applied uniform load.

   $$w_{rest} = w\cdot\sigma$$

   where

   $$\sigma = \frac{C1\frac{\left(\frac{I_{xy}}{I_x}\cos\theta\right)L^4}{EI_{my}} + \frac{((\delta b+m)\cos\theta)d}{2}\tau + \frac{\alpha\cdot Np\cdot L^2\sin\theta}{8G'Bay}}{C1\frac{L^4}{EI_{my}} + \frac{d^2}{4}\tau + \frac{\alpha\cdot\eta\cdot L^2}{8G'Bay}} \qquad \text{(Eq. 5.5.4-51)}$$

   Since I_{xy} = 0, for C-sections, the above equation reduces to

   $$\sigma = \frac{\frac{((\delta b+m)\cos\theta)d}{2}\tau + \frac{\alpha\cdot Np\cdot L^2\sin\theta}{8G'Bay}}{C1\frac{L^4}{EI_{my}} + \frac{d^2}{4}\tau + \frac{\alpha\cdot\eta\cdot L^2}{8G'Bay}}$$

a. End bay – half-span adjacent to Frame Line 1 (approximated as a simple-fixed beam with warping free ends).

   C1 = 1/185, α = -1, η = -12 (purlins facing downslope)

$$\sigma = \frac{\frac{\left(\left(\frac{2.5\text{in}}{3}+1.05\text{in}\right)\cos\left(2.39°\right)\right)9.0\text{in}}{2\cdot\text{rad}}0.0040\frac{\text{rad}}{\text{lb}}+\frac{(-1)(12)(300\text{in})^2\sin(2.39°)}{8\cdot\left(2500\,{}^{\text{lb}}/_{\text{in}}\right)(660\text{in})}}{\frac{(300\text{in})^4}{185\cdot\text{E}\cdot0.828\text{in}^4}+\frac{(9.0\text{in})^2}{4\cdot\text{rad}}0.0040\frac{\text{rad}}{\text{lb}}+\frac{(-1)(-12)(300\text{in})^2}{8\cdot\left(2500\,{}^{\text{lb}}/_{\text{in}}\right)(660\text{in})}} = 0.016$$

b. End bay – half-span adjacent to Frame Line 2 (approximated as a simple-fixed beam with warping fixed ends).

C1 = 1/185, α = -1, η = -12 (purlins facing downslope)

$$\sigma = \frac{\frac{\left(\left(\frac{2.5\text{in}}{3}+1.05\text{in}\right)\cos\left(2.39°\right)\right)9.0\text{in}}{2\cdot\text{rad}}0.0036\frac{\text{rad}}{\text{lb}}+\frac{(-1)(12)(300\text{in})^2\sin(2.39°)}{8\cdot\left(2500\,{}^{\text{lb}}/_{\text{in}}\right)(660\text{in})}}{\frac{(300\text{in})^4}{185\cdot\text{E}\cdot0.828\text{in}^4}+\frac{(9.0\text{in})^2}{4\cdot\text{rad}}0.0036\frac{\text{rad}}{\text{lb}}+\frac{(-1)(-12)(300\text{in})^2}{8\cdot\left(2500\,{}^{\text{lb}}/_{\text{in}}\right)(660\text{in})}} = 0.014$$

c. Interior bay – between Frame Lines 2 and 3 (approximated as a fixed-fixed beam with warping restrained at each end).

C1 = 1/384, α = 1, η = 12 (purlins facing upslope)

$$\sigma = \frac{\frac{\left(\left(\frac{2.5\text{in}}{3}+1.05\text{in}\right)\cos\left(2.39°\right)\right)9.0\text{in}}{2\cdot\text{rad}}0.0036\frac{\text{rad}}{\text{lb}}+\frac{(1)(12)(300\text{in})^2\sin(2.39°)}{8\cdot\left(2500\,{}^{\text{lb}}/_{\text{in}}\right)(660\text{in})}}{\frac{(300\text{in})^4}{384\cdot\text{E}\cdot0.698\text{in}^4}+\frac{(9.0\text{in})^2}{4\cdot\text{rad}}0.0036\frac{\text{rad}}{\text{lb}}+\frac{(1)(12)(300\text{in})^2}{8\cdot\left(2500\,{}^{\text{lb}}/_{\text{in}}\right)(660\text{in})}} = 0.029$$

d. Interior bay – between Frame Lines 3 and 4 (approximated as a fixed-fixed beam with warping restrained at each end).

C1 = 1/384 α = -1, η = -12 (purlins facing downslope)
$\sigma = 0.023$

e. Right end bay – half-span adjacent to Frame Line 4 (approximated as a simple-fixed beam with warping fixed ends).

C1 = 1/185 α = 1, η = 12 (purlins facing upslope)
$\sigma = 0.017$

f. Right end bay – half-span adjacent to Frame Line 5 (approximated as a simple-fixed beam with warping free ends).

C1 = 1/185, α = 1, η = 12 (purlins facing upslope)
$\sigma = 0.019$

2. Calculate the overturning forces generated by each purlin.

a. End bay – half-span adjacent to Frame Line 1 (approximated as each end warping free).

Local deformation reduction factor

$$R_{local} = \frac{k_{mclip}}{k_{mclip} + \frac{Et^3}{3d}} = \frac{3600\,{}^{lb\cdot in}/_{rad\cdot ft}}{3600\,{}^{lb\cdot in}/_{rad\cdot ft} + \frac{E\cdot(0.070in)^3}{3\cdot 9.0in}\left(12\,{}^{in}/_{ft}\right)} = 0.445 \qquad \text{(Eq. 5.5.4-50)}$$

Typical purlins (Purlins 2-11), facing downslope, α = -1 and w = 115 lb/ft

$$P_i = \frac{wL}{2d}\cdot\left[\left(\delta b\cos\theta\left(1-R_{local}\right)+\tfrac{2}{3}k_{mclip}\tau\left(\sigma\frac{d}{2}-\left(\delta b+m\right)\cos\theta\right)\right)\alpha - d\sin\theta\right] \qquad \text{(Eq. 5.5.4-49)}$$

$$P_{2-11} = \frac{(115\,{}^{lb}/_{ft})(25ft)}{(2)(9in)}\cdot\left[\begin{array}{l}\left(\begin{array}{l}\frac{2.5in}{3}\cos(2.39°)(1-0.445)\\ +\frac{2}{3}\left(\frac{3600\,{}^{lb\cdot in}/_{rad\cdot ft}}{12\,{}^{in}/_{ft}}\right)\left(0.0040\frac{1}{lb}\right)\left[(0.016)\frac{9.0in}{2}-\left(\frac{2.5in}{3}+1.05in\right)\cos(2.4°)\right]\end{array}\right)(-1)\\ -(9.0in)\sin(2.39°)\end{array}\right]$$

$$P_{2-11} = 98\text{ lb}$$

Purlins 1 and 12. The load on Purlins 1 and 12 is half that of Purlins 2-11, the overturning force is half that of Purlins 2-12, or

$$P_{1,12} = 49\text{ lb}$$

b. End bay – half-span adjacent to Frame Line 2 (approximated as each end warping fixed).

Local deformation reduction factor

$$R_{local} = 0.445$$

Typical purlins (Purlins 2-11), facing downslope, α = -1 and w = 115 lb/ft

$$P_{2-11} = \frac{(115\,{}^{lb}/_{ft})(25ft)}{(2)(9in)}\cdot\left[\begin{array}{l}\left(\begin{array}{l}\frac{2.5in}{3}\cos(2.39°)(1-0.445)\\ +\frac{2}{3}\left(\frac{3600\,{}^{lb\cdot in}/_{rad\cdot ft}}{12\,{}^{in}/_{ft}}\right)\left(0.0036\frac{1}{lb}\right)\left[(0.014)\frac{9.0in}{2}-\left(\frac{2.5in}{3}+1.05in\right)\cos(2.4°)\right]\end{array}\right)(-1)\\ -(9.0in)\sin(2.39°)\end{array}\right]$$

$$P_{2-11} = 75\text{ lb}$$

Purlins 1 and 12. The load on Purlins 1 and 12 is half that of Purlins 2-11, the overturning force is half that of Purlins 2-12, or

$$P_{1,12} = 38\text{ lb}$$

c. Interior bay between Frame Lines 2 and 3 (approximated as each end warping fixed).

Local deformation reduction factor

$R_{local} = 0.572$

Typical purlins (Purlins 2-11), facing upslope, $\alpha = 1$ and w = 115 lb/ft

$P_{2-11} = -204$ lb

Purlins 1 and 12. The load on Purlins 1 and 12 is half that of Purlins 2-11, the overturning force is half that of Purlins 2-12, or

$P_{1,12} = -102$ lb

d. Interior bay between Frame Lines 3 and 4 (approximated as each end warping fixed).

Local deformation reduction factor

$R_{local} = 0.572$

Purlins 2-11 $\alpha = -1$ and w = 115 lb/ft

$P_{2-11} = 88$ lb

Purlins 1 and 12. The load on Purlins 1 and 12 is half that of Purlins 2-11, the overturning force is half that of Purlins 2-12, or

$P_{1,12} = 44$ lb

e. End bay – half-span adjacent to Frame Line 4 (approximated as each end warping fixed).

Local deformation reduction factor

$R_{local} = 0.445$

Typical purlins (Purlins 2-11), facing upslope, $\alpha = 1$ and w = 115 lb/ft

$P_{2-11} = -195$ lb

Purlins 1 and 12. The load on Purlins 1 and 12 is half that of Purlins 2-11, the overturning force is half that of Purlins 2-11, or

$P_{1,12} = -98$ lb

f. End bay – half-span adjacent to Frame Line 5 (approximated as each end warping free).

Local deformation reduction factor

$R_{local} = 0.445$

Typical purlins (Purlins 2-11), facing upslope, $\alpha = 1$ and w = 115 lb/ft

$P_{2-11} = -217$ lb

Purlins 1 and 12. The load on Purlins 1 and 12 is half that of Purlins 2-11, the overturning force is half that of Purlins 2-11, or

$$P_{1,12} = -109 \text{ lb}$$

3. Calculate the stiffness of the anchorage devices

The stiffness of each anchorage device is

$$K_{device} = 40 \text{ kip/in}$$

The net stiffness of the anchorage device must include the configuration stiffness which accounts for the flexibility of the web of the purlin between the top of the device and the top flange of the purlin.

a. Frame Line 1

Configuration stiffness

$$K_{config} = \frac{E b_{pl} t^3}{(d-h)^3} \cdot \frac{d}{h} = \frac{E(5 \text{ in})(0.070 \text{ in})^3}{(9 \text{ in} - 7 \text{ in})^3} \cdot \frac{9 \text{ in}}{7 \text{ in}} = 8.1 \text{ kip/in} \qquad \text{(Eq. 5.5.4-32)}$$

Net restraint stiffness

$$K_{rest} = \frac{\left(\frac{h}{d}\right)^2 K_{device} K_{config}}{\frac{h}{d} K_{device} + K_{config}} = \frac{\left(\frac{7 \text{ in}}{9 \text{ in}}\right)^2 (40 \text{ kip/in})(8.1 \text{ kip/in})}{\frac{7 \text{ in}}{9 \text{ in}}(40 \text{ kip/in}) + 8.1 \text{ kip/in}} = 5.0 \text{ kip/in} \qquad \text{(Eq. 5.5.4-30)}$$

b. Frame Line 2

To account for the purlins at the lap, the combined purlins are given an equivalent thickness.

$$t_{lap} = \sqrt[3]{t_1^3 + t_2^3} = \sqrt[3]{(0.070 \text{ in})^3 + (0.059 \text{ in})^3} = 0.082 \text{ in}$$

Configuration stiffness

$$K_{config} = \frac{E(5 \text{ in})(0.082 \text{ in})^3}{(9 \text{ in} - 7 \text{ in})^3} \cdot \frac{9 \text{ in}}{7 \text{ in}} = 13.0 \text{ kip/in}$$

Net anchorage device stiffness

$$K_{rest} = \frac{\left(\frac{7 \text{ in}}{9 \text{ in}}\right)^2 (40 \text{ kip/in})(13.0 \text{ kip/in})}{\frac{7 \text{ in}}{9 \text{ in}}(40 \text{ kip/in}) + 13.0 \text{ kip/in}} = 7.1 \text{ kip/in}$$

c. Frame Line 3

Equivalent thickness at lap

$$t_{lap} = \sqrt[3]{t_2^3 + t_2^3} = \sqrt[3]{(0.059\text{in})^3 + (0.059\text{in})^3} = 0.074\,\text{in}$$

Configuration stiffness

$$K_{config} = \frac{E(5\text{ in})(0.074\text{ in})^3}{(9\text{ in} - 7\text{ in})^3} \cdot \frac{9\text{ in}}{7\text{ in}} = 9.7\,{}^{\text{kip}}\!/_{\text{in}}$$

Net anchorage device stiffness

$$K_{rest} = \frac{\left(\frac{7\text{ in}}{9\text{ in}}\right)^2 \left(40\,{}^{\text{kip}}\!/_{\text{in}}\right)\left(9.7\,{}^{\text{kip}}\!/_{\text{in}}\right)}{\frac{7\text{ in}}{9\text{ in}}\left(40\,{}^{\text{kip}}\!/_{\text{in}}\right) + 9.7\,{}^{\text{kip}}\!/_{\text{in}}} = 5.8\,{}^{\text{kip}}\!/_{\text{in}}$$

4. Calculate the stiffness of the system.
a. Calculate the stiffness of the panels.

$$K_{panel} = \frac{k_{mclip} L}{d}\left(\frac{\frac{1}{4} E t^3}{0.38 k_{mclip} d + 0.71 \frac{E t^3}{4}}\right)\left(1 - \tfrac{2}{3} k_{mclip} \tau\right) \qquad \text{(Eq. 5.5.4-37)}$$

i. End bay. It is conservative to use the torsional coefficient, τ, for a warping free ends.

$$K_{panel} = \frac{3600\,{}^{\text{lb}\cdot\text{in}}\!/_{\text{rad}\cdot\text{ft}}(25\,\text{ft})}{9.0\text{ in}}\left(\frac{\frac{E(0.070\text{ in})^3}{4}}{(0.38)\frac{3600\,{}^{\text{lb}\cdot\text{in}}\!/_{\text{rad}\cdot\text{ft}}}{12\,{}^{\text{in}}\!/_{\text{ft}}}(9.0\,\text{in}) + (0.71)\frac{E(0.070\,\text{in})^3}{4}}\right) \text{x}$$

$$\left(1 - \left(\tfrac{2}{3}\right)\frac{3600\,{}^{\text{lb}\cdot\text{in}}\!/_{\text{rad}\cdot\text{ft}}}{12\,{}^{\text{in}}\!/_{\text{ft}}}\left(0.0040\frac{\text{rad}}{\text{lb}}\right)\right)$$

$$K_{panel} = 1791\,{}^{\text{lb}\cdot\text{in}}\!/_{\text{in}}$$

ii. Interior bay

$$K_{panel} = \frac{3600\,{}^{\text{lb}\cdot\text{in}}\!/_{\text{rad}\cdot\text{ft}}(25\,\text{ft})}{9.0\text{ in}}\left(\frac{\frac{E(0.059\text{ in})^3}{4}}{(0.38)\frac{3600\,{}^{\text{lb}\cdot\text{in}}\!/_{\text{rad}\cdot\text{ft}}}{12\,{}^{\text{in}}\!/_{\text{ft}}}(9.0\,\text{in}) + (0.71)\frac{E(0.059\,\text{in})^3}{4}}\right) \text{x}$$

$$\left(1 - \left(\tfrac{2}{3}\right)\frac{3600\,{}^{\text{lb}\cdot\text{in}}\!/_{\text{rad}\cdot\text{ft}}}{12\,{}^{\text{in}}\!/_{\text{ft}}} \cdot 0.0036\frac{\text{rad}}{\text{lb}}\right)$$

$$K_{panel} = 2019\,{}^{\text{lb}\cdot\text{in}}\!/_{\text{in}}$$

b. Calculate stiffness of the connection between the rafter and the C-section (flange bolted connection).

$$K_{rafter} = 0.45\frac{Et^3}{2d} \qquad \text{(Eq. 5.5.4-36)}$$

Exterior Frame Line

$$K_{rafter} = 0.45\frac{E(0.070\text{ in})^3}{2(9\text{ in})} = 253\ ^{\text{lb}\cdot\text{in}}\!/_{\text{in}}$$

At the interior frame lines, the equivalent thickness of the laps is used.

First Interior Frame Line

$$K_{rafter} = 0.45\frac{E(0.082\text{ in})^3}{2(9\text{ in})} = 404\ ^{\text{lb}\cdot\text{in}}\!/_{\text{in}}$$

Second Interior Frame Line

$$K_{rafter} = 0.45\frac{E(0.074\text{ in})^3}{2(9\text{ in})} = 303\ ^{\text{lb}\cdot\text{in}}\!/_{\text{in}}$$

5. Calculate the total stiffness of the system attributed to each anchorage device location (frame line).

$$K_{total} = \sum_{N_a} K_{rest} + \frac{\sum_{N_p} K_{panel} + \sum_{N_p - N_a} K_{rafter}}{d} \qquad \text{(Eq. 5.5.4-48)}$$

a. At Frame Line 1, the stiffness includes three anchorage devices, the rafter stiffness of nine purlins flange bolted to the rafter, and the panel stiffness of half of the end bay for twelve purlins.

$$K_{total} = 3(5.0\ ^{\text{kip}}\!/_{\text{in}}) + (12)\frac{1791\ ^{\text{lb}\cdot\text{in}}\!/_{\text{in}}}{(2)(9\text{ in})1000\ ^{\text{lb}}\!/_{\text{kip}}} + (9)\frac{253\ ^{\text{lb}\cdot\text{in}}\!/_{\text{in}}}{(9.0\text{ in})1000\ ^{\text{lb}}\!/_{\text{kip}}} = 16.5\ ^{\text{kip}}\!/_{\text{in}}$$

b. At Frame Line 2, the stiffness includes three anchorage devices, the rafter stiffness of nine purlins flange bolted to the rafter, and the panel stiffness of half of the end bay and half of the interior bay for twelve purlins.

$$K_{total} = 3(7.1\ ^{\text{kip}}\!/_{\text{in}}) + (12)\frac{1791\ ^{\text{lb}\cdot\text{in}}\!/_{\text{in}}}{(2)(9\text{ in})1000\ ^{\text{lb}}\!/_{\text{kip}}} + (12)\frac{2019\ ^{\text{lb}\cdot\text{in}}\!/_{\text{in}}}{(2)(9\text{ in})1000\ ^{\text{lb}}\!/_{\text{kip}}} + (9)\frac{404\ ^{\text{lb}\cdot\text{in}}\!/_{\text{in}}}{(9\text{ in})1000\ ^{\text{lb}}\!/_{\text{kip}}} = 24.2\ ^{\text{kip}}\!/_{\text{in}}$$

c. At Frame Line 3, the stiffness includes three anchorage devices, the rafter stiffness of nine purlins flange bolted to the rafter, and two times the panel stiffness of half of the interior bay for twelve purlins.

$$K_{total} = 3(5.8\ ^{\text{kip}}\!/_{\text{in}}) + (12)\frac{2019\ ^{\text{lb}\cdot\text{in}}\!/_{\text{in}}}{(9\text{ in})1000\ ^{\text{lb}}\!/_{\text{kip}}} + (9)\frac{303\ ^{\text{lb}\cdot\text{in}}\!/_{\text{in}}}{(9\text{ in})1000\ ^{\text{lb}}\!/_{\text{kip}}} = 20.4\ ^{\text{kip}}\!/_{\text{in}}$$

6. Distribute the overturning forces to each anchorage device.

a. Frame Line 1

The total load generated by the end bay half-span adjacent to Frame Line 1 is

$$\sum_{N_p} P_i = \left(P_1 + 10P_{2-11} + P_{12}\right) = \left(49\text{ lb}\right) + 10\left(98\text{ lb}\right) + \left(49\text{ lb}\right) = 1078\text{ lb}$$

Distribution to each anchorage device along Frame Line 1

$$P_L = \sum_{N_p} P_i \left(\frac{K_{rest}}{K_{total}}\right) = \left(1078\text{ lb}\right)\frac{5.0\,{}^{kip}\!/_{in}}{16.5\,{}^{kip}\!/_{in}} = 327\text{ lb} \qquad \text{(Eq. 5.5.4-46)}$$

Anchorage force at the height of the anchorage device

$$P_h = P_L \frac{d}{h} = \left(327\text{ lb}\right)\frac{9\text{ in}}{7\text{ in}} = 420\text{ lb} \qquad \text{(Eq. 5.5.4-47)}$$

b. Frame Line 2

The total load generated by each half-span adjacent to Frame Line 2 is

$$\sum_{N_p} P_i = \left(P_1 + 10P_{2-11} + P_{12}\right)_{Left} + \left(P_1 + 10P_{2-11} + P_{12}\right)_{Right}$$

$$\sum_{N_p} P_i = \left(38\text{ lb}\right) + 10\left(75\text{ lb}\right) + \left(38\text{ lb}\right) + \left(\left(-102\text{ lb}\right) + 10\left(-204\text{ lb}\right) + \left(-102\text{ lb}\right)\right) = -1418\text{ lb}$$

Distribution to each anchorage device along Frame Line 2

$$P_L = \sum_{N_p} P_i \left(\frac{K_{rest}}{K_{total}}\right) = \left(-1418\text{ lb}\right)\frac{7.1\,{}^{kip}\!/_{in}}{24.2\,{}^{kip}\!/_{in}} = -416\text{ lb} \qquad \text{(Eq. 5.5.4-46)}$$

Anchorage force at the height of the anchorage device

$$P_h = P_L \frac{d}{h} = \left(-416\text{ lb}\right)\frac{9\text{ in}}{7\text{ in}} = -535\text{ lb} \qquad \text{(Eq. 5.5.4-47)}$$

c. Frame Line 3

At Frame Line 3, it is assumed that half of the force generated at each bay adjacent to the frame line is distributed to the interior frame line.

$$\sum_{N_p} P_i = \left(\left(-102\text{ lb}\right) + 10\left(-204\text{ lb}\right) + \left(-102\text{ lb}\right)\right) + \left(44\text{ lb}\right) + 10\left(88\text{ lb}\right) + \left(44\text{ lb}\right) = -1276\text{ lb}$$

Distribution to each anchorage device along Frame Line 3

$$P_L = \sum_{N_p} P_i \left(\frac{K_{rest}}{K_{total}}\right) = \left(-1276\text{ lb}\right)\frac{5.8\,{}^{kip}\!/_{in}}{20.4\,{}^{kip}\!/_{in}} = -363\text{ lb} \qquad \text{(Eq. 5.5.4-46)}$$

Anchorage force at the height of the anchorage device

$$P_h = P_L \frac{d}{h} = \left(-363\text{ lb}\right)\frac{9\text{ in}}{7\text{ in}} = -467\text{ lb} \qquad \text{(Eq. 5.5.4-47)}$$

d. Frame Line 4

At Frame Line 4, it is assumed that half of the force generated at each bay adjacent to the frame line is distributed to the interior frame line.

$$\sum_{N_p} P_i = \big(\big(44\text{ lb}\big)+10\big(88\text{ lb}\big)+\big(44\text{ lb}\big)\big)+\big(\big(-98\text{ lb}\big)+10\big(-195\text{ lb}\big)+\big(-98\text{ lb}\big)\big) = -1178\text{ lb}$$

Distribution to each anchorage device along Frame Line 4

$$P_L = \sum_{N_p} P_i\left(\frac{K_{rest}}{K_{total}}\right) = \big(-1178\text{ lb}\big)\frac{7.1\,{}^{kip}\!/_{in}}{24.2\,{}^{kip}\!/_{in}} = -346\text{ lb} \qquad \text{(Eq. 5.5.4-46)}$$

Anchorage force at the height of the anchorage device

$$P_h = P_L\frac{d}{h} = \big(-346\text{ lb}\big)\frac{9\text{ in}}{7\text{ in}} = 445\text{ lb} \qquad \text{(Eq. 5.5.4-47)}$$

e. Frame Line 5

At Frame Line 5, it is assumed that half of the force generated at the bay adjacent to the frame line is distributed to the exterior frame line.

$$\sum_{N_p} P_i = \big(-109\text{ lb}\big)+10\big(-217\text{ lb}\big)+\big(-109\text{ lb}\big) = -2388\text{ lb}$$

Distribution to each anchorage device along Frame Line 5

$$P_L = \sum_{N_p} P_i\left(\frac{K_{rest}}{K_{total}}\right) = \big(-2388\text{ lb}\big)\frac{5.0\,{}^{kip}\!/_{in}}{16.5\,{}^{kip}\!/_{in}} = -724\text{ lb} \qquad \text{(Eq. 5.5.4-46)}$$

Anchorage force at the height of the anchorage device

$$P_h = P_L\frac{d}{h} = \big(-724\text{ lb}\big)\frac{9\text{ in}}{7\text{ in}} = -931\text{ lb} \qquad \text{(Eq. 5.5.4-47)}$$

7. Check the deflection of the system and compare to the limits specified in AISI S100 Section I6.4.1.

a. Lateral deflection of the purlin top flange

Allowable deflection limit (ASD)

$$\Delta_{tf} \le \frac{1}{\Omega}\frac{d}{20} = \frac{1}{2.00}\frac{9\text{ in}}{20} = 0.23\text{ in} \qquad \text{(AISI S100 Eq. I6.4.1-9a)}$$

Frame Line 1

$$\Delta_{rest} = \frac{P_L}{K_{rest}} = \frac{327\text{ lb}}{5.0\,{}^{kip}\!/_{in}} = 0.07\text{ in} \le 0.23\text{ in}\ \ \text{OK} \qquad \text{(Eq. 5.5.4-52)}$$

Frame Line 2

$$\Delta_{rest} = \frac{P_L}{K_{rest}} = \frac{\big(-416\text{ lb}\big)}{7.1\,{}^{kip}\!/_{in}} = -0.06\text{ in} \le 0.23\text{ in}\ \ \text{OK} \qquad \text{(Eq. 5.5.4-52)}$$

Frame Line 3

$$\Delta_{rest} = \frac{P_L}{K_{rest}} = \frac{(-363\text{ lb})}{5.8\,{}^{kip}\!/\!_{in}} = -0.06\text{ in} \leq 0.23\text{ in OK} \quad \text{(Eq. 5.5.4-52)}$$

Frame Line 4

$$\Delta_{rest} = \frac{P_L}{K_{rest}} = \frac{(-346\text{ lb})}{7.1\,{}^{kip}\!/\!_{in}} = -0.05\text{ in} \leq 0.23\text{ in OK} \quad \text{(Eq. 5.5.4-52)}$$

Frame Line 5

$$\Delta_{rest} = \frac{P_L}{K_{rest}} = \frac{(-724\text{ lb})}{5.0\,{}^{kip}\!/\!_{in}} = -0.14\text{ in} < 0.23\text{ in OK} \quad \text{(Eq. 5.5.4-52)}$$

b. Mid-Span deflection of the diaphragm relative to the ends of the span

Allowable deflection limit

$$\Delta_{ms} \leq \frac{L}{360} = \frac{25\text{ft}\,{}^{12\text{in}}\!/\!_{\text{ft}}}{360} = 0.83\text{ in}$$

$$\Delta_{diaph} = \Sigma(w(\alpha\sigma - \sin\theta))_i \frac{L^2}{8G'Bay} \quad \text{(Eq. 5.5.4-53)}$$

End bay (between Frame Line 1 and 2)

Use the average uniform diaphragm force between the two half-spans.

$$\bar{\sigma} = \tfrac{1}{2}(0.016 + 0.014) = 0.015$$

$$\Delta_{diaph} = \left[(11)(115\,{}^{lb}\!/\!_{ft})((-1)0.016 - \sin(2.39°))\right]\frac{(25\text{ ft})^2}{8(2500\,{}^{lb}\!/\!_{in})(55\text{ ft})} = -0.04\text{ in} \leq 0.83\text{ in OK}$$

Interior bay (between Frame Lines 2 and 3)

$$\Delta_{diaph} = \left[(11)(115\,{}^{lb}\!/\!_{ft})((1)0.029 - \sin(2.39°))\right]\frac{(25\text{ ft})^2}{8(2500\,{}^{lb}\!/\!_{in})(55\text{ ft})} = -0.01\text{ in} \leq 0.83\text{ in OK}$$

Interior bay (between Frame Lines 3 and 4)

$$\Delta_{diaph} = \left[(11)(115\,{}^{lb}\!/\!_{ft})((-1)0.023 - \sin(2.39°))\right]\frac{(25\text{ ft})^2}{8(2500\,{}^{lb}\!/\!_{in})(55\text{ ft})} = -0.05\text{ in} \leq 0.83\text{ in OK}$$

End bay (between Frame Lines 4 and 5)

Use the average uniform diaphragm force between the two half-spans.

$$\bar{\sigma} = \tfrac{1}{2}(0.017 + 0.019) = 0.018$$

$$\Delta_{diaph} = \left[(11)(115\,{}^{lb}\!/\!_{ft})((1)0.018 - \sin(2.39°))\right]\frac{(25\text{ ft})^2}{8(2500\,{}^{lb}\!/\!_{in})(55\text{ ft})} = -0.02\text{ in} \leq 0.83\text{ in OK}$$

8. Calculate the shear force in the connection between the panels and purlin at the anchorage device location.

$$P_{sc} = P_L + \frac{wL}{2}(0.9\sigma\alpha + \sin\theta) - P_i \qquad \text{(Eq. 5.5.4-54)}$$

Frame Line 1

$$P_{sc} = 327 + \frac{(115\ {}^{lb}\!/\!{}_{ft})(25\ ft)}{2}\left(0.9(0.016)(-1) + \sin(2.39°)\right) - (98\ lb) = 268\ lb$$

Frame Line 2

$$P_{sc} = -416 + \frac{(115\ {}^{lb}\!/\!{}_{ft})(25\ ft)}{2}\left(0.9(0.014)(-1) + \sin(2.39°)\right) - (75\ lb)$$

$$+\frac{(115\ {}^{lb}\!/\!{}_{ft})(25\ ft)}{2}\left(0.9(0.029)(1) + \sin(2.39°)\right) - (-204\ lb) = -148\ lb$$

Frame Line 3

$$P_{sc} = -363 + \frac{(115\ {}^{lb}\!/\!{}_{ft})(25\ ft)}{2}\left(0.9(0.029)(1) + \sin(2.39°)\right) - (-204\ lb)$$

$$+\frac{(115\ {}^{lb}\!/\!{}_{ft})(25\ ft)}{2}\left(0.9(0.023)(-1) + \sin(2.39°)\right) - (88\ lb) = -120\ lb$$

Frame Line 4

$$P_{sc} = -346 + \frac{(115\ {}^{lb}\!/\!{}_{ft})(25\ ft)}{2}\left(0.9(0.023)(-1) + \sin(2.39°)\right) - (88\ lb)$$

$$+\frac{(115\ plf)(25\ ft)}{2}\left(0.9(0.017)(1) + \sin(2.39°)\right) - (-195\ lb) = -127\ lb$$

Frame Line 5

$$P_{sc} = -724 + \frac{(115\ plf)(25\ ft)}{2}\left(0.9(0.019)(1) + \sin(2.39°)\right) - (-217\ lb) = -423\ lb$$

5.5.5 Frame Element Stiffness Model

The computer model presented here was used to develop and calibrate the calculation procedure presented in AISI S100. It can be used to analyze conditions that are beyond the scope of the available manual procedures or when a better understanding of the behavior is needed. The stiffness mode replicates the physical geometry of the roof system with simple frame elements and has been validated by comparing the resulting forces to test results.

5.5.5.1 Source of Test Data

The computer model was built in a way that closely mimics the physical properties of the actual system, so it was expected that the model behavior should mimic the behavior of the physical system. To verify the model results and to calibrate some of the model properties, the model results were compared to the available test results. Previously proposed calculation procedures were calibrated to tests of flat roof systems performed at the University of Oklahoma by Curtis and Murray (1983) and Seshappa and Murray (1985). Since the development of the previously proposed procedures, additional tests including sloped roofs have been performed at Virginia Tech by Lee and Murray (2001) and Seek and Murray (2004a). These later tests were used as the primary source of data when verifying the calculation procedure.

5.5.5.2 Selection of Computer Model

The work by Elhouar and Murray (1985), which formed the basis of the procedure in previous editions of AISI S100, utilized a first order elastic stiffness model with a combination of frame and truss elements to model the roof system. This model was later modified slightly by Neubert and Murray (2000) and was further updated as a result of research at Virginia Tech (Seek 2007 and Sears 2007). Seek also developed a separate computer model that utilizes finite elements and agrees very well with the results of tests. This model is summarized in Section 5.5.6.

5.5.5.3 Development of Stiffness Model

The computer stiffness model utilizes linear frame elements to model the purlins and a combination of frame and truss elements to model the panels. The material properties of all elements in the model are taken as isotropic steel with a modulus of elasticity of 29,500 ksi. Shear deformations and the effects of warping under torsion are neglected. The analysis solution is strictly linear-elastic and neglects all material and geometric non-linearity.

5.5.5.3.1 Local and Global Axes

For defining the attributes of the model, a global coordinate system is defined, and a local system of axes is defined for each element type. The global Y-axis is aligned normal to the plane of the roof panels, the global Z-axis parallel to the purlin span, and the global X-axis up the slope of the roof, perpendicular to the purlin web. The local axes of each element are oriented so that the local x-axis lies along the length of the element. The y axis and z axis are as shown in Figure 5.5.5-1.

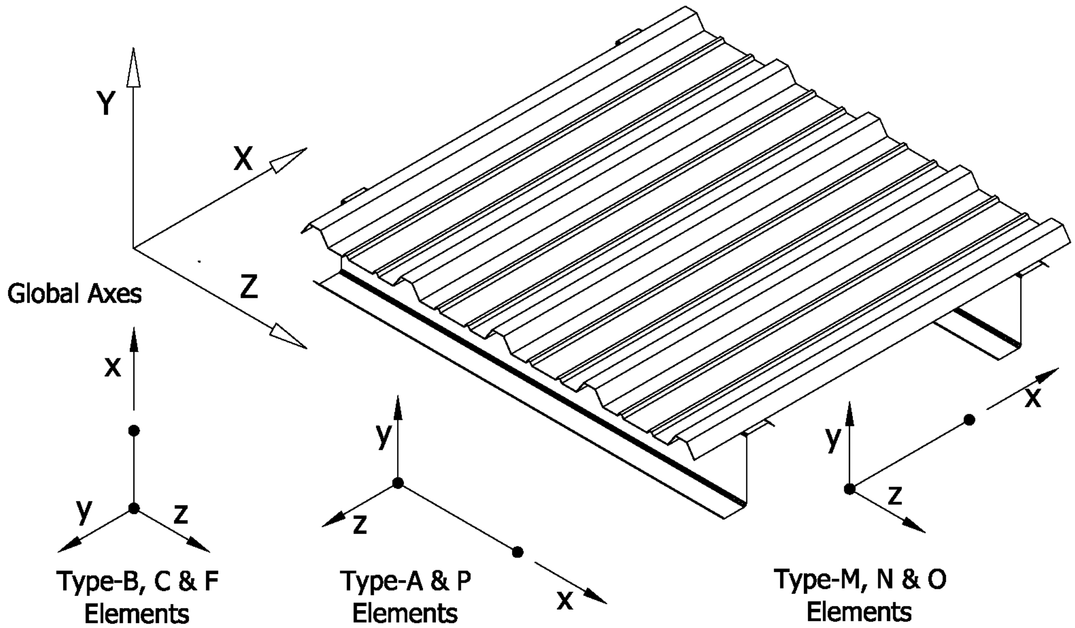

Figure 5.5.5-1 Local and Global Axes Orientations

5.5.5.3.2 Modeling of Purlins

In the computer model, the purlins are represented by a series of frame elements along the axis of the purlin in the plane of the web. The length of the purlin is divided into twelve equal

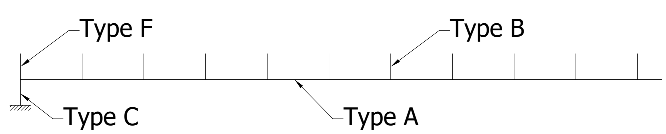

Figure 5.5.5-2 Purlin Frame Elements

segments to provide nodes for discretizing the roof diaphragm and for providing nodes at one-third points or one-quarter points for the attachment of anchorage devices. The geometry of a purlin is represented by four element types as shown in Figure 5.5.5-2.

Table 5-1 Type A Element Properties

Stiffness Model Property	Purlin Property Assigned to Type A Element
Area	Area
I_{yy}	I_{x2}
I_{zz}	I_{y2}
J	10 in.^{4}
x-axis rotation	θ

The longitudinal, Type A, elements are assigned the gross area and principal bending moments of inertia of the purlin section being modeled. Table 5-1 shows how the purlin properties given in AISI D100 correlate to the properties used in the stiffness model. Also, the axes of the Type A elements are rotated by the principal axis angle, θ_p. The torsional constant, J, is assigned an arbitrarily high value of 10 in.[4] because the torsional flexibility of the purlin is modeled by the Type B, Type C and Type F elements. Because the purlin cross-section may vary between bays, the element property input must typically include a definition for each bay (e.g. A1, A2, A3…).

For roof systems with multiple spans, the purlins from adjacent bays are typically lapped. To simplify the modeling and the user input, the lapped sections are assumed to extend into each bay for one-twelfth of the bay span. Within this region the area and the moments of inertia of the Type A elements are taken as the sum of the values for the two adjacent bays. The principal axis angle, θ_p, is taken as the average of the two values.

The Type B and Type F elements are included to provide the link between the plane of the roof panels and the neutral axis of the purlin and to model the weak-axis bending deformations of the purlin web. A moment release for the moments about the y-y axis is added to the element end at the connection between the Type A elements and the vertical elements. This eliminates the Vierendeel truss action that would artificially stiffen the system. The properties of the Type B elements are assigned to be consistent with a flat plate with a width equal to one-twelfth of the span and a thickness equal to the purlin thickness (see Table 5-2). For simple span purlins and end bays, the Type F elements have properties equal to one-half of the Type B elements. At interior supports in multi-span systems, the purlins are assumed to extend into the adjacent bays. Therefore, the properties of the Type F elements are found by the same principles as the Type B elements with the two purlins assumed to act as two non-composite sections. The resulting properties are summarized in Table 5-3.

Table 5-2 Type B Element Properties

Stiffness Model Property	Purlin Property Assigned to Type B Element
Area	L/12 x t
I_{yy}	0.0001
I_{zz}	$(L/12 \times t^3)/12$
J	I_{x2}
x-axis rotation	Zero

Table 5-3 Type F Element Properties

Stiffness Model Property	Purlin Property Assigned to Type F Element at Ends	Purlin Property Assigned to Type F Element at Laps
Area	L/24 x t	$(L_1+L_2)/12 \times (t_1 + t_2)$
I_{yy}	0.0001	0.0001
I_{zz}	$(L/24 \times t^3)/12$	$((L_1+L_2)/12 \times (t_1^3+t_2^3))/12$
J	I_{x2}	$(I_{x2})_1 + (I_{x2})_2$
x-axis rotation	Zero	Zero

At the purlin end, the Type C elements provide the connection to the support and model the behavior of the lower half of the purlin web in the vicinity of the support. A moment release is assigned to the end of the element at the connection to the Type A and Type F elements to eliminate bending in the plane of the purlin web (M_{ZZ}-moment). The properties of the Type C elements are formulated in a similar fashion as the Type F elements and have properties associated with the end one-twelfth of the span. The resulting properties for the Type C elements are summarized in Table 5-4.

Table 5-4 Type C Element Properties

Stiffness Model Property	Purlin Property Assigned to Type C Element at Ends	Purlin Property Assigned to Type C Element at Laps
Area	L/24 x t	$(L_1+L_2)/12$ x $(t_1 + t_2)$
I_{yy}	0.0001	0.0001
I_{zz}	$(L/24 \times t^3)/12$	$((L_1+L_2)/12 \times (t_1^3+t_2^3))/12$
J	I_{x2}	$(I_{x2})_1 + (I_{x2})_2$
x-axis rotation	Zero	Zero

5.5.5.3.3 Modeling of Roof Panels

The model developed by Seek (2007), which accurately models the axial, shear and flexural

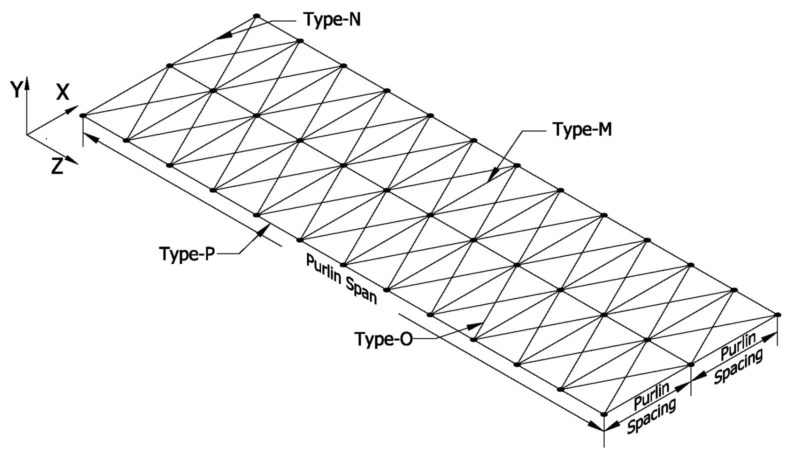

Figure 5.5.5-3 Panel Truss Elements

stiffness of the roof diaphragm, is used to model the roof panels. This formulation, shown in Figure 5.5.5-3, uses four element types. The diagonal Type O members are modeled with pinned end truss elements which provide the shear stiffness of the diaphragm. The cross-sectional area of the Type O elements is taken as

$$A_O = \frac{G' z(\alpha^2 + 1)^{1.5}}{2E\alpha^2} \qquad \text{(Eq. 5.5.5-1)}$$

where G′ is the shear stiffness of the panels, z is the purlin spacing and α is the module aspect ratio, z/(L/12). The "posts" of the truss are modeled with Type M and Type N elements. The cross-sectional area of these elements is calculated to yield the appropriate axial stiffness using the following.

$$A_N = \frac{\sqrt{b^2 + 4ac} - b}{2a} \qquad \text{(Eq. 5.5.5-2)}$$

$$A_M = 2A_N \qquad \text{(Eq. 5.5.5-3)}$$

where

$$a = 2zE\alpha(\alpha^2 + 1)^{1.5} \qquad \text{(Eq. 5.5.5-4)}$$

$$b = 2A_O zE(\alpha^4 + 1) - K_{axial} z^2 \alpha(\alpha^2 + 1)^{1.5} \qquad \text{(Eq. 5.5.5-5)}$$

$$c = K_{axial} A_O z^2 \qquad \text{(Eq. 5.5.5-6)}$$

$$K_{axial} = \frac{A_p E}{z} \qquad \text{(Eq. 5.5.5-7)}$$

and A_p is the cross-sectional area of the roof panels per unit width. To model the bending stiffness of the panels, the Type M and Type N elements are assigned a moment of inertia, I_{zz}, equal to the moment of inertia of the panels within the width tributary to the element. Moment releases are added at both ends of the Type M and Type N elements to eliminate bending about the y-y axis and torsion. The longitudinal Type P "chords" of the truss are modeled as axial-only truss elements with a cross-sectional area equal to product of alpha and A_N.

The above formulation works well for systems with through-fastened panels. The test results (Lee and Murray 2001; Seek and Murray 2004) for standing seam systems show a significant reduction in anchorage force when compared to through-fastened systems. This reduction is not seen in the computer model using the above diaphragm model. The transfer of shear forces in a standing seam system is fundamentally different from that of a through-fastened system due to slip between the individual panels. To represent this in the model, a hybrid treatment of the panel truss is used. For the effects of the load that acts in the plane of the purlin web, the panels are modeled as described above. Then a separate analysis is executed with the Type O elements removed and the torsional and downslope loads applied. The results of these two analyses are then superimposed.

5.5.5.3.4 Modeling of Loads

The loads applied to the model are calculated based on an input uniform total roof load distributed with a tributary area approach. In the physical roof system, the gravity loads are applied to the roof panels. In the computer stiffness model, the loads are represented by a series of distributed line loads and torsional moments. Typically, the roof system will have some slope; however, the geometry in the computer model is constructed with the plane of the roof parallel to the X-Z plane. To account for the slope, the applied gravity load is separated into vector components acting normal to and in the plane of the roof panels, resulting in

$$w_{normal} = w\cos\theta \qquad \text{(Eq. 5.5.5-8)}$$

$$w_{ds} = w\sin\theta \qquad \text{(Eq. 5.5.5-9)}$$

The load in the plane of the panels, w_{ds}, is applied as a uniform line load acting in the negative X direction along the Type P elements.

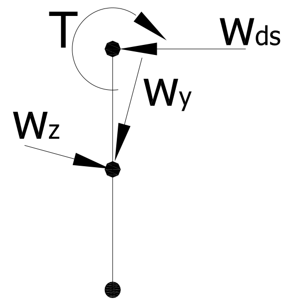

Figure 5.5.5-4 Summary of Loads

The component of the load that acts normal to the panels acts in a plane eccentric to the shear center of the purlin and causes torsion in the purlin. The gravity loads are transferred from the panels to the purlin by bearing on the purlin top flange. The true load distribution across the width of the flange is not known. Previous models have assumed a triangular distribution, and therefore a resultant force a distance of b/3 from the purlin web, where b is the width of the purlin flange. The latest research in the application of the frame element stiffness model (Sears 2007) found that an eccentricity of b/4 agreed better with tests. For sections, such as channels, where the shear center is not located in the plane of the purlin web, the eccentricity is m+b/4, where m is the distance between the shear center and the plane of the web. To model this torsion in the computer stiffness model a uniform torsion is applied along the length of the Type P elements. The magnitude of this moment is taken as,

$$T = w_{normal}\frac{b}{4} \quad \text{For Z-section purlins} \quad \text{(Eq. 5.5.5-10a)}$$

$$= w_{normal}\left(m + \frac{b}{4}\right) \quad \text{For C-section purlins} \quad \text{(Eq. 5.5.5-10b)}$$

For Z-sections the principal axes are inclined with respect to the geometric axes. Therefore, the applied load must be translated into vector components that act in the planes of the principal axes.

$$w_y = w_{normal}\cos\theta_p \quad \text{(Eq. 5.5.5-11)}$$

$$w_z = w_{normal}\sin\theta_p \quad \text{(Eq. 5.5.5-12)}$$

5.5.5.3.5 Modeling of the Purlin-to-Panel Connection

With the direct consideration of the axial and flexural stiffness of the panels included in the model, it is also important to represent the connection between the panels and the purlin. Therefore, linear springs in the local y-axis at the top of the Type B and Type F elements are added and assigned a stiffness of 5000 lb/in. for standing seam systems and 100,000 lb/in. for through-fastened systems. Rotational springs are placed at the ends of the Type M and Type N elements and have a stiffness of 1500 in.-lb/radian per foot of width for both roofing systems. The stiffness values are based on the calibration of this modeling with test results.

5.5.5.3.6 Modeling of Anchorage Devices

Spring supports are used at the top of the Type B or Type F elements at user selected locations in the model. By using spring supports, the finite stiffness of various anchorage devices can be accurately represented. Due to the indeterminate nature of the roof system, reduction in device stiffness can greatly affect the predicted anchorage forces. Modeling the points of anchorage with discrete nodal supports accurately represents typical construction details for anchorage devices at the frame lines, and for certain cases when anchorage devices are located along the purlin span. However, lines of anchorage constructed so that displacement at a line of anchorage is coupled with the displacement of other lines of anchorage, such as 1/4 point anchors connected to a beam at the eave, are difficult to represent accurately with this method of modeling.

5.5.6 Shell Finite Element Models to Predict Anchorage Forces

5.5.6.1 Components of Finite Element Model

A finite element model was developed for the prediction of anchorage forces. The model is the most complete representation of a purlin supported roof system for the prediction of anchorage forces. The model has been validated by comparisons to the test results of Lee and Murray (2001) and Seek and Murray (2004) and was used in the development of the component stiffness method.

The model is composed of four basic elements. Shell elements are used to represent the purlin and the panels. Frame elements are used to represent the anchorage devices and strap bracing. Connection between the purlin and the panels is made using a two node link element. A representation of the elements comprising the model and the global axes are shown in Figure 5.5.6-1.

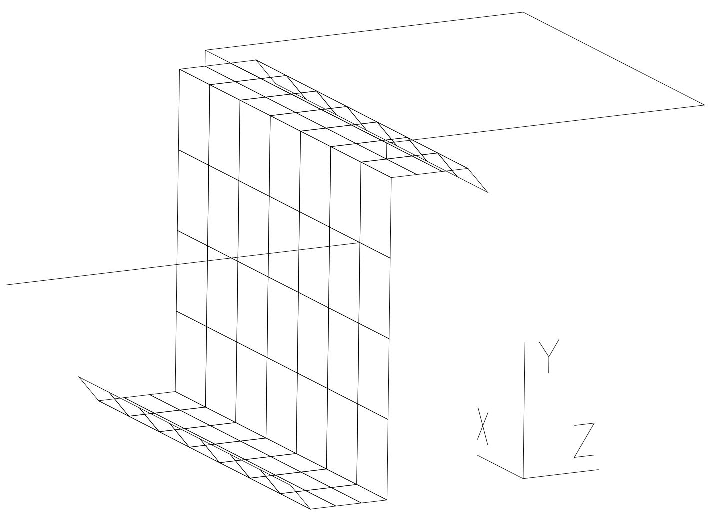

Figure 5.5.6-1 Representative Elements of Finite Element Model

5.5.6.1.1 Finite Element Representation of Purlin

To represent the purlin with finite elements, the web is discretized into four elements, the flanges into three elements, and the lips into single elements. Discretization along the length of the purlin should be chosen to maintain a maximum aspect ratio of 4:1.

The elements representing the purlins are assigned a membrane thickness and a bending thickness equal to the nominal thickness of the purlin. In the case of a multi-span system in which the purlins are lapped, the modeled purlin is given a membrane thickness equivalent to the sum of the thicknesses of the two purlins at the lap. The bending thickness of the element at the lap is equivalent to the combined moment of inertia of the two purlins comprising the lap. That is,

$$t_{lap,bending} = \sqrt[3]{t_1^3 + t_2^3} \qquad \text{(Eq. 5.5.6-1)}$$

where t_1 and t_2 are the thicknesses of each purlin at the lap.

5.5.6.1.2 Finite Element Representation of the Panels

The panels are represented in the finite element model by a shell element discretized into 12 in. segments along the length of the purlin and divided into five equal segments between the purlins. The elements representing the panels are given a membrane thickness equal to the material thickness of the panels. To account for the bending stiffness provided by the panel ribs, the bending thickness of the element equivalent to the gross moment of inertia of the deck is calculated by:

$$t_{panel,bending} = \sqrt[3]{12 \cdot I_{panel}} \qquad \text{(Eq. 5.5.6-2)}$$

To allow for variations in panel diaphragm stiffness, the panel elements are designated as orthotropic material and the shear modulus is adjusted. For the two material directions in the plane of the panels, the panel shear modulus, G, for a desired diaphragm shear stiffness, G′, is

$$G = \frac{G'}{t} \qquad \text{(Eq. 5.5.6-3)}$$

For the material direction perpendicular to the plane of the panels, the shear modulus of steel (11,300 ksi) is used.

5.5.6.1.3 Link Connection Between Purlin and Panels

The connection between the purlin and the panels is made by a 2-node link element at 1 ft intervals along the length of the purlin and at an eccentricity of 1/3 of the flange width. The link element allows for the translational and rotational stiffness between two joints to be defined about three axes. The link element also provides an efficient means to track forces transferred between the purlin and the panels. Because there is some rotational flexibility in the connection between the purlin and the panels about the axis parallel to the length of the purlin, the link rotational stiffness about this axis will typically range between 500 lb-in./radian and 10000 lb-in./radian. To prevent the purlin and the panels from behaving like a composite section, the translational stiffness of the link element about the axis parallel to the length of the purlin is released.

In standing seam systems, the connection between the purlin and the panels is made by a clip screwed to the purlin and sandwiched in the seam between two adjacent panels. There is some translational slip in this connection parallel to the seam, whether it is intentional in a sliding clip or inadvertent due to a loose seam. Although the stiffness of this connection is nonlinear, it can be approximated by assigning the link element a linear stiffness in the axis perpendicular to the web of the purlin. The stiffness of this connection is assumed to range between 250 lb/in. and 5000 lb/in. for most standing seam systems. The flexibility of this connection has the effect of reducing the diaphragm stiffness of the system.

5.5.6.1.4 External Restraints

An external restraint representing the connection to the rafter is applied at a single node at the base of the purlin at the intersection of the web and bottom flange of the purlin based on a web plate connection. An external restraint can be located elsewhere to model different rafter connection configurations, which could create additional eccentricities and consequential forces.

Translational restraint is applied in the global Y and Z directions and rotational restraint is applied about the global X axis.

External anchorages are modeled as axial loaded frame elements between the web of the purlin and an external support. The location of the anchorage device along the height of the web should reflect the actual device modeled. The total stiffness of the anchorage is the combined stiffness of the anchorage device and the stiffness of the purlin web transferring this force to the anchorage. The stiffness of the anchorage can be modeled in one of two ways. The first is to model the anchorage with the combined device and configuration stiffness. Using the stiffness derived from the test in Section 5.5.4.5, restraint is applied at the top flange of the purlin and assigned the linear spring stiffness of the test specimen. The second is to treat the configuration and device stiffness separately. The restraint is applied in the model at the same height along the web as the actual specimen. For example, the top row of bolts in an anti-roll anchorage device is considered the anchorage height. The restraint is assigned a linear spring stiffness equivalent to that of the device itself. This stiffness can be determined by testing the device itself or utilizing mechanics to estimate the stiffness. The configuration stiffness will be captured by the model itself because the web will deform as it transfers the anchorage force between the top flange and anchorage device. The model will typically overestimate this deformation of the web, which will cause the configuration stiffness to be underestimated. The flexibility of the web between the top of the restraint and the top flange of the purlin when modeled in this way will typically underestimate the configuration stiffness.

5.5.6.2 Model Loading

Load is applied directly to the panels in the model as a uniformly applied area loading. To account for roof slope, a uniform load is applied both normal and parallel to the panels (downslope). The vertical gravity load, W, is then divided into normal, W_{normal}, and downslope, $W_{downslope}$, components according to the roof slope, or

$$W_{normal} = W \cos\theta \qquad \text{(Eq. 5.5.6-4)}$$

$$W_{downslope} = W \sin\theta \qquad \text{(Eq. 5.5.6-5)}$$

where θ is the angle of the roof with respect to the horizontal.

5.5.6.3 Finite Element Model Example

The following example shows the development of a shell finite element model to predict anchorage forces based on the roof system of Example 3.3.2.1

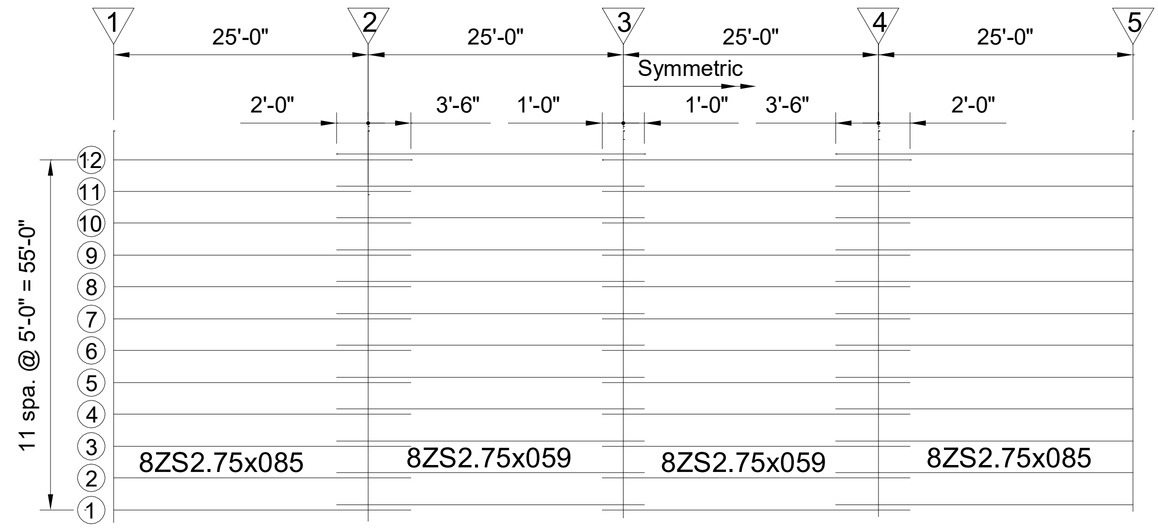

Figure 5.5.6-2 Roof Layout for Finite Element Model

Given

1. Twelve purlin lines spaced at 5 feet. The top flange of the first purlin closest to the eave faces downslope. The top flanges of the remaining purlins face upslope. Roof slope is a 1/2 on 12 pitch and the gravity loads are 3 psf dead and 20 psf live.
2. The system of purlins is a four-span continuous system symmetric about the center frame line. Each span is 25 ft. In the end bays, the purlins are 8ZS2.75x085. In the interior bays the purlins are 8ZS2.75x059. Laps are as shown in Figure 5.5.6-2.
3. The roof covering is attached with standing seam panel clips along the entire length of the purlins. The panel is a 26 gage (0.0179 in.) rib type panel profile with fixed clips and a mechanical seam. The gross moment of inertia of the panel is 0.254 in.^{4}/ft. The panels have a diaphragm stiffness G′ = 1000 lb/in. and the rotational stiffness of the standing seam panel clips, k_{mclip} = 2500 lb-in./(rad-ft).
4. There are no discrete bracing lines. Anti-roll clips are provided at each support at every fourth purlin line (lines 4, 8 and 12). Each anti-roll anchorage device is attached to the web of the Z-section with two rows of two 1/2 in. diameter A307 bolts. The bottom row of bolts is 3 in. from the bottom flange and the top row is 6 in. from the bottom flange. The stiffness of each anti-roll anchorage device, K_{device} = 40 kip/in. The width of the anti-roll anchorage device is b_{pl} = 5.0 in.
5. Purlin flanges are bolted to the support member with two 1/2 in. diameter A307 bolts through the bottom flange.

Required

1. Anchorage forces along each frame line at the top of the anchorage device due to gravity loads.

2. Lateral deflection of the top flange of the Z-section along each frame line and at the purlin mid-span.
3. Shear force in the standing seam panel clips at each anchorage device.

Solution

Assumptions for Analysis

a. The model is first order linear elastic.
b. Purlin and panels are modeled as shell elements with thin plate behavior. Purlins are modeled with a zero bend radius.
c. Connection between the purlin and the panels is made through a single spring connection.
d. Connections to rafters are made at a single node at the junction of the purlin web and bottom flange.

1. Model Properties

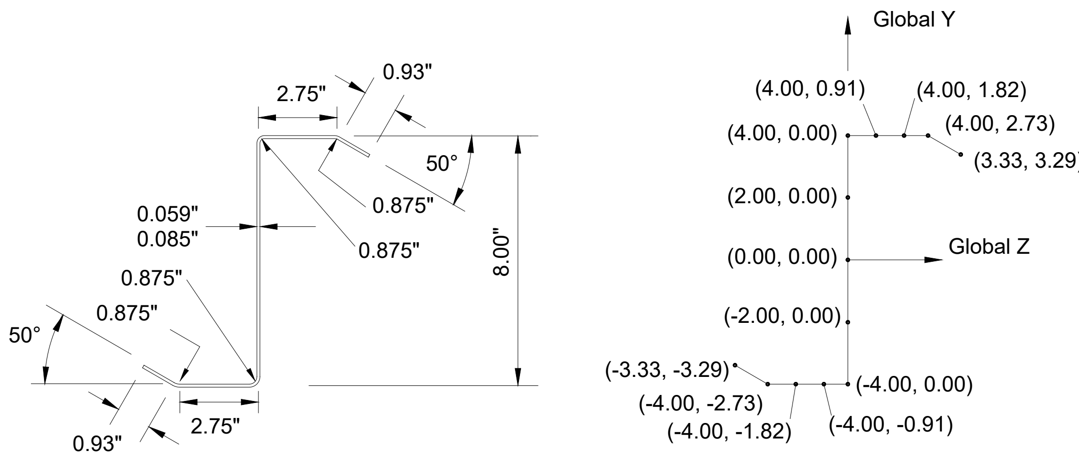

a) Cross Section Dimensions **b) FE Model Discretization**

Figure 5.5.6-3 Purlin Cross Section

a. Purlins

The purlin cross section is discretized as shown in Figure 5.5.6-3(b). Along the span of the purlin, the purlin is discretized in 2 in. increments. The purlin is modeled as a shell element with thin plate behavior. Along the interior of the span, the nominal thickness of the purlin is assigned to the membrane and bending thickness of the elements. At the lap, a single element is used to approximate the two purlins in the lapped region. In the lapped region, the membrane thickness is the sum of the thicknesses of the two purlins, and the bending thickness is an equivalent thickness such that the single plate thickness has the same moment of inertia of the sum of the moments of inertia of the individual plate thicknesses.

End bay

$t_{membrane}$ = 0.085 in.

$t_{bending}$ = 0.085 in.

First interior lap

$t_{membrane}$ = 0.085 in. + 0.059 in. = 0.144 in.

$t_{bending} = \sqrt[3]{(0.085in)^3 + (0.059in)^3}$ = 0.094 in.

Interior bay

$t_{membrane}$ = 0.059 in.

$t_{bending}$ = 0.059 in.

Second interior lap

$t_{membrane}$ = 0.059 in. + 0.059 in. = 0.118 in.

$t_{bending} = \sqrt[3]{(0.059in)^3 + (0.059in)^3}$ = 0.074 in.

b. Diaphragm Elements

The diaphragm is discretized into 12 in. by 12 in. elements. Each element is modeled as a shell element with thin plate behavior. The membrane thickness of the panel elements is the nominal thickness of the panel (26 ga. panel, t = 0.0179 in.). To account for the diaphragm stiffness, the shear modulus of the material is adjusted.

$t_{membrane}$ = 0.0179 in.

$G = \frac{G'}{t} = \frac{1000 \, {}^{lb}\!/_{in}}{0.0179in}$ = 55,866 psi.

The panel has a gross moment of inertia of I_{panel} = 0.254 in.^{4}/ft. The bending thickness of the panels is adjusted to give an equivalent moment of inertia.

$$t_{panel,bending} = \sqrt[3]{12I_{panel}} = \sqrt[3]{12\left(0.254\,{}^{in^4}\!/_{ft}\right)\left(\frac{1ft}{12in}\right)} = 0.633 \text{ in.} \qquad \text{(Eq. 5.5.6-2)}$$

c. Link Elements

The diaphragm is located 0.1 in. above the top flange of the purlin. Link elements provide the connection between the panel elements and purlin elements at 12 in. increments along the length of the purlin at the panel element joints. The link elements are attached to the purlin at the node at 1/3 the distance from the purlin web to model the eccentricity of the gravity loads acting on the purlin top flange. Link elements are convenient because they allow for the stiffness of the connection between the purlin and the panels to be specified directly and quickly adjusted. The link element local axes are shown in Figure 5.5.6-4. The rotational stiffness of the connection between the purlin and the panels is assigned to the local 3 axis. The connection is considered translationally rigid in the local 1 and 2 directions and rotationally rigid about the local 2 axis. To prevent the purlin from acting like a composite member, translational stiffness in the local 3 direction is reduced to a negligible value. Rotational stiffness about the local 1 axis is also reduced to a negligible value. The link stiffness values are tabulated below. Because the links are located at 12 in. intervals along the span of the purlin, tabulated stiffness values are considered per foot along the length of the purlin.

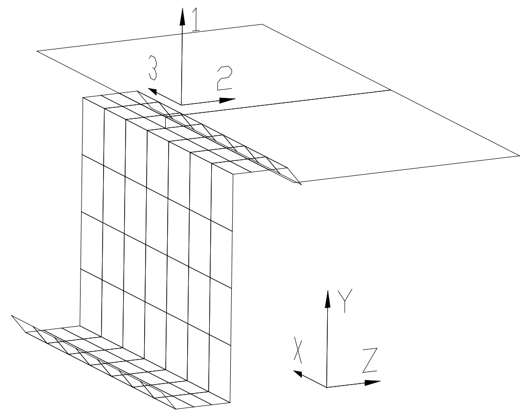

Figure 5.5.6-4 Link Element Local Axes

Summary of link element properties.

Translation	Rotation
U1 = $1x10^7$ lb/in.	R1 = 1.0 lb-in./rad
U2 = $1x10^7$ lb/in.	R2 = $1x10^7$ lb-in./rad
U3 = 0.1 lb/in.	R3 = 2500 lb-in./rad

d. Connection to the rafter

The connection to the rafter is modeled as a single node joint restraint at the junction of the bottom flange and web at the centerline of the frame line. The joint is restrained from translation in the global Y and Z axes (refer to Figure 5.5.6-4) and restrained from rotation about the global X axis. The remaining degrees of freedom are released.

e. Anchorage Device

The anchorage device has a stiffness of 40 kip/in. This stiffness is considered at the top row of bolts of the anchorage device (6 in. from the bottom flange). Therefore, a spring restraint with a stiffness of 40 kip/in. in the global Z direction is applied to a node at 6 in. from the base of the purlin. To account for the width of the anchorage device and the stiffening effect it has on the purlin web, frame elements were added to the web of the purlin as shown in Figure 5.6.5-5. Frame element 1 was modeled as a bar 1/2 in. x 4 in. and frame element 2 was modeled as a bar 1/4 x 2 in. The thickness of the elements was oriented in the same direction as the thickness of the purlin. To prevent moment transfer at the base of the purlin, the rotational stiffness of the frame elements was released at the connection at the base of the purlin web.

Note, if the stiffness of the anchorage device includes the deformation of the purlin web, as can be determined by the test discussed in Section 5.5.6.1.4, a spring restraint with the stiffness determined from the test should be applied at the top flange of the purlin.

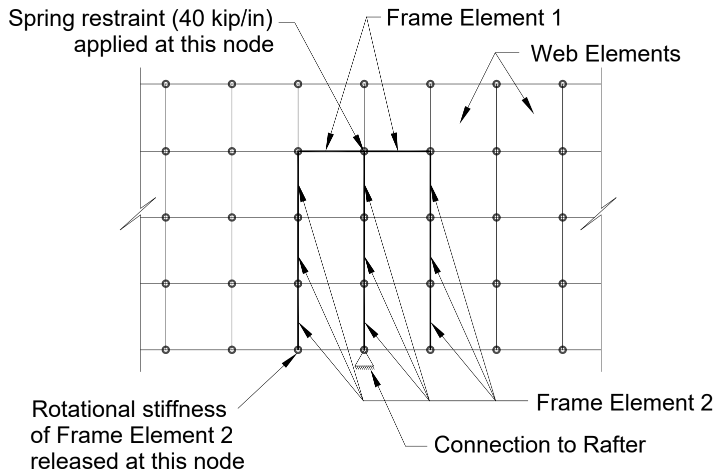

Figure 5.5.6-5 Frame Elements to Represent Anti-roll Anchorage

2. Loading

Gravity loads are applied as uniform area loads on the panels. The total gravity load, dead plus live, is 23 psf. To account for the slope of the roof, the gravity load is broken into components normal to the panels and in the plane of the panels.

$U_{normal} = U \cos\theta = (23\text{ psf}) \cos(2.39°) = 22.98\text{ psf}$

$U_{downslope} = U \sin\theta = (23\text{ psf}) \sin(2.39°) = 0.959\text{ psf}$

3. Model Solution

a. Anchorage Forces

Frame Line 1

Purlin 4 P_h = 432 lb
Purlin 8 P_h = 410 lb
Purlin 12 P_h = 406 lb

Frame Line 2

Purlin 4 P_h = 415 lb
Purlin 8 P_h = 391 lb
Purlin 12 P_h = 431 lb

Frame Line 3

Purlin 4 P_h = 380 lb
Purlin 8 P_h = 367 lb
Purlin 12 P_h = 435 lb

b. Lateral Deflection of Z-section

Positive values indicate upslope translation.
Lateral deflection extracted from the Purlin 4 model.

Top flange at Frame Line 1 $\Delta = 0.111$ in.

AISI S100 deflection limit $$\Delta_{tf} \le \frac{1}{\Omega}\frac{d}{20} = \frac{1}{2.00}\frac{8\text{ in}}{20} = 0.20\text{ in} > 0.111\text{ in OK}$$

Top flange at the centerline of the end bay $\Delta = 0.382$ in.
Bottom flange at the centerline of the end bay $\Delta = 0.629$ in.

AISI S100 deflection limit $$\Delta_{ms} \le \frac{L}{360} = \frac{25\text{ft}\left(12\ {}^{\text{in}}\!/_{\text{ft}}\right)}{360} = 0.83\text{ in} > 0.382\text{ in. OK}$$

Approximate rotation at the centerline of the end bay $\phi \approx (0.382\text{ in.} - 0.629\text{ in.})/8\text{ in.} = -0.031$

Top flange at Frame Line 2 $\Delta = 0.14$ in.

AISI S100 deflection limit $$\Delta_{tf} \le \frac{1}{\Omega}\frac{d}{20} = \frac{1}{2.00}\frac{8\text{ in}}{20} = 0.20\text{ in} > 0.14\text{ in OK}$$

Top flange at the centerline of the interior bay $\Delta = 0.310$ in.
Bottom flange at the centerline of the interior bay $\Delta = 0.649$ in.

AISI S100 deflection limit $$\Delta_{ms} \le \frac{L}{360} = \frac{25\text{ft}\left(12\ {}^{\text{in}}\!/_{\text{ft}}\right)}{360} = 0.83\text{ in.} > 0.310\text{ in. OK}$$

Approximate rotation at the centerline of the end bay $\phi \approx (0.310\text{ in.} - 0.649\text{ in.}/8\text{in} = -0.042$

Top flange at Frame Line 3 $\Delta = 0.110$ in.

AISI S100 deflection limit $$\Delta_{tf} \le \frac{1}{\Omega}\frac{d}{20} = \frac{1}{2.00}\frac{8\text{ in}}{20} = 0.20\text{ in.} > 0.110\text{ in OK}$$

Vertical deflection extracted from the Purlin 4 model.

Top flange at the centerline of the end bay $\Delta = -1.189$ in.
Top flange at the centerline of the interior bay $\Delta = -0.515$ in.

c. Shear Forces in the purlin to panel connection

The shear forces in the link connection are plotted in Figure 5.5.6-6 from the exterior frame line to the centerline of the system (Frame Line 3) for both Purlin 3 and Purlin 4. The spikes in fastener forces occur at the frame lines. For comparison to the calculation in the component stiffness method of the shear force in the purlin to panel connection, P_{sc}, the total fastener force is the sum of the forces at 12 in. to either side of the frame line. This total fastener force can be considered to be distributed evenly between each of the fasteners within 12 in. of the frame line. The forces along the length of the span represent the uniform restraint force in the panels, w_{rest}, calculated in the component stiffness method.

Fastener forces for Purlin 3 (typical purlin).

Frame Line 1 P_{sc} = 148 lb + (-19.0 lb) = 129 lb

Frame Line 2 P_{sc} = 68.6 lb + 93.0 lb + 69.9 lb = 232 lb

Frame Line 3 P_{sc} = 55.5 lb + 58.2 lb + 55.5 lb = 169 lb

Along the span of Purlin 3, the uniform restraint force in the panels is the average of forces along the length.

End bay w_{rest} = 29.6 lb/ft

Interior bay w_{rest} = 25.2 lb/ft

Fastener forces for Purlin 4 (directly anchored).

Frame Line 1 P_{sc} = 453 lb + 44.0 lb = 497 lb

Frame Line 2 P_{sc} = 130 lb + 305 lb + 131 lb = 566 lb

Frame Line 3 P_{sc} = 107 lb + 270 lb + 107 lb = 484 lb

Along the span of Purlin 4, the uniform restraint force in the panels is the average of forces along the length.

End bay w_{rest} = 29.1 lb/ft

Interior bay w_{rest} = 24.4 lb/ft

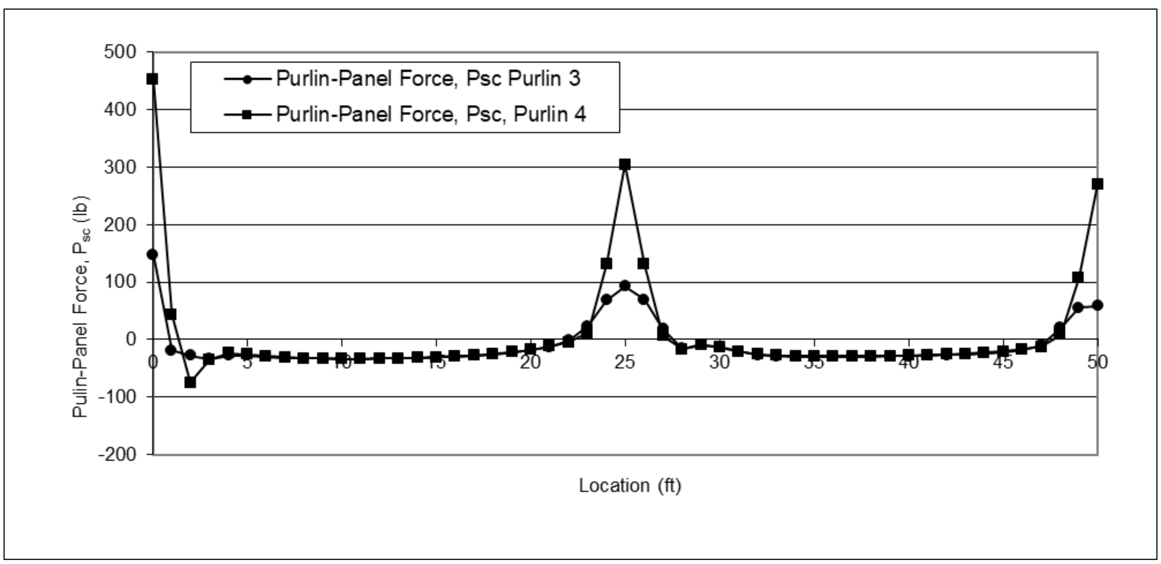

Figure 5.5.6-6 Shear Force Transfer Between Purlin and Panels

d. Panel Moment

The total moment in the connection between the panels and the purlin is plotted from Frame Line 1 to the centerline of the system (Frame Line 3) for Purlins 3 and 4 in Figure 5.5.6-7. This total moment includes the parabolic moment in the panels due to torsion effects, $M_{torsion}$, the moment due to local deformations, M_{local}, and the moment due to the deformation of the anchorage, M_{panel}.

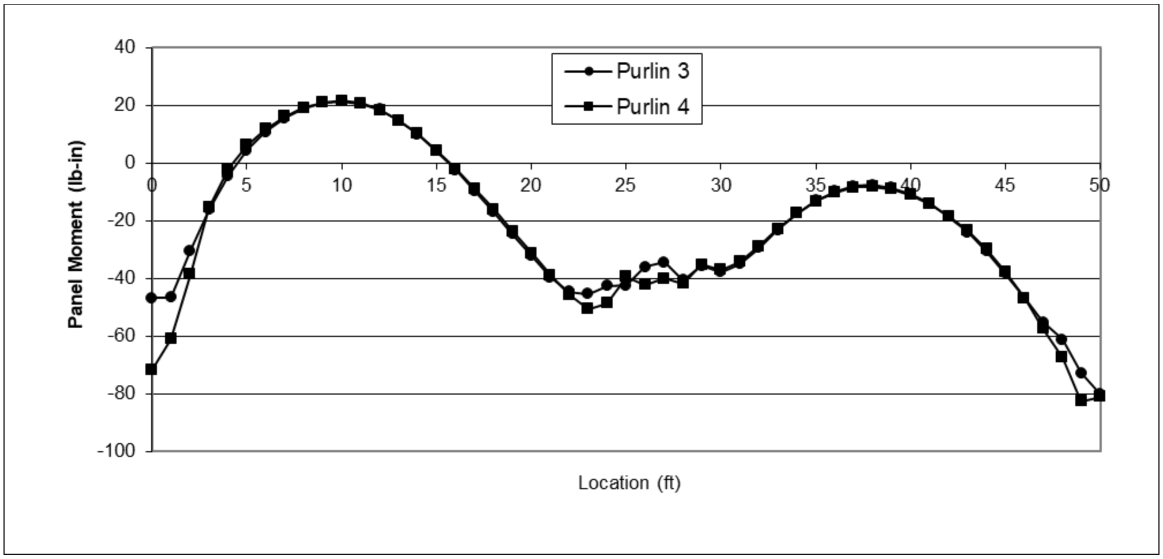

Figure 5.5.6-7 Moments in Connection Between Purlin and Panels

e. Comparison to analytical solution of Section 5.5.4.7.1

The finite element model example provided in this section is the same as the model solved by the analytical solution in Section 5.5.4.7.1 with the exception that the anchors are located along different purlin lines. The difference in anchorage location results in negligible differences. A comparison is made for the calculated values of analytical model relative to the results of finite element model.

Anchorage forces

The calculated anchorage forces, P_h, for a purlin connected to an anchorage device are provided in the table below for Purlins 5 and 9 from the analytical solution versus the average of Purlins 4, 8 and 12 from the finite element model. The forces from the finite element model are almost uniform, indicating that there is some sharing of forces between the adjacent frame lines. The forces from the analytical solution look at each frame line individually. This results in overpredicting the forces at Frame Line 2 versus slightly underpredicting the forces at 1 and 3.

Table 5.5.6-1 Comparison of Anchorage Force

	Anchorage force at height of anchor, P_h	
Location	Analytical Solution (lb)	FE Model Average (lb)
Frame Line 1	396	416
Frame Line 2	529	412
Frame Line 3	339	394

Anchor deflection at frame line

The calculated deflection at the top of the purlin along each frame line, Δ_{rest}, is compared between the analytical model and the finite element model in Table 5.5.6-2. The finite element model predicts larger deflections than the analytical model. The equations for the analytical model were developed to overestimate the stiffness at the anchor location, which will result in higher predicted anchorage forces in the analytical model. As the system deflects at the frame line, forces will be distributed to other components in the system. Because the anchors are so much stiffer than other components in the system and the magnitude of the difference in deflection between the finite element model and the analytical solution is small, the difference in the forces distributed to the system is small and thus, the anchorage forces are very similar between the finite element model and analytical solution.

Table 5.5.6-2 Comparison of Deflection at Anchorage

	Deflection of top flange of purlin at anchor, P_h	
Location	Analytical Solution (in.)	FE Model (in.)
Frame Line 1	0.040	0.111
Frame Line 2	0.044	0.114
Frame Line 3	0.045	0.110

Uniform restraint force in panels and lateral deflection of the purlins

The calculated uniform restraint force between the purlin and the panels, w_{rest} is shown in Table 5.5.6-3. Although not explicitly calculated in the analytical solution example from Section 5.5.4.7.1, it can be calculated by Eq. 5.5.4-5. The analytical solution predicts a higher uniform restraint force in the panels. This may be due to other mechanisms in play in the finite element model such as tension field action and the approximations made in the analytical model regarding the force transitions near the frame line. As a result of the higher forces in the panels predicted by the analytical solution, the lateral deflections predicted by the analytical solution are slightly higher than those predicted by the finite element model. Ultimately, the analytical model results in conservative approximations of both force in the panels and lateral deflection of the purlins.

Table 5.5.6-3 Comparison of Uniform Restraint Force in the Panels

	Analytical Solution		FE Model Average (in.)	
Location	w_{rest} (lb/ft)	Δ_{diaph} (in.)	w_{rest} (lb/ft)	Δ_{diaph} (in.)
End Bay	33.9	0.40	29.6	0.382
Interior Bay	32.2	0.375	25.2	0.310

Fastener forces in connection between panel and purlin

The forces in the connection between the purlin and the panel, P_{sc}, at a typical anchor location (Purlin 5 in analytical model, Purlin 4 from FE model) are provided in Table 5.5.6-4 below. The forces calculated by the analytical method are greater than those determined from the finite element model for several reasons. The analytical method predicts a larger uniform restraint force along the length of the purlin which must be resolved at the frame lines. The analytical method also conservatively assumes that all of the force is transferred very close to the frame line whereas the finite element model shows a more gradual transition of the forces over a greater length of the purlin. Finally, as previously discussed the analytical solution evaluates the forces transferred to each frame line individually, whereas in the finite element model there is some force transfer between the frame lines, which results in a more uniform magnitude of forces between adjacent frame lines.

Table 5.5.6-4 Comparison of Force in Connection Between Purlin and Panel at Anchorage

	Connection force between purlin and panel, P_{sc}	
Location	Analytical Solution (in.)	FE Model (in.)
Frame Line 1	512	497
Frame Line 2	869	566
Frame Line 3	748	484

CHAPTER 6 MISCELLANEOUS TOPICS

6.1 Standing Seam Roofs on Steel Joists

The 2020 SJI *Standard Specification for Open Web Steel Joists, K- Series, and LH- Series* (SJI, 2020) contains in Section 5.9.7 the following provision relative to standing seam roofs:

> "Where the roof systems do not provide lateral stability for the steel joists in accordance with Section 5.9.5 sufficient stability shall be provided to brace the steel joists laterally under the full design load. For this condition, the compression chord design shall include the effects of both the in-plane and out-of-plane buckling of the steel joist (e.g., buckling about the vertical axis of the steel joist cross section). In any case where the attachment requirement of Section 5.9.5 is not achieved, out-of-plane strength shall be achieved by adjusting the bridging spacing and/or increasing the compression chord area and the y-axis radius of gyration. The effective slenderness ratio about the vertical axis equals 0.94 L/r_y; where L is the bridging spacing in inches (millimeters) and r_y is the radius of gyration of the top chord in inches (millimeters). The maximum bridging spacing shall not exceed that specified in Section 5.5.3.
>
> Horizontal bridging members attached to the compression chords and their anchorages shall be designed for a compressive axial force. P_{br}, given in Equation 5.9-1.
>
> $$P_{br} = 0.001nP + 0.004P\sqrt{n} \geq 0.0025nP\text{, kips (N)} \qquad \text{(SJI Eq. 5.9-1)}$$
>
> Where n is the number of joists between end anchors and P is the chord design force in kips (N).
>
> The attachment force between the horizontal bridging member and the compression chord shall be 0.01P. Horizontal bridging attached to the tension chords shall be proportioned so that the slenderness ratio between attachments does not exceed 300. Diagonal bridging shall be proportioned so that the slenderness ratio between attachments does not exceed 200."

Some joist manufacturers have conducted proprietary tests to determine the strength of their joists with various standing seam roof systems. Currently there are no standardized test procedures to determine the lateral bracing effectiveness of the standing seam panel.

Without supportive test data, joist manufacturers must design the joist chords based on the SJI provisions cited above.

6.2 Standing Seam Roofs with Roof Top Units or Hanging Loads

The lateral support provided to purlins from a standing seam roof is available from roof clips, friction and panel envelopment. The amount of support provided by each of these effects is unknown. Since the base test is conducted in an air chamber, whereby the loads are applied through the standing seam roof to the purlins, the stability effect of concentrated loads applied to the purlin flanges is unknown. Thus, purlins supporting concentrated loads should be braced independently of the standing seam roof system. From a practical point of view, the stability forces from small collateral loads such as sprinkler lines, ceiling, etc. may be neglected.

REFERENCES

AISC (2016), *Specification for Structural Steel Buildings*, American Institute of Steel Construction, Chicago, IL, 2016.

AISI (2016), AISI S100, *North American Specification for the Design of Cold-Formed Steel Structural Members,* American Iron and Steel Institute, Washington, DC, 2016.

AISI (2017a), AISI D100, *Cold-Formed Steel Design Manual*, American Iron and Steel Institute, Washington, DC, 2017.

AISI (2017b), AISI S901, *Test Standard for Determining the Rotational-Lateral Stiffness of Beam-to-Panel Assemblies*, American Iron and Steel Institute, Washington, DC, 2017.

AISI (2017c), AISI S907, *Test Standard for Determining the Strength and Stiffness of Cold-Formed Steel Diaphragms by the Cantilever Method*, American Iron and Steel Institute, Washington, DC, 2017.

AISI (2017d), AISI S908, *Test Standard for Determining the Flexural Strength Reduction Factor of Purlins Supporting a Standing Seam Roof System*, American Iron and Steel Institute, Washington, DC, 2017.

AISI (2017e), AISI S912, *Test Standard for Determining the Strength of a Roof Panel-to-Purlin-to-Anchorage Device Connection*, American Iron and Steel Institute, Washington, DC, 2017.

AISI (2020), AISI S310, *North American Standard for the Design of Profiled Steel Diaphragm Panels*, American Iron and Steel Institute, Washington, DC, 2020.

ASCE (2016), *Minimum Design Loads for Buildings and other Structures,* ASCE Standard 7-16, American Society of Civil Engineers, Reston, VA, 2016.

Bryant, M. R. and T. M. Murray (2000), “Investigation of Inflection Points as Brace Points in Multi-Span Purlin Roof Systems”, Research Report No. CE/VPI-ST-00/11, Department of Civil and Environmental Engineering, Virginia Polytechnic Institute and State University, Blacksburg, VA, 2000.

Curtis, L. and T. M. Murray (1983), "Simple Span Z-Purlin Tests to Determine Brace Force Accumulation", Fears Structural Engineering Laboratory Research Report FSEL/MBMA 83-02, University of Oklahoma, Norman, OK, 1993.

Center for Cold-Formed Steel Structures (CCFSS) (1992), Bulletin, Vol. 1, No. 2, August 1992.

Ellifritt, D. S., T. Sputo and J. Haynes (1992), “Flexural Capacity of Discretely Braced C’s and Z’s,” *Proceedings of the Eleventh International Specialty Conference on Cold-Formed Steel Structures*, University of Missouri-Rolla, Rolla, MO, October 1992.

Elhouar, S. and T. M. Murray (1985), "Stability Requirements of Z-Purlin Supported Conventional Metal Building Roof Systems," *Annual Technical Session Proceedings*, Structural Stability Research Council, Bethlehem, PA, 1985.

Ghazanfari, A., and T. M. Murray (1983), "Prediction of the Lateral Restraint Forces of Single Span Z-purlins with Experimental Verification." Fears Structural Engineering Laboratory Research Report No. FSEL/MBMA 83-04, University of Oklahoma, Norman, OK.

Heinz, D. A. (1994). "Application of Generalized Beam Theory to the Design of Thin-Walled Purlins", *Thin Walled Structures*, 19, pp. 311-335, 1994.

Lee, S. and T. M. Murray (2001), "Experimental Determination of Required Lateral Restraint Forces for Z-Purlin Supported, Sloped Metal Roof Systems." Research Report CE/VPI-ST 01/09, Department of Civil and Environmental Engineering, Virginia Polytechnic Institute and State University, Blacksburg, VA, 2001.

Murray, T. M. and S. Elhouar (1994), North American Approach to the Design of Continuous Z- and C-Purlins for Gravity Loading with Experimental Verification, *Engineering Structures*, Elsevier, Vol. 16, No. 5, pp. 337-341, 1994.

Neubert, M. C. and T. M. Murray (2000), "Estimation of Restraint Forces for Z-Purlin Roofs under Gravity Loads," *15th International Specialty Conference on Cold-Formed Steel Structures*, St. Louis, MO, 2000.

Seaburg, Paul A. and Carter, Charles J. (1997), *Steel Design Guide Series 9, Torsional Analysis of Structural Steel Members.* American Institute of Steel Construction, Chicago, IL, 1997.

Sears, J. M. (2007), "Development of Prediction Methods for the Lateral Anchorage Requirements in Metal Building Roof Systems", MS Thesis, Department of Civil and Environmental Engineering, Virginia Polytechnic Institute and State University, Blacksburg, VA, 2007.

Sears, J. M. and T. M. Murray (2007), "Proposed Method for the Prediction of Lateral Restraint Forces in Metal Building Roof Systems," *Annual Stability Conference Proceedings*, Structural Stability Research Council, New Orleans, LA, April 19-21, 2007.

Seek, M. W. (2007), "Prediction of Lateral Restraint Forces in Sloped Z-Section Supported Roof Systems Using the Component Stiffness Method" PhD Dissertation, Department of Civil and Environmental Engineering, Virginia Polytechnic Institute and State University, Blacksburg, VA, 2007.

Seek, M. W. (2016), "Displacement Compatibility Solutions for Discrete Bracing of Cold-Formed C- and Z-Sections in Flexure." *Annual Stability Conference Proceedings*, Structural Stability Research Council, University of Missouri-Rolla, Rolla, MO, 2016.

Seek, M. W. (2022), "Exploring the effects of clip flexibility on the behavior or standing seam diaphragms to brace cold formed steel purlins." *Annual Stability Conference Proceedings*, Structural Stability Research Council, University of Missouri-Rolla, Rolla, MO, 2022.

Seek, M. W. and Avci, O. "A system analysis methodology for the practical design of cold-formed steel purlin supported roof systems with paired torsion braces using the Direct Strength Method" *Conference Proceedings*, Structural Stability Research Council Annual Stability Conference. 2021. Structural Stability Research Council, American Institute of Steel Construction, Chicago, Illinois.

Seek, M. W. and T. M. Murray (2004a), "Testing of the Lateral Restraint Force Requirements of Sloped Z-Purlin Supported Standing Seam and Through-Fastened Roof Systems with Two, Four and Six Purlin Lines." Research Report CE/VPI-ST-04/01, Department of Civil and Environmental Engineering, Virginia Polytechnic Institute and State University, Blacksburg, VA, 2004.

Seek, M. W., and T. M. Murray (2004b), "Computer Modeling of Sloped Z-Purlin Supported Roof Systems to Predict Lateral Restraint Force Requirements." *Conference Proceedings, 17th International Specialty Conference on Cold-Formed Steel Structures*, Department of Civil Engineering, University of Missouri-Rolla, Rolla, MO, 2004.

Seek, M. W., and T. M. Murray. (2006). "Component Stiffness Method to Predict Lateral Restraint Forces in End Restrained Single Span Z-Section Supported Roof Systems with One Flange Attached to Sheathing." *Conference Proceedings, 18th International Specialty Conference on Cold-Formed Steel Structures*, Department of Civil Engineering, University of Missouri-Rolla, Rolla, MO, 2006.

Seek, M. W. and T. M. Murray (2007), "Component Stiffness Approach to Determine Lateral Forces in Z-Section Roof Systems," *Annual Stability Conference Proceedings*, Structural Stability Research Council, New Orleans, LA, April 19-21, 2007.

Seshappa, V. and T. M. Murray (1986), "Study of Thin-Walled Metal Building Roof Systems Using Scale Models", *Proceedings of the IABSE Colloquium on Thin-Walled Metal Structures in Buildings*, IABSE, Zurich, Switzerland, pp. 177-183, 1986.

SJI (2020), SJI 100, *Standard Specification for K-Series, LH-Series, DLH-Series Open Web Steel Joists and for Joist Girders*, Steel Joist Institute, Florence, SC, 2020.

Trout, A. M. and T. M. Murray (2000), "Reduced Number of Base Tests," Research Report CE/VPI-ST00/17, Department of Civil and Environmental Engineering, Virginia Polytechnic Institute and State University, Blacksburg, VA, 2000.

MBMA

METAL BUILDING MANUFACTURERS ASSOCIATION®

Research | Leadership | Education

1300 Sumner Avenue
Cleveland, OH 44115-2851
Phone: (216) 241-7333

mbma.com